In collaboration with

PRESENTS

2012 International Conference on Clean Technology & Engineering Management (ICCEM 2012)

2012 INTERNATIONAL CONFERENCE

ON

CLEAN TECHNOLOGY AND CONTEMPORARY ENGINEERING MANAGEMENT

NOVEMBER 12 – 15, 2012

@

COVENANT UNIVERSITY, OTA

CONFERENCE AGENDA

Conference Chair:
Engr. Prof. F.A Oyawale

Conference Secretary:
Engr. S.O Oyedepo

© Mechanical Engineering, Covenant University, Ota, Nigeria

CONFERENCE PROGRAMME

November 12 - 15, 2012

Day One: Monday, November 12, 2012
Venue: Mechanical Engineering Building
2:00pm – 6:00pm: Registration of Participants /Arrival of Invited Guests

Day Two: Tuesday November 13, 2012
Session 1: Plenary Opening Ceremony
THEME: INNOVATIONS, CLEAN TECHNOLOGY AND CONTEMPORARY ENGINEERING MANAGEMENT
Venue: African Leadership Development Center, Covenant University, Ota

10:00am – 10:05am: National Anthem
10:05am – 10:10am: University Anthem
10:10am – 10:15am: Opening Prayer (**University Chaplain**)
10:15am – 10:30am: Introduction of Guests/Dignitaries (**Dr. Ogunsina B.S**)
10:30am – 10:40am: Welcome Address (**Dean CST**)
10:40am – 11:00am: Goodwill Message (**Prof. C.K Ayo**, Vice Chancellor, Covenant University)
11:00am – 11:05am: Goodwill Message (Engr. M.B Shehu, President, Nigerian Society of Engineers)
11:05am – 11: 10am: Goodwill Message (Engr. A. Fanimokun, Chairman, Nigerian Institution of Mechanical Engineers)
11:10am- 11:40am: Special Keynote Address (Ogbeni (Engr.) Rauf Aregbesola, Executive Governor of Osun State
11:40am – 12:20pm: Keynote Address (Prof. Onwalu, P, Director General, Raw Materials Research and Development Council)
12:20pm – 12:30pm Remark from Deputy Dean, Sch. of Engrg – Dr. Agboje
12:30pm – 12:40pm: Vote of Thanks (Prof. F.A Oyawale, Chairman (LOC))
12:40pm – 12:45pm: Closing Prayer (Dr. Ajayi, O.O)
12:45pm – 1:00pm: Group Photograph/Departure
1:00pm – 3:00pm: Lunch Break/Exhibition of Students Projects
3:00pm – 5:00pm: Plenary session 2

3:00pm – 5:00pm: First Concurrent Session

Technical Session A

THEME FOCUS: CONTEMPORARY ENGINEERING MANAGEMENT

Tract 1 ***Building Services***
Venue: 500 Lecture Hall, Mechanical Engineering Department Building

Chairman: Prof. T.O. Mosaku
Secretary: Dr. S.T. Adedokun
Rapporteurs: Mr. Banjo Solomon & Mr. Abidakun, O.A.

Speakers/Papers:

Paper A1: **Mr. Adekeye, Engr. S.O. Oyedepo & Oyebanji**
Design & Development of Vapour Absorption Refrigeration System for Rural Dwellers.

Paper A2: **P.O. Babalola**
Electromechanical Systems in Building Services Engineering

Paper A3:

Paper A4:

Track 2 ***Applied Mechanics/Management***
Venue: ***Computer Lab, Mechanical Engineering Department Building***

Chairman: **Dr. Osheku, C.A**

Secretary: **Dr. R.J.O Ekeocha**
Rapporteurs: **Engr. Oyebanji, J.A & Mr. Ocheja, J.P**

Paper A5: **Razak I. Adeniji and Olawale O.E. Ajibola**
Resolving Energy Crisis through Communication: The Case of PHCN.

Paper A6: **Olateju O.I, Oyeobu A.J and Nwatulegwu B.I**

Effects of project management techniques on primary health care delivery

Paper A7: **Diji, C.J.**
Sustainability Assessment of Electricity Production and Consumption in Nigeria

Paper A8: **Loto M.A. & Ojakinwa TB**
Human Capital Formation Technological Diffusion and Economic Growth In Sub-Saharan African Countries: Evidence From Panel Data Analysis

Paper A9: **OLATEJU O.I, HOTEPO O.M and OYEOBU A.J**
An evaluation of total quality management practices on business performance of the Nigerian telecommunication sector

Paper A10: **Alamutu S.A, Hotepo O.M, Oyeobu A.J and Nwatulegwu B.I**

An evaluation of total quality management practices on business performance of the Nigerian telecommunications sector: a case study of MTN Nigeria Limited

Paper A11: **Olateju, O.I, Olateju, R.O and Mohammed, T.O**
Effects of project management techniques on the performance of the oil sector

Track 3 ***Mechatronics***
Venue: ***Conference Room, Mechanical Engineering Department Building***

Chairman: **Prof. Katende, J**
Secretary: **Engr. R. O Leramo**
Rapporteurs: **Engr. Omotosho, O.A & Mr. Babarinde Taiwo**
Speakers/Papers:

Paper A11: **Aru, O.E and Opara, F.K.**
Applying intelligent Systems in medical Diagnosis

Paper A12: **C. A. Bolu**
Integrating Mechatronics into Mechanical Engineering Curriculum in Nigeria

Paper A13: **V.O.S. Olunloyo, O.O.E. Ajibola and O. Ibidapo-Obe**
Active fuzzy control of tall civil engineering structures

DAY THREE: Wednesday, November 14, 2012

9:00am – 12:00pm: Second Concurrent Session

Technical Session B

THEME FOCUS: **CLEAN TECHNOLOGY AND ENVIRONMENTAL SCIENCE & TECHNOLOGY**

Tract 1 ***Clean Technology/Environmental Science & Technology***
Venue: ***CNC Lab, Mechanical Engineering Department Building***

Chairman: **Engr. Awoyele**
Secretary: **Engr. O.S. Ohunakin**
Rapporteurs: **Mr. Gbenebor,P.O & Mr. Abioye, P.O**

Speakers/Papers:

Paper B1: **Engr. Abolarin, T.S**
Identification of Major Noise Donors, A Sure Way To Abating Noise.

Paper B2: **Antai E.E**
Environmental Liquid Effluent, a Novel Approach for Treatment Of Industrial Waste Water

Paper B3: **Olukani D.O and Akinyinka O.N**
Environment Health and Wealth: Towards Analysis of Municipal Waste Management in Ota

Paper B4: **Ovri J.E.O**
Design and Construction of an Anearobic Digester for the Production of Biogas

Paper B5: **Ekpeni L.E.N. and Olabi A.G.**
Homogenisation In High Pressure Homogenizer (HPH) - A Deviced Technique for Biomass Conversion in Biogas

Paper B6: **Inegbenebor, A.I., Aruwajoye I.O. and Inegbenebor, A.O.**
Evaluation of homogeneity from ore-bodied in Nigeria for secondary mineral prospective

Paper B7: **Babalola P.O.**
Design and construction of parabolic solar heater using polymer matrix composite

Paper B8: **Tunde F. Adepoju, Adeyinka O. Adetunji, Emmanuel M. A. Olatunji and Bello J. Olatunde**
HCME: An environment-friendly I.C. engine fuel

Paper B9: **Ogunsina, B.S, Ojolo S.J, Ohunakin, O.S, Oyedeji, O.A, Matanmi, K.A**

Potentials for generating alternative fuels from empty palm fruit bunches by pyrolysis

Track 2 ***Nanoscience and Materials***
Venue: ***300 Lecture Hall, Mechanical Engineering Department Building***

Chairman: **Engr. Prof. C.A Loto**
Secretary: **Engr. J.O. Okeniyi**
Rapporteurs: **Mr. Ajayi, C.O & Mrs. Joseph, O.O**

Speakers/Papers:

Paper B10: **Gbenebor, P.O. Aasa, S.A, Inegbenebor, A.O.**
Effect of Pouring Temperature on Solidification Profiles of Aluminium Alloy

Paper B11: **O. Sanni, A.P.I. Popoola and C.A. Loto**
Inhibition Effect of Ferrous Gluconate on the Electrochemical Corrosion Behaviour of Aluminium Alloy in H_2SO_4

Paper B12: **C.A Loto and R.T. Loto**
Corrosion Polarisation Susceptibility Behaviour of Duplex (α β) Brass in Nitric Acid Concentrations

Paper B13: **Ovri J.E.O**
Corrosion Inhibition of Stainless Steel Using Molasses

Paper B14: **O.S.I Fayomi, A.P.I Popoola, C.A Loto and O.M Popoola**
Morphology and Properties of Zn-Al-TiO_2 Composite on Mild Steel

Paper B15: **C .A. Loto and R. T. Loto**
Corrosion resistance evaluation of Ferritic stainless steel and αβ (duplex) Brass in strong acids and acid chloride environments

Track 3 ***Renewable Energy Systems***
Venue: ***Conference Room, Mechanical Engineering Department Building***

Chairman: **Prof. A.S. Sambo**
Secretary: **Dr. R.J.O Ekeocha**
Rapporteurs: **Engr. Makun, T.O.K & Mr. Ocheja, J.P**

Speakers/Papers:

Paper B16: **Aasa S.A, Gbenebor O.P and Ajayi O.O**
Thermodynamics Charcterisation of Density Models For Solar Water Heater Sizing.

Paper B17: **Sobamowo, M. G, Ogunmola, B.Y, Ogbemhe, J. A and Adeoye S.A.**
Analysis of a wind-tidal power generating system for marine environment

Paper B18:

Paper B19:

Track 4 ***Thermal Engineering / Power***
Venue: ***Computer Lab, Mechanical Engineering Department Building***

Chairman: **Prof. S.S Adefila**
Secretary: **Dr. S.T. Adedokun**
Rapporteurs: **Mr. Banjo Solomon & Mr. Abioye, P.O.**

Speakers/Papers:

Paper B20: **Omorogiwa Eseosa and Odiase O.F**
Sensitivity studies in the Nigeria restructured 330KV Power network using FAT devices

Paper B21: **Sobamowo, M.G and Ogunmola, B.Y**
Transient Heat transfer analysis in longitudinal straight fin of rectangular profiles

Paper B22: **Diji, C.J.**
Exergoeconomic Analysis of a Steam – Fired Power Plant in Nigeria

Paper B23: **Oyedepo S. O and Kilanko**
Thermodynamic analysis of a gas turbine power plant modeled with an evaporative cooler

Tract 5 ***Industrial Engineering / Manufacturing***
Venue: ***500L Lecture Hall, Mechanical Engineering Department Building***

Chairman: **Prof. Charles Owaba**
Secretary: **Engr. O.A. Abidakun**
Rapporteurs: **Engr. Olugboye, D.O & Mr. Babarinde Taiwo**

Speakers/Papers:

Paper B24: **Oyebanji J.A, Oyedepo, S.O and Adekeye, T**
Performance evaluation of two palm kernel nut cracker machine

Paper B25: **Adeyemo, J. A**
Investigation of drillware and tool life in Cutting sintered powdered steel materials

Paper B26: **Oyawale F. A and Fashola, A. A**
Quality Characteristics of Concrete Poles manufactured in the Ibadan Metropolis, South West, Nigeria

Paper B27: **Adekunle, A.S. Odusote, J.K. and Rabiu, A.B.**
Effect of Using Vegetable Oils As Quenching Media For Pure Commercial Aluminium

Paper B28: **Babalola P.O., Inegbenebor, A.O.**
Design and construction of tilting furnace for producing aluminium matrix composites

Paper B29: **Christian A. Bolu, Ademisoye O. Tolulade and Alimi Adeshina**
University Optical Fibre Network Access Optimisation: A Case Study

2:00pm – 5:00pm: Third Concurrent Session
Technical Session C

Track 1 ***Nanoscience and Materials***
Venue: ***Computer Lab, Mechanical Engineering Department Building***

Chairman: **Engr. Prof. A.O. Inegbenebor**
Secretary: **Engr. R. O Leramo**
Rapporteurs: **Engr. Makun, T.O.K & Mr. Olugboye, D.O**

Speakers/Papers:

Paper C1: **C.A. Loto**
Influence of *Ananascomosus* Juice Extract as Additive on the Electrodeposition of Zinc on Mild Steel in Acid Chloride Solution

Paper C2: **Okeniyi, J.O., Oladele I.O., Ambrose, I.O., Omoniyi, O.M., Okpala, S.O., Loto C.A. and Popoola, A.P.I.**
Effects Of Na2Cr2O7 Inhibitor On The Corrosion Potentils Response Of Steel Reinforced Concrete In Saline Medium

Paper C3: **R.T. Loto, C.A. Loto and A.P.I. Popoola**
Inhibitive effect of Di-Metyl-Aminiethanol on the Corrosion of Austenitic Stainless Steel Type 304 in Acidic Media

Paper C4: **Ajayi, O.O., Joseph, O.O., Omotosho, O.A. and Olabowale, T.O**
Rauvolfia vormitoria Effect on the Degradation of Aluminium Alloy in 2.5 M Hydrochloric Acid Solution

Paper C5: **Fayomi, O. S. I, Abdulwahab, M., Gbenebor, O. P and Popoola, A. P. I.**
Physio-Chemical and Mechanical Behaviour of (*Pinussylvestris)* as Binders on Foundry Core Strength

Paper C6: **C.A. Loto and R.T. Loto**
Electrochemical Corrosion Resistance Evaluation of Ferritic Stainless Steel in HCl

Track 2 ***Engineering Innovations***
Venue: ***500L Lecture Hall, Mechanical Engineering Department Building***

Chairman: **Engr. Prof. F.A. Oyawale**
Secretary: **Mr. S.A. Aasa**
Rapporteurs: **Engr. Oyebanji, J.A. & Mr. Adelekan, D.S**

Speakers/Papers:

Paper C7: **Abidakun, O.A.**
Effect of expression conditions on the yield of dika nut (*irvingia gabonesis*) oil under uniaxial compression

Paper C8: **James Katende and Abubakr Sadiq Bappah**
An autotuner for industrial PID control loops

Paper C9: **Olateju O.I, Oyeobu A.J and Nwatulegwu, B.I**
Effects of project management techniques on primary health care delivery

Paper C10: **Ilori, T.A., Dauda.,T.O., Raji.A.O, and Kilanko,. O. O**
Occupational Mobility in Engineering Profession (Craftman and Artisan) in Oyo State, Nigeria

Track 3 ***Modelling & Simulations***
Venue: ***Conference Room, Mechanical Engineering Department Building***

Chairman: **Dr. Anake, T.**
Secretary: **Mrs. O.O. Joseph**
Rapporteurs: **Engr. Adekeye, T. & Engr. Kilanko, O.**

Speakers/Papers:

Paper C11: **David O. Olukanni, Kenneth O. Adekalu and Joel J. Ducoste**
Hyderaulic modelling and optimisation of a waste water treatment system for developing nations using CFD

Paper C12: **Ramalingam Periasamy**
Mathematical model of alternate methods of dispersion of fluid gases from Power generation units

Paper C13: **Katende, J, Awelewa, A.A, Samuel, I.A and Iyiola, S.O.**
Root Locus-Based Magnetic Levitation System Stabilization: An Undergraduate Control System Design Approach

Paper C14: **M. G. Sobamowo, S.O. Ismail and A.M. Ayerin**
Experimental and numerical investigations of free convection heat transfer in solar ovens

Paper C15: **Tunde F. Adepoju, Eriola Betiku, Bamidele O. Solomon, Bello J. Olatunde and Emmanuel M. A. Olatunji**
Statistical approach to optimization of the transesterification reaction from sorrel (*hibiscus sabdariffa*) oil

Inhibitive effect of ferrous gluconate on the electrochemical corrosion of aluminium alloy in H_2SO_4 solution

O Sanni[(1)], A.P.I. Popoola[(1)], C.A. Loto[(2)]
[1]Department of Chemical and Metallurgical Engineering, Tshwane University of Technology, Pretoria, South Africa
[2]Department of Mechanical Engineering, Covenant University, Ota, Nigeria
E-mail address: tayo.sanni@yahoo.com

Abstract
The use of ferrous gluconate as corrosion inhibitor on aluminium alloy in 0.5M H_2SO_4 solution was studied using gravimetric and potentiodynamic polarization measurements. The surface morphology of the aluminium alloy was studied after exposure to 0.5 M H_2SO_4 solution in the presence and absence of inhibitor using high resolution scanning electron microscopy equipped with energy dispersive spectroscopy (HRSEM – EDS). The adsorption behaviour of the inhibitor was investigated. The results of the investigation show that increase in concentration of ferrous gluconate corresponds to an improvement on inhibition efficiency. Equally, the results showed the ferrous gluconate to be an effective corrosion inhibitor for the aluminium in the acidic medium. The results obtained from the two methods used were found to correlate with each other.

***Key words**: Corrosion test, Ferrous gluconate, Inhibition efficiency, Adsorption*

1. Introduction
Corrosion of metals/alloys can be defined as the deterioration or disintegration of materials due to their interaction with the environment. The subject has continued to receive attention over the years. Corrosion scientists are relentless in seeking better and more efficient ways of combating the corrosion of metals /alloys [Fontana, 1987].
Aluminium and its alloys are generally light, cheap, good conductors of heat and electricity and resist corrosion at moderate temperatures. They are therefore used widely as materials for cooking utensils, electricity cables, bottle tops, food and beverage containers, roofing sheets [Uppal and Bhatia, 2001]. Bottle tops of most alcoholic and non-alcoholic drinks, industrial machine parts are found to corrode rapidly in moist air thus constituting a health hazard to the end users. Although the oil and gas, beverage and metallurgical industries sink a large sum of money in an attempt to control corrosion of their engine parts and products, however, the problem still persist. In some chemical industries, equipment becomes corrosive after few years. In view of this, the need to research into the field of corrosion inhibition becomes necessary [Onen et al, 2010].

Inhibitors are chemical compounds that, when added to a fluid or gas decreases the corrosion rate of the metal or an alloy [Asuke, 2008]. The effectiveness of a corrosion inhibitor is a function of many factors like: fluid composition, quantity of water and flow regime [Asuke, 2008; Scamans et al, 1989; Schmitt, 1984]. In the oil extraction and processing industries, inhibitors have always been considered to be one of the defences against corrosion [Thomas, 1980; Fontana and Greene, 1987].

Various methods namely weight loss and gasometric [Ekpe et al, 1995; Ita et al, 1997; Ebenso et al 2004; El-Naggar, 2007; Ait Chikh et al, 2005; Ebenso et al, 1999; Ekpe et al, 2001; Obot et al, 2010; Ebenso et al, 2008], electrochemical and analytical [Ait Chikh et al, 2005] and polarization [Abdulwahab et al, 2012] have been employed in the determination of corrosion rates and inhibition studies. There have been several studies on corrosion inhibition of aluminium, mild steel, copper, and zinc in acidic and other medium. Some corrosion inhibitors such as synthetic compounds [Ait Chikh et al, 2005; Ebenso et al, 1999; Ekpe et al, 20011], natural products [Obot et al 2010] and dyes [Ebenso et al, 2004; Ebenso et al, 2008] have been investigated and reported as good corrosion inhibitors. In this work, the use of

ferrous gluconate (FG) as corrosion inhibitor was investigated for aluminium alloy in sulphuric acid solution using gravimetric and potentiodynamic polarization methods

2. Experimental methods

2.1 Materials and Methods

As – received aluminium alloy of dimension 12 x 12 x 2 mm with chemical composition shown in Table 1 was used. A 3.0mm diameter hole was drilled about 5 mm from the top of the 12 mm edge. The gravimetric test specimens were degreased in ethanol, dried, weighed and stored in desiccators for further tests. Selected specimens were connected to an insulated flexible wire and cold mounted in methyl methacrylate resin. They were subsequently used for potential measurement. A concentration of 0.5M H_2SO_4 was prepared as required for the experiment. FG as inhibitor was used in H_2SO_4 medium. The molecular structure of the inhibitor is presented in Figure 1. The experiment was conducted at 28^0C.

Table 1: Chemical composition of the aluminium used.

Si(%)	Fe(%)	Cu(%)	Mn(%)	Mg(%)	Zn(%)	Ni(%)	Cr(%)	Ti(%)	Ag(%)
0.157	0.282	0.0025	0.024	0.51	<0.0010	<0.0010	0.023	0.0046	<0.0001

B(%)	Be(%)	Bi(%)	Ca(%)	Cd(%)	Co(%)	Li(%)	Na(%)	p(%)	Pb(%)
0.0007	<0.0001	<0.0010	0.0011	0.0005	<0.0010	<0.0002	0.0005	<0.0010	<0.0005

Sn(%)	Sr(%)	V(%)	Zr(%)	Al(%)
<0.0010	<0.0001	0.0035	0.002	99

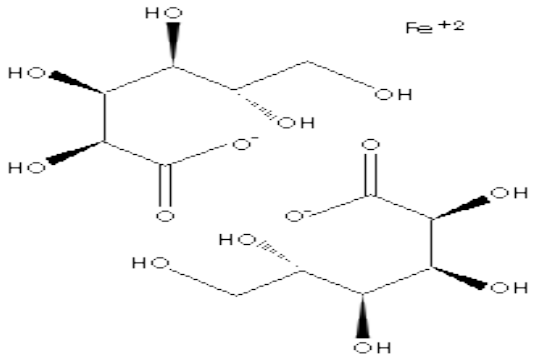

Figure 1: Molecular structure of ferrous gluconate

2.2 Gravimetric measurements

Corrosion test was carried out on the previous weighed samples in the presence and absence of inhibitor and one of the samples was used as control (i.e. without inhibitor) while other samples were with inhibitor. The ferrous gluconate was dissolved in 0.5 M H_2SO_4, the experiment was repeated with varying concentration of inhibitor (0.5 – 2.0) % g/v.

For each experiment, the samples were washed, dried and weighed over a period of twenty – eight days. The weight loss measurements were taken at an interval of 48h. The corrosion rate, degree of surface coverage and inhibitor efficiency were determined. The weight loss was determined by finding the difference between the initial weight of the samples and the final weight after 48 h using the equation below

$$W = W_O - W_F \quad (1)$$

Where:

W = weight loss in mg, W_O= initial weight, W_F= final weight.

The corrosion rate was determined in millimeter per year (mm/yr)

$$CR\ (mm/yr) = \frac{87.6W}{DAT} \quad (2)$$

Where W = weight loss in mg, D = density of the materials in g/cm^3, T = time of exposure in hours and A = area of specimen in cm^2

The degree of coverage and efficiency of the inhibitor was determined using the relationship reported elsewhere [Halambek et al, 2010]

2.3 Electrochemical measurement

The potentiodynamic polarization techniques were used to evaluate the corrosion rate of the aluminium alloy in FG-H_2SO_4 solution. All electrochemical measurements were obtained using Autolab frequency response analyzer (FRA) coupled to potentiostat and connected to a computer system as source of data acquisition. A standard corrosion cell was used as described elsewhere [Abdulwahab et al, 2012]; saturated Ag/Ag reference electrode and aluminium sample as working electrode were used for the electrochemical study. The working electrode samples were positioned at the glass corrosion cell kit, leaving 1 cm^2 surfaces in contact with the solution. Polarization test was carried out at 28^0C in 0.5 M H_2SO_4 solution using a 668 VA AUTOLAB potentiostat with 1.8 NOVA software package; a scan rate of 0.0016V/sec was used. From the Tafel corrosion analysis, the corrosion rate, potential and linear polarization resistance data were obtained in a static solution.

2.4 Surface morphology

The as – received and as – corroded aluminium alloy surfaces were examined with high resolution scanning electron microscopy equipped with energy dispersive spectroscopy (HR SEM/EDS) Model : (Joel JSM – 7600F) was used to assess the surface of the corroded samples.

3. Results and discussion

3.1 Weight loss measurement

The results obtained for the variation of corrosion rate, inhibition efficiency and degree of surface coverage with exposure time for the aluminium alloy specimens immersed in 0.5 M sulphuric acid with varied concentrations of FG are represented in Figures 2 and 3.

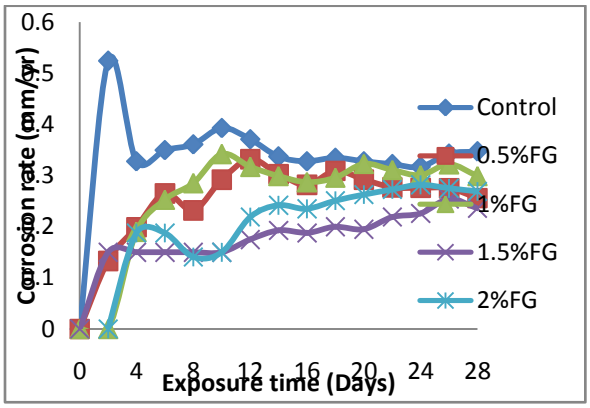

Figure 2: Variation of corrosion rate with exposure time for the aluminium specimen immersed in sulphuric acid for different concentration of inhibitor.

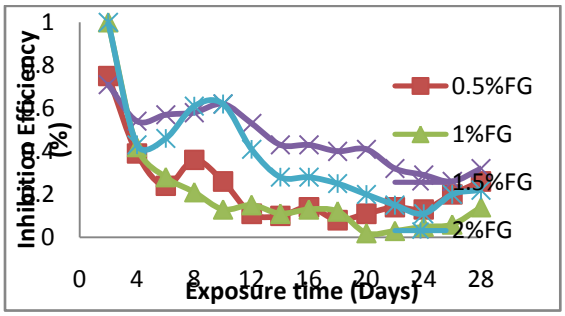

Figure 3: Variation of inhibition efficiency with exposure time for the aluminium specimen immersed in sulphuric acid for different concentration of inhibitor.

The corrosion rates of the aluminium coupons in 0.5M H_2SO_4 in the presence and absence of different concentrations of inhibitor (FG) were determined using equation 2. The results obtained are presented in Figure 2. The corrosion rates decreased with addition of ferrous gluconate. This indicates that (FG) in the solution inhibits the corrosion of aluminium in acidic medium and that the extent of corrosion inhibition depends on the amount of the ferrous gluconate present.

The percentage inhibitor efficiency shown in Figure 3 shows the variation of inhibitor efficiency with time at different concentrations of the inhibitor. The inhibition efficiency decreases with increase in exposure time with final values of 26%, 14%, 32%, and 22% when inhibitor concentration was increased from 0.5% to 2% with 0.5% incremental range. It shows that

percentage inhibition efficiency of ferrous gluconate progressively decreases with increase in time of exposure.

3.2 Potentiodynamic polarization

The potentiodynamic polarization measurement for aluminium alloy in 0.5 M H_2SO_4/ferrous gluconate is presented in Table 2. Potentiodynamic polarization –corrosion rate (PP-CR), potentiodynamic polarization corrosion density (PP-Icorr) and linear polarization resistance (LPR) data were used as criteria for evaluation of corrosion resistance of aluminium alloy in the medium.

Table 1: Electrochemical corrosion data obtained for aluminium alloy in 0.5 M H_2SO_4- varying concentration of ferrous gluconate at 28^0C.

S/N	C (% g/v)	Icorr (A/cm2)	ba(v/dec)	bc (v/dec)	LPR Rp(Ω cm2)	Ecorr (V)	CR (mm/yr)
1	0	1.73 E-05	0.025 551	0.124 93	5.33E +02	- 0.33 054	0.559 600
2	0.5	4.27 E-06	0.111 520	0.225 70	7.60E +03	- 0.35 751	0.138 000
3	1.0	6.30 E-09	0.892 180	1.727 60	4.06E +07	- 0.34 318	0.000 206
4	1.5	5.43 E-06	0.042 048	0.035 871	1.55E +03	- 0.33 054	0.175 710
5	2.0	6.05 E-09	1.958 100	0.748 74	3.90E +07	- 0.34 318	0.000 197

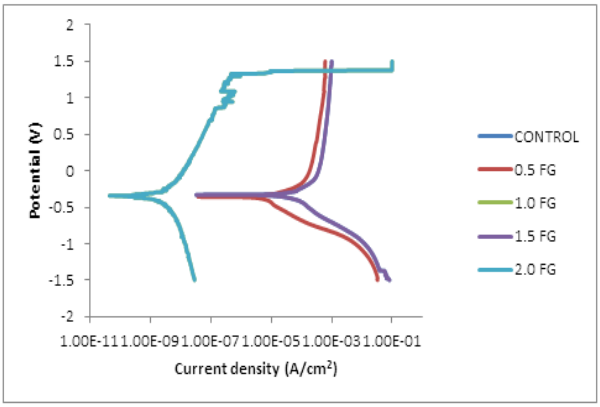

Figure 4: Linear polarization of aluminium in 0.5M H_2SO_4 solution / ferrous gluconate environment at 28^0C.

Figure 4 shows the polarization curves for 0.5 M H_2SO_4-Ferrous gluconate. The environment demonstrated a decrease in the corrosion rate and current density with addition of the inhibitor.

While the corrosion potential (Ecorr) and polarization resistance increases with inhibitor concentrations. The trend in the corrosion under this study is similar with the previous report [Abdulwahab et al, 2012]. The inhibited aluminium in 0.5M H_2SO_4 –Ferrous gluconate revealed that corrosion rate decreases from 0.17571 mm/yr to 0.138, 0.000206 and 0.000197 at 1.5% g/v, 0.5% g/v,1.0% g/v and 2.0% g/v ferrous gluconate. Corrosion rate of aluminium alloy –H_2SO_4 is lower in 2.0% g/v and 1.0%g/v ferrous gluconate when compared to 0.5% g/v and 1.5% g/v respectively. Also, the changes in anodic and cathodic region suggest the mixed –type corrosion inhibition for aluminium alloy-0.5M H_2SO_4/ferrous gluconate.

3.3. Corroded surface analysis

The SEM microstructure of aluminium surface is shown in Figure 5 to 6. The as - received aluminium alloy sample Figure 6, shows that ferrous gluconate was able to exhibit some degrees of inhibition which retard the corrosion rate of aluminium in H_2SO_4 solution.

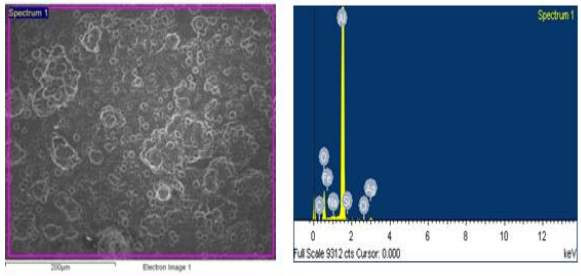

Figure 5: SEM micrograph of the as-received aluminium sample with the EDS spectrum

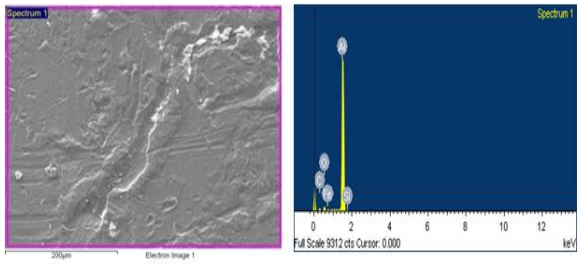

Figure 6: SEM micrograph of aluminium in 1.0%g/v ferrous gluconate in 0.5M H_2SO_4 with the EDS spectrum

3.4. Efficiency of Inhibitor and adsorption isotherms

The percentage inhibitor efficiency (%IE) of the aluminium alloy –ferrous gluconate in H_2SO_4 solution was computed using the equation reported elsewhere [Halambek et al, 2010] .The

computed data for the IE using potentiodynamic polarization corrosion rate (PP-CR), potentiodynamic polarization-corrosion density (PP-Icorr), linear polarization resistance (LPR) and gravitational method (GM) are presented in Figure 7 for 0.5M H_2SO_4/ferrous gluconate. The result revealed that the highest %IE of ferrous gluconate was achieved at 1.0 and 2.0%g/v and there was a correlation in all the methods used. The adsorption mechanism was shown from the variation between log θ with log C indicating linearity for the environment and the adsorption behavior is believed to have obeyed Freundlich adsorption isotherm.

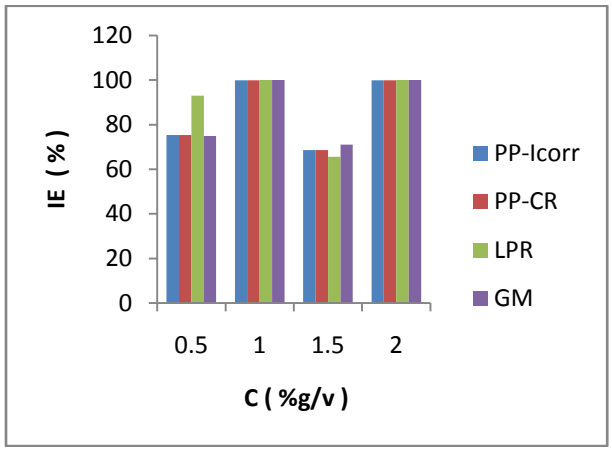

Figure 8: Comparism of inhibitor efficiency (IE) for 0.5M H_2SO_4 solution / ferrous gluconate concentration obtained from gravimetric method and potentiodynamic polarization.

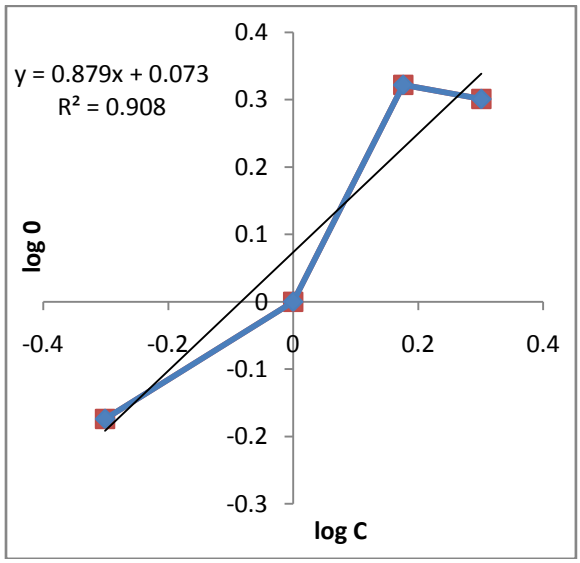

Figure 9: Freundlich isotherm for the adsorption of ferrous gluconate on the aluminium alloy in 0.5 M H_2SO_4 solution obtained from gravimetric method at 28^0C.

4. Conclusion

The deductions from the experimental investigations show that ferrous gluconate (FG) acts as a good inhibitor for the corrosion of aluminium in 0.5M H_2SO_4 because the inhibitor was able to reduce the corrosion rate. Potentiodynamic polarization curves reveals that ferrous gluconate is a mixed – type inhibitor. The adsorption of ferrous gluconate follows Freundlich adsorption isotherm.

References

Abdulwahab, M., Kasim, A., Fayomi, O.S.I., Asuke, F. and Popoola, A. P. I. (2012): Inhibitive effect of Arachis hypogeae on the corrosion of mild steel in sulphuric acid solution, J. Mater. Environ. Sci., 3(6), pp. 1177 – 1182.

Ait Chikh, Z., Chebabe, D., Dermaj, A., Hajjaji, N., Srhiri, A., Montemor, M.F., Ferreira, M.G.S. and .Bastos, A.C. (2005): Electrochemical and analytical study of corrosion inhibition on carbon steel in HCl medium by 1,12-bis(1,2,4-triazolyl)dodecane, Corros. Sci.47 pp. 447-459.

Asuke, F (2008): Corrosion Characteristics of Al- Si/Sic composite using palmwine and propagyl as inhibitors, an Unpublished MSc degree thesis, Department of Metallurgical and Materials Engineering, Ahmadu Bello University, Zaria, Nigeria.

Ebenso, E. E., Okafor, P. C., Ekpe, U. J., Ibok, U. J. and Onuchukwu, A. I. (2004): The joint effects of halide ions and methylene blue on the corrosion inhibition of aluminium and mild steel in acid corrodent, Journal of Chemical Society of Nigeria. 29(1), 15-25

Ebenso, E. E., Ekpe, U. J., Ita B. I., Offiong, O.E. and Ibok U. J. (1999): Effects of molecular structure on the efficiency of amides and TSC used for corrosion inhibition of mild steel in HCl. Materials Chemistry and Physics ,Elsevier Science, Holland, 60, pp. 79-90.

Ebenso, E.E., Hailemicheal Alemu, Umoren, S.A. and Obot, I.B. (2008): Inhibition of mild steel corrosion in sulphuric acid using Alizarin Yellow GG dye and synergistic iodide additive, International Journal of Electrochemical Science 3, pp. 1325-1339.

Ekpe, U. J., Ibok, U. J., Ita, B. I., Offiong O. E. and Ebenso, E. E. (1995): Inhibitory action of methyl and phenyl thiosemicarbazone derivatives on the corrosion of mild steel in HCl. Material Chemistry and Physics, Elsevier Science, Holland, 40; 87-93.

Ekpe, U. J., Okafor, P. C., Ebenso, E. E., Offiong, O. E. and Ita, B. I. (2001): Mutual effects of TSC derivatives on the acidic corrosion of aluminium. Bulletin of Electrochemistry, Cecri, India, 17(3), pp.131-135.

El-Naggar, M.M. (2007): Corrosion inhibition of mild steel in acidic medium by some sulfa drugs compounds, *Corrosion Science*, vol. *49* (5), pp. *2226*–2236.

Fontana, M. G. (1987): Corrosion Engineering, Mc-Graw-Hill Book Company, 3rd Edition, Boston, pp. 143-160.

Fontana, M. G. and Greene, N. D. (1987): Corrosion Engineering, McGraw-Hill book Company, New York.

Halambek, J., Berkovic, K. and Vorkapic – Furac. J. (2010): The influence of Lavandula angustifolia L. oil on corrosion of Al-3Mg alloy, *Corrosion Science,* Vol. *52,* pp. 3978–3983.

Ita, B. I. and Offiong, O. E. (1997): The inhibition of mild steel corrosion in hydrochloric acid by 2, 2 pyridil and a-pyridoin, Mater. Chem. Phys, 51, pp.203 – 210.

Obot, I.B., Obi-Egbedi, N.O., Umoren, S.A. and Ebenso, E. E. (2011): Adsorption and kinetic studies of fluconazole for the corrosion of aluminium in HCl solution, Chemical Engineering Communications, 198, pp. 711-725.

Onen, A.I., Nwufo, B. T., Ebenso, E.E. and Hlophe, R.M. (2010): Titanium (IV) oxide as corrosion inhibitor for aluminium and mild steel in acidic medium, Inter. Jour. Electrochem. Sci. 5. 1564.

Scamans, G. M., Hunter, J. A. and Holroyd, N. J. (1989): Corrosion of aluminium – a new approach, proceeding of 8th Inter. Light metals Congress, Leoban Wien, pp. 699-705.

Schmitt, G. M. (1984): Application of inhibitors for acid media. British Corrosion Journal, 19, pp.165-176.

Uppal, M. M. and Bhatia, S. C. (2001): Engineering Chemistry, Khana Publishers, 6th edition, Delhi, pp. 860.

Inegbenebor et al: Proc. ICCEM (2012) 7 - 12

Evaluation of homogeneity from ore-bodied in nigeria for secondary mineral prospective

*A.I Inegbenebor *I.O. Aruwajoye and **A.O. Inegbenebor

College of Science and Technology, Covenant University, Canaan Land, Ota, Ogun-State

*Chemistry Department **Mechanical Engineering Department

Corresponding Author: *A.I. Inegbenebor*

Abstract

Samples from ore–bodied areas at different locations in Papalanto and Ifo in Ogun-State, South-West of Nigeria, where Ewekoro cement industry is situated, were analyzed so as to recover some secondary minerals of economic value. The following parameters were evaluated, conductivity, turbidity, colour, pH and other chemical parameters. Variations of Dissolved Oxygen (DO), Chemical Oxygen Demand (COD), sulphate, nitrate, phosphate, chloride ion contents, and temperature were also studied. Mineral-forming heavy metals were in the ranges Fe: 89.0–1080 mg/l; Mg: 869–1120 mg/l; Pb: 23–80 mg/l; Zn: 180-480 mg/l. The concentration of nitrate is 20-35 mg/l; phosphate: 8-80mg/l; Dissolved Oxygen (DO): 30–45 mg/l; Total Dissolved Solids (TDS): 89-900 mg/l; pH: 6.1-8.5; Conductivity: 10-18µs/cm^3 and temperature ranged between 25-27^{o}C. Also in the tabulation are the results of the homogeneity of four geochemical explorations from other Nigerian ore-bodied environments for comparison. Correlations of some of the physical and chemical parameters have been established with the view of providing conditions for the formation of secondary minerals and the types of such minerals expected from the studied areas. The minerals may include the following groups of minerals: Adelite, Melilite, Cancrinite and Copriapite. The study apart from the present knowledge on ore-based baseline also present information on the pollution studies of the area under investigation.

***Key words**: Secondary Minerals, Homogeneity. Oxide-zone and Ore*

1. Introduction

The study of minerals has led to rapid development of material technology which is a key enabling area for economic and social well being. Materials with new and improved properties, and innovative methods if processing them, give industries competitive advantage in world markets. The products lead to better medical care, enhanced safety in infrastructural projects, improved and safer transport, sporting and leisure facilities and more environmentally friendly operation. These materials are from secondary minerals. Emphasis is therefore placed on secondary minerals of economic importance in this work since mostly all of the chemical reactions that take place in oxidizing sulfide beds ores involve homogeneous or heterogeneous systems. When compounds crystallized from aqueous solutions, redox processes that occur between various dissolved species, and dissolved gases especially oxygen and carbon dioxide, play central roles in the formation of many secondary minerals in most cases.

Although, the general mode of mineral formation in the oxide zone may involve dehydration of previously crystalline oxide, or oxide derivative, other compounds formation can also occur in the process. This phenomenon has been expressed (Williams 1992) in the way Jerosite $PbFe_3\ (SO_4)_2\ (OH)_6$, and Cerrusite $Pb_3(CO_3)_2(OH)_2$ are formed from aqueous solutions, as shown in the equations below for example.

$$Pb^{2+}{}_{(aq)} + \frac{2}{3}CO_{2\,(g)} + \frac{4}{3}H_2O_{\,(l)} \rightleftharpoons \frac{1}{3}Pb_3(CO_3)_2(OH)_{2\,(S)} + 2H^+{}_{(aq)}$$

Hydrocerussite

$$MFe_3(SO_4)_2(OH)_{6\,(S)} + 6H^+{}_{(aq)} \rightleftharpoons M^+{}_{(aq)} + 3Fe^{3+}{}_{(aq)} + 2SO_4{}^{2-}{}_{(aq)} + 6H_2O_{(l)}$$

Jerosite

Here, M can be H_3O, Na^+, K^+, Ag^+, $NH_4{}^+$, and 0.5 Pb^{2+}.

Ogun-State is an agrarian state, where fertilizers are frequently in use to boost the agricultural products. As a result of these activities, there is increase in acidity as well as that of level of other elements when ores are leached, some of which are toxic.

For these reasons, it is thought to examine some of the aspects of homogeneity and invariably prospective for ores so as to recover secondary minerals of economic importance. The result obtained would provide parameters of embodies baseline, especially those of heavy metals in waters of the study areas. The aim was to study the metallogenesis and other parameters in homogeneity of South Western Nigeria ore bodied environment in order to prospect for secondary minerals for industrial use.

2. Material and instrumentation

Sample Collection

To avoid inhomogeneous distribution during sample collection, spot collection was selected at Ewekoro because it is an active site for cement production, while at Papalanto and Ifo stations base-line collection was carried out. However, at Ifo samples were collected in a type of graduation. Units of oxide zone grade rock types are intercalated or mixed. Such relations indicate, that genetic conditions oscillated between extremes as they changed or possibly that materials were mixed grossly. Papalanto samples were collected by locating midpoint of particular bedrock. Notwithstanding, a unit was chosen which crop out where other components of the gradational zone are not. The top of the uppermost bed above flow is 10 ft. Samples were collected at Ewekoro, Papalanto and Ifo at close intervals along banks of the active channels.

The concept of the density flow [Wilson 1971] was applied in the collection of the sample. Here, two fluid bodied of different density were mixed together, the dense fluid tend to move above the denser one. Conversely, the denser fluids tend to flow downwards. Aqueous density flows were as a result of differences of temperature, salinity, and suspended sediment. Turbid bodies of water with large loads of suspended sediment frequently move as density flows beneath clear water.

Ten samples were collected in many series from each of the locations. Some were used for tests. Before sampling began, the homogeneity within several sections of units was tested. This is done by collecting channels chip and stratified samples of typical sections and comparing analysis made from them. Some of the homogeneous samples change appreciably when exposed for some time on the surface. The samples were put in dust-proof bag that was labeled clearly. These samples were registered in a sample book that was numbered in duplicate with sample numbers. The question then arose here whether the results of test samples were in close range. The interpretation of such was pertinent because change were compared especially at different temperatures.

The pH of the samples was determined on site by the use of an electrode pH meter (see Table 1). The temperature (^{o}C) of all the samples was measured in situ by the use of a graduated thermometer. Standard conductivity meter (us/cm) was used to determine the conductivity of the homogeneity while PCU was employed in detecting the colour of the water samples. Titration method was carried out for determination of alkalinity with measured volume of sample with H_2SO_4. Turbidity was measured using the graduated turbidity meter (NTU) by use of a standard solution (blank). The corresponding values of the instrument after sample was placed give the actual turbidity of the homogeneity. Elemental analyses were carried out by the use of atomic absorption spectrophotometric procedure (Thermo Corporation Model) for the determination of metals. The instrument was set at appropriate wavelength current, flame type and then calibrated by the use of standard solutions for each metal. Nitrates, sulphates and phosphates were also determined. The nitrate contents of the sample were analyzed by Brucine method. The other types of equipment used and manufacturers are recorded in Table 1.

3. RESULTS AND DISCUSSION

The amounts of the contents of major and minor elements in homogenous solution of selected geochemical environment from Ogun-State, Nigeria are listed in Tables 2 and 3, columns 1-3. The results of recent relative works carried out from other states in Nigeria, that is, Enugu, Delta, Sokoto and Abuja (columns 4-7) on the

tables are included for comparison because of the climatic difference within the country.

Table 1: Equipment

EQUIPMENT	MANUFACTURERS	MODEL
TDS	Hanna microprocessor	conductivity/TDS meter HI 9835
Conductivity	Hanna microprocessor	conductivity/TDS meter HI 9835
Salinty	Hanna microprocessor	conductivity/TDS meter HI 9835
Turbidity	Hanna	fast tracker(HI 98703)
Total hardness	Hanna	Multiparameter Bench Photometer (c 99)
Colour	Hanna	Multiparameter Bench Photometer (c 99) PUC
Dissolved oxygen	Hanna	Multiparameter Bench Photometer (c 99)
COD	Hanna	Multiparameter Bench Photometer (c 99)
Acidity		Done By Titration
pH	Hanna	pH 211 microprocessor pH meter
Temperature	Hanna	Thermometer
BOD		P Selecta Incubator (Medi Low)
AAS		Thermo Corporation S series AA Spectrometer
UV	For single beam	Thermo Corporation Genesys 10 UV scanning
UV	For single beam	Thermo Scientific HELLOS ZETA UV-VIS

Table 2: Selected Physico-Chemical Properties of Ore-bodied homogeneity from some states in Nigeria

CONSTITUENTS	CONTENT IN mg/l							
	1	2	3	4	5	6	7	8
SALINITY	NA	NA	NA	NR	35	NR	NR	1
TURBIDITY	350	150	180	10	20	0.2	1.34	<500
BIOLOGICAL OXYGEN DEMAND (BOD)	50	25	30	6	3.01	NR	5.8	
CARBON OXYGEN DEMAND(COD)	500	670	650	30	821	NR	NR	
TOTAL DISOLVED SOLID(TDS)	350	900	89	NR	20	46	491	500
TOTAL HARDNESS	20	50	95	NR	NR	4.5	0.08	250
COLOUR				NR	NR	70	NR	colourless
TEMPERATURE	26	25	27	NR	26	43	26	25-26
CONDUCTIVITY				NR	0.47	NR	17.3	1000µs/m
DISSOLVED OXYGEN(DO)	35	40	45	NR	74.5	NR	NR	

Table 3: Analysis of percolating homogeneity from Ore-zones of some states in Nigeria

CONSTITUENTS	CONTENT IN mg/l							
	1	2	3	4	5	6	7	8
pH	8.5	6.1	6.5	7.5	7.8	7.8	6.43	<8.0
Cl^-	20	15	28	0.1	12	15.9	0.9	200
NO_3^-	35	20	15	40	0.18	NR	NR	10
PO_4^{3-}	8.5	45	80	3.5	0.3	NR	NR	5
SO_4^{2-}	5.5	30	18	500	481	2.1	NR	250
NH_4^+	1.5	2	1.5	2	0.2	NR	NR	
CO_3^{2-}	35	32	29	NR	24	NR	NR	100
Na	7.5	890	185	NR	1359	4.2	NR	
Ca	1120	960	950	NR	326	NR	NR	
Mg	890	1080	500	NR	51	493	NR	20
Fe	80	45	23	NR	1.51	20	NR	3.0
Pb	9.5	250	ND	NR	0.01	NR	NR	0.01
Zn	181	480	380	NR	NR	1281	NR	3.0
K	1550	120	850	NR	106	1.9	NR	

(1) Ewekoro; (2) Papalanto; (3) Ifo; (4) Enugu, (Obuzor and Nduka 2010); (5) Delta, (Umudi and Awatefe 2010); (6) Sokoto, (Uba, Gwandy, Izuwagie and Sadiq 2010); (7) Abuja, (Aremu, Ozonyia and Ikokoh 2010) (8) WHO (2004, 2007) NA=Not Analyzed; NR=Not Recorded.

The results in the tables showed varying values for both physical and chemical constituents. Noticeable from the results in Table 1, is the relatively acidic pH of 6.1 and 6.5, conductivity of 18 and 13.5 at Papalanto and Ifo environments. The amount of dissociation of water depends on pH which invariably can lead to chemical reactions of waters and its dissolved solutes as well as the physical break down of the bedrock. The principal types of chemical reactions in such oxide zone in acidic medium are hydration (i.e. absorption of water), hydrolysis (chemical reaction to produce or consume H^+ or OH^- ions), oxidation and simple solution (Bartholomew et al. 1973, Garrels and Christ 1965). It is worth pointing out that pH of 8.5 (column 1) at Ewekoro may be a result of dissociation of carbonate equilibrium involving calcium carbonate or dimorph aragonite. With a high value of Pb, Mg and Fe of 80, 1120, and 890mg/l respectively at Ewekoro, it would not be surprising if secondary carbonate minerals are widely spread in this area, especially mineral containing more common base-metals such as lead, magnesium and iron which are frequently found in the oxidize zone of sulphide ore-bodies. Such may include the minerals with general formula $AB(XO_4)(OH)$; A=Ca, Pb; B=Fe^{2+}, Mg, X=P^{5+}; As^{5+},V^{5+} that is the Adelite group for example, also the Melilite, A_2BSiO_7; A=Na, Ca, B=Mg, Z=Al, Si, the Cancrinite group, $A_{6\text{-}9}(Si, Al)_{12}O_{24}(SO_4),(CO_3)$, $C_{l2}(OH)_{2\text{-}4}.nH_{2O}$, A=Ca, K, Na and the Copiapite group $A^{2+}Fe_4^{3+}(SO_4)_6(OH)_2 .2H_2O$ A=Ca, Fe, Mg, Zn; B^{3+}= Fe, Al. This type of observations and conclusions does not invalidate the general conditions of formation of

the group of minerals based on equilibrium of the M_nO_2–SO_3–H_2O system for example in aqueous solutions, while bearing reactants and transporting products and reactants, as well as furnishing in water necessary reagent in many cases, control chemical speciation, solute components and thus the solubility of secondary mineral species.

The value of COD at Ewekoro is 500, Papalanto 670 and Ifo, 600 are high when compared with TDS of 850 at Ewekoro and 900 for Papalanto. These constituents can be affected by additional CO_2 which are introduced into the homogenous from the atmosphere via rainfall, leaching from soil and bedrock, running from agricultural land, the stream and uncultivated lands. This is however a reflection of high solubility of the bulk solutes in water and the relative geochemical abundance. It is not surprising the presences of high dissolved oxygen, carbon dioxide and humic complexes as have earlier been reported (Bartholomew et al. 1973) to greatly increase the corroding power on solids in solutions.

Similar arguments can be made to explain the high amounts of total dissolve solid (TDS), 46ppm at Sokoto while temperature is 43^oC. Under arid conditions chemical weathering is minimal and physical processes are dominant. For example, temperature influences the rate of chemical reaction and affects the availability of water by increasing evaporation at high temperature. However, some elements such as Si of detrimental quartz grains characteristically can occur as component of insoluble secondary minerals during chemical reaction.

There are high amounts of Na, 1359mg/l and SO_4^{2-} ; 481 mg/l for example at Delta, the values of other parameters in this area are minimum compare with the zone analyzed in this present work. It should be therefore possible to explain the pollution of waters in this location and of course the formation of secondary minerals. Where major constituents are present in high amount, pollution is minimal, because the major constituents affect the dispersal of minor elements (see Table 2) in solution primarily by providing reactants, either for the precipitation of insoluble secondary minerals or for the formation of soluble complex in ions with minor elements (Wilson 1972).

Nevertheless, as rivers at the ore-bodied environ provide water for drinking, fishing and other purposes for the communities living around them, there is need to monitor periodically these parameters because of possibility of their accumulation especially the heavy metals often mineral forming.

4. CONCLUSION

Since the above explanation is consistence with the observation, therefore as a result of these studies, it is possible to delimit quickly and more or less precisely, the area of interest where to concentrate detailed exploration. The economic value of the suspected groups of minerals would be enormous, when they may be prospective for materials in industrial use, most especially in the areas of microprocessors, memories, superconductors and other systems. The study apart from the present knowledge on ore-based baseline also present information on the pollution studies of the area under investigation where WHO values are comparable. More intensive work is in progress in conjunction with the geological, geophysical and geochemical surveyors of the study location.

Acknowledgement

The authors acknowledge the contribution of T. Owoeye, Technologist, Chemistry Department, Covenant University.

References

Aremu, M.O., Ozonyia, G.N. and Ikokoh, P.P. (2010), Chemical Society of Nigeria, Proceeding of the 33rd Annual Conference, pages 24-27.

Bartholomew, P., Evrard, P., Katekesha, F., Lopez-Ruiz, J. and Ngogo, M. (1973), Viagenetic ore-forming processes at Komoto, Katanga, Republic of Congo. In “Ores in sediments (Amstutz G.C. and A.J. Bernard, A.J. Eds.) Springer-Verlag, Heidelberg pages 21-41.

Garrels, R.M. and Christ, L.C. (1965), Solutions, Minerals and Equilibria, pages 371-372.

Obuzor, G. U. and Nduka, J. O. (2010), Chemical Society of Nigeria, Proceeding of the 33rd Annual Conference, pages 9-12.

Uba, A. and Gwandy, A.A., Izuagie, T. and Sadiq, I.S., (2010) Chemical Society of Nigeria, Proceeding of the 33rd Annual Conference, pages 67-68.

Umudi, E.Q. and Awatefe, K. J., (2010), Chemical Society of Nigeria, Proceeding of the 33rd Annual Conference, pages 60-63.

Williams, P.A. (1992), Oxide-zone Geochemistry, Ellis Harwood Inorganic Chemistry.

Wilson, I.J. (1972), Relian bed forms, their development and origins Sedimentry, Vol.19, pages 173-210.

Wilson, I.G. (1971). Desert sand flow basins and a model for the development of Ergs., Geogrl. J. 137, pages180-199.

World Health Organization (2004), Guide lines for for Drinking Water Quality, International Standard, 3rd Edition, Geneva, Vol. 1.

World Health Organization, (2007), Water for Pharmaceutical Use In: Quality Assurance of Pharmaceutical. A compendium of Guidelines and related Materials. 2nd Update Edn. World Health Organization Geneva, pages 170-187.

Prospero, J.M. and Carlson, T.N. (1972), Vertical and areal distribution of Saharan dust over the Western Equatorial North Atlantic Ocean, J. geophys. Res. 77, pages 5255-5265.

Abolarin: Proc. ICCEM (2012) 13 - 20

Identification of major noise donors, a sure way to abating noise

Abolarin, Thomas Sunday

Mechanical Engineering Department, Kwara State Polytechnic Ilorin, Nigeria

08035066410, 08055823910; athomvice2012@gmail.com

Abstract

A Study was conducted to ascertain the specific noise emitted by presumed noisy environments. This was achieved by direct measurement of the noise with the use of an integrated sound level meter in which a built-in frequency filter or weighting network is incorporated. Ten (10) environments were selected in Ilorin and Akure towns in Nigeria, in which sixty (60) readings were taken at intervals of 30 seconds for 30minutes separately at each location. This amounted to an overall reading of six hundred (600) readings. The results show that the Lawn Mower emits noise with the highest Equivalent sound level, L_{Aeq} of (98.55dB (A)) followed by the Food Milling Machine (93.80dB (A)). The lowest L_{Aeq} value of (61.76dB (A)) obtained in the study was arrived at with the measurements taken while standing 20 meteres away from a generating set. These values are extremely outside those recommended for community noise by the WHO. Signal analysis obtained with the measurements indicates the complex and non-periodic signal of noise. Identifying this fact therefore, calls for direct efforts at abating noise emitted by these known donors of noise. This effort will ensure that better equipment are designed to free the environment from the influx of noise, which has been identified as major source of environmental pollution. This will enhance the creation of clean products and ultimately a clean technology.

Key words: Noise, Noise donors, Equivalent sound level, integrated sound level meter, signal analysis, weighting network

1. Introduction

The word noise is derived from the Latin term nausea. It has been defined as unwanted sound [Hasall et al., 1979; Jaiswal, 2003; Omubo-Pepple, et al., 2010]; an undesirable by-product of society's normal day-to-day activities. In physical terms, Hasall et al., defined sound as the "Mechanical vibration of gaseous, liquid or solid elastic medium through which energy is transferred away from the source by progressive sound waves". He added that, "whenever an object moves or vibrates, a small proportion of the energy involved is lost to the surrounding medium as sound" (Hasall and Zaveri, 1979).

Noise could also be defined as an available acoustic energy that adversely affects the physiological and/or psychological well-being of people, or which disturbs or impairs the convenience or peace of any person. (Saadu, 1987).

Noise is defined as unwanted sound (Laurent et al, 1977; Enger, et al, 2002). Sound, which pleases the listeners, is music and that which causes pain and annoyance is noise. At times, what is music for some can be noise for others [Parivesh, 1996].

A decibel (dB) is the standard for the measurement of noise. The zero on a decibel scale is at the threshold of hearing, the lowest sound pressure that can be heard. 20 db is whisper, 40 db the noise in a quiet office. 60 db is normal conversation, 80 db is the level at which sound becomes physically painful. "Decibel scales are logarithmic, rather than linear". Therefore, an increase in loudness from 40dB to 80dB is a ten-thousandth percent rise in the loudness of the noise (Enger, et al, 2002).

According to Encyclopedia Britannica; **an acoustic noise is defined as any undesired sound.** In chambers 21st Century Dictionary the definition of noise has undergone a change. Noise pollution stands carved out as phrase separately from noise. The two are defined as follows: **Noise**- a sound; a harsh disagreeable sound, or such sound; a din. **Noise Pollution**- This is an excessive or annoying degree of

noise in a particular area, eg from traffic or aero plane engines.

Noise can be described as sound without agreeable musical quality or as an unwanted or undesired sound. Thus, noise can be taken as a group of loud, non-harmonious sounds or vibrations that are unpleasant and irritating to ear. [Jaiswal, 2003] The audiologist says noise is a meaningless sound; the communicator says it is any barrier to effective communication Dunmoye, (2011).

In the sciences, especially in physics and telecommunication noise is fluctuations in, and the addition of external factors to the stream of target information (signals) being received at a detector.

Noise can be created deliberately for some communication effects e.g. jamming of a radio or TV signal. However, it is still regarded as an undesired interference with intended operations. Natural and deliberate noise sources can provide both or either of random interference or patterned interference.

Environmental noise is a worldwide problem. However, the way the problem is handled differs immensely from country to country and is very much dependent on culture, economy and politics. It is saddening that the problem persists even in areas where extensive resources are being used for regulating, assessing, and damping noise sources, and or for creation of noise barriers.

Noise has been identified as a pollutant. Section 2(a) of the Environment (Protection) Act, 1986 of India; states that: **air pollution** means any solid, liquid or gaseous substance including noise present in the atmosphere in such concentration as may be or tend to be injurious to human beings or other living creatures or plants or property or environment.

Pollution is a word derived from the verb pollute. Section 2 (c) of the Act defines **environmental pollution** to mean the presence in the environment of any environmental pollutant. Section 2 (b) defines **environmental pollutant** to mean any solid, liquid or gaseous substance present in such concentration as may be ,or tends to be injurious to environment. Section 2 (a) of the Air (Prevention and Control of Pollution) Act, 1981 includes noise in the definition of 'air pollutant'.

Studies have shown that noise has a significant impact on the quality of life, and in that sense, it is a health problem in accordance with the World Health Organization (WHO) definition of health which includes total physical and mental well-being, as well as the absence of disease. A 1971 WHO working group stated, that: "Noise must be recognized as a major threat to human well-being," (Ali andTamura, 2003).

The U.S. Department of Housing and Urban Development (HUD) (Oyedepo and Saadu, 2011)
recommends the following noise levels for residential areas, measured outdoors:

LAeq ≤ 49 dBA
—clearly acceptable
49 < LAeq ≤ 62 dBA (or LDN≤65 dBA)
—normally acceptable
62 < LAeq ≤ 76 dBA (or 65 < LDN≤ 75 dBA) —normally unacceptable
LAeq > 76 dBA (or 75 dBA< LDN)
—clearly unacceptable

Researchers throughout the world have been conducting investigations with a view to tackling the problem of noise pollution in cities. (Oyedepo, et al 2008; Morillas et al., 2005; Zannin et al., 2002) It is no news again that noise causes a great deal of discomfort in lives of people. This has long been established (Ozer, et al, 2009; Marius et al., 2005).

Physical, physiological, psychological and effects on work performance are the four categories of health effects on human. As in all form of pollution, the degree of the effects of noise pollution depends on the dose in terms of the amount and duration of exposure (Yilmaz, et al., 2005).

Instances such as hearing defects (physical effects); irregularity of heart rhythms, increased blood pressure and ulcers (physiological effects), insomnia and going to sleep late, disorders, irritability and stress (psychological effects); and lastly misunderstanding of instructions and reduction of productivity (effects on work performance) are observed in human. (Evans and Hygge, 2000; Passchier-Vermeer and Passchier, 2000;). Nigerian researchers are not taking the back seat in the

quest to curb noise pollution problems. In 1998 Saadu, et al carried out a study on "Road Traffic Noise Survey and Analysis of some Major Urban Centres in Nigeria". Anomohanran,et al (2008), Omubo-Pepple, et al (2010), Oyedepo and Saadu, (2008); Saadu, (1987); Saadu et al, (1998) and many more have also worked on different cities in Nigeria; such as Ilorin, Kwara State, Abraka Delta State, Port Harcourt, Rivers State etc. These studies have generally revealed that generators, loudspeakers, food milling machines, Worship centres actually dole out the highest level of the community noise.

The outpouring of noise into the Nigerian Cities calls for lots of research to evaluate the effects of the public noise on residents. This will help to checkmate the current and imminent adverse effects resulting from the noise. It has been observed from the studies that, many families in the Nigeria have generators which give uncontrolled noise to the neighbourhood. The effects of noise from such if not identified and checked, may lead to a chronic situation which may be difficult to subdue.

This study is therefore, carried out to measure and ascertains the actual values of noise emitted by these sources. In addition, since what is music for some can be noise for others; it is necessary to make an objective measurement of the noise produced by the sources so that the noise level can be compared adequately with the world standard, which is not subjective and not subjected to human limitations.

Environmental noise is the one resulting from neighborhood activities. It is different from industrial noise, which results from industrial, production activities. However, in many Nigerian cities, there seems to be no discernable difference between the two, because the few industries in the towns are embedded in the residential areas and residential houses have smuggled themselves into the designated industrial areas (Abolarin, 2012).

1.1 Sources of Noise Pollution:-

Noise pollution like other pollutants is also a by-product of industrialization, urbanization and modern civilization. Most leading noise sources will fall into the following categories: roads traffic, aircraft, railroads, construction, industry, noise in buildings, and consumer products

1.2 Road Traffic Noise:

In many cities in the world, the leading source of noise is the traffic noise (Yilmaz and Ozer, 2005). These are emitted by the motors and exhaust system of automobiles, smaller trucks, buses, and motorcycles. Panadya, (2003) cited in social surveys that: this type of noise is the major source of nuisance and annoyance.

1.3 Aircraft Noise: -

According to Omubo-Pepple et al., (2010), rail and aircraft noise are acoustically characterized by high noise levels of relative short duration. Increasing noise of airport and motorway traffic in the city centres have become a part of modern life (Passchier-Vermeer, 1996). Now-a-days, the problem of low flying military aircraft has added a new dimension to community annoyance. The only succour to these is the submission of Omubo-Pepple et al, which identified noise pollution of aircraft as of short duration. It has to be noted also that airport in many cities in Nigeria is far from the city centre; therefore the dose per person living in the city is negligible. However, noise is a problem for residents of villages near the airport (Yilmaz and Ozer, 2005)

1.4 Noise from railroads: -

The noise from locomotive engines, horns and whistles, and switching and shunting operation in rail yards can impact neighboring communities and railroad workers. For example, rail car retarders can produce a high frequency, high level screech that can reach peak levels of 120 dB at a distance of 100 feet (30.48m), which translates to levels as high as 138, or 140 dB at the railroad worker's ear. As cited for Erzurum city in Turkey, noise from the railway is especially dominant in the area near the railway, where noise level was over 90 dB (A) (Yilmaz and Ozer, 2005).

1.5 Construction Noise: -

The noise from the construction of highways, city streets and buildings is a major contributor to the urban scene. However, use of manpower rather than mechanical power means that the noise of construction is less of a problem. Construction noise sources include pneumatic hammers, air compressors, bulldozers, loaders,

dump trucks (and their back-up signals), Quarries, mining explosives and pavement breakers.

1.6 Noise in Industry: -

Although industrial noise is one of the less prevalent community noise problems, neighbours of noisy manufacturing plants can be disturbed by sources such as fans, motors, and compressors mounted on the outside of buildings Interior noise can also be transmitted to the community through open windows and doors, and even through building walls.

1.7 Noise in building: -

Apartment dwellers are often annoyed by noise in their homes, especially when the building is not well designed and constructed. In this case, internal building noise from plumbing, boilers, generators, air conditioners, and fans, can be audible and annoying. Improperly insulated walls and ceilings can reveal the sound of-amplified music, voices, footfalls and noisy activities from neighboring units. External noise from emergency vehicles, traffic, refuse collection, and other city noises can be a problem for urban residents, especially when windows are open or insufficiently glazed.

1.8 Noise from Consumer products: -

Certain household equipment, such as vacuum cleaners and some kitchen appliances have been and continue to be noisemakers, although their contribution to the daily noise dose is usually not very large.

A consumer product, which may eventually break the long apathy of the public to noise pollution, is the headphones, which are also called headsets. It is highly probable to see someone with a headset wire drooping down from his or her ear in nearly all environment one finds him or herself. It is often discovered that the person is hearing a sound with heavy percussion turned to maximum volume. Many a times the individual is unconscious of the events around him. (Adeniji, 2011)

Earphones are placed in the outer part of the ear normally in circumstances where solitude is required by an individual to either prevent interference by other sounds or prevent him from disturbing others. However, they cannot be said to have the capacity to entirely muffle external sounds, as a result, the user increases the volume thereby raising the risk of hearing loss. Headphones are often connected to devices such as cell phones, computers and radio sets as well as media players. A recent survey by Australia's National Acoustic Laboratories revealed that about 25 percent of people addicted to portable music players experienced daily noise level capable of causing hearing damage.

1.9 Loudspeaker: -

The indiscriminate use of loudspeakers in the urban centres calls for caution. This is because the noise emitted by these electronic devices are usually of high intensity which could seriously and adversely impact on the health of the hearers. Citing (Oyedepo and Saadu, 2008, Abolarin, 2012), the use of loudspeaker is common at transporters' loading points, where they are used to call prospective passengers. Survey also revealed that marketers of some household products such as local/traditional herbs use public address system (PAS) as mode of advertising their market not minding the loudness of the speaker. "In fact the louder it is the happier they are".

Churches, Mosques and prayer grounds are increasingly noisy in Nigeria with public address systems. In a survey conducted in Port Harcourt, (Omubo-Pepple et al, 2010) it was discovered that the use of loudspeaker which may be comfortably merged with religious activities ranked second to the use of generator as source of noise.

1.10 Electric Power Generating Sets: -

This is a major producer of community noise in our nation. At market places, neighbourhoods, etc dwellers are often annoyed by noise created by the next neighbour. Even at social gatherings and official events, the use of these appliances as stand-by source of power infuriates participants. It is amazing that this major source of noise in Nigeria is never mentioned in many literatures from Asian and European countries. In a study conducted by Omubo-Pepple et al, in 2010; sources of noise were verified from residents of Port Harcourt in Rivers State Nigeria. Eighty Five percent of respondents agreed that generator supplies the highest noise to the environment.

This survey has clearly shown that noise from generators affects residents of urban cities in Nigeria more than any other form of noise. This finding also corroborates the view of Anomohanran et al, 2008; in the investigation of environmental noise pollution level of Abraka, Delta State Nigeria. The researchers observed that noise level in the town was non-conducive at night owing to the use of power generating set.

1.11 Internal Combustion Engines (ICE)

A group of noise generator that is appropriate under this heading is comprised of domestic food milling machines, chainsaw and the lawn mower. This group is powered by diesel or gasoline powered internal combustion engines (ICE) which at times generate more noise than the common generating set. In fact, the effect of these other engines could be more hazardous because the users are very close to the source, while the generating set is commonly placed some metres away from users.

2.0 Materials and methods

The study focuses on the results obtained from outdoor and indoor sound level measurements carried out between August 2011 and May 2012 at 10 different locations in Ilorin, Kwara State and Akure, Ondo State of Nigeria. Table 1 shows the Selected Noise Sources for the measurements while Table 2 shows the raw data obtained.

2.1 Procedure for Noise Measurement

The digital noise level metre was used to measure noise level emitted by the selected noise producers. The noise level meter is an integrated A-weighted measuring instrument with internationally standardized networks. It is a lightweight hand-held instrument, the type ANSI S1.4; pointed to the direction of the major source of noise in each location and being very sensitive equipment it gave the accurate readings, which were recorded from the meter screen (liquid crystal display, LCD in 4-digit and 0.1dB resolution). It has an accuracy of $\pm$ 2.0dB (under reference conditions). The noise level was recorded at a regular interval of thirty (30) seconds for a period of thirty (30) minutes; with a total of sixty (60) readings at each location.

2.2 The Digital Sound Level Meter:

The noise level metre has a dynamic characteristics setting facility that allows measurement for slow/fast responses and maximum hold. It belongs to the very large group of sound level metres meeting the *Precision* requirements of IEC 651. It is supplied with $1/2$ inch electric condenser microphone and $1/3$ -octave filter for which a windshield could be used. This gives the metre a display dynamism enabling it to measure very large measuring range and especially for a widely fluctuating noise. The digital display eliminates the uncertainties of visual averaging and provides a repeatable value when measuring fluctuating noise levels. It displays with 0.1dB steps on a 4-digit LCD.

Proper care was taken against reflected sound waves from the operators' body when using the sound level meter. This was achieved by ensuring that the microphone is adequately pointed away from the user.

Table 2 shows the data obtained from the readings including the Equivalent sound level, L_{Aeq} The maximum and minimum values. Where L_{Aeq} is the A-weighted equivalent noise pressure level which is the A-weighted energy mean of the noise level averaged over the measurement period as defined by Hassall, et al1979.

The 10 randomly selected points were picked as measurement points with reference to the following guides.

Table 1: Selected Noise Sources

Location	Noise Sources	Location
1.	Generator	0 metre
2.		6 metres
3.		20 metres
4.	Mower	0 metre
5.	Food Milling	0 metre
6.		2 metres
7.	Ramadan Lecture	
8.	Crusade Ground	
9.	Celebrating Indoor	
10	Student Union Building	

Table 2: Raw data obtained from 10 selected locations

GENERATOR			MOWER	FOOD MILLING		WORSHIP			
0m	6m	20m	0m	0m	2m	CRUSADE	RMDN LECT	CELEBRATING	SUB
92.2	70	60	100	94.8	77.9	78.8	59.9	80.3	62
91.9	71.3	67	96	94.6	87.7	68.7	60.5	80.1	72
92	70.6	61.5	95	94.7	78	81	60.4	65.5	69.9
91.9	70.6	59.7	97	94.9	78.2	72.3	85.2	70.8	67
92.2	70.9	60.2	102	94.1	78.3	82.6	87	84.4	69.6
91.8	70.8	60.4	99	94.5	78.8	92.2	61.4	78.6	75.3
92	71.1	61.4	90	95	78.4	88.4	60	82.1	62.1
93.3	71	60	99.8	95.2	78.5	91.5	59.3	70	73.2
92.3	70.2	59.3	98.3	95.3	78.9	95.4	59.9	86.6	65.6
92.6	71.3	59.9	99.1	94.4	79	63.9	61.1	89	68
92.2	71.6	61.1	103.2	94.1	77.9	73.7	60	79.1	63
92	71.1	60	97	94	78.1	75.4	57.9	84.5	76.6
92.2	70.1	57.9	100	95.6	78.5	82.1	51.7	84	70.5
91.7	71	60.5	96.7	96.2	78.6	85.6	48.9	82.2	77.5
92	70.8	59	98.1	96.3	78.7	83	59.9	83.2	69.8
92.5	70.6	62.3	99.2	96.2	79	77.3	59	81	71.8
91.8	73	65	97	96	79.2	70.7	60.5	61	62
92.1	75	51.7	100.2	96.4	79.1	62	59	62.3	59
92.3	75.7	64.8	103	98.5	79.3	84.4	62.3	69.7	61.5
91.8	74.4	59.9	99.1	99.2	79.3	75.6	65	61.3	66.7
91.7	75.3	59	98.8	99	79	71.4	51.7	70.7	60.4
91.9	75.2	62.1	95.5	100.8	79.2	85.8	64.8	61.4	73
93.1	74.9	60.2	99	100.9	79.1	83.5	50.6	63	68.5
93.2	76	59.6	97.7	100.3	78.1	79.3	59	73.9	72.1
92.5	75.1	63	97.1	100.5	78.2	86.6	62.1	78.9	69.9

GENERATOR			MOWER	FOOD MILLING		WORSHIP			
0m	6m	20m	0m	0m	2m	CRUSADE	RMDN LECT	CELEBRATING	SUB
93	74.7	62.5	97.9	101	78.3	74.6	60.2	71.1	60.8
93.3	75.9	59.6	100.3	97	78	82.1	59.6	70.2	61
92.9	74.4	73.2	98	96	78.8	80	63	78.2	59.7
93	74.8	67	110	82	78.4	81.2	62.5	79	81.9
93.1	75.1	59.4	99.4	85.3	79.5	78.8	59.6	66.6	61.6
93.6	76	60.4	99.7	84.4	90.2	78.2	73.2	77	58.4
93.9	75.9	58.7	96.1	84.3	79.1	73.8	67	67.5	60.5
92.6	76.3	62.1	97.8	86.2	78.6	66.4	59.4	79.9	61.4
92.7	74.2	78.8	90.9	84.9	78.8	84.9	60.4	85.9	62.4
93.9	74.7	74.9	96.6	90	78.9	66.1	98.6	74.4	65.1
91	75.1	60	99.7	99.4	78.6	69.7	62.1	78.8	71
93	75.2	61.1	98.1	99.7	78.7	84.3	78.8	64	57
92.9	76.1	66.9	95.3	96.1	78.1	83	74.9	72.2	62
92.8	75.8	59.6	104.6	97.8	78.4	77.2	60	81	76.3
93.1	74.7	60.3	101.8	90.9	78	92.9	61.1	66.8	59
94	75.2	61.2	95.9	96.6	78.3	95.7	66.9	80.2	60.2
93	74.8	60	100.5	99.7	89.7	83.6	59.6	80.8	63.9
92.9	75.4	60.7	98.8	98.1	87.8	96	60.3	73	66.6
92.6	76.5	59.6	99.9	86.3	87.9	95.9	61.2	79.5	65.8
93.1	74.1	60.2	92.6	86.6	87.6	88	60	81.1	68.5
93.4	74.2	59.7	94	86.2	87.2	78.2	60.7	77.7	75.5
94.3	75	63.7	98.6	86	89.4	77.7	59.6	85.9	66.5
92.7	74.3	61.5	97.9	87.1	89.1	92.5	60.2	79.4	60.5
92.3	73.8	71	96.5	86.1	89.6	94	59.7	72.2	88.1
92.8	77.3	59.4	106.6	87.3	89.9	76.8	63.7	76.1	70.9
92.9	75.9	66	101.1	87.5	89.8	75.9	61.5	80.3	70.5
92.7	77.2	59.7	95	98.8	89.1	85.6	71	79.6	75
93	77.8	61	98.1	99	77.9	80.1	59.4	86	76.3
93.3	74.3	61.1	97	90	79.2	79.9	66	81.9	74.4
92.8	75.5	60.1	99.1	99.8	78.6	88.4	59.7	82.2	60.1
92.6	76.8	60.4	98	98.3	78.7	80.1	61	81.7	61.8
93.1	74.8	59.8	95.6	99.1	78.1	79.6	61.1	80	60.9
92.9	75	60	97.3	89.7	78.6	91.4	60.1	70.3	60.2
93.3	74.9	59.7	97.1	89.1	78.4	79.8	60.4	78.8	65.7
93	75	60.6	109.1	90.2	78.8	79	59.8	80	88
Av92.68	74.07	61.76	98.55	93.80	80.82	81.04	62.66	76.38	67.41
Mx94.30	77.80	78.80	110.00	101.00	90.20	96.00	98.60	89.00	88.10
Mn 91.00	70.00	51.70	90.00	82.00	77.90	62.00	48.90	61.00	57.00

3. Results and discussion

Table 2 shows that the maximum and the minimum noise level recorded are 110.00dB (A) and 48.90dB (A) respectively. The highest was recorded while standing by a lawn mower and the lower from a worship centre. The result of this study shows that the equivalent noise levels (L_{Aeq}) of the ten locations surveyed are not within acceptable standard. 50% falls in the normally unacceptable range and the other 50% are in the clearly unacceptable range.

The World Health Organization (WHO) recommends a noise level limit of about 55dB (A) as a general health goal for outdoor noise in residential areas, (Oyedepo et al, 2008 & 2011). This is usually considered as a comfortable environment with little or no annoyance so that no negative physical and mental influence will be caused to essential activities such as working leisure and sleeping (Dai et al, 2005; Dhananjay & Prashant, 2005). It is observed that the values recorded in this study are generally of high noise level higher than the recommended values by the WHO.

3.1 Signal Analysis: Figure 1 shows the typical noise graph with the noise level plotted against the frequency of measurement. The figure is a true reflection of the non-sinusoidal nature of noise waves, which is a subset of sound. This also shows the accuracy of the data in its own right. This graph was plotted with the Microsoft Excel software. The root and the peak of the wave is 62(dB) and 96(dB)A respectively.

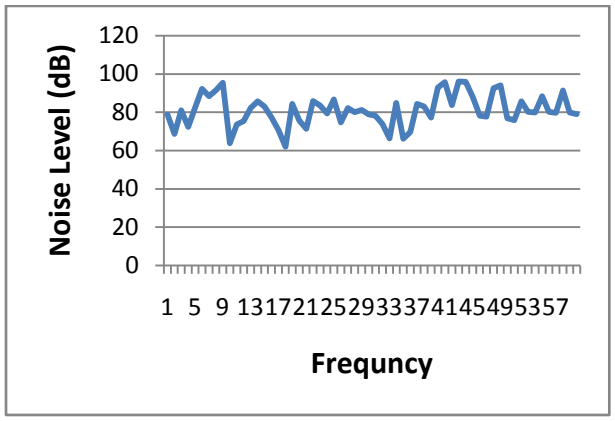

Fig 1: Typical Noise Graph (Measurement at a crusade ground)

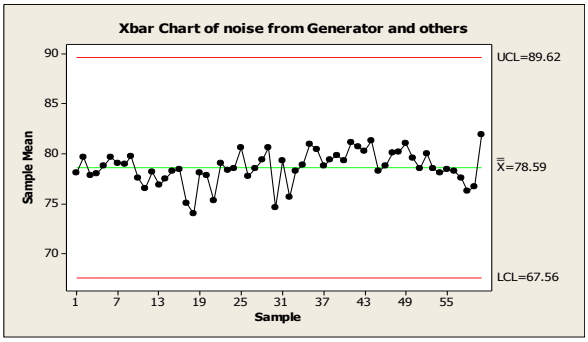

Figure 2: Control Charts for Variables (Noise sources)

The analysis of the data by the Control Chart figure 2, obtained through the SPSS software revealed that the noise emitted by the different sources have a generally high noise level. These noise level from the isolated sources is so high and therefore should be treated as occupational noise which requires greater attention. This actually corroborates the unacceptability of the equivalent noise levels.

4.0 Conclusion

This study has clearly shown the various sources of noise and has been able to establish that some sources pose more threat to citizenry than others do. It is therefore imperative for engineers and the public to work towards abating noise from internal combustion engines (ICE) as there is no visible end to their use in Nigeria with unreliable state of the national power supply. Efforts should also be geared towards utilizing other noiseless sources of power such as solar. Working in this direction will enhance the design of clean products thereby and ultimately a clean technology for a clean environment.

References

Abolarin, T. S. (2012): Monitoring of Noise Pollution in Ilorin Metropolis, Proceedings of the 1st Joint National Conference, Kwara State Polytechnic Ilorin, Nigeria. Vol.1, 2012 pp 124-132.

Adeniji, Gbenga, (2011): 'Feature: Headphones can cause hearing loss, columnist in the Punch Newspaper, 01/09/11

Ali, S. A., Tamura, A (2003): Road traffic noise levels, restrictions and annoyance in greater Cario, Egypt. Appl. Acoustics. 64(8): 815-823.

Anomohanran, O., Iwegbue, C. M. A., Oghenerhoro, O., and Egbai, J. C. (2008): 'Investigation of Environmental Noise Pollution Level of Abraka in Delta State Nigeria, Trends in Applied Sciences Research 3(4), 292-297.

Dai .L, Cao.J, Fan.L and Mobed .N, (2005) "Traffic Noise Evaluation and Analysis in Residential Areas of Regina", *J. of Environmental Informatics* 5(1), 17–25.

Dhananjay, K. P. and Prashant, B. N (2007) "Assessment and ANN Modeling of Noise Levels at Major Road Intersections in an Indian Intermediate City", *J. of Research in Science, Computing, and Engineering* 4(3), 39–49.

Dunmoye, S (2011): Department of Oto-Rhino-Laryngology, University of Ilorin Teaching Hospital (UITH), Ilorin, Nigeria. Oral Communication

Evans, G. W. and Hygge, S. (2000): Noise and performance in children and adults. In D. Prasher (Ed.), Handbook of noise and health

Hassall, J. R. & Zaveri K. (1979): Acoustic Noise Measurements, Bruel & Kjaer Publications, N/Erum, Denmark.

Jaiswal, P.S. and Nistha Jaiswal (2003): Environmental Law, Second Ed., p.327.

Laurent, H. H. Rinehart, I and Winston, R.(1977): Environmental Pollution 2nd Ed. Iowa State University, Library of Congress Cataloguing Publication Data. pp.147-160

Marius A, Tijunelis, M. D., Fitzsullivan, B. A., Sean, O. & Henderson, M.D.(2005): Noise in the ED. Am. J. Emerg. Med. 23(3): 332-335.

Morillas, B. J. M., Escobar GV, Vaquero JM, Sierra MJA, Gómez VR (2005): Measurement of Noise Pollution in Badajoz City, Spain. Acta Acustica United with Acustica; 91(4): 797-809.

Omubo-Pepple, V. B., Briggs-Kamara, M. A. and Tamunobereton-ari, I. (2010): 'Noise Pollution in Port Harcourt Metropolis: Sources, Effects and Control, the Pacific Journal of Science and Technology, Vol. 11, No. 2, pp. 592-600.

Oyedepo, O S., & Saadu, A. A. (2008): Changing Noise Climate of Ilorin Metropolis. Environmental Engineering Science, 25(6), 797-808.

Oyedepo, O S., & Saadu, A. A. (2011): Noise Map: Tool For Abating Noise Pollution in Urban Areas, Proceedings of the National Engineering Conference of the Nigerian Society of Engineers.

Ozer, S., Yilmaz, H., Yesil, M. and Yesil, P. (2009): 'Evaluation of noise pollution caused by vehicles in the city of Tokat, Turkey', Scientific Research and Essay, Vol. 4, No. 11, pp. 1205-1212.

Panadya, G. H.: (2003): 'Assessment of traffic noise and its impact on the community, International Journal of Environmental Studies 60(6), 595–602.

Parivesh (1996): News-Letter: Central Pollution Control Board, New-Delhi, India.

Passchier-Vermeer W, Passchier WF (2000): Noise exposure and public health. Environ.Health Perspect. Suppl. 108 (1): 123-131.

Saadu, A.A. (1987): Community and Occupational Noise Survey and Analyses of some selected Nigerian Cities and Industries. Ph.D Thesis, University of Benin, Benin-City, Nigeria.

Yilmaz, H. and Ozer, S. (2005): 'Evaluation and Analysis of Environmental Noise Pollution in the City of Erzurum, Turkey', Int. J. Environment and Pollution, Vol. 23, No. 4, pp. 438-448

Zannin, P. H. T., Calixto, A., Diniz, F. and Ferreira, J.A. (2002): 'A Survey of Urban Noise Annoyance in a Large Brazilian City: The Importance of Subjective Analysis in Conjunction with an Objective Analysis', Environmental Impact Assessment Review 22.

Ajayi et al: Proc. ICCEM (2012) 21 - 29

Rauvolfia vormitoria Effect on the Degradation of Aluminium Alloy in 2.5 M Hydrochloric Acid Solution

Ajayi, O.O., Joseph, O.O., Omotosho, O.A.* and Olabowale, T.O

Mechanical Engineering Department, Covenant University, P.M.B. 1023, Ota, Nigeria

*Corresponding author: olugbenga.omotosho@covenantuniversity.edu.ng;Tel: +2348033382752

Abstract

The deterioration of aluminium alloy in 2.5 M hydrochloric acid in the presence Rauvolfia vormitoria extract was examined using both gasometric and gravimetric techniques. Aluminium coupons measuring 4 cm by 1 cm were introduced into test solutions of uninhibited acid and also those containing extract quantities of 10, 20, 30 and 40 cm^3 at ambient temperature of 25^0C for a total cumulative period of 117 minutes. The volumes of hydrogen gas evolved and weight loss readings were recorded and analyzed to obtain weight loss and corrosion rate for each coupon at specific time intervals. The results however, showed that while extract quantity was increasing; weight loss measurements increased but inhibitor efficiency decreased. Also, the metal surface-phytoconstituent interaction mechanism was consistent with the Temkin adsorption isotherm and the 3 minutes curve showed the best exposure time for phytochemicals to adsorb to alloy surface. Furthermore, microstructural studies showed an indirect relationship between metallic degradation and extract quantity, while uniformity of the irregular intermetallic phases increased with increasing extract quantity.

Key words-Environmentally induced failure, green inhibitors, hydrogen evolution, Aluminium alloy, adsorption isotherm.

1. Introduction

A material usually a metal is said to undergo chemical degradation otherwise called corrosion when it experiences a change in its properties as a result of an interaction with its environment. Corrosion is a natural process. For instance steel or iron has a natural tendency to combine with other chemical elements to return to their lowest energy states. Iron or steel normally combine with oxygen and water to return to lower energy states. This combination leads to the formation of hydrated iron oxides otherwise called rust and similar in chemical composition to the original iron ore. Corrosion processes leads to losses and affects society on a regular basis causing degradation and damage to household appliances, automobiles, airplanes, highway bridges, energy production and distribution systems. Corrosion is the major factor influencing the durability and dependability of pipelines that transport crucial energy through the country.

Presently, most of the aging infrastructure in the form of bridges, buildings, roads and tanks are reaching the end of their design lifetime in Nigeria. Structural deficiency resulting from corroded steel and steel reinforcement has been fingered as the major factors responsible for these damages (Omotosho, 2011). The cost of controlling this naturally occurring phenomenon and cost associated with the damage it causes is substantial with figures rising yearly in developed countries like the U.S. The current per capita direct cost of corrosion for U.S residents based on 2001 figures is approximately $970 per person per year (Koch et al, 2001). This amount does not include indirect/user cost which will essentially double that amount and is put at 6% of the Gross Domestic product (GDP) (Koch et al, 2001). However, these costs could be saved if optimum corrosion management techniques are employed. Thus, corrosion protection and control is a potent and vital tool for the techno-industrial and socio-economic development for any country that is determined to protect public safety, prevent damage to property and the environment and conserve funds.

Acids are utilized for rust removal and pickling; degreasing/desludging of petrochemical equipment; oil well acidizing and descaling; and the removal of calcareous deposit from steam

boilers and cooling tower units. These acids are known to have damaging effects on their substrates. Several established methods for preventing and controlling the damages depend on specific material to be protected, environmental concerns, type of product to be transported. The most generally used methods include organic and metallic protective coatings, corrosion resistant alloys, plastics and polymers, cathodic protection and corrosion inhibitors. However, bulk of the corrosion inhibitors available are synthetic chemicals, expensive and very hazardous to the environment. Therefore, it is desirable to source for environmentally safe and cheap green inhibitors (Ajayi et al., 2011a, Ajayi et al., 2011b, Ajayi et al., 2011c, Omotosho et al. 2012a, Omotosho et al. 2012b, Ajayi et al., 2012, Omotosho and Ajayi, 2012, Omotosho et al. 2011).

Various assessment studies have been carried out to ascertain the potential of various inhibitors on different metals in the presence of variety of acids, most of them using either gasometric or gravimetric method (Ebenso et al, 1998; Ebenso and Ekpe 1996; Ekpe et al, 1994; Martinez and Tagljar, 2002; Ebenso et al, 2004; Oguzie, 2006; Njoku et al, 2006; Abiola et al, 2007; James and Akaranta, 2009; Saratha et al, 2009; Okafor et al, 2010; Ajayi et al., 2011a; Ajayi et al., 2011b; Ajayi et al., 2011c; Omotosho et al. 2012a; Omotosho et al. 2012b; Omotosho and Ajayi, 2012; Ajayi et al., 2012 and Omotosho et al. 2011). Amongst the studies considered, none has yet worked on the effect of *Rauvolfia vormitoria* (RV) on Aluminium alloy in the presence of 2.5 M Hydrochloric acid (HCl). Thus, the aim of this study is to investigate the effect of RV on the deterioration of aluminium alloy in the presence of 2.5 M HCl at ambient temperature of 30 degrees celsius. The technique adopted in this study is the gasometric and gravimetric methods. Moreover, attempts were made to determine the mechanism of interaction between the aluminium sample and extract phytochemical.

2. Materials and Methods

Aluminium alloy specimens with dimension 4 x 1 cm were employed for the determination of corrosion inhibition of RV extract in 2.5 M Hydrochloric acid (HCl). Specimens were prepared by degreasing in ethanol and cleaning in acetone. It was then allowed to dry. The composition of the aluminium alloy samples was analyzed using Optical Emission Spectrometer (OES) and the result is presented in Table 1.

Table 1. Chemical composition of Aluminium alloy sample utilized for the investigation

Elements	% Chemical Composition	Elements	% Chemical Composition
Silicon	0.157	Cadmium	0.0005
Iron	0.282	Calcium	0.0011
Copper	0.0025	Cobalt	<0.001
Manganese	0.51	Lithium	<0.0002
Magnesium	0.51	Sodium	0.0005
Zinc	<0.001	Phosphorus	<0.001
Nickel	<0.001	Lead	<0.0005
Chromium	0.023	Tin	<0.001
Titanium	0.0049	Strontium	0.0001
Silver	0.0004	Vanadium	0.0063
Boron	0.0007	Zirconium	0.002
Beryllium	0.0001	Aluminium	99
Bismuth	0.001		

The acidic extracts of RV were prepared from fresh leaves which were air dried and ground into powder, of which 20g was put into a 1000ml volumetric flask containing 1000 ml of ethanol. The resulting solution was left for 48hrs after which it underwent an evaporation process in the rotary evaporator to remove most of the ethanol. The remaining solution was then left for another 48 hours to allow the further evaporation of the remaining ethanol so that what is left afterwards, is the actual extract obtained from the leaves; which is considered as the phyto-chemical. In order to obtain the inhibited test solution, 1000ml of 2.5 M HCL is then mixed with 10, 20, 30 and 40 ml of the extract. The experimental set up is similar to the technique adopted elsewhere (Okafor et al. 2010; Ajayi, et al. 2011a; Ajayi, et al. 2011b; Ajayi et al. 2011c; Omotosho et al. 2011; Omotosho and Ajayi, 2012; Omotosho et al. 2012a and Omotosho et al. 2012b). The time was recorded and H_2 evolved was collected in a calibrated tube by downward displacement of water per time for

each coupon used. A plot of H_2 evolved per unit area (ml cm^{-2}) against time (minute) in the presence of different concentrations of RV was obtained as shown in Figure 2. The inhibition efficiency was then determined using Equation 1 below obtained from literature (Okafor et al. 2010; Ajayi, et al. 2011a; Ajayi, et al. 2011b; Ajayi et al. 2011c; Omotosho et al. 2011; Omotosho and Ajayi, 2012; Omotosho et al. 2012a; Omotosho et al. 2012b; Omotosho et al. 2012c) [1]

$$I.E(\%) = \frac{(V_H - V_{HI})}{V_H} \times 100 \quad (1)$$

Where, V_H is the volume of H_2 evolved without inhibitor (i.e control experiment) and V_{H1} is the volume of H_2 evolved with inhibitor.

Weight loss experiments were conducted by first weighing the sample before immersion and recording the weight. Thereafter, the weight was obtained after completion of the hydrogen evolution experiment but before this was done the sample was separated from the test solution, washed with deionised water and acetone; and dried finally with a stream of air. From the weight loss results, the corrosion rate (R), inhibition efficiency (%I) of the inhibitor and degree of surface coverage (θ), were calculated using equations 2, 3 and 4, respectively.

$$R\ (g\ h^{-1}\ cm^{-2}) = W/At \quad (2)$$

$$\%\ I = (1 - W_1/ W_2) \times 100 \quad (3)$$

$$\theta = 1 - W_1/ W_2 \quad (4)$$

Where W_1 and W_2 are the weight losses (g/dm^3) for the sample in the absence and presence of the inhibitor in HCl solution, respectively, and θ is the degree of surface coverage of the inhibition.

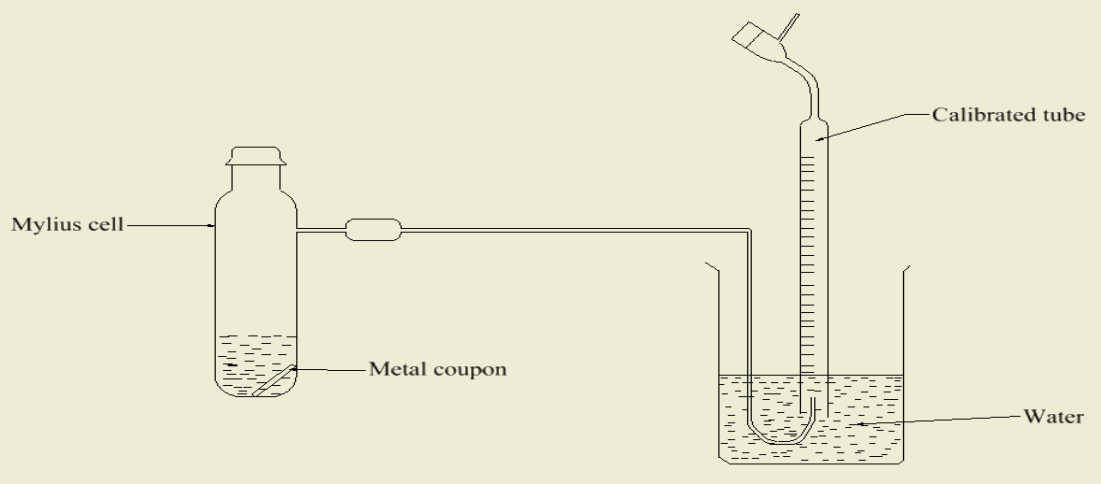

Figure 1: Schematic diagram of the experimental set up

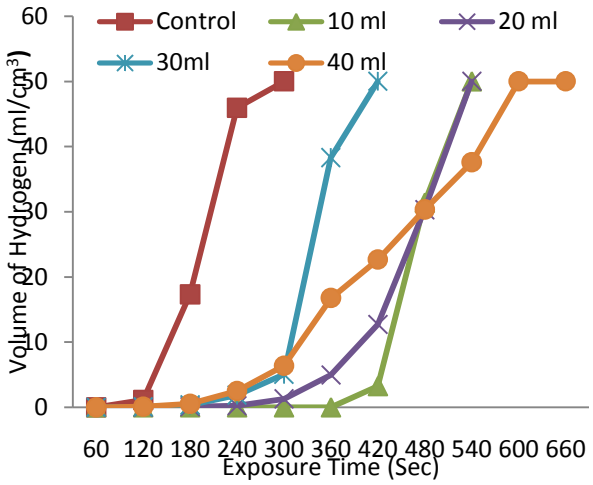

Figure 2: Variation of volume of hydrogen (cm^3) evolved with time (sec) of Al coupons for varying quantities of RV extract in 2.5 M HCl at room temperature of 27°C using gasometric method

It is known that H_2 gas is one of the products of reaction when Al-alloy reacts with HCl, it is thus, suitable to predict the rate of reaction by determining the rate of H_2 gas evolution from the system. By inference, the rate of reaction corresponds to the rate of corrosion damage of the Al-alloy in HCl in the presence of RV extract. This therefore means that, modeling the rate of corrosion from the direction of rate of hydrogen gas evolution is indirectly a way to model the rate of material loss when the relationship between the weight loss and hydrogen gas evolution is known. The foundation for this is as represented in Equation (5) (Ajayi, et al. 2011a; Ajayi, et al. 2011b; Ajayi et al. 2011c; Omotosho et al. 2011; Omotosho and Ajayi, 2012; Omotosho et al. 2012a; Omotosho et al. 2012b):

$$\Delta V \alpha \Delta W$$

$$\frac{d\Delta V}{dt} \alpha \frac{d\Delta W}{dt}$$

$$\text{but } R \alpha \frac{d\Delta W}{dt} \alpha \frac{dV}{dt} \quad (5)$$

Where α = proportionality sign.

ΔV = volume of hydrogen gas evolved

ΔW = metal weight loss due to corrosion

R = Rate of corrosion

t = time (s)

Thus to determine Equation (5), it is necessary to develop a relationship between volume evolved and the time of evolution. This was arrived at by a polynomial regression analysis of the volume of hydrogen gas against time leading to Equation (6) (Ajayi, et al. 2011a; Ajayi, et al. 2011b; Ajayi et al. 2011c; Omotosho et al. 2011; Omotosho and Ajayi, 2012; Omotosho et al. 2012a; Omotosho et al. 2012b):

$$V = c + bt + at^2 \quad (6)$$

Thus,

$$R = \frac{dV}{dt} = b + 2at \quad (7)$$

A particular case of this study will involve adapting Equations (6) and (7) to the volume-time measurement for individual quantity. For instance, for measurements relating to 5ml extract quantity, the corrosion rate model is presented as Equation (9) (Ajayi, et al. 2011a; Ajayi, et al. 2011b; Ajayi et al. 2011c; Omotosho et al. 2011; Omotosho and Ajayi, 2012; Omotosho et al. 2012a; Omotosho et al. 2012b):

$$V = 0.450t^2 + 0.352t - 3.104 \quad (8)$$

$$dV/dt = 0.9t + 0.352 \quad (9)$$

3. Results and discussion

An analytical look at Figure 2 revealed that the corrosion rate of Aluminium alloy as indicated by the amount of H_2 evolved reduced in the presence of RV when compared to the control. The amount of H_2 evolved in the presence of increasing volume of the extract did not follow a particular trend. However, based on the observations of the graph the trend of corrosion rate reduction starting from the least is as follows; 30<40<20<10<control. This indicates that the RV extract in the solution has an inhibitive effect on the corrosion of Aluminium in HCl and that the extent of inhibition depends on the amount of RV extract present.

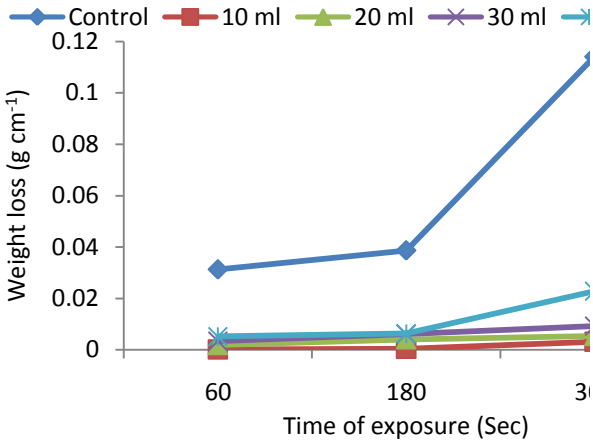

Figure 3: Curves of weight loss of varying quantities of RV extract with time (minutes) on aluminium coupon in 2.5M HCl solution at room temperature

Figure 3 shows a better picture of the weight loss measurements as the curves do not cross over each other as in Figure 2. From Figure 3 the trend of weight loss measurement starting from the least is as follows; 10<20<30<40 ml<control. This same behavior was also observed in Figure 4 which shows the percentage inhibition efficiency (% I.E). The sample immersed in the 10 ml test solution showed best performance for the entire 5 minutes of the experiment as the inhibitor efficiency attained a hundred percent throughout. The sample immersed in the 20 ml test solution showed the same performance as that in the 10 ml test solution for the first two minutes of the experiment as 100 % inhibitor efficiency was attained; however after the second minute, the inhibitor efficiency began to decrease from that time till the end of the experiment. The sample immersed in the 30 and 40 ml test solution showed best performance for the first minute of the experiment as the inhibitor efficiency attained 100%; however after the first minute; the inhibitor efficiency began to decrease from that time till the end of the experiment. The order of inhibitor efficiency starting with the least is thus: 40 < 30 < 20 < 10 ml.

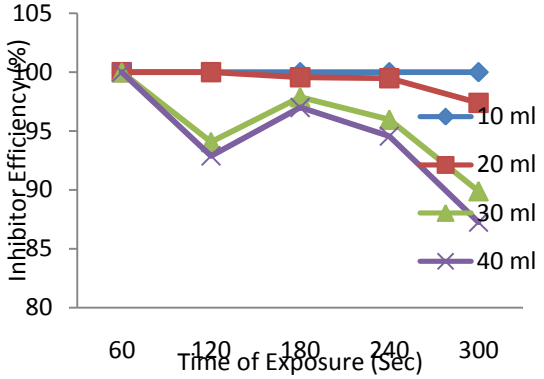

Figure 4: Percentage inhibition efficiency of varying concentrations of RV extract with time (minutes) on aluminium coupon in 2.5M HCL solution at room temperature of 27°C using gasometric method

In Figure 5, corrosion rate values for all the varying inhibitor additions were very low at the beginning of the experiment, with the 10 and 20 ml extract additions having sub-zero values for the first 4 minutes, while the 30 and 40 ml extract additions had above-zero values after the 3rd and 1st minute of the experiment respectively. However, the control experiment maintained above-zero values throughout the experiment with value increasing as the experiment progressed.

The order of performance is as follows: 40 < 30 < 20 < 10 ml. At the beginning of the experiment, the samples which were immersed in the 10, 20 and 30 ml test solutions had just adsorbed to the surface of the metal and since the bond was still strong at this timing of the experiment, corrosion rate was greatly reduced with no noticeable corrosion occurring. This explains the negative corrosion rate on the graph (Figure 5).

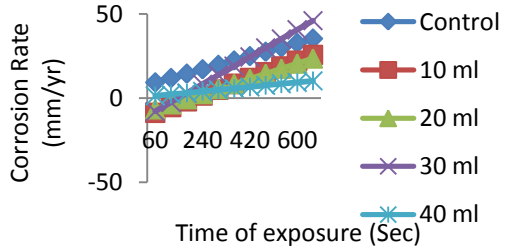

Figure 5: Corrosion rate of varying amounts of RV extract with time (minutes) on aluminium coupon in 2.5M HCl solution at room temperature of 27°C using gasometric method.

This same behavior was also observed in Figure 6 which shows the percentage inhibition efficiency (% I.E). The inhibitor performance followed the order: 40 < 30 < 20 < 10 ml.

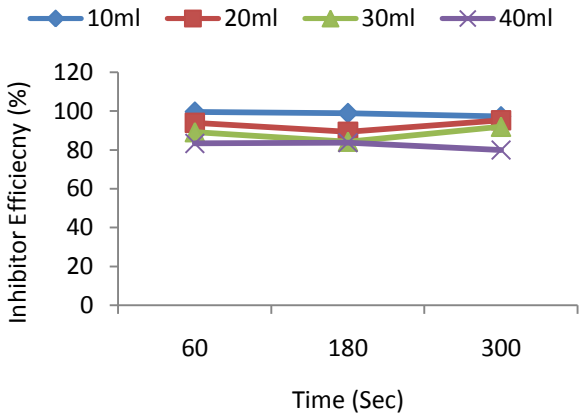

Figure 6: Inhibitor efficiency of varying amounts of RV extract with time (minutes) on aluminium alloy coupon in 2.5 M HCl solution at room temperature using weight loss method.

According to the observation in Figure 7, which is the graph of corrosion rate against time for the experiment based on weight loss measurements the same behavior that was shown by the graph for corrosion rate based on gasometric technique. The order of performance is thus as follows: 40 < 30 < 20 < 10 ml. This is exactly the same as that of Figure 5. The only difference is the level of responsiveness.

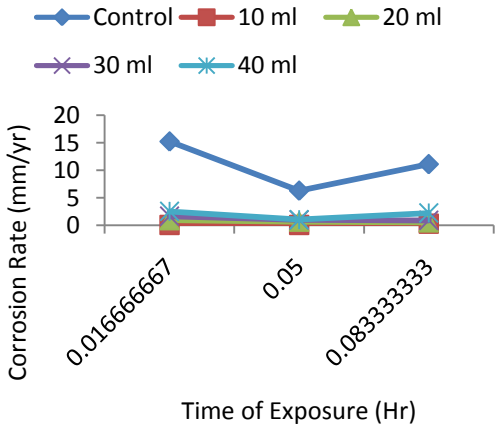

Figure 7: Corrosion rate of varying concentrations of RV extract with time on aluminium coupon in 2.5 M HCl solution at room temperature of 27 °C using weight loss method.

Adsorption studies

The interaction between the phytochemicals in the RV extract and the metal surface suggests the existence of a relationship. This was thoroughly investigated by deploying various adsorption isotherms amongst which are Langmuir, Freundlich, Frumkin and Temkin. Surface coverage values, θ, for the changing extract volumes were appraised on the measurement of the volume of H_2 gas evolved while fitting the θ values with the different adsorption isotherms were conducted, however, the Temkin isotherm was discovered to be best fitted to the θ values at different time intervals. The Temkin isotherm has been reported (Febrianto et al, 2009) to be superior in the prediction of gas phase equilibra. The plot of θ as a function of logarithm of concentration of RV is shown in Figure 8. This result justifies the notion that the corrosion inhibition of the RV extract is credited to the adsorption of phytochemical molecules on the metal surface by the chemisorption process. In this process which is a known tribological consideration in metal surface preparation a covalent bond is formed between phytochemicals and aluminium alloy.

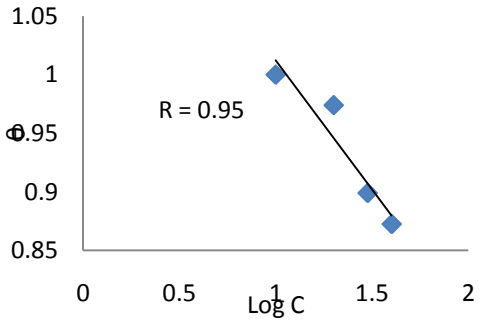

Figure 8: Plot of surface coverage (θ) with logarithm of concentration of acid extract of RV at a temperature of 300K in accordance with Temkin isotherm

Furthermore, the surface coverage strength study was conducted for different extract volume utilized at different time intervals of 1, 2, 3, 4 and 5 minutes as shown in Figure 9 to investigate if there are any influence of exposure times to the connection between θ and C. The 2, 3, 4 and 5 minutes time curve showed the highest θ value at extract volume of 10 cm^3, while the 1 minute curve showed the least value at extract volume of 10 cm^3. However, all the time curves showed a downtrend from the beginning to the end of the experiment as extract quantity increased. An

observation of Figure 9 shows that the surface coverage trend at different times can be depicted in the following order, 1 min < 5 min < 2 min < 4 min < 3 min.

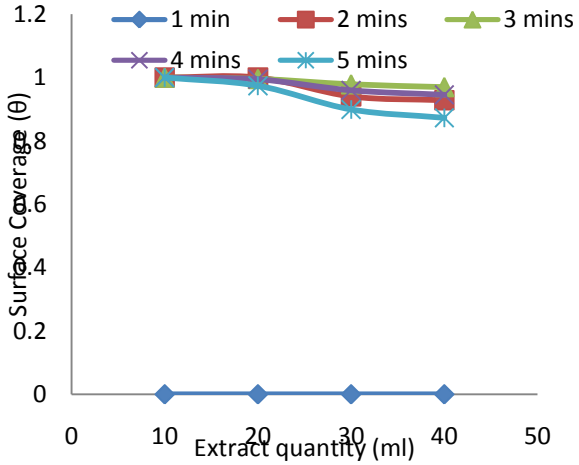

Figure 9: Variation of surface coverage (θ) with extract volume (cm^3) at a temperature of 300K for different time intervals.

In addition, the values of θ were also plotted against ln C in Figure 10. Investigations on the adsorption phenomenon involved linking θ with ln C (natural logarithm of extract volume) using Equation 10 (Pandey et al, 2010):

$$\theta = \xi + \lambda \ln C \qquad 10$$

$$\text{where; } \xi(\text{ml/ml}) = \frac{RT}{b}\ln a \qquad (11)$$

$$\lambda = \frac{RT}{b}$$

a = Temkin constant related to the maximum adsorption capacity.

b = Temkin constant related to the energy of adsorption.

θ = Surface coverage

C = Extract quantity

R and T are the gas constant (8.314 J mol^{-1} K^{-1}) and temperature (300 K) respectively. By comparing equation 10 to the straight line equation of the graph, it was possible to estimate the values of the energy of adsorption, b, and the maximum adsorption capacity, a, in terms of volume of hydrogen evolved to be 26,117.3 J mol^{-1} and 2.494 x 10^{-6} respectively.

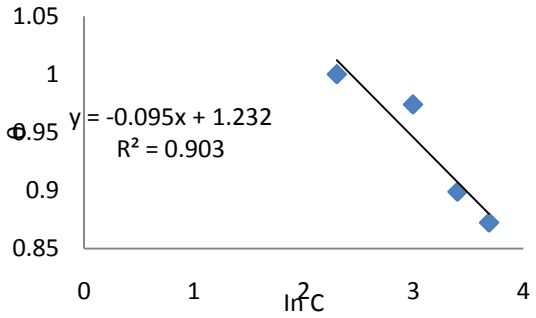

Figure 10: Plot of surface coverage (θ) with natural logarithm of extract quantity (ml) at a temperature of 300K.

The superficial effects of HCl action on the metal in the absence and presence of RV extract were investigated using optical microscope. Moreover, the studies were conducted on these samples with the aim of assessing the condition of the Al-alloy surface and grain structure. Nevertheless, the examinations were carried out on five metal samples which include that of the control experiment (having no inhibitor present) and samples from the 10, 20, 30 and 40 ml extract quantities. Superficial analysis was carried out and the micrograph of the alloy before the experiment as observed in Figure 11a, indicate the presence of three phases, which were the α-Al (white) phase, the Mg_5Al_8 (grey) phase and the thick spotted coarse Mg_2Si (black) phase. The first two mentioned phases were observed to be finely dispersed. In Figure 11b, which is the control sample, the micrograph indicate the presence of irregular flakes of the intermetallic phase along the grain boundaries which eventually resulted in deterioration. The effect of 10, 20, 30 and 40 ml acid extract of RV for over 60 minutes on the aluminium sample as shown in Figs. 11c, 11d, 11e and 11f respectively indicate that intergranular and pitting corrosion may not have occured rather there were indication of noticeable grain roughening and/or reformation. The presence of surface flakes was ostensibly suppressed with increasing quantity of inhibitors than without. It was also shown that the irregular intermetallic phases were more regular after exposure to increasing quantity of inhibitors due to the adsorption efficiency of the RV extract which controls the acidic and cathodic processes that may affect the grain structure. Therefore, by comparing Figs. 11c, d, e and f, it is observed that the addition of RV extract has obviously slowed down the metal deterioration rate. It is therefore clear that the higher the RV extract

quantity the slower the degradation rate and the longer the life of the alloy.

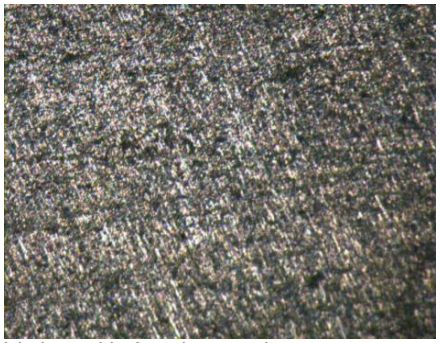

(a)Al metal before the experiment

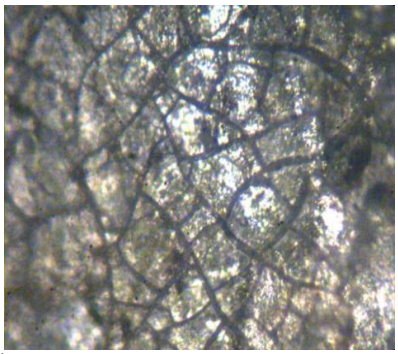

(b) Control

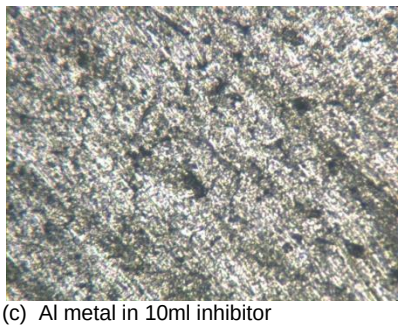

(c) Al metal in 10ml inhibitor

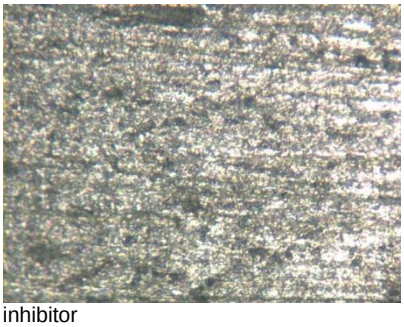

(d) Al metal in 20ml inhibitor

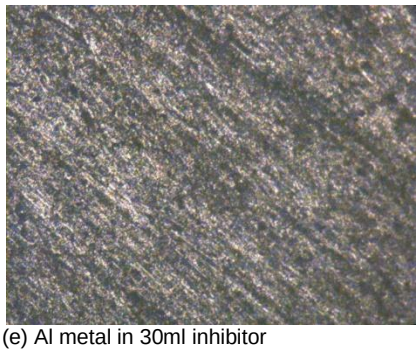

(e) Al metal in 30ml inhibitor

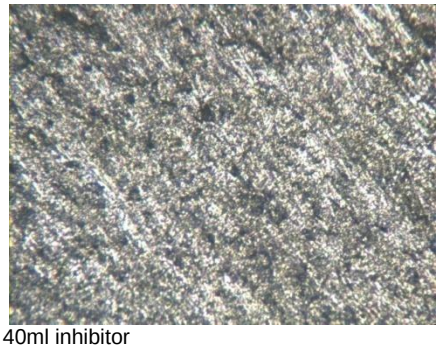

(f) Al metal in 40ml inhibitor

Figure 11: Micrographs for mild steel surface (a) before immersion in 2.5 M HCl solutions (b) after immersion in 2.5 M HCl for 60 min (c) after immersion in 10cml of RV extract (d) after immersion in 20 ml of RV extract.

4. Conclusions

The study investigated the environmentally induced damaged of Al-alloy by HCl acid in the presence of RV extract using gasometric and gravimetric techniques. Attempts were made to ascertain if any relationship existed: between H_2 evolved and time; inhibitor efficiency and concentration; corrosion rate and time; hydrogen evolved and weight loss; and adsorption mechanism with concentration. Several indices that portrayed the performance of the metal in the medium at different inhibitor concentrations were pinpointed. The results showed that as extract concentration was increasing, H_2 evolution and corrosion rate increased, while only inhibitor efficiency reduced both for gasometric and gravimetric methods. The phytoconstituent-metal surface interaction mechanism was best described by the Temkin isotherm. The 3 minutes curve showed itself as

the best time for extract phytochemicals to adsorb to the alloy surface.

References

Abiola, O.K., Oforka, N.C., Ebenso, E.E. & Nwinuka, N.M., (2007), Ecofriendly Corrosion Inhibitors: The Inhibitive Action of *Delonix regia* Extract for the Corrosion of Aluminium in Acidic Media, Anti-Corrosion Methods and Materials, 54 (4), 219-224,

Ajayi O. O., Omotosho O. A., Ajanaku K. O., Olawore B. O., (2011a), Degradation Study of Aluminium Alloy in 2.5 M Hydrochloric Acid in the Presence of *Chromolaena odorata*, Journal of Engineering and Applied Sciences 6 (1), 10-17.

Ajayi O. O., Omotosho O. A., Ifepe, V.O., (2011b), Acid Failure of Mild Steel in 2 M Sulphuric Acid in the Presence of *Vernonia amygdalina*, Journal of Materials and Environmental Science, 2 (2), 186-195

Ajayi, O. O., Omotosho, O. A., Ajanaku, K.O., Ifepe, V.O., (2012), Environment Induced Failure of Mild Steel in 2 M Sulphuric Acid Using *Chromolaena odorata*, Journal of Materials and Environmental Science, 3(1), 66-75.

Ajayi, O.O., Omotosho, O.A., Ajanaku, K. O., Olawore, B. O., (2011c), Failure evaluation of Aluminium Alloy in 2 M HCl in the presence of *Cola acuminata*, Environmental Research Journal, 5 (4), 163-169.

Ebenso, E.E. & Ekpe, U.J., Kinetic Study of Corrosion and Corrosion Inhibition of Mild Steel in H2SO4 using *Parica Papaya* Leaves Extract, W. Afri. J. Biol. Appl. Chem., 41, pp. 21-27, 1996.

Ebenso, E.E., Ekpe, U.J. & Ibok, U.J., (1998) Studies on The Inhibition of Mild Steel Corrosion by Some Plant Extracts in Acidic Medium, Discov. And Innov., 10, 52-59,

Ebenso, E.E., Ibok, U.J., Ekpe, U.J., Umoren, S., Ekerete, J., Abiola, O.K., Oforka, N.C., Martinez, S., (2004), Corrosion Inhibition Studies of Some Plant Extracts on Aluminium in Acidic Medium, Trans. of SAEST, 39, 117-123.

Ekpe, U.J., Ebenso, E.E. & Ibok, U.J., (1994), Inhibitory Action of *Azadirachta indica* Leaves Extract on The Corrosion of Mild Steel in H_2SO_4, J.W. Afri. Sci. Assoc., 37, 13-30,

Febrianto, J., Kosasih, A.N., Sunarsob, J., Ju, Y., Indraswati, N., Ismadji, S., (2009), Equilibrium and Kinetic Studies in Adsorption of Heavy Metals Using Biosorbent: A Summary of Recent Studies, Journal of Hazardous Materials, 162, 616–645.

James, A.O. & Akaranta, O., (2009), Corrosion Inhibition of Aluminium in 2.0M Hydrochloric Acid Solution by The Acetone Extract of Red Onion Skin, African Journal of Pure and Applied chemistry, 3 (12), 262-268.

Koch, G. H., Brongers, M. P. H., Thompson, N. G., Virmani, P., Payer, J.H. F.HWA-RD-01-156 (2001) [available at http://www.corrosioncost.com/pdf/main.pdf] accessed 15/10/2012.

Martinez, S., Tagljar, I. (2002), Correlation Between the Molecular Structure and the Corrosion Inhibition Efficiency of Chestnut Tannin in Acidic Solutions, Journal of Molecular structure, THEOCHEM, 640 (1-3), 167-174.

Njoku, P.C., Oguzie, E.E. & Nwaogu, U.C., (2006), Inhibitive Effect of Aqueous Extracts of Chromolaena Odorata and Vigna Radiata on the Corrosion of Aluminium in Acidic Medium, Journal of Chemical Society of Nigeria, 89-95.

Oguzie, E. E., (2006), Studies on The Inhibitive Effect of *Occimum viridis* Extract on The Acid Corrosion of Mild Steel, Material Chemistry and Physics, 99 (2/3), 441-446.

Okafor, P.C., Ebenso, E.E. & Ekpe, U.J., (2010), *Azadirachta indica* Extracts as Corrosion Inhibitor for Mild Steel in Acid Medium, International Journal of Electrochemical Science, 5, 978-993.

Omotosho, O.A., (2011), Assessing the Performance of Potassium Dichromate and Aniline on Concrete Steel Rebar Deterioration in Marine and Microbial Media, Research Journal of Applied Science, 6 (3), 143-149.

Omotosho, O.A., Ajayi, O.O., (2012), Investigating the Acid Failure of Aluminium Alloy

in 2 M Hydrochloric Acid in Using *Vernonia amygdalina*, ITB Journal of Engineering Science, 44 (1), 77-92.

Omotosho, O.A., Ajayi, O.O., Fayomi, O., Yussuff, O.O. (2012b), Degradation Evaluation of Zinc in 2 M Hydrochloric Acid in the presence of *Bambusa bambos,* Singapore Journal of Scientific Research, 2(1), 14-24.

Omotosho, O.A., Ajayi, O.O., Fayomi, O.S., Ifepe, V.O. (2011), Assessing the Deterioration Behavior of Mild Steel in 2 M Sulphuric Acid Using *Bambusa glauscescens*, International Journal of Applied Engineering Research, Dindigul, 2(2), 406-418.

Omotosho, O.A., Ajayi, O.O., Fayomi, O.S., Ifepe, V.O. (2012a), Evaluating the Deterioration Behaviour of mild steel in 2M sulphuric acid in the presence of *Butyrospermum parkii*, Asian Journal of Applied Sciences, 5 (2), 74-84.

Pandey, P.K., Sharma, S.K., Sambi, S.S., (2010), Kinetics and Equilibrium Study of Chromium Adsorption on ZeoliteNaX, International Journal of Environmental Science Technology, 7(2), 395-404.

Saratha, R., Priya, S.V., Thilagavathy, P., (2009), Investigation of *Citrus aurantifolia* Leaves Extract as Corrosion Inhibitor for Mild Steel in 1 M HCl, E-Journal of Chemistry, 6(3), 785-795.

Sobamowo et al: Proc. ICCEM (2012) 30 -50

Analysis of dynamic behaviour and power generation of a wind-tidal system for marine environment

[1]M. G. Sobamowo, [2]B.Y. Ogunmola, [3]J. A. Ogbemhe

[1,2] Department of Mechanical Engineering, University of Lagos, Akoka, Lagos, Nigeria.
[3]Department of Systems Engineering, University of Lagos, Akoka, Lagos, Nigeria.
Corresponding Author: M.G. Sobamowo E-mail- mikegbeminiyiprof@yahoo.com

Abstract

This work presents the analysis of dynamic behaviour and power generation of a wind-tidal hybrid system. Mathematical models and system design approach were used to investigate the feasibility, reliability and economic impact of the system. From the system design analysis carried out, by harnessing the tidal energy with wind energy in marine environment, the total power generated (approximately 180KW) by the hybrid power system showed a significant improvement over a wind turbine system which only generates a maximum power of 25KW at the rotor diameter as reported in literature. The effects of aerodynamics and hydrodynamics forces on the structure were investigated through the analysis of dynamic behaviour of the system under different loads and at various sites in the marine environment. The stability and the optimum turbine design were found to depend on the wind and tidal speed distribution of the specific site in the environment. The long term benefit of this work is aimed at meeting the energy needs of coastal dwellers by implementing the hybrid power system. Also, the gridless system could be used to generate power for both large and small scale industries in the marine environment.

***Key words**: Wind Energy; Tidal Energy; Hybrid Power System; Dynamic behaviour; Power generation; Marine Environment*

1. Introduction

Growing concerns over the threat of global energy security and climate change have strengthened interest in harnessing renewable energy resources as a response to the global energy challenge. The inadequate supply or the epileptic nature of electricity generation in developing countries has also given rise to research into other source of energy generation like wind, tidal, solar etc. The rapid world population growth and the advancement in economy in no doubt resulted in rapid increase in energy demands. Moreover, the limited nature of fossil energy and its pollution on the enviroment has given rise to contradiction among energy providing, environment protection and economic development. The energy available from the renewable resources, with the availability of its renewability and non-pollution, will grow to be an effective and practical choice to guarantee the future developing countries of the world. On the other hand, the renewable energy sources like wind energy, solar energy, etc. is seasonal, periodic or unpredictable and most often such energy is affected by factors beyond human control. Also, in most cases such seasonal, intermittent and periodic renewable energy systems are backed up by conventional sources of energy or energy storage devices (which in consequent, gives rise to additional production, operation and maintenance costs) in order to ensure continuity of the energy supply. One of the solutions to combating the problem is to hybridize two or more energy sources for efficient and effective performance. Actually, the technique of hybrid power system is one of

the currently most explored techniques for power generation which focuses on the generation of power from two different energy sources and it has proven to solve the power crisis in many countries around the world to a very large extent.

From the literatures for these two renewable energy sources, the power generation from wind turbines has already been studied extensively and very much literature on the topic exists. Wasynczuk et al (1981) investigated the dynamic behaviour of a class wind turbine generator during random wind fluctuations. Rajib and Ranganathan (2002) used a doubly fed wound rotor induction machine for a variable-speed wind power generation. Eduard and Butterfield (2001) presented pitch-controlled variable-speed wind turbine power generation. Antonios et al (2004) developed mathematical models for the dynamic performance and control for a grid-connected variable speed wind turbine. Erlich et al (2007) showed that with properly designed crowbar and DC-link chopper even zero voltage-through is possible using a Doubly-Fed Induction Generator, Fault-Ride through (DFIG) based wind turbines. Jonathan and Hiskens (2008) developed a model for estimating wind turbine parameters and quantifying their effects on dynamic behavior. Yuwei Li et al (2012) presented a simulation result of an overset computational fluid dynamics for wind turbine. Also, various work on the use of Tidal waves or currents for power generations have been presented in literatures [1, 3, 4, 8, 10, 13, and 16]. On the dynamic analysis of a Hybrid system, Gillie and Leithead (2003) developed dynamic models for the synchronous generator and induction generator of a hybrid generation system referred as a virtual power plant which consists of a wind farm and a gas turbine driven synchronous generator whose outputs are combined before connecting to the grid. With the various efforts towards energy generation through renewable energy sources, generating power with a hybridized power system operating on wind and tidal turbines to best of our knowledge has not been researched into. Consequently, in this work, we analyzed the dynamic behaviour and power generation of a hybrid system comprising wind and tidal sources that could operate in complementing or supplementing each other. Wind and Tidal energy are forms of renewable energy sources which contain clean and abundant source of energy. They provide a vast potential for renewable electric power generation and industrial energy supply. Since tides are generated by endless cycles of the rotation of the moon about the Earth, resulting in an almost limitless supply of energy, this gives the tidal power system a distinct advantage over other power systems. Moreover, the Wind power system produced by wind energy found at high altitudes where continuous wind speeds of over one hundred and sixty kilometer per hour occur is also very dependable. The hybridized system of these renewable energy sources posseses some advantages to its credit. It needs no fuel to maintain, and free of charge, totally no pollution, unlike fossil fuels, it produces no greenhouse gases or other waste. It is a predictable source of energy as compared with wind and solar hybridized system. It is independent of weather and climate change and follows the predictable relationship of the lunar orbit. It is more efficient and reliable than wind or tidal power generation system. It will protect a large stretch of coastline against damage from high storm tides. The disadvantages could be overcome and mitigated by proper design and practice. The development and utilization of such a hybrid system will

enhance the reduction in major health risks through reduced air, land and water pollution. Adverse effects of global warming on weather and climate can be mitigated by reduced CO_2 emissions. As a result, there will be reduction in health care costs and the impact of likely stricter federal emission standards in the future. Such a healthy environment achieved by the proper utilization of wind-tidal turbines attracts and retain business and also encourages the tourist industry. Large and Small scale industries on the coast can benefit by using it. Thereby increasing their marginal profit and reducing their down time. Educational institutions can also benefit from the use of the plant since they can run their laboratory equipment on it. It will also give the institution an opportunity to explore, relocate and train its faculty and students in an emerging environmental technology. Consequently this will drastically reduce the over-dependent on petrol and the effects of petroleum scarcity in our nation if the work is properly supported and developed. Moreover, the fact that the proposed hybrid system has highly efficient process, flexibility in applications over a range of output ratings, comparable low initial investment, low cost of power production, better process control and convenience, and low maintenance cost gives the study undeniable advantages over the high-grade energy generated from fossil fuels.

As pointed out before, this effort seems to be the first attempt into such form of hybridized renewable energy system. Therefore, the possibilities and potentialities of the power generation by the system worth serious considerations. This will help to measure, mitigate and control negative consequences on the system. Since this work is basically designed to be an off-grid system, our main focus is to generate power for both large and small scale industries along the coast where the hybrid system is installed. Consequently, in remote and isolated areas far from the coast, it may not be an economically viable option to supply electric power from the coast. This is due to the high cost of transmission lines and higher transmission losses that accompany distribution of centrally generated power to remote areas.

2. The off-grid hybrid power system

Fig. 1 presents in block diagram, the hybrid power generating system. The components of the hybrid power system could however be classified into the wind power system components, the tidal power system components and an intelligent hybrid controller as shown in the block diagram.

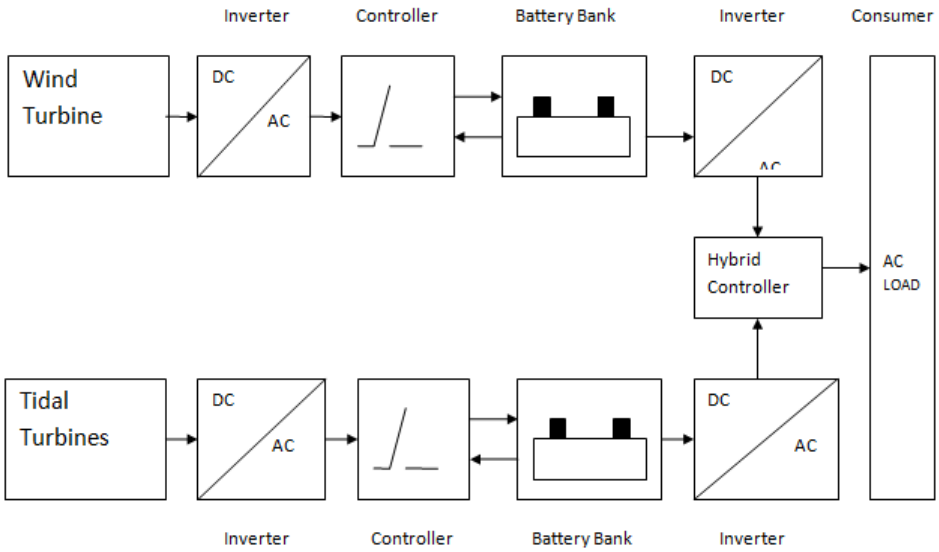

Fig. 1 Block diagram of the Wind-Tidal Power generating system

The off-grid hybrid energy system is battery based. It is limited in capacity by the size of the generating sources (wind turbine, tidal generator, etc.), the resources available, and the battery bank size. The users learn to live within the limitations of the system capacity.

3. Modeling the power generation by the system

Our first attempt in this work is to model the power generation by the system. This will be done by considering different power sections of the system.

3.1 Modeling the power generation by the wind turbine

Power Extraction from the air stream by the turbine is given as

$$P_{Wi} = \tfrac{1}{2}\rho . A V^3 C_P \qquad 1$$

Where C_p is the fraction of the upstream wind power which is captured by the rotor blades and it has theoretical maximum value of 0.59. It is referred as the power coefficient of the rotor or the rotor efficiency in practical designs. The maximum achievable C_P is between 0.4 and 0.5 for high-speed, two – blade turbines and 0.2 and 0.4 for slow speed turbines with more blades.

An improved model for the rotor for the power coefficient varying with tip speed ratio, $\lambda = \frac{\omega R}{V}$ (the ratio between the blade tip speed V_t and product of the wind speed upstream of the rotor v) is given as

$$P_{Wi} = 0.22\left(\frac{125V}{\omega R} - 6.69\right) A V^3 e^{\left(\frac{16.5V}{\omega R} + 0.33\right)} \qquad 2$$

R is the rotor blade radius in meter, ω is the rotor angular speed in $rad/\sec$.

.

The thrust from the air to the rotor is

$$T_{Wi} = 0.22AV^2\left(\frac{125V}{\omega R} - 6.69\right)e^{\left(\frac{16.5V}{\omega R}+0.33\right)} \quad 3$$

For a wind turbine using a doubly fed induction generator, it shows that the performance coefficient C_p is not only dependent on the tip speed ratio λ, as before but also on the pitch angle $\theta[\deg]$. This is caused by the fact that variable speed wind turbines are assumed to be equipped with a pitch angle controller as in normally the case.

$$P_{Wi} = 0.365\rho A_r V^3\left[151\left(\frac{1}{\lambda - 0.02\theta} + \frac{0.003}{\theta^3 + 1}\right) - 0.58\theta - 0.002\theta^{2.14} - 13.2\right] \times e^{18.4\left(\frac{1}{\lambda-0.02\theta}+\frac{0.003}{\theta^3+1}\right)} \quad 4$$

$$T_{Wi} = 0.365\rho A_r V^2\left[151\left(\frac{1}{\lambda - 0.02\theta} + \frac{0.003}{\theta^3 + 1}\right) - 0.58\theta - 0.002\theta^{2.14} - 13.2\right] \times e^{18.4\left(\frac{1}{\lambda-0.02\theta}+\frac{0.003}{\theta^3+1}\right)} \quad 5$$

In the previous section in this work, the power generated by waves and tidal has been referred to as the power generated by tidal. For the purpose of proper analysis and explanations in this section, a separation is made.

Energy Content of the Wind

$$EC = 0.00001073\rho A\sum_{i=1}^{N_m} V_i^3 \quad 6$$

EC is the energy content of the wind in kWh, V_i is the hourly wind speed in km/h, for hour *i*, N_m is the total number of hours in the specified period

3.2 Modeling the Power generated by the Water Waves

The condition on the free surface for the water waves is given by:

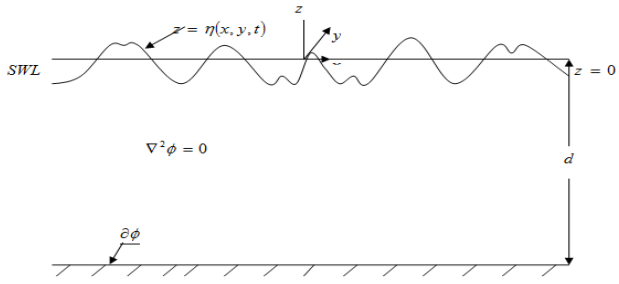

Fig. 2 condition on the free surface for the water waves

If we consider a fluid on which disturbances of height $\eta(x, y, t)$ above still water level are propagating. The vertical velocity at the free surface, taking into consideration at the surface moves with the fluid, is

The stream function,

$$\phi = \frac{ga_0}{\omega} f_0(z)\sin(\omega t - Kx) \quad 7a$$

where $\omega^2 = gK\tanh Kd$, and we have written

$f_0(z)$ for the usual $\frac{\cosh[K(z+d)]}{\cosh Kd}$

a_0 is the airy wave amplitude

Hence

$$V_x = \frac{\partial\varphi}{\partial x} = \frac{g}{\omega}Ka_0\exp[-i(Kx - \omega t)]\frac{\cosh[K(z+d)]}{\cosh Kd}$$

$$V_z = \frac{\partial\varphi}{\partial z} = \frac{ig}{\omega}Ka_0\exp[-i(Kx - \omega t)]\frac{\sinh[K(z+d)]}{\cosh Kd} \quad 7b$$

7c
Generally, we have;

$$\eta(x) = -i\frac{\omega\varphi(x)}{g} = a_0 \exp(-ikx)$$

$$\phi(x,z,t) = \frac{ig}{\omega}\eta(x)\frac{\cosh[K(z+d)]}{\cosh Kd}\exp(i\omega t)$$

$$V_x = \frac{\partial\phi}{\partial x} = \frac{g}{\omega}K\frac{\cosh[K(z+d)]}{\cosh Kd}\exp(i\omega t)\eta(x)$$

$$V_y = 0$$

$$V_z = \frac{\partial\phi}{\partial z} = \frac{ig}{\omega}K\frac{\sinh[K(z+d)]}{\cosh Kd}\exp(i\omega t)\eta(x)$$

$$V_t = \frac{\partial\varphi}{\partial t} = -\frac{g}{\omega}a_0 \exp[-i(Kx-\omega t)]\frac{\cosh[K(z+d)]}{\cosh Kd}$$

8a-f

The average rate at which work is done is P over wave period T, then P can be given as

$$P_{Wa} = \frac{1}{T}\int_0^T\int_{z=-d}^{z=0}\rho\left(-\frac{\partial\varphi}{\partial t}\right)\left(\frac{\partial\varphi}{\partial x}\right)dzdt \qquad 9$$

which gives

$$P_{Wa} = \frac{\rho a_o^2 g^2}{2\omega\cosh^2(Kd)}\left(\frac{\sinh(2Kd)}{4}+\frac{Kd}{2}\right) \qquad 10$$

Where $k = 2\pi/L$, a_0 is the amplitude and ω is the angular speed

3.3 Modeling the Power generated by Tides is given as

Tidal Energy or tidal power is the power achieved by capturing the energy contained in moving water mass due to tides. Two types of tidal energy can be extracted: kinetic energy of currents between ebbing and surging tides and potential energy from the difference in height between high and low tides. Moving water has kinetic energy similar to wind. The energy per second intercepted by a device of frontal area A(m²) in water of density ρ, and current velocity V (m/s) is therefore given by:

$$P = \tfrac{1}{2}\rho.A.V(t)^3 C_P \qquad 11$$

Assuming a gearbox transmission efficiency of η_T and generator efficiency of η_G then the electrical power output is given as:

$$P = 0.5\eta_T\eta_G\rho.A.V(t)^3 C_P \qquad 12$$

Tidal currents are not constant. Generally they are a combination of quasi-steady marine currents and flows induced by the tides. Consequently, the estimation of energy capture therefore becomes a fairly complex procedure. However for most sites the flows are purely tidal, making it possible to parameterize the tidal currents as series of simple sinusoids. Assuming the current velocity *v(t)* follows a cyclic pattern then:

$$V(t) = V_{\max}\sin\omega t$$

$$where \quad \omega = \frac{2\pi}{T} \qquad 13$$

Vmax is the maximum current speed at the surface
ω is the angular velocity of the tide
T is the period of the cycle, typically 12h 25 min or 745 minutes.

$$P = \eta_T\eta_G C_P\rho A V_{\max}^3\sin^3\omega t \qquad 14$$

The energy captured during one half of each half tidal cycle is:

$$E_T = \int P(t)dt = \int_{T_1}^{T_2} (0.5\eta_T \eta_G C_P \rho A V_{\max}^3 \sin^3 \omega t)dt + P_{rated}(T_m - T_2) \quad 15a$$

which gives,

$$E_T = \eta_T \eta_G C_P \rho A V_{\max} \left[9\sin\left(\frac{\pi}{T}(T_1 + T_2)\right)\sin\left(\frac{\pi}{T}(T_1 - T_2)\right) + \sin\left(\frac{3\pi}{T}(T_1 + T_2)\right)\sin\left(\frac{3\pi}{T}(T_1 - T_2)\right)\right] + P_{rated}(T_m - T_1) \quad 15b$$

where

T_1 and T_2 are the times at which cut-in and rated power occur (relative to the start of the cycle)

The design analysis of the power generated by the system is presented in the appendix

4. Models for the dynamic behaviour of the structure

When designing a wind or tidal turbine it is extremely important to calculate in advance how the different components will vibrate, both individually, and jointly. It is also important to calculate the forces involved in each bending or stretching of a component.

A 50 meter tall Hybrid wind-tidal turbine tower will have a tendency to swing back and forth, say, every three seconds. The frequency with which the tower oscillates back and forth is also known as the eigenfrequency of the tower. The eigenfrequency depends on both the height of the tower, the thickness of its walls, the type of steel, and the weight of the nacelle and rotor. Each time a rotor blade passes the wind/tidal shade of the tower, the rotor will push slightly less against the tower. If the rotor turns with a rotational speed such that a rotor blade passes the tower each time the tower is in one of its extreme positions, then the rotor blade may either dampen or amplify (reinforce) the oscillations of the tower.

The rotor blades themselves are also flexible, and may have a tendency to vibrate, say, once per second. So, it is very important analyse the dynamic behaviour of the in order to design a safe system that does not oscillate out of control

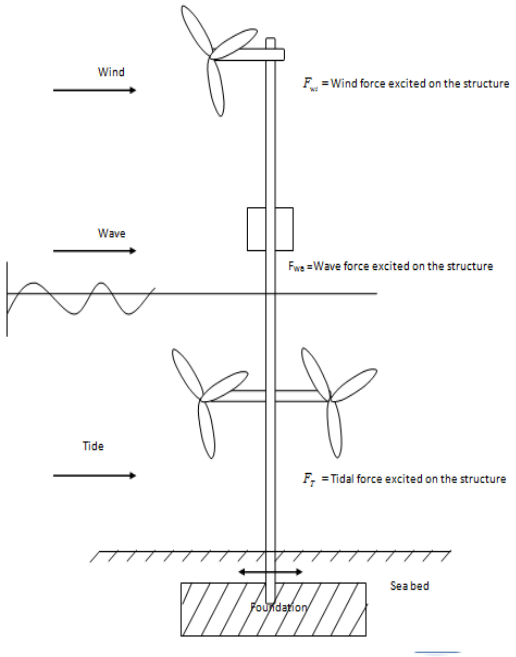

Fig.3 Environmental loads on the hybrid power-system structure.

In deriving the equation governing the vibration in the structure (modelled as flexure beam), the following assumptions were

i. Vibration occurs in one of the principal planes of the beam.
ii. The effects of rotatory inertia and transverse shear deformation are neglected.
iii. The gravity forces are neglected by measuring the displacement from the position of static equation of the beam.

After derivations, the governing differential equation becomes

$$EI\frac{\partial^4 u}{\partial z^4}+\rho A\frac{\partial^2 u}{\partial t^2}=F(z,t) \qquad 16$$

where

$$F(z,t)=F_{wind}(z,t)+F_{waves}(z,t)+F_{tides}(z,t)$$

Where

$F(z,t)$ are the applied forces along the beam

E is the modulus of electricity of the beam and I is the moment of inertia,

I is the moment of inertia;

u are the transverse displacement

A is the cross-sectional

One way of finding an approximate solution for these equations is by weighing equation and the boundary condition in the following way

$$\int_0^l -\left(EI\frac{\partial^4 u}{\partial z^4}+\rho A\frac{\partial^2 u}{\partial t^2}-P(z,t)W\ dz\right)=\left[\left(\overline{M}-M\right)\frac{dW}{dz}\right]_{s_2}+\left[\left(\overline{Q}-Q\right)W\right]_{s_2} \qquad 17$$

Where W are weighting functions that are assumed to satisfy the essential boundary conditions, that is W and $\frac{dW}{dz}$ are identically zero on s_1.The essential or primary displacement condition on the s_1 part of the boundary is $u=0$ at $z=0$

The natural or force or secondary condition on the s_2 part of the boundary which are moment M and shear Q.

$$\overline{M}=EI\frac{d^2u}{dz^2}=0 \qquad \text{at } z=l$$

$$\overline{Q}=-EI\frac{d^3u}{dz^3}=0$$

$$\frac{du}{dz}=0 \text{ at } z=0$$

18a-c

Assuming that the shapes of the W functions are the same as the u functions, which was taken as approximate solutions, this leads to the following form of the principle of virtual displacement.

$$\int_0^l\left(EI\frac{\partial^4 u}{\partial z^4}+\rho A\frac{\partial^2 u}{\partial t^2}-P(z,t)\partial u\ dz\right)=\left[\left(\overline{M}-M\right)\frac{d\ \partial u}{dz}\right]_{s_2}+\left[\left(\overline{Q}-Q\right)\partial u\right]_{s_2} \qquad 19$$

Integrating equation (19) by parts twice, we obtain the best-known expression for virtual displacements, that is

$$\int_0^l \left(EI\left(\frac{d^2u}{dz^2}\right)\left(\frac{d\ \partial u}{dz^2}\right) + \rho A\ddot{u} \right) dz = \int P\ \partial u dz + \left[\overline{M}\ \frac{d\ \partial u}{dz} \right]_{s_2} + \left[\overline{Q}\ \partial u \right]_{s_2} \qquad 20$$

On putting the boundary condition we have the principle of virtual displacements for the equation (20) as

$$\int_0^l \left[EI\left(\frac{d^2u}{dz^2}\right)\left(\frac{d\ \partial u}{dz^2}\right) + \rho A\ddot{u} \right] dz = \int P\ \partial u dz \qquad 21$$

With the function u satisfying the essential boundary conditions at z=0, that is the part of the boundary s_2. Assuming an approximate function for u, such that

Where u represent the horizontal displacement at the top of the tower and $g(z)$ is a "shape" function that represents the shape of the tower substituting 14a and 14b into 5, we find

$$\partial u\left[\int_0^l EI\left(\frac{d^2g}{dz^2}\right)^2 dz\ u + \int_0^l \left(\rho A(g)^2 dz\ \ddot{u}\right) \right] = \partial u\left[\int_0^l \rho g\ dz \right] \qquad 22$$

As ∂u is arbitrary, we can simply write

$$Ku + M\ddot{u} = F \qquad 23$$

Where

$$\left.\begin{aligned} K &= \int_0^l EI\left(\frac{d^2g}{dz^2}\right)dz \\ M &= \int_0^l \rho A(g)^2 dz \\ F &= \int_0^l \rho g\ dz \end{aligned}\right\} \qquad 24$$

$K,\ M,\ and\ F$ are the equivalent stiffness, mass and force coefficients for the one – degree of freedom system.

We can similarly include the damping term into the equation. Therefore more general equilibrium equation will then be

$$Ku + C\dot{u} + M\ddot{u} = F \qquad 25$$

Where

$$C = \int_0^l c(g)^2 dz \qquad 26$$

$$M\ddot{u} + C\dot{u} + Ku = F \qquad 27$$

where M is the mass of the tower, the mass of the platform and the hydrodynamic mass. The term C includes the structural

and hydrodynamic damping. K include the structural and hydrodynamic stiffness. u is the displacement at the top of the column $x = L$.

The Force F in equation has three components, that is $F = F_{Wi} + F_{Wa} + F_T$

$$F = \left[\left(C_I v_x + C_D\sqrt{\frac{8}{\pi}}\sigma_{vx} v_x\right)^2 + \frac{1}{4}\rho^2 D^2 v_m^4\left(\sum_{n=1}^{N} C_1^n \cos\left(m\omega_0 + \varphi_n\right)\right)^2\right]^{\frac{1}{2}}$$
$$+ 4\rho_{air} v^2 D\left(\sqrt{C_D^2 C_L^2}\right)(z)^{2\alpha_s}\left(\frac{H_0}{D_0}\right) f(t) + F_{ZNB}\delta(z-1) + M_{YNB}\eta(z-1) - m_T\frac{\partial^2\omega}{\partial t^2} - g_2\frac{\partial\omega}{\partial t}$$
$$+ 4\rho_{water} v_x^2 D\sqrt{C_D + C_L^2}\, x^{2\alpha_s} + 2F_{TNB}\delta(z-1) + 2M_T\eta(z-1)$$

28

Thus, we have

$$M\ddot{u}_t + C\dot{u} + Ku = \left[\left(C_I v_x + C_D\sqrt{\frac{8}{\pi}}\sigma_{vx} v_x\right)^2 + \frac{1}{4}\rho^2 D^2 v_m^4\left(\sum_{n=1}^{N} C_1^n \cos\left(m\omega_0 + \varphi_n\right)\right)^2\right]^{\frac{1}{2}}$$
$$+ 4\rho_{air} v^2 D\left(\sqrt{C_D^2 C_L^2}\right)(z)^{2\alpha_s}\left(\frac{H_0}{D_0}\right) f(t) + F_{ZNB}\delta(z-1) + M_{YNB}\eta(z-1) - m_T\frac{\partial^2\omega}{\partial t^2} - g_2\frac{\partial\omega}{\partial t} \qquad 29$$
$$+ 4\rho_{water} v_x^2 D\sqrt{C_D + C_L^2}\, x^{2\alpha_s} + 2F_{TNB}\delta(z-1) + 2M_T\eta(z-1)$$

This model seems complex in obtaining the closed form solution due to the non-linear nature of the force function. One of the ways of approximating the force function is neglect the effect of wind load on the structure. This approximation is justified if we compare the effect wind load to that of wave and tidal loads on the structure.

Morison et al [1950] postulated an empirical formula for the forces on vertical cylinders in the presence of surface waves. They postulated that the force had two components;

- the drag force, proportional to the square of the water-particle velocity, the constant of proportionality being a drag co-efficient having substantially the same value as for steady state
- An inverted or virtual – mass force, proportional to the horizontal component of acceleration of the water particles.

So, the force per unit length in the x direction (horizontal direction) at depth z is

$$F(z,t) = C_m(\dot{v}_x - \ddot{u}) + C_A\dot{v}_x + C_D(v_x - \dot{u})|v_x - \dot{u}| \qquad 30$$

This force is in the direction of the wave advance and the water – particle velocities and acceleration v and $\dot{v}_x$ are

evaluated at the cylinder axis. C_I is a constant due to inertia constituting of two terms; one due to the "hydrodynamic" mass contribution and the other to the variation of the pressure gradient within the accelerating fluid.

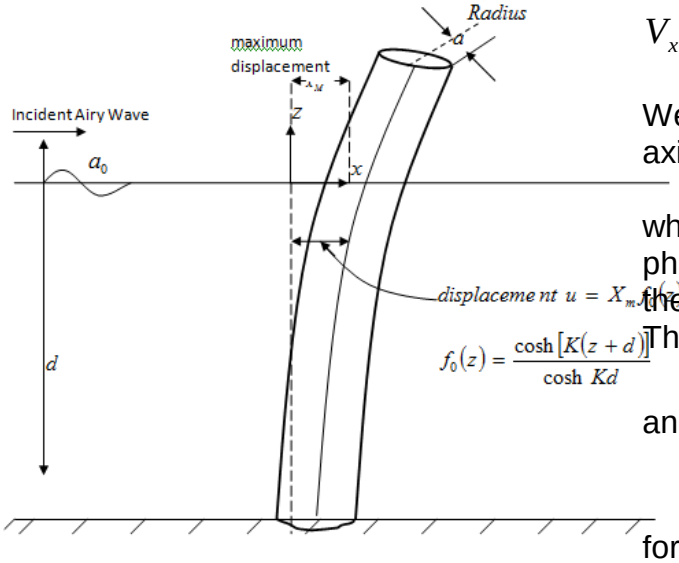

Fig. 4 Physical model for the bending and vibration of the structure

Recall from equation (7b);

$$V_x = \frac{\partial \varphi}{\partial x} = -\frac{Kga_0}{\omega} f_0(z)\cos(\omega t - Kx)$$

$$V_x = Kga_0 f_0(z)\sin(\omega t - Kx)$$

We have for displacement of the column axis:

where α is the angle representing the phase difference between the motion of the column and the wave.

The velocity of the column axis is:

$$\dot{u} = \omega X_m f_0(z)\cos(\omega t + \alpha)$$

and the acceleration is given by

$$\ddot{u} = -\omega^2 X_m f_0(z)\sin(\omega t + \alpha)$$

for a circular cylinder radius a, taking

$$C_m = C_A = C_d = 1,\ C_m = \pi a^2 \rho, \qquad C_A = \pi a^2 \rho, \qquad C_m = a\rho \qquad 31$$

Hence, the Morison's equation,

$$F(z,t) = \pi a^2 \rho f_0(z)\left[2gKa\sin(\omega t) + \omega^2 X_m \sin(\omega t + \alpha)\right] \times \rho a\left[f_0(z)\right]^2 \left[\frac{gKa_0}{\omega}\cos(\omega t) + \omega X_m \cos(\omega t + \alpha)\right] \times \left|\left[\frac{gKa_0}{\omega}\cos(\omega t) + \omega X_m \cos(\omega t + \alpha)\right]\right| \qquad 32$$

For deep water, $f_0(z) \approx \exp(Kz)$ and $\omega^2 = gK$, then we have

$$F(z,t) = \exp(Kz)\pi a^2 \rho\omega\left[2a_0 \sin(\omega t) + X_m \sin(\omega t + \alpha)\right] \times -\exp(2Kz)\rho a\omega^2\left[a_0 \cos(\omega t) + X_m \cos(\omega t + \alpha)\right] \times \left|a_0 \cos(\omega t) + X_m \cos(\omega t + \alpha)\right| \qquad 33$$

The total force on the cylinder (tower) $F_t(t)$ is obtained from F by integrating $F(z,t)$ from $z = -d$ *to* $z = 0$ in equ. 33

$$F_t(t) = \int_{-d}^{0} F(z,t)dz$$

$$F_t(t) = \int_{-d}^{0} \left[\exp(Kz)\pi a^2 \rho\omega\left[2a_0 \sin(\omega t) + X_m \sin(\omega t + \alpha)\right] - \exp(2Kz)\rho a\omega^2\left[\cos(\omega t) + X_m \cos(\omega t + \alpha)\right] \times \left|a_0 \cos(\omega t) + X_m \cos(\omega t + \alpha)\right|\right]dz$$

$$F_t(t) = \left[K\pi a^2\left[2a_0 \sin(\omega t) + X_m \sin(\omega t + \alpha)\right] - 2K\rho a\omega^2\left[a_0 \cos(\omega t) + X_m \cos(\omega t + \alpha)\right]\right](1 - \exp(-Kd)) \times \left|a_0 \cos(\omega t) + X_m \cos(\omega t + \alpha)\right|\Big]$$

34

For a stationary tower (cylinder), $X_m = 0$

So,

$$F_t(t) = 2\pi a^2 \rho g K a_0 f_0(z)\sin\omega t + \rho a\left[f_0(z)\right]^2 \frac{g^2 K^2 a_0^2}{\omega^2}\cos\omega t\left|\cos\omega t\right| \qquad 35$$

For deep water, $f_0(z) \approx \exp(Kz)$

$$F_t(t) = \left[2\pi a^2 \rho g K^2 a_0 \sin\omega t + \frac{2\rho a g^2 K^2 a_0^2}{\omega^2}\cos\omega t\left|\cos\omega t\right|\right](1 - \exp(-Kd)) \qquad 36$$

On substituting this into equation (27) and solve analytically,

The closed form solution for the vibration of the tower is given by

$$u(t) = e^{-\gamma\omega_n t}\left[\frac{u(0)+\gamma\omega_n u(0)}{\omega_n\sqrt{1-\gamma^2}}\sin\left(\sqrt{1-\gamma^2}\right)\omega_n t + u(0)\cos\left(\sqrt{1-\gamma^2}\right)\omega_n t\right] +$$

$$\frac{2\pi a^2\rho g K^2 a_0\left(M\omega^2 - K\right)\sin\omega t}{K\left(M\omega^2 - K\right) - M\omega^2\left(M\omega^2 - K\right) - \left(C\omega\right)^2} +$$

$$+\frac{2\pi a^2\rho g K^2 a_0\left(M\omega^2 - K\right)CM\omega^2\cos\omega t}{M\omega\left(M\omega^2 - K\right)\left[K\left(M\omega^2 - K\right) - M\omega^2\left(M\omega^2 - K\right) - \left(C\omega\right)^2\right]} +$$

$$+\frac{\rho a K^3 g^2 a_0\left(\exp\left(Kd\right)-1\right)\left(M\omega^2 - K\right)}{K\left(M\omega^2 - K\right) - M\omega^2\left(M\omega^2 - K\right) - \left(C\omega\right)^2}\sin 2\omega t +$$

$$\frac{\rho a K^3 g^2 a_0\exp\left[\left(Kd\right)-1\right]\left(M\omega^2 - K\right)CM\omega^2\cos 2\omega t}{M\omega\left(M\omega^2 - K\right)\left[K\left(M\omega^2 - K\right) - M\omega^2\left(M\omega^2 - K\right) - \left(C\omega\right)^2\right]}\cos 2\omega t +$$

$$+\frac{\rho a K^3 g^2 a_0}{\omega^2}\exp\left[\left(Kd\right)-1\right] \qquad 38$$

5. Dynamic analysis of the foundation

The vertical oscillation of the foundation of the hybrid power system can be modeled using Dashpot-spring-mass system.

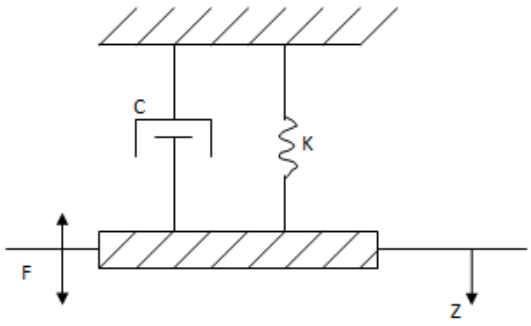

Fig.5 Physical model for foundation vibration.

$$M_{eff}\ddot{z} + C\dot{z} + Kz = F$$

40

For the Harmonically exciting force, we can write

$$F = P\sin\omega t$$

41

Hence:

$$M_{eff}\ddot{z} + C\dot{z} + Kz = P\sin\omega t$$

42

Where P the amplitude of the exciting force and ω is the forced frequency. M. Hanler etal gave the following relationship

$$C = \frac{3.4r^2\sqrt{G\rho}}{1-v} \text{ and } K = \frac{4Gr}{1-v}$$

G is the shear modulus of the foundation, v is the poisson ratio

On putting this into equation 43, we have

44

$$M_{eff}\ddot{z} + \frac{3.4r^2\sqrt{G\rho}}{1-\nu}\dot{z} + \frac{4Gr}{1-\nu}z = P\sin\omega t$$

Thus the complete solution is

$$z(t) = \frac{P}{\sqrt{M_{eff}\left\{\left[4\left(\frac{Gr}{1-\nu}\right) - M_{eff}\omega^2\right]^2 + \left[11.56\left(\frac{r^2\omega\sqrt{G\rho}}{1-\nu}\right)\right]^2\right\}}}\sin\left\{\omega t - \tan^{-1}\left[\frac{3.4r^2\sqrt{G\rho}}{4Gr - M_{eff}\omega^2(1-\nu)}\right]\right\}$$

45

The amplitude of the vibration is given as

$$Z = \frac{P}{\sqrt{M_{eff}\left\{\left[4\left(\frac{Gr}{1-\nu}\right) - M_{eff}\omega^2\right]^2 + \left[11.56\left(\frac{r^2\omega\sqrt{G\rho}}{1-\nu}\right)\right]^2\right\}}}$$

46

The phase angle is given by

$$\phi = \tan^{-1}\left[\frac{3.4r^2\sqrt{G\rho}}{4Gr - M_{eff}\omega^2(1-\nu)}\right]$$

47

The power generated by the turbines, the dynamic response of the structure to the wind, wind and tidal loads and the vibration of the foundation were investigated were simulated and the results were presented as follows.

6.0 economic models of the hybrid power gerating system

For the success and commercialization of any new technology, it is essential to know whether the technology is economically viable or not. Therefore, an attempt was made to evaluate economics of the Hybrid system. The merits and the economic potential and analysis of the technology can be evaluated in terms of the following indices:

i. Net Present Value (NPV): The present worth of the project
ii. Benefit Cost Ratio (BCR): The benefits from the project which are in proportion with the costs involved
iii. Pay Back Period (PBP): The years it will take to get the investment back from the project i.e is the year in which the net present value of all costs equals with the net present value of all benefits. It could also be defined as the minimum period over which the investment for the project is recovered

iv. Internal Rate of Return (IRR): The real return of the project or the maximum rate of interest at which capital can be arranged for the project

The Net Present Value (NPV) is given by the following:

$$NPV = B_A\left[\frac{(1+I)^n-1}{I(1+I)^n}\right]-\left[C_I\left\{1+m\left(\frac{(1+I)^n-1}{I(1+I)^n}\right)\right\}\right] \quad 48$$

The economic viability is established when the NPV is greater than 0

The Benefit Cost Ratio (BCR) is given by the following:

$$BCR = \frac{B_A}{C_l}\left[\frac{\frac{(1+I)^n-1}{I(1+I)^n}}{1+m\left(\frac{(1+I)^n-1}{I(1+I)^n}\right)}\right] \quad 49$$

The project is acceptable if BCR is greater than 1.

The Pay Back Period of the project is given by

$$n = -\frac{In\left(1-\frac{IC_l}{B_A-mC_l}\right)}{In(1+I)} \quad 50$$

The Internal Rate of Return (IRR) is determined from the following model using Numerical methods such as Newton-Raphson:

$$B_A\left[\frac{(1+IRR)^n-1}{IRR(1+IRR)^n}\right]=\left[C_I\left\{1+m\left(\frac{(1+IRR)^n-1}{IRR(1+IRR)^n}\right)\right\}\right] \quad 51$$

The cost of kWh of biomass gasification electricity generated is given by

$$C = \frac{C_l}{Nn}\left[\left(\frac{1}{P_R C_F}\right)\left\{1+m\left(\frac{(1+I)^n-1}{I(1+I)^n}\right)\right\}\right] \quad 52$$

Annual energy production (E) is given by

$$E = NP_R C_F \quad (53)$$

Annual revenue (AR) from the sale of electricity is given by

$$AR = \frac{C_l}{n}\left[\left\{1 + m\left(\frac{(1+I)^n - 1}{I(1+I)^n}\right)\right\}\right] \quad (54)$$

Where, AR is the Annual revenue, B_A Benefit delivered annually, BCR Benefit Cost Ratio, C Cost of kWh of biomass gasification electricity generated, C_F Site capacity factor, C_I Capital Investment of the Project, E Annual Electricity Production from the plant, I Real rate of return, IRR Internal Rate of Return, N Annual hour of the plant, n Life in Years of Plant NPV Net Present Value, PBP Pay Back Period of Investment, P_R Plant installed capacity

7.0 Result and Discussion

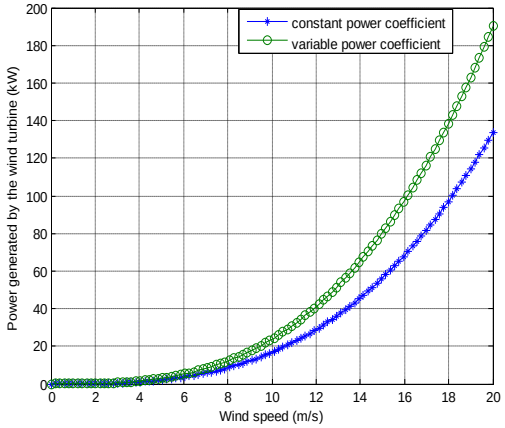

Fig.5 Effects of wind speed on power the generation by the wind turbine.

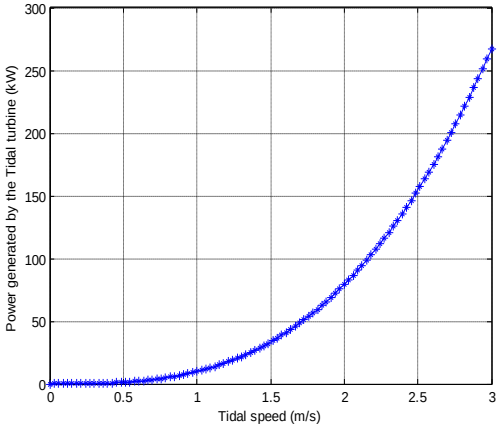

Fig.6 Effects of tidal speed on power the generation by the tidal turbine

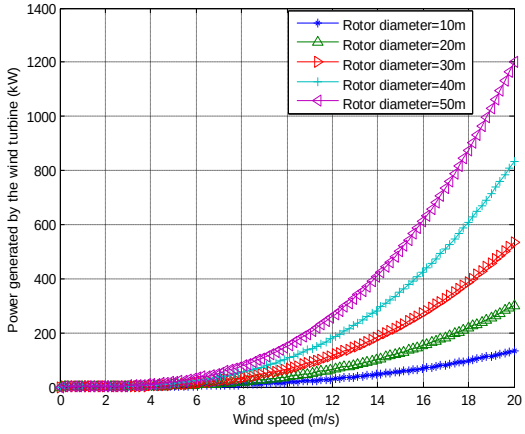

.

Fig.7 Effects of rotor diameter on power the generation by the wind turbine of constant C_p

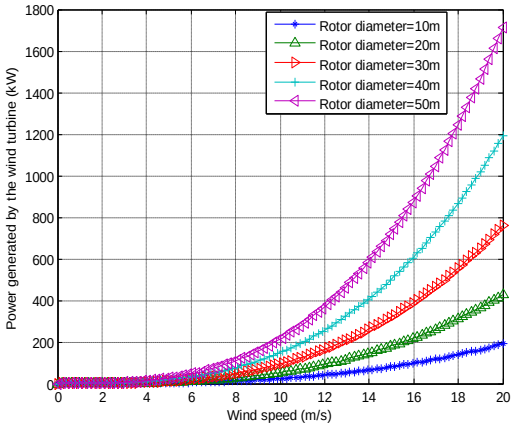

Fig.8 Effects of rotor diameter on power the generation by the wind turbine of variable C_p.

Fig. 5 and 6 depict that the power generated by the wind turbine and the tidal turbine increases with wind and tidal speed respectively. Fig. 7 and 8 show the effects of rotor diameter on the power generated by the wind turbine. From the figures, the power generated by the wind turbine increases with increase in rotor diameter. This is because, as the rotor diameter increases, the swept area of the turbine increases and more power are extracted by the rotor from the wind. Also from the model, it is shown that the power absorption and operating condition of a turbine are determined by the effective area of the rotor blades, wind speed and wind flow condition at the rotor. The output power of the turbine can be varied by the effective area and by changing the flow condition of the rotor system, which forms the basis of control of wind energy conversion system. Tip speed Ratio (TSR) is related to the wind turbine operating point for extracting power. The maximum rotor efficiency C_P is achieved at a particular TSR, which is speed to the aerodynamics design of a given turbine. The rotor must turn at high – speed at high – wind and at low – speed at low – wind, to keep TSR constant at the optimum level at all times. The larger the TSR, the faster is the rotation of the wind turbine rotor at a given wind speed. High (rotational) speed turbines are preferred for efficient electricity generation. From the tip speed ratio equation, for a particular value of speed v, turbine with large blade radius R results in low rotational speed, and vice versa. For operation over wide range of wind speeds, wind turbines with high tip speed ratios are preferred.

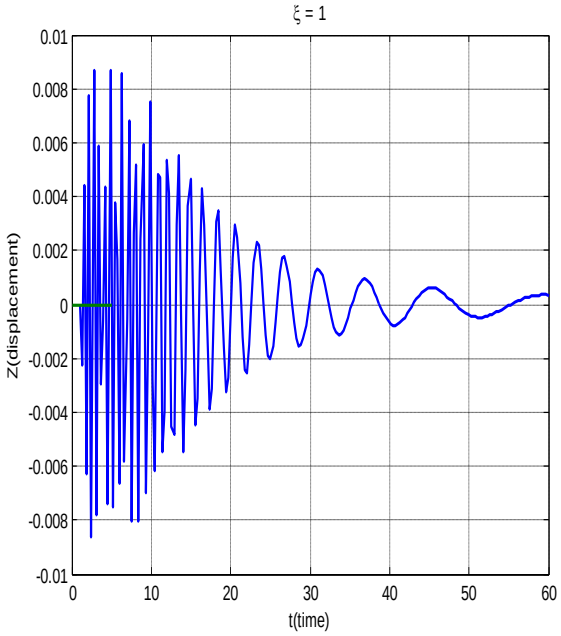

Fig.9a

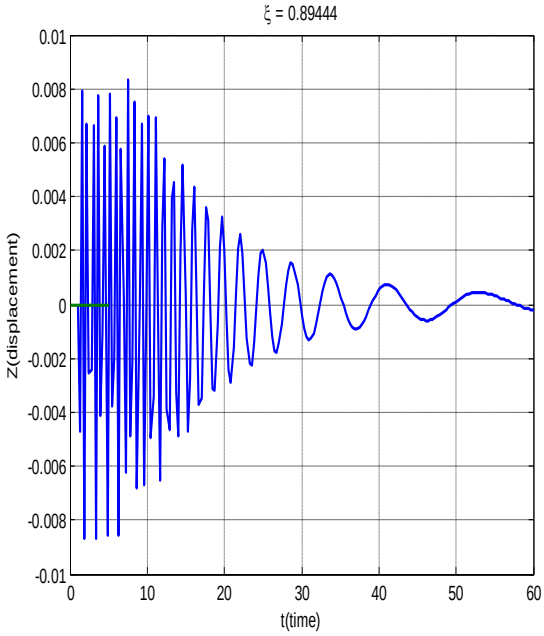

Fig.9b

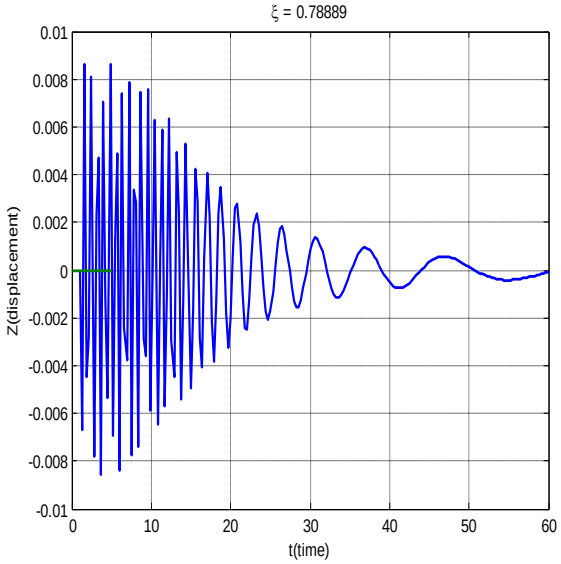

Fig.9c

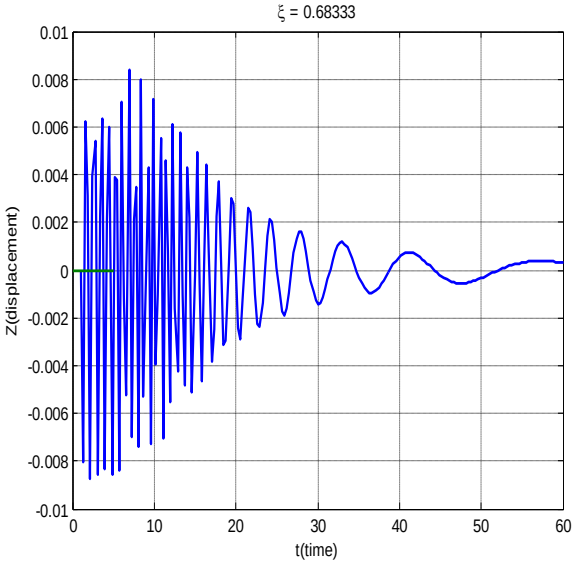

Fig.9d

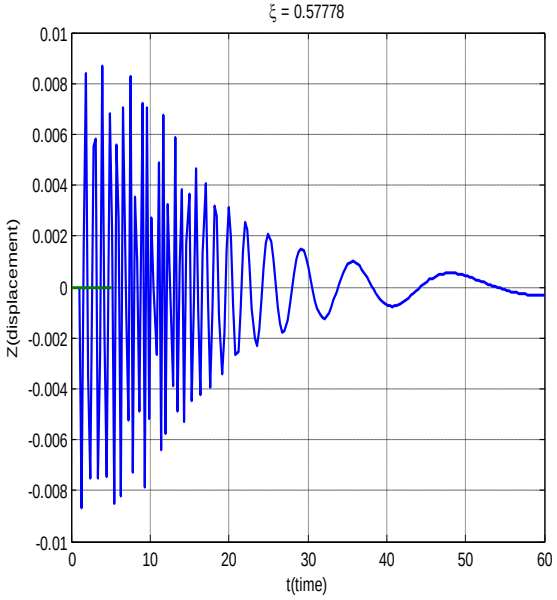

Fig.9e

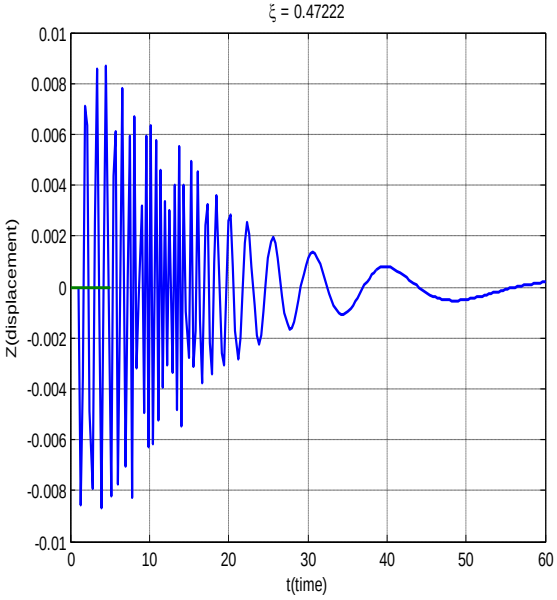

Fig.9f

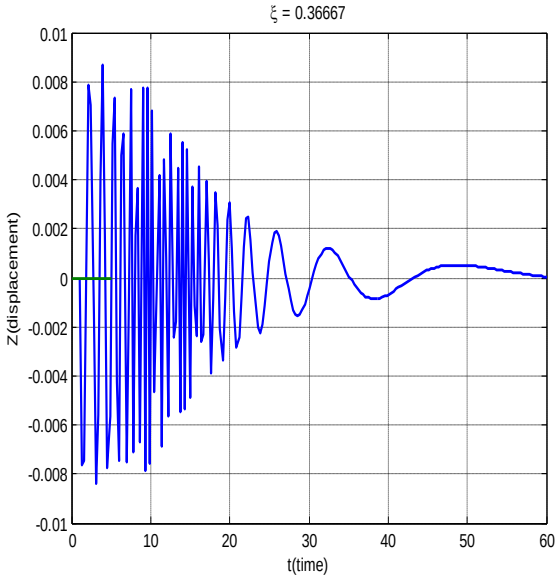

Fig.9g

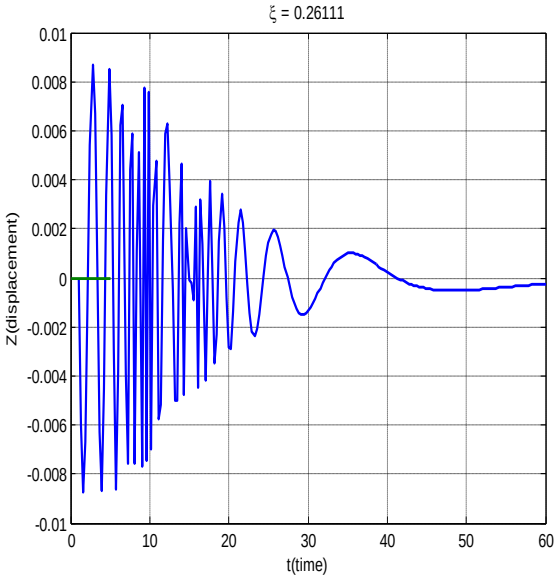

Fig.9h

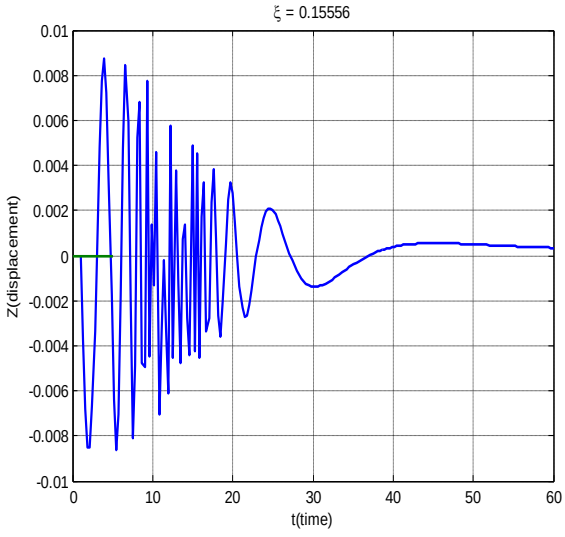

Fig.9i

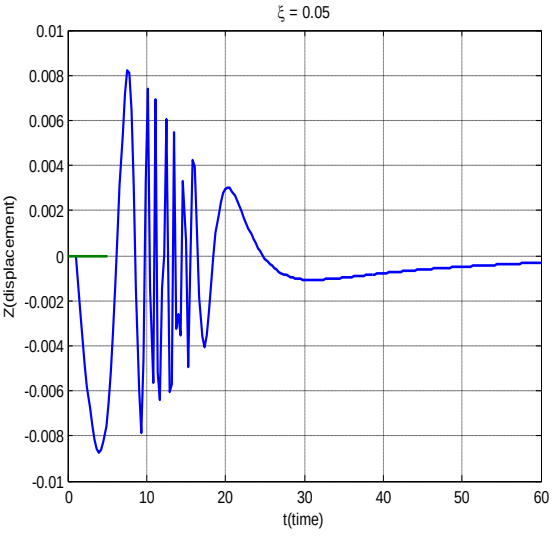

Fig.9j

Fig.9a-9j Effects of damping ratio on the vibration of structure for different damping ratio.

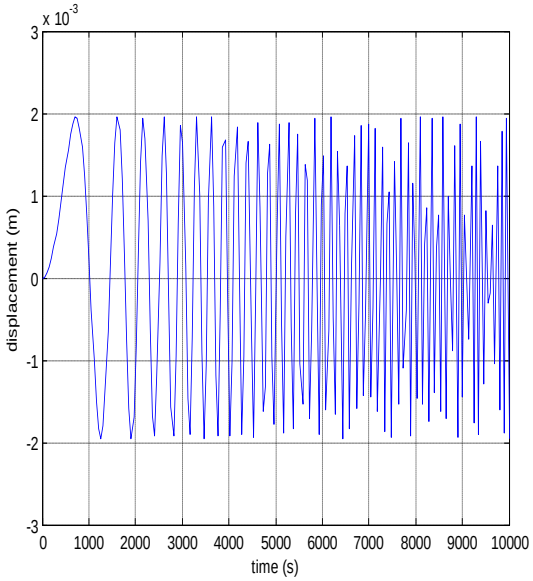

Fig.10a

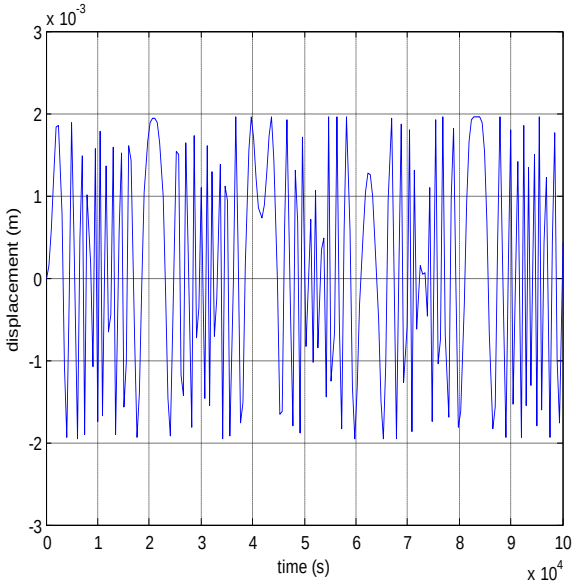

Fig.10b

Fig.10a-10b Effects of damping ratio on the vibration of structure.

Fig.9a-9j show the effects of damping ratio on the vibration of structure while Fig.10a-10b depict the effects of damping ratio on the vibration of structure.

8.0 Conclusion

In this work, the analysis of dynamic behaviour and power generation of a wind - tidal hybrid system were investigated. The power generated by 10m diameter rotor was used to investigate the potential power generated wind and tidal turbines. The effects of aerodynamics and hydrodynamics forces on the structure were investigated through the analysis of dynamic behaviour of the system under different loads and at various sites in the marine environment. The stability and the optimum turbine design were found to depend on the wind and tidal speed distribution of the specific site in the environment. It could be established from the work that the wind and tides provide vast sources of potential energy resources, and as renewable energy technologies develop, investment in wind and tidal energy is likely to grow. These sources have the potential to help alleviate the global climate change threat, but the ocean environment should be protected while these technologies are developed. Renewable energy sources from the wind and ocean may be exploited without harming the marine environment if projects are sited and scaled appropriately and environmental guidelines are followed. The utilization of these energy sources will abate over-dependent on fossil fuel as sources of power generation in Nigeria as it will meet the energy needs of coastal dwellers especially of those in remote areas.

REFERENCES

American Fisheries Society. “Tidal Power Development in Estuarine and Marine Environments”. http://www.fisheries.org/resource/page15.htm

Antonios E. Haniotis; Konstantinos S. Soutis, Antonios G. Kladas, and John

A. Tegopoulos, “Grid connected variable speed wind turbine modeling, dynamic performance and control,” in *IEEE PES Power Syst. Conf. Expos*., vol. 2, pp. 759-764, Oct 10-13 2004, New York, NY, United States.

Bahaj, A S and Myers, L E (2003), Fundamentals applicable to the utilisation of marine current turbines for energy production, Renewable Energy 28, 2205-2211.

E Van Walsom, “Barriers against tidal power,” *International Water and Dam Construction*, September3, 2003,

Eduard Muljadi and C. P. Butterfield, “Pitch-controlled variable-speed wind turbine generation,” *IEEE Transactions on Industry Applications* , vol. 37, no. 1, pp. 240-246, Jan/Feb 2001.

Erlich, H. Wrede and C. Feltes Dynamic Behavior of DFIG-Based Wind Turbines during Grid Faults 1-4244-0844X/07/ 2007 IEEE.

Gillie M.F. and Leithead E.F. “Operation and regulation of a wind and gas virtual power plant,” in *17th intl. conf. Electricity Dist*., Barcelona, May 20003.

Gray, T.J., and O.K. Gashus, eds. Tidal Power. Proceedings of an International Conference on the Utilization of Tidal Power, May 24-29, 1970, Atlantic Industrial Research Institute of Nova Scotia Technical College. New York: Plenum Press, 1972.

Jonathan Rose and Ian A. Hiskens Estimating Wind Turbine parameters and Quantifying Their Effects on Dynamic Behavior Power and Energy Society General meeting 2008 IEEE/RSJ Las Pittsburgh, PA July 2008.

Lenihan, J. and William W. Fletcher eds. The Marine Environment. New York: Academic Press, 1977.

Morison J.R. , Johnson J.W., O’Brien M.P. and Schaaf S.A. (1950). The force exited by surface waves on Piles, Petroleum Transaction, American Institute of Mining Engineers, vol. 189, TP 2846,pp. 149-154

Rajib Datta and V. T. Ranganathan, “Variable-speed wind power generation using doubly fed wound rotor induction machine – A comparison with alternative schemes,” *IEEE Transactions on Energy Conversion*, vol. 17, no. 3, pp. 414-420, Sept. 2002.

UES tests tidal generation,” *International Water and Dam Construction*, November 29, 2006.

Wasynczuk O., Man D. T. and Sullivan J. P., “Dynamic behavior of a class of wind turbine generators during random wind fluctuations,” *IEEE Transactions on Power and Apparatus and Systems*, vol. PAS-100, no. 6, pp. 2837-2845, June 1981.

Yuwei Li, Kwang-Jun Paik, Tao Xing, and Pablo M. Carrica. Dynamic Overset CFD Simulations of Wind Turbine Aerodynamics. Renewable Energy 37 (2012) 285-289.

Zhang Liang, “Activities For Ocean Energy Exploration In China” presentation at 11th IEA-OES meeting Lisbon, Portugal, November 14-15, 2006,

APPENDIX

1. Design for a 10m Diameter Wind Turbine

Power in the area swept by the wind turbine rotor:

$P = 0.5 \times \rho \times A \times V^3$

where:

P = power in watts (746 watts = 1 hp) (1,000 watts = 1 kilowatt)

ρ = air density (about 1.225 kg/m^3 at sea level, less higher up)

A = rotor swept area, exposed to the wind (m^2)

V = wind speed in meters/sec (20 mph = 9 m/s) (mph/2.24 = m/s)

This yields the power in a free flowing stream of wind. Of course, it is impossible to extract all the power from the wind because some flow must be maintained through the rotor (otherwise a brick wall would be a 100% efficient wind power extractor). On including some additional terms to get a practical equation for a wind turbine.

Wind Turbine Power:

$P = 0.5 \times \rho \times A \times Cp \times V^3 \times Ng \times Nb$

where:

Ng = generator efficiency (50% for car alternator, 80% or possibly more for a permanent magnet generator or grid-connected induction generator)

Nb = gearbox/bearings efficiency (depends, could be as high as 95% if good)

$P = 0.5 \times 1 \times 78.55 \times 0.35 \times 14^3 \times 0.8 \times 0.90 = 21.7444KW$

2. Design for two 10m Diameter Tidal Turbines

Tidal Turbine Power:

$P = 0.5 \times 1000 \times 78.55 \times 0.35 \times 2^3 \times 0.8 \times 0.90 = 79.178KW$

From the Fig. 2, two tidal turbines are to be used in the system. The total power to be generated by the two turbines is 2×79.178 = 158.356KW

Total power generated by the system = 158.356 + 21.744 = 180.1kW

Hydraulic Modelling and Optimization of a Wastewater Treatment System for Developing Nations Using Computational Fluid Dynamics

David O. Olukanni [a*], Kenneth O. Adekalu [b] and Joel J. Ducoste [c]

[a] Department of Civil Engineering, Covenant University, P.M.B. 1023, Ota, Ogun State, Nigeria.
[b] Department of Agricultural Engineering, Obafemi Awolowo University, Ile-Ife, Osun State, Nigeria.
[c] Department of Civil, Construction and Environmental Engineering, North Carolina State University, Raleigh,
North Carolina, USA.
E-mail: david.olukanni@covenantuniversity.edu.ng+234-08030726472; koadekalu2002@yahoo.co.uk

+234-08052365079 and jducoste@ncsu.edu; +1(919)-515-8150

Abstract:

Waste stabilization pond (WSP) is globally one of the most popular wastewater treatment options because of its high efficiency and low cost. However, no rigorous assessment of WSPs that account for cost in addition to hydrodynamics and treatment efficiency has been performed. A study was conducted that utilized Computational Fluid Dynamics (CFD) coupled with an optimization program to optimize the selection of the best WSP configuration based on cost and treatment efficiency. Several designs generated by the CFD/optimization model showed that both shorter and longer baffles, alternative depths, and reactor length to width ratios could improve the hydraulic efficiency of the ponds at a reduced overall construction cost. In addition, a study was conducted on the optimized WSP which consisted of an anaerobic, facultative, and a maturation stage whose baffle orientation, length to width ratio, was specified by a CFD model prediction and was compared with a three stage WSP designed according to literature suggested reactor geometric configurations. Experimental tests were performed on a pilot scale version of the three-stage WSP where the removal performance was based on a number of parameters (Faecal coliform, pH, TDS, and Conductivity). Results showed that the significantly lower cost design based on the optimized CFD simulations displayed slightly better removal performance compared to the standard WSP design developed from literature data. The results of this study clearly showed that unit treatment process designs based on rigorous numerical optimization can aid in producing cost effective designs that make it more possible for developing nations to incorporate adequate and effective sanitation.

Key words: *Wastewater, Waste Stabilization Pond, CFD, Reactor design and Pond-configuration*

1. Introduction

The construction cost for a standard wastewater treatment plant has been a major barrier for the implementation of modern technologies by local authorities in many African nations (Agunwamba, 1994 and 2001b; Olukanni and Aremu, 2008; Olukanni and Ducoste, 2011). In addition, these technologies require considerable technical expertise, which is often not available in developing nations to successfully operate these treatment facilities. Consequently, developing nations are unable to incorporate these technologies as part of a wastewater treatment master plan. It is therefore imperative to develop treatment systems that are economical and sustainable.

Among the current processes used for wastewater treatment, WSP has been identified and consistently selected as the unit process choice for wastewater treatment in developing nations due to their low cost and efficient operation in tropical regions (Agunwamba, 2001a; Mara, 1997, 2004; Abbas et al., 2006; Kaya et al., 2007; Naddafi et al., 2009; Olukanni and Ducoste, 2011). Babu et al (2010) and Mara (2004) describe a WSP as a chemical reactor used for the reduction of solids, organic matter as well as pathogenic organisms. The WSP system usually consists of a series of continuous flow anaerobic, facultative, and maturation ponds. The

anaerobic pond is designed for eliminating suspended solids and some of the soluble organic matter while the faclcultative pond is designed for further removal of the residual organic matter through the activity of algae and heterotrophic bacteria. The final stage of pathogens and nutrients removal takes place in the maturation pond (Olukanni and Ducoste, 2011; Mara, 2004; Babu, et al., 2010). WSPs are most suited for tropical and subtropical countries since the sunlight irradiance and ambient temperature are key factors for the WSP process efficiency (Mara, 2004; Mara 2001; Mara and Pearson, 1998). However, the application of WSP is limited by its large area requirement (Agunwamba, 1991 and 2001a). In addition, no rigorous experimental assessment of WSP that account for cost along with hydrodynamics and treatment efficiency has been performed (Olukanni and Ducoste, 2011). The goal of any WSP designer would be to optimize pond design by minimizing cost and land required while maintaining treatment effluent standards.

Previous studies have shown that the WSP treatment efficiency is often hydraulically compromised (Shilton and Mara, 2005; Shilton and Harrison, 2003a; Persson and Wittgren, 2003). Majority of the hydraulic studies on WSPs have been performed on full-scale field ponds, which have transient flows and large surface areas exposed to wind and temperature variations (Marecos and Mara, 1987; Moreno, 1990; Agunwamba, 1992; Fredrick and Lloyd, 1996). However, it was observed that operation and weather variations that occur during field experimental tests limit the study of reactor mixing characteristics only with lab-scale models studied under controlled conditions (Antonini et al., 1983; Shilton and Bailey, 2006), in which its results could be used to produce an optimal WSP design for field scale ponds performance.

The treatment of wastewater through WSPs has been an important research area over the past decades (Agunwamba, 1994; 2001a; Mara, 2004; Olukanni and Ducoste 2011). Oke, et al (2006) assessed the physical and engineering properties of a WSP system in Ahmadu Bello University (ABU), Zaria (Nigeria). The WSP system consisted of facultative and maturation ponds in series with hydraulic retention time of 24- and 6-days, hydraulic loading 15.34 and 10.2 ($m^3/m^2.d$) and BOD loading of 0.75 and 4.59 (kg/ha.d) respectively. Influent and effluent wastewater qualities were monitored from their system for one year. Oke et al.'s results revealed an average fecal coliform removal efficiency of 99% and an average reduction in suspended solids by 66%. The ammonia and phosphate concentrations of the raw influent were reduced on average by 88 and 81%, respectively, and an overall COD reduction of 96%. Oke et al (2006) confirmed that under tropical conditions, the WSPs are suitable compared to the modern and mechanized treatment systems such as trickling filters and activated sludge, because of the ease of operation and maintenance. Hodgson (2000) achieved similar results of a biological treatment plant at Akuse (Ghana) where the WSP system produced a 65% BOD reduction, 99.99% fecal removal, 46% reduction of suspended solids, and 92% and 94% of ammonia and phosphate removal, respectively.

Mohammed (2006) carried out the design and performance evaluation of a numerical model of a waste stabilization system that was comprised of one facultative pond, three maturation ponds, and a contact filtration unit all operated in series. The facultative and maturation ponds have hydraulic retention times of 11- and 4-days respectively. The numerically predicted microbial removal from each stage of the WSP system was greater than the experimentally measured percent removal. The numerical predicted removal of 62% and 91% was recorded for facultative and maturation ponds while experimental observed results were 45% and 84%, respectively. The deviation between the experimental and numerical results was likely due to the numerical assumptions, which assumed completely mixed reactors for the ponds. Other reasons for the deviation could be the values of the reaction coefficients used in the design.

Recently, Olukanni and Ducoste (2011) performed a study that utilized computational fluid dynamics (CFD) coupled with an optimization program to optimize the selection of the best WSP configuration based on cost and treatment efficiency. The numerical results of monitoring the fecal coliform concentration at the reactor outlet showed that the conventional 70%

pond-width baffle pond design was not consistently the best pond configuration as previously reported in the literature. The study concluded that target effluent log reduction can be achieved by reducing the amount of construction material and tolerating some degree of fluid mixing within the pond. Several other designs generated by the CFD/optimization model showed that both shorter and longer baffles, alternative depths, and reactor length to width ratios could improve the hydraulic efficiency of the ponds at a reduced overall construction cost. Olukanni and Ducoste (2011), however, did not experimentally validate the CFD model predictions. Experimental validation in terms of microbial pollutant and nutrient removal of CFD generated WSP configurations are still scarce, especially for lab-scale ponds. The main focus of this study has been the need for a cost effective designs that will not jeopardize the treatment efficiency and to validate the predicted results of an optimized WSP discussed in Olukanni and Ducoste, 2011. In addition, a parameter sensitivity analysis was performed to determine the influence of the first order constant (k) and temperature (T) on the design configurations.

2. Materials and methods

2.1 Design and construction of a Laboratory-scale WSP

The initial length to width dimensions of the reactors are (950 mm × 320 mm) (A_o = 0.3 m^2), (2100 mm × 700 mm) (A_o = 1.5 m^2) and (2470 mm × 830 mm) (A_o = 2.1 m^2) for the anaerobic, facultative, and maturation ponds, respectively, as shown in Figure 1. The three sets of laboratory-scale reactors for WSP design configurations from Olukanni and Ducoste (2011) CFD model was compared with the Simplex and MOGA II design specifications. The SIMPLEX method was based on a modified single objective algorithm that takes into account discrete variables and constraints (mode-FRONTIER Manual, 2009). The Simplex solver produces an optimal result based on a single objective function while MOGA-II is a multi-objective genetic algorithm that uses a multi-search elitism (Silva, 2003; Olukanni and Ducoste, 2011). This elitism operator preserves some near optimal solutions without bringing premature convergence to a local-optimal (Fonseca and Fleming, 1993 and 1995). The five set of reactors had cost area ratio, wastewater depth, length, width, baffle length dimensions and number of baffles as presented in Table 1 (a-c) for the anaerobic, facultative, and maturation ponds, respectively. It was understood from practice that several other items make up for the construction costs of ponds which could have been incorporated into the design calculation, conversely, for the purpose of simplicity and in coupling computational fluid dynamics (CFD) with an optimization program to optimize the selection of the best WSP configuration based on cost and treatment efficiency, a 2 mm galvanized metal gauge plate was considered for the construction of the reactors including the baffle walls. Since the baffle walls were made with the same material as the reactor and matched the reactor depth, the cost of material per unit surface area was used as the only measure of the cost and excludes labor and other costs associated with the construction of the ponds.

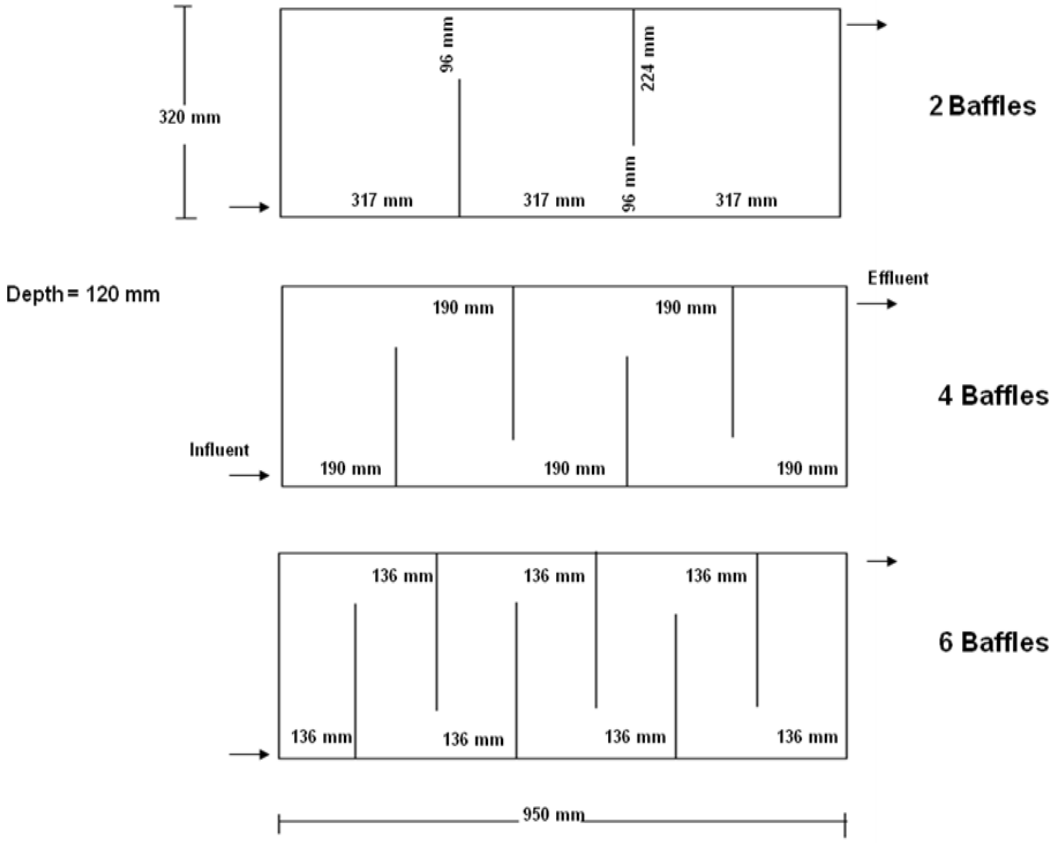
320 mm
96 mm
224 mm
96 mm
317 mm
317 mm
317 mm
2 Baffles
Depth = 120 mm
Effluent
190 mm
190 mm
190 mm
190 mm
190 mm
4 Baffles
Influent
136 mm
136 mm
136 mm
136 mm
136 mm
136 mm
6 Baffles
950 mm

(1a)

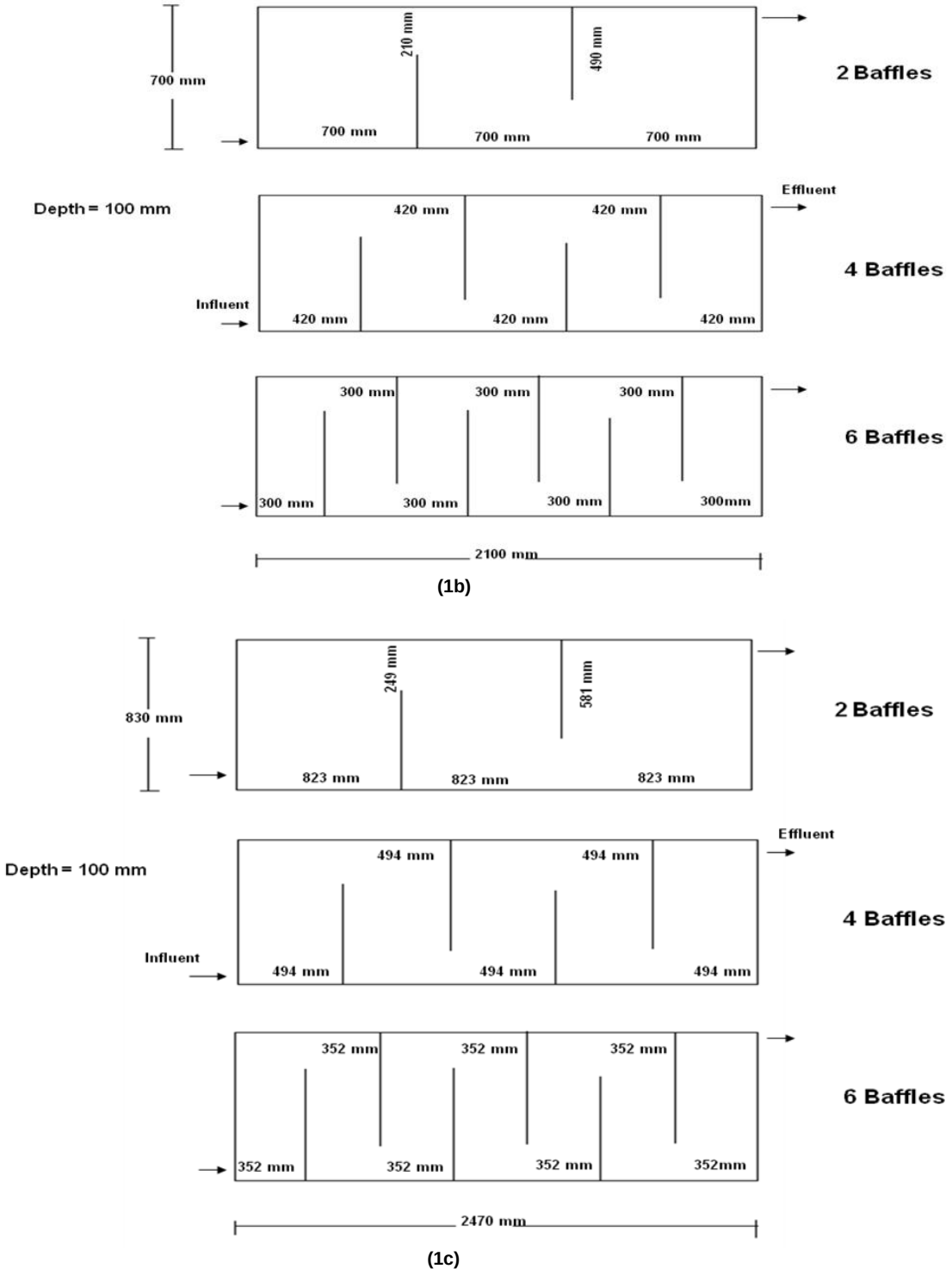

Figure 1 Different baffle arrangements with 70% pond width a) Anaerobic, b) facultative, c) maturation reactors

Table 1a. Anaerobic reactor configurations

	Six-baffle 70% pond-width transverse lab-scale reactor	Four-baffle 70% pond-width transverse lab-scale reactor	Four-baffle 70% pond-width longitudinal lab-scale reactor	Simplex transverse optimized designs	MOGA-II transverse optimized designs
Cost (N)	1, 669	1, 582	1, 926	1, 297	1, 234
Area ratio	3:1	3:1	3:1	3:1	2:1
Depth (m)	0.065	0.065	0.065	0.115	0.120
Length (m)	0.950	0.950	0.950	0.717	0.574
Width (m)	0.320	0.320	0.320	0.239	0.287
Baffle length (m)	0.224	0.224	0.665	0.117	0.166
Baffle ratio	70%	70%	70%	49%	58%
Number of baffles	6	4	4	3	2

Table 1b. Facultative reactor configurations

	Six-baffle 70% pond-width transverse lab-scale reactor	Four-baffle 70% pond-width transverse lab-scale reactor	Four-baffle 70% pond-width longitudinal lab-scale reactor	Simplex longitudinal optimized designs	MOGA-II transverse optimized designs
Cost (N)	5, 563	5, 431	5, 960	5, 091	4, 988
Area ratio	3:1	3:1	3:1	1:1	1:1
Depth (m)	0.045	0.045	0.045	0.048	0.048
Length (m)	2.10	2.10	2.10	1.17	1.17
Width (m)	0.70	0.70	0.70	1.17	1.17
Baffle length (m)	0.49	0.49	1.47	0.97	0.62
Baffle ratio	70%	70%	70%	83%	53%
Number of baffles	6	4	4	2	2

Table 1c Maturation reactor configurations

	Six-baffle 70% pond- width transverse lab-scale reactor	Four-baffle 70% pond-width transverse lab-scale reactor	Four-baffle 70% pond-width longitudinal lab-scale reactor	Simplex transverse optimized designs	MOGA-II transverse optimized designs
Cost (N)	7, 360	7, 221	7,772	7, 221	7, 221
Area ratio	3:1	3:1	3:1	3:1	3:1
Depth (m)	0.04	0.04	0.04	0.04	0.04
Length (m)	2.47	2.47	2.47	2.47	2.47
Width (m)	0.83	0.83	0.83	0.83	0.83
Baffle length (m)	0.58	0.58	1.73	0.58	0.58
Baffle ratio	70%	70%	70%	70%	70%
Number of baffles	6	4	4	4	4

2.2 Cost Estimation Model

As mentioned earlier, the impact of the water depth was included in the model simulation by adjusting the influent velocity while maintaining a constant flow rate through the WSP. In this study, initial water depths of 65mm, 45mm, and 40mm were used for the anaerobic, facultative, and maturation, respectively. Figure 2 shows the layout of the reactors as described in Olukanni and Ducoste, 2011 while Equations 1-6 describe the WSP optimization criteria used in estimating

the cost for the model. The objective function was based on minimizing the cost of construction of the pilot scale WSP.

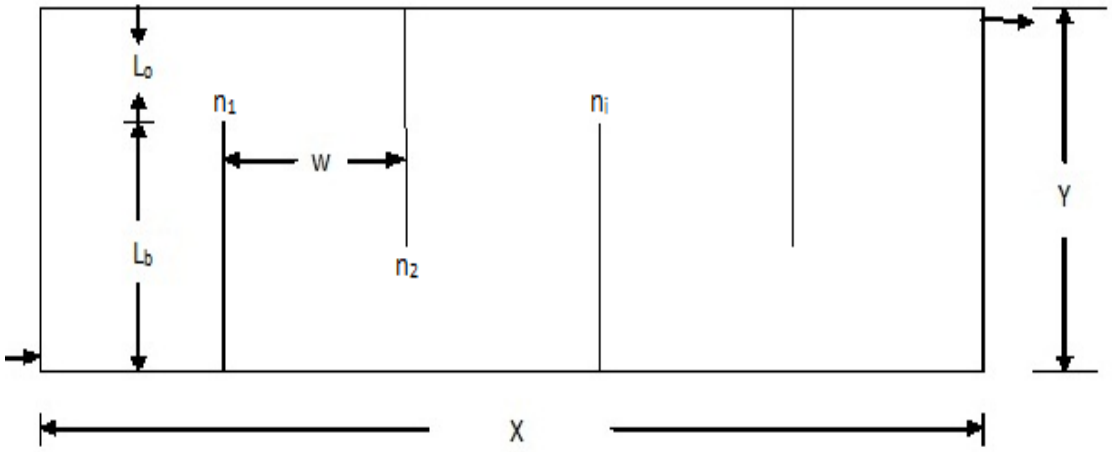

(2a)

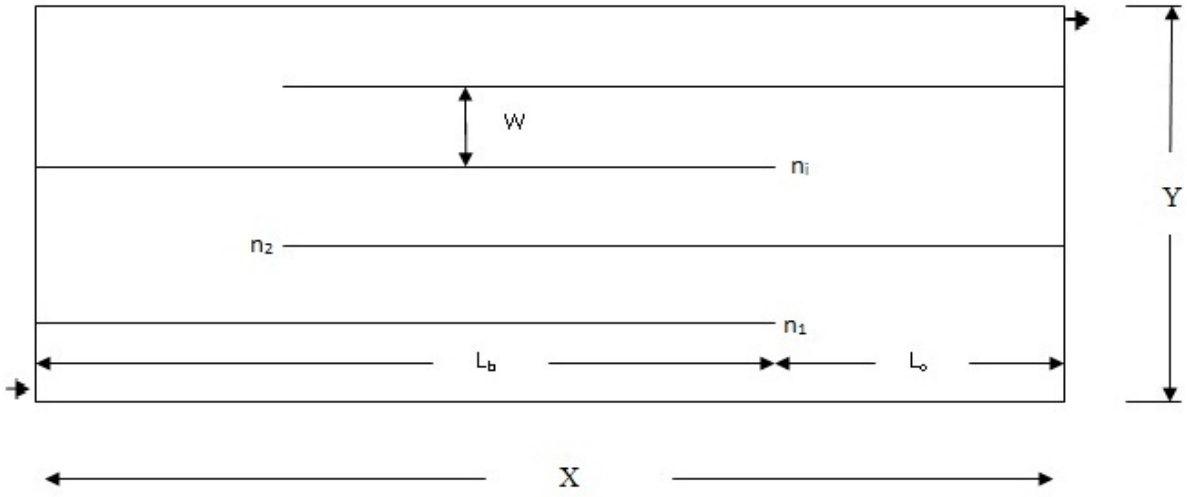

(2b)

Figure 2 Geometric design parameters for the baffled lab-scale WSP

Minimize Cost = $3000 \times (2hX + 2hY + XY + bn \times L_b \times h)$ (1)

Subject to (Constraints)

$A \leq A_o$ (2)

where A = XY

$h_{min} \leq h \leq h_{max}$ (3)

$0 \leq bn \leq 8$ (4)

Log (C_o/C) ≥ 0.6, 1.5 and 1.5 (5)

for anaerobic, facultative and maturation, respectively.

$1 \leq r \leq 4$ (6)

where r = X/Y

Table 1 Range of adjusted parameter values

Parameters	Anaerobic	Facultative	Maturation
Flow rate (constant)	1.39×10^{-6} m^3/s	1.39×10^{-6} m^3/s	1.39×10^{-6} m^3/s
Volume	0.0197 m^3	0.066 m^3	0.082 m^3
Depth (h)	0.048m – 0.12m	0.024m – 0.048m	0.024m – 0.04m
Reactor L/W ratio (r)	1:4	1:4	1:4
Baffle number (bn)	0 - 8	0 - 8	0 - 8
Baffle length ratio(L_b)	5% - 95%	5% - 95%	5% - 95%

In Equations 1-6, the cost function is in Naira (**N**); A is the surface area in (m^2); Co and C are the fecal coliform concentration at the pond inlet and outlet, respectively; X, Y, and h are the pond length, width, and depth, respectively; A, r, bn, and L_b are pond area, L/W ratio, baffle number, and baffle length, respectively. These values were specified in the optimization algorithm. The cost estimate was based solely on the construction material cost and excludes labor and other costs associated with the construction of the ponds. Equation (5) expresses the minimum required effluent log removal constraint that must be satisfied for each of the three reactors in series before the program is terminated. Details of the optimization set up and problem formulation for the optimization loop are expressed in Olukanni and Ducoste (2011).

3. CFD Model Application

A finite element-based commercial CFD code COMSOL Multiphysics was used in this study with the simulations performed under steady state conditions. The simulation of fecal coliform and fluid transport within the WSP requires the solution of the conservation of mass (continuity), momentum (Navier-Stokes) and convective-diffusion equations (Olukanni and Ducoste, 2011). Although a 2D model was used in this study, the impact of water depth was included in the model simulation by adjusting the influent velocity while maintaining a constant flow rate through the WSP. An unstructured mesh consisting of triangular elements was selected for the 2D geometry. The accuracy of the CFD solutions depends also on the quality of the grid. The grid size was determined through successive refinement in the grid and evaluating the impact of that size on the local fecal coliform concentration and mean velocity at selected points in the reactors. The final maximum grid size was specified as 5 percent of the width of each reactor, which was small enough to produce a grid-independent solution without significantly impacting the computational cost. The simulations were performed on a desktop computer (Intel ® Core(TM) 2 Duo CPU E6550 with 2048MB RAM). For the CFD optimization set up, ModeFRONTIER, an optimization tool was used to predict an optimal design using a single objective (SIMPLEX) and Multi-objective genetic algorithm (MOGA-II). Figure 3 describes the hydrodynamic result (Velocity streamlines and FC concentration maps) showing clear image of the CFD model before optimization. This range of baffle lengths were initially simulated to review the impact of baffle number, placement, and arrangement on the effluent log reduction as discussed in the literature without optimizing for cost. Details of the hydrodynamic result and the FC map of CFD model of the optimized designs are expressed in Olukanni and Ducoste, 2011.

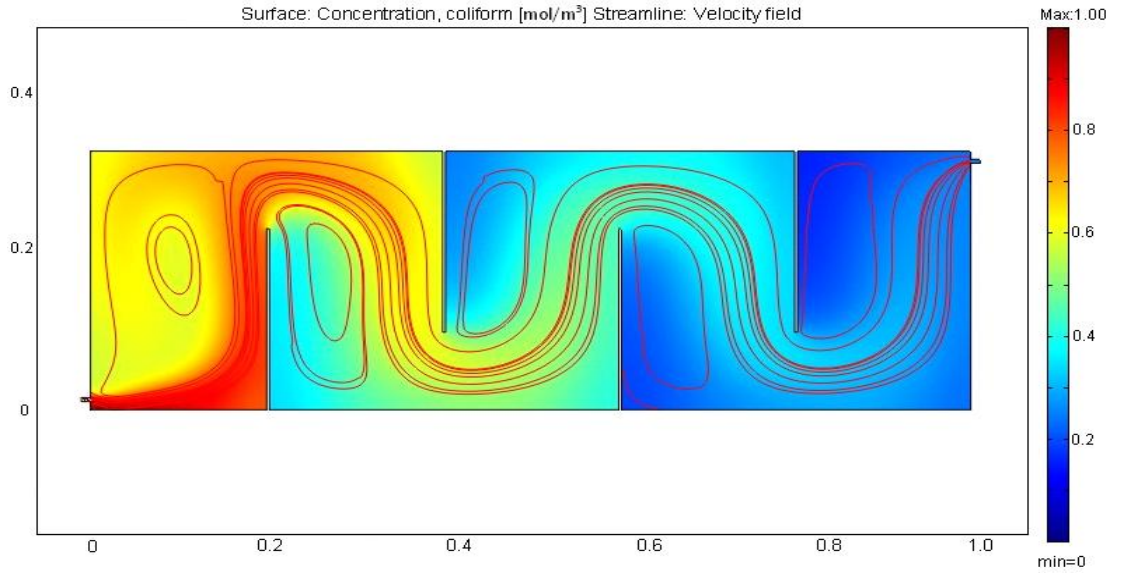
Surface: Concentration, coliform [mol/m³] Streamline: Velocity field
Max:1.00
0.8
0.6
0.4
0.2
min=0
0.4
0.2
0
0
0.2
0.4
0.6
0.8
1.0

(3a)

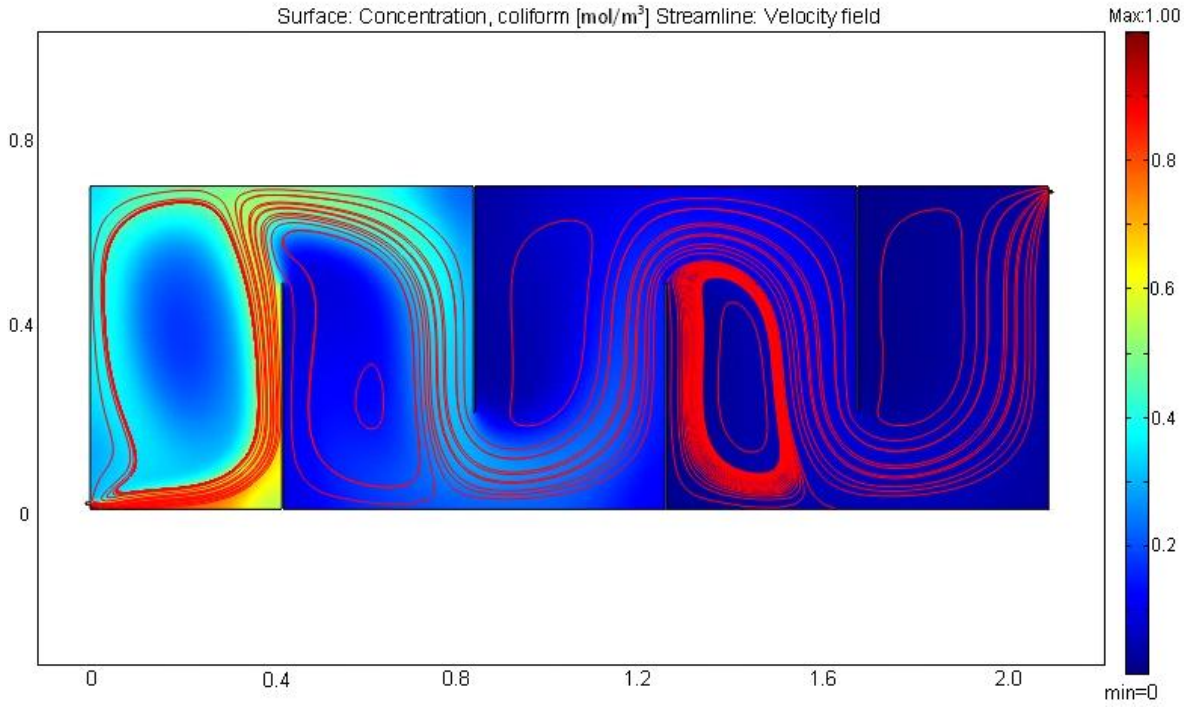
Surface: Concentration, coliform [mol/m³] Streamline: Velocity field
Max:1.00
0.8
0.6
0.4
0.2
min=0
0.8
0.4
0
0
0.4
0.8
1.2
1.6
2.0

(3b)

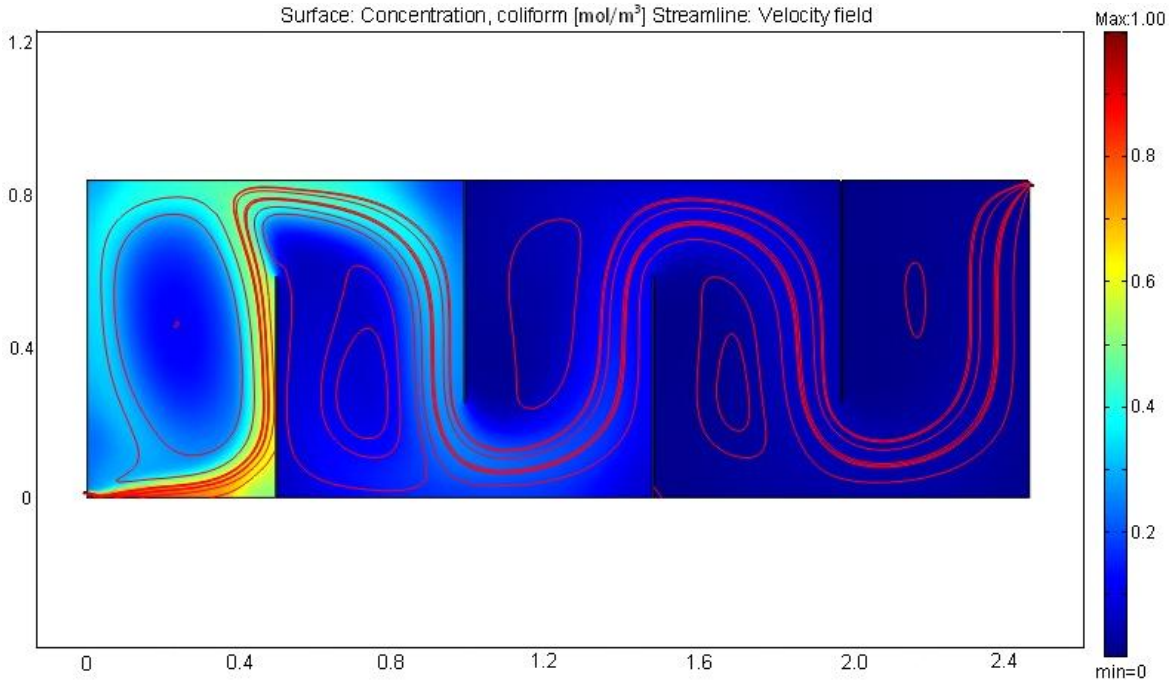

(3c)

Figure 3 Velocity streamline and coliform inactivation for the 4 baffle 70% pond width baffle arrangement in a) anaerobic, b) facultaive, and c) maturation reactors.

3.1 Laboratory methods

Experimental tests were performed at the Civil Engineering hydraulics laboratory of Covenant University. Samples of the campus wastewater were collected at both the inlet and outlet position of each pond in series for the analysis of Fecal coliform, Total Dissolved Solids, Conductivity, and pH. The fecal coliform bacteria for the influent and effluent samples were determined by the membrane filter procedure (method no.: 9222D, APHA, 1998), which uses an enriched lactose medium and incubation temperature of 44.5 ± 0.2°C for selectivity. The total dissolved solid (TDS) and conductivity measurements were performed using the HANNA C99 Multiparameter Bench photometer. The pH was measured using the HANNA Instruments pH meter. The operating condition of the lab where the lab-scale pilot experiment was performed has a room temperature of 24^0C with the ponds hydraulic retention times of 0.165 day, 0.563 day, and 0.683 day for anaerobic, facultative and maturation ponds, respectively, that correspond to a flow rate of 0.12 m^3 per day. At this flow rate, the Re number for the three ponds was 304, which suggest that the WSP operates well within the laminar flow regime. The observed influent concentration into the three stage reactors were 59×10^3 per 100 ml for fecal coliform and a mean value of 342 (ppm), 695 (µS), and 7.47 for TDS, conductivity, and pH, respectively. Figure 4 displays the laboratory set up for the experiment that compares the initial design without cost and the optimized designs.

Figure 4 Different tested laboratory-scale reactor configurations during the experiment

$$\rho\frac{\partial C}{\partial t}+\rho\sum_j\frac{\partial\left(U_jC\right)}{\partial x_j}=\rho\sum_j\frac{\partial}{\partial x_j}\left(\frac{\nu}{Sc_l}\frac{\partial C}{\partial x_j}\right)-kC \quad (7)$$

where:

ρ = fluid density (kg/m^3)

U = mean velocity (m/s)

t = time (s)

u = kinematic viscosity (m^2/s)

C = fecal coliform or tracer concentration (mol/m^3)

Sc = Schmidt number

k = first order decay of fecal coliform (d^{-1})

where:

$k^1 = k^1_{old}$ (1 ± 0.5); (k^1 = 4.55 at T = 24^{0}C). Therefore, k = 6.825 (1.19) $^{24\text{-}20}$ = 13.686 (day^{-1}) at the upper bound and

k = 2.275 (1.19) $^{24\text{-}20}$ = 4.562 (day^{-1}) at the lower bound

For the sensitivity assessment on temperature, a 20 percent variation was evaluated based on the temperature range that may be possible in Nigeria. Equation 10 expresses how T value was varied while maintaining k^1 equal to 4.55.

$$k = k^1_{old}(1.19)^{T^1-20} \quad (10)$$

where:

$$T^1 = T^1_{old} \pm 4^0 c$$

Therefore, k = 4.55(1.19) $^{28\text{-}20}$ = 18.297 (day^{-1}) at the upper bound and k = 4.55(1.19) $^{20\text{-}20}$ = 4.55 (day^{-1}) at the lower bound.

3.2 SENSITIVITY ANALYSIS

A sensitivity analysis was performed with the optimization tool for the single objective (SIMPLEX) and Multi-objective genetic algorithm (MOGA-II) to determine the influence of the first order constant (k) and temperature (T) on the optimal design configurations. A 50 percent variation was made on the values of k proposed and adopted by Banda (2007). Equation 7 expresses the relationship k, in the convective-diffusion equation (Olukanni and Ducoste, 2011) as:

The simulations were performed at steady state and the reaction term in Equation 7 was used for characterizing the fecal coliform inactivation kinetics. Banda (2007) fecal coliform first-order decay rate constant was adopted in this study due to its reasonable goodness of fit for baffled WSPs. The goodness of fit as measured with R^2 between the predicted CFD fecal coliform counts and the measured effluent fecal coliform concentration from his baffled pilot-scale ponds was 0.83 when the following rate constant expression:

$$k = 4.55(1.19)^{T-20}day^{-1} \quad (8)$$

$$k = k^1(1.19)^{T-20}day^{-1} \quad (9)$$

4.0 Results and Discussion

4.1 Evaluation of the Three-Stage WSP designs

Table 2 displays the comparison of the CFD predicted results and experimental data of the effluent fecal coliform log kill for the six-baffle 70% pond-width transverse, four-baffle 70% pond-width transverse, and longitudinal reactors with the CFD/optimized Simplex and MOGA II WSP designs. The CFD model reasonably predicts well the experimental fecal log kill for the anaerobic pond but over predicts the log kill for the facultative and maturation reactors. Possible reasons for these discrepancies include a slight difference in the experimental fecal 1st order rate constant, operating temperature, and the wastewater density (ρ) as compared to the values used in the model simulations. The

literature reports that temperature and 1st order rate constant are factors that significantly affect experimental performance of WSPs (Shilton and Harrison, 2003a; Fredrick and Lloyd, 1996; Brissaud *et al.,* 2000, 2003).

It was recognized that the results in Table 2 are almost the same for the most part with little difference in the fecal coliform results for the different reactor configuration. Only that the model was able to show how to reduce the cost and still achieve similar effluent quality. The main prominent difference in the overall three-stage reactors in series is the cost for each of the different set of designs. For the anaerobic reactors, the simplex optimal design had the highest fecal log kill (0.35) as compared to other configurations followed by the four-baffle and Six-baffle 70% pond-width lab-scale reactors with 0.34 and 0.32, respectively. The MOGA II design configuration performed with a reduced fecal log kill as compared to the Simplex design (0.30 vs 0.35). For the facultative reactors, the same value of log removal was observed for Four-baffle 70% pond-width transverse reactor and the Simplex optimized design (0.81 log unit). The Simplex optimized design for the facultative reactor performed better than the remaining configurations with a log unit of 0.81 with an additional cost (N103) over the MOGA II design as compared to 0.74 and 0.75 in the six-baffle transverse and Four-baffle 70% pond-width longitudinal reactors, respectively. Surprisingly, there was no difference in the treatment performance for the six baffle transverse and four baffle longitudinal maturation reactors (0.70 fecal log kill). The same performance was observed in the four-baffle 70% pond-width transverse reactor, Simplex, and MOGA II optimized design with 0.60 fecal log kill.

While each design seemed to have produced similar log-kill removal results, the CFD optimized configuration led to designs that were cheaper in cost. A cost of N1, 297 and N1, 234 were achieved for the optimized designs for the anaerobic reactors as compared to N1, 669, N1, 582 and N1, 926 for the literature arranged designs. The same pattern of cost reduction was achieved for the facultative reactors except for the maturation reactor where the CFD/optimized designs (MOGA II and Simplex) have the same cost (N7, 221) with the four-baffle 70% pond-width transverse reactor configuration. This similar result confirms that the four baffle 70% pond-width maturation reactor could be considered a cost effective design that was suggested in the literature. However, the six-baffle 70% pond-width configuration displayed only a marginally higher cost (N7, 360) with a higher log reduction of 0.70 fecal log kill.

While the results of the simulated models in this study is expected to enhance the understanding of field-scale ponds and to aid in the estimation of some parameters that are useful in the design and evaluation of the performance of field-scale ponds, it is important to stress that most variables affecting ponds performance are very complex and may not be straightforwardly analyzed in which environmental, pond geometry and flow conditions are very paramount (Marcos do Monte and Mara, 1987; Agunwamba, 1992). Hence, the variation that could occur in performance between laboratory-scale model and field scale prototype of WSPs. This is because model ponds are often subjected to hydraulic flow, operating and boundary conditions that are not encountered in practice. Therefore, adequate consideration should then be given to these factors during the modeling phase in addition to the interpretation and application of the results of the models in the design and construction of field-scale ponds.

Parameter Feacal coliform (FC/100ml) at k = 4.56 d^{-1}	**Six-baffle 70% pond-width lab-scale reactor**	**Four-baffle 70% pond-width transverse lab-scale reactor**	**Four-baffle 70% pond-width longitudinal lab-scale reactor**	**Simplex optimized designs**	**MOGA-II optimized designs**
		Anaerobic reactors			
Experimental Log-removal	0.32	0.34	0.31	0.35	0.30
CFD Simplex log-removal	-	-	-	0.32	-
CFD MOGA II log- removal	-	-	-	-	0.30
Cost of construction (N)	1, 669	1, 582	1, 926	1, 297	1, 234
		Facultative reactors			
Experimental Log-removal	0.74	0.81	0.75	0.81	0.76
CFD Simplex log-removal	-	-	-	1.01	-
*CFD MOGA II lo-*removal	-	-	-	-	0.71
Cost of construction (N)	5, 563	5, 431	5, 960	5, 091	4, 988
		Maturation reactors			
Experimental Log- removal	0.70	0.60	0.70	0.60	0.60
CFD Simplex log-removal	-	-	-	1.08	-
CFD MOGA II log-removal	-	-	-	-	0.81
Cost of construction (N)	7, 360	7, 221	7, 772	7, 221	7, 221

Table 2 Comparison of the CFD-predicted results and Experimental data of the effluents of fecal coliform log kill

4.2 Results of sensitivity analysis for Simplex design at upper and lower boundary.

Tables 3-6 show WSP configurations that were generated due to changes in the fecal coliform 1st order rate constant and temperature. The results in Tables 3-6 displayed that changing these two parameters not only impacts the effluent fecal coliform concentration, which was expected, but also the WSP system configuration. In Tables 3-6, there are differences in the baffle length, area ratio, reactor depth, baffle orientation and baffle number. The result in Table 3 of the sensitivity analysis performed using the single objective simplex program at the higher k value displays a significant change in fecal coliform log removal with an appreciable difference in the associated cost at the higher disinfection rate constant.

Table 3 Simplex sensitivity analysis optimal design results for k = 13.686 d^{-1} at T = 24^0C

	Anaerobic Transverse SA1			**Facultative Longitudinal SA1**			**Maturation Transverse SA1**		
	Optimal design	Min. FC removal	Max FC removal	Optimal design	Min. FC removal	Max FC removal	Optimal design	Min. FC removal	Max FC removal
Cost (₦)	**1, 200**	1, 211	1, 767	**5, 184**	5, 184	5, 265	**7, 891**	7, 993	7, 992
Log removal	**0.82**	0.80	0.98	**2.32**	2.32	2.92	**2.34**	2.01	2.77
Area ratio	**3:1**	3:1	2:1	**2:1**	2:1	2:1	**2:1**	4:1	2:1
Depth (m)	**0.113**	0.113	0.062	**0.048**	**0.048**	**0.048**	**0.036**	0.035	0.036
Baffle ratio	**8%**	10%	71%	**70%**	70%	87%	**64%**	45%	68%
Number of baffles	**3**	4	7	**2**	2	2	**5**	4	6

Table 4 displays the results that were found at the lower bound of the k value used in the sensitivity analysis. The same order of optimal design solutions are recorded (Transverse-, Longitudinal- and Transverse-baffle arrangement). There is a significant change in FC log removal with little difference in the associated cost as compared to the simplex optimal design result in Table 3. This is due to the higher values of first order kinetic rate constant that was used in the simulation. A higher value of log removal also can be seen on the max FC removal columns for the three reactors. It can be said that the 8% pond-width baffle shown in anaerobic is as good as no baffles. An additional simulation was performed to verify the same configuration without the use of the 8% pond-width baffles and the results recorded were indeed the same. This is an indication that baffles may not be required in the anaerobic pond at that k value and it suggests that for efficient treatment, combinations in the order of transverse, longitudinal and transverse baffle arrangement may be a optimal solution for the anaerobic, facultative and maturation reactors respectively. The 14% baffle in the anaerobic pond was also evaluated and found to produce no significant difference compared to a no baffle configuration at the lower bound k value. The maturation reactors requires were found to require more number of baffles than both the anaerobic and facultative as shown in Tables 3 and 4. Also, only 2-baffles were achieved for the optimal solution in all the k values used in the facultative reactor. This may not be unconnected to the fact that the the final stage of pathogens and nutrients removal takes place in the maturation pond with wider surface area, shallow depth, and more number of baffles (Hamzeh and Ponze, 2007).

Table 4 Simplex sensitivity analysis optimal design results for k = 4.562 d^{-1} at T = 24^0C

	Anaerobic Transverse SA2			Facultative Longitudinal SA2			Maturation Transverse SA2		
	Optimal design	Min. FC removal	Max FC removal	Optimal design	Min. FC removal	Max FC removal	Optimal design	Min. FC removal	Max FC removal
Cost (₦)	**1, 192**	1, 237	1, 579	**5, 220**	5, 220	5, 750	**7, 991**	8, 698	8, 071
Log removal	**0.32**	0.30	0.33	**1.01**	1.01	1.16	**1.08**	1.02	1.30
Area ratio	**3:1**	3:1	4:1	**2:1**	2:1	3:1	**4:1**	3:1	4:1
Depth (m)	**0.12**	0.098	0.074	**0.048**	**0.048**	**0.048**	**0.036**	0.032	0.036
Baffle ratio	**14%**	16%	52%	**77%**	77%	95%	**70%**	49%	74%
Number of baffles	**2**	2	7	**2**	2	3	**6**	5	7

Table 5 displays the sensitivity analysis based on the multi-objective program at the upper bound value of k. Transverse, transverse and longitudinal baffle arrangements were obtained for the three reactors in series which is not the same as the configuration pattern predicted at the lower bound value of k = 4.562 d^{-1}. Table 6 shows that all configurations recorded transverse baffle arrangement for the three reactors in series. There is also a significant change in FC log removal with little difference in the associated cost. This same observation was made in the case of the simplex sensitivity analysis results in Tables 3 and 4. This observation is as a result of the higher values of 1^{st} order kinetic rate constant that was used in the simulation. However, the number of baffles was significantly reduced for the MOGA II results as compared to the simplex sensitivity analysis results in both instances of higher and lower values of first order kinetic rate constants.

Table 5 MOGA-II Sensitivity Analysis Optimal Design Results k = 13.686 d^{-1}

	Anaerobic Transverse SA1			Facultative Transverse SA1			Maturation Longitudinal SA1		
	Optimal design	Min. FC removal	Max FC removal	Optimal design	Min. FC removal	Max FC removal	Optimal design	Min. FC removal	Max FC removal
Cost (₦)	**1, 219**	1, 369	1, 539	**4, 966**	4, 966	5, 235	**7, 727**	8, 457	7, 873
Log removal	**0.81**	0.80	1.00	**1.90**	1.90	2.48	**2.28**	2.01	2.98
Area ratio	**1:1**	1:1	1:1	**1:1**	1:1	1:1	**1:1**	4:1	2:1
Depth (m)	**0.115**	0.117	0.115	**0.048**	0.048	0.046	**0.036**	0.036	0.036
Baffle ratio	**46%**	66%	79%	**46%**	46%	68%	**74%**	62%	76%
Number of baffles	**2**	3	4	**2**	2	2	**2**	4	2

Table 6 MOGA-II Sensitivity Analysis Optimal Design Results k = 4.562 d^{-1}

	Anaerobic Transverse SA2			Facultative Transverse SA2			Maturation Transverse SA2		
	Optimal design	Min. FC removal	Max FC removal	Optimal design	Min. FC removal	Max FC removal	Optimal design	Min. FC removal	Max FC removal
Cost (₦)	**1, 188**	1, 476	1, 538	**4, 931**	4, 974	5, 385	**7, 623**	9, 566	9, 626
Log removal	**0.30**	0.30	0.35	**0.71**	0.71	1.1	**0.81**	0.80	1.42
Area ratio	**2:1**	3:1	1:1	**2:1**	3:1	1:1	**1:1**	3:1	1:1
Depth (m)	**0.11**	0.062	0.074	**0.048**	0.048	0.048	**0.036**	0.028	0.028
Baffle ratio	**29%**	33%	82%	**11%**	10%	85%	**42%**	90%	86%
Number of baffles	**2**	2	3	**6**	6	4	**2**	3	3

As presented in Table 2, even though the simplex and MOGA II designs produced similar fecal log reduction results, they achieved the results at a significantly reduced cost, which was the desired goal of this study. This observation suggests that the first order kinetic rate constant k for the laboratory experiment may perhaps be closer to the ones at lower range of k value and that the low end of the sensitivity analysis performed on the rate constant is actually quite good. While each design seemed to have produced similar results, the CFD optimized designs were cheaper in cost. Therefore, this approach to developing a cost effective design has been validated.

The experimental data of Physico-chemical (PH, conductivity and Total dissolved solids) parameters in the influent and effluent samples are presented in Tables 7-9 for anaerobic, facultative, and maturation laboratory scale WSPs, respectively.
The associated cost for each reactor configuration for nutrient removal performance is presented in Tables 7-9. Although the optimized design results and the standard configuration produced similar removal performance, the cost is vastly different. Table 7 displays the experimental pH that was measured in all the reactor configurations. The measured pH in all the reactor configurations compare well with the expected pH found in literature (Pearson et al, 1987; Parhad and Rao, 1974). Many chemical and biological reactions in wastewater treatment are pH dependent and rely on pH control. Table 7 shows that as the wastewater moves through the reactors in series, the pH of the effluent from the reactors increases from pH 7.5-7.9.

Table 8 shows that the experimental data of total dissolved solids in the influent was in the range of 340-343 (Avg = 341) ppm while the effluent concentration was in the range of 273-315 ppm, respectively. The CFD/optimized configuration performed well as compared to other configurations with TDS effluent of 275 ppm in Simplex and 293 ppm MOGA II optimized designs. The four-baffle 70% pond width transverse performed well as compared to the six-baffle transverse arrangement and the four baffle longitudinal arrangement.

Table 9 shows that the anaerobic reactor had minimal reduction in conductivity values as compared to the performance of the maturation reactors which gave a significant reduction in the conductivity of the effluents. The four-baffle 70% pond width transverse lab-scale reactor series gave the optimal conductivity reduction for the entire configuration (557 µS) followed by the simplex optimized design with a conductivity value of 562 µS. It is evident that the Simplex design is reasonably predicting more of pollutant reduction in the entire set of laboratory-scale WSPs. Continuous measuring systems are employed to monitor the salt load at the influent and effluent of wastewater treatment facilities. At present, the conductivity of wastewater is one of

the important parameters used to determine the suitability of wastewater for irrigation (Crites and Tchobanoglous, 1998; Metcalf and Eddy 2003).

Table 7 Experimental data of PH variation for all the reactor configurations

Parameter pH	Six-baffle 70% pond width reactor	Four-baffle70% pond width transverse reactor	Four-baffle 70% pond width longitudinal reactor	Simplex optimized design	MOGA-II optimized design
Influent pH	7.43	7.47	7.47	7.50	7.50
Anaerobic Effluent pH	7.69	7.54	7.53	7.62	7.58
Facultative Effluent pH	7.81	7.86	7.81	7.80	7.84
Maturation Effluent pH	7.88	7.89	7.85	7.82	7.89
Cumulative cost (N)	14, 592	14, 234	15,658	13,609	13,443

Table 8 Experimental data of TDS removal for all the reactor configurations

Parameter TDS (ppm)	**Six-baffle 70% pond width reactor**	**Four-baffle 70% pond width transverse reactor**	**Four-baffle 70% pond width longitudinal reactor**	**Simplex optimized design**	**MOGA-II optimized design**
Influent TDS	342	340	340	343	343
Anaerobic Effluent TDS	340	334	333	338	338
Facultative Effluent TDS	326	313	309	315	318
Maturation Effluent TDS	302	273	285	275	293
Percentage Removal (%)	12	20	16	20	15
Cumulative Cost (N)	14, 592	14, 234	15,658	13,609	13,443

Table 9 Conductivity experimental data for all the reactor configurations

Parameter Conductivity (µS)	Six-baffle 70% pond width reactor	Four-baffle70% pond width transverse reactor	Four-baffle 70% pond- width longitudinal reactor	Simplex optimized design	MOGA-II optimized design
Influent conductivity	700	690	690	697	697
Anaerobic Effluent conductivity	693	682	662	689	691
Facultative Effluent conductivity	656	627	642	653	639
Maturation Effluent conductivity	625	557	581	562	598

Percentage Removal (%)	11	19	16	19	14
Cumulative cost (N)	14, 592	14, 234	15,658	13,609	13,443

The result of the effluent quality tested for pH, conductivity and TDS showed that the WSPs performed well with different levels of pollutant removal. The model results of the fecal coliform log removal at the low end rate constant compared well with the experimental results that were carried out in the entire set of reactors in the laboratory-scale WSPs. The significance of the CFD validation is that regulators and designers can use CFD confidently both as a reactor model and as a hydraulic tool to develop an optimal design that meets the treatment efficiency of baffled WSPs at a reduced cost. The results of this research will directly impact the possible design decisions that wastewater treatment engineers must make related to WSPs design in developing nations.

5. Conclusions

Characteristics of a CFD-based model that incorporates the effects of different foot print size, baffle configuration, and baffle length on the treatment performance of the WSP has been explored. The use of CFD has proven to be a powerful tool to facilitate the design and evaluation of new and existing WSP systems. However, the modeling performed in this study did not include potential physics and biodegradable build-up that may occur in field WSPs such as surface wind shear, variable flow rate, variable climatic condition, and sludge deposits that may impact WSP design decisions. It was also observed that even though hydraulic similarity was achieved in the laboratory scale model which is intended to represent a full scale pond, other physical and biochemical phenomena such as sunlight penetration along the depth, temperature gradients, gas transfer and removal of other nutrient parameters could not be incorporated into this CFD model because the removal of these parameters depends on various processes such as algae uptake, sedimentation, vaporization and denitrification, which are more complex to model as several sub-models and empirical measurement would be required. In addition, it would also be difficult to test and verify the results of such complex models. The optimized solution was based only on the disinfection process, the kinetics of fecal coliform, and an explicit cost objective function along with the associated constraints. The realization of this practical limitation of CFD modeling is a very important consideration for practicing engineers applying CFD result to full-scale pond design. However, since designs can be compared with each other, then it might be possible to determine the best design among a possible list of alternatives. Therefore, CFD/optimization technique is seen as a sign tool or protocol to achieving a cost effective designs that will not jeopardize the treatment efficiency.

Rigorous assessment of WSPs that account for cost in addition to treatment efficiency utilizing CFD coupled with an optimization program to efficiently optimize the selection of the best WSP configuration has been performed. In addition, a sensitivity analysis with the first order rate constant (k) and the temperature (T) parameters was carried out. The most important result of this study has been that a cost effective designs was produced by the simplex and MOGA II optimization techniques that do not jeopardize the treatment efficiency of the three stage reactors. While each design seemed to have produced similar results, the CFD optimized designs were significantly lower in cost. Therefore, this approach to developing a cost effective design has been validated.

In view of the experimental data obtained from the laboratory-scale waste stabilization ponds and the CFD modeling, further work is required:

1. Verification of results achieved from the laboratory-scale to a full-scale construction of waste stabilization pond. This type of experience would provide valuable insight on the real investment and operational costs as well as the real requirements of operation and management for this technology.
2. The data obtained from the full-scale construction of WSP would allow the sustainability of the technology to be assessed under real conditions. The result of the full-scale experimentation would serve as guide to physical planning units of institutions for the design of treatment systems that will enhance environmental quality and protection.

The results of this study have indicated that the WSP geometry can be optimized to achieve a target effluent contaminant reduction using CFD coupled with an optimization algorithm. Finally, this work has demonstrated the use of CFD coupled with an optimization algorithm to provide an efficient assessment of alternative pond configurations, thereby, addressing a potential knowledge gap in waste stabilization pond design.

Acknowledgement

The author would like to acknowledge the US Department of States through the Institute of International Education for the Fulbright scholarship to carry out the modeling and optimization aspect of this research in the Hydraulic Laboratory of North Carolina State University. Covenant University provided the platform for which the data to design a field-scale pond was made available and subsequently the experimental data to verify and validate the model results.

References

Abbas, H., Nasr, R. and Seif, H., 2006. Study of waste stabilization pond geometry for wastewater
treatment efficiency. Ecological Eng, 28: 25-34.

Agunwamba, J. C., 1991. Simplified optimal design of waste stabilization pond, Water, Air and Soil
pollution, 59: 299-309.

Agunwamba, J. C., 1992. Field pond performance and design evaluation using physical models.
Water resources, 26 (10), 1403-1407.

Agunwamba, J. C., 1994. Capacity expansion of waste stabilization ponds. Journal of Indian association
for environmental management, vol. 21(1): 17-23.

Agunwamba, J.C., 2001a. Effect of tapering on the performance of waste stabilization ponds.Wat. Res,
35(5): 1191-1200.

Agunwamba, J.C., 2001b. Analysis of Socioeconomic and Environmental Impacts of Waste Stabilization
Pond and Unrestricted Wastewater Irrigation: Interface with Maintenance. Environmental
Management, 27 (3): 463-476.

Antonini, G., Brunier, E., Houang, P., Schaegger, M., Zoulalian, A., 1983. Analyse des D.T.S dans les
systemes hydrauliques de type lagunaire. Scale-Up of Water and Wastewater Treatment
Processes. Schmidtke, N. and Smith, D. (Eds). Butterworth Publishers; Edmonton, Canada; 73-86.

American Public Health Association (APHA), 1998. Standard Methods for the Examination of
Water and Wastewater (20th ed.), APHA, Washington, DC.

Banda, C. G., 2007. Computational fluid dynamics modeling of baffled waste stabilization Ponds. PhD
Thesis, School of Civil Engineering, University of Leeds, UK, Leeds.

Babu, M. A., Hes, E. M. A., van der Steen, N. P., Hooijmans, C.M., Gijzen, H. J., 2010. Nitrification rates
of algal–bacterial biofilms in wastewater stabilization ponds under light and dark conditions.
Ecological Eng, 36: 1741–1746

Brissaud, F., Lazarova, V., Ducoup, C., Joseph, C., Tournoud, M., 2000. Hydrodynamic behaviour and
faecal coliform removal in a maturation pond. Water Science and Technology 42 (10/11), 119-
126.

Brissaud, F., Tournoud, M. G. Drakides, C., Lazarova, V., 2003. Mixing and its impact on faecal coliform
removal in a stabilization pond. Water Science and Technology 48 (2), 75-80.

Crites, R. and Tchobanoglous, G., 1998. Small and Decentralized Wastewater Management Systems.
McGraw-Hill Series, San Francisco, USA.

Elenkova, N. G. Tsoneva, R. A. and Nedelcheva, T. K., 1980. New turbidimetric method for

determination of sulphate. Talanta 27(1), 67-68

Frederick, G., Lloyd, B., 1996. An evaluation of retention time and short-circuiting in waste stabilization ponds using Serratia marcescens bacteriophage as a tracer. Water Science and Technology, 33(7): 49-56.

Hamzeh, R., Ponce, V. M., 2007. Design and Performance of Waste Stabilization Ponds. http://www.ponce.sdsu.edu (Accessed May 2007).

Hodgson, O.A., 2000. Treatment of domestic sewage at Akuse (Ghana), Water SA., 26, 413-416.

Kaya, D., Dilek, F. B., Gokcay, C. F., 2007. Reuse of lagoon effluents in agriculture by post-treatment in a step feed dual treatment process. Desalination, 215: 29-36.

Mara, D. D., 1997. Design Manual for Waste stabilization ponds in India. Lagoon Technology International Ltd., Leeds, England.

Mara, D., Pearson, H., 1998. Design Manual for Waste Stabilization Ponds in Mediterranean Countries, Leeds Lagoon Technology International Ltd. Leed, UK.

Mara, D. D., 2001. Appropriate wastewater collection, treatment and reuse in developing countries Proceedings of the Institutions of Civil Engineers, London. Pp. 299-303.

Mara, D. D., 2004. Domestic Wastewater Treatment in Developing Countries. Earthscan Publications, London, England, ISBN 1844070190

Marecos do Monte, M.H.F., Mara, D.D., 1987. The hydraulic performance of waste stabilization ponds in Portugal. Water Science and Technology, 19 (12), 219-227.

Metcalf and Eddy 2003. Wastewater Engineering: Treatment and Reuse, McGraw-Hill Series in Civil and environmental engineering, 4th ed. New York, USA.

Mohammed, B., 2006. Design and Performance Evaluation of a Wastewater Treatment Unit AU J.T. 9(3): 193-198.

Moreno, M., 1990. A tracer study of the hydraulics of facultative stabilization ponds, Water Research 24(8), 1025–1030.

Naddafi, K., Hassanvand, .A. S., Dehghanifard, E., Faezi Razi, D., Mostofi, S., Kasaee, N.,Nabizadeh, R, Heidari, M., 2009. Performance evaluation of wastewater stabilization ponds in Arak-Iran, Iran. J. Environ. Health. Sci. Eng., Vol. 6, No. 1, pp. 41-46.

Oke, I. A., Otun, J. A., Okuofu, C. A., Olarinoye, N.O., 2006. Efficacy of biological treatment plant at Ahmadu Bello University Zaria, Research Journal of Agriculture and Biological Sciences, 2(6), 452-459.

Olukanni, D. O., Aremu, S.A., 2008. Water hyacinth based wastewater treatment system and its derivable bye-product. Journal of research information in Civil Engineering, Vol.5, No.1 43-55.

Olukanni, D.O., Ducoste, J.J., 2011. Optimization of Waste Stabilization Pond Design for Developing Nations using Computational Fluid Dynamics. Ecological Eng, 37: 1878–1888.

Parhad, N.M. and Rao, N.U., 1974. Effect of pH on survival of Escherichia coli. Journal of the Water Pollution Control Federation, 46 (5) 980-986.

Pearson, H. W., Mara, D. D., Konig, A., De Oliveira., and Silva, S.A., 1987. Water column sampling as a rapid and efficient method of determining effluent quality and performance of waste stabilization ponds. Water Science and Technology, 19 (12), 100-119.

Persson, J., Wittgren, H. B., 2003. How hydrological and hydraulic conditions affect performance of ponds. Ecological Eng. 21: 259–269.

Shilton, A., Bailey, D., 2006. Drogue tracking by image processing for the study of laboratory scale pond

hydraulics. Flow Measurement and Instrumentation, 17 (2006) 69–74.
Shilton, A.N., Mara, D.D., 2005. CFD (computational fluid dynamics) modeling of baffles for optimizing
tropical waste stabilization ponds system. Water Science and Technology 51(12) 103-106.
Shilton, A., Harrison, J., 2003a. Guidelines for the Hydraulic Design of Waste Stabilization ponds.
Institute of Technology and Engineering, Massey University. Palmerstone North.

*Corresponding author at: Department of Civil Engineering, Covenant University, P.M.B. 1023, Canaan Land, Ota,
Ogun State, Nigeria.
E-mail addresses: david.olukanni@covenantuniversity.edu.ng (D.O. Olukanni). Tel.: +234-08030726472.
Work done as a Visiting Research Scholar, North Carolina State University, Raleigh, USA.

Loto et al: Proc. ICCEM (2012) 72 - 88

Inhibition effect of N, N'-Dimethylaminoethanol on the Corrosion of Austenitic Stainless steel type 304

Loto, R.T[1]*, Loto, C.A[1, 2] and Fedotova, T.[1]
1Department of Chemical and Metallurgical Engineering
Tshwane University of Technology, Pretoria, South Africa
2 Department of Mechanical Engineering, Covenant University, Ota, Nigeria
E-mail address: tolu.loto@gmail.com

Abstract

The effect of N,N'-dimethylaminoethanol on the corrosion of austenitic stainless steel type 304 in 3M H_2SO_4 has been studied by weight-loss method and linear polarization measurement in different concentrations of the compound. The inhibition efficiencies of the inhibitor compound on the corrosion of the stainless steel were evaluated through assessment of the anodic and cathodic polarization curves of the alloy, the spontaneity of the electrochemical process, inhibition mechanism and adsorption isotherm. The inhibitor efficiency increased with increase in the inhibitor concentration. Results obtained reveal that the inhibitor performed effectively on the stainless steel providing good protection against pitting and uniform corrosion in the chloride containing acidic solutions. The compound act through physiochemical mechanism on the stainless steel surface and obeyed Langmuir adsorption isotherm. The values of the inhibition efficiency calculated from the two techniques are in reasonably good agreement. Polarization studies showed that the compounds behave as mixed type inhibitor in the aggressive media.

Key words: *N, N'-dimethylaminoethanol, corrosion, stainless steel, tetraoxosulphate(vi) acid, inhibitor*

1.0 INTRODUCTION

Corrosion of metals is a major industrial problem that has attracted numerous investigations and researchers (Tarab and Al.Turkustani, 2006, Eddy and Ebenso, 2010). Millions of dollars are lost each year because of corrosion (Kadry, 2008). Much of this loss is due to the corrosion of iron and steel. The problem with steel as well as many other metals is that the oxide formed by oxidation does not firmly adhere to the surface of the metal and flakes off easily causing "pitting". Extensive pitting eventually causes structural weakness and disintegration of the metal (Kadry, 2008). Stainless steel derives their corrosion resistance from a thin durable layer of chromium oxide that forms at the metal's surface and gives stainless steel its characteristic 'stainless quality'. The passive film on stainless steel surface consists of a mix of iron oxide and chromium oxide (Tuthill and Avery, 1992). The formation of this film is instantaneous in an oxidizing atmosphere such as air, water, or other fluids that contain oxygen. Once the layer has formed, the metal becomes "passivated" and the oxidation or "rusting" rate will slow down significantly. Breakdown of the protective films leads to localized corrosion failures. The corrosion of stainless steel in acidic solutions has received considerable amount of attention (Abdallah, 2003). The highly corrosive nature of aqueous mineral acids on most metals requires degree of restraint to achieve economic maintenance and operation of equipment, minimum loss of chemical product and maximum safety conditions. Acidic solutions are aggressive to this film layer and results in severe pitting formation (Galal et al., 2005, Fouda et al., 2010). Several mineral acid solutions such as sulphuric acid are widely used for various treatments of materials in industry. Sulphuric acid is used for pickling, descaling, acid cleaning; oil-well acidizing, etc (Ahamad et al., 2010) Sulphuric acid is generally the choice in steel surface treatment basically due to its lower cost, minimal fumes and non-corrosive nature of the SO_4^{2-} ion. Since steel could be attacked by the acidic media during its various application processes, the presence of corrosion inhibitors in the solutions is of utmost importance to keep the surface of steel intact (Hosseini et al., 2009). The use of inhibitors is one of the most practical methods of metallic protection against corrosion (Umoren ey al., 2009). Most of the efficient inhibitors used in industry are organic compounds, which mainly contain nitrogen, oxygen, sulphur atoms, and heterocyclic compounds containing functional groups and conjugated double bonds, and multiple bonds in the molecule through which they are adsorbed on metal surface by the formation of an adherent

film (Abd El-Maksoud and Fouda, 2005, Aljourani et al., 2010, Hasanov et al., 2010, Abd El-Maksoud, 2003, Xu et al., 2008, Abboud et al., 2007, Awad and Gawad, 2005, Chetouani, 2003) . The compounds containing both nitrogen and sulphur can provide excellent inhibition, compared with compounds containing only nitrogen or sulphur (Aljourani et al., 2010, Abboud et al., 2007). Generally, inhibitor molecules may physically or chemically adsorb on a corroding metal surface. In any case, adsorption is generally over the metal surface forming an adsorption layer that functions as a barrier protecting the metal from corrosion (Elayyachy et al., 2005, Bouklah et al., 2006). It has been commonly recognized that an organic inhibitor usually promotes formation of a chelate on a metal surface, by transferring electrons from the organic compounds to the metal and forming a coordinate covalent bond during the chemical adsorption (Ajmal et al., 1994). In this way, the metal acts as an electrophile; and the nucleophile centers of inhibitor molecule are normally heteroatoms with free electron pairs that are readily available for sharing, to form a bond (Fang et al., 2002). The power of the inhibition depends on the molecular structure of the inhibitor. Organic compounds, containing functional electronegative groups and π-electron in triple or conjugated double bonds, are usually good inhibitors. Heteroatoms, such as sulphur, phosphorus, nitrogen, and oxygen, together with aromatic rings in their structure are the major adsorption centers. The planarity and the lone electron pairs in the heteroatoms are important features that determine the adsorption of molecules on the metallic surface (Quraishi and Sharma, 2002).

The inhibition efficiency of organic compounds is strongly dependent on the structure and chemical properties of the layer formed on the metal surface under particular experimental conditions.

Different classes from organic compounds are used as corrosion inhibitors for iron alloys in various acid media (Growcock et al., 1998, Hettiarachchl et al., 1989, Gad Alla and Tamous,1990, Agrawal, and Namboodhiri, 1990, Moretti, 1996, Agrawal and Namboodhiri, 1997, Abdel-Aal and Morad, 2001, Mthar et al., 2002, Selvi et al,. 2003, Bentiss et al., 2004, Noor, 2005, Yurt et al., 2005) . Unfortunately, most of the organic inhibitors used are very expensive and health hazards. Their toxic properties limit the field of their application. Thus, it remains an important objective to find low-cost inhibitors of the non-hazardous type for the protection of metals against corrosion.

N,N-dimethylethanolamine belongs to the group of alkanolamines, chemical compounds that carry hydroxy (-OH) and amino (-NH_2, -NHR, and -NR_2) functional groups on an alkane backbone. Alkanolamines have the combined physical and chemical characteristics of both alcohols and amines in one molecule, which makes them useful intermediates in the synthesis of various target molecules for use in many diverse areas such as pharmaceutical, urethane catalysts, coatings, personal care, products, Water treatments and gas treating industries, Dimethylaminoethanol used specifically for the synthesis of dyestuffs, textile auxiliaries and pharmaceuticals [such as procaine] contributing to its extensive industrial utilization and low cost (N,N DIMETHYLETHANOLAMINE). A major problem with evaluating these inhibitors is that they are commonly used as part of complex formulations, marketed under trade names, whose compositions are uncertain.

This study aims to investigate the corrosion inhibition effect of N, N dimethylethanolamine an amino alcohol compound and its ability to provide protection against pitting and uniform corrosion at different concentrations in 3M H_2SO_4 solution using linear polarization and weight loss techniques.

2.0 EXPERIMENTAL PROCEDURE

2.1 Material

Commercially available Type 304 austenitic stainless steel was used for all experiments of average nominal composition; 18.11%Cr, 8.32%Ni and 68.32%Fe. The material is cylindrical with a diameter of 1.80cm (18mm).

2.2 Inhibitor

N, N-Dimethylaminoethanol (DMAE) a colorless, transparent liquid is the inhibitor used. The structural formula of DMAE is shown in Fig. 2. The molecular formula is $C_4H_{11}NO$, while the molar mass is 89.14 g mol^{-1}.

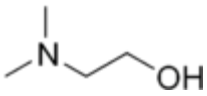

Fig. 1 Chemical structure of N, N Dimethylaminoethanol (DMAE)

DMAE was prepared in various concentrations of 0%, 2.5%, 5%, 7.5%, 10%, 12.5% and 15% was used as the inhibiting medium

2.3 Test Media

3M tetraoxosulphate (VI) acid with 3.5% recrystallised sodium chloride of Analar grade were used as the corrosive medium

2.4 Preparation of Test Specimens

The cylindrical stainless steel (1.80cm dia.) was mechanically cut into a number of test specimens of different dimensions in length ranging from 1.78 and 1.88cm coupons. The two surface ends of each of the specimen were ground with Silicon carbide abrasive papers of 80, 120, 220,800 and1000 grits. They were then polished with 6.0*u*m to 1.0*u*m diamond paste, washed with distilled water, rinsed with acetone, dried and stored in a dessicator for further weight-loss test and linear polarization.

2.5 Weight-loss Experiments

Weighted test species were fully and separately immersed in 200ml of the test media at varying concentrations of the inhibitor for 18days at ambient temperatures. Each of the test specimens was taken out every three days (72 hours), washed with distilled water, rinsed with acetone, dried and re-weighed. Plots of weight-loss (mg) and corrosion rate (mmpy) versus exposure time (hours) (Figs. 2 & 3) and those of percentage inhibition efficiency (%IE) (calculated) versus exposure time (hours) and percentage inhibitor concentration (Fig. 4 & 5) were made from Table 1.

The corrosion rate (R) calculation is from this formula:

$$R = \left[\frac{87.6W}{DAT}\right] \quad \text{eqn. 1}$$

Where W is the weight loss in milligrams, D is the density in g/cm^2, A is the area in cm^2, and T is the time of exposure in hours. The % inhibitor efficiency, (I.E), was calculated from the relationship.

$$\left[\frac{W1-W2}{W1}\right] \times 100 \ldots\ldots\text{eqn. 2}$$

Where W_1 and W_2 are the corrosion rates in the absence and the presence respectively of a predetermined concentration of inhibitor. The %IE was calculated for all the inhibitors on the 18th day of the experiment [Table 1], while the surface coverage is calculated from the relationship:

$$\theta = \left[1 - \frac{W2}{W1}\right] \ldots\ldots\ldots\text{eqn. 3}$$

Where θ is the substance amount of adsorbate adsorbed per gram (or kg) of the adsorbent, the unit of m is mol.g^{-1}. W_1 and W_2 are the weight loss of austenitic stainless steel coupon in free and inhibited acid solutions, respectively.

2.6 Linear polarization Resistance

Linear polarization measurements were carried out using, a cylindrical coupon embedded in resin plastic mounts with exposed surface of 2.54 cm^2. The electrode was polished with different grades of silicon carbide paper, polished to 6*u*m, rinsed by distilled water and dried with acetone. The studies were performed at ambient temperature with Autolab PGSTAT 30 ECO CHIMIE potentiostat and electrode cell containing 200 mL of electrolyte, with and without inhibitor. A graphite rod was used as the auxiliary electrode and silver chloride electrode (SCE) was used as the reference electrode. The steady state open circuit potential (OCP) was noted. The potentiodynamic studies were then made from -1.5V *versus* OCP to +1.5 mV *versus* OCP at a scan rate of 0.00166V/s and the corrosion currents were registered. The corrosion current density (*j* corr) and corrosion potential (*E* corr) were determined from the Tafel plots of potential *versus* log *I*. The corrosion rate (*r*), the degree of surface coverage (θ) and the percentage inhibition efficiency (% *IE*) were calculated as follows

$$r\ (mmpy) = \frac{0.00327\ x\ icorr\ x\ eq.wt}{D} \quad \text{eqn.4}$$

Where *icorr* is the current density in *u*A/cm^2, D is the density in g/cm^3, eq. is the specimen equivalent weight in grams;

The percentage inhibition efficiency (% IE) was calculated from corrosion current density values using the equation.

$$\%I.E = 1 - \left[\frac{c2}{c1}\right] 100 \quad \text{eqn.5}$$

where C1and C2 are the corrosion current densities in absence and presence of inhibitors, respectively.

3. Results and Discussion

3.1 Weight-loss measurements

Weight-loss of austenitic stainless steel at various time intervals, in the absence and presence of different concentrations of (DMEA) in 3M sulphuric acid at 25^{o}C was studied. The values of weight-loss (wt), corrosion rate (CR) (mmpy) and the percentage inhibition efficiency (IE %) are presented in Table 1. It is clear that the decreasing corrosion rate is associated with increase in the inhibitor concentration which indicates that more inhibitor molecules are adsorbed on the metal surface, thereby providing wider surface coverage (Emregul, 2003). Fig. (2, 3 & 4) shows the variation of weight-loss, corrosion rate and percentage inhibition efficiency with exposure time at different inhibitor concentration while fig. 5 shows the variation of %IE with inhibitor concentration. The curves obtained indicate progressive increase in %IE with increase in inhibitor concentration accompanied by a reduction in corrosion rate.

Table 1. Data obtained from weight loss measurements for austenitic stainless steel in 3M H2SO4 in presence of different concentrations of the DMEA at 312hrs

Sample	Inhibitor Concentration (%)	Weight Loss (mg)	Corrosion Rate (mmpy)	Inhibition Efficiency (%)
A	0%	5345	49.1071	0
B	2.5%	2006	11.8126	62.45
C	5%	1774	11.7695	66.81
D	7.5%	1082	7.4023	79.76
E	10%	725	4.1509	86.44
F	12.5%	518	3.4562	90.31
G	15.0%	542	3.2186	89.86

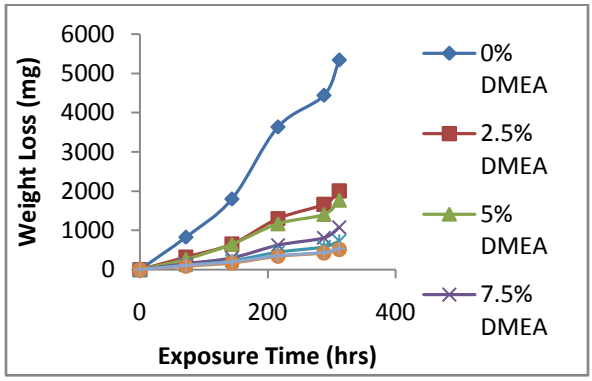

Fig. 2 Variation of weight-loss with exposure time for samples (A – G) in (0% -15%) DMEA concentrations.

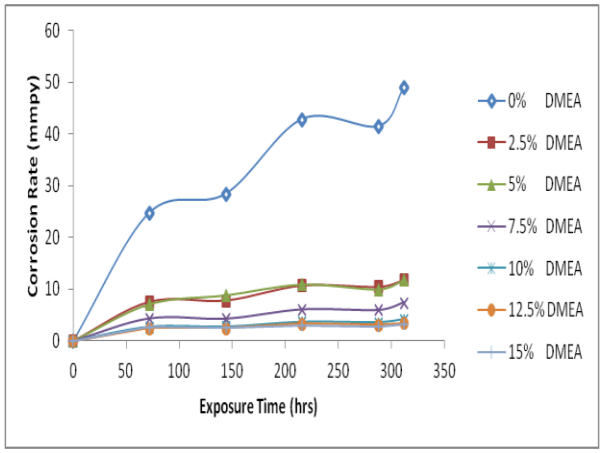

Fig. 3 Effect of percentage concentration of DMEA on the corrosion rate of austenitic stainless steel.

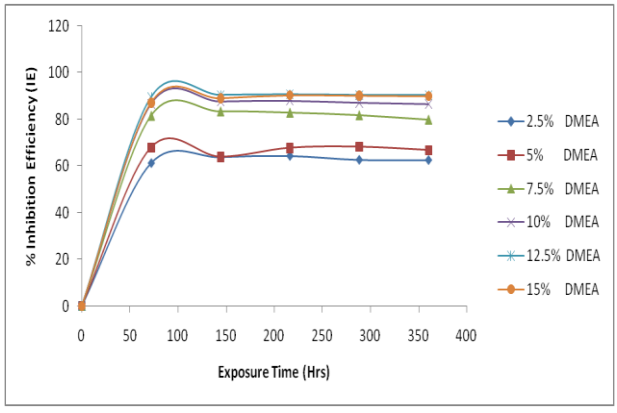

Fig. 4. Plot of inhibition efficiencies of sample (A-G) during the exposure period

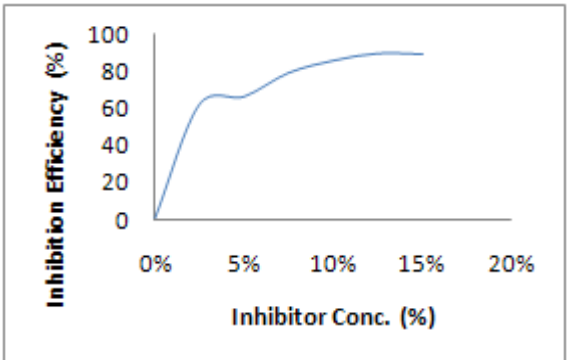

Fig. 5 Percentage inhibition efficiency of DMEA at varying concentrations from weight loss.

3.2 Polarization studies

The potential was scanned from –1.50 to 1.50 V vs. SCE at a rate of 0.0166 mV s^{-1}, which allows the quasi-stationary state measurements. The effect of the addition of DMEA on the anodic and cathodic polarization curves of austenitic stainless steel type 304 in 3 M H_2SO_4 solutions at 25 °C was studied. Fig. 6 (a & b) shows the polarization curves of austenitic stainless steel in absence and presence of DMEA at different concentrations. Anodic and cathodic currents were inhibited effectively with increasing concentrations of inhibitor. The inhibitor appeared to act as mixed type inhibitor since anodic [metal dissolution] and hydrogen evolution reactions were significantly influenced by the presence of compounds in the corrosive medium. Generally, all scans exhibit slightly similar behavior over the potential domain examined, indicating similar electrochemical reactions took place on the metal. The electrochemical parameters such as, corrosion potential (E_{corr}), corrosion current (i_{corr})corrosion current density (I_{corr}), cathodic Tafel constant (*bc*), anodic Tafel slope (*ba*) , surface coverage ~~θ~~ and percentage inhibition efficiency (%IE) were calculated and given in Table 2. These results show that the %IE increased while the corrosion current density generally decreased with the addition of DMEA until 10% and 12.5% concentration where there was a sharp increase before decreasing at 15% concentration. The corrosion current density (I_{corr}) and corrosion potential (E_{corr}) were determined by the intersection of the extrapolating anodic and cathodic Tafel lines, % IE was calculated from Eq. 6

$$\% \text{ I.E} = \frac{CR1 - CR2}{CR1}\% \quad \text{eqn. 6}$$

Table 2 Data obtained from polarization resistance measurements for austenitic stainless steel in 3M H2SO4 in presence of different concentrations of the DMEA

Inhibitor Conc. (%)	Inhibitor Conc. [Molarity]	Corrosion Rate (mmpy)	Inhibition Efficiency (%)	Rp	Ecorr	i (A)	I(A/cm2	bc	ba
0%	0	7.995	0	2.269	-328	1.979x10 -2	7.782x10-3	0.456	0.227
2.5%	0.00028	2.765	65.42	3.499	-243	6.843x10-4	2.691x10-4	0.210	0.026
5%	0.00056	2.074	74.06	9.107	-263	5.133x10-4	2.018x10-4	0.185	0.058
7.5%	0.00084	1.556	80.54	8.448	-317	3.851x10-4	1.514x10-4	0.207	0.036
10%	0.00112	1.241	84.48	5.146	-348	3.072x10-2	1.208x10-2	0.434	0.084
12.5%	0.00140	1.051	86.85	1.513	-364	2.601x10-2	1.023x10-2	0.572	0.158
15%	0.00168	1.003	87.46	3.888	-364	2.483x10-3	9.762x10-4	0.249	0.089

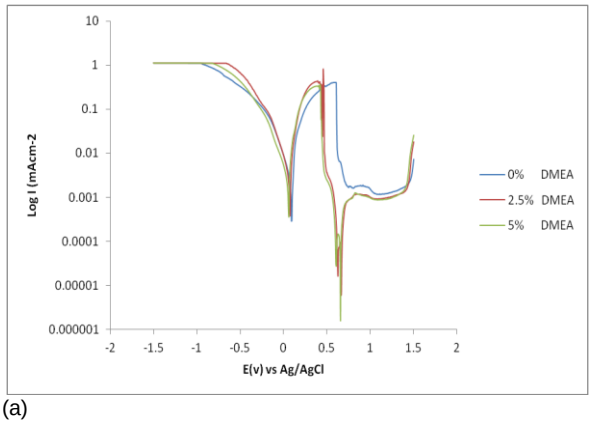

(a)

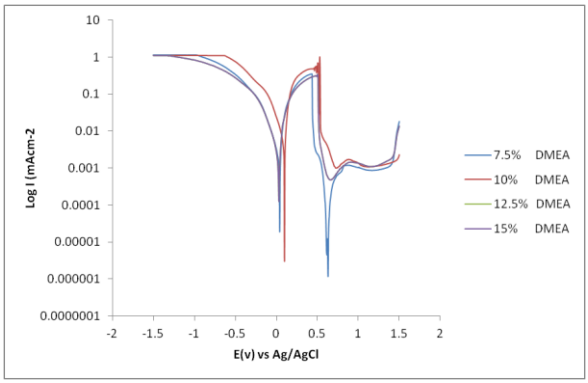

(b)

Fig. 6 Comparison plot of cathodic and anodic polarization scans for austenitic stainless steel in 3M H_2SO_4 + 3.5% NaCl solution in the absence and presence of different concentrations of DMEA at 25°C. (a) 0% - 5% DMEA (b) 7.5% - 15% DMEA

Anodic and cathodic currents were inhibited effectively with increasing concentrations of DMEA. This compound appeared to act as a mixed type inhibitor since both cathodic (hydrogen evolution) and anodic (metal dissolution) reactions were influenced by the presence of DMEA in the corrosive medium, with the anodic effect being more significant suppressed than the cathodic reactions.

As shown in Table 2, the values of cathodic Tafel slope constants (bc) varied differentially in the presence of DMEA concentrations, indicating changes in the mechanism of its inhibition. This suggests that inhibitor affects the mechanism of cathodic reaction (hydrogen evolution and oxygen reduction reaction) which is the main cathodic process under activation control and the addition of DMEA modifies and suppresses the reaction. Results suggests that the inhibition mode of the tested DMEA is by simple blockage of the surface via adsorption, accompanied by an increase in the number of adsorbed organic molecules on the steel with increase in inhibitor concentration, which impede more the diffusion of ions to or from the electrode surface as the degree of surface coverage (θ) increases (Mohamed et al., 2009).

The anodic Tafel lines (ba) are observed to change with addition of inhibitors suggesting that the inhibitor were first adsorbed onto the metal surface and impedes the passage of metal ions from the oxide-free metal surface into the solution, by merely blocking the reaction sites of the metal surface thus affecting the anodic reaction mechanism. Increasing the concentration of the inhibitor gives rise to a consistent decrease in anodic and cathodic current densities indicating that DMEA acts as a mixed type inhibitor (Muralidharan et al., 1995).

Corrosion potentials slightly shifted in the positive direction. A compound can be classified as an anodic- or a cathodic-type inhibitor when the change in the Ecorr value is larger than 85mV (Musa et al., 2010, Li et al., 2010). If displacement in Ecorr is <85, the inhibitor can be seen as mixed type. In this study the maximum displacement in Ecorr value was 54mV.. Small changes in potentials can be a result of the competition of the anodic and the cathodic inhibiting reactions (Fouda et al., 2010). However, in the anodic range from the corrosion potential, the current density starts to increase very steeply due to active metal dissolution reaction, and then stabilizes over a passivation zone extending to ~1000 mV indicating strong resistance to pitting corrosion before it starts again to increase faster due to breakdown of the passive film and pit initiation.

The values of the anodic Tafel slope can be attributed to surface kinetic process rather than a diffusion-controlled one (Amin et al., 2010), where the inhibitor molecules are adsorbed via their polycentric adsorption sites on to the steel surface forming a protective layer. Furthermore, the results in Table 2 demonstrate clearly demonstrate the inhibitory effect of DMEA on the stainless steel corrosion whereby both i_{corr} and CR decreases, accompanied by a decrease in polarization resistance (*R*p). The inhibition mechanism of these DMEA compounds is a combination of surface blockage and electrostatic repulsion between adsorbed species and chloride ions. The adsorption of DMEA depends on the inhibitors concentrations. DMEA act on both anodic and cathodic sites and reducing the corrosion rate without a significant change in the corrosion potential, generally by surface adsorption over the surface of the steel in contact with the inhibitor and consequently forming a thin protective layer. It is clear that the cathodic reaction [hydrogen evolution] is inhibited and the inhibition increases along with the inhibitor concentration (Soeda and Ichimura, 2003). This controls corrosion by attacking cathodic activity, blocking sites where oxygen picks up electrons and is reduced to hydroxyl ion (Gaidis, 2004). The variable constancy of this cathodic slope can indicate that the mechanism of proton discharge reaction changes by addition of the DMEA to the acidic media.

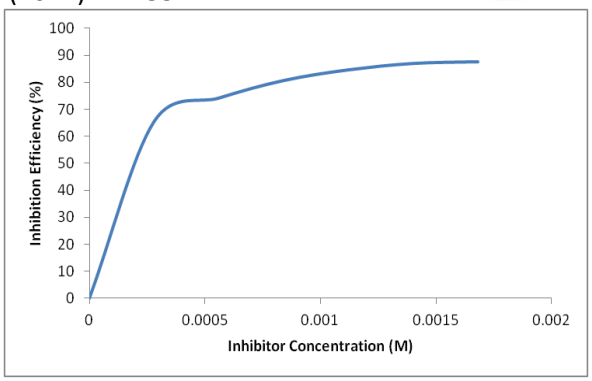

Fig. 7. The relationship between % IE and inhibitor concentration for polarization test

3.3 Mechanism of inhibition

As far as the inhibition process is concerned, the adsorption of the inhibitors at the metal solution interface is the first step in the action mechanism of inhibitors in aggressive acid media. Inhibition of austenitic stainless steel in H2SO4 solution by the DMEA can be explained on the basis of adsorption. Adsorption depends on the nature and the state of the metal surface on the type of corrosive medium and on the chemical structure of the inhibitor. Studies report that the adsorption of the organic inhibitors mainly depends on some physicochemical properties of the molecule related to its functional groups, to the possible steric effects and electronic density of donor atoms; adsorption is suppose also to depend on the possible interaction of p-orbitals of the inhibitor with d-orbitals of the surface atoms, which induce greater adsorption of the inhibitor molecules onto the surface of carbon steel, leading to the formation of a corrosion protecting film (Cruz et al, 2004).

Four types of adsorption may take place involving organic molecules at the metal solution interface (i) electrostatic attraction between charged molecules and the charged metal, (ii) interaction of *n* electrons with the metal, (iii) interaction of uncharged electron pairs in the molecule with the metal and (iv) a combination of the above (Ajmal et al., 1994). It is apparent that the adsorption of DMEA on the steel surface could occur directly on the basis of donor acceptor between the lone pairs of the heteroatoms, the extensively delocalized π electrons of the DMEA molecule and the vacant d-orbitals of iron surface atoms (Abdel-Aal and Morad, 2001). The functional group responsible

for DMEA adsorption on metal surface is the lone pair of the nitrogen atom: iron ions on metal surface act as a Lewis acid because they accept electrons from a donor group. Amines adsorption is influenced by the electronic properties of the functional groups, R, bound to the nitrogen atom (Ormellese et al., 2009).

In acidic solution, these compounds can exist as protonated species; these protonated species may adsorb on the cathodic sites of the stainless steel and decrease the evolution of hydrogen. These compounds are able to adsorb on anodic sites through N atoms, which is an electron donating groups. The adsorption of these compounds on anodic sites decreases anodic dissolution of stainless steel by the electron-rich heteroatoms in DMEA which adsorbs on the anodic site through their lone pairs of electrons of nitrogen thus reduces the anodic dissolution of metal. The performance of DMEA is also attributed to the presence of OH

Inhibition of the stainless steel corrosion DMEA was also found to depend on its stability in acidic solutions. Transfer of lone pairs of electrons on the nitrogen to the surface to form coordinate type linkage is favored by the presence of vacant orbital in iron atom of low energy. Polar character of substituent in the changing part of the inhibitor molecule seems to have a prominent effect on the electron charge density of the molecule. The presence of one active adsorption centers [one N-atoms] do not necessarily impact on the electron charge density on the molecule but increase in the inhibition efficiency as this occurs with increasing concentration of the compound. The presence of chloride ion in some way increases this migration; the passive barrier becomes less effective at holding iron ions inside. Finally, at some point, the film ceases to exist and is replaced by an anodic site. The mechanism by which chloride ion accelerates corrosion of steel is complex, but one or more of the following descriptions (Abd El-Maksoud and Fouda, 2005) may be appropriate:

(1) Penetration of oxide film by chloride ion.
(2) Adsorption of chloride ion rather than a passivating species.
(3) Field effect of chloride ion pulling ferrous ions out of the metal.
(4) Catalysis of corrosion reaction by a bridging structure.
(5) Complex formation between chloride ion and some form of iron (Trauenberg and Foley, 1971)

Some of the inhibition mechanisms identified by a previous study in aqueous solutions suggested that DMEA was able to displace chloride ions from the steel surface and to protect the surface passive film. This differed from the finding from the study in aqueous solutions (Welle et al., 1997), where the DMEA-to-chloride concentration ratio was much higher and a durable passivating film was formed by DMEA on the steel surface. DMEA effectively delayed the onset of steel corrosion and inhibited the steel corrosion even when the passive film was compromised. According to (Hansson et al 1998) the strong absorption of DMEA onto the steel surface inhibited the cathodic reaction of steel corrosion by limiting the access of oxygen to the steel.

Generally, the adsorption of organic compounds can be described by two main modes of interaction: physisorption and chemisorption. The former requires the presence of electrically charged metal surface and charged species in the bulk of solution, while the latter involves charge-sharing or charge-transfer from the inhibitor molecules to the metal surface to form a co-ordinate type of a bond (Donahue and Nobe, 1965, Moretti et al., 2004, Zhao and Mu, 1944)

3.4 Adsorption isotherm

The mechanism of corrosion protection may be explained on the basis of adsorption behavior (Allam, 2007). Adsorption isotherms are very important in determining the mechanism of organo-electrochemical reactions. The adsorptive behavior of a corrosion inhibitor is an important part of this study, as it provides important clues to the nature of the metal-inhibitor interaction (Emregul et al., 2003).Interaction information between the inhibitor molecule and metal surface can be provided by adsorption isotherm (Emregul et al., 2006). For an inhibitor to have a high surface coverage on the surface, a chemical bond between the inhibitor and the metal atom stronger than the one for water molecules should be formed. The adsorption of corrosion inhibitors at the metal/solution interface is due to the formation of either electrostatic or covalent bonding between the adsorbates and the metal surface atoms. Langmuir adsorption isotherm

was applied to describe the adsorption mechanism for DMEA compounds as it fits the experimental results at 25 ^{o}C.

The conventional form of the Langmuir isotherm is,

$$\left[\frac{\theta}{1-\theta}\right] = K_{ads}C \qquad \text{eqn.7}$$

where θ is the degree of coverage on the metal surface, C is the inhibitor concentration in the electrolyte, and K_{ads} is the equilibrium constant of the adsorption process. The plots of $\frac{C}{\theta}$ versus the inhibitor concentration were linear (Fig. 8) indicating Langmuir adsorption.

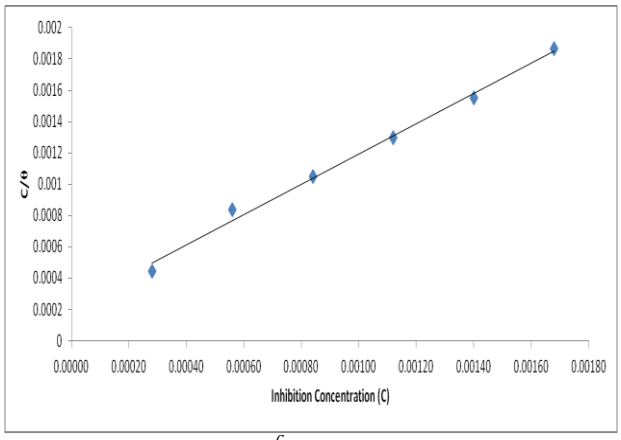

Fig. 8 Relationship between $\frac{C}{\theta}$ and inhibitor concentration (C)

The deviation of the slopes from unity is attributed to the molecular interaction among the adsorbed inhibitor species, a factor which was not taken into consideration during the derivation of the Langmuir equation. Langmuir isotherm assumes that:

(i) The metal surface contains a fixed number of adsorption sites and each site holds one adsorbate.

(ii) ΔG_{ads} is the same for all sites and it is independent of θ.

(iii)The adsorbates do not interact with one another, i.e. there is no effect of lateral interaction of the adsorbates on ΔG_{ads} (Villamil et al, 1999).

Table 3 Data obtained for the values of Gibbs free energy, Surface coverage and equilibrium constant of adsorption at varying concentrations of DMEA

Inhibitor Concentration (M)	**Free energy of Adsorption (ΔGads)**	**Surface Coverage (θ)**	**Equilibrium Constant of Adsorption (K_{ads})**
0	0	0	0
0.00028	31.52	0.625	6009.62
0.00056	30.24	0.668	3591.40
0.00084	30.91	0.798	4694.12
0.00112	31.38	0.864	5684.21
0.00140	31.76	0.903	6639.71
0.00168	31.20	0.899	5288.24

The free energies of adsorption, ΔGads, were calculated from the equilibrium constant of adsorption using the following equation as shown in table 3

ΔG_{ads}=-2.303RTlog [55.5K]

Where 55.5 is the molar concentration of water in the solution, R is the universal gas constant and T is the absolute temperature. Generally, values of ΔG_{ads} around -20 kJ/mol or lower are consistent with the electrostatic interaction between the charged molecules and the charged metal [physisorption]; those around -40 kJ/mol or higher involve charge sharing or transfer from organic molecules to the metal surface to form a coordinate type of bond (Obot et al., 2009). The value of ΔGads reflects the

strong adsorption capability. The negative values of **Δ**Gads

showed that the adsorption of inhibitor molecules on the metal surface is spontaneous (Hosseini et al., 2003). The values of ΔG_{ads} calculated ranges between −30.24 and −31.76 kJ mol^{-1} for DMEA. Accordingly, the values of ΔG_{ads} obtained in the present study indicate that the adsorption mechanism of DMEA on austenitic stainless steel involves two types of interaction, chemisorption and physisorption. Indeed, due to the strong adsorption of water molecules on the surface of stainless steel, one may assume that adsorption occurs first due to the physical forces. The removal of water molecules from the surface is accompanied by chemical interaction between the metal surface and the adsorbate, and that turns to chemisorptions (Vračar, L.M and Dražić, 2002). It is assumed from observation that the adsorbed layer was of one-molecule thickness at all sites, resulting in equal energies and enthalpies of adsorption. The intermolecular bonding to the adsorption sites can be either chemical or physical, but is sufficiently strong to prevent displacement of adsorbed molecules along the surface (Da˛browski, 2001).

The nitrogen and oxygen atoms of the inhibitor molecules are readily adsorbed onto the metal surface, forming insoluble stable films on the metal surface, thus decreasing metal dissolution Saliyan (V.R and Adhikari, 2008).

4. Conclusions

(i) N,N'-dimethylaminoethanol is a inhibitor for austenitic stainless steel in acidic chloride environment

(ii) The inhibition efficiency increases with inhibitor concentration.

(iii) The investigated compound inhibits corrosion by adsorption of the inhibitor on the steel surface blocking the active sites and inhibition of the hydrogen evolution reactions.

(iv) The adsorption of the compounds on the stainless steel surface was found to obey Langmuir adsorption isotherm.

(iv) The order of the inhibition efficiency of inhibitor at varying concentration as given by linear polarization measurements is in good agreement with that obtained from weight loss measurements.

(v) N,N'-dimethylaminoethanol provide protection against pitting corrosion of austenitic stainless steel in presence of chloride ions.

(vi) The free energy of adsorption indicates that the process was spontaneous and inhibition was due to physiochemical reactions on the steel surface.

References

Abboud, Y; Abourriche, A; Saffaj, T; Berrada, M; Charrouf, M; Bennamara, A; Al Himidi, N and Hannache, H. 2, 3-Quinoxalinedione as a novel corrosion inhibitor for mild steel in 1 M HCl, Mater. Chem. Phys.105 (2007)1

Abd El-Maksoud and Fouda, A. S. Some pyridine derivatives as corrosion
inhibitors for carbon steel in acidic medium", Mater. Chem. Phys.Mater. Chem. Phys. 93 (2005) 84

Abd El-Maksoud, S. A. The influence of some Arylazobenzoyl acetonitrile
derivatives on the behaviour of carbon steel in acidic media. Appl. Surf. Sci. 206 (2003)129

Abdallah, M. Corrosion behaviour of 304 stainless steel in sulphuric acid solutions
and its inhibition by some substituted pyrazolones. Mater. Chem. Phys. 82(2003)786

Abdel-Aal, M.S and Morad, M.S. Inhibiting effects of some quinolines and organic phosphonium compounds on corrosion of mild steel in 3M HCl solution and theiradsorption characteristics, Br. Corros. J., 36 (2001)253

Agrawal, R and Namboodhiri, T.K.G. The inhibition of sulphuric acid corrosion of 410 stainless steel by thioureas, Corr. Sci., 30 (1990) 37

Agrawal, R and Namboodhiri, T.K.G. Inhibition of corrosion and hydrogen
embrittlement of HSLA steel in 0.5m H2SO4 by nitrile compounds, J. Appl.
Electrochem., 27 (1997)1265

Ahamad, I and Quraishi, M. A. Mebendazole: New and efficient corrosion inhibitor for
mild steel in acid mediumCorros. Sci. 52 (2010) 651-656

Ajmal, M; Mideen, A.S and Quraishi, M.A. 2-Hydrazino-6 methylbenzothiazole as an effective inhibitor for corrosion of carbon steel in acidic solutions, Corr. Sci 36 (1994) 79

Aljourani, J; Golozar, M. A and Raeissi, K. The inhibition of carbon steel corrosion in hydrochloric and sulfuric acid media using some benzimidazole derivatives, Mater. Chem. Phys.121 (2010) 320

Allam, N.K. Thermodynamic and quantum chemistry characterization of the adsorption of triazole derivatives during Muntz corrosion in acidic and neutral solutions, Appl. Surf. Sci. 253 (2007) 4570

Amin, M.A; Khaled, K.F and Fadl-Allah, S.A. Testing validity of the Tafel extrapolation method for monitoring corrosion of cold rolled steel in HCl solutions –Experimental and theoretical studies Corros. Sci. 52 (2010) 140

Awad,H. S; Gawad, S. A. Mechanism of inhibition of iron corrosion in hydrochloric acid by pyrimidine and series of its derivatives, Anti-Corros. Method. M. 52(2005) 328

Bentiss, F; Traisnel, M; Vezin, H; Hildebrand, H.F and Lagrenee, M. 2, 5-Bis (4- dimethylaminophenyl)-1, 3, 4-oxadiazole and 2, 5-bis (4-dimethylaminophenyl)-1, 3, 4-thiadiazole as corrosion inhibitors for mild steel in acidic media Corros. Sci., 46 (2004) 2781

Bouklah, M; Hammouti, B; Lagrenée, M and Bentiss, F. Thermodynamic properties of 2,5-bis(4-methoxyphenyl)-1,3,4-oxadiazole as a corrosion inhibitor for mild steel in normal sulfuric acid medium Corr. Sci 48(2006) 2831

Chetouani, A; Aouniti, A; Hammouti, B; Benchat, N; Benhadda, T and Kertit, S.Corrosion inhibitors for iron in hydrochloride acid solution by newly synthesised pyridazine derivatives, Corros.Sci. 45 (2003) 1675

Cruz, J; Martínez, R; Genesca, J and García-Ochoa, E. Experimental and theoretical study of 1-(2-ethylamino)-2-methylimidazoline as an inhibitor of carbon steel corrosion in acid media."J. Electroanal. Chem., 566(1) (2004) 111-121

Da˛browski, A. Adsorption—From theory to practice, Adv. Colloid Interface Sci., 93 (2001)135–224

Donahue, F. M and Nobe, K. Theory of organic corrosion inhibitors, J. Electrochem. Soc. 112 (1965) 886-891

Eddy, N.O and Ebenso, E.E;Corrosion inhibition and adsorption properties of ethanol extract of Gongronema latifolium on mild steel in H_2SO_4, Pigment and Resin Tech. 39 (2010) 77.

Elayyachy, M; Hammouti, B and El Idrissi. New telechelic compounds as corrosion inhibitor for steel in 1M HCl. Appl. Surf. Sci. 249 (2005)176-182

Emregul, K. C; Duzgun, E and Atakol, O. The application of some polydentate Schiff base compounds containing aminic nitrogens as corrosion inhibitors for mild steel in acidic media, Corros. Sci. 48 (2006)3243

Emregul, K.C; Kurtaran, R and Atakol, O. An investigation of chloride-substituted Schiff bases as corrosion inhibitors for steel, Corros. Sci., 45 (2003) 2803–2817

Fang, J and Li, J.Quantum chemistry study on the relationship between molecular structure and corrosion inhibition efficiency of amides, J Mol Struct. [THEOCHEM] 2002, 593, 179

Fouda, A. S; Abdallah, M; Al-Ashrey, S. M and Abdel-Fattah, A. A. Some crown
ethers as inhibitors for corrosion of stainless steel type 430 in aqueous solutions, Desalination 250 (2010) 538

Fouda, H. A. Mostafa, H. M. El-Abbasy, , Antibacterial drugs as inhibitors for the corrosion of stainless steel type 304 in HCl solution, J. Appl. Electrochem. 40
(2010)163

Gad Alla, A.G and Tamous, H.M. Structural investigation of pyrazole derivatives as corrosion inhibitors for delta steel in acid chloride solutions, J. Appl. Electrochem., 20 (1990) 488

Gaidis, J.M. Chemistry of corrosion inhibitors, Cem Concr Com, 26 (2004)181–189

Galal, A; Atta, N. F; Al-Hassan, M. H. S. Effect of some thiophene derivatives on the Electrochemical behavior of AISI 316 austenitic stainless steel in acidic solutions containing chloride ions I. Molecular structure and inhibition efficiency relationship, Mater. Chem. Phys. 89 (2005) 38

Growcock, F.B; Lopp, N.R and Jasinski, R. Corrosion Protection of Oilfield Steel
With 1-Phenyl-2-Propyn-1-Ol, J. Electrochem. Soc., 135 (1988) 823

Hansson, C.M. Mammolite, L and Hope, B.B Corrosion inhibitors in concrete – Part I: the principles", Cement Concrete Research, 28 (1998)1775-81

Hasanov, R; Bilge, S; Bilgiç, S; Gece, G and Kıl,ıç, Z. Experimental and theoretical calculations on corrosion inhibition of steel in 1 M H2SO4 by crown type polyethers,Corros. Sci. 2010, 52, 984

Hettiarachchl, S; Chan, Y.W; Wilson Jr. R.B and Agarwal, V.S. Macrocyclic
Corrosion Inhibitors for Steel in Acid Chloride Environments, Corrosion, 44 (1989) 30

Hosseini, M.G; Mertens S.F.L. and M.R. Arshadi, Synergism and antagonism in mild steel corrosion inhibition by sodium dodecylbenzenesulphonate and hexamethylenetetramine, Corros. Sci., 45 (2003) 1473

Hosseini, S. M. A; Salari, M and Ghasemi, M. 1-Methyl-3-pyridine-2-yl-thiourea as inhibitor for acid corrosion of stainless steel, Mater. Corr. 60 (2009) 963

Kadry, S. Corrosion Analysis of Stainless Steel, European Journal of Scientific Research 22 (2008) 508-516

Li, W; Zhang, Q; Pei, S; and Hou, B. Some new triazole derivatives as inhibitors for mild steel corrosion in acidic mediumJ. Appl. Electrochem. 38 (2008) 289

Mohamed, A.K; Mostafa, H.A; El-Awady G.Y and Fouda, A.S.Use of 1-phenylamine-3-(4-phenylthiosemicarbazone)-butan-1,3-diones derivatives as corrosion inhibitors for Carbon steel in acidic chloride solution, Port. Electrochim. Acta, 18 (2000) 99

Moretti, G; Quartarone, G; Tassan, A and Zingales, A. 5-amino- and 5-chloro-
indole as mild steel corrosion inhibitors in in sulphuric acid, Electrochem. Acta, 41 (1996) 1971

Mthar, M; Ali, H and Quraishi, M.A.. Corrosion inhibition of carbon steel in
hydrochloric acid by organic compounds containing heteroatoms, Br. Corros. J., 37 (2002)155

Muralidharan, S; Phani, K.L.N; Pitchumani, S; Ravichandranand S and Iyer, S.V.K Polyamino-quinone polymers: A new class of corrosion inhibitors for mild steel, J. Electrochem. Soc. 142(1995)1478

Musa, A. Y; Kadhum, A. A. H; Mohamad, A. B; Takriff, M. S; Daud, A. R and Kamarudin, S. K. On the inhibition of mild steel corrosion by 4-amino-5-phenyl-4H- 1, 2, 4-trizole-3-thiol, Corr. Sci. 52(2010) 526

Moretti, G; Guidi, F and Grion, G. Tryptamine as a green iron corrosion inhibitor in 0.5 M deaerated sulphuric acidCorros. Sci. 46 (2004) 387-403

Noor, E.A. The inhibition of mild steel corrosion in phosphoric acid solutions by
some N-heterocyclic compounds in the salt form Corros. Sci., 47 (2005) 33

N,N DIMETHYLETHANOLAMINE *available a*t http://www.chemicalland
21.com/industrialchem/organic/N,N-DIMETHYLETHANOLAMINE.htm

Obot, I.B; Obi-Egbedi, N.O and S.A. Umoren. Experimental and theoretical
investigation of clotrimazole on corrosion inhibitor for aluminium in hydrochloric acid and effect of iodide ion addition, Der Pharma Chemica 1(2009) 151-166

Ormellese, M; Lazzari, L; Goidanich, S; Fumagalli G and Brenna, A. A study of organic substances as inhibitors for chloride-induced corrosion in concrete, Corrosion Sci. 51(2009) 2959-2968

Quraishi, M.A and Sharma, H.K. 4-Amino-3-butyl-5-mercapto-1, 2,4-triazole: a new corrosion inhibitor for mild steel in sulphuric acid, Mater Chem Phys 78(2002)18

Saliyan, V.R and Adhikari, A.V. Quinolin-5-ylmethylene-3-f[8-[trifluoromethyl]- quinolin-4-yl]thiogpropanohydrazide as an effective inhibitor of mild steel corrosion in HCl solution, Corros. Sci.50 (2008) 55–61

Selvi, S.T; Raman, V and Rajendran, N. Corrosion inhibition of mild steel by
benzotriazole derivatives in acidic medium, J. Appl. Electrochem., 33 (2003) 1182

Soeda, K and Ichimura, T. Present state of corrosion inhibitors in Japan, Cem Concr Com, 25 (2003)117–122

Tarab, S and Al.Turkustani**,** A.M. Corrosion Inhibition of Steel in Phosphoric Acid by Phenacyldimethyl Sulfonium Bromide and some of its p-Substituted Derivatives, Portugaliae Electrochimica Acta 24 (2006) 53

Trauenberg, S.E and Foley, R.T. J. Electrochem. Soc., 118(1971) 1066

Tuthill, A.H and Avery, R.E. Specifying stainless steel surface treatments (NiDl)
Technical Series No 10068), The Nickel Development Institute (NiDl), Toronto,
Ontario, Canada.

Umoren, S. B.Obot, A;I and Obi-Egbedi, N.O. Raphia hookeri gum as a potential
eco-friendly inhibitor for mild steel in sulfuric acid, Mater. Sci. 44(2009) 274-279

Villamil, R.F.V; Corio, P; Rubin, J.C and Agostinho, S.M.I. Effect of sodium
dodecylsulfate on copper corrosion in sulfuric acid media in the absence and presence of benzotriazole, J. Electroanal. Chem., 472 (1999)112–119

Vračar, L.M and Dražić, D.M. Adsorption and corrosion inhibitive properties of some organic molecules on iron electrode in sulfuric acid, Corros. Sci., 44 (2002) 1669

Welle, A; Liao, J.D; Kaiser, K; Grunze, M; Blank, N and Maäder, U."Interactions of N,N′-dimethylaminoethanol with steel surfaces in alkaline and chlorine containing solutions", Applied Surface Science, Vol. 119 (1997) 185-98

Xu, F. ; Duan, J. ; Zhang, S and Hou, B. The inhibition of mild steel corrosion in 1 M hydrochloric acid solutions by triazole derivative, Mater. Lett. 62 (2008) 4072

Yurt, A; Bereket, G; Balaban, A.B and Erk, E. Effect of Schiff Bases Containing
Pyridyl Group as Corrosion Inhibitors for Low Carbon Steel in 0.1 M HCl, J. Appl.
Electrochem., 35 (2005) 1025

Zhao, T. P and Mu, G. N. The adsorption and corrosion inhibition of anion surfactants on aluminium surface in hydrochloric acid Corros. Sci. 41 (1999)1937-1944

Babalola: Proc. ICCEM (2012) 89 - 114

Electromechanical Systems in Building Services Engineering

P.O. Babalola
Department of Mechanical Engineering, College of Science and Technology, Covenant University, Canaan Land, Km 10, Idiroko Road, PMB 1023, Ota, Ogun State.
phillip.babalola@covenantuniversity.edu.ng; phillgail@yahoo.com

Abstract

There are myriad of electromechanical systems in domestics, commercial and industrial buildings. Part or most of these systems hardware are hidden from the public though they do account for between 50% to 75% of the total construction cost and take up to 15% of the building volume. This paper is aimed at enumerating their functions as a prerequisite for designing (including modelling and simulation), selecting, integrating, managing and reduction in energy usage. The electromechanical systems included in this paper are cold and hot water supplies, heating, ventilation, air conditioning, drainage, sanitation, refuse and sewage disposal, gas, electricity, access control, communication, oil installation, fire fighting and transportation.

Key words: building services engineering, water supply, air conditioning, fire fighting

1. Introduction

The capital and installation costs of building services in modern buildings can take up 50% of the total construction budget. For highly serviced buildings such as sports centres, this figure can easily exceed 75%. Services can also take up 15% of a building's volume. Therefore building services cannot be ignored. Architects have learnt to accept and accommodate the increased need for pipes, ducts and cabling encroaching on to their designs. Building services are the dynamics in a static structure, providing movement, communications, facilities and comfort. As they are unavoidable, it is imperative that architects, surveyors, builders, structural engineers, planners, estate managers and all those concerned with the construction of buildings have a knowledge and appreciation of the subject.

This paper incorporates a wide range of building services. The services included in this paper are cold and hot water supplies, heating, ventilation, air conditioning, drainage, sanitation, refuse and sewage disposal, gas, electricity, oil installation, fire services, transportation, accommodation for services, energy recovery and alternative energy. Illustrations shall be used to show the principles and operations of various services. The building services industry is based on engineering principles that are applied to the construction of buildings and the built environment. Its origins as a science and technology are well documented, not least the use of Archimedes ` spiral for movement of water ' and the concept of under floor heating in Roman palaces. More recently, it has evolved in response to the demands of population growth and the expectation of comfortable shelter, convenience and a healthy home and workplace environment. As an industry it is vast in terms of the diversity of professions and trades that it encompasses.

The industry is generally divided between design and installation. Design is undertaken by specialist consultancies and installation undertaken by specialist contractors. The latter sub-contracted on site under the overall administration of a construction management main contractor.

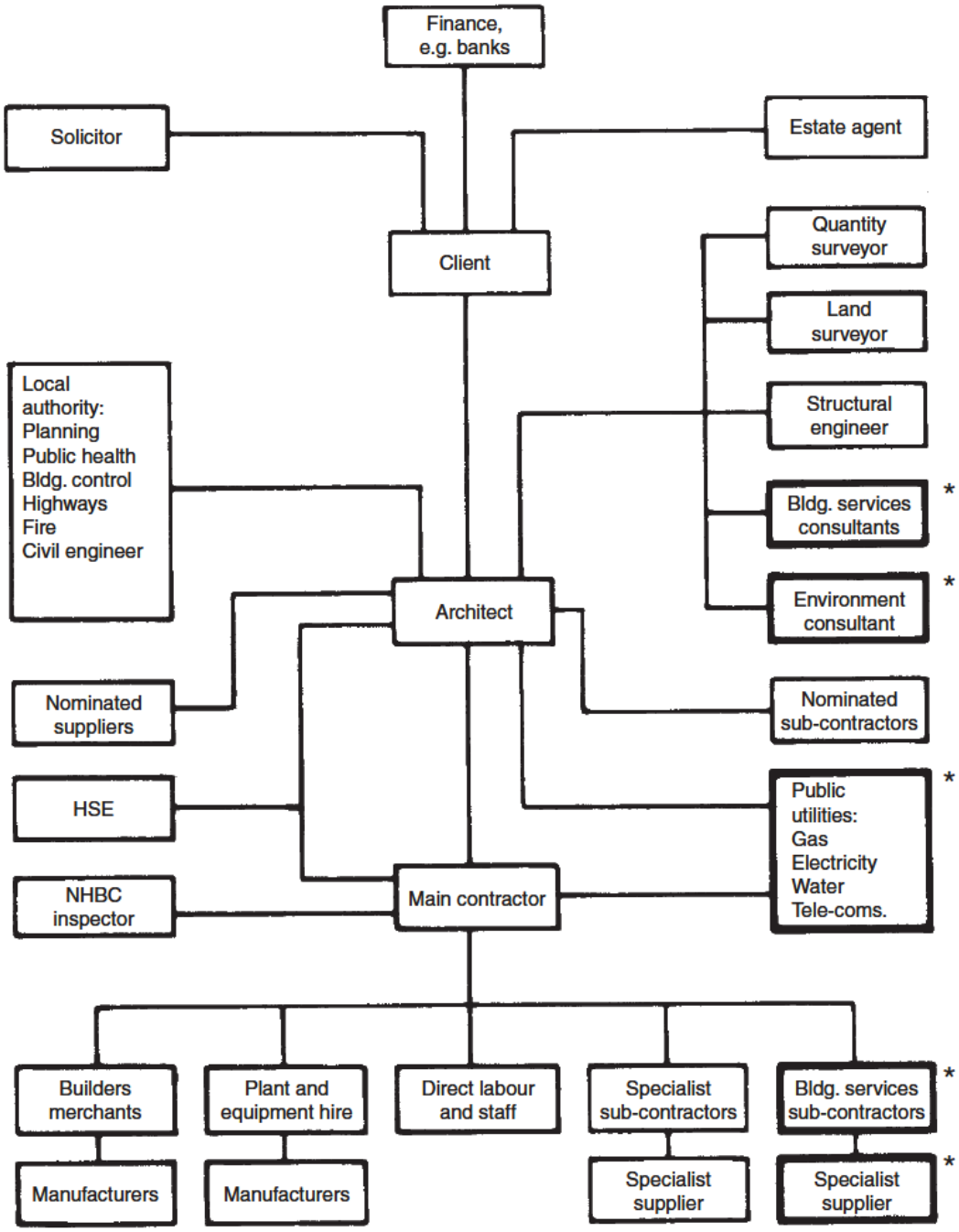

Figure 1. The Building Industry (Greeno and Hall, 2009)

2. The Electromechanical Systems

The electromechanical systems are cold and hot water supplies, heating, ventilation, air conditioning, drainage, sanitation, refuse and sewage disposal, gas, electricity, access control, communication, oil installation, fire fighting and transportation. Table 1 Typical Plumbing Schedule

PLUMBING FIXTURE CONNECTION SCHEDULE

SYM	DESCRIPTION	CONNECTION SIZE			
		W	V	CW	HW
WC–1	WATER CLOSET : ARMITAGE SHANKS 'TIFFANY' RANGE, WHITE CLOSED COUPLED WASHDOWN UNIT IN VITREOUS CHINA COMPRISING OF; (i) TIFFANY WC PAN (1043E4) (ii) CISTERN (1775FK) FOR BOTTOM SUPPLY AND OVERFLOW WITH 'FREE–FLOW' PLASTIC SYPHON FITTINGS 19mm MICROVALVE HP/LP BALLVALVE WITH WHISPERFLOW REFILL UNIT AND CLOSE–COUPLING FITMENT, WITH CHROME–PLATED SIDE LEVER (iii) SATURN SEAT AND COVER (0980BF) (iv) EDMEX SCREWS (7503BX) (v) S AND P TRAP PANSITA CONNECTORS (9014D30 AND 9013D20 RESPECTIVELY)	100	50	15	–
L–1	LAVATORY WASHBASIN : ARMITAGE SHANKS 'TIFFANY' RANGE (1201H4), WHITE GENERAL PURPOSE WASHBASIN IN VITREOUS CHINA, COMPLETE WITH A SINGLE TAP HOLE FOR MONOBLOC FITMENT, CONCEALED HANGERS, MILLENA 15mm MONOBLOC MIXER AND 32mm POP–UP WASTE (9124DX)	50	32	15	15
U–1	URINAL BOWL: ARMITAGE SHANKS SANURA WALL URINAL IN VITREOUS CHINA COMPRISING MURA AUTO CISTERN IN VITREOUS CHINA COMPLETE WITH FITTINGS– 9.0 LITRES CAPACITY (1734DW) SANURA 450mm URINAL (3911BC), TOP INLET SPREADER (7434AA/C), CONCEALED STEEL HANGERS (7220DSS), 40mm PLASTICS BOTTLE TRAP WITH 76mm SEAL (7523BQA), 40mm PLASTICS DOMED WASTE (9056BNC), DIHEDH WITH HANGER AND SCREW (2853DXX)	50	32	15	–
SH–1	SHOWER TRAY: ARMITAGE SHANKS TREM SHOWERS (L2174), WHITE LINCOLN CAST ACRYLIC SHEET,FULLY REINFORCED, FOUR UPSTANDS, FRONT AND END PANEL, AND 1 1/2 IN STRAINER WASTE,COMPLETE WITH TREM SHOWER KIT (TJ815AA), CHATTY SLIDE BAR, SOAP SHELF AND WALL CONNECTION (BW/TV SHOWER KIT FOR BUILT–IN OR EXPOSED SHOWER MIXER) CHROME PLATED	50	40	15	15
RD–1	ROOF DRAIN: GENERAL PURPOSE, 430 MM DIAMETER BODY, FLASHING CLAMP,GRAVEL STOP AND DOME, UNDERDECK CLAMP, SUMP RECEIVER, ALL COMPONENTS OF CAST IRON CONSTRUCTION JR.SMITH 1010	100	–	–	–
FD–1	FLOOR DRAIN: CAST–IRON BODY WITH ADJUSTABLE ROUND POLISHED NICKEL BRONZE TOP, STRAINER DIAMETER 165 MM VANDAL–PROOF SCREWS, TRAP PRIMER CONNECTION, PROVIDED WITH P–TRAP (JR.SMITH 2035–A) TRAP PRIMER, CAST BRASS TRAP SEAL PRIMER VALVE WITH AUTOMATIC VACUUM BREAKER JR.SMITH 3999	50	–	–	–
EWH–1	ELECTRIC WATER HEATER; CORROSION PROOF STEEL CENTRIC, ENAMEL STONE FINISH, ARISTON ENAMEL SERIES ST 50 CAPACITY: 150 LITRES	–	–	15	15
EWH–2	ELECTRIC WATER HEATER (UNDER SINK TYPE), GLASS–LINED TANK WITH POLYURETHANE FOAM INSULATION, STAINLESS STEEL ELEMENT CAPACITY: 15 LITRES	–	–	15	15
EWH–3	INSTANTANEOUS ELECTRIC WATER HEATER COLD WATER FEED, FLOW CONTROL, RINNAI MODEL 606N, FLOW RATE: 1.0 GPM (16.3 LPM)	–	–	15	15
S–1	KITCHEN SINK: 18 GUAGE STAINLESS STEEL, SINGLE DRAINER WITH 40mm WASTE OUTLET AND OVERFLOW HOLE FITTINGS, POLISHED CHROMEPLATED FINISH CONCEALED FIXED– JUST S1–2407–A–DR JR.SMITH 1010 BOTTLE TRAP: TWYFORDS 'M' BARKOP PILLAR TAPS: 15mm HIGH–NECK PILLAR TAPS–TWYFORDS SF 5211 CP	40	50	15	15
H–1	SLOP HOPPER: 18 GUAGE STAINLESS STEEL, WITH BUCKET GRATING AND REMOVABLE SUMP GRID, S–STRAP OUTLET (5320SGR) ARMITAGE SHANKS DU–S LEVER	100	75	15	–
GT–1	GREASE TRAP: INTERCEPTOR GRADE POLYETHYLENE GREASE TRAP HAVING A FLOW RATE OF 7gpm AND GREASE CAPACITY OF 144lbs, SEAMLESS CONSTRUCTION INSTALLATION ABOVE GROUND OR FLUSH TO THE FLOOR, 316Ti CONTINUOUS SERVICE WITH POLYETHYLENE DOMED SECURED BY STAINLESS STEEL SCREWS, O–RING GASKET AND INLET AND OUTLET FITTINGS OF 50mm, FLOW CONTROL DEVICE AND INTERNAL AIR–RELIEF	50	25	–	–

EQUIPMENT SCHEDULE

SYMBOL	DESCRIPTION	ELECTRICAL
DTP–1	DIESEL TRANSFER PUMP : 3.5L/S AT A HEAD OF 20m MAKE : STORK	1.5kW 230V/1PH/50Hz
CWP–1	COLD WATER PUMP : CAPACITY : 2.5xL/S AT 40m HEAD MAKE : PULLEN PUMP , MODEL : HYDROFIX 5V5	4.0kW 400V/3PH/50Hz
SP–1	SUMP PUMP : 1.5L/s AT A HEAD OF 9m MAKE : PULLEN PUMP , MODEL : AS 10–2 CS	2.2kW 230V/1PH/50Hz
DST–1	BULK STORAGE DIESEL TANK ; CAPACITY :– 45m³ SIZE :– 2.75m Dia x 7.69m LENGHT	–
DT–1	DIESEL OIL DAY TANK; CAPACITY:– 2m³ SIZE:– 2mLx2mWx2mH	–
WTP–1	WATER TREATMENT PLANT; CAPACITY :– 5m³/Hr SIZE:– 5.0mLx1.67mWx2.06mH, SATEC MODEL WS 84	2.5kW 400V/3PH/50Hz
STP–1	SEWAGE TREATMENT PLANT (GALVANISED STEEL) ; SATEC MODEL SO S 144 SIZE :– 7.0mLx4.95mWx3.05mH, WEIGHT FULL :– 84 TONNES	3.0kW 400V/3PH/50Hz
OHT–1	OVERHEAD WATER STORAGE TANK TYPE :– SPHEROIDAL; CAPACITY :– 45m³ SIZE :– 7.32mLx4.88mWx7.32mH	–
UHT–1	UNDERGROUND CONCRETE WATER TANK; CAPACITY :– 120m³ SIZE :– 9.0mLx8.0mWx1.7mD	–
BH–1	BOREHOLE INCLUDING DRILLING AND CONSTRUCTION COMPLETE WITH SUBMERSIBLE PUMP & PIPE WORK CAPACITY :– 5.0m³ /hr HEAD ; – 100m, MAKE:– LOWARA 4SS22T OR APPROVED EQUAL	3.0kW 440V/3PH/50Hz
AE–1	AERATOR SIZE :– 500mmDx2817mmH	–
PSF–1	PRESSURE SAND FILTER; 5m³/hr COMPLETE WITH 2No PRESSURE GUAGE, RELIEF VALVE, AUTOMATIC AIR VALVE AND FILTRATION MEDIA :– SAND,GRAVEL OF VARYING GRADES. MAKE:– SATEC MODEL PAL 30/L OR APPROVED EQUAL. MAXIMUM OPERATING PRESSURE:– 63m MINIMUM OPERATING PRESSURE:– 20m SIZE:– 800mmW x 2820mmH	–
PSF–2	PRESSURE SAND FILTER ; SAME AS PSF–1 BUT FILTRATION MEDIA TO CONSIST OF ACTIVATED CARBON AND VARYING GRADES OF SAND/GRAVEL. MAKE:– SATECTS MODEL PAL 30/L OR APPROVED EQUAL. MAXIMUM OPERATING PRESSURE:– 63m MINIMUM OPERATING PRESSURE:– 20m SIZE:– 800mmW x 2820mmH	–
AT–1	STEEL AERATION TANK SIZE:– 5.0mL X 1.672mW X 2.089mH	–
DP–1	DOSING PUMP WITH MIXING DRUM, LEVEL INDICATOR, CHEMICAL (FITKIT) AGITATOR AND LOW LEVEL SWITCH CAPACITY :– 15.75L/Hr HEAD :– 45m. MAKE :– GRUN–TECH SERIES 150, MODEL:– 130 OR APPROVED EQUAL.	1/4kW 240V/1PH/50Hz
DP–2	DOSING PUMP WITH MIXING DRUM, LEVEL INDICATOR, CHEMICAL (ALUM) AGITATOR AND LOW LEVEL SWITCH CAPACITY :– 15.75L/Hr HEAD :– 45m. MAKE :– GRUN–TECH SERIES 150, MODEL:– 130 OR APPROVED EQUAL.	1/4kW 240V/1PH/50Hz
DP–3	DOSING PUMP WITH MIXING DRUM, LEVEL INDICATOR, CHEMICAL (CHLORINE) AGITATOR AND LOW LEVEL SWITCH CAPACITY :– 15.75L/Hr HEAD :– 45m. MAKE :– GRUN–TECH SERIES 150, MODEL:– 130 OR APPROVED EQUAL.	1/4kW 240V/1PH/50Hz
TP–1	WATER TRANSFER PUMP CAPACITY :– 5.0m³/hr. HEAD :– 33.0m. MAKE :–PULLEN, MODEL:– KD5SL	1.5kW 230V/1PH/50Hz
BP–1	BACKWASH PUMP CAPACITY :– 5.0m³/hr. HEAD :– 33.0m. MAKE :–PULLEN, MODEL:– KD5SL	1.5kW 230V/1PH/50Hz
AC–1	AIR COMPRESSOR CAPACITY :– 5.0m³/hr. MAKE: ATLAS COPCO HEAD:– 50m.	1.5kW 230V/1PH/50Hz
DF–1	ELECTRIC HOT/COLD WATER DISPENSER WITH WOODEN RACK AND BOTTTLES CAPACITY : 19 LITRES, ASTRAL MODEL SNOW	230V/1PH/50Hz
HD–1	HAND DRIER INTEA–SEC SENSOR SYSTEM AND FULLY AUTOMATIC OPERATION MAKE: AIRDRI COMPACT SERIES AIR VOLUME :– 160m³/hr. DRYING TIME : 25 SECONDS	1.5kW 220–240V/1PH/50Hz
TD–1	PROVIDE ALLOWANCE OF 250mmW x 200mm IN DRAIN FOR TRENCH DRAIN	–
CWP–2	COLD WATER PUMP COMPLETE WITH PRESSURE VESSEL CAPACITY :– 2.5L/S HEAD :– 16.0m MAKE :–PULLEN KD 4S.	1.1kW 230V/1PH/50Hz

Table2. Typical Equipment Schedule-HVAC

AIR HANDLING UNIT SCHEDULE

MARK	FAN SECTION: AIR FLOW L/S	TSP KPa	RPM	WHEEL TYPE	FAN POWER KW	MOTOR KW	V	Φ	HZ	AIR SIDE SENS. KW	AIR SIDE TOTAL KW	COOLING COIL L/S	E.A.T. DB °C	E.A.T. WB °C	L.A.T. DB °C	L.A.T. WB °C	MAX P.D. KPa	ROWS NO.	FIN MAX (F/in)	COIL FACE VEL (m/s)	HOT DECK/ REHEAT COIL KW	SUPPLY AIR DISCHARGE	FILTER SECTION	OUTSIDE AIR (L/S)	UNIT SIZE USED IN DESIGN CARRIER MODEL	MAX. UNIT WEIGHT. KG	REMARKS
AHU–1	6654	1.55	1696	AIR FOIL	16.5	24	460	3	60	143.8	213.8	6654	31.5	22.8	13.29	13.20	0.282	8	14	2.4	—	VERTICAL	FLAT AND BAG CARTRIDGE	1500	39T32	—	VERTICAL DRAW THRU UNIT

EQUIPMENT SCHEDULE

SYMBOL	DESCRIPTION	ELECTRICAL
CDU–1	PACKAGED OUTDOOR AIRCOOLED CONDENSING UNIT 274KW COOLING CAPACITY AT 10°C AND 35°C OUTDOOR TEMPERATURE UNIT TO HAVE MINIMUM (2) COMPRESSORS 6–STEP CONTROL REDUCED VOLTAGE STARTING TYPE COMPRESSOR MOTOR. WEIGHT : 1728KG UNIT MODEL: CARRIER TYPE 30AH074	89.3kW 460V/3PH/60HZ
SU–TI	FLOOR MOUNTED INDOOR SPLIT UNIT AIRCONDITIONER COOLING CAPACITY: 3.30KW WEIGHT: 58KG UNIT MODEL: CARRIER 42VRC012	1.2kW 230V/1PH/50HZ
CU–TI	OUTDOOR CONDENSING UNIT WEIGHT: 41KG UNIT MODEL: CARRIER 38CH–012	

DIFFUSER, REGISTER AND GRILLE SCHEDULE

SYMBOL	TYPE	FACE	FRAME	DAMPER	FINISH	MODEL NO.	REMARKS
CD–1	CEILING DIFFUSER	LOUVERED	T–BAR	NONE	WHITE	TITUS TDC–AA	600x600 SURFACE MOUNTED TYPE WITH UNIFORM FACE APPEARANCE
CRG–1	CEILING RETURN GRILLE	LOUVERED	T–BAR	NONE	WHITE	TITUS TDC–AA	600x600 SURFACE MOUNTED TYPE WITH UNIFORM FACE APPEARANCE
CEG–1	CEILING EXHAUST GRILLE	LOUVERED	T–BAR	NONE	WHITE	TITUS TDC–AA	600x600 SURFACE MOUNTED TYPE WITH UNIFORM FACE APPEARANCE
SR–1	SIDE WALL SUPPLY GRILLE	DOUBLE DEFLECTION	32mm BORDER	NONE	WHITE	TITUS 272FS	ALUMINUM CONSTRUCTION
RG–1	SIDE WALL RETURN GRILLE	FIXED BAR 0° DEFLECTION	32mm BORDER	NONE	WHITE	TITUS 3FL	ALUMINUM CONSTRUCTION
EL–1	EXTENAL AIR LOUVRE	SURFACE MOUNTED	32mm BORDER	NONE	WHITE	TITUS 350FL	FIXED DEFLECTION ALUMINUM CONSTRUCTION

EXHAUST FAN SCHEDULE

SYMBOL	SERVICE	L/S	T.S.P. KPa	FAN POWER KW	MOTOR 50 HZ VOLTS	MOTOR 50 HZ PHASE	MAX. SONES AT 1.5 METRE	TYPE	REMARKS
EF–1	TOILETS	733	0.10	0.830	230	1	5.5	CEILING MOUNTED EXTRACT FAN	GREENHECK MODEL CSP–265
EF–2	TOILETS	498	0.10	0.455	230	1	5.5	CEILING MOUNTED EXTRACT FAN	GREENHECK MODEL CSP–262
EF–3	TOILET CONTROL TOWER	120	0.1	0.129	230	1	5.5	CEILING MOUNTED EXTRACT FAN	XPELR MODEL XDFAS–200

VAV TERMINAL UNIT SCHEDULE

SYMBOL	AREA SERVED	L/S MAX	MIN INLET STATIC PRESSURE LOSS Pa	MAX. No AT ΔSP = 250Pa
VB–1.1	HELICOP.HALL 017, DISPATCHER 018, SNACKS 014	1412	50	33
VB–1.2	CREW RM 008, OFFICE 006, 005, CORR.014, KIT.013 TOILETS 016, 010, 015, 011, TELECOMS ROOM 037	1012	50	31
VB–1.3	DEPART. CON.003, CHECK–IN–AREA	983	50	31
VB–1.4	BAGGAGE DISPATCH 019	369	50	31
VB–1.5	FIXED WING DEPT. HALL 021, SNACKS 023	899	50	31
VB–1.6	AIRPORT DIRECT.020, OFFICE 024, CREW RM. 029, V.I.P 030 HANGRAT. 031, CORR. 032, TOILETS 025, 026, 027, 028	1068	50	31
VB–1.7	FIXED WING ARRIV.HALL 022, PROCESS 032, EXIT 034	984	50	31

NOTES:
1. ΔSP IS STATIC PRESSURE DIFFERENCE FROM INLET TO DISCHARGE
2. UNIT MODEL : CARRIER MODEL 35DA
3. ALL TERMINAL UNITS TO BE EQUIPPED WITH ANALOG ELECTRONIC CONTROLS, SPACE TEMPERATURE SENSOR / THERMOSTAT AND CONTROL TRANSFORMER.

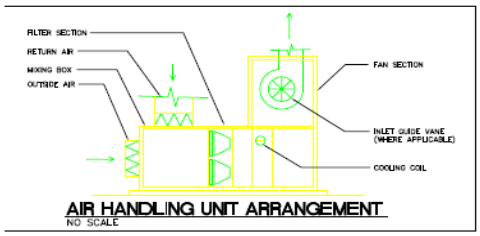

2.1 Cold water and supply systems

Water piping systems to distribute potable water throughout the building from source (borehole), treatment plant and storage tanks.

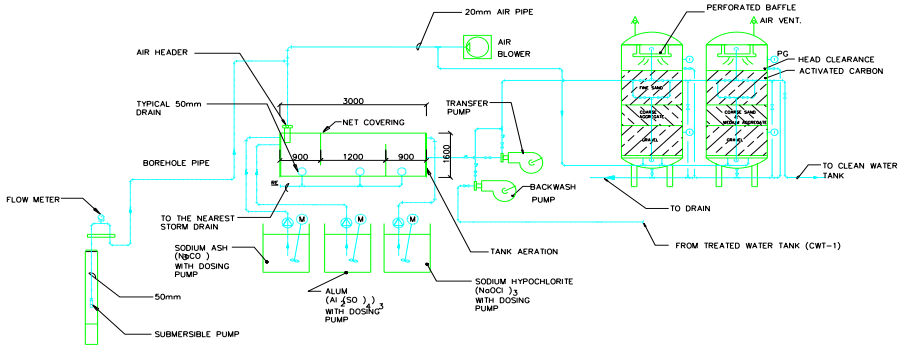

Figure 2. Water treatment plant

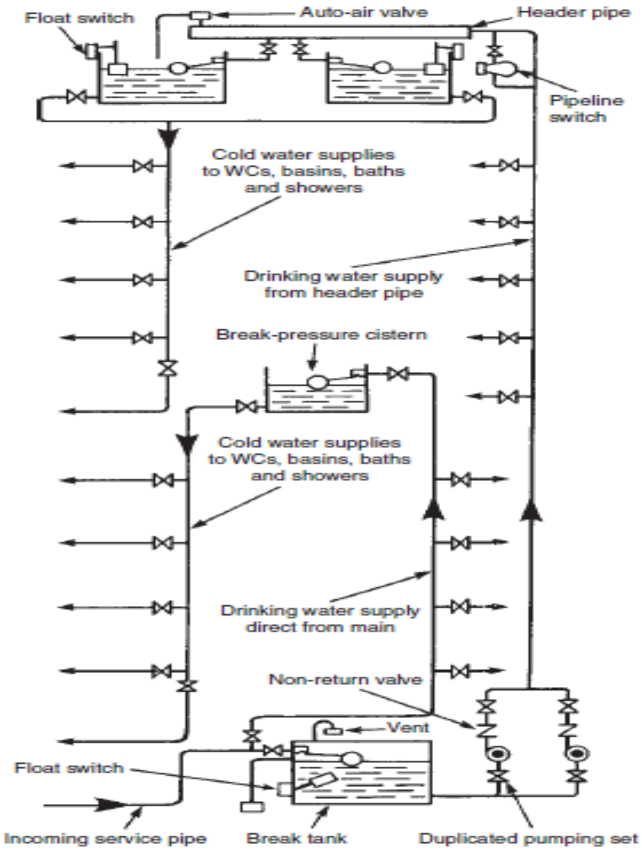

Figure 3. Typical Boosted Cold Water System (Greeno and Hall, 2009)

2.2 Hot Water Supply Systems

Hot water from water heater is connected to the hot water fixtures in the domestic building, kitchen, laboratory, laundry and so on. The water heater may be wall hung water heater, calorifier and boiler. Energy source may be electrical, gas, liquid or solid fuels depending on the application and the magnitude of the project.

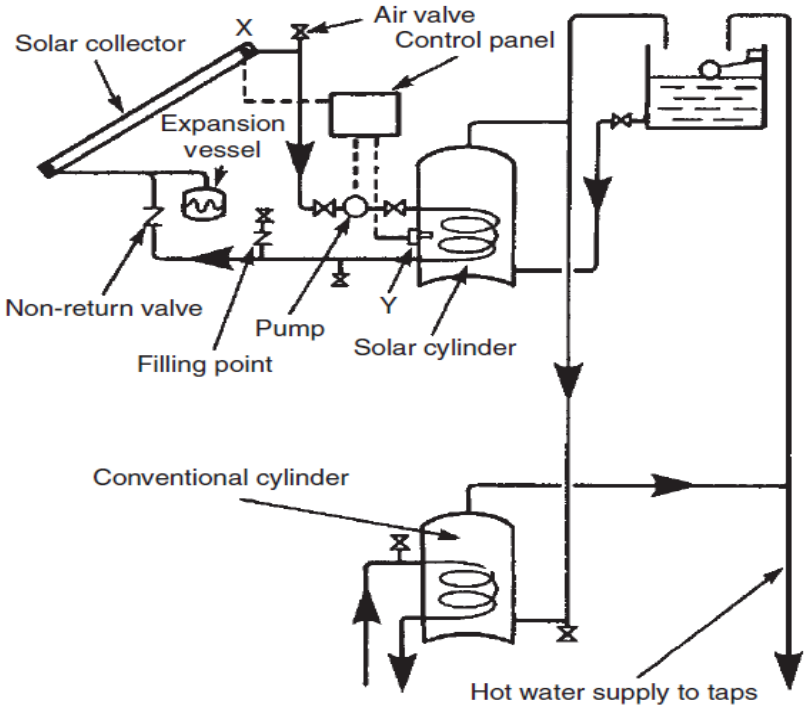

Figure 4. Typical Hot Water System with integral solar collected (Greeno and Hall, 2009)

2.3 Heating systems

Heating systems for human comfort is less desire in the tropical region and hence will not be given adequate attention. However, heat energy sources may be electrical, gas, liquid, solid fuels or heat pump.

2.4 Fuel Supply Systems

The system involves piping, pump and fuel storage tank to the point of use. Point of use may be power generator, calorifier, boiler et cetera.

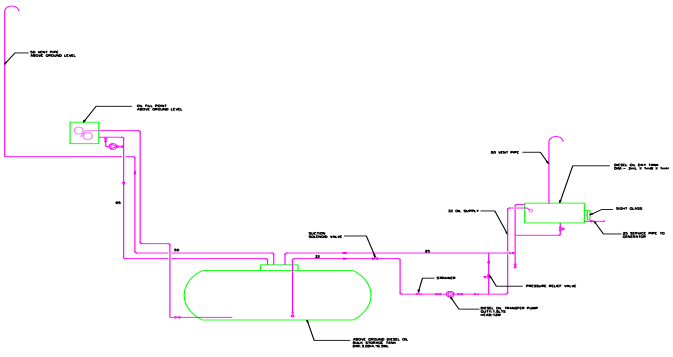

Figure 5. Fuel storage

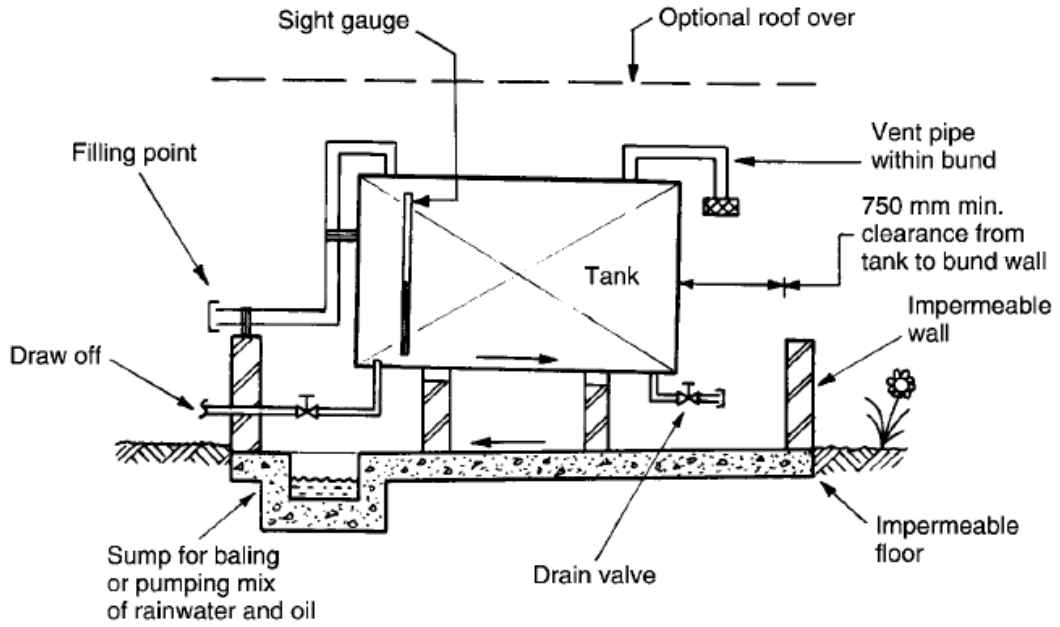

Figure 6. Oil Tank in bund wall

2.5 *Ventilation Systems*

Ventilation system is an integral part of air conditioning. It is the removal of unwanted or spent air from occupied zone. Some ventilation systems address safety issue during fire outbreak in high rise buildings.

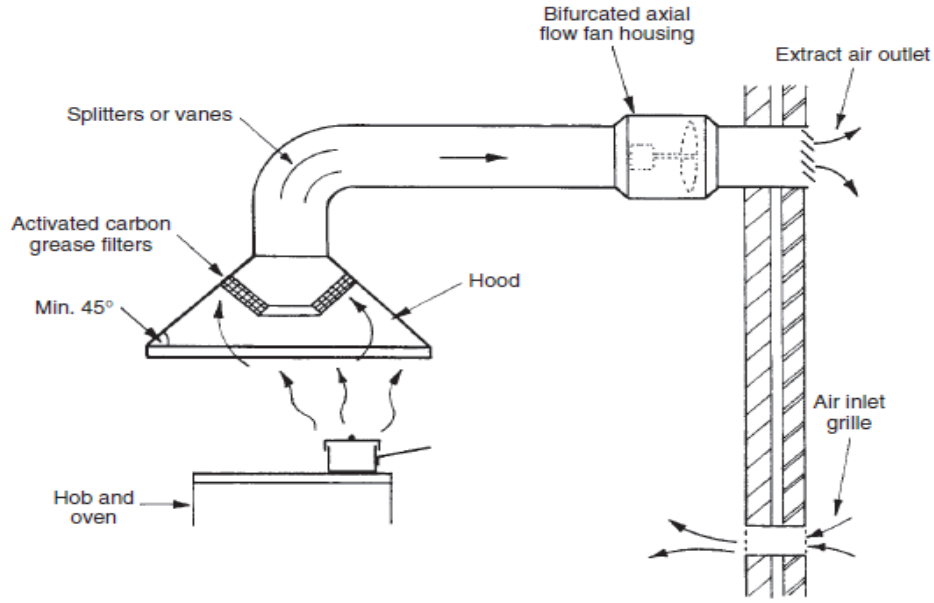

Figure 7. Typical ventilation application

Table 3. Air changes rate for room/building/accommodation (Greeno and Hall, 2009)

Room/building/accommodation	Air changes per hour
Assembly/entrance halls	3–6
Bathrooms (public)	6*
Boiler plant rooms	10–30†
Canteens	8–12
Cinema/theatre	6–10
Classrooms	3–4
Dance halls	10–12
Dining hall/restaurants	10–15
Domestic habitable rooms	approx. 1*
Factories/garages/industrial units	6–10
Factories – fabric processing	10–20
Factories (open plan/spacious)	1–4
Factories with unhealthy fumes	20–30
Foundries	10–15
Hospital wards	6–10
Hospital operating theatres	10–20
Kitchens (commercial)	20–60*
Laboratories	6–12
Laundries	10–15
Lavatories (public)	6–12*
Libraries	2–4
Lobbies/corridors	3–4
Offices	2–6
Smoking rooms	10–15
Warehousing	1–2

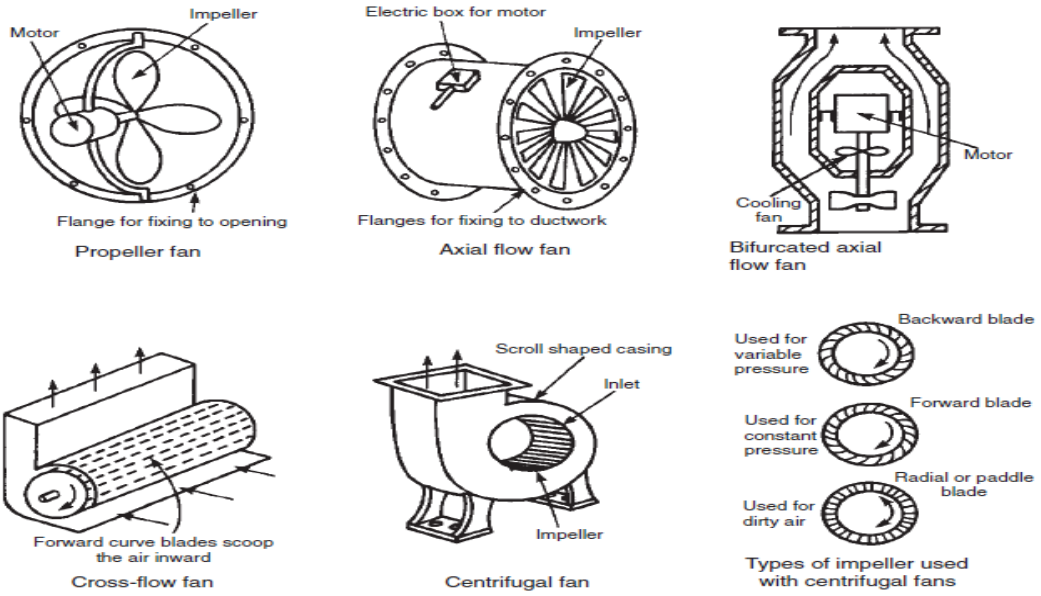

Figure 8. Types of fan

2.6 Air Conditioning

Air conditioning equipment are used to enhance the air quality, quantity and characteristics for human comfort. For buildings with human occupancy, the design specification is likely to include an internal air temperature of 19 – 23 ^{0}C and relative humidity between 40 and 60%.

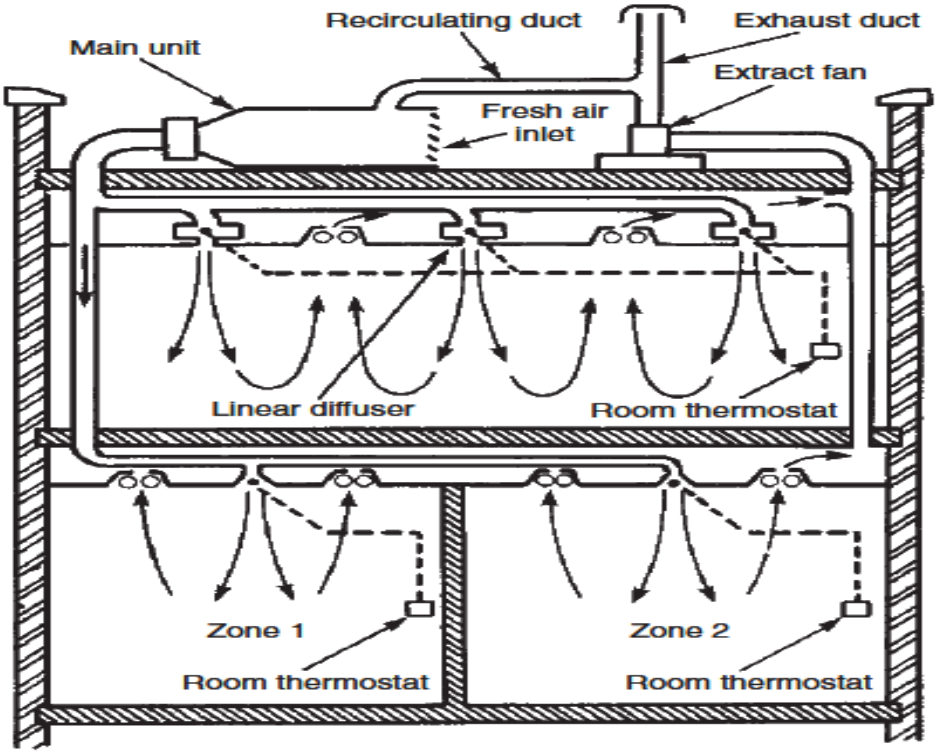

Figure 9. Typical (Air Conditioning) layout of variable air volume system

2.7 Drainage Systems, Sewage Treatment and Refuse Disposal

Drainage systems are the piping network conveying liquid sewer from sanitary appliances to the point of sewage treatment. Sewage treatment, depending on the magnitude of the generated sewer might be kept simple as in septic tank and soak away pit or elaborate treatment plant. Solid wastes in high rise buildings are conveyed to the ground or basement floor through the refuse chute.

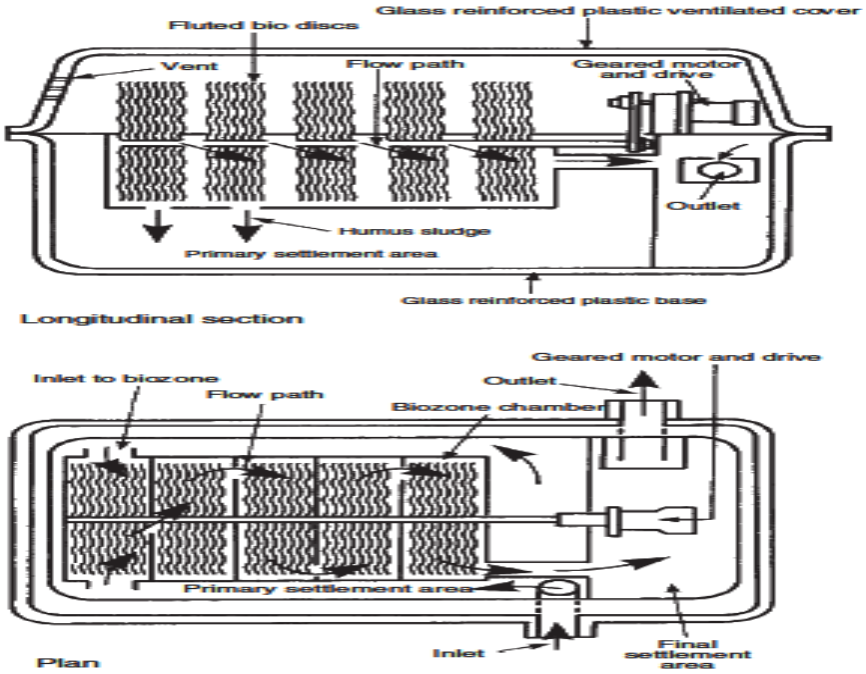

Figure 10. Biodisc sewage treatment plant

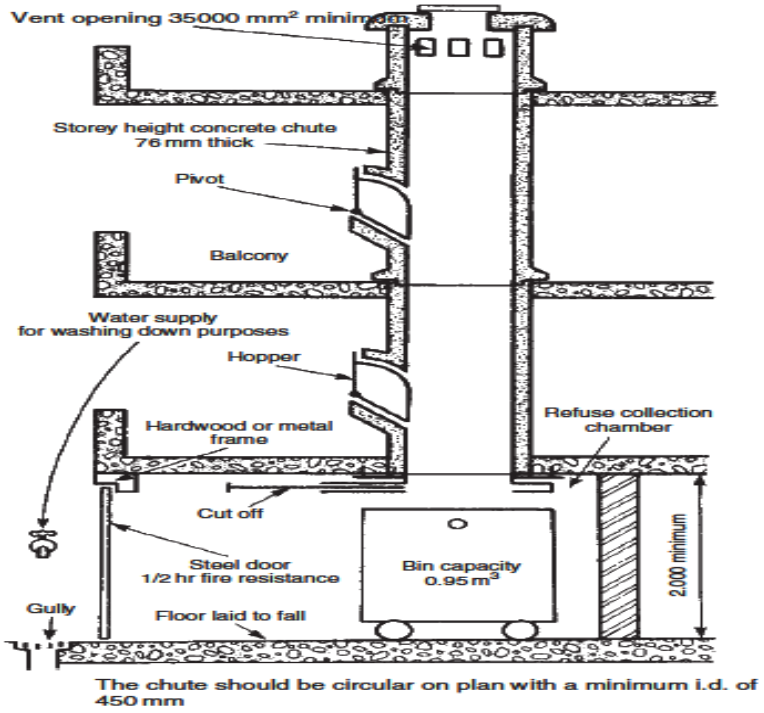

Figure 11. Refuse chute

2.8 Sanitary Appliances: Discharge and Waste Systems

Sanitary appliances have transformed from pure mechanical appliances to mechanical, electrical and electronic fixtures. For example, Jacuzzi is a glorified bath tub which is now not only bigger, but now has

inbuilt pumps, electric heater, water filter, water spray nozzles and electronic controls.

WC	7	discharge units
Shower	1	discharge unit
Basins	2	discharge units
Sinks	12	discharge units
Group	14	discharge units
Washing machine	4	discharge units
Dishwasher	4	discharge units

Total = 44 discharge units × 500 dwellings = 22000 discharge units.

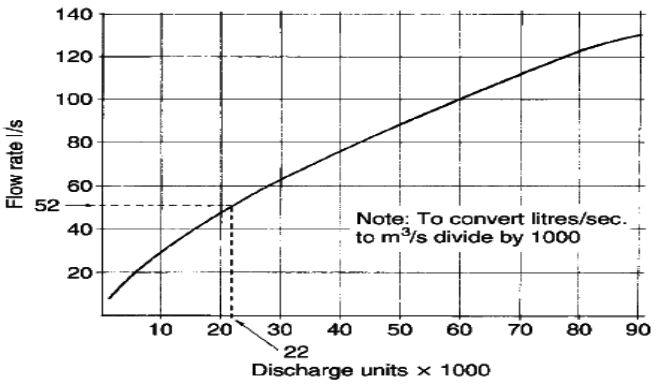

Figure 12. Calculation of drainage flow rate

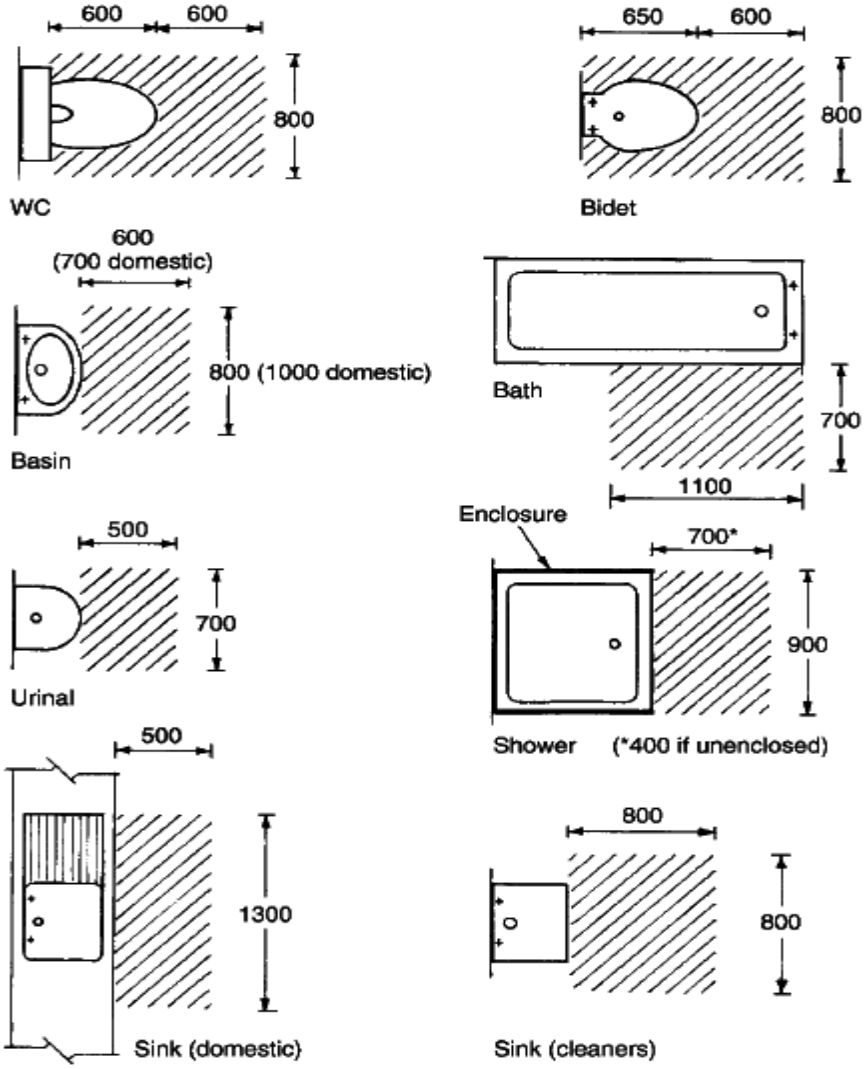

Figure 13. Typical activity spaces (mm) for plumbing fixtures

2.9 Gas Supply and Installation

Gas are stored under high pressure in pressure vessel and piped to point of use in the kitchen, laboratory, workshop or other applications.

2.10 Electrical Supply and Installations

This installation includes electricity distribution, power and lighting circuits, earthing system, light sources, lamps and luminaires and extral-low-voltage and telecommunications installation.

Table 4. Minimum provision of power sockets in domestic accommodation

Location	Minimum quantity of sockets
Living rooms	8
Kitchen	6
Master bedroom	6
Dining room	4
Study bedroom	4
Utility room	4
Single bedrooms	4
Hall and landing	2
Garage/workshop	2
Bathroom	1 – double insulated shaver socket

Maximum appliance load (watts) and plug cartridge fuse (BS 1362) selection for 230 volt supply:

Maximum load (W)	Plug fuse rating (amp)
230	1
460	2
690	3
1150	5
1610	7
2300	10
2900	13

Calculated from: Watts = Amps × Voltage.

Table 5. Examples of illumination levels and limiting glare indices for different activities:

Activity/location	Illuminance (lux)	Limiting glare index
Assembly work: (general)	250	25
(fine)	1000	22
Computer room	300	16
House	50 to 300*	n/a
Laboratory	500	16
Lecture/classroom	300	16
Offices: (general)	500	19
(drawing)	750	16
Public house bar	150	22
Shops/supermarkets	500	22
Restaurant	100	22

*Varies from 50 in bedrooms to 300 in kitchen and study.

2.11 Mechanical Conveyors- Lifts, Escalators and Travelators

To transport men, goods and food in the building, passenger lift, good lift, escalator, travelator and cleaning cradle are used.

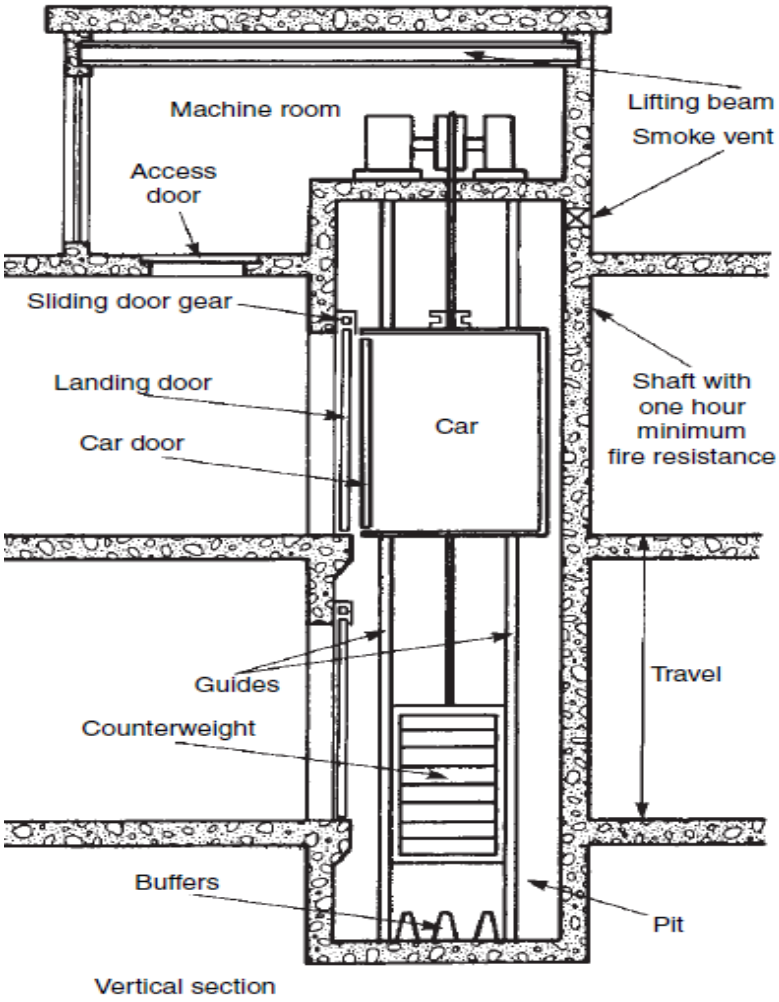

Figure 14. 2Electric Lift Installation

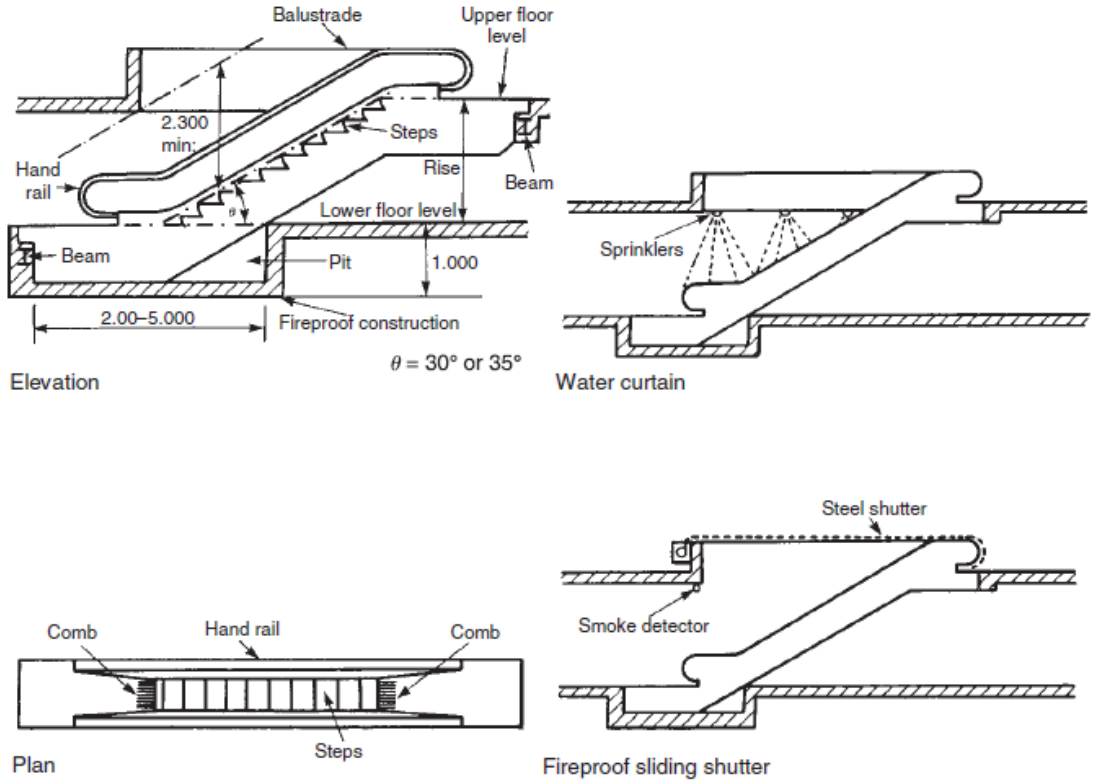

Figure15. Escalator

2.12 Fire Protection Systems

These are systems used to prevent, detect or fight fire outbreak. They include but not limited to fire hose reel, fire hydrant, automatic fire sprinkler systems, portable fire extinguishers, FM200 system, form installations, smoke, fire and heat detectors, fire alarms and fire pumps.

Fire outbreaks result in deaths, more injuries and loss of valuable properties. About a
tenth of all fires occur in homes resulting in deaths and injuries. An early warning device to detect smoke and fire could significantly reduce the number of human casualties. There smoke, heat, light obscuring and radiation detecting devices.

Smoke detectors are available in two basic types. Each can be powered by a simple battery cell or by mains electricity. The latter will normally have battery backup if the mains supply fails.

- Ionisation: an inexpensive device, sensitive to tiny smoke particles and fast burning fires such as a flaming chip pan.
- Light scattering or optical: this is more expensive but more sensitive in slow burning and smouldering fire produced by burning fabrics or upholstery and overheating PVC wiring.
- Combined: a unit containing both ionisation and optical detection.

Heat detectors are used where smoking is permitted and in other
situations where a smoke detector could be inadvertently actuated by process work in the building, e.g. a factory. Heat detectors are designed
to identify a fire in its more advanced stage, so their response time is longer than smoke detectors.

*Fusible type: has an alloy sensor with a thin walled casing fitted with heat collecting fins at its lower end. An electrical conductor passes through the centre. The casing has a fusible alloy lining and this functions as a second conductor. Heat melts the lining at a pre-determined temperature causing it to contact the central conductor and complete an alarm relay electrical circuit.

Bi-metallic coil type: heat passes through the cover to the bi-metal coils. Initially the lower coil receives greater heat than the upper coil. The lower coil responds by making contact with the upper coil to complete an electrical alarm circuit.

Light obscuring: a beam of light is projected across the protected area close to the ceiling. The light falls onto a photo-electric cell which produces a small electrical current for amplification and application to an alarm circuit. Smoke rising from a fire passes through the light beam to obscure and interrupt the amount of light falling on the photo-electric cell. The flow of electric current from the cell reduces sufficiently to activate an alarm relay.
A variation is the light-scatter type. In normal use the light is widely dispersed and no light reaches the photo-electric cell receptor. In the presence of smoke, particulates deflect light on to the receptor to energize the cell.

Laser beam: a band of light which can be visible or infra-red projected onto a photo-electric cell. It does not fan out or diffuse as it travels through an uninterrupted atmosphere. The beam can operate effectively at distances up to 100 m. If a fire occurs, smoke and heat rises and the pulsating beam is deflected away from the cell or reduced in intensity. As the cell is de-energised, this effects on alarm relay.

In addition to producing hot gases, fire also releases **radiant** energy in the form of visible light, infra-red and ultra-violet radiation. Radiant energy travels in waves from the fire.
Infra-red detector : detectors have a selective filter and lens to allow only infra-red radiation to fall on a photo-electric cell. Flames have a distinctive flicker, normally in the range of 4 to 15 Hz. The filter is used to exclude signals outside of this range. The amplifier is used to increase the current from the photo-electric cell. To reduce false alarms, a timing device operates the alarm a few seconds after the outbreak of fire.

Ultra-violet detector: these detectors have a gas-filled bulb which reacts with ultra-violet radiation. When the bulb receives radiant energy, the gas is ionised to produce an electric current. When this current exceeds the set point of the amplifier the alarm circuit closes to operate the alarm system.

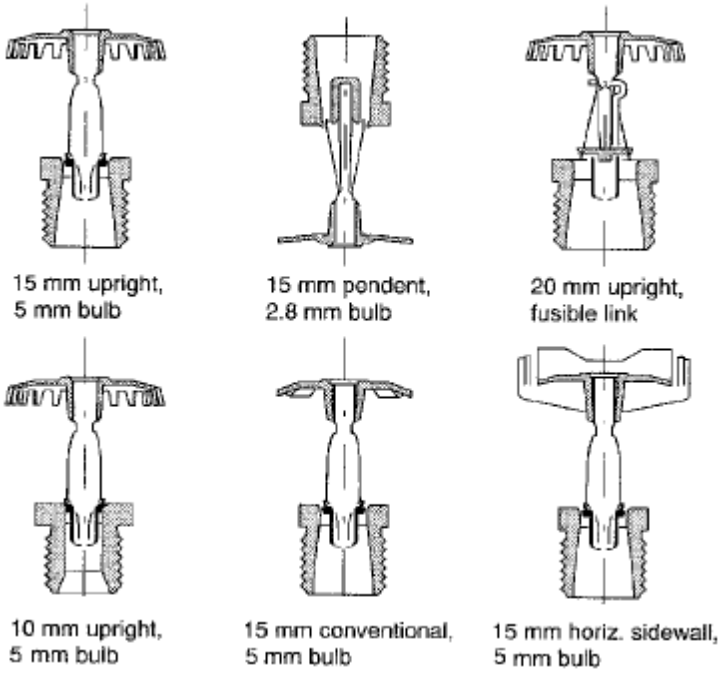

Figure16. Typical sprinklers (Knight and Jones, 2004)

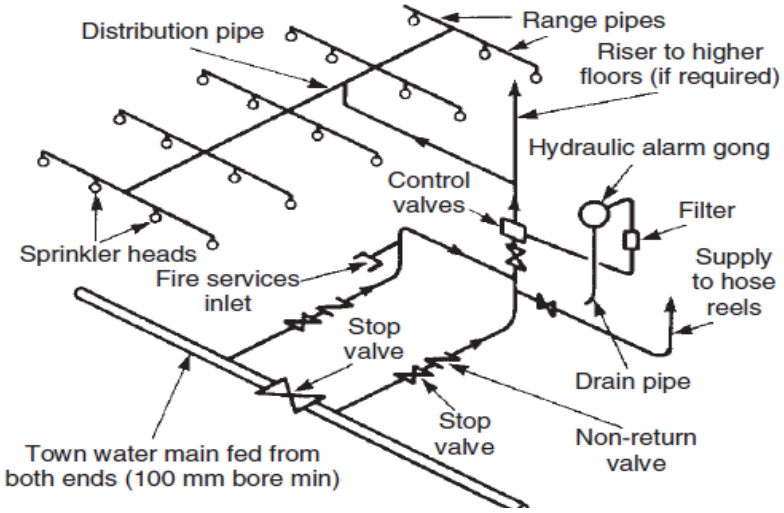

Figure 37. Wet Sprinkler Installation

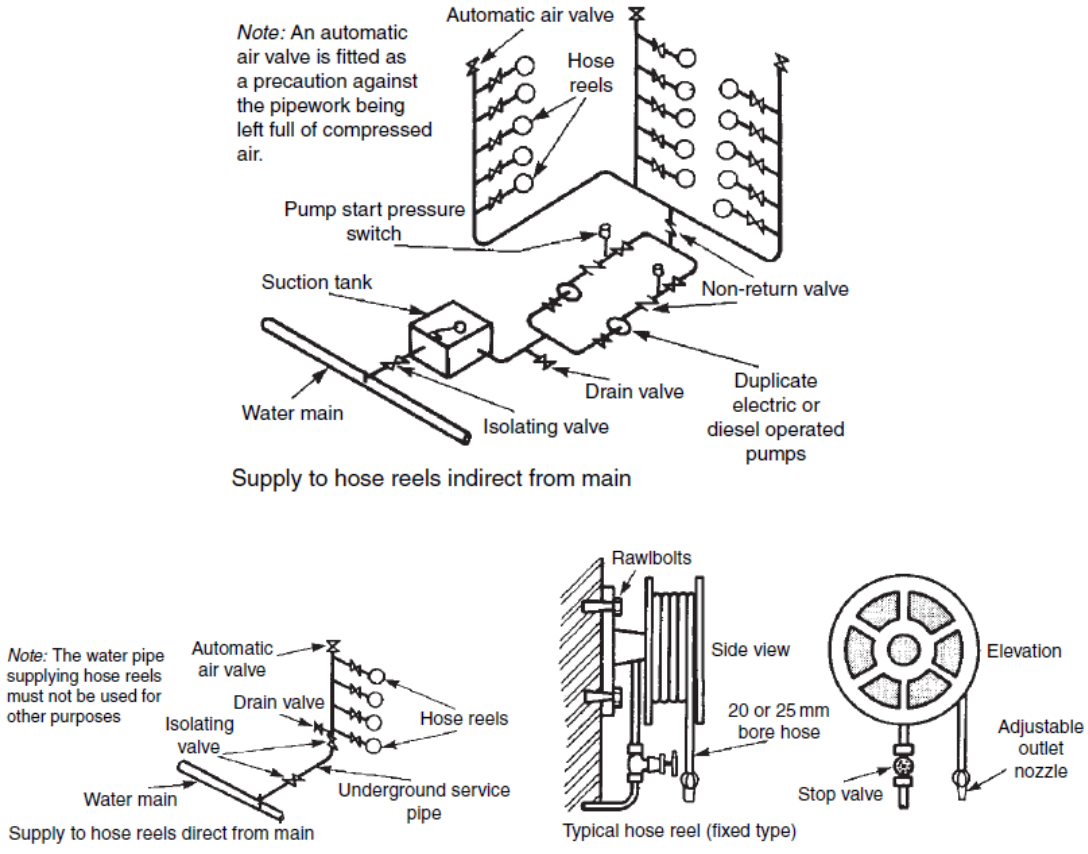

Figure 48. Hose Reel Installations

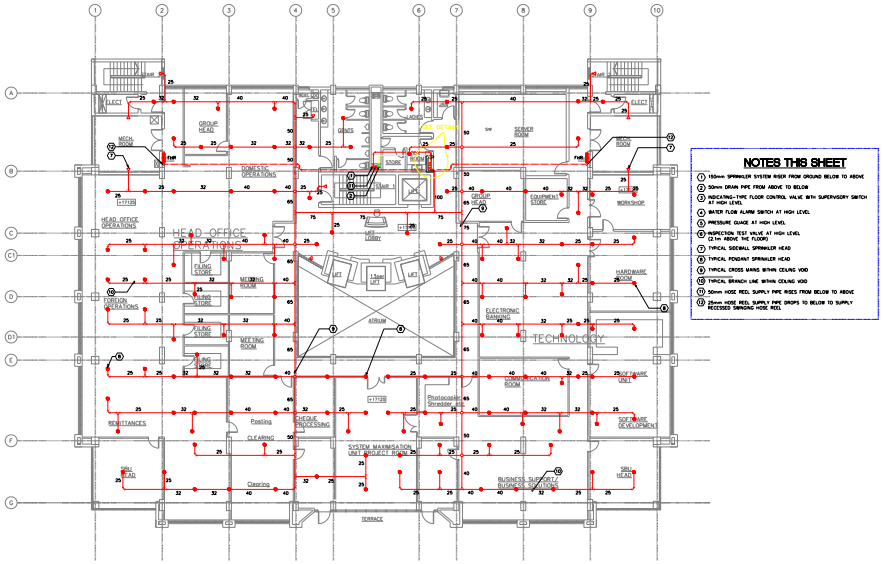

Figure 19. Sprinkler and Hose Reel System

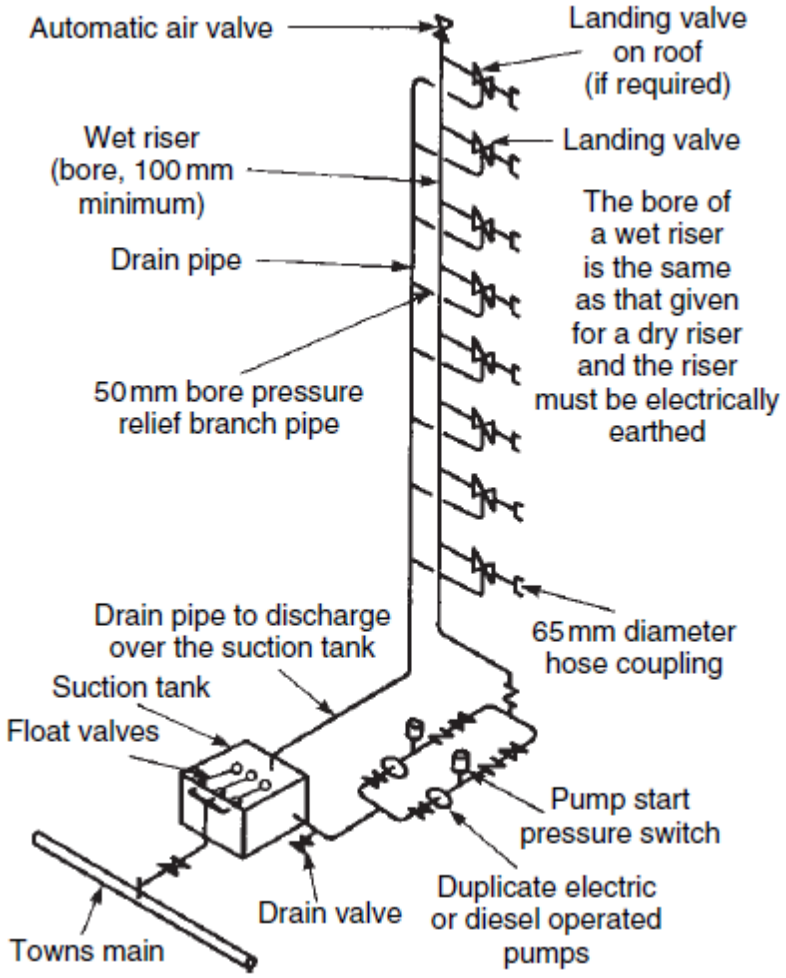

Figure 50. Typical arrangement of a wet riser

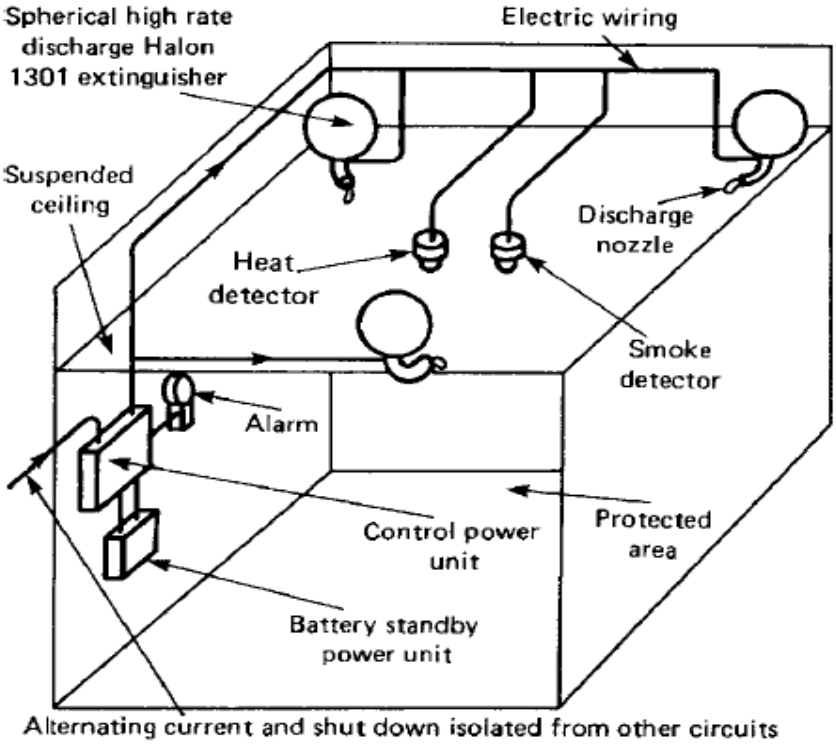

Figure 21.6 Gas Extinguishing Systems

2.13 Security Installations

Security installation includes access control devices (reader in- reader out), CCTV, intruder alarms, infra-red detectors, lightning protection fittings et cetera.

Intruder alarms have developed from a very limited specialist element of electrical installation work in high security buildings to the much wider market of schools, shops, offices, housing, etc. This is largely a result of the economics of sophisticated technology surpassing the efficiency of manual security. It is also a response to the increase in burglaries at a domestic level. Alarm components are an alarm bell or siren activated through a programmer from switches or activators.

Power is from mains electricity with a battery back-up. Extended links can also be established with the local police, a security company and the facility manager's central control by telecommunication connection.

Selection of switches to effect the alarm will depend on the building purpose, the extent of security specified, the building location and the construction features. Popular applications include:

- Micro-switch
- Magnetic reed
- Radio sensor
- Pressure mat
- Taut wiring
- Window strip
- Acoustic detector
- Vibration, impact or inertia detector

The alternative, which may also be integrated with switch systems, is space protection. This category of detectors includes:

- Ultrasonic
- Microwave
- Active infra-red
- Passive infra-red

2.14 Accommodation for Building Services

Building services are the dynamics of the building hence pathway must be provided and concealed from the occupant and general public as much as possible.

These are medium and large horizontal ducts, floor and skirting ducts, raised access floors, suspended and false ceilings, and subways.

Major equipment like power generator, air conditioning plant, water pump et cetera are kept in the plant room.

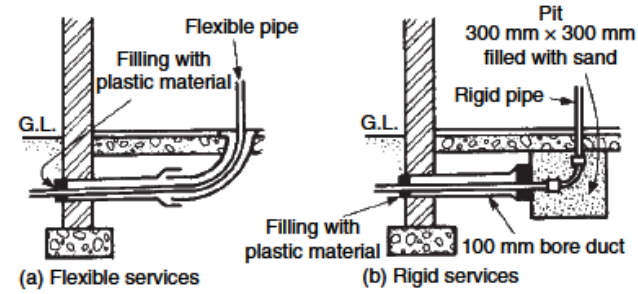

Ducts for entry of services into the building

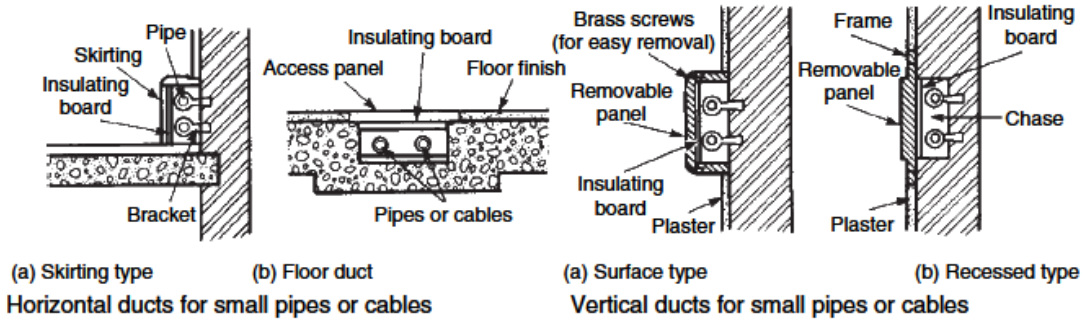

Horizontal ducts for small pipes or cables

Vertical ducts for small pipes or cables

Figure 72. Sleeves, horizontal and vertical ducts for pipes or cables

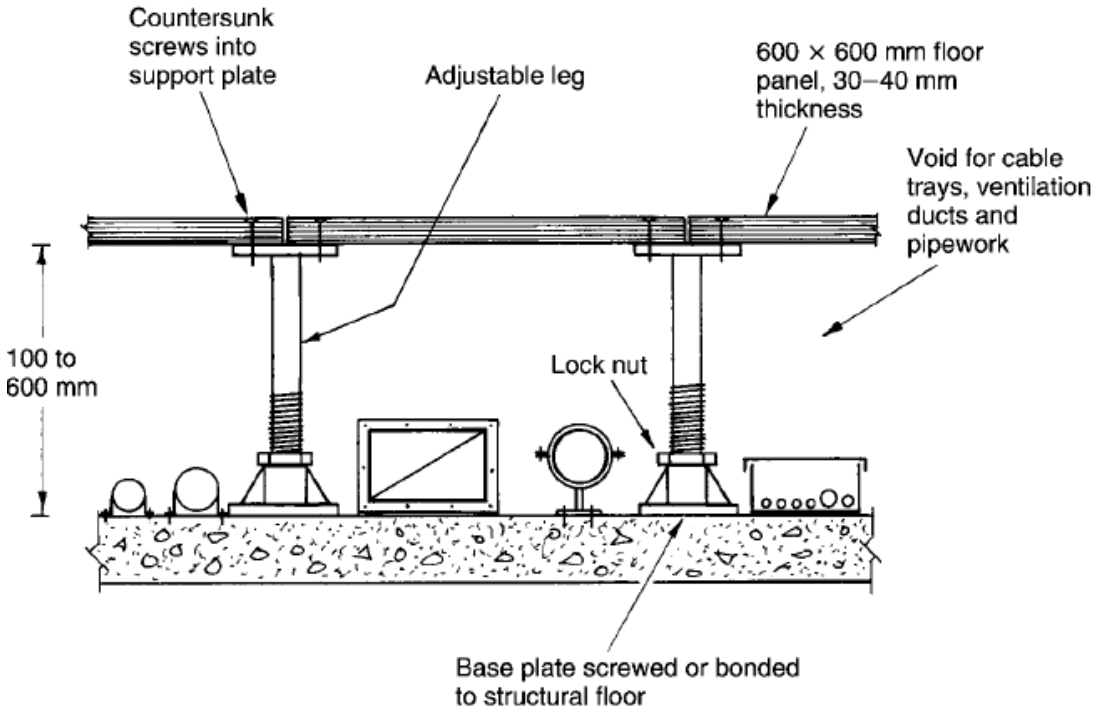

Figure 83. Raised accessed floor

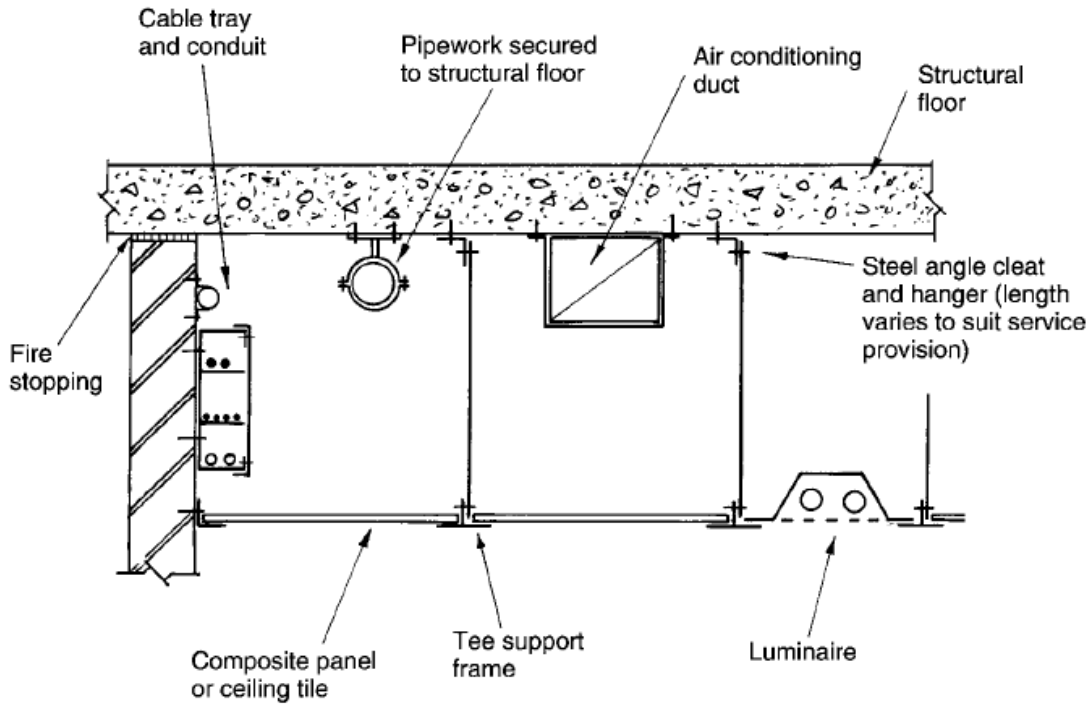

Figure 94. Typical suspended ceiling

3.0 Alternative and Renewable Energy

There quite a number of alternative and renewable energy sources such as wind, fuel cells, water power, geothermal, solar power, photovoltaic and biomass/biofuel.

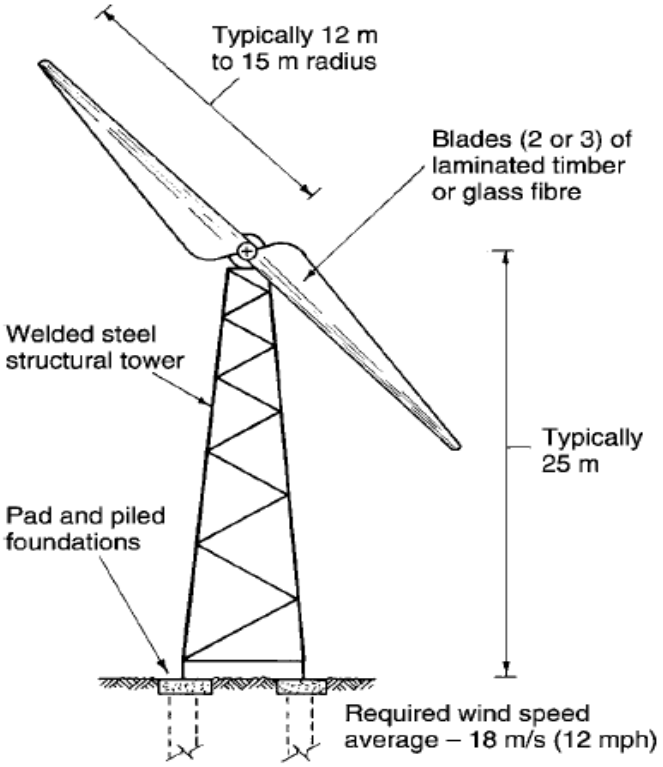

Figure 25. Wind power generator

Solar Pond (Babalola,2009):

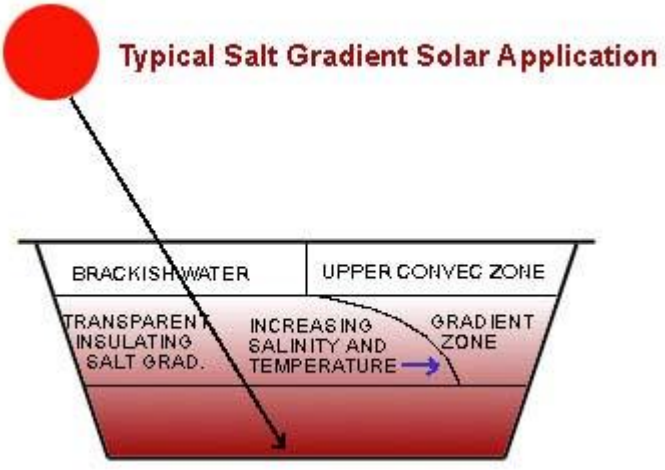

Figure 26. Generic solar pond showing density and temperature gradient

Due to diffusion (though very small indeed) of salt upwards from the higher to lower concentration, the salt gradient will be affected gradually. The rate of movement of salt flux upwards q_s is given by:

$$q_s = vs - k_s \frac{\partial s}{\partial z}$$

where k_s is the coefficient of salt diffusivity, v is the velocity, s is salt concentration and z is depth. Thus, if water is removed from the bottom of the pond to give v a value

$$v = \frac{1}{s}\left(k_s \frac{\partial s}{\partial z}\right)$$

then $q_s = 0$ and salt remain stationary in space. This is known as 'falling pond' concept (19). A flow system to carefully add salt to the bottom at the top had been developed.

Some recent ponds used salt (e.g. borax or potassium nitrate) which exhibits a high increase in solubility with increase in temperature. The pond is filled with a saturated solution with left over at the bottom. When the pond is heated up, more salt goes into solution and convection does not occur. Even some are with transparent membranes that separate the layers. This pond does not even need salt at all.

Generally, inexpensive layer of transparent plastic over the water will suppress heat loss to the environment.

Solar radiation incident upon a horizontal surface of the earth is a function of latitude, the day of the year, the time of the day and the atmospheric conditions. The energy is received as both direct and diffuse radiation and is distributed over the spectrum in the ultraviolet, visible, and infrared.
Fraction of the radiation reaching the surface of the pond will be reflected and the remainder that penetrate the pond result in thermal energy. This fraction in a day can be calculated from the following equations which are obtained from Fresnel's equation (22):

$$E = 2n(a^2 + b^2)\cos i \cos r$$

$$a = 1/(\cos r + n\cos i)$$

$$b = (\cos i + n\cos r)$$

where E is the ratio of radiation penetrating the water surface and incident upon a horizontal plane just below the surface to the radiation incident upon a horizontal plane above the water surface and incident upon a horizontal plane just below the surface to the radiation incident upon a horizontal plane above the water surface; i = the angle made by the incident radiation with the normal (solar zenith distance); n = indexes of refraction of the salt-water solution at the surface (≈1.33 for very dilute solution); and r = the angle made by the refracted ray with the normal.

From Snell's law: $\sin i = n \sin r$

Fraction of diffuse radiation $2\int_0^{\pi} E \cos i \sin i \, \partial i$

The solar zenith distance can be measured or calculated by

$$\cos i = \cos \emptyset \cos \delta \sin 2\pi (t-6)/24 + \sin \emptyset \sin \delta$$

t = time in hours (noon =12)

Ø = declination of the sun ≈

$\delta \sin 2\pi D/365.25$
δ_0 = declination of the sun at equinox

= 23 degree, 27 minutes

D = number of days

From Bonguer's law, transmitted radiation

$$q_\lambda^t = q_\lambda^i e^{-\alpha Z}$$

Where q_λ^i is the intensity of the incident radiation of wavelength λ

α_λ is spectral absorption coefficient

z is the thickness of homogeneous absorber.

Therefore, the spectral transmittance is

$$\tau_\lambda = q_\lambda^t / q_\lambda^i = e^{-\alpha_\lambda Z}$$

and the spectral absorption coefficient is expressed by

$$\alpha_\lambda = \left(\frac{1}{s}\right) \ln \tau_\lambda$$

The heat transfer processes in the solar pond is governed by one-dimensional time-dependent heat conduction equation

$$\frac{\partial T}{\partial t}\rho c = \frac{\partial (K \frac{\partial T}{\partial z})}{\partial z} + q - q_s$$

in which ρ is the fluid density; c is specific heat of fluid; T is temperature; t is time; z is vertical coordinate; K is coefficient of heat diffusion; q is source of thermal energy and q_s is removal rate of thermal energy. A complete treatment is of course complex because of the large number of variables involved.

According to Hull , the thermal efficiency of solar pond is

$$= \alpha\tau = \frac{K\Delta T}{Z_{NCZ} H_S}$$

where ΔT is the temperature difference across the NCZ and H_S is the surface insolation.

Various methods are employed to extract heat energy from the pond. This may be done by applying heat-exchanger equations:

$$q = m_c C_{pc} (T_{co} - T_{ci}) \quad (1)$$

$$q = m_h C_{ph} (T_{hi} - T_{ho}) \quad (2)$$

$$q = UA\Delta_c T_{LM} \quad (3)$$

subscripts c, h refer to cold and hot fluid,

i, o denote inlet and outlet

Another way is the use of hydrodynamic layer flow principle where by the hot fluid
is removed at one end into a heat-exchanger external to the pond and then returns the solution to the other end of the pond.

Some applications of solar ponds are for heating and cooling of buildings, and power production.

Heat energy stored in the pond may be used for space heating during the harmattan season. The heat energy is transferred into Air Handling Unit (AHU) containing heat exchanger coil and fan that blows heated air into the space. This arrangement can be incorporated into office complex and estate in the future. Also, hot water can be extracted from the pond for domestic or industrial needs. A typical application is heating of greenhouse in U.S.A.

Cooling can be achieved by absorption refrigeration system with generator heated with solar pond. The chiller side of the refrigerator will then be part of A.H.U.

With suitable fluid (Freons) and two heat exchangers-one on the upper cold water and one on the lower hot water, it is possible to operate a heat engine for power production . This is the most promising application of solar pond especially for small developing countries.

4. Conclusion.

Most electromechanical systems in building are energy consuming. However, with proper design, energy consumption can be reduced or totally eliminated. Also, energy required could be totally met or at least augmented using appropriate renewable energy sources peculiar to the location.

Reference

Babalola P.O., 2009. Non-convective solar pond as a thermal energy source, International Conference/Workshop on Renewable Energy and Climate Change Mitigation, Covenant University, Ota, Nigeria

John Knight and Peter Jones, 2004. Newnes Building Services Pocket Book, Elsevier Limited, Second Edition, Amsterdam, pp.313

Roger Greeno and Fred Hall, 2009. Building Services Handbook, Butterworth- Heinemann, Oxford, pp.3
http://www.engineeringtoolbox.com/electrical-equipment-power-consumption- d_119.html.

Antai: Proc. ICCEM (2012) 115 - 125

Title of Paper: Environmental Liquid Effluents, A Novel Approach For Treatment Of Industrial Waste Water

Antai, E.E.
Department of Mechanical Engineering, Akwa Ibom State University, Ikot Akpaden-Mkpat Enin, Akwa Ibom State. Nigeria Email: antai4eisl@yahoo.com

Abstract

Nutrient enrichment or eutrophication of aquatic ecosystems can cause an increase in algae and aquatic plants, loss of component species, and loss of ecosystem function. For these reasons, numerous studies were focused on nitrogen and phosphorus removal from wastewater streams. Most of these studies were based on biological processes and different combinations of anaerobic, aerobic, and anoxic zones such as Bardenpho, A_2O, UCT, and their modifications. Hence phosphate recovery from sewage is in synergy with reducing other environmental impacts and making it a long term economic resource. The aim of the novel treatment process is to highlight on studies investigated for the nutrient removal performance using Chorella-vulgaris at different nitrogen and phosphorus concentrations. The effect of ammonia nitrogen and phosphorus concentration on removal of these nutrients from synthetic wastewater by algae Chorella-vulgaris in batch cultivation have been investigated in this study and kinetic coefficients were determined. It is observed that an effluent may contain specific nutrients valuable for recovery and this observation may lead to the idea or understanding of treating an effluent from industrial source as a useful resource instead of the general idea of treating the effluent as waste products, and in the same process losing money in terms of expenses on chemicals and energy. Treatment and discharge of effluents into the receiving streams should not be an issue that will be considered as usual because there are specified standards required by the legislation, in terms of the quality and characteristic of the effluent before it is discharged into the waterways.

***Key words**: Liquid Effluents, Municipal waste water, Chorella-vulgaris, kinetic coefficients*

1. Introduction

For simplicity and clarity, the subject of waste water may be divided into three categories namely; domestic or sewage, industrial and municipal waste water. However municipal liquid effluents may further be classified as effluents from both domestic sewage and industrial sources.

Waste water contains a mixture of complex organic and inorganic matters combined with man- made substances. It also contains material washed from road and roofs as well as contaminated underground water which may run into the sewer system; thereby forming a complex waste water which will inevitably require some form of treatment before being discharged into receiving streams. According to Gray (1999), the strength and composition of sewage varies on hourly, daily and seasonal basis which also depends on individual water usage, infiltration, surface run off, local habits and diet.

The constituents of waste water may be categorized into physical, chemical and biological parameters. Physical include temperature, odour, turbidity, oil and grease etc. Solids are classified into dissolved, suspended as well as organic (volatile) and inorganic, (fixed) fractions.

Chemical organic parameters are BOD, COD, TOC, TOD and inorganic parameters may include pH acidity and Alkanity, salinity, chloride nitrate, ionized metals etc.

Biological parameters are Coli-forms, specific pathogen and viruses. All the constituents and concentration vary with time and local conditions (Metcalf and Eddy, 1991). But Kiely (1998) considers oil and grease as chemical organic and also Bacteria, Algae and protozoa are included as bacteriological parameters. Hence the characteristics of waste water may depend on the season of the year and may also vary in weekdays and holidays. Summer period discharges 10 – 20% more than winter and Industries discharges minimized on Sundays.

1.1 Composition Municipal Waste Water

The waste water composition contains about 70% organic matter and 30% inorganic. The volume of the domestic effluents discharged into

sewer in a community varies from 50 to 250 gal per person depending on the sewer uses (Gray, 1999). Municipal effluents are low strength waste compared with industrial waste water that contains high strength waste of hazardous chemicals like phenols etc (Kiely, 1998). The solids content found in urban waste water can be classified into suspended and filterable solid. The suspended solid consist of settleable and non settleable accounting for 30.5% of the total solid. The filterable solid comprises of colloidal and dissolved solids given as 69.5% (Boari et al, 1997). Municipal waste water contain 75% SS and greater than 50% filterable solids of organic in nature and their sources are from animal, plants and synthesis of organic compounds. The organic material found in effluent include protein 40-60%, carbohydrates 25 – 50%, fats and oil -10% and some traces of phosphorus, sulphur compounds etc (Boari et al, 1997)

The composition of inorganic substances can have metal contents of salts associated with it, which include nitrate phosphorus, sulphur, chlorine and their compounds. The source of nitrate and phosphorus in domestic sewage is from human excreta and phosphorus specifically due to the use of detergents. The total nitrogen is categorised into organic (containing biodegradable and non-biodegradable) account for 25% and inorganic nitrogen given as 75% containing ammonia nitrogen (Boari et al, 1997). In UK, the nutrient production per capita is 5.9g N per day and 2.0g P per day (Gray, 1999).

Table 1.0 *Major Composition of untreated Domestic waste water*

Constituents	Concentration mg/l Weak	Medium	Strong
Total solid (TS)	350	720	1200
Total dissolved solid (TDS)	250	500	850
Suspended solid (SS)	100	220	350
Nitrogen (N)	20	40	85
Phosphorus (P)	4	8	15
Chloride	30	50	100
Alkalinity (as $CaCO_3$)	50	100	200
Grease	50	100	150
BOD at 20^{o}C Over 5 days	110	220	400
COD	250	500	1000

Source: Adapted from Metcalf and Eddy inc. 1991

1.2 Composition Industrial Waste Water

Within municipal limits it is often a conventional practice for Industries to pre-treat their effluents before discharge into sewer system due to the nature of toxicity and treatability of the waste water. It considerably varies from one industry to another (Gray, 1999).

It is quite normal for Industrial waste water to have a strong odour due to the presence of phenol and sulphur compounds etc. generated in gas industries, refineries and other chemical processing plants.

The color of industrial waste water is also affected due to the presence of organic materials such as blue copper and green nickel. Yellow and brown iron may also be found in industrial waste effluent from textile, paper, and food processing industries. (Boari et al, 1997) mentioned that, the coloring may also be due to the presences of oily material such as fat and lubricants found in the waste water.

Recent studies (Hammer et al, 2004) show the average characteristics of selected Industrial waste waters. It is advisable that the pre-treatment process at industrial site must be considered for high strength waste water, different from domestic waste water. By comparing effluents from domestic sources with some selected industries listed in table 1.1, it is observed that the BOD contents is 5- 20 times greater than domestic effluent and the level of total solids vary significantly. (Hammer et al, 2004).

Table 1.1 Average characteristics of selected Industrial waste waters

Constituents	Milk Processing	Meat Packing	Synthetic Textile	Chlorophenolic Manufacture
BOD, mg/l	1000	1400	1500	4300
COD, mg/l	1900	2100	3300	5400
Total solids, mg/l	1600	3300	8000	53000
Suspended solids, mg/l	300	1000	2000	1200
Nitrogen, mg N/l	50	150	30	0
Phosphorus, mg/l	12	16	0	0
pH	7	7	5	7
Temperature ^{o}C	29	28	-	-
Grease, mg/l	-	500	-	-
Chloride, mg/l	-	-	-	27, 000
Phenols, mg/l	-	-	-	140

Source: Hammer et al. water and Waste water Technology. International Ed.

1.3 Environmental Effects

(Mara et al, 1992) and (Sung et al, 1977), in their study mentioned that the presence of endocrine in municipal sewage treatment plant (STP) is responsible for the environmental effect observed in the aquatic environment concerning the reproductive system. For instance feminisation of male fishes within the STP effluents. They explained that the chemical substance responsible for this harmful effects are yet unknown and still under investigations; but the presence of substance like nonylphenols, phthalic esters, PCB`s, Dioxins. Phyto-estrogens and human estrogens are suspected to influence the hormonal system. (Russell and Gordon,1971).

From hypothesis (Richardson et al, 2001).based on the statistically derived data; commented on the disorder relating to male infertility, low sperm count, testicular cancer, etc. to be caused by the intake of estrogens in drinking water. This they explained that as drugs are used in medicine to influence the endocrine (hormonal)system e.g. contraceptives used as ingredients of birth control pills are excreted after ingestion into the municipal sewage.

In general these pharmaceuticals and natural hormones would have to pass through an STP prior to entering rivers or streams. Hence a precise quantification of natural estrogens and contraceptives in STP effluents is essential for risk assessment regarding the endocrine disruption in aquatic environment.

1.4 Application of Nutrient Recovery from Wastewater Streams

The detergent phosphate industry recognises that phosphate is the only recyclable components in detergents. More importantly weather phosphate is used for detergent or not the fact remains that the bulk of phosphate in sewage comes from natural human emissions.

Practically, biological-removal in sewage works is a process which may require higher investment cost and requires better process engineering; but the advantage is such that it avoids chemical consumption and subsequent disposal can be combined with different technologies with recovery of the phosphate and nitrogen for recycling.

This therefore makes it a target for sustainable sewage treatment i.e., making sewage a resource rather than continue to treat it as a waste with the loss of nutrients and increasing energy consumption, chemical use and greenhouse emissions.

The Ostara process, developed by the University of British Columbia has been proved to be a success in many sewage plants in Canada and USA and it is now being tested in China, Israel and the UK. The process allows for the recovery of phosphate from sewage world operating biological P- removal, as struvite, a high quality slow release fertiliser with high economic value.

Recycling of phosphate, Nitrogen and organics from wastewater such as municipal sewage treatment plants or even animal manure directly

contributes to reducing green house gas emissions.

1.5 Other Application Process

- ***1.5.1*** *Direct recycling of sewage nutrients*
- ***1.5.2*** *Phosphorus recovery by precipitation*
- ***1.5.3*** *Operational Struvite recovery*
- ***1.5.4*** *Calcium phosphate precipitation*
- *1.5.5 Sludge incineration by ash*

2. Review of Relevant Literature

2.1 A Novel Approach

Novel treatment approaches have been developed for treatment of effluents either from industrial and municipal sewage treatment plants. The studies reveals that the Novel processes being developed are capable of extracting and recovering several nutrients like phosphorus, Nitrogen, Organic, Estrogens', indirubin, etc; from wastewater streams.

An international conference on nutrient recovery form wastewater streams held in Vancouver May 10^{th} to 13^{th} 2009; confirmed the increasing recognition that recycling of Phosphorus and Nitrogen will be essential for a sustainable development.

To this end, a novel approach was tested in Oregon, involving the online monitoring of ammonia in Municipal STP`s. Also the batch kinetics of nitrogen and phosphorus removal from synthetic wastewater using algae has also been tested.

Due to the broad scope, quantity and application of both industrial and municipal wastewater effluents; the future role of the use of sewage effluent for irrigation in the Middle East has been considered. Hence based on these studies, the physiochemical treatment of both industrial and municipal effluents as a process can be optimised to treat an effluent according to the specific makeup or characteristics of the contamination.

Examples of some innovative processes or novel approaches may combine two or more operational steps easily performed on site. A more practical example was the study of the behaviour and occurrence of estrogens in municipal STP`s, this novel process which was investigated in Germany, Canada and Brazil was found to be effective in quantifying the level and amount or quantity of estrogens in municipal sewage samples.

Using the method for investigating the behaviour and occurrence of natural estrogens and synthetic contraceptives in municipal STP`s, it was discovered that the mean recoveries of the analytes in ground water after extraction ,clean-up and derivation was generally above 75%.

In recent study (Clayton et al, 1999) a sewage treatment plant in Germany close to Frankfort main was determined to have been contained with 17β-estradiol and estrogens with mean concentrations' 0.015µg/L and 0.027µg/L respectively. Similarly investigations carried out in Canada and Brazil also discovered that the STP discharges estrogens

Studies on treatment of industrial liquid effluents (Daniels et al ,1977) laid emphasis on the fact that Global biochemical cycles have been largely affected by human activities thus increasing the input of nutrients into biochemical cycles through agricultural practices, urbanization, industrialization, and other alterations, especially nitrogen and phosphorus.

The aim of these studies was to evaluate the ammonium nitrogen removal performance of algae culture (*Chlorella vulgaris)* in a novel approach using an immobilized photo-bioreactor system under different operating conditions and to determine the bio-kinetic coefficients using the Stover-Kincannon model.

In these approaches batch experiments were performed to determine the effect of initial nitrogen and phosphorus concentration on nutrients removal performance of microalgae (*chorella vulgaris)* and to obtain bio-kinetic coefficients such as K, reaction rate constant K_m, half reaction rate constant and yield coefficients using "Michaells-Menten" rate expression.

Other study (Curtis, 1994) reveals that Immobilization techniques have been applied to algae to solve harvesting problems encountered in suspended growth systems. Internal immobilization (of *Chlorella vulgaris)* in sodium-alginate beads provided higher nutrient removal from raw sewage treatment compared to external immobilization on polyurethane foam.

3. Materials and Methods

3.1 Microorganism

The green algae (*C. Vulgaris)* should be used for the process. The diagram below shows the cycle of nutrient flow in the proposed treatment system, where manure from dairy cows in free-stall barns could be mechanically scraped (or flushed with water) and the resultant manure slurry subjected to a solid separation step prior to treatment of the solids by composting and treatment of the effluent by anaerobic digestion and algal scrubbing. Values for input N and P, was emphasised in (Van Horn et al., 1994). Biomass from the algal scrubbers can either be recycled into farm operations as a feed supplement or fertilizer or exported from the farm.

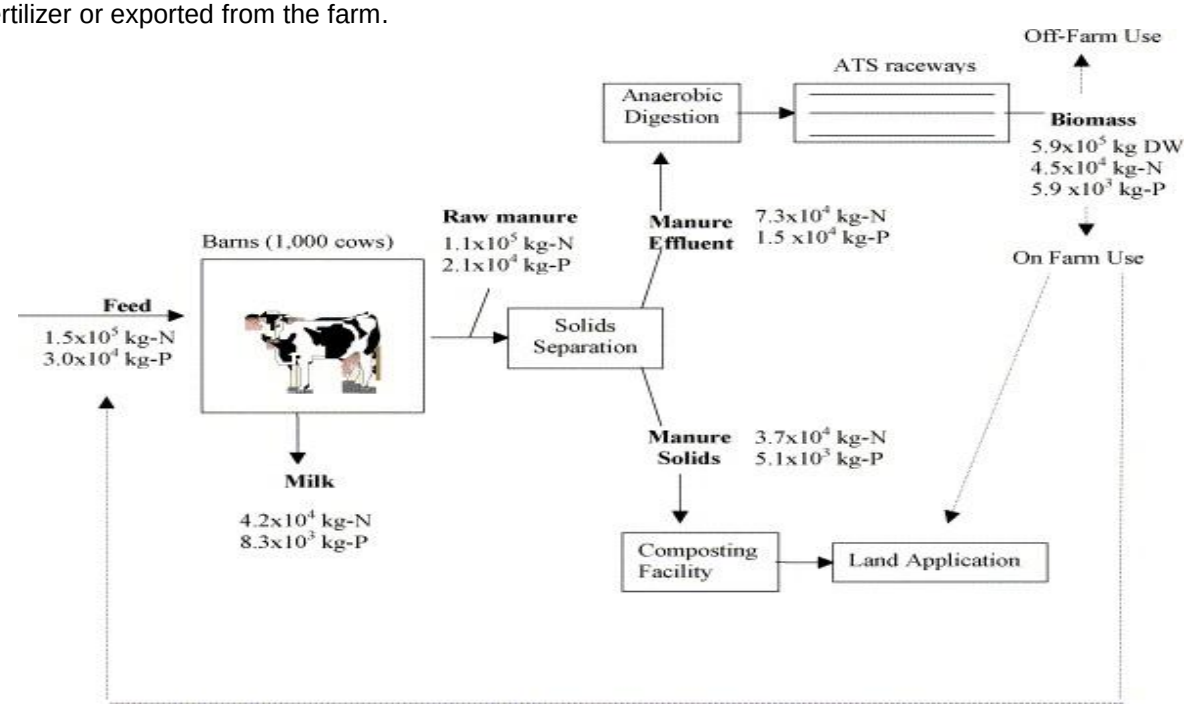

Figure 3.1 *Schematic diagram of nutrient flow in the proposed treatment system. Source: Van Horn et al, 1994*

Figure 3.2 below shows a Schematic diagram of an algae turf scrubbers (ATS) unit with associated equipment and water reservoir. Manure effluent is added continuously to the equalization reservoir. Algal biomass is harvested weekly, removed from ATS effluent using a mechanical rake, dewatered with a screw press, and dried using a belt drier. A 1000-animal farm-scale system would be composed of eleven ATS units that would share reservoirs and the harvesting, dewatering, and drying equipment.

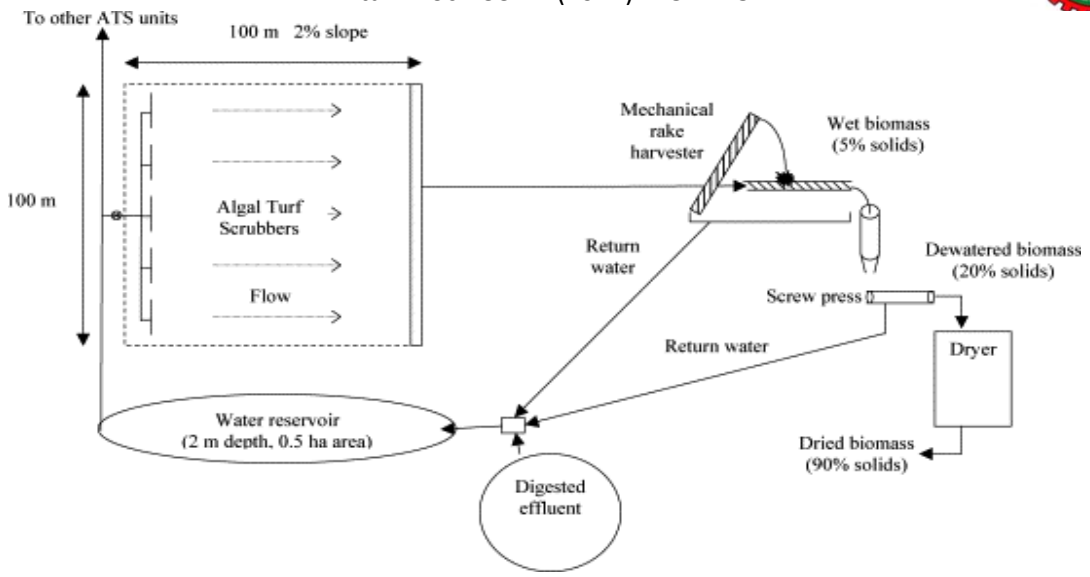

Figure 3.2 *Schematic diagram of 1ha ATS unit with associated equipment and water reservoir*
Source: Van Horn et al, 1994

3.2 Culture Medium

Synthetic wastewater was used throughout the experiments. The growth media contained: $MgSO_4 \cdot 7H_2O$, 1000 mg l^{-1}; $CaCl_2$, 84 mg $l^{-1}$and 0.5 ml of trace elements.

NH_4Cl and KH_2PO_4 were used as nitrogen and phosphorus sources, respectively. The trace elements were composed of H_3BO_3, 57 mg l^{-1}; $FeSO_4 \cdot 7H_2O$, 25 mg l^{-1}; $ZnSO_4 \cdot 7H_2O$, 44 mg l^{-1}; $MnCl_2 \cdot 4H_2O$, 7 mg l^{-1}; MoO_3, 35 mg l^{-1}; $CuSO_4 \cdot 5H_2O$, 8 mg l^{-1}; $Cu(NO_3)_2 \cdot 6H_2O$, 2.5 mg l^{-1}; Na_2EDTA, 250 mg l^{-1}; and $NaHCO_3$, 2500 mg l^{-1}.

3.3 Experimental Set-Up

The experiments were conducted in batch by using 1000 ml flasks. At the beginning of each series of experiments, 800 ml of culture medium was inoculated to flasks with a suspension of pre-cultured cells.

The initial chlorophyll *a* (chl *a*) concentration was kept constant around 3.5 ± 0.5 mg l^{-1} throughout the experiments. NH_4-N concentration was varied between 13.2–410 mg l^{-1} while PO_4-P concentration was between 7.7–199 mg l^{-1} by keeping N/P ratio around 2/1.

The flasks were aerated to provide CO_2 and for mixing via an air pump. The pH was maintained at 6.5–7.0 by the addition of 5% potassium hydroxide (KOH) and 10% acetic acid (CH_3COOH) solutions. Illumination was provided continuously from one side of the flasks by using 36 W/54 fluorescent lamps with 4100 flux and continuous illumination.

Light intensity was measured by a digital light meter (Luxeron LX-1108). The experiments were conducted at room temperature (20 ± 2 °C) for 10 days.

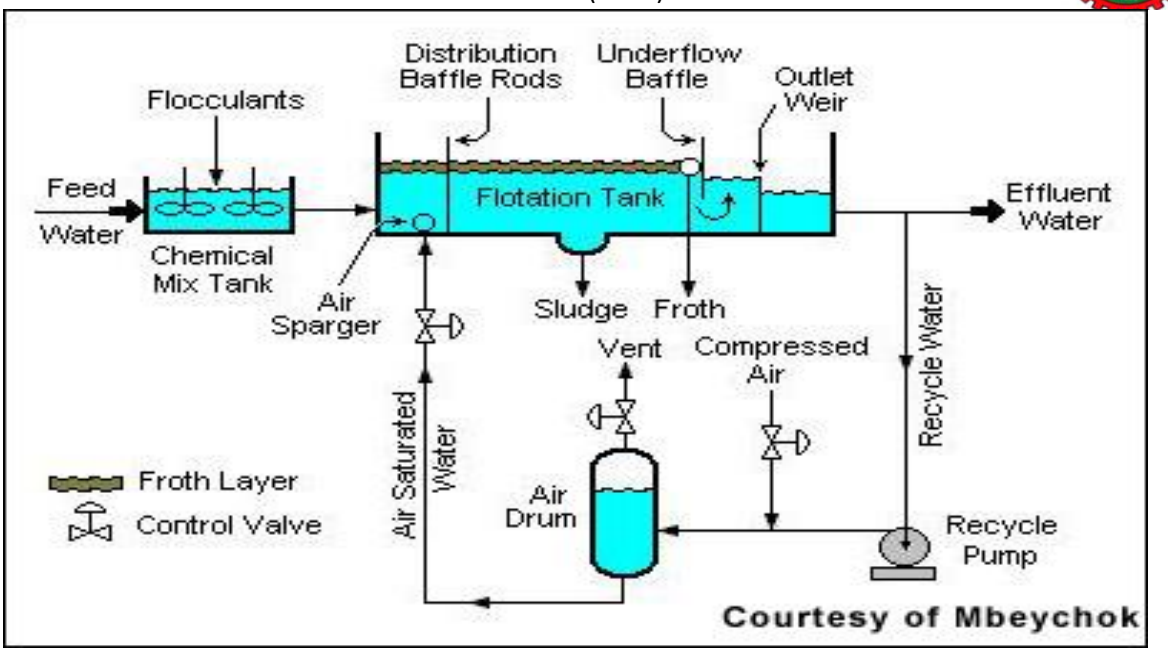

Figure 3.3 *Schematic diagram shows typical flow arrangement for effluent treatment incorporating recycle water fed back via a recycle pump.*
Source: http://www.water-technology.net/projects/tianjinjejuan/tianjinjejuan2.html

3.4 Analytical methods

Ammonia, nitrogen, phosphorus, and Chlorophyll a concentrations were monitored on the samples. Daily samples withdrawn from flasks were centrifuged at 5000–6000 rpm to separate algae. NH_4-N and PO_4-P measurements were carried out in clear supernatant by colorimetric method using phenate and vanadomolybdolo-phosphoric acid with standard deviations of ±0.025 and ±0.08, respectively (Culp et al,1978)

To determine the Chlorophyll a content, 10 ml of algal suspension was centrifuged at 3000 rpm for 30 min and the supernatant was discarded. The algae were suspended in 3 ml of methanol and heated for about 5 min in a water bath. The samples were cooled to room temperature and then the volume was made up to 5 ml by adding methanol. The chl a concentration in the extract was calculated by reading the absorption (A) of the pigment extract in a spectrophotometer at the given wavelength against a solvent blank by using the equation:
Chlorophyll a (mg/L) = $(16.5 \times A_{665}) - (8.3 \times A_{650})$ (Culp et al,1978).
The result of the above experiment showed that batch kinetics coefficients of NH_4-N and PO_4-P removal by C. vulgaris were determined by changing the initial concentrations of corresponding nutrients in the media. The initial Chlorophyll a content was 3.0 ± 0.5 mg l^{-1} at all experimental conditions. Variations of nutrient concentrations were monitored daily and the specific substrate utilization rates were calculated.

4. Discussion of Results

A photo bioreactor was continuously operated at different initial ammonium nitrogen concentrations (NH_4-N_0 = 10-48 mg L^{-1}), hydraulic retention times (HRT = 1.7-5.5 days) and nitrogen/phosphorus ratios (N/P = 4/1-13/1).
Effluent NH_4-N concentrations varied between 2.1 ± 0.5 mg L^{-1} and 26 ± 1.2 mg L^{-1} with increasing initial NH_4-N concentrations from 10 ± 0.6 mg L^{-1} to 48 ± 1.8 mg L^{-1} at θ_H = 2.7 days. The maximum

removal efficiency was obtained as 79 ± 4.5% at 10 mg L^{-1} NH_4-N concentration.
Operating the system for longer HRT improved the effluent quality, and the percentage removal increased from 35 ± 2.4% to 93 ± 0.2% for 20 mg L^{-1} initial NH_4-N concentration.
The N/P ratio had a substantial effect on removal and the optimum ratio was determined as N/P = 8/1.
Saturation value constant, and maximum substrate utilization rate constant of the Stover-Kincannon model for ammonium nitrogen removal by *C. vulgaris* were determined as K_B = 10.3 mg L^{-1} d^{-1}, U_{max} = 13.0 mg L^{-1} day^{-1}, respectively.
Experimental results indicated that C. vulgaris can completely remove up to 21.2 mg l^{-1} ammonia-nitrogen concentration. However the tolerance to PO_4-P was lower.
The culture was able to remove only 7.7 mg l^{-1} initial PO_4-P concentration with 78% efficiency. The main reason for low removal performance at high nutrient concentrations could be the light limitation because of excess Chlorophyll *a* concentrations in this study.
In addition, the optimization of other parameters such as N/P ratio and light–dark cycle may enhance the nutrient removal capability of C. vulgaris at high nitrogen and phosphorus concentrations.

4.1 NH_4-N and PO_4-P removal

The variation of NH_4-N concentration with time at different initial NH_4-N concentration for 10 days of batch operation was obtained. The NH_4-N was completely removed from the media when the initial concentration was between 13.2 and 21.2 mg l^{-1}.
However, the NH_4-N removal efficiency was around 50% for $(NH_4\text{-}N)_o$ = 41.8–92.8 mg l^{-1} and it further decreased to less than 24% when the NH_4-N concentration was higher than 129 mg l^{-1}.
Since the pH was kept constant around pH 7, no significant ammonia removal was observed in control experiments. The final phosphorus concentration was around 1.7 mg l^{-1} with 78% removal efficiency for $(PO_4\text{-}P)_o$ = 7.7 mg l^{-1}.
The higher concentrations resulted in mostly less than 30% removal. Although nitrogen and phosphorus uptake by algae did not provide efficient removal of these nutrients from the synthetic media at high concentrations of nutrients, final chl *a* content of the culture significantly increased from 10.7 mg l^{-1} to 27.3 mg l^{-1} with the increase in $(NH_4\text{-}N)_0$ = 13.2 mg $l^{-1}$to $(NH_4\text{-}N)_0$ = 410 mg l^{-1}.
The light limitation due to excess amount of Chlorophyll *a* could be one of the reasons for low removal efficiencies at high nutrient concentrations. These results indicate that *C. vulgaris* is very effective in removing nutrient concentrations as $NH_4\text{-}N_0$ < 22 mg l^{-1} and $PO_4\text{-}P_0$ < 7.7 mg l^{-1}.

4.2 Determination of batch kinetic coefficients

The Michaelis–Menten kinetic relationship was used in determination of kinetic coefficients, K_m, saturation constant, *k*, and reaction rate constant. The substrate concentration corresponds to half reaction rate gives the saturation constant.
Based on the experimental data, batch kinetic coefficients of ammonia nitrogen removal by C. vulgaris were determined as k = 1.5 mg NH_4-N mg^{-1}, Chlorophyll *a* d^{-1} and K_m = 31.5 mg l^{-1}.
Similarly, kinetic coefficients for PO_4-P removal were found as k = 0.5 mg PO_4-P mg^{-1} Chlorophyll *a* d^{-1} and K_m = 10.5 mg l^{-1}. So, ammonia nitrogen removal rate is higher than that of phosphorus.
Yield coefficient for NH_4-N was Y_N = 0.15 mg chl a mg^{-1} NH_4-N and Y_P = 0.14 mg Chlorophyll *a* mg^{-1} PO_4-P for phosphorus. This result indicates that almost the same amounts of Chlorophyll *a* a are produced from phosphorus and nitrogen in C. vulgaris.

4.3 Groundwater Remediation, Odour And Vapour Control

It is common knowledge that nitrogen is essential for all living things, but high levels of nitrate-nitrogen in waters destined for portable drinking purpose can pose serious health risk, especially for infants and pregnant women. Novel treatment approaches developed for wastewater treatment are capable of recovering nutrients like phosphorous, nitrogen and organics. Hence treatment of ground water for the removal of organics may vary based on the intended uses. Therefore novel applications have been developed to meet the increasing technological demands for wastewater treatment.
With respect to the case study developed for investigating the behaviour and occurrence of natural estrogens and synthetic contraceptives in municipal STPs. This study became necessary due to the

observation relating to the feminization of male fishes within a municipal sewage treatment plant. It was discovered that the natural hormones excreted by humans and flushed into the sewers had an effect on the aquatic life style; hence extraction was necessary.
In most cases even trace elements of the contaminants require some level of extraction to meet drinking water standard or makeup the water quality requirements.

4.4 A Case Study – Pharmaceutical Industry

A characteristic of the pharmaceutical industries is the diversity of their process operations, which gives rise to a wide variation in liquid wastes. There is little similarity between effluents from different factories and individual effluents may alter continually as a result of process changes. This lack of homogeneity leads to a difficulty in categorising wastes of this type, preventing any real standardisation of treatment methods and necessitating a detailed and individual approach to effluent assessment. Many individual effluents arise from insufficient processes or spillages and thus the initial site investigation work is aimed at recovery methods to reduce the volume of effluent to be treated. (Callely et al, 1977).
As a result of the complexity of many of the pharmaceutical wastes, the resultant treatment plants may be multi – stage and in some cases may consist of two or more completely separate plants situated on the same works, with a complicated collection and balancing system (Callely et al, 1977).

4.4.1 Waste Characteristics

The majority of organic chemical which may be found in any significant amount in many of these process waste are readily biodegradable. Certain waste constituents often present in small amounts are extremely toxic to bacteria and may be produced as biocides. Due to the considerable difference between works effluents, it is impossible to describe each type of waste which may be encountered individually. It is therefore most beneficial to discuss the major trends in waste stream characteristics and apply these collectively to specific applications (Callely et al, 1977).

4.4.2 Carbohydrate Products

Sterile products. These effluents contain mainly dextrose and salt solutions. A sterile area with container washing shows a flow of 1-8m3/h with a BOD of 12 – 85 mg/l and suspended solids level of 16 – 2400mg/l.

4.4.3 Production of pastilles

These contain sugar and starch washed from equipment and Starch moulds Contain 2250mg/l BOD and 150mg/l suspended solids level.

4.4.4 Acid and Alkali Effluents.

These contain little or no organic matter and pollutants load in terms of BOD may be negligible.

i. Dissolved salts. The most predominate one are sulphates and chlorides, which may be found in concentrations of 25 000 – 30 000 mg/l
ii. General process liquors
iii. Strong process liquors
iv. Emulsions

4.4.5Waste Assessment

i. Site survey
ii. Chemical Analysis: Effluent composition
iii. Treatability Studies

4.4.6 Waste Treatment Processes

i. Segregation and Balancing
ii. Neutralisation and Pre – treatment

5. Conclusion

Useful conclusions obtained from studies of treatment processes show that integrated wastewater treatment processes can be considered as an alternative to single stage algal pond systems to improve algal separation and nutrient removal. Combination of *C. vulgaris* with water hyacinth *Eichhornia crassipes* resulted in 23% more nitrogen removal.

With the novel approach, *C. vulgaris* was co-immobilized with the growth promoting bacterium *Azospirillum brasilense* in small alginate beads and enhanced ammonia and phosphorus removal were obtained.

Results also indicated that the algae-immobilized photo bioreactor system had an effective nitrogen removal capacity when the operating conditions were optimized. The optimal conditions for the immobilized photo bioreactor system used in this study can be summarized as HRT = 5.5 days, N/P = 8 and NH_4-N_0 = 20 mg L^{-1} initial nitrogen concentration to obtain removal efficiency greater than 90%.

Advantages

a. The advantages of using algae for that purpose include: the low cost of the operation,
b. The possibility of recycling assimilated nitrogen and phosphorus into algae biomass as a fertilizer avoiding a sludge handling problem.
c. The discharge of oxygenated effluent into the water body. In addition, the process has no carbon requirement for nitrogen and phosphorus removal, which is attractive for the treatment of secondary effluents

References

Boari, G. Mancini, I. M and Trulli, E. (1997) *Technologies for waste water treatment, Italy, Potenza*

Callely, A. G., Foster, C. F., and Stafford, D. A., (1977), *Treatment of Industrial Effluents* ;London, Hodder and Stoughton.

Clayton A., Spinaldi G. and Williams R. (1999), *Policies for Cleaner Technology: A New Agenda for Government and Industry*, P.1 – 51, 218 – 288. London, Earthscan.

Culp, R.L., Wesner, G. M and Culp, G. L., (1978), *Handbook of Advanced Wastewater Treatment*, 2nd ed. New York, Van Nostrand Reinhold. Company

Culp, R. L. and Culp, G. L., (1971), *Advanced Wastewater Treatment*, New York, Van Nostrand Reinhold Company.

Curtis, T.P. (1994). *The Effect of Sunlight on Mechanisms for the Die-off of Faecal Coliform Bacteria in Waste Stabilization Ponds. Ph.d thesis.* School of Civil Engineering, University of Leeds. Leeds, UK

Daniels, S. L., Carmouche, L. N. and Driscoll, E. D., (1977), *Chemical Treatment as a Cost Effective Alternative for Wastewater Treatment: Operating vs. Capital Costs, in Water* – 1976: 1. Physical, chemical wastewater treatment, 166, volume 73, 1977, Edited by Bennett, G. F., NY: AIChE

Finger, R.E.; Harrington, D.; and Paxton, L.A (1985). *Development of an On-Line Zero Chlorine Residual Measurement and Control System*. Fulltext (online), Journal of the Water pollution Control Federation. 57 (1985) 1068-1073. [Accessed 25th April, 2010].

Gray, N. F., (1999) *Water Technology: An Introduction for Scientists and Engineers,* London, Hodder Headline Group.

Hammer Mark J., Hammer Mark J. Jr, (2008), *Waste and Wastewater Technology*, 6th edition, Harlow, Prentice Hall P.139-142, 359-374, 509-524

Hammer J. M and Hammer, Jr. J. M (2004), *Water and Waste Water Technology*, 5th edition New Jersey, Pearson Education LTD.

Kiely G. (1998) *Environmental Engineering,* International edition, UK,McGraw – Hill Book International Limited.

Mara, D.D., Alabaster, G.P., Pearson, H.W. and Mills, S.W. (1992). *Waste Stabilization Ponds: A Design Manual for Eastern Africa,* Leeds, England, Lagoon Technology International.

Metcalf and Eddy, (1991) *Waste Water Engineering* 3rd edition, Available from: www.escwa.un.org/information/publications [accessed 18th April 2010]

Metcalf and Eddy, (1991), *Wastewater Engineering: Treatment, Disposal, and Reuse*. 3rd edition, London, McGraw-Hill. P.190 – 207, 242 – 245

Pena M.R. (2002), *Advanced primary treatment of domestic wastewater in tropical countries: development of high-rate anaerobic pond`.Ph.D thesis*. School of Civil Engineering, University of Leeds. Leeds, United Kingdom.

Richardson, J.F., Harker, J.H and Blackhurst, J. (2001), *Particle Technology and Separation,* 5th edition, Processes, Chemical Engineering Vol. 2, Buttermouth Heinemann.

Russell L. Culp and Gordon L. Culp (1971), *Advanced Wastewater Treatment*, New York, New Van Nostrand Reinhold Company. chap.7: p 133-161, chap.8: pp 162-173.

Sung, R. D., Cotter, J., Neal, L. G. and Prien, C. H., (1977), *An Evaluation of the Pollution Abatement Technologies Available For Treatment of Wastewater from Oil Shale Processing in Water* – 1976:

Physical, chemical wastewater treatment, 166, volume 73, 1977, Edited by Bennett, G. F., NY: AIChE

Acknowledgement

The authors would like to thank the research group Environmental and Energy Engineering (Alpha consultants 2010) University of Sheffield, United Kingdom for the team spirit and effort in carrying out this research and for their assistance in the preparation of this paper.

Adepoju et al: Proc. ICCEM (2012) 126 - 137

HCME: An environment-friendly I.C. engine fuel

Tunde F. Adepoju[a,*], [b]Adeyinka O. Adetunji, [c]Emmanuel M. A. Olatunji, [a]Bello J. Olatunde
[a]Chemical Engineering Department, Landmark University, Omu-aran, P.M.B. 1001, Kwara State, Nigeria.
[b]National Biotechnology Development Agency, 16, Dunukofia Street, Area 11, Garki, P. M. B. 5118, Wuse, Abuja, Nigeria.
[c] Department of Industrial Chemistry, Landmark University, Omu-aran, P.M.B. 1001, Kwara State, Nigeria.
*Address of Correspondence: avogadros2002@yahoo.com, Tel: +234-803-39404673

Abstract

The study revealed that Hura crepitans oil is a good candidate for Hura crepitans methyl ester (HCME) production. Two steps (esterification and transesterification) production stages influenced the high yield of HCME. Three possible experimental runs were performed in each step, the best of the three conditions were 1.45 (% v/v) for H_2SO_4 conc., 5:1 for methanol/oil molar ratio, 40 min for reaction time which gave 1.06 % for FFA in the first step, in the second step, 92.70 %(w/w) of HCME was obtained at 0.55% KOH, 5:1 methanol/oil molar ratio, 60 ^oC temperature and 30 min reaction time. The produced HCME had fuel properties which satisfied both ASTME D6751 and EN 1424 standards. The fatty acid profile of the HCME revealed the dominant fatty acids were linoleic (64.50%), oleic (17.54%) and palmitic (12.70%). Exhaust emissions from an internal combustion (I.C.) engine revealed that there is 60% decreased in CO, 58% decreased in NOx, 60% decreased in HC, 39% decrease in smoke opacity and 42% decreased in BSFC at B20, respectively. Flue gas temperature increased by 12% at B20, 45% increased in BTE at B50 when compared to pure diesel (AGO). Hence, it can be concluded that
B20 (20% HCME + 80% AGO) will provides the best emission reduction at the lowest cost.

Keywords: *Hura crepitans methyl ester (HCME), Esterification, Transesterification, Fatty acids, I.C. engine, Exhaust emissions*

1. Introduction

Few people realize that vegetable oilseeds can be used for more than frying fast food. Indeed, Rudolph Diesel's first public exhibition of the internal combustion technology that was to later bear his name featured an engine running on peanut oil. He envisioned freeing small businesses from the monopolistic coal and steam power of the day by using organic fuels in his engine. Unfortunately, it turned out that his engine also lent itself to burning low-grade fractions of petroleum, and the rest is history. Diesel engine manufacturers optimized the design for lighter oils, and the use of vegetable oil never really got a chance. But, experimenters throughout the world have been reviving Diesel's vision, and vegetable oilseeds is finding increasing use, particularly in the US, UK, Germany, and Australia.

Because of this heritage, the fuel injection pump and the fuel injectors in modern diesel engines won't work on room temperature vegetable oilseeds because of its thickness. However, there are three common ways to thin vegetable oilseeds so it can be used in diesel engines, this includes; blend the vegetable oil with a lighter fuel, heat the vegetable oil until it becomes thin enough and changing the chemical composition of the vegetable oil.

Blending is fraught with problems, and although some enthusiasts swear by it, others end up

swearing at it, as they damage expensive injection pumps with the heavier fluid. Some have suffered explosions when trying to mix extremely lighter fuels, like gasoline, with vegetable oil. Those reporting success seem to be limited to a mix no more than 50/50 with petro-diesel at no colder than "shirt sleeve" temperatures, on a few engines that have very robust injection pumps. Meanwhile, heating vegetable oil to about 80°C (or about 180°F), it's viscosity is only a bit above that of normal diesel fuel, and so can make its way through pumps and injectors, cools down and gels, thereby causing damage to the engine. It can also results in a lot of heat wastage, presence of impurities in the oil and water in the fuel which can cause expensive engine damage, this method is not preferable. But, the act of changing the chemical composition, also known as transesterification process (biodiesel), is safe, reliable, and cost effective, reduces pollution, and will work in almost any diesel engine without modification.

Internal combustion (I.C.) engines play a major role in transportation, industrial power generation and in the agricultural sector. There is a need to search and find ways of using alternative fuels, which are preferably renewable and also emit low levels of gaseous and particulate pollutants in internal combustion engines. As per the literature survey, fuels like vegetable oils, biodiesel (transistorized vegetable oils to methyl esters), alcohols, natural gas, biogas, hydrogen, liquefied petroleum gas (LPG), etc. are being investigated by researchers for engine applications. In the case of agricultural applications, fuels that can be produced in rural areas in a decentralized manner, near the consumption points will be favoured. The permissible emission levels can also be different in rural areas as compared to urban areas on account of the large differences in the number density of engines. Many researchers have done work on conversion of edible and non-edible vegetable oilseeds such as beniseed (*Sesamum indicum*), sorrel oil (*Hibiscus sabdariffa*), coconut oil, linseed, Jatropha, Karanja (*Pongamia glabra*), kusum (*Schlerlchera trijuga*), pongamia, etc, to biodiesel, separately to study the performance and emission characteristics of I.C. engine [1,2,3,4,5,6]. However, competitions for commercial edible vegetable oilseeds which are obtainable from just about a dozen species of plant have necessitated the search for oils from underutilized tropical plants such as *Hura crepitans* (Sandbox). Despite the potential of this under-utilized species as a source of less consumed food and medicine, to authors' best knowledge, sparse information is available on the suitability of it biodiesel in I.C. engine and whose emission characteristics hitherto remains untapped. Therefore, the study is aimed at investigating the emission characteristics of *Hura crepitans* (Sandbox) methyl ester (HCME) biodiesel in I.C. engine.

2. Materials and Methods

2.1 Materials

The *Hura crepitans* oil used for this study was collected from the Department of Agricultural Engineering, University of Markudi, Nigeria. The convectional fuel (AGO) was purchased from Obafemi Awolowo University's petrol station in Ile-Ife. All chemicals such as Methanol (CH_3OH), potassium hydroxide (KOH), anhydrous calcium

chloride ($CaCl_2$), sulphuric acid (H_2SO_4), sodium hydroxide pellet (NaOH) etc, were all of analytical grade.

2.2 Experimental procedure

2.2.1 Pretreatment – Acid catalyzed esterification

The crude unrefined *Hura crepitans* oil was golden yellow in colour. The FFA was determined through the standard titrimetric method. The initial acid value of the oil was obtained to be 4.22 ± 0.01 mg KOH/g oil (FFA level of 2.11 ± 0.01 %), which is far above the < 1.50 specification limit for satisfactorily alkaline catalyst transesterification reaction. Hence, the FFAs were first esterified with catalyst (H_2SO_4). Using the standard AOAC method, the acid value of separated product at the bottom was determined. This process was repeated in triplicate and the product having acid value < 2.11 ± 0.01 mg KOH/g (FFA = 1.06) oil was used for the alkalis transesterification stage (step 2). Table 1 shows the reaction time, concentration of acid (H_2SO_4) and methanol/oil molar ratio used with the acid value and FFAs computed.

2.2.2 Alkalis catalyzed transesterification

According to the method of [7], the reaction was carried out with 5:1 methanol/oil molar ratio using 0.55% KOH as an alkaline base catalyst. The amount of KOH (5.5 g/l of preheated *Hura crepitans* oil) was reached based on the amount needed to neutralize the unreacted acids (2.11 mg KOH/g oil) in this stage. The reaction was carried out at 60 ^{o}C for 30 min in a reactor. At the completion of the reaction, the product was transferred to a separating funnel for glycerol and HCME separation. Glycerol was tapped off and the HCME left was washed with ionized water to remove residual catalyst, glycerol, methanol and soap. The washed HCME was further dried over heated $CaCl_2$ powder. The HCME yield was determined gravimetrically as described in Eq.1. The experiment was carried out in triplicate in order to select the best optimum condition with highest yield (Table 2).

$$HCME\ Yield\ \%(w/w) = \frac{Weight\ of\ Hura\ crepitans\ \text{oil used (g)}}{Weight\ of\ HCME\ obtained\ (g)} \quad 1$$

2.3 Physicochemical analysis of the Hura crepitans (Sandbox) oil and HCME

The evaluation of physicochemical and other properties of the oil and HCME were determined by [8], method, Wijs method and the methods reported by [9]. The quality of biodiesel is very important for the performance and emission characteristics of a diesel engine. Thus, the HCME produced was sent to the Nigeria National Petroleum Company (NNPC) Laboratory for chromatography analysis of fatty acids present in the HCME quality testing using standard methods.

2.4 Emission Characterization of HCME on I.C. engine

The blend of HCME and AGO were mixed in different proportions such as B10, B20, B30, B40 and B50. The same procedure was repeated for 100% AGO (B0) and 100% HCME (B100).The emissions (CO, NOx, HC, Smoke

opacity and Flue gas temperature) were recorded using EGA4 palm top flue gas analyzer having Ni-MH rechargeable battery, opacity of smoke was measure using smoke meter. Brake specific fuel consumption (BSFC) and brake thermal efficiency were computed.

3. Results and Discussion

3.1 Oil production characteristics

3.1.1 Pretreatment process - Acid catalyzed esterification

This section describes a series of tests that were conducted to develop the acid–catalyzed pretreatment process. Since Hura crepitans oil tends to have variable properties that could influence the repeatability of the tests, the pretreatment step was repeated in triplicate and the mean value of yield (acid values) was titrimetrically obtained. % FFA was computed (Table 1). The results obtained shows that the FFA of 1.06 mg KOH/g oil at the following working variable, reaction time, 40 min, methanol/oil molar ratio, 5:1 and 1.45 (% v/v) H_2SO_4 conc. were suitable for the best yield in the second step alkalis transesterification process.

3.1.2 Alkalis catalyzed transesterification process

The yield of HCME obtained during the alkalis catalyzed transesterification process was 92.70% (w/w) at the following variable conditions, 0.55% KOH, 5:1 Methanol/oil molar ratio, 60 ^oC reaction temperature and 30 min reaction time. The validity of the HCME was confirmed by carrying out three independent replicates experiments (Table 2).

3.2 Physicochemical analysis and other properties of Hura crepitans oil and HCME

3.2.1 Physical properties of the Hura crepitans oil and HCME

In order to evaluate the quality of the crude *Hura crepitans* oil and HCME, the content and compositions of the oil and HCME was subjected to physicochemical analysis and the results obtained were shown in Table 3. At room temperature, the oil was golden yellow in colour and the HCME was light yellow. The refractive index increases but the moisture content decreases after conversion of oil to HCME, indicating a good shelf life characteristic of oil. Observations on the colour, moisture content and refractive index of the oil and HCME agreed with previously published report [10]. The specific gravity of the oil was determined as 0.93 which was reduced to 0.86 after conversion, indicates that the oil and HCME are less dense than water with refractive index of 1.480 and 1.490, respectively. Although, [11], reported mean value of 0.98 on specific gravity for the same oil, [12] reported a range between 0.874-8.2312 for most of the vegetable seed oils. The viscosity, which is a measure of the resistance of material to shear, was determined to be 6.32 mm^2/s and 2.78 mm^2/s, respectively. The higher value obtained for the oil in this study indicates the oil could be used as lubricant in engine parts in the tropics if left overnight as solidification temperature of the oil is below 10 ^oC at any season [13]. The densities obtained in this present work were in line with what was obtained by [10].

3.2.2 Chemical properties of the Hura crepitans oil and HCME

Table 3 contains results obtained for the chemical properties of crude *Hura crepitans* oil and HCME. The high acid

value of the seed oil and HCME showed that it is non-edible and is a good candidate for biodiesel production. This can be used to check the level of oxidative deterioration of the oil and biodiesel by enzymatic or chemical oxidation. The acid value is expected to range from 0.00 - 3.00 mg KOH/g material, before it can find application in industries but the value is high for oil under study. That is why acid value was made fit by subjecting the oil to biodiesel and this may also improve its quality for industrial purposes [11]. A high Saponification value obtained for the seed oil, suggesting high concentration of triglycerides suitable for biodiesel production. The iodine value of the seed oil was high (125.90 g of I_2/100 g of oil), which signified the oil contained a substantial level of unsaturation and could be used to quantify the amount of double bonds present in the oil which reflects the susceptibility of oil to oxidation before conversion to biodiesel. Peroxide value measures the content of hydro-peroxides in the oil and its low value indicates high resistance to oxidation. The value obtained for the seed oil and HCME in this work were well within the limit stipulated for vegetable oils and biodiesel. This shows that the oil is not rancid and considered stable [14]. The HHV determined for the oil was 39.28 MJ/kg and it is within the range earlier reported [15] for vegetable oils (37.47 – 40.62 MJ/kg). The rise in the HHV after conversion of oil to HCME is a proved that the oil is not only good for biodiesel production, but can be suitably used as fuel in I.C. engine.

3.2.3 Other properties of the Hura crepitans oil and HCME

Additional fuel properties such as cetane number, API, diesel index, means molecular mass and aniline point of the seed oil and HCME were determined (Table 3). Cetane number is a measure of the fuel's ignition delay and combustion quality. Standard specification for cetane number biodiesel is 40 minimum [16]. The cetane number of the seed oil (45.05) showed that it have high fuel potential before being converted to HCME (cetane number- 50.40). The cetane number reported for most vegetable oils range from 27.6 to 52.9 [15,17]. The API, diesel index and aniline point of the oil and HCME were comparable with other reported work [9]. The two steps transesterification of the oil improved its fuel properties.

3.3 Fatty acid profile of the Hura crepitans oil and HCME

Gas chromatography analysis of fatty acids present in the seed oil and HCME was showed in Table 4. The results indicated that the oil is highly unsaturated. The dominant fatty acids were linoleic (58.52%), oleic (20.31%), palmitic (16.01%), stearic (3.10%), linolenic acid (C18:3) (1.60%) and others (0.46%). Whereas, the dominant fatty acids found in HCME were linoleic (64.50%), oleic (17.54%), palmitic (12.70%), stearic (1.74%), linolenic acid (3.50%) and others (0.02%) The values observed in this work are within the ranges previously reported [18,19]. This indicates that fatty acid composition will play a dominant role in establishing the cetane number [19,20].

3.4 Emission characterization

The test were conducted on a four stroke, air cooled, single cylinder direct injection diesel engine, developing a power output of 3.23 kW at a constant of

2600 rpm. Table 5 shows the specifications of the engine. The characterization of fuel behavior with respect to emissions and performance was carried out by determined the CO, NOx, HC, Smoke opacity, Flue gas temperature, BSFC and BTE.

3.4.1 Carbon monoxide (CO) emission (ppm)

CO is only a very weak direct greenhouse gas, but has important indirect effects on global warming. CO is an ozone precursor, but to a lesser extent than unburned hydrocarbons or nitrogen oxides. Biomass burning and fossil fuel use are the main sources of man-made CO emission. The most potential control is through direct reduction in fossil fuel use. Since the emission of CO depended on rotational speed, it decreased with increased in concentration of biodiesel.

Figure 1 shows the variation of CO with blends at different speed of revolution of I.C. engine. At the speed range of 800-1000 rpm, the CO emission was found to be highest at B0, followed by B10, B50 and B100. The CO decreases with increases in concentration of biodiesel blends as fuel [21]. At speed range of 1000-1200 rpm, the emission of B0 and B10 was found to be the highest compared with blends of B20 and B100. B50 has the lowest emission at this speed range. It was also observed that at highest speed range (1200-1400 rpm), the CO emission concentration was lowest at B50 while B0 has the highest emission concentration. Therefore, the CO emission concentration at B20 is the lowest with 60% emission reduction when compare with B0 (100% AGO).

3.4.2 NOx emission

NOx should not be confused with N_2O, which is a greenhouse gas. It is the total concentration of NO and NO_2. When NOx and volatile organic compounds (VOCs) react in the presence of sunlight, they form photochemical smog, a significant form of air pollution, especially in the summer. It adverse effect is damage to the lung tissue and reduction in lung function [22]. It can also forms nitric acid which contributes to acid rain if the combustion emission is not regulated in the environmental. NOx also increase in proportion to ignition advance, regardless of variations in the air/fuel ratio.

Figure 2 shows the variation of NOx emission concentration with the blends at different speed ranges. B20 at the highest speed range (1200-1400 rpm) has the lowest NOx concentration, followed by B10, B50, B0 and B100. At 1000-1200 rpm, B10 and B20 were found to have the same NOx concentration been the lowest, followed by B0, B50 and B100. Similarly, the highest NOx concentration was observed at B100 within the range of 800-1000 rpm, followed by B0, B50, B10 and B20. Hence, B20 at highest speed range has the lowest NOx emission concentration with 58% reduction compared to B0.

3.4.3 HC (Hydrocarbon) emission

The exhaust gases emitted by 4-cycle spark I.C. engine does not operate at 100% efficiency, and the air/flue mixture when burned produces exhaust gases containing various pollutants. Among these are the HC made up of principally of minute particles of unburned gasoline; these particle react photo-chemically with sunlight to produce smog; and NOx which combines with water to produce so-called acid rain.

HCs are measured in ppm (parts per million). Their presence in the exhaust stream is a result of unburned or partly burned fuel, and engine oil. HC emissions increase in proportion to ignition advance, except at very lean air/fuel ratios. Factors such as poor mixture distribution, ignition misfires and low engine temperatures, will all cause significant increases in HC.

Figure 3 shows the variation of HC emission with the blends at different speed ranges. The figure showed that at all speed ranges, the HC emission was found to be the highest at B0; this is followed by B100, B50, B10 and B20. B20 at a speed range of 1000-1200 rpm has the lowest HC emission with 60% reduction when compare with B0.

3.4.4 Smoke opacity emission (%)

Smoke opacity is a measurement of smoke density from 0% – clean and 100%– dirty. Smoke opacity can be in many shades including grey/black (unburnt fuel), blue (burnt oil – worn engine) or white (water condensation). It is the level of peak smoke opacity for diesel-powered motor vehicles. The level of opacity measurement remains the core of federal, state and local air pollution control effort as more visible emission observers verify now than ever before.

Figure 4 shows the variation of smoke opacity with the blends ratio at various speed ranges. B0 at the speed range of 1200-1400 rpm has the highest smoke opacity, followed by B100, B50, B10 and B20. B20 has the lowest smoke opacity at speed range 1000-1200 rpm. Whereas, B0 at the lowest speed (800-1000 rpm) range has the lowest emission of smoke opacity with 64% reduction.

3.4.5 Brake specific fuel consumption (BSFC) emission

The BSFC is the amount of fuel which an engine consumed for each unit of break powers per hour. It indicates the efficiency with which the engine develops the power from fuel. Majorly used to compare the performance of different engine but always tends to be the same for similar engine.

Figure 5 shows the graph of variation of BSFC with the blends at various speed ranges. B50 at all speed ranges has the highest BSFC with 36% increase when compared with B0. Although, the BSFC is the same at all speed ranges for B0. B20 at the speed range of 800-1000 rpm has the lowest BSFC with 42% reduction when compared with B0.

3.4.6 Flue gas temperature (deg. C)

In the low temperature combustion region the exhaust temperature is critical even for diesel fuel due to its negative effects on turbocharger performance, so the lower exhaust temperature observed for neat biodiesel could be an important drawback for its applicability in future diesel engines.

Figure 6 shows the flue gas temperature variation with the blends ratio. B20 has the lowest at the speed range of 800-1000 rpm. B10 at the speed ranges of 1000-1200 rpm and 1200-1400 rpm has the highest flue gas temperature as well as B20 at 1000-1200 rpm and B100 at 1200-1400 rpm, respectively. This is due to lower cetane number and higher ignition delay of the blend [23]. Hence, the highest flue gas temperature was found at 1000-1200 rpm for B10, B20 and B100 with 12% increase.

3.4.7 Brake thermal efficiency (BTE)

BTE is the ratio of output to that of input energy in the form of fuel. It gives the efficiency with which the chemical energy of fuel is converted into mechanical work. It shows that all chemical energy of fuel is not converted to heat energy. The fuel efficiency tend to peak at higher engine speeds [24].

Figure 7 therefore shows the BTE variation with the blends at various speed ranges. The BTE decreases as the blend ratio increases at all speed ranges. However, B100 at speed range of 800-1000 rpm has the lowest BTE with 23% reduction when compared with B0 at the same speed range. B50 has the highest BTE at the speed range 1200-1400 rpm, these shows 45% increased in the BTE when compared with B0.

4. Conclusion

The results obtained in this study revealed that *Hura crepitans* oil is a good candidate for HCME production. Two steps production processes influenced the high yield of HCME. Three possible experimental runs were performed in each step, the best of the operating conditions were 1.45 (% v/v) for H_2SO_4 conc., 5:1 for Methanol/oil molar ratio, 40 min Reaction time which gave 1.06 % for FFA in the first step, in the second step, 92.70 %(w/w) of HCME at 0.55% KOH, 5:1 methanol/oil molar ratio, 60 ^oC temperature and 30 min reaction time was achieved.

The produced HCME had fuel properties which satisfied both ASTME D6751 and EN 1424 standards. Emission assessment revealed 60% decreased in CO, 58% decreased in NOx, 60% decreased in HC, 39% decrease in smoke opacity and 42% decreased in BSFC at B20, respectively. Flue gas temperature increased by 12% at B20. Meanwhile, there is 45% increased in BTE at B50.

Acknowledgment

The help of Laboratory staffs of Nigeria National Petroleum Company (NNPC) in conducting the GC analysis in the company laboratories is highly valued. The effort of technical staffs of Mechanical engineering departmental at workshop is highly appreciated.

Table 1: Pretreatment process - Acid catalyzed esterification

Variables	Values		
H_2SO_4 conc. (% v/v)	1.30	1.45	1.60
Methanol/oil molar ratio	4	5	6
Reaction time (min)	30	40	50
Titrimetric acid values (mg KOH/ g oil)	3.20	2.11	2.54
% FFA	1.60	1.06	1.27

Table 2: Alkalis catalyzed transesterification process

KOH (%)	Methanol/oil molar ratio	Reaction temp. (^oC)	Reaction time (min)	HCME yield % (w/w)
0.55	5:1	60	30	92.40
0.55	5: 1	60	30	92.50
0.55	5:1	60	30	92.70

Table 3: Properties of *Hura crepitans* (Sandbox) oil and HCME Comparison to Biodiesel Specification

Parameters	Hura crepitans oil (sandbox)	HCME	ASTM D6751	EN 14214
Physical properties				

Colour	Golden yellow	Light yellow		
Moisture content %	0.40 ± 0.001	0.001 ± 0.001	0.05 max	0.02
Specific gravity	0.930 ± 0.01	0.860 ± 0.015	0.86-0.90	0.85
Viscosity (mm^2/s) at 40°C	6.32 ± 0.01	2.78 ± 0.02	1.9-6.0	3.5-5.0
Density (g/cm^3) at 25°C	1.42 ± 0.01	0.92 ± 0.02	0.84	0.86-0.90
Chemical properties				
Iodine value (g I_2/100g)	125.90 ± 0.10	116.40 ± 1.40	-	120 max
Acid value (mg KOH/g oil)	4.22 ± 0.10	2.34 ± 0.15	< 0.80	0.5 max
%FFA (as oleic acid)	2.11 ± 0.01	1.17 ± 0.02	-	-
Saponification value (Mg KOH/g oil)	201.60 ± 0.50	180.20 ± 0.10	-	-
Peroxide value	3.04 ± 0.10	2.48 ± 0.10	-	-
Other properties				
Cloud point °C	-	8.00	6	12 max
Flash point °C	-	112.00	100 min	>120
Pour point °C	-	-14.00	- 15	-
Diesel index	48.68 ± 0.20	56.11 ± 0.11	50.40	-
API	20.65 ± 0.14	33. 03 ± 0.40	36.95	-
Mean molecular mass	277.78 ± 1.60	310.77 ± 1.45		
Cetane number	45.05 ± 4.80	50.40 ± 1.20	47 min	51 min
HHV (MJ/kg)	39.28 ± 0.30	40.30 ± 010	-	-
Aniline point	235.74 ± 0.13	169.88 ± 0.50	331.00	-

values are means of triplicate determination ± standard deviation of mean

Table 4: Fatty Acids Compositions of the *Hura crepitans* (Sandbox) oil and HCME Produced

Parameters	Compositions %	
	Oil	HCME
Palmitic acid (C16:0)	16.01	12.70
Stearic acids (C18:0)	3.10	1.74
Oleic acids (C18:1)	20.31	17.54
Linoleic acids (C18:2)	58.52	64.50
Linolenic acid (C18:3)	1.60	3.50
Other	0.46	0.02
Total	100	100

Table 5: Engine specifications

Parameter	Specification
Type of engine	Single cylinder
Engine brand name	165F, Direct injection, four-stroke, Internal Combustion Engine.
Stroke length	0.11 m
Bore and stroke	87.5 mm x 110 mm
Cooling method	Air
Injector operating pressure	200 bar/ 23 °C BTDC
Dynamometer current	Eddy current
Compression ratio	16.5:1
Response time	4 micro seconds
Rated speed	2600 rpm
Resolution in 1 degree	360 degree encoder with a resolution of 1
Rated power	3.2 kW

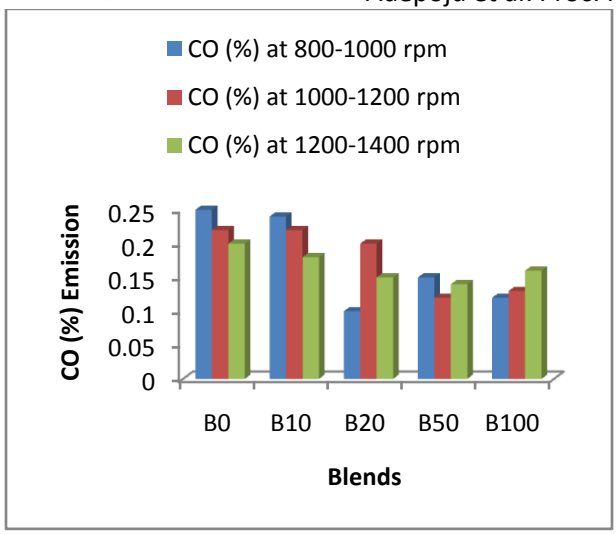

Figure 1: CO emission vs. blends

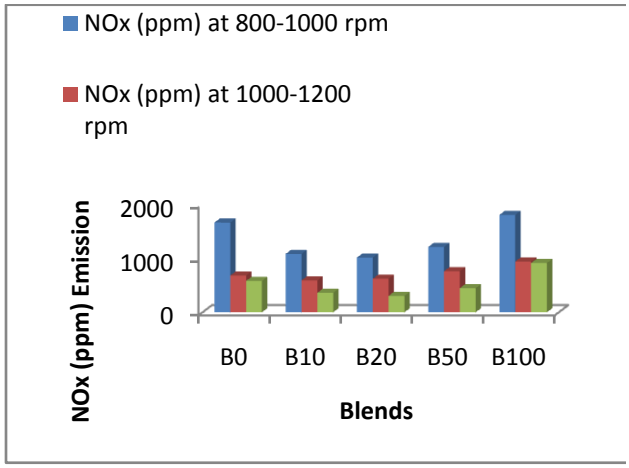

Figure 2: NOx emission vs. blends

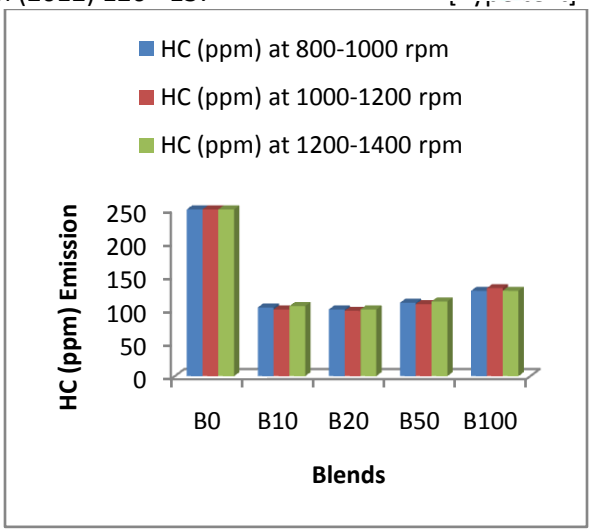

Figure 3: HC emission vs. blends

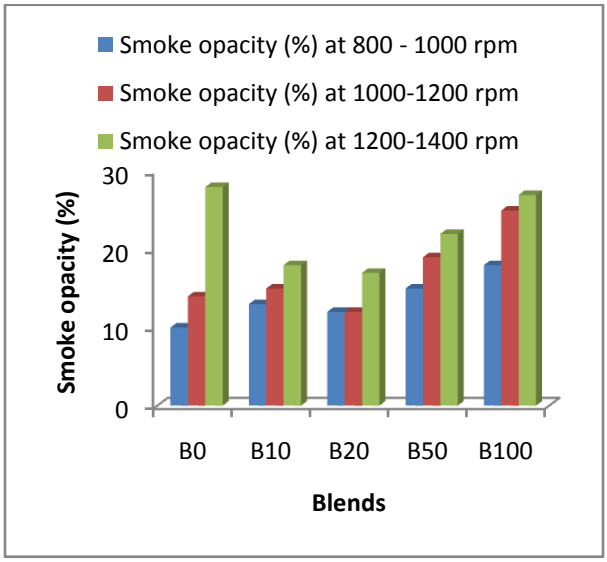

Figure 4: Smoke opacity vs. blends

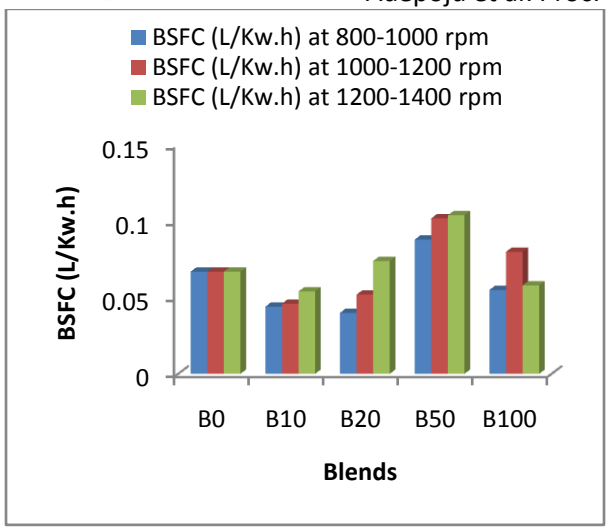

Figure 5: BSFC vs. blends

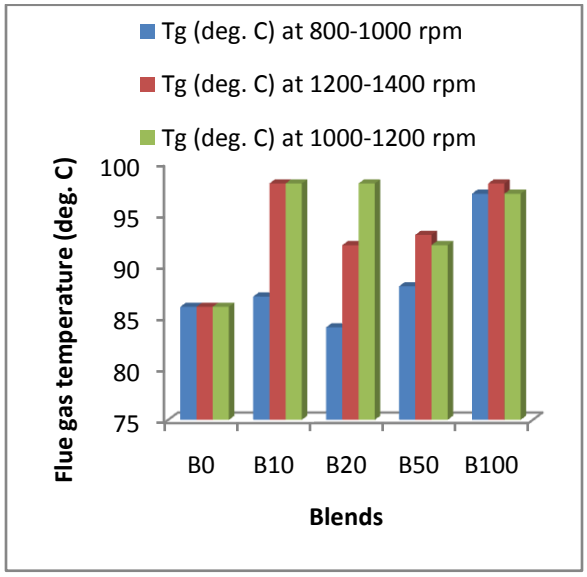

Figure 6: Flue gas temperature vs. blends

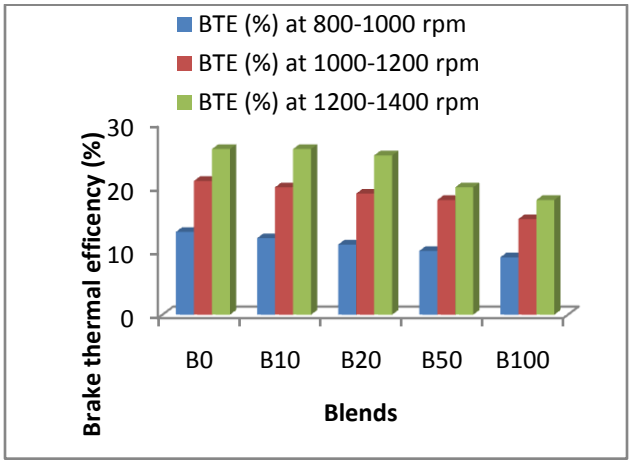

Figure 7: Brake thermal efficiency vs. blends

References

[1] Alcantara A, Amores J, Canoira L, Fidalgo E, Franco MJ, Navarro A. Catalytic production of biodiesel from soybean oil, used frying oil and tallow. Biomass Bioenergy 2000; 18: 515-527.

[2] Dorado MP, Ballesteros E, López FJ, Mittelbach M. Optimization of alkali catalyzed transesterification of Brassica Carinata oil for biodiesel production. Energy Fuel 2004; 18:77–83.

[3] Mittelbach M, Remschmidt C. Biodiesel. The comprehensive handbook. Vienna: Boersedruck Ges.m.b.H.; 2004.

[4] Karmee, SK, Chadha. Preparation of biodiesel from crude oil of Pongamia pinnata.

Bioresour Technol 2005; 13 (96): 1425-1429.
[5] Leung D, Guo Y. Transesterification of a neat and used frying oil: Optimization for biodiesel
production. Fuel Process Technol 2006; 87: 883-890.
[6] Wang L, Stevenson DG, Eller FJ, Jane JL, Wang T, Inglett G. Oil and tocopherol content and
composition of pumpkin seed oil in 12 cultivars. J AGR FOOD CHEM 2007; 55: 4005-
4013.
[7] Tiwari AK, Kumar A, Raheman H. Biodiesel production from jatropha oil (Jatropha curcas)
with high free fatty acids: An optimized process. Biomass Bioenergy 2007; 31: 569-575.
[8] AOAC - Official methods of analyses of the Association of Official Analytical Chemists
(1998). 16th Ed., Washington DC, USA, Association of Official Analytical Chemists.
[9] Haldar SK, Ghosh BB, Nag A. Utilization of unattended *Putranjiva roxburghii* non-edible oil
as fuel in diesel engine. Renewable energy 2009; 34: 343-347.
[10] Igbum OG, Eloka-Eboka AC. Nwadinigwe CA. Effects of Transesterification Variables on
Yields and Properties of Biodiesel Fuels Produced from Four Virgin Tropical Seeds Oils.
IJEE 2012; 1(2): 119-130.
[11] Olatidoye OP, Adeleke AE, Adegbite SA, Sobowale SS. CHEMICAL COMPOSITION
AND NUTRITIONAL EVALUATION OF SANDBOX (Hura crepitan) SEED FLOUR
FOR DOMESTIC CONSUMPTION AND INDUSTRIAL. J Med Appl Biosciences 2010; 2:
72-83.
[12] Eze OS. Physico-chemical properties of oil from some selected underutilized oil seeds
available for biodiesel preparation. AJB 2012; 11(42): 10003-10007.
[13] Oyekunle JAO, Omole AA, Akinnifasi JO. Physical properties of oils extracted from
Nigerian Non conventional oilseeds. J Appl Scienc 2007; 7(6):835-840.
[14] Ajayi IA, Dawodu FA, Adebowale KO, Oderinde RA. Chemical composition of
Pentaclethra macrophylla seed and seed oil grown in Nigeria. Riv. Ital. Sostanze Grasse.
2002; 74:183-185
[15] Demirbas A. Fuel properties and calculation of higher heating values of vegetable oils. Fuel
1998; 7:1117-1120.
[16] Ramos MJ, Fernández CM, Casas A, Rodríguez L, Pérez Á. Influence of fatty acid
composition of raw materials on biodiesel properties, Bioresourc Technol 2009; 100:261–
268.
[17] Njoku OU, Boniface JAE, Obitte NC, Odimegwu DC, Ogbu HI. Some nutriceutical
potential of beniseed oil. Int J Appl Res Nat Prod 2009; 2(4):11-19.
[18] Knothe G, Matheaus AC, Ryan III TW. Cetane numbers of branched and straight-chain
fatty esters determined in an ignition quality tester. Fuel 2003; 82:971–975.

[19] Bamgboye AI, Hansen AC. Prediction of Cetane number of biodiesel fuel from the fatty acid methylester (FAME) composition, IAPPP 2008; 22: 21-29.

[20] Knothe G. "Dependence of biodiesel fuel properties on the structure of fatty acid alkyl esters" Fuel Process Technol, vol. 86, pp. 1059–1070, 2005

[21] Lenin HA, Azhagesan N, Selva Rex, CR, Thyagarjan K. Performance of Diesel Engine with Pongamia Methyl Esters as Biodiesel. AJSR 2012; 5(3): 153-161.

[22] "Methodology for Thermal Efficiency and Energy Input Calculations and Analysis of Biomass Cogeneration Unit Characteristics, U.S. Environmental Protection Agency Office of Air and Radiation"- Retrieved, 2012-09-20.

[23] Rao VT, Rao GP, Reddy KHC. Experimental investigation of Pongamia, Jatropha and Neem methyl esters as biodiesel on C.I. engine. Jordan J. Mech. Ind. Eng 2008; 2: 117-122.

[24] Health and Environmental impacts of NOx. United State Environmental Protection Agency, Retrieved, 2012-09-20.

Olukanni and Akinyinka: Proc. ICCEM (2012) 138 – 145

Environment, Health and Wealth: Towards an Analysis of Municipal Solid Waste Management in Ota, Ogun State, Nigeria

David O. Olukanni and Michael O. Akinyinka

Department of Civil Engineering, Covenant University, P.M.B. 1023, Ota, Ogun State, Nigeria.
E-mail: david.olukanni@covenantuniversity.edu.ng +234-08030726472

Abstract

The management of municipal solid waste is one of the challenges facing the developing countries because governments, institutions, and private sectors have given solid waste management low priority and ignoring the implication it has on the general public. This is characterized by inefficient collection methods, insufficient coverage of the collection system and improper disposal. This paper presents the current solid waste management method adopted in Ado-Odo Ota local government and its associated challenges. Four locations (Iganmode area, Joju area, Ota market and toll gate area) were selected. These sites are points where the waste bins are located. A field work that involves the characterization and types of the waste generated, and frequency of collection from each site was carried out. A representative sample of 280 kg was used for the waste characterization and the result shows that about 64% of the wastes are recyclable with lots of organic waste that comprises of food and agricultural waste which can be used as compost. The only dump site in Ota was visited in order to obtain useful information concerning the present state of solid waste management. The study revealed that there is presently no investment made to the existing development plan to introduce a modern waste management system. The study suggests new approach that could be used by institutions and government agencies for municipal solid waste management to achieve sustainable and effective sanitation.

Key words: *Ota, Municipal solid waste, waste characterization, effective sanitation, recycling, disposal*

1. Introduction

Ota metropolis, Ogun State in South-Western Nigeria has witnessed a rapid urbanization over the past decades providing a large market for manufacturing industries and organizations. Its population growth has led to the rapid expansion of the city which has resulted in urban sprawl and uncontrolled increase of occupancy ratios in existing housing units and infilling of vacant plots in existing residential area. However, the lack of proper and comprehensive land use planning has hindered effective sanitation thus reeling under indiscipline and haphazard way of dumping refuse in an objectionable manner. The waste generated include refuse from households, non-hazardous solid waste from industries, commercial and institutional establishments (including hospitals), market waste, yard waste, and street sweepings. The general practice in the municipality has been indiscriminate disposal of solid waste thereby creating unsanitary environments in many part of the metropolis. In addition, the waste disposal site is faced with poorly developed dumping ground that is potentially threatening to public and environmental health. Agunwamba (1998; 2003) expressed that political, economical and sociological factors among other factors are attributable to an inadequate formulated and poorly implemented environmental policy that complicates such problems. The public health consequences of poor management of solid waste in the city are becoming enormous while on the other hand the need to minimize wastages and make the most valuable use of some materials from the generated waste is attracting interest.

Ogwueleka (2009) pointed out that solid waste management in Nigeria is characterized by inefficient collection methods, insufficient coverage of the collection system and improper disposal of solid waste. The mountainous heaps of solid wastes that deface Nigerian cities and the continuous discharges of industrial contaminants into streams and rivers without treatment motivated the federal government of Nigeria to promulgate Decree 58 for the establishment of a Federal Environmental Protection Agency (FEPA) in 1988. A national policy on the environment was formed and the goals of the policy include:

securing for all Nigerians a quality of environment adequate for their health and well being, raising public awareness and promoting understanding of the essential linkages between the environment and development, and to encourage individual and community to participate in environmental protection and improvement efforts (FEPA, 1989 in Agunwamba, 1998). As fallout of this decree, many States of the Federation established their own waste management authorities for the safety and development of the environment within their jurisdiction: Ondo State Integrated Waste Recycling and Treatment Project (OSIWRTP), Lagos Waste Management Authority (LAWMA), Ogun State Environmental Protection Agency (OGEPA), Oyo State Environmental Protection Agency (OSEPA), Kaduna State Environmental Protection Agency (KASEPA), River State Environmental Protection Agency (RSEPA), Enugu State Environmental Protection Agency (ESEPA) and Anambra State Environmental Protection Agency (ANSEPA) among others. The agencies are charged with the responsibility of handling, employing and disposing of solid waste generated. These agencies generate fund from subvention from state governments and internally generated revenue through sanitary levy and stringent regulations with heavy penalties for offenders of illegal dumping and littering of refuse along streets (Ogwueleka, 2003; 2009). In addition, the federal government instituted national integrated municipal solid waste management intervention programme in seven cities of Nigeria. The seven cities are Maiduguri, Kano, Kaduna, Onitsha, Uyo, Ota, and Lagos (Ogwueleka, 2009). However, development project may be judged unsustainable and not cost-effective if it threatens human health. The goal of municipal solid waste management is to promote the quality of the urban environment, generate employment and income, protect environmental health and support the efficiency and productivity of the economy (Ogwueleka, 2003).

Agunwamba (2003) expressed that planned recycling does not exist in Nigeria as it does in developed countries and suggested that waste recycling and composting activities should be encouraged since this approach is considered to be the right measure in attaining sustainability in waste management. However, recycling measures are still faced with many problems such as lack of financial resources, collection and transportation facilities and lack of advanced technology. Recycling reduces the amount of waste needed to be collected, transported and disposed of, and extends the life of disposal facilities, which saves money to environmental agency. Birly and Lock (1998) pointed out that good waste management is frequently concerned with identifying problems, assessing their importance and proposing solutions. It was further stressed that collection and disposal of refuse can consume up to 50 per cent of a municipal operating budget. Where markets for solid waste exist there is usually a thriving trade which supports many destitute people who may live or work on refuse dumps that are often cited in peri-urban areas (Furedy, 1996; Birly and Lock, 1998). Proper management of municipal solid waste at all stages of a project is expected to be beneficial to the health and sustainable development as well as economic well-being of a community. Ogwueleka (2009) pointed out that a different approach is required for developing countries in the management of solid waste because most developing countries have solid waste management problems different from those found in developed countries in areas of composition, density, waste amount, access to waste collection, awareness and attitudes, political and economic framework.

While stressing the need for recycling, it is also important to discuss the health implications of improper waste disposal. Health impact assessment consists of identifying health hazards, assessing health risks and proposing risk mitigation measures. There are potential risks to the environment and human health from improper handling of solid wastes. Direct health risks concern mainly the workers in this field, who need to be protected, as far as possible, from contact with wastes. Epidemiological studies have shown that a high percentage of workers who handle refuse, and of individuals who live near or on disposal sites, are infected with gastrointestinal parasites, worms and related organisms. Disease transmission by houseflies is greatest where inadequate refuse storage, collection and disposal is accompanied by inadequate sanitation. Once collected in poorly designed or poorly operated disposal sites, rubbish may contaminate groundwater with nitrates, heavy metals and other chemicals. Incineration of wastes may pollute the air with particulates and oxides of sulphur and nitrogen.

The slag and ashes from incinerators may result in leachate that is rich in heavy metals and other potentially toxic substances (WHO, 1985). This study emanates from the need to address the solid waste management problem in Ota. The major thrust of this investigation is to assess the solid waste management problem and document the potential environmental and health implications, and resources that could be annexed from the municipal solid waste generated in Ota, Ogun State, Nigeria.

2. Materials and Method

Study Area

Ota is the capital of the Ado-Odo/Ota local government area and has the third largest concentration of industries in Nigeria (Salako, 1999). It covers an area of 878 square kilometers and lies between latitude 6°41′N and 6°68′N and longitude 3°41′E and 3°68′E. Ado-Odo/Ota Local Government has an estimated population of 527,242 (Male 261,523 and Female 265,719) (2006 Census) with about four hundred and fifty (450) towns, villages and settlements. Other towns and cities include Ado-Odo, Igbesa, Agbara, Sango-Ota, and Itele. It also possesses a large market and an important road junction, found north of the Tollgate on the Lagos-Abeokuta expressway. Ota is also well known to be the location of the Canaan Land where the mega church Winner's Chapel, renowned as the world's largest single auditorium is situated. Ota is gradually becoming a busy place because of its proximity to Lagos thereby increasing the migration of people it.

Field Work

This study is both quantitative and descriptive with field works and assessment that involved the characterization of the waste from four waste bin locations. Data were collected from both primary and secondary sources. The location of the collection points, type of waste generated, collection duration and frequency were collected. The dump site was visited which happen to be the only one in Ota. Discussion and interviews were held with some of the residents, scavengers and key officials in order to confirm the practice and problems facing solid waste management. The Ota township map is presented in Figure 1 with the four collection points labeled for identification while Table 1 shows the description of the selected locations.

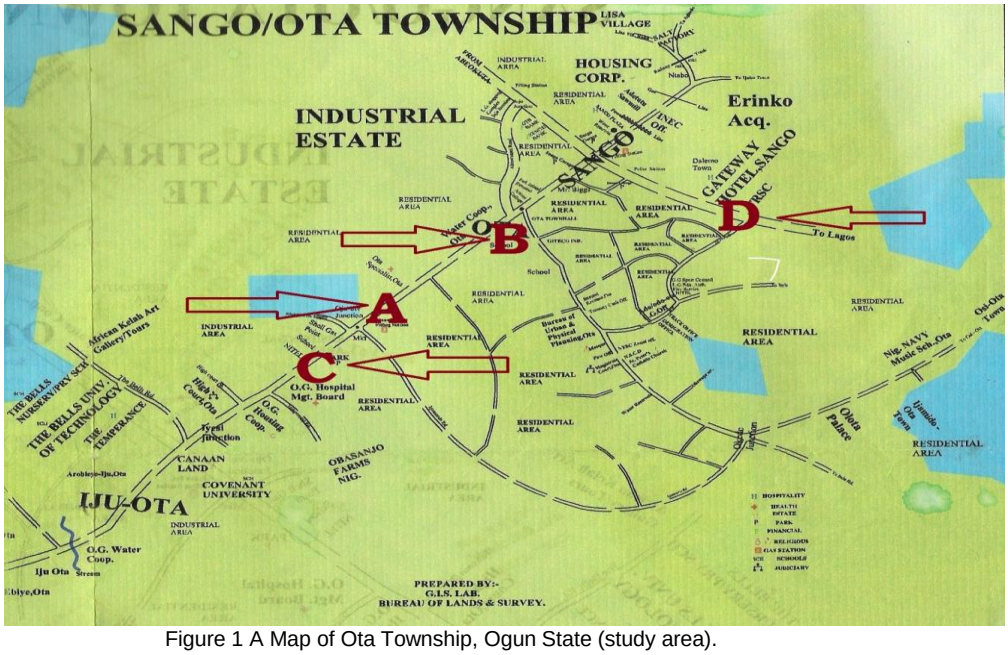

Figure 1 A Map of Ota Township, Ogun State (study area).

The indiscriminate disposal of waste in Ota is a concern to the Ado-Odo Ota local government waste management agency and this gave rise to the provision of waste bin along the road side for

ease of generation and collection. The volume of the waste bin provided by the local government waste management authority is $7m^3$. A representative sample of 280 kg was collected from a loaded $7m^3$ waste bin and its surrounding in each of the location to represent the municipal solid waste generated. The weighing scale was used in determining the weight of solid waste collected. Glove and nose guard were used for safety measure. Thereafter, sorting of the waste was done in order to classify the waste into glass, food waste, textile, rubber, plastics, cartoon, paper etc., and subsequently, the characterized waste was weighed and recorded for each of the sites. The quantity of characterized waste varies with site.

Table 1 Selected sites in Ota and quantities of waste bins provided.

Site	Location	Quantity of bins
A	Iganmode Grammar School.	4
B	Joju Junction.	2
C	Ota Market.	3
D	Toll Gate.	1

The quantity of waste bins supplied is based on the population and the activity in such area. Iganmode area has four waste bins because it is a residential/commercial area, while Ota market also has three due to the commercial activities there. Joju has two waste bins because it is also a residential area and toll gate has only one waste bin because it is a transition point with varying population for motorist and people moving in and out of Ota. Figure 2 shows the manual collection of waste around the waste bin and bagged to be disposed.

2a 2b

Figure 2 Waste Collection bin provided by the Local Government and the ad-hoc workers parking the waste into sacks for unward tranfer into the bin.

Characterization of Waste Composition (%)

$$Characterisation..of..Waste..Composition.(\%) = \frac{Weight..of..Waste..Composition.(kg)}{Weight..of..Total..Solid..Waste.(kg)} \times 100\%$$

3. Results

From observation and inquiries made, the local government provides waste bins for the storage of waste to reduce the indiscriminate disposal of solid waste on the road side. These waste bins are generally at open spaces along street ends or junctions. Tables 2-4 show the composition of the inorganic and organic wastes of the 280 kg from the collection points.

Table 2 Composition of inorganic and organic waste of the 280 kg from collection points

LOCATION	TYPE OF WASTE	
	Inorganic (%)	Organic (%)
Igannode Grammar School	60.28	39.72
Joju Junction.	65.38	34.62
Ota Market.	63.51	36.49
Toll Gate.	61.11	38.89

Results in Table 2 shows that a larger percentage of the waste generated by the people of Ota is inorganic which the same is relative over the entire sampling points.

Table 3 Representative Composition of Inorganic Waste in Ado-Odo Local Government

LOCATION → / MATERIAL ↓	Igannode Grammar School Site A Percentage (%)	Joju Junction Site B Percentage (%)	Ota Market Site C Percentage (%)	Toll Gate Site D Percentage (%)
PAPER	4.55	3.92	4.26	3.03
CARTON	11.36	11.76	14.89	9.09
PLASTICS	9.09	5.88	12.77	18.18
TEXTILE	13.64	9.8	6.38	9.09
RUBBER	6.82	5.88	10.64	12.12
GLASS	11.36	15.69	8.51	21.21
TIN CAN	4.55	7.84	12.77	12.12
SACKS	9.09	9.8	17.02	9.10
NYLON	29.55	29.41	12.77	6.06
TOTAL	100	100	100	100

As shown in Table 3, carton, plastic, textile, glass and nylon dominated the waste stream, followed by rubber, tin and sacks. This data informed on the kind of materials used mostly by the inhabitants. These waste all have potential for recycling if they are all sorted out from source as done in developed nations.

Table 4 Representative Composition of Organic Waste in Ado-Odo Local Government

LOCATION	Igannode Site A	Joju Site B	Ota Market Site C	Toll Gate Site D
MATERIAL	Percentage (%)	Percentage (%)	Percentage (%)	Percentage (%)
FOOD WASTE	31.03	59.26	48.15	38.09
AGRICULTRAL WASTE	6.89	3.7	14.81	4.76
OTHERS(DECOMPOSED)	62.07	37.04	37.04	57.14
TOTAL	100	100	100	100

Table 4 shows that food waste takes a significant amount of the organic waste stream which when used appropriately could be of great benefit in composting. The remaining decomposed waste stream if annexed could be used to generate biogas or could serve as an alternative energy source**.**

Discussion

Planning and Management of the Waste Management Authorities in Ota

Private participation in waste management has not been successful in Ota because such companies are profit driven and they are not monitored or regulated by government. The initiative for the private sector to participate in the waste management is to strengthen the system. Waste management in Ota has this facility but suffers funding as such it is not stable. Funding has made the waste management to experience a step back because solid waste management is very expensive. There is little financing even for the private sector participation. Therefore, waste management agencies cannot meet the demand of collection effectively. The present analysis highlighted that the existing system of waste collection and its disposal within the municipality is not only inadequate and insufficient but also unscientific. Proper management of municipal solid waste should have minimum effect on environment. The role of the informal sector in waste collection is significant. This sector could be responsible for removing a significant percent of total generated waste in the urban areas. In some public places and markets, people pay scavengers to clean the front of their shops. Scavengers salvage repairable and rentable materials to sell for recycling. To achieve sustainable and effective waste management of municipal solid waste, there is need to consider the political, institutional, social, economic and technical aspects. It is imperative that the local government realizes that increasing environmental education and awareness are key factors to changing the current paradigm.

High-income earners consume more packaged products, which results in a higher percentage of inorganic materials – metals, plastics, glass, and textile. Waste characteristics also vary according to season, income level, population, social behaviour, climate, and industrial production, the size of markets for waste materials and the extent of urbanization, effectiveness of recycling, and work reduction. The organic fraction of municipal solid waste is an important component, not only because it constitutes a sizeable fraction of the solid waste stream, but also because of its potentially adverse impact upon public health and environmental quality. A major adverse impact is due to its attraction of rodents and vector insects for which it provides food and shelter. Impact on environmental quality takes the form of foul odors, unsightliness, land, water and air pollution. Unless an organic waste is appropriately managed, its adverse impact will continue until it has fully decomposed or otherwise stabilized.

Environmental status of collection points and disposal sites

Waste management's agency determines the frequency of the collection. The collection in Ota is designed to be on a weekly basis but unfortunately, the weekly basis is not adhered to which then causes the indiscriminate disposal around the waste bin and individuals hipping up bags of waste along the road side. Due to the numbers of waste bin and location, it would be suggested that collection should be twice a week and consistency should be enforced. The population, consumption and frequency of waste generation have made it obvious that the waste bins in Ota are not enough to serve the disposal

need of the community. Other locations should be created for more generation point. The collection system is also not efficient due to the inadequate collection vehicle. Infrequent collection and rapid decomposition of wastes provide an attractive feeding and breeding site for flies, rats and other scavengers. The collection system is the conventional hauled container system and there is no form of processing. The waste accumulates in open dumps at roadsides. The open dumps provide harborage for diseases causing organisms, bacteria, insects, and rodents. Some individuals use the waste bins provided by the local government as generation point. There is no form of on-site sorting of waste at the generation or collection point and as such different waste are dumped. The waste is collected and taken by collection vehicles directly to the disposal site. There is no house-to-house service and most cases, residents pack their waste in bag and sacks and placed by road sides which last for days before the local authorities come to pack them. Residents also are in the habit of dumping waste at any vacant plot, public space, and river or burn it in their backyard, thereby polluting the air.

Cart pushers also dispose waste collected at a certain fee from house-holds that do not have access to the provided waste bin. Because of the frequency of disposal, there is always spill of waste around the bin which is non-hygienic. The transportation is such that waste bins are taken directly to the dump site emptied and returned to their original location. The disposal site, owned by the local government, is a steep land whereby waste disposed are pushed and burnt. This site emanates foul smell and become a breeding ground for flies, rodent and pest. These impacts are not confined merely to the disposal site. On the contrary, they pervade the area surrounding the site and wherever the wastes are generated, spread or accumulated.

Reuse and Recycling

Recycling is a means of using some waste materials as a substitute for virgin materials for production of goods. It is the recovery and reuse of materials from wastes. Recycling reduces the amount of waste that needs to be collected, transported, and disposed of which ultimately extends the life of disposal facilities. In Ota, there is no form of sorting of the collected waste from the generation sources to the disposal site, but scavengers pick materials which are reused and the bulk of the waste are burnt. A significant number of scavengers pack refuse for a fee and salvage any recyclable prior to the disposal of the waste. Other repairable items (old furniture, waste paper, bottles and glass, and metal scraps) are bought by the scavengers in some cases. Waste materials can be put back into the raw product stream, either as base material, as with glass, plastics and paper, or as reusable product as with returnable milk bottles. Some scavengers go around the town pushing their trucks and pay individuals that has some recyclable materials like metal scraps and plastics. Facilities could be provided where sorting of materials to be recycled is carried out. The recovery of materials in this way would reduce the need to use natural resources directly, and may reduce emissions from extraction and processing of raw materials. These could offset the benefits of recycling to some extent. Food from households is feed to animals, some are home composted and used to condition the soil. The waste could be converted to compost or used to generate biogas or used as fertilizer. It is apparent that the local government takes responsibility for their waste and should begin to incorporate recycling and reuse into their solid waste management plans.

The amount of energy that is wasted by not recycling paper, printed material, glass, plastic and aluminum and steel cans could be much. Plastic can be recycled and reused depending on the quality. Recycling process of plastics involves washing, shredding, drying, wet grinding; extrusion, pelletizing and the final product are package and sold to consumers. Paper recycling saves the forest of trees which would produce new paper. It reduces the quantity of solid waste disposed and the pollution also reduces during manufacturing because the fibers have been processed once. Reuse of aluminum saves precious natural resources, energy, time and money. It is sustainable metal that can be recycled again and again. It involves re-melting scrap aluminum after its initial production. Compost/organic fertilizer can be obtained from the food waste by converting biowaste into organic fertilizer. This is an aerobic process whereby micro-organism decomposes biodegradable waste to produce organic fertilizer in the presence of ample oxygen.

This waste has its usefulness rooted in fertilizer generation which would be of great benefit and in fact cheap for farmers.

Health Impact of Waste Management

There are potential risks to environment and health from improper handling of solid wastes. The environmental problem arising from unscientific and indiscriminate disposal of municipal garbage is a real menace for the whole society. Direct health risks concern mainly the workers in this field, who need to be protected, as far as possible, from contact with wastes. The main risks to health are indirect and arise from the breeding of disease vectors, primarily flies and rats. The most obvious environmental damage caused by municipal solid wastes is aesthetic, the ugliness of street litter and degradation of the urban environment and beauty of the city. Foul odor is emitted at the disposal site due to continuous decomposition of organic matter and emission of methane, hydrogen sulphide and ammonia. Odor is also emitted at the collection points if quick removal of wastes is not practiced. Spreading of the waste in the area adjacent to the dustbin due to activity of rag pickers causes degradation of aesthetic quality.

4. Conclusion

Environmental management Ota metropolis requires collaboration at all levels between different stakeholders and pooling of all expertise to be involved in the entire sanitation process. It is important that resources for running the waste management are harnessed and attention should be paid to storage, collection, transport, and intermediate transfer to bulk transport and final disposal. The frequency of collection and route planning for collection vehicle should be developed for the ease of collection from all generation point. The public should be sensitized on the locations for disposal of waste and there should be stringent policies to facilitate it. Solid waste recycling should be integrated with other solid waste management options to abate degradation in the environment. This can be achieved through promotion of economical, efficient and environmentally sound practices in managing municipal waste. Recycling also can be promoted by encouraging separation at source. The best way of waste separation at source can be stimulated by financial incentives, legislation and to raise environmental awareness. It is recommended therefore, that the existing open dumping system in Ota metropolis be converted to a sanitary landfill with proper environmental protection measures in order to minimize environmental pollution. However, it is also proposed that the government, if possible, should adopt the waste-to-energy treatment system since it is not possible by sanitary landfill to eliminate all the negative impacts to the environment.

Reference

Agunwamba, J. C. (1998) Solid Waste Management in Nigeria: Problems and Issues. Environmental Management. Volume 22 (6): 849-856.

Agunwamba, J. C. (2003) Environmental Assessment: Analysis of Scavengers' Activities and Recycling in Some Cities of Nigeria. Environmental Management. Volume 32 (1):116-127.

Asomani-Boateng, R and Haight, M (1999). Reusing organic solid waste in urban farming in African cities: a challenge for urban. Third World Planning Review. Volume 21, Number 4

Birley, M. H. and Lock, K (1998). Health and peri-urban natural resource production Environment and Urbanization, Vol. 10, No. 1

Furedy, C. (1996), "Solid waste reuse and urban agriculture - dilemmas in developing countries: the bad news and the good news" in Association of Collegiate Schools of Planning and Association of European Schools of Planning, Joint International Congress, Myerson Polytechnic University, Toronto.

Jeevan Rao, K. and M.V. Shantaram (1995), "Contents of heavy metals in crops treated with urban solid wastes", Journal of environmental Biology Vol.16, No.3, pages 225-232.

Ogwueleka, T.C., (2003). Analysis of urban solid waste in Nsukka, Nigeria. Journal of Solid Waste Technology and Management, 29 (4): 239-246.

Ogwueleka, T.C., (2003). Municipal Solid Waste Characteristics and Management in Nigeria *Iran. J. Environ. Health. Sci. Eng., Vol. 6 (3): 173-180*

WHO (1985), Environmental Pollution Control in Relation to Development, World Health Organization, Geneva.

Okeniyi et al: Proc. ICCEM (2012) 146 – 154

Effects of $Na_2Cr_2O_7$ Inhibitor on the Corrosion Potential Response of Steel Reinforced Concrete in Saline Medium

Okeniyi, J.O. [*1], Oladele I.O. [1], Ambrose, I.O. [1], Omoniyi, O.M.[1], Okpala, S.O. [1], Loto C.A. [1] and Popoola, A.P.I. [2]

[1]Mechanical Engineering Department, Covenant University, Ota, Nigeria

[2]Chemical and Metallurgical Engineering Department, Tshwane University of Technology, Pretoria, South Africa

Abstract

Electrochemical monitoring method of the open circuit potential was used to investigate the effect of the concentrations of $Na_2Cr_2O_7$ on the corrosion potential response of steel reinforced concrete in sodium chloride medium. In the study, five different concentrations of $Na_2Cr_2O_7$ admixtures were employed in a system of replicated samples of steel-reinforced concrete specimens partially immersed in 3.5% NaCl to simulate marine and saline environments. Forty days measured responses from these were subjected to the statistical analyses of the Normal and the Weibull distribution functions and tested using the Kolmogorov-Smirnov goodness of fit criteria. Results obtained from the analyses identified 4 g $Na_2Cr_2O_7$ with optimal averaged potential response inhibition performance by the Normal model which showed better agreements in its models of $Na_2Cr_2O_7$ potential test data than that obtained from the Weibull model of the same data. These bear pertinent implications on the need for suitability studies of appropriate statistical distribution for studying performance of corrosion inhibitors even as suggestions were proffered for addressing results conflicts among replicates of steel reinforced concrete samples employed.

*Corresponding author: joshua.okeniyi@covenantuniversity.edu.ng; Tel: +234-806-983-6502

1. Introduction

Corrosion degradation of reinforcing steel in concrete is a major cause of service failure in reinforced concrete infrastructure worldwide. Usually, steel embedded in concrete is protected from corrosion degradation by the high alkalinity of the concrete pore structure which is at a pH greater than 12.5 (Tang et al, 2012; Nürnberger, 2007). However, the reduction of this alkalinity could be induced by environmental agents of corrosion the major of which include chloride ingress through natural sources of marine environments or man-made saline sources of de-icing salts applications on concrete infrastructures. This renders reinforcing steel in concrete susceptible to corrosion deterioration and consequent premature dilapidation of the reinforced concrete structures. Maintenance, repair and restoration to forestall grievous and unprecedented collapse of these concrete structures usually constitute considerable portion of the budget of many countries globally (Tang et al, 2012; Sideris and Savva, 2005).

The ubiquitous nature of corrosion of reinforcing steel in concrete structures and its insidious grave consequences had necessitated the propositions of many methods for delaying corrosion initiation and arresting the progressive deterioration of steel reinforcement in concrete. From these, the use of corrosion inhibitors had been identified in studies as a viable means of mitigating corrosion menace in reinforced concrete structures. According to ISO 8044 1989, a corrosion inhibitor could be defined as a chemical substance that decreases the corrosion rate when present in the corrosion system at suitable concentration (Söylev and Richardson, 2008). From this definition, two important requirements could be identified for a chemical substance that would qualify as a corrosion inhibitor. These requirements include reduction of corrosion rate by the chemical substance and its presence, at suitable concentration, in the corrosion system.

Both ascertaining corrosion rate reduction and determination of suitable concentration for the optimal reduction of corrosion rate require effective monitoring of the corrosion system. Such monitoring techniques usually require electrochemical and non-destructive methods of measurement and subsequent comparison, especially in different corrosion systems, of the corrosion status of reinforcing steel in concrete

structures. A lot of these electrochemical measuring methods for monitoring corrosion of steel in concrete had been described in literature (Song and Saraswathy, 2007). Many of them, however, require very costly and highly sophisticated equipments. Also, a good number of them suffer the setback of been applicable for monitoring laboratory setup of corrosion system only but find no suitability for monitoring corrosion in field applications of reinforced concrete structures.

The open circuit potential (OCP) monitoring system has been known as a good monitoring method that is both suitable for monitoring probability that corrosion is occurring in steel reinforcement embedded in concrete. This method, which had been employed in many studies (Loto, 2012; Okeniyi et al 2012a; Omotosho et al, 2011; Loto 2011a; Loto, 2011b, Omotosho et al, 2010; Burubai and Dagogo, 2007; Song and Saraswathy, 2007), utilizes simple equipments which are very easy to setup both in the laboratory as well as in the field applications for diagnosing corrosion risks in reinforced concrete structures. Also, standard for interpreting measurements from the OCP monitoring method exists, especially, that which had been provided by the American Society for Testing and Materials (ASTM) generally known as ASTM C876 (Song and Saraswathy, 2007).

Although the open circuit potential measuring method has been studied for relationship between its potential measurements and corrosion rate in well established laboratory conditions, the generalization of the results had not been possible (Song and Saraswathy, 2007). This is both due to the wide variation of corrosion rate that could be possible within narrow range of open potential readings and the stochastic response in the potential readings that could results in the dynamic active-passive mechanism of the corrosion system. The consequences from these had included prevalent conflicting interpretations and contradicting reports in corrosion inhibitor studies.

According to Haynie (2005), variations and stochastically differing results require the use of statistical methods of probability distributions for the treatment of corrosion data for assessing the prevalent conditions in the corrosive environments. However, this approach had been identified as a neglected one among the tools for interpreting and requisite treatment of corrosion data. By this, there is paucity of studies in literature deliberating on suitability or otherwise of statistical probability distribution for studying performance of inhibitor admixtures on the corrosion of steel reinforcement in concrete. This paper therefore studies the suitability of the Normal and Weibull modeling tool applications for investigating corrosion potential performance of $Na_2Cr_2O_7$ on the corrosion of reinforcing steel in concrete immersed in NaCl, simulating marine or saline environments.

2. Materials and Methods

Reinforced concrete blocks

Twelve reinforced concrete block samples used for the experiment were produced as replicates blocks of size 100 mm × 100 mm × 200 mm. Embedded in each block was 150 mm length of steel rebar which was symmetrically placed across the width of the block with the remaining length of the rebar protruding for electrochemical connections. Each of the concrete blocks was made of water and a mixture of Portland cement, sand and granite stones in a mix proportion of 1:2:4 (C:S:G). The formulation used for the reinforced concrete specimens was 300.0 kg/m^3 of cement, 149.7 kg/m^3 of water, 890.6 kg/m^3 of sand, and 1106.3 kg/m^3 of granite stones. The water/cement (w/c) ratio was 0.499. For these reinforced specimen samples, the $Na_2Cr_2O_7$ admixture concentrations were varied from 0 g (for the control specimen replicates) in increments of 2 g up to 10 g of $Na_2Cr_2O_7$. The inhibitor admixed concrete blocks were moulded with wood covered with non-absorbent material that is non-reactive with concrete and cured in a curing room for 28 days. The rebar protrusion was painted with glossy paint.

2.1 Experimental Procedure

Corrosion test setup

Steel reinforced concrete samples were partially immersed, longitudinally, in plastic bowls containing 3.5% NaCl solution (Zhou et al, 2012; Zafeiropoulou et al, 2011). In each bowl, the test solution was made up to just below the reinforcing steel rebar but was not touching it. From these, open circuit potential (OCP) measurements were taken versus $Cu/CuSO_4$ electrode (CSE), using a high impedance digital multimeter according to ASTM C876, in five days interval through an experimental period of forty days.

Data Analysis

Probability distribution modelling

Test data of the potential response from the corrosion test setup were subjected to statistical analysis of the Normal and the Weibull distribution functions (Okeniyi et al, 2012a; Okeniyi et al, 2012b; Omotosho et al, 2011). While the application of the Normal distribution for modelling data had been described elsewhere (Okeniyi et al, 2012b), the Weibull distribution is an extreme-value modelling distribution with probability density function, pdf (Omotosho et al, 2011; Montgomery and Runger, 2003):

$$f(x)=\frac{k}{c}\left(\frac{x}{c}\right)^{k-1}\cdot\exp\left\{-\left(\frac{x}{c}\right)^{k}\right\} \quad 1$$

Where k is the shape parameter and c is the scale parameter. Estimations of these parameters were done as described in Omotosho et al (2010) and these find usefulness for computing the Weibull predictions of the mean μ_W and the standard deviation σ_W, respectively, using the relationships (Murthy et al, 2004; Montgomery and Runger, 2003):

$$\mu_W = c\Gamma\left(1+\frac{1}{k}\right) \quad 2$$

$$\sigma_W = \sqrt{c^2\left\{\Gamma\left(1+\frac{2}{k}\right)-\left[\Gamma\left(1+\frac{1}{k}\right)\right]^2\right\}} \quad 3$$

where $\Gamma(\cdot)$ is the gamma function of $(\cdot)$.

Goodness-of-fit test statistics

To ascertain the compatibility of the OCP data to each of the statistical distributions employed, the Kolmogorov–Smirnov (K-S) goodness of fit test (Thas, 2010; Soong, 2004; Izquierdo et al, 2004; Roberge, 2003) was used. This measures the absolute difference between empirical distribution function $F^*(x)$ and theoretical distribution function $F(x)$ (Thas, 2010; Soong, 2004) through the statistics

$$D_n = D(x_1,...,x_n) = \sup_{-\infty<x<\infty}\left|F^*(x)-F(x)\right| \quad 4$$

The D-value evaluation from Equation **Error! Reference source not found.** was used for direct computation of the K-S p-value using procedures that had been described in Okeniyi and Okeniyi (2011). By this, criteria could be set such that, for α = 0.05 significant level, K-S p-value < α for a probability distribution model of corrosion test data indicate that such data did not follow that distribution while K-S p-value ≥ α showed that the test data followed the distribution model.

3. Results and discussions

Measured experimental data

Plots of the measured data of open circuit corrosion potential response through the forty days experimental period are presented in Fig. 1 for the reinforced concrete samples admixed with different replicated concentrations of $Na_2Cr_2O_7$ and immersed in 3.5% NaCl. While it could be deduced from the plots, that the corrosion potential response of the control samples had, by the fortieth day overshot the potential response of the remaining samples with inhibitor admixture, thus depicting inhibition, the plots still exhibit stochastic variability among the samples. This variability could make interpretation or evaluation of the performance of the concrete admixture on the rebar corrosion difficult, hence, re-affirming the need for the use of statistical modeling tool for evaluating this variability and aiding result interpretations.

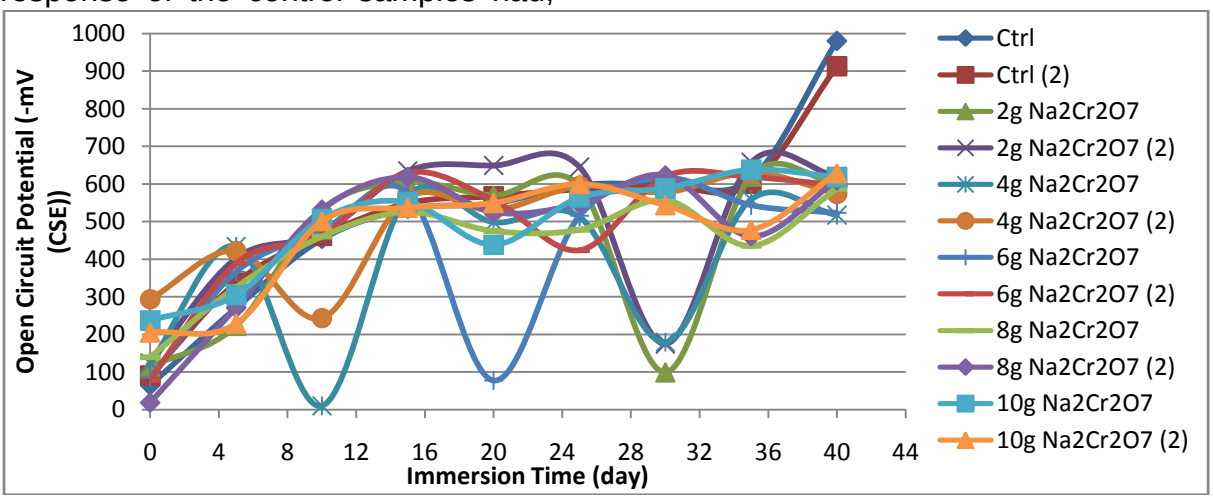

Fig. 1 Corrosion potential response of $Na_2Cr_2O_7$ admixtures in reinforced concrete samples

Statistical modeling and analyses

Results of the Normal pdf and that of the Weibull pdf models of the potential response data of $Na_2Cr_2O_7$ admixture concentrations in steel reinforced concrete samples are presented in ranking order in Fig. 2. In this figure, rankings by the Normal model are shown in Fig. 2(a) while that by the Weibull model are shown in Fig. 2(b). From these, it could be observed that while the Normal pdf model identified the 4 g $Na_2Cr_2O_7$ sample with optimal, more positive corrosion potential inhibition ranking, the Weibull pdf modeled this same sample as exhibiting corrosion potential even more negative (and higher corrosion probability) than the replicate samples of control specimens. Also, while the Normal model agrees in the ranking order of the effectiveness of the replicate samples of the 8 g $Na_2Cr_2O_7$ replicate samples, Fig. 2(a), the Weibull model identified one of these samples with optimal corrosion potential inhibition performance and its replicate as exhibiting the most negative corrosion potential (and the highest or most severe corrosion probability) in all the samples studied in this work, Fig. 2(b). Thus, while the Normal pdf model were in agreement that all concrete samples admixed with $Na_2Cr_2O_7$ exhibited better corrosion potential performance than the control samples though with slight

discrepancies in the ranking order of replicate samples, the Weibull pdf model identified two samples admixed with $Na_2Cr_2O_7$ performing exhibiting worse performance than the two replicates of control samples. A close observation of the plots showed that these two samples, the 4 g $Na_2Cr_2O_7$ and the replicate of 8 g $Na_2Cr_2O_7$, both exhibited very high values of Weibull pdf model standard deviations (Weibull σ) which were even higher than the Weibull mean models for these samples. This portends wide range of scattered corrosion potential data in the Weibull model of these test data, even as it genders questions on how well these sets of data followed the Weibull distribution modeling function.

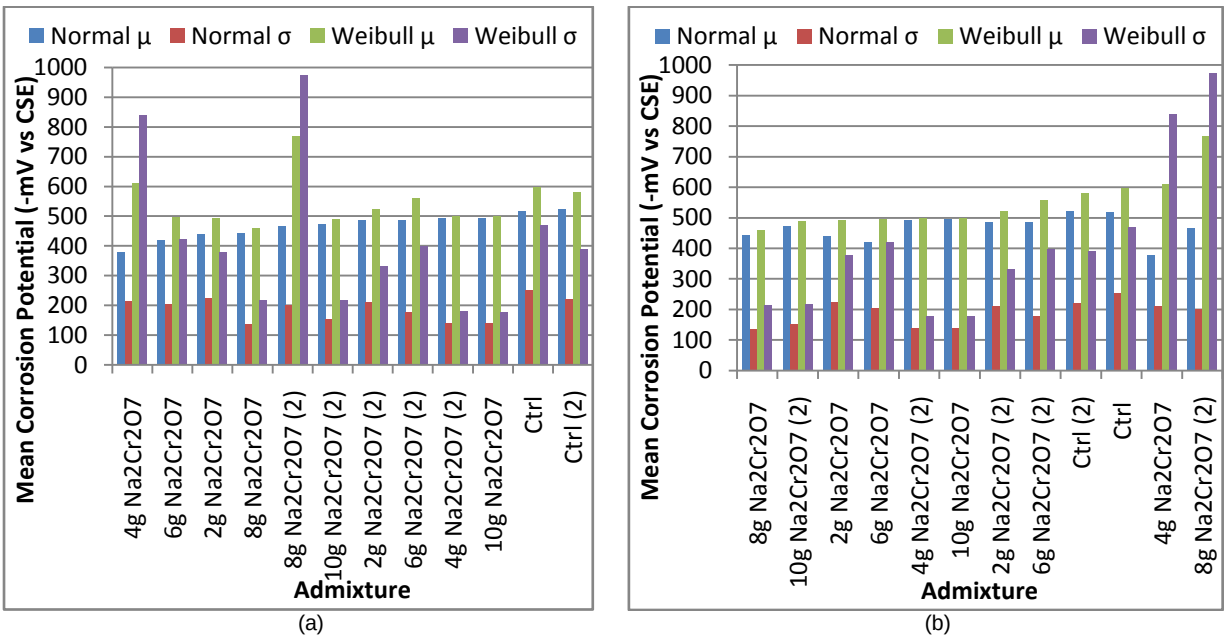

(a) (b)

Fig. 2 Ranking models of $Na_2Cr_2O_7$ inhibition performance by potential response in reinforced concrete samples (a) Normal pdf model (b) Weibull pdf model

The results of testing how well the modeled data followed each of the statistical distribution models employed in this paper, using the Kolmogorv-Smirnov goodness of fit statistics, are presented in Fig. 3. This showed that all the modeled data of corrosion potential response of steel reinforced concrete samples followed both the Normal pdf model and the Weibull pdf model at the significance level of α = 0.05, shown in the figure. By this, it could be surmised that discrepancies observed in the pdf models depend more on the applied pdf model than on the corrosion potential data. Thus, because the Normal pdf exhibited better agreements in its models of these data than the Weibull pdf, it is adjudged as the suitable pdf model for describing the performance of the $Na_2Cr_2O_7$ admixtures on the corrosion potential of the concrete reinforcing steel specimens in this study.

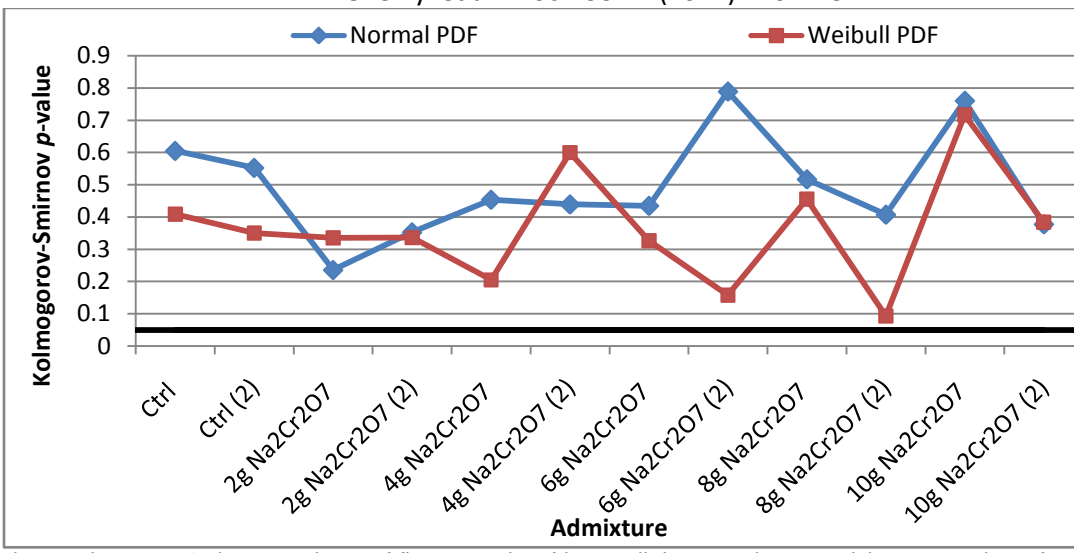

Fig. 3 Kolmogorov-Smirnov goodness of fit test results of how well the corrosion potential response data of $Na_2Cr_2O_7$ admixtures in reinforced concrete samples follows the Normal and the Weibull distribution functions

From the foregoing considerations, the Normal pdf model results are employed for estimating averaged model of $Na_2Cr_2O_7$ performance on the corrosion potential response of steel reinforced concrete immersed in saline media, in this study. The plots of this averaged performance model are presented in Fig. 4. From this figure, the 4 g $Na_2Cr_2O_7$ admixture is modeled as exhibiting optimal corrosion potential inhibition performance among all the samples studied in this experimental work. This was followed in order by the 6 g $Na_2Cr_2O_7$, the 8 g $Na_2Cr_2O_7$, the 2 g $Na_2Cr_2O_7$ and then the 10 g $Na_2Cr_2O_7$ before the control sample.

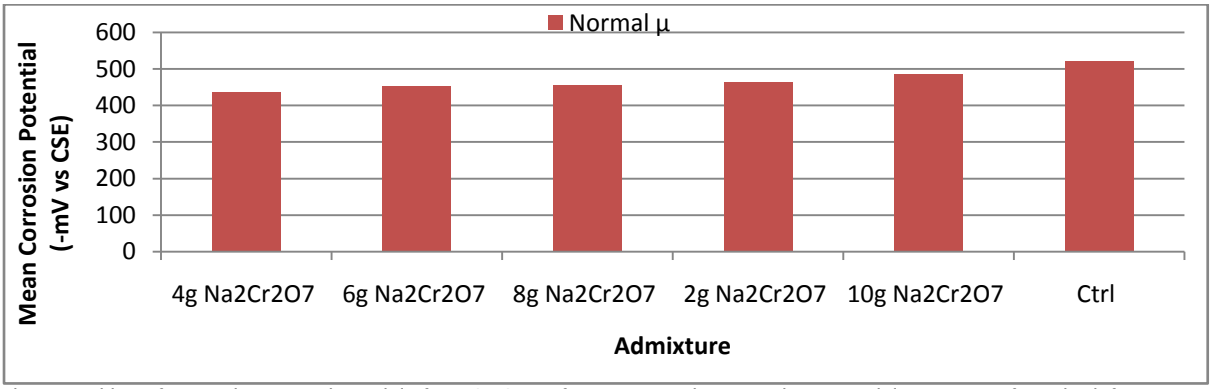

Fig. 4 Ranking of Normal averaged model of $Na_2Cr_2O_7$ performance on the corrosion potential response of steel reinforcement in concrete

These results bear implications on the need for studying suitability of statistical distribution functions for tackling inherent variability in corrosion test data and for aiding interpretation of the prevailing conditions in these datasets. Also, there is need for further studies deliberating on suitable statistical tools for handling discrepancies in results observed among replicate samples admixed with similar concentrations of inhibitor admixtures. Such studies would be useful for assessing significance or otherwise of observed or modeled discrepancies and which could serve as important tools for avoiding conflicting and contradictory reports of corrosion inhibitor performance.

4. Conclusions

Effects of $Na_2Cr_2O_7$ admixtures on the corrosion potential response of steel

reinforced concrete in immersed saline medium had been studied using the Normal and the Weibull distribution functions. From these, the following conclusions can be drawn:

- The non-destructive test data of corrosion open circuit potential response, measured through the experimental period, exhibited stochastic data which require probability density fittings for modeling order and interpreting inhibitor performance;
- Results of Normal pdf model of the test data of corrosion potential response exhibited better agreements among the replicates of steel reinforced concrete samples studied than the results obtained from the Weibull pdf of the same datasets;
- The test data of corrosion potential response followed the Normal distribution and the Weibull distribution model at $\alpha = 0.05$ significant level, through the Kolmogorov-Smirnov goodness of fit statistics, by this, the discrepancies observed in the statistical models of the corrosion test data in the study were surmised to be due to the suitability of the statistical probability model for describing the test datasets, thus, because the Normal pdf exhibited less of these discrepancies, it was adjudged as the suitable pdf model for interpreting inhibitor performance in the corrosion setup system;
- By these, considerations, the application of the Normal pdf model identified the 4 g $Na_2Cr_2O_7$ admixture as exhibiting optimal more positive corrosion potential and thus the admixture with optimum inhibition performance, on the corrosion of steel reinforcement in concrete, among the other $Na_2Cr_2O_7$ admixture studied in this work;
- These bear implications of the need for studying suitability of statistical probability distribution models for requisite analyses and interpretation of corrosion test data results in the performance studies of corrosion inhibitor in steel reinforced concretes, even as these also genders suggestions for the use of further applications of necessary statistical tools for studying significance of discrepancies encountered among the replicates samples admixed similar concentrations of inhibitor admixtures.

References

Burubai, W. and Dagogo, G. 2007. Comparative Study of Inhibitors on the Corrosion of Mild Steel Reinforcement in Concrete, *Agricultural Engineering International: The CIGR Ejorunal, Manuscript BC 06 008*, **9:** 1–10.

Haynie, F. H. 2005. Statistical treatment of data, data interpretation, and reliability. In: Baboian, R. (ed.) *Corrosion Tests and Standards: Application and Interpretation – second edition*, ASTM International, West Conshohocken, PA, 83–88.

Izquierdo, D., Alonso, C., Andrade C. and Castellote, M. (2004) 'Potentiostatic determination of chloride threshold values for rebar depassivation: Experimental and statistical study', *Electrochimica Acta*, Vol. 49: 2731–2739.

Loto, C. A. 2012. Electrode Potential Evaluation of Effect of Inhibitors on the Electrochemical Corrosion Behaviour of Mild Steel Reinforcement in Concrete in H_2SO_4. *Journal of Materials and Environmental Science* **3(1):** 195–205.

Loto, C. A. Loto R. T. and Popoola, A. P. I. 2011a. Electrode Potential Monitoring of Effect of Plants Extracts Addition on the Electrochemical Corrosion Behaviour of Mild Steel Reinforcement in Concrete. *International Journal of Electrochemical Science* **6:** 3452–3465.

Loto, C. A., Omotosho, O. A. and Popoola, A. P. I. 2011b. Inhibition effect of potassium dichromate on the corrosion protection of mild steel reinforcement in concrete. *International Journal of the Physical Sciences* **6(9):** 2275–2284.

Montgomery, D.C. and Runger, G.C. (2003) *Applied Statistics and Probability for Engineers, 3rd edition*, John Wiley & Sons, Inc.

Murthy, D.N.P., Xie, M. and Jiang, R. (2004) *Weibull Models*, John Wiley & Sons, Inc., Hoboken, New Jersey.

Nürnberger, U. 2007. Corrosion of metals in contact with mineral building materials. In: Raupach, M., Elsener, B., Polder R. and Mietz J. (eds.) *Corrosion of reinforcement in concrete: Mechanisms, monitoring, inhibitors and rehabilitation techniques.* England: Woodhead Publishing and Maney Publishing on behalf of Institute of Materials, Minerals and Mining.

Okeniyi, J. O. and Okeniyi E. T. 2011. Implementation of Kolmogorov-Smirnov p-value computation in Visual Basic®: implication for Microsoft Excel® library function. *Journal of Statistical Computation and Simulation* doi:10.1080/00949655.2011.593035

Okeniyi, J. O., Obiajulu, U. E., Ogunsanwo, A. O., Odiase, N. W. and Okeniyi, E. T. 2012b. CH_4 emission model from the waste of Sus Domesticus and Gallus Domesticus in Nigerian local farms: environmental implications and prospects. *Mitigation and Adaptation Strategies for Global Change* doi: 10.1007/s11027-012-9365-7

Okeniyi, J.O., Omotosho, O. A., Ajayi, O. O., James, O. O. and Loto, C. A. 2012a. Modelling the Performance of Sodium Nitrite and Aniline as Inhibitors in the Corrosion of Steel-reinforced Concrete. *Asian Journal of Applied Sciences* **5(3):** 132–143.

Omotosho O. A, Loto C. A., Ajayi O. O. and Okeniyi J. O. 2011. Aniline effect on concrete steel rebar degradation in saline and sulfate media. *Agricultural Engineering International: CIGR E-Journal Manuscript No.1830* **13(2):** 1–17.

Omotosho, O. A., Okeniyi, J. O. and Ajayi, O. O. 2010. Performance Evaluation of Potassium Dichromate and Potassium Chromate Inhibitors on Concrete Steel Rebar Corrosion. *Journal of Failure Analysis and Prevention* **10:** 408–415.

Roberge, P.R. (2003) 'Statistical Interpretation of Corrosion Test Results', In: Cramer, S.D. and Covino, B.S., *Corrosion: Fundamentals, Testing, and Protection*, *ASM Handbook, Vol. 13A*, ASM International, pp. 425−429.

Sideris, K.K. and Savva, A. E. 2005. Durability of mixtures containing calcium nitrite based corrosion inhibitor. *Cement & Concrete Composites* **27:** 277–287.

Song, H. -W. and Saraswathy, V. 2007. Corrosion monitoring of reinforced concrete structures: A review. *International Journal of Electrochemical Science* **2:** 1–28.

Soong, T.T. (2004) *Fundamentals of probability and statistics for engineers*, John Wiley & Sons Ltd, England.

Söylev, T. A. and Richardson, M. G. 2008. Corrosion inhibitors for steel in concrete: State-of-the-art report. *Construction and Building Materials* **22:** 609–622.

Tang, Y.M., Miao, Y.F., Zuo, Y., Zhang, G.D. and Wang, C.L. 2012. Corrosion behavior of steel in simulated concrete pore solutions treated with calcium silicate hydrates. *Construction and Building Materials* **30:** 252–256.

Thas, O. (2010) *Comparing Distributions*, Springer Science+Business Media, LLC.

Zafeiropoulou, T., Rakanta, E. and Batis, G. 2011. Performance evaluation of organic coatings against corrosion in reinforced cement mortars. *Progress in Organic Coatings* **72:** 175– 180.

Zhou, X., Yang, H. and Wang, F. 2012. Investigation on the inhibition behavior of a pentaerythritol glycoside for carbon steel in 3.5% NaCl saturated $Ca(OH)_2$ solution. *Corrosion Science* **54:** 193–200.

An evaluation of total quality management practices on business performance of the Nigerian telecommunications sector: a case study of MTN Nigeria Limited

Alamutu S.A, Hotepo O.M, Oyeobu A.J. and Nwatulegwu B.I.
Lagos State University, Department Of Business Administration and Management Technology

Abstract

This study examines the effects of The Total Quality Management practices on Business Performance of the Nigerian Telecommunications Sector. A review of literatures on TQM shows that no study has been carried out on its application in the Nigerian Telecommunication sector hence the need for this research. To assess the situation One hundred and fifty (150) questionnaires were administered to customers of MTN Limited within the Lagos environ. These customers were randomly selected from five (5) different MTN customer care centres within the five divisions of Lagos State. These divisions include Epe, Ikorodu, Lagos Island, Lagos Mainland and Badagry. Thirty (30) questionnaires were administered at each centre. Fifty (50) questionnaires were also administered to employees of MTN and a total of twenty (20) questionnaires were administered to top management in the same organizations.

The data collected were analyzed using descriptive statistics and regression analysis. Our finding revealed that 90.7% of the changes that occurred in employees' satisfaction could be traced to the policy and commitment of top management. It also shows that 69.4% of the changes in customer satisfaction could be attributed to continuous training in quality. The study recommended among other things the training of telecommunications personnel on Total Quality Management practices and the adoption of alternative renewable sources of energy like solar to address their energy problems.

***Key words**: Total Quality Management, Telecommunication industry, top management commitment, continuous training in quality, employee satisfaction, customer satisfaction*

1. Introduction

In a competitive market, the demand for quality is emerging as the single most critical factor for companies to survive in the ever-expanding global market place.

One of the major reason quality has gained such prominence is because organizations have gained an understanding of the cost of poor quality. Quality affects all aspects of an organization and has serious cost implications. The most obvious is when poor quality cause customer dissatisfaction and consequently lack of patronage. There are two major cost element associated with quality, namely: quality control cost and quality failure cost. The quality control cost is made up of prevention cost and appraisal cost while quality failure cost is made up of internal failure cost and external failure cost. Research has shown that quality control cost is considerably less than quality failure cost.

Another reason adduced for emphasis on quality is because of the phenomena of globalization and competition. As trading barriers are collapsing all over the world and firms are competing for markets that were previously controlled by monopolist; the issue of satisfying the customer has taken centre stage and companies must seek ways to offer the customer better products at cheaper prices. Companies which cannot do this become extinct. The attempt to produce better products at cheaper prices has made the concept of quality imperative as a survival strategy for organizations operating in the 21st century.

2. History of Total Quality Management

The concept of quality has existed for many years though its meaning has changed and evolved over time. Quality can be traced back to the craftsmen era. This was before the industrial revolution. During this era products were produced by skilled craftsmen who set up guilds to ensure that products conformed to standard. The second was the standardization, mass production and quality assurance era (1900-1930). This happened with the formation of factories and increasing automation and as work became progressively deskilled and more repetitive. Thus inspectors were employed to do 100% inspection and differentiate between conforming and non conforming items. This was also the era of Frederick Winslow Taylor who introduced the concept of scientific management with emphasis on work output, labour efficiency and introduction of work study. The third era was the quality control era (1930-1950) when the principal focus was replacing inspection with more informative process control systems which aimed at reducing variation in outputs and delivering more consistency by focusing on inputs. Next was the total quality management (TQM) era (1950-1970) which emphasized organizational quality driven by management. After this was the Standards and Awards Era (1970-1990). This was a period of standardization of the principles of TQM. Examples of standards are BS 5750 and ISO 9000 Quality systems standard. They are externally audited and accredited standards. Finally, we are in what can be termed the initiatives era which started in 1990 until the Present time. This involves the appearance of mega initiatives of which Lean and Six-Sigma are of.

3. Total Quality Management

Ciampa (1992) describes TQM as "the state of an organization in which all the activities of all functions are designed and carried out in such a way that all external customer requirements are met while reducing internal time and cost, and enhancing the workplace climate".

TQM can be defined as a holistic management philosophy aimed at continuous improvement in all functions of the organization and satisfaction of customers' needs and requirements by providing quality services under the leadership of top management (Demirbag, Taloglu, Tekinkus, and Zaim 2006). According to Ooi, Arumugam, Loke and Lorraine (2006) TQM is significant because its implementation brings about positive impact on the organization and its employees.

In the case of Deming (1986) he posits that TQM is a philosophy that involves everyone in an organization on continuous effort to improve quality and achieve customer satisfaction. Juran (1995) however suggests that TQM is a description of the culture, attitude and organization of a company that strives to provide customers with products and services that satisfy their needs.

4. Overview of Nigerian telecommunications sector

The Telecommunications industry is a strategic and critical sector of the Nigerian economy. It has security implications. It is also a source of employment and livelihood to millions of Nigerians.

The development of Telecommunication in Nigeria can be traced back to 1851 when the British Post Office established its postal branch in the country. Following this was the establishment of the ''key & Sounder'' system of telecommunication in 1885 used by the colonial masters for effective administration and contact with London Home office. Within this year also local telecommunication using this system was introduced by the colonial government in 1885

under the Public Works Department. The first direct telegraph services between Lagos and London was finally commenced in September 1886.

By 1950 Nigeria had 98 exchanges with 15,063 telephone instruments. The exchanges were of the Magnetic and Central Battery type. In this year also General Electric Corporation installed 600 lines automatic exchange in Port Harcourt which was followed by 500 lines exchange in Lagos by 1953. In 1963 the satellite exchanges of Ikeja with 400 lines, Ebute Metta with 500 and Apapa with 600 commenced. After Nigeria's independence, the sector has undergone several development stages. The first stage was 1962-1968 during which 2,000 direct exchange lines were provided instead of 90,000 that was projected. This period was however interrupted by the civil war. During the period between (1970-1974) the National Telex/Gentex Network, 19 crossbar Telephone Exchanges, Subscriber Trunk Dialing (STD) facilities, between Lagos, Ibadan, Kaduna, Enugu and Benin were developed. Thereafter, the Contingency Plan (1973-1975) was launched with a total of 52,000 lines against the planned 184,000. The next phase was 1975-1980 in which 188,000 of the planned 750, 000 lines was achieved. Between the periods 1981-1985 telephone lines increased to 400,000 instead of the projected 612,000.

In 1985 Nigerian Telecommunications Limited (NITEL) was born by merging the Telecommunication arm of Post & Telecommunication with Nigerian External Telecommunication in 1985. NITEL was given the mandate to provide efficient and reliable telecommunications services for the country at a marginal profit. This mandate could not be achieved as NITEL services were characterized by low call completion, low investment rate, uneconomic investment patterns and management.

With the Global trend in telecommunication moving towards deregulation government was compelled to liberalize the telecommunication sector with the establishment of a regulator, Nigerian Communications Commissions (NCC). Despite the creation of NCC, NITEL still enjoyed a monopoly status with its services still characterized by inaccurate and irredeemable bills. There were also incidences of contested bills. Subscription rates for phone services were also very exorbitant.

With these problems bedeviling NITEL, many private telephone operators like Intercellular, Mobitel, Reltel were licensed but could not deliver as expected.

With the pent up demand and global adoption of GSM technology the door was opened for licensing of GSM operators. The first set of GSM operators, namely MTN, ECONET, NITEL were issued licenses in early 2001 and in August 2001 Econet (now Airtel Bharti) and MTN launched commercial services.

There are presently 8 major telecom companies in Nigeria in Nigeria, namely: MTN, Globacom, Airtel, and Etisalat who offer Global Systems Mobile communication (GSM) while another four namely Visafone, Zoom, Multilinks, Starcoms offer Code Division Multiple Access (CDMA). These companies offer voice, data and video services.

According to Nigerian Telecommunication Commission (2011) as at December 2011 the number of fixed and fixed wireless lines available was 95,886, 714 compared with the 400,000 lines fifteen years ago.

According to Nigerian Pilot (2012) the Executive Vice-Chairman, NCC, Mr. Eugene Juwah, while speaking at a forum said "Nigeria's growth has been mirrored by a concomitant boom in telecommunications in recent time, because the

industry is a sector that holds the key to the realisation of Nigeria's ambition to truly emerge as a dominant developing economy. The importance of communication in any country whether developed or developing is so obvious. In fact the inter-relationship between the economic development of a country and effective telecommunication services is so interwoven that it is difficult to tell which one comes first. Communications has remained permanently visible, with its applicability to almost every human endeavor from agriculture, to food security, to manufacturing, energy and physical infrastructure sectors in all its ramifications for governance, e-commerce and the provision of public and social services".

The figure for active subscribers in mobile networks is around 100 million lines and may surpass 105 million by end of December, 2012

5. MTN Telecommunications Ltd

MTN Nigeria is the largest member of MTN group, a South African company with many subsidiaries spread across the world (21 countries in Africa and Middle East). In Nigeria, the company just marked its 11 years of operation. The company's vision is to be the country's leading telecommunications service provider while its mission is to provide 1st class network quality, customer service and value.

MTN communications Ltd was one of the three (3) initial GSM companies licensed by NCC to provide telecommunications services to the Nigerian public. It commenced operations in August 2001 and has been the largest in all of Nigeria.

MTN has invested billions of dollars in telecoms equipment and infrastructure providing base stations, and other amenities. It has also created job for hundred of thousand of Nigerians directly and indirectly.

In the area of products and services MTN offers various services like MTN happy hour, MTN family and friends etc. It provides services like internet browsing, international roaming, enterprise solutions and airtime services. It also provides MTN blackberry services, data bundle, MTN video calling, fast link, mobile internet. Among all the mobile phone networks, MTN is the most widely spread in terms of coverage and availability.

Successful implementation of TQM in the Nigerian Telecommunications sector will result in improved employee involvement, improved communication, increased productivity, improved quality of service, reduced cost, customer satisfaction, and improved competitive advantage.

6. Statement of the Problem

Even though the Nigerian Telecommunications sector has grown significantly in the past ten years, yet customers still complain of poor customer service, drop calls, high call rate, network blockage or congestion, and service quality problems. Piqued by these falling standard of quality of services the Nigerian Telecommunications Commission had to slam a whopping sum of N1.17billion fine on all four (4) GSM operators (Guardian May 10th 2012). This problem of quality may be due to non-adoption of TQM practices by the Telecommunications companies. There is however a scarcity of literature on factors responsible for this development; hence we intend to appraise the TQM practices in this industry and to develop a model for applying TQM practices for better

delivery of services in the Nigerian telecommunication sector.

Objectives of this research

1. To examine if Total Quality Management is being practiced in the Nigerian Telecommunications sector
2. To assess the impact of Top management commitment on employee satisfaction
3. To assess the impact of continuous training in quality on customer satisfaction

Research question

1. Would the Top management commitment lead employee satisfaction?
2. Would quality training in quality lead to customer satisfaction?

Literature Review

Theoretical Framework

Walter A. Shewart laid the foundation for the application of Statistical quality control to quality management while W. Edwards Deming followed with 14 principles of implementing total quality management. These points are namely:- The fourteen points proposed by Deming are to create constancy of purpose towards improvement of product and service; adopt the new philosophy of we can no longer live with commonly accepted levels of delays, mistakes, and defective workmanship; cease dependence on mass inspection. Instead, require statistical evidence that quality is built in; end the practice of awarding business on the basis of price; find problems because it is management's job to work continually on the system; institute modern method of training on the job; institute modern methods of supervision of production workers; the responsibility of foreman must be changed from numbers to quality; drive out fear, so that everyone may work effectively for the company; break down barriers between departments; eliminate numerical goals, posters and slogans for the workforce asking for new levels of productivity without providing methods; eliminate work standards that prescribe numerical quotas; remove barriers that stand between hourly worker and their right to pride of workmanship; institute a vigorous programme of education and retraining; create a structure in top management that will push on the above point every day. Deming was also reported to have introduced a systematic approach to problem solving and promoted the widely known Plan, Do, Check, Act (PDCA) cycle

Joseph M. Juran is the next quality guru. In terms of contribution, Juran concentrated not just on the end customer but also on other external and internal customers. According to him each person along the chain, from product designer to final user is a supplier and a customer. In addition the person will be a process, carrying out more transformation or activity.

Another leader is Armand V. Feigenbaum who looked at Quality using the system approach. He emphasized the idea of a work environment where quality development is integrated throughout the entire organization. He defined is total quality control as an "An effective system for integrating quality development, quality maintenance and quality improvement efforts in various groups within an organization so as to enable production and service at the most economical levels that allow full customer satisfaction". Faigenbaum saw it as business method and proposed three steps to quality which are quality leadership; modern quality technology; organizational commitment.

Following Feigenbaum was Phillip B. Crosby who emphasized the concepts of "zero defects" and "do it right the first time".

Kaoru Ishikawa is best known for his development of quality tools like “fishbone” diagram. He also emphasized the concept of “internal customer” and the use of “quality circles” to solve quality problems.

Genichi Taguchi contribution was in product design. According to him, 80 percent of defective products are caused by poor product design. He developed the “Taguchi Loss function” which shows that the cost of quality increase as a quadratic function as conformance values moves away from the target. There are also numerous contributors to total quality which will be considered below.

In the study by Brah, Wong and Rao (2000) 11 different concepts of TQM were suggested, which are customer focus, process improvement, quality improvement rewards, cleanliness and organization, service design, benchmarking, employee empowerment, top management support, customer focus, employee involvement, employee training, supplier quality management. Bayraktar, Tatiglu, and Saim (2008) were able to identify 11 critical success factors (CSFs) for the implementation of TQM, which are employee involvement, recognition and award, education and training, quality system improvement, student focus, program design, process control and improvement, measurement and evaluation, vision, other stakeholder focus, leadership. In the case of Talib, Rahman and Quresh (2010) they posited that there are 17 practices needed for the successful adoption of TQM in the service sector which are: top management commitment, customer focus, training and education, continuous improvement, and innovation, supplier management, employee involvement, information and analysis, process management, quality system, benchmarking, quality culture, human resource management, strategic planning, employee encouragement, teamwork, communication, process and service design. Sureshchandar et al (2002) in his work argued that there are 12 major practices which comprise top management commitment and visionary leadership, human resource management, technical system, information and analysis system, benchmarking, continuous improvement, customer focus, employee satisfaction, union intervention, social responsibility, servicescapes, and service culture. According to Mehra, Hoffman and Sirias(2001) there are 45 elements that affect TQM which are : top management commitment, suppliers involvement, small supplier base, total employee involvement, teams, training, leadership, customer focus, human resource, management style, organizational structure, ownership, continuous improvement, consultants, business culture, process oriented, statistical tools, quality audits, empowerment, quality planning, quality data, mechanism to set priorities, mechanism to coordinate activities, quality council or steering committee, written policy on quality, measurement of key result areas, reward system tied to key measures, customer oriented reward system, recognition and celebration, deployment of key information to all employees, quality related goals, flatter organizations, group incentive systems, decentralization of operational decisions, lateral communication, decisions based on data, benchmarking, measurement of cost of quality, customer oriented product development, long term employment, technical competence of senior corporate executive, board of directors involvement, management tools, right brain thinking, recognition of environmental issues. All these 45 elements he was able to summarize under 5 headings which are: human resource focus, management structure, quality tools, supplier support, customer orientation.

Performance Measurement

Numerous studies have examined the positive and negative (or non-significant) relationships or

contributions between TQM practices and various performance measures. This section examines different performance measures. Hermann et al (2006) considered quality performance, reduction in cost and shorter R&D time as performance measures whereas in the case of Yang (2006) he measured quality performance by using the following indicators namely: Employee satisfaction, employee quality awareness, customer satisfaction and company image.

Conceptual Framework

Through the comprehensive review of TQM literature, the present study identified a set of 8 essential TQM practices on which the conceptual framework of this study will be based. They are: - top management commitment, customer focus, strategic focus, process focus, employee empowerment, training, continual improvement, and managing suppliers' quality. The reasons for selecting these practices are:

- They constitute practices that represent the hard and soft components of TQM
- Have been used frequently by different researchers in the service industry

Hence, it is believed that these practices are suitable to the used in the Nigerian service sector.

Top management commitment to TQM

The involvement and commitment of top management is topmost in the implementation of total quality management as agreed by different authors as cited above. According to Mehra et al (2001) top management provides both the physical and leadership needs of the organization and most organizational changes and training needs require top management approval. He said further that in addition, top management behavior signals to all employees the importance of TQM and that the job of top management is coaching and facilitating

Continuous Training in Quality

Training is the single most significant component in trying to improve quality (0akland, 1989). He argues that ''quality training must be continuous to meet not only changes in technology but also changes involving the environment in which an organization operates, its structure, and perhaps most important the of all the people who work there".

According to Brown (1994) and Patel (1993) effective TQM implementation requires a training policy which will be part of the overall quality Strategy with the aims of improving the necessary skills for continuous quality improvement. According to Wagoner (n.d) one of the key elements affecting TQM success or failure is knowledge and understanding. He argues further that for TQM to succeed employees must understand what TQM is, what it can do and why its being pursued by the organization. According to the study by Olian & Rynes (1991) it was found that the most mentioned topic found in training for TQM, presented in order of frequency were interpersonal skills, quality improvement processes and problem solving, team leading and building, running meetings and statistical analysis.

Customer satisfaction

According to Fornell(1992) a key motivation for the growing emphasis on customer satisfaction is that high customer satisfaction lead to a stronger competitive position resulting in higher market share and profit. Deng et al (2009) posits that the ability of a service provider to create a high degree of satisfaction is crucial for product differentiation and developing strong relationship with customers. The service a brand offer and the price it charges actually determine

the level of satisfaction among its customer than any other measure (Turel and Serenko 2006). According to Eklof and Westlund (2002) using the European Customer Satisfaction Index (ECSI) customer satisfaction is caused by some factors such as perceived quality (PQ), perceived value (PV), expectation of customers and image of a firm.

Employee satisfaction

Rousseau (1978) identified three elements of employee satisfaction which are organization characteristics, personal characteristics and job task factor. According to the study by Judge et al (1993) employee satisfaction is the degree to which a person feels satisfied by his/her job and positively correlated with motivation, job involvement, organizational citizenship behavior, organizational commitment, life satisfaction, mental health, and job performance and negatively related to absenteeism, turnover and perceived stress on the job.

Research Methods

For this research work, survey design was adopted. One hundred and fifty (150) questionnaires were administered to customers of MTN Limited within the Lagos environ. These customers were randomly selected at five (5) different MTN customer care centres within the five divisions of Lagos State. These divisions include Epe, Ikorodu, Lagos Island, Lagos Mainland and Badagry.

Thirty (30) questionnaires were administered at each centre. Fifty (50) questionnaires were also administered to employees of MTN and a total of twenty (20) questionnaires were administered to top management in the same organizations. The data collected were analyzed using descriptive statistics and regression analysis.

Model Summary

Model summary of Top Commitment and Employee Satisfaction

Model Summary

Model	R	R Square	Adjusted R Square	Std. Error of the Estimate	Change Statistics		
					R Square Change	F Change	Sig. F Change
1	.953[a]	.907	.876	31.192	.907	29.379	.012

a. Predictors: (Constant), TOP MANAGEMENT COMMITMENT

Table 1

Model Summary of Continuous Training in Quality and Customer Satisfaction

Model Summary

Model	R	R Square	Adjusted R Square	Std. Error of the Estimate	Change Statistics		
					R Square Change	F Change	Sig. F Change
1	.833[a]	.694	.592	50.354	.694	6.801	.080

a. Predictors: (Constant), CONTINUOUS TRAINING IN QUALITY

Table 2

Findings

From the Model Summary 1 above, the coefficient of determination (R^2) gave a value of 0.907 This value reveals that 90.7% of the changes or variation that occurred in the employees' satisfaction could be traced to the policy and commitment of top management of MTN. Also, the value of 0.694 representing the coefficient of determination in Model Summary 2 indicates 69.4% of the changes or variation that occurred in customer satisfaction could be attributed to the continuous training in quality in MTN.

Discussion

The Telecommunications industry is a strategic and critical sector of the Nigerian economy. It has security implications and also is a source of employment and livelihood to millions of Nigerians. Its performance is therefore vital for social and economic wellbeing of the nation.

Implementation of TQM in this critical sector will enhance its performance which will in effect have positive social and economic implications.

Our findings in this study show that there is a positive correlation between top management commitment and employee satisfaction. This implies that top management in MTN is committed to the implementation of TQM and that this leads to employee satisfaction. This is in agreement with the findings of Mehra et al (2001) that top management commitment which is demonstrated in form of coaching and facilitating the quality process leads to employees' participation and satisfaction.

In the same vein, there is a positive correlation between continuous training in quality and customer satisfaction. This implies that continuous training in quality is practiced at MTN leading to customer's satisfaction. This agrees with the opinion of Wagoner (n.d) that one of the key success factors for successful implementation of TQM is knowledge and understanding which is gained through continuous training. The successful implementation of TQM leads ultimately to customer satisfaction. This also agrees with the position of Oakland (1989) that training is the single most important significant component in trying to improve quality.

Conclusion and Recommendation

Based on our research findings TQM is being practiced in the Nigerian Telecommunications sector. The reason for customers' complaints is due to lack of adequate power supply and vandalisation of its infrastructure which affects the operational capacity of these organizations and their quality of service. This agrees with the position of several stakeholders in the industry. According to ThisDay (2012), Dr Ekuwem, former President of ATCON (Association of Telecommunications of Nigeria) posited that the greatest threat to the growth of telecommunications and information technology sector is insufficient and epileptic public power supply. Also, according to Nigerian Pilot (2012) Engr Gbenga Adebayo, Chairman ATLON (Association of Licensed Telecommunications Operators of Nigeria opined that fines or penalties will not solve the problems with service of telecommunications companies, and that the fundamental problems are issues of power and protection of telecom infrastructure.

A large proportion of Telecom operators' expenses are used to procure and power generators and also to replace damaged telecom infrastructure. These generators, diesel, and equipment are imported thereby leading to loss of foreign exchange which is not healthy for the growth of the industry and the economy. Consequently, this study wishes to make the following recommendations:-

1. Training of Telecommunications personnel especially low and middle level management to appreciate the importance of total quality

management as a cost reduction strategy

2. There is need for telecommunications companies in addressing their energy problem to adopt renewable energy options like solar power.
3. There is the need for government to work assiduously to improve power supply
4. There is the need for telecommunication company to co-locate their telecommunication masts
5. There is also the need for security agencies like the Nigerian Police and State Security Services to be well equipped and funded to prevent vandalisation of telecommunications infrastructure.

References

Akao, Y. (1990). *Quality Function Deployment* Cambridge, MA: Productivity Press

Baidoun, S. (2003). An Empirical Study of Critical Factors of TQM in Palestinian Organizations. *Logistics information management*. 16(2) 156-171.

Bayraktar,E; Tatiglu, E & Saim, S. (2008). An Instrument for Measuring the Critical Factor of TQM in Turkish Higher Education. *Total Quality Management and Business Excellence* 19(6) 551-574.

Besterfield,H.D., Besterfield-Michna,C., Besterfield, H.G., & Besterfield-Sacre,M. (1999). *Total quality management* (2nd ed.).London: Prentice Hall

Bounds, G.M. (1995). *Management: A Total Quality Perspective*. Cincinnati: South Western College

Brah, S.A; Wong, J.L. & Rao B.M.2000. TQM and Business Performance in the Service Sector: A Singapore Study. *International Journal of Operations and Production Management* 19(4) 1293-1312

Brown,A. (1994). *TQM:* Implications for Training. *Training for Quality.* 2(3). 4-10

Chou, C.M & Chang, S.C. (2006). Factors Affecting China Mobile Customer Satisfaction. http//www.decisionsciences.org/proceedings/DS12008/docs/17-9824

Deming, W.E (1986). Out of Crisis. Cambridge. MIT USA

Demirbag,M., Taloglu,E., Tekinkus, M., and Zain, S (2006). An analysis of the relationship between TQM implementation and organizational performance. Journal of manufacturing Technology Management. 30 (6) 29-49

Deng, Z., Lu, Y; Wei, K. K & Zhang, J. (2009). Understanding Customer Satisfaction and Loyalty: An Empirical Study of Mobile Instant Messages in China. *International Journal of Information Management*. 30 289–300

***Department of Trade and Industry (n.d): *The original quality gurus*. www.dti.gov.uk/quality/gurus. March 19, 2012

Eklöf, J. and Westlund, A.H. (2002). The European Customer Satisfaction Index: It's Background and the Role of Private Concerns and Public Utilities in Fabris, G., Rolanda, S. (Eds.), La customer satisfaction. Nel settore pubblico, Franco Angeli Publishers, Milano

Fornell, C. (1992). A National Satisfaction Barometer: The Swedish Experience. *Journal of Marketing* 56, 6–21

Goetsch, D.L & Davis, S.B (2010). *Quality Management for Organizational Excellence: Introduction to Total Quality*. Pearson. NJ

Gustafsson, A., Johnson, M.D., & Roos, I. (2005). The Effects of Customer Satisfaction, Relationship Commitment Dimensions, and Triggers on Customer Retention. *Journal of Marketing.* 69, 210–218.

Hanif, M; Hafeez, S & Riaz, A. (2010). Factors Affecting Customer Satisfaction.

International Research Journal of Finance and Economics. 60, 44-52.

Hermann, A., Huber, F., Algesheime, R & Tomezak, T. (2006). An Empirical Study of Quality Function Deployment On Company Performance. *International Journal of Quality & Reliability Management.* 23, 345-366.

Irianto. D. (2005). Quality *Management Implementation: A Multiple Case Study in Indonesian Manufacturing Firms*. University of Twente, The Netherlands.

Judge, T.A & Hulin, C.L. (1993). Job Satisfaction as a Reflection of a Disposition: A Multiple Source Causal Analysis. *Organizational Behaviour and Human Decisions Processes*, 56, 388-421.

Juran, J. M., (1974), Quality control handbook. London. McGraw-Hill

Juran, J.M., Gryna, F.M (1999). Quality planning and analysis. McGraw-Hill. 5th

***Karia. N., Asaari .M.H.A.H. (2003). TQM Practices: Continuous Improvement and Problem Prevention. International Business Information Management Conference*, Refereed Proceeding*, Cairo, Egypt, 498-502. Support of Non-Financial Management Accounting Practices. Utah State University, Utah, USA

Khan, M.A., (2010). Evaluating the Deming Management Model of TQM in Telecommunication Industry in Pakistan-An Empirical Study. *International Journal of Business and Management*. 5(9), 46-58.

Knowles, G. (2011). *Quality management: Bookboon.com* Graeme Knowles &Ventus Publishing Alps.

Lascelles, D. and Dales, B. (1989). The Buyer-Supplier Relationship in Total Quality Management. *Journal of Purchasing and Materials Management*. Summer. 10-19.

Mehra S., Hoffman. J.M., Sirias .D. (2001). TQM as a management strategy for the next millennia. *International journal of operations & production management*. 21(5/6) 855-876

Munro, R. (2000). Linking six sigma with QS-9000. *Quality Progress*, May. 47-53.

Nigerian Telecommunications Commission (2011): *Quarterly Summary Of Telecom Subscriber in Nigeria*

Nosakhare.J.O. (2000). *Organizational Approach to Total Quality Management in Nigeria*. Unpublished Ph.D thesis, St. Clements University

Oakland, J. (1989). *Total quality management*. Oxford, UK: Heinemann.

Oakland, J. (2000). *Total Quality Management, Text With Cases*, 2nd ed., Butterworth Heinemann, Oxford

Olian,J.D & Rynes,S.L. (1991). Making Total Quality Work: Aligning Organizational Process, Performance Measures And Stakeholders. Human Resource Management 30, 303-333

Ooi,K,B., Arumugam .V., Loke K.Y., Lorraine.S.V (2006) Relationship of TQM practices and employees propensity to remain: an emphirical case study. TQM magazine. 18(5) 528-541

Osland, A (1997). Impact of Total Quality Management Training and Work Context on attitudes towards supervisors. *The international Journal of organizational analysis* 5(3) 291-301

Patel, A (1993) Total Quality Management: Paving The Way for Future Training. *Industrial and Commercial Training*. 25(2), 23-32.

Parzinger,M.J., & Nath, R. (2000). A Study of the Relationship between Total Quality Management Implementation Factors and Software Quality. *Total Quality Management*. 11(3). 353-371.

***Rosemary R.F. (2006). Thesis PHD: Financial Consequence of Implementation of Lean Manufacturing With the???

Rousseau, D. (1978). Characteristics of Departments, Positions, And Individuals: Contexts for Attitudes and Behaviors, *Administrative Science Quarterly.* 23, 521–540.

Samat, N;Ramayah, T & Saad, M; (2006). TQM Practices, Service Quality, and Market Orientation. *Management Research News* 29(11), 713-728.

Sajjad F & Amjad S. (2012). Role of Benchmarking in Total Quality Management: A Case Study of Telecom Services Sector of Pakistan. Business Management Dynamics 1(8,) 34-44.

Su, C.T., Chen, M.C., & Cheng, G.C. (2001). TQM in Taiwan's Computer and Its Peripheral Industry, Industrial Management and Data Systems. 101(7), 357-362.

Slack.N., Chambers, S.; Johnstone, R.,& Betts, A.(2006.) Operations and Process Management. Prentice Hall, London.

Stenberg, A. & Deleryd, M. (1999). Implementation of Statistical Process Control and Process Capability Studies: Requirements or Free Will?. *Total Quality Management*, 10 (4), 439-46.

Sit, W.Y., Ooi, K.B., Lin, B & Chong, A.Y.L (2009). TQM and Customer Satisfaction in Malaysia's Service Sector. *Industrial Management and Data systems*. 109(7), 957-975.

Soedarso, S.W. (2009). Doctor of Business Administration Thesis. TQM Extension Practices and Performance: a case study Malaysian aerospace industry???

Sureshchandar, G.S., Rajendran,C & Anantharaman, R.N. (2002). The Relationship between Management's Perception of Total Quality Service and Customer Perception of Service Quality. *Total Quality Management*. 13(1) 69-88.

Taguchi, G. (1979). *Introduction to Off-Line Quality Control*. Japanese Standards Association, Tokyo.

Talib, F; Rahman, Z & Quresh, M.N (2010). The relationship between total quality management and quality performance in the service industry: a theoretical model. *International Journal of Business, Management and social sciences* 1(1), 113-118.

The Guardian Newspaper. www.ngrguardiannews.com Accessed. 28/10/2012

The Punch Newspapers.www.punchng.com. Accessed.28/10/2012

Turel, O. & Serenko, A. (2006). Satisfaction with Mobile Services in Canada: An Empirical Investigation. Telecommunication Policy 30(5) 314-331.

Ukodie, A. (2010): *50 years of ICT in Nigeria: The st ory, the players.* Lagos: eworld Magazine

Vavra.T.G. (2002). ISO 9001:2000 and customer satisfaction. Quality progress, 35(5), 69-75.

***Wagoner Rick (n.d) Role of Leadership and the Employees on the Success and Failure of TQM. Morehead State University

Wilkinson, A. (1998). Empowerment: Theory and Practice. Personnel Review, 27(1), 40-56.

Zairi, M. (1997).Business process management: a boundary less approach to modern competitiveness. *Business process management journal* 3(1) 64-80

Zairi, M. & Baidoun, S. (2003) Working Papers. Understanding the essentials of total quality management: A best practice approach part 2 3(5)

***Zaim, H & Zaim, S. (n.d) Measuring Employee Satisfaction in Small and Medium Sized Enterprises

Zaim, S; Turyilmoz, A;Ucar, B & Akkas, Oguz (2010). Measuring Customer Satisfaction in Turks Telecom Company Using Structural Equation Modeling Technique. *Journal of Global Strategic Management***.** 7, 89-99.

Yang C.C. (2006). The impact of Human Resource Management Practices in the Implementation of TQM: An Empirical Study on High-Tech Firms. *The TQM magazine* 18(2), 166-173.

Aasa et al: Proc. ICCEM (2012) 167 – 171

Thermodynamics Characterization of Density models for an Effective Solar Water Heater Sizing

Aasa, S.A, Gbenebor, P.O. and Ajayi, O.O.

Department of Mechanical Engineering Covenant University, Otta, P.M.B. 1023 Ogun state Nigeria
*Correspondence: oluwashina.gbenebor@covenantuniversity.edu.ng

Abstract

The problem faced in Sizing of an effective Solar Water Heater (SWH) by engineers to meet certain design requirement is highly enormous. Using the thermodynamic characterization relation and the knowledge of Solar Water Heater (SWH) density's model; various design were evaluated. The result shows that density model actually predicts adequately and providing alternative means of estimating these design parameters. Also, the properties of the system, such as entropy and enthalpy (specific heat capacities), which cannot be determined directly from experimental axiom, were evaluated. These evaluations therefore, give room to express the thermodynamics properties of the system and consequently improve the design performance. Further comparisons with experimental results reveal a better outfit. Therefore through the knowledge of thermodynamic relation an efficient Solar Water Heater is operated and empirical data is expanded.

***Key words**: Thermodynamic Relation, Density Model, SWH parameters, thermodynamic and dimensionless properties.*

1. Introductions

Thermosyphon solar water heater is a naturally operated system that performs using the force of gravity. It is the oldest form of the system but less utilized due to its system efficiency. Though it could be highly effective if proper optimized and operated in most temperate developing countries where less power are supplied, low income purchasing for active equipments and less ability to procure require measuring equipment for system optimization; Agbo, (2012). As a result of this; evaluation models are developed to obtain various data whose equipment is not readily available. Density model is one of those models in solar water heater to ease the evaluation of system parameters which are difficult to obtain during experimentations. But despite the use of these models by various researchers, (Aasa and Ajayi 2012, Agbo and Unachukwu 2007), some thermodynamics properties are yet to be evaluated. These parameters, (specific capacity, entropy and enthalpy etc) are of immense important during system optimizations which give us rooms for maneuvering the energy available during the proper system sizing. Further to this, thermodynamics characterizations give room for analysis and calculation of various system parameters which are difficult to obtain during experimentations. Many researchers have used the ability of this skill to obtain parameters that cannot be estimated during the course of experiment. Reiner and Harns, (1994) used the standard formulation of thermodynamic properties to present the fundamental equation of state for helmholtz free energy their results gave a good correlation with the annex 18 research group of IEA. The exergetic evaluation of the thermal performance was also carried out by Gang et al, (2012). In their experiment first and second laws of thermodynamic were employed for optimum determination of the work potential performance. Ma et al, (2010); Liang et al, (2011) and Dufie, (1980) used the energy balance to evaluate the thermal performance of an evacuated tube solar water heater.

The high rate of socio political development plays a lot on the need for an improved performance of solar water heater to meet up the

domestic and industrials processes. Improving on solar water heater performance required mend operation process which takes into critical analyses of the performance parameters. In doing that, this study analyses the various thermodynamic property parameters using thermodynamic relation of Clausius Clapeyron analysis.

2. Material and Methods

Using Maxwell knowledge of thermodynamic relation the p-v- T surface for water in Solar water heater is analysed based on continuous and discontinuities that occurred during the process. Hence, according to Winterborne, (1997) the relationships apply over the major regions of the surface, but not across the boundaries is expressed for a continuous surface z = z(x, y).

$$dz = \left(\frac{dz}{dx}\right)_y dx + \left(\frac{dz}{dy}dy\right)_x \qquad 1$$

$$dz = Mdx + Ndy \qquad 2$$

Given: $M = \left(\frac{dz}{dx}\right)$, $N = \left(\frac{dz}{dy}\right)$

Following this particular relation as explained by Maxwell and Clausius Clapeyron thermodynamic relations for entropy, volume, pressure and temperature is express as follows;

$$\left(\frac{ds}{dv}\right)_T = \left(\frac{dp}{dT}\right)_v \qquad 3$$

Where; s = entropy; v = volume; p = pressure; T = Temperature

For a change of state in which a constant temperature and pressure is observed

$$\frac{ds}{dv} = \frac{s_2 - s_1}{v_2 - v_1} \qquad 4$$

Thus,

$$\frac{dp}{dT} = \frac{s_2 - s_1}{v_2 - v_1} \qquad 5$$

During phase changes therefore, the ratio of change of enthalpy, h, of a system to change in entropy is expressed as;

$$\frac{\partial h}{\partial s} = T \qquad 6$$

$$\therefore h_2 + h_1 = T(s_2 - s_1) \qquad 7$$

Substituting equation (5) to equation (7)

We have;

$$\frac{h_2 + h_1}{v_2 - v_1} = T\frac{dp}{dT} \qquad 8$$

Following the proposition of first law of thermodynamic, the energy efficiency was not ascertained unlike the second law which expresses the production of entropy in a system as the difference between the sum of stream entropy flows and entropy flows by heat transfer leaving the system and the sum of stream entropy flows and entropy flows by heat transfer entering the system.

$$\sum_{\text{out of system}} \left(\text{ns} + \frac{\text{Q}}{\text{T}_\text{s}}\right) - \sum_{\text{into system}} \left(\text{ns} + \frac{\text{Q}}{\text{T}_\text{s}}\right) = \Delta\text{S}_{\text{irr.}} \qquad 9$$

n =molar flow rates; Q =heat transfer T_s =System temperature; $\Delta\text{S}_{\text{irr.}} = \text{entropy production in a system or irriversible entropy.}$

In addition to this its gives the analysis of available energy which is further expressed as;

For stream available functions the expression is as follows;

$$\text{b} = \text{h} - \text{T}_\text{o}\text{S} \qquad 10$$

b= stream available function

Therefore, lost work, LW, is expressed as;

$$\text{LW} = \text{T}_\text{o}\Delta\text{S}_{\text{irr.}} \qquad 11$$

The system efficiency according to second law is the ratio of minimum works of separation to equivalent actual work of separation and therefore expressed as;

Therefore knowing the inlet and outlet temperature of a system of solar water heater the nature of it phase behaviour could actually be predicted using the analogy of the pressure and density model presented by Aasa and Ajayi, (2012).

For the pressure model;

$$P(T) = 0.0001T^2 - 0.006T + 0.1738 \quad (12)$$

And the density model;

$$\rho(T, P) = 1.0118 - 0.0004T - 0.0177P \quad (13)$$

These models are going to be used in evaluating the various thermodynamic properties of the system.

3. Results

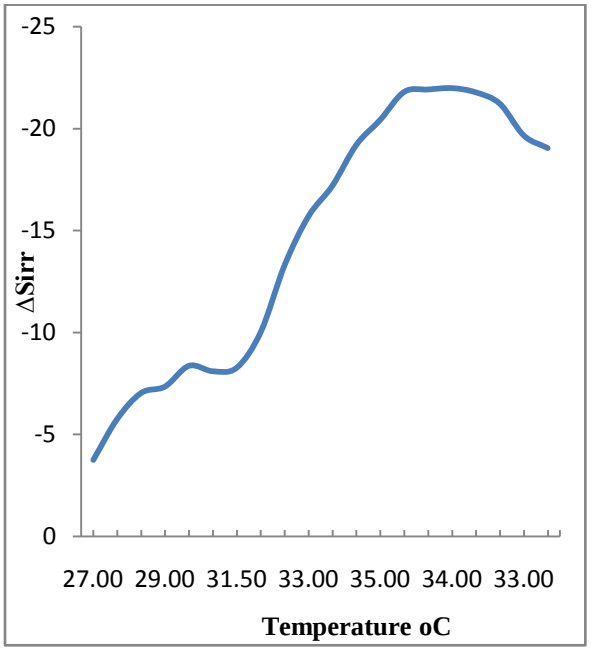

Fig. 1: Plot of Entropy minimization against Temperature variations

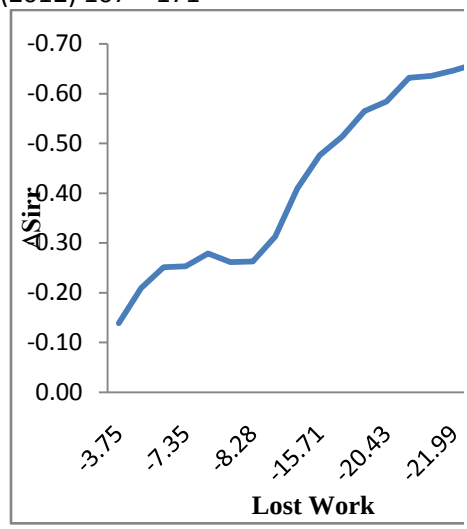

Fig.2: Plot of Entropy minimization against Lost Work

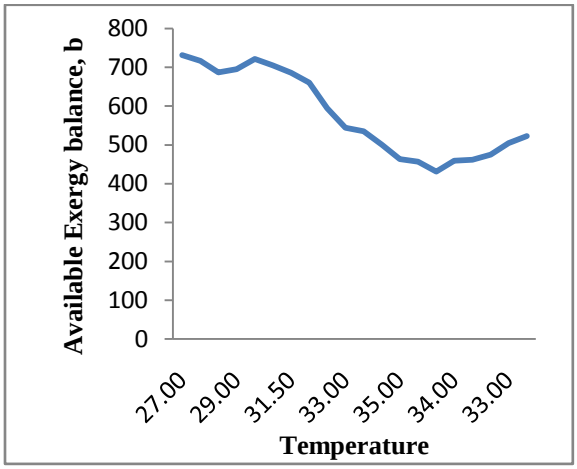

Fig. 3: Plot of Available Exergy balance against Temperature

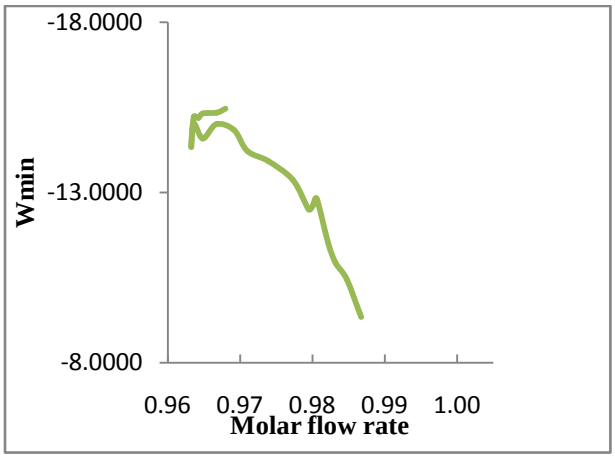

Fig. 4: Plot of Minimum work against Molar flow rate

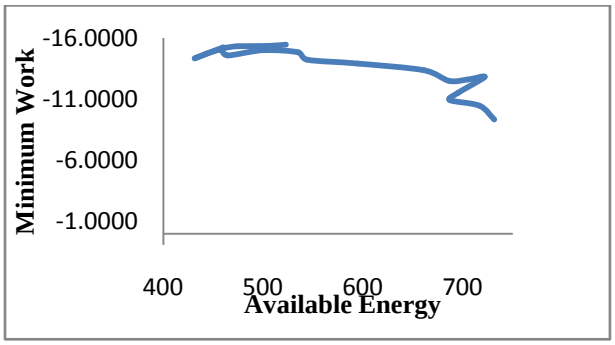

Fig. 5: Plot of Minimum against available Exergy

4. Discussions

Figures 1-5 present the plots of various analyses carried out for the system characterization of density model present by Aasa and Ajayi, (2012). Figure 1 analysis the change in the entropy irreversibility as temperature of the fluids is improved. The plot shows that the irreversibility decreases as the fluid flows absorbs heat energy, this is explained by the negative values display by the change in the irreversibility.

Plot 2 further strengthens the rate of change of the irreversibility and lost work, the graph shows that at maximum heat absorbs by the fluid in the system; the entropy generation and the lost work is minimum. This gives implication for optimum available energy (Exergy) of the system.

In addition to this, figure 3 analyses the available energy as system temperature of the system changes it was noticed that maximum energy was obtained at the top of the day when the highest heat absorption take place. Therefore considering the level of heat absorption and the exergetic nature of energy obtained it could be stated that the higher the heat radiation heat the higher the absorb heat and consequently the available energy.

Figure 4 explains the minimum work done and the amount of mass flow rate effects. A minimum work is done at maximum mass flow of the fluid; this implies low lost work at the optimum absorption because virtually all the heat is absorbed. The density which is responsible for the flow process occurs at its peak and a maximum flow rate at minimum work done is realised.

Finally, figure 5 explains work done in respects of the available energy. A maximum available energy of 731.4J was achieved at the least work done of 9.34J and a minimum available energy of 431.43J was achieved at a maximum work of 14.34J.

5. Conclusions

Thermodynamic relationships between properties have been developed which are independent of the particular fluid. This has been used to evaluate derived properties from primitive ones and to extend empirical data. Therefore an optimum available energy of 731.4J was achieved at the least work done of 9.34J and a minimum available energy of 431.43J was achieved at a maximum work of 14.34J. Also, at a optimum lost work of 14.34J a mass flow rate of corresponding density of 0.9633Kg/m^{3}s was obtained and at 10.45J lost work, 0.9833Kg/m^{3}s.

To sum it up, using the thermodynamics characterization relations of Clausius Clapeyron and basic experimental data of solar water heater (temperature) various performance evaluations have been accessed. Hence, analysis for optimum design operation can now be achieved by simply taking temperature, a domineering

parameter, of solar water heater experiment and empirical data have been stretched.

References

Aasa and Ajayi (2012); Evaluation of the Temperature Effects of A Thermosyphone Solar Water Heater. Canadian Journal of Pure and Applied Sciences; 6(1) pp1855-1862.

Agbo S. (2011); Analysis of the performance profile of the NCERD thermosyphon solar water heater. Journal of Energy in South Africa Vol 22(2) pp 22-26.

Agbo and Unachukwu, (2007); Design and Performance Features of a Domestic Thermosyphon Solar water Heater for an Average Sized Family in Nssuka Urban. Trend in Apply sciences 2(3) 224-230.

Ma, L.; Lu, Z.; Zang, J.; Liang, R (2010); Thermal Performance analysis of the glass evacuated tube solar collector with U-Tube. Build. Environ; 45 pp1959-1967

Liang, R.; Ma, L,; Zhang, J Zhao, D. (2011); Theoretical and experimental investigation of the filled type evacuated tube solar collector with U-Tube. Sol. Energy 85 1735-1744.

Reiner Tillner-Roth and Hans Dieter Baehr, (1994); An International Standard Formulation for Thermodynamics Properties of HFC-134 for Temperature from 170K to 455K and Pressure up to 70MPa. J. Phy. Chem. Vol 23 (5) pp 657-729.

HernaÂn A. Makse & Jorge Kurchan (2002); Testing the thermodynamic approach to granular matter with a numerical model of a decisive experiment. Nature Vol 415 (2) pp 614-616 (www. nature com).

Gang Pei; Guiqiang L; Xi Zhou Jie Ji and Yuehoug Su (2012); Comparative Experimental Analysis of the Thermal Performance of Evacuated Tube Solar Water Heater Systems With and Without a Mini-Compound Parabolic Concentrating (PC) Reflector(C<1). Journal of Energy 5, 911-924.

Winterborne, D.E. (1997); Advanced Thermodynamics For Engineers. John Wiley and Son., inc 605 Third Avenue. New York City NY 10158-0012.

Fayomi et al: Proc. ICCEM (2012) 172 - 174

Physio-Chemical and Mechanical Behaviour of(*Pinussylvestris)* as Binders on Foundry Core Strength

Fayomi, O. S. I[1,2*], Abdulwahab, M.[1], Gbenebor, O. P.[2] Popoola, A. P. I. [1]

[1]Department of Chemical and Metallurgical Engineering, Tshwane University of Technology, Pretoria, P.M.B. X680, South Africa 0001
[2]Department of Mechanical Engineering, Covenant University, Canaan land, Ota, Ogun State, Nigeria
*Corresponding author: sunnyfayomi@yahoo.co.uk, popoolaapi@tut.ac.za

Abstract
The mechanical potential of sand core binders made withPinussylvestris has been examined. Ota silica base sand bonded with 6% of cassava starch in admixed proportion of Pinussylvestris was tested for tensile, compressive strength and permeability to establish the binding efficiency. Tensile strength of the green baked core were oven baked at 50°C, 100°C, 150°C and 200°C.The cylindrically shaped permeability specimens were tested with permeability meter. Study revealed thatPinussylvestris showed an improve properties at 6% cassava starch at 200°C.
Keywords:*PinusSylvestris foundry cores, cassava starch.*

1. Introduction
Suitable molding raw materials for core making have been of great interest recently. Industries have showninterest in the use of locally sourcing binders for productions in order to boost the ailing economy [1-8]. Cores are made of core sand mixtures from sand grains and binders[6-11]. A proper and formulated admixture gives good green compressive strength and adequate baked strength to prevent premature collapse during usage. Binders are introduced into the molding and core mixtures in order to improve their properties especially the strength [5-11]. The usage of *Manihotesculentacrantz* (Cassava Starch) for sand core processes has not been widely study in the literature, and hence the continue need to investigate its prospective with other binding additive such as pine oil in this respect is considered necessary. Cassava starch has therefore been chosen for the study because is easily sort for and cheap with excellent bonding features. Equally, cassava starch and pine oil has no negative health implication; they are environmental friendly for the production of sand cores and most importantly reduce the total addiction on foreign materials to promote the development of indigenous technology.This study aimed at producing sand cores locally using Ota silica sand, cassava starch and pine oil as binder and examining their suitability and behavior during casting process.

2. Experimental procedures
2.1 Materials
Base material used for this work was collected from Ota in Ado-odo Local Government in Ogun state, Nigeria. Binders which are cassava starch, was extracted from cassava tubers obtained from Arobieye in Ota, Ogun State, Nigeria. The pine oil was purchased from South Africa market. Equipment such as universal strength testing machine, weighing balance, mixer, measuring cylinder, specimen rammer, permeability meter, oven, shaker, sets of sieve, crucible furnace, hack saw machine, mould box, core box and wire brush were used.

2.2 Method
2.2.1 Preparation of Manihotesculentacrantz
Peeled and washed cassava tubers were grinded into pulp and water was added for extraction. The admixed particulate was left to stay for 180 minutes before the water above was poured. The starch residue was properly dried to white in line with (Popoola, 2011).
2.2.2 Sand preparation
The silica sand was collected from the Ota river side, washed to remove clay and dirt. The processed silica sand was dried and sieved using shaker of different meshes and aperture. The obtained and dried sand was studied with ED X-ray fluorescence analyzer for mineralogical composition is shown in Table 1.

Table 1: Mineralogical composition of the foundry sand used for the study

Composition	SiO_2	Al_2O_3	K_2O	CaO	$Ti0_2$	Cr_2O_3	MnO	Fe_2O_3	MgO	CuO	Na_2O
Wt%	Balance	0.58	0.08	0.34	1.60	0.02	0.02	0.45	0.16	0.04.	0.04.

2.2.3 Sieve Analysis

Standard sieve test of Bs 410 series to remove all coarse particles according to Popoola, 2011 was used. Weight of sieved sand sample values in Table 2 were used to calculate grain fineness number ($GFN = \frac{TotalProduct}{Total\ \%\ of retained grain}$) and fines (%).

Core mixture and core making

The mixtures constituent and % composition of the mixed oils are shown in Table 2 below.

Table 2: Composition of the mixed oils and starch

S/No	% Mixture
1	3% Starch + 2% pine oil + 3% water
2	3% Starch + 6% pine oil + 3% water
3	6% Starch + 2% pine oil + 3% water
4	6% Starch + 6% pine oil + 3% water

The blended admixed constituent was gradually put into 45 mm diameter by 50 mm height and immediately rammed with a rammer. Subsequent to the ramming, the core specimen was ejected directly from the sleeve by a piston. Thereafter the ejected core was transferred to an electric oven with temperature of about 1200^{o}C capacity.

3. Results and discussion

3.1 Sand mineralogy study

From the ED X-ray fluorescence analyzer for mineralogical composition during sand preparation it shows that the Ota sand contains 0.45%Fe_20_3, 0.58% Al_20_3 and 95.50% $Si0_2$. The silica content value is in line with the acceptable value suggested for moulding and core sands between 85% and 97%. According to Popoola, (2011) higher silica content is essential to resist the heat from molten metal during casting operation.

3.2 Comparative effect of baking temperature on foundry properties at various binders composition.

In Figure 1, the variation in foundry properties; CM, PM and B/SS as a result of the composition admixture are compared along with baking temperatures. From the Figure, it is observed that these properties increased with change in composition at various levels of binder additions. Specifically, composition of 3% starch with 2%pine oil binder in all the baking temperature considered. While an increase in the starch content at 6% significantly improved the foundry properties for various levels of pine oil binders (see Figure 1 and 2). It can however be said that all investigated properties are favored at 150^{o}C for most composition at all temperatures.

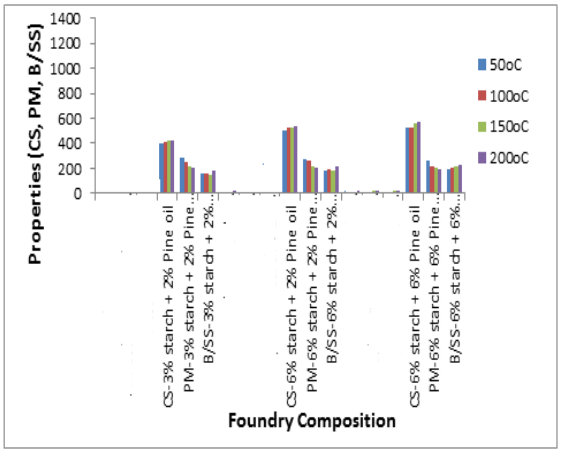

Figure 1: Comparative chart for combined foundry composition with 3%H_2O

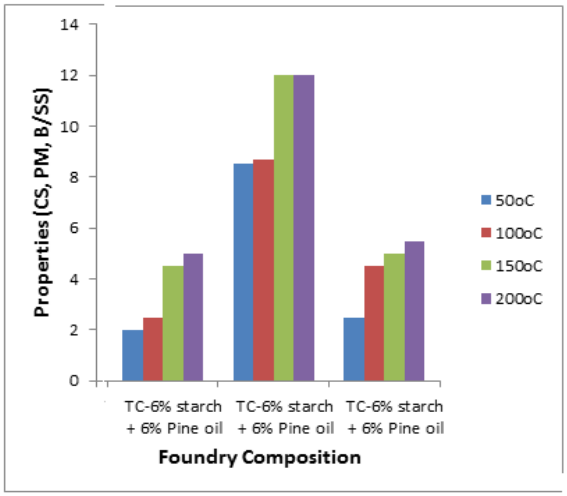

Figure 2: Comparative chart for TCs of different composition and at various temperatures

4. Conclusions

1. The use of pine oil (*Pinussylvestris)*as potential binders on foundry core strength have been established to significantly improve foundry properties at different baking temperatures
2. The higher foundry properties can be obtained at 150^{o}C baking temperature and that TC increases and decreases for some foundry compositions
3. It can be said that higher starch and oil additions favored PM value for pine oil in all admixtures. Higher TCfor pine oil in all compositions is obtainable at 200^{o}C baking temperature.

References

Fayomi, O.S.I, Ajayi, O.O, Popoola, A.P.I. (2011). Suitability of local binder compositional variation on silica sand for foundry core making. *Int. Jour. of Physical Sci.,* 6(8):1940-1946.

Paul, A., Jecob, J., Hamisu, M. (2007). The use of LP simplex method in the determination of the minimized cost of a newly developed core. J. Mat. Sci. 155–162.

Nuhu, A. A. (2010). Evaluation of the tensile strength of foundry cores made with hybridized binder composed of neon oil. *Inter. Journal of Physical Science.* Vol.5 (5):555-563.

Olakanmi, E.O., Arome, A.O. (2009). Characterization of the core binding properties of fatty based oil. *Inter. J. Physical Science* Vol.4 (11) pp, 623-628.

Silver, F., Maria, C. Z. (2007). Foundry waste reuse and recycling in concrete production. *Envi. J of Science*, 3(3):135-142.

Fayomi, O.S.I., Popoola, A.P.I., Ojo,O..I. (2011).Investigating Nigeria Ochadamu Silica Sand, Clay and Local oils for foundry core making. *Int. Journal of Physical Sciences,* Vol. 6(8):1894- 1904.

Abdulwahab, M., Gaminana, J. O., Bello, K. A. and Ochuokpa, E.O. (2008); Prospect of Local Core Binders in Foundry Industries. Proceedings of Nigerian Metallurgical Society. 25th Annual conference,Akure, Pp 210-213.

Ayoola, W. A., Adeosun, S. O., Oyetunji,A. and Olodoye, A.M. (2010). Suitability of Oshogbo Sand Deposit as Moulding Sand. *The Kenya Journal of Mechanical Engineering*, 6(1):33-41.

Charles, E. B. (2004); Advances in Core Making Technology. Penton media, Inc. Britain. P 2026. *Journal of Emerging Trends in Engineering and Applied Sciences* (JETEAS) 3(1):25-32

Tunji, A.**,** Bankole, L.K. and Alhassan, A.O. (2009). Binding Characteristics of Mbushi and Ewekoro Clays of Nigeria in Foundry Moulding Sand. *Global Journal of Engineering and Technology.*2(4):509-514.

Popoola, A.P.I. 2011. Effect of molasses, cassava starch and arabic gum on mechanical strength of foundry core. *Journal of Scientific and Industrial Research*, 5: 1029-1032.

Oyawale and Fashola: Proc. ICCEM (2012) 175 - 180

Quality characteristics of concrete poles manufactured in the Ibadan metropolis, southwest Nigeria

Oyawale F. A[1]. and A. A. Fashola[2]
[1]Mechanical Engineering Department, Covenant University, Ota
[2]Industrial & Production Engineering Department, University of Ibadan

Abstract

In Nigeria, power is transmitted by overhead transmission lines fixed on wooden or concrete poles. Often times these poles collapse under excessive loads occasioned by storm and accidents. This project work is to determine the quality characteristics of concrete electric poles used to carry overhead conductors in the Ibadan metropolis of Nigeria. Samples of broken concrete poles were collected from various sites within Ibadan metropolis. Core, permeability, cube and tensile tests were carried out on samples of stumbled poles and fresh concrete mix collected from companies producing poles. This was to check the conformance of the poles to the standard set by the regulatory authority. The test results showed that all the samples on which the core and permeability tests were carried out fell short of the required standard of 37,000KN/m. For the core test, only one sample had the average values of 46,200KN/m and 50,400KN/m^2 at 7days and 28days respectively which exceeded the standard minimum value. The results showed that the manufacturers did not use the right ratio of materials, the mode of mixing of the aggregates was not adequate and casting allowed voids/air space which made the poles permeable and the period of curing (the number of days) of the poles was not adequate. Almost all the poles were found to be below standard

***Key words**: aggregate, crushing strength, crushing load, concrete curing, overhead conductors*

1. Introduction

In recent times, efforts have been geared towards the production of electric poles that meet the international quality standards. With the level of development in Nigeria, the use of electric poles has been on the increase as a result of the rural electrification programme. In effect, efforts have been made to provide quality facilities and amenities for the production of poles in the rural and urban areas.

Reinforced concrete is a strong and durable building material that can be formed into various shapes and sizes. It's utility and versatility are achieved by combining the best features of concrete and other materials. In Nigeria, electricity is transmitted by conductors carried overhead by concrete and wooden poles. Concrete Pole design is dependent on the power and voltage that is to be transmitted. In Nigeria, 33/11/0.415kv is usually transmitted generally by overhead conductors; hence the wooden and concrete pole types are suitable for use (Ilochi et al 1996). The design of poles is mainly based on the principle of conductor loading. However, sag-tension calculation is quite involved due to the varying loading effect on conductors and the nature of conductor materials. The calculations would be simpler if the conductor could be regarded as being subjected to a fixed loading. This however, is not the case since the conductors may be subjected to a gale or may only be acted upon by their own weight in still air. As a result of varying conditions, the overhead line design engineer must be able to design the support to carry the conductor under different conditions. The stumbling/falling and cracking of the poles have constituted a great nuisance in the environment and also endangered the lives of people residing in the vicinity.

The objective of this paper is to examine the quality characteristics of poles produced locally in the Ibadan metropolis in Nigeria with an aim to establishing causes of failure and conformance or otherwise of the poles to infrastructure quality standards. Only one of the outfits studied in Ibadan was owned by government and this had since gone out of production.

2. Theoretical background

The tensile strength of concrete is only about 10% of the compressive strength. As a result of this, nearly all reinforced concrete are designed on the assumption that concrete does not resist any tensile force. Reinforcement is designed to carry these tensile forces, which are transferred

by bonds between the interface of the two materials (i.e. concrete and the reinforcing steel bar). If this bond is not adequate, the reinforcing bars will slip within the concrete and there will not be a composite action. Thus, the members should be detailed, so that the concrete can be well compacted around the reinforcement during construction. This is further facilitated by the use of bars that are ribbed or twisted to produce an extra mechanical grip.

In the analysis and design of the composite reinforced concrete section, it is assumed that there is a perfect bond so that the strain in the reinforcement is identical to the strain in the adjacent concrete. This ensures that there is what is known as "compatibility of strains'' across the cross-section of the member. The coefficients of thermal expansion for steel and for concrete were of the order of 10 x 10^{-6} per ^{0}C and 7– 12x10^{-6} per ^{0}C respectively. (Mosley et al 1990).

The span length, height of support and the strength of support required are functions of the conductor Sags and tension. (Ilochi et al 1996).

Whenever tension occurs, it is likely that cracking will take place. This cracking, however, does not detract from the safety of the structure provided there is good reinforcement bond to ensure that the cracks are restrained from opening so that the embedded steel continues to be protected from corrosion. In determining the strength of a pole, the pole is considered as a cantilever beam anchored at one end i.e. the pole is designed for bending strength (Akala.. 2002). When the compressive or shearing forces exceed the strength of the concrete, steel reinforcement must again be provided to supplement the load carrying capacity of the concrete. To prevent these bars from buckling, steel binders are used to assist the restraint provided by the surrounding concrete.

Total bending moment on pole at ground level,

$$BM = (P.h.W.H/2)\ kg.m \quad \text{.....1}$$

Where

H = the height of pole above the ground level

h = height of centre of gravity of conductor loading in meter above ground level

P = total horizontal conductor loading in Newton acting at height h meters above the ground level

Assuming a maximum fiber stress of $8000kg/mm^2$ on the pole;

Max. allowable fibre stress

$$F = \frac{8000}{S}\ kg/mm^2 \quad \text{.....}$$

2

Where S = factor of safety.

Moment of inertia for circular pole

$$I = \frac{\pi D_g^4}{64} mm^4 \quad \text{..... 3}$$

Section modulus $Z = \dfrac{I}{D_g/2} = \dfrac{\pi D_g^3}{32} mm^3$

..... 4

Allowable Stress = $F = \dfrac{BM(10)}{Z} = \dfrac{BM(10)(32)}{\pi D_g^3}$ 5

Pole Diameter at ground level = D_g

$$\therefore D_g = \sqrt[3]{\frac{BM(102)}{F}}\ mm \quad \text{..... 6}$$

Poles are not designed to withstand such impact strength that might occur when a moving vehicle hits a pole. Poles should, if at all possible, be sited to minimize this possibility (NZE: 3115:1980).

The minimum requirement for reinforced concrete pole should be high grade with a specified strength of 30mpa, and in prestressed concrete poles the specified strength is 40mpa. The deflection of the top of the pole under specified working load should not exceed the distance from the ground line to the top of the pole divided by 50. The cover to all steel reinforcement including stirrups and prestressed tendons should not be less than 20mm except for spun poles. Thus minimum cover may be reduced to 12mm. The position and size of holes are to be specified by the purchaser. Holes should be within 5mm of the specified position and should be 4mm larger in diameter than the intended bolt size. Provision for earthing should be made only when specified by the purchaser. Prestressed steel must not be used for earthing purpose. All poles must be clearly and indelibly marked with the following:

(a) Date of manufacture at approximately 3m from the butt end.

(b) The specified working load, in kilo Newton and at approximately 3m from the butt end.

(c) A warning notice, when requested by the purchaser.
(d) A horizontal mark to show the designated ground line position
(e) The design lifting points.

Where it is not obvious in which direction a pole is to be placed on site, the pole should be marked to give an indication of the required orientations.

3. Methodology

Plate 1: Fracture at 1,200 mm

Plate 2 Clean fracture at 900mm

Plate 3 A fracture and a tear

Plate 4 Multiple fracture

The core and permeability tests were carried out on them. The tests were carried out to determine the crushing strength and the rate of water absorption of the concrete.

Cubes were made from samples of concrete mix collected from water absorption. The bars in the concrete were also tested to determine the tensile stress.

The sample of concrete from broken poles used in this study were collected from various parts of the Ibadan metropolis (see plates 1 – 6).

Avery Universal testing machine 600KN capacity, Diamond Cutting machine, meter rule and the specimens (concrete) were used for the test.

Plate 5: Stumbled Pole wires unbroken Plate 6: Stumbled Pole

3.1 Procedure

The samples were cut into equal sizes using a diamond cutting machine. The cube length was 0.150m; the breadth was 0.2m and the cross sectional area calculated was 0.03m^2. The core and permeability tests were carried out on the cubes on different days ranging from 4 to 20 days.

3.2 Core test

The concrete was placed flat down in the compressive side of the machine. The machine was switched on and was gradually loaded until the specimen was crushed. The core test was carried out on the hardened concrete poles and the result was recorded as follows

TABLE 1 Core Sample

Sample	Crushing Load KN/m^2	Cross sectional area (m^2)	Crushing strength (KN/m^2)
A	392	0.03	13,067
B	438	0.03	14,600
C	680	0.03	22,667

3.3 Permeability test

The samples were weighed before being submerged in water and were tested on different days after removal from the water and reweighed; the weight and the crushing load values were recorded. This was done in order to determine the rate of water absorption.

Some of the identified problems that led to the collapse of some of the remnants of broken poles picked up in the Ibadan metropolis included permeability to continuous rainfall, poor compaction/consolidation and inadequate curing.

The results showed that the samples tested were not up to the required standard of 37,000kN/m^2 set by the regulatory body; therefore. Hence they did no show conformity to the standard set for poles manufactured in Nigeria.

Table 2 Permeability test result for sample A

No Of ys	Approximate Cross Sectional Area (m^2)	**Crushing Load KN/m^2**	**Weight in Air (Kg)**	**Weight in Water (Kg)**	**Crushing Strength (KN/m^2)**	**% of Water Absorbed**
4	0.03	**320**	**8.00**	**8.20**	**10,667**	**2.5**
8	0.03	**288**	**8.00**	**8.22**	**9,600**	**6.25**
12	0.03	**273**	**8.02**	**8.70**	**9,100**	**8.48**
16	0.03	**263**	**8.06**	**8.80**	**8,834**	**9.18**
20	0.03	**260**	**8.08**	**9.0**	**8,667**	**12.00**

Table 3 Permeability test result for sample B

No Of Days	Approximate Cross Sectional Area (m^2)	Crushing Load KN/m^2	Weight in Air (Kg)	Weight in Water (Kg)	Crushing Strength (KN/m^2)	% of Water Absorbed
4	**0.03**	**420**	**9.00**	**9.04**	**14,000**	**0.45**
8	**0.03**	**400**	**9.05**	**9.12**	**13,334**	**0.77**
12	**0.03**	**395**	**9.07**	**9.13**	**13,167**	**0.66**
16	**0.03**	**390**	**9.10**	**9.14**	**13,000**	**0.44**
20	**0.03**	**390**	**9.11**	**9.15**	**13,000**	**0.44**

Table 4 Permeability result for sample C

No Of Days	Approximate Cross Sectional Area (m^2)	Crushing Load KN/m^2	Weight in Air (Kg)	Weight in Water (Kg)	Crushing Strength (KN/m^2)	% of Water Absorbed
4	**0.03**	**660**	**8.00**	**8.01**	**22,000**	**0.12**
8	**0.03**	**650**	**8.00**	**8.04**	**21,667**	**0.50**
12	**0.03**	**645**	**8.00**	**8.05**	**21,500**	**0.63**
16	**0.03**	**610**	**8.02**	**8.08**	**20,334**	**0.75**
20	**0.03**	**636**	**8.03**	**8.10**	**20,534**	**0.87**

Sample A: was the most permeable; the concrete absorbed water at a very fast rate when immersed in water for a period ranging from four days to twenty days thereby increasing the weight by the percentage of water absorbed.

Sample B: Though the concrete, absorbed water at a fast rate when it was immersed in water between the fourth day and the eighth day when it was reweighed and tested, the absorption rate became reduced by the twelfth day and finally became constant between the sixteenth and the twentieth day.

Sample C: the absorption rate was not as fast, compared to samples A and B. From the fourth day the absorption was a bit fast but it became reduced between the twelfth and the twentieth day.

The above results revealed that the concrete pole was not produced according to the specification given by the regulatory body. Though the poles have been in use over time they were still found permeable and this was as a result of the void present because the concrete mix was not well compacted.

4. Conclusion

From the test results, only one sample showed full compliance with the specified standard by the regulatory body. Concrete poles that were not cured for the recommended 28 days before use aged fast and were weakened with time and had a shorter useful life. All but one of the samples tested failed to meet the minimum crushing strength of $37,000KN/m^2$ specified by the NIS. It was established that the manufacturers only cured the poles for 5 to 7 days instead of the 28 days specified. The poles were not well bonded and as a result weakened in situations where there was continuous rainfall leading to failure regardless of their age due to the voids present. The tensile test showed that all the samples were reinforced with 4mm reinforcing bars, which normally was above the minimum required standard of $0.48KN/mm^2$. However, the failed poles showed that the reinforcing bars were inadequate for the excessive load during failure. There is no central testing and licensing authority for concrete pole manufacturers and government does not have any regulatory authority to enforce compliance with laid down standards.

References

Toff consultancy (1982): A feasibility study on manufacturing of prestressed of concrete

Mosley W.H. and Bungey J.H.: Reinforced concrete design 1990

Ilochi E.E., Onoh G.N. and Okafor E.C. (1996): NSE technical Transaction

Akala A. (2002). N.E.P.A.: Technical Training Report NIS: Standard for Steel Bars for the reinforcement of Concrete (reviewed NIS 117-1992)

British Standard: Steel Fabrication for concrete reinforcement B.S. 1221: 1945.

British standard: Specification for reinforced concrete pole. BS 607: 1960.

Adams E.C. Science in building for craft student and technician Volume 3: publish by Anchor press Ltd .1974.

Bernard. H Knight and Rens. G. Knight .Builders material: 3rd edition: publish by Edward Arnold Ltd. 1967.

New Zealand standard: Specification for concrete poles for Electric Transmission and Distribution. NZE 3115: 1980.

Kong. F. K. and Evans. R.H. Reinforced and Prestressed concrete. 3rd edition: 1993.

Charles E Reynolds and James. C. Steedman. Reinforced concrete designer's handbook.9th edition: 1981.

Bassett. C.R. Experimental building craft science, Clearer Hume Press Ltd. 1961

RUS Bulletin 1724E-216: Guide Specification for Standard Class Spun Prestressed Concrete Pole 2000.

Habib Dagher, University of Maine and Ron Randle, EDM International: science of Pole Selection 2003.

Standard Australia: Concrete Structures, AS 3600 -2001, Standards Australia International Sydney. 2001

McDonald S. "Building Pathology" Concrete, Blackwell Science Oxford. 2003

Standard Australia 2003, Concrete Structures, AS 3600 -2001/ Amdt 1-2003, Standards Australia International Sydney. 2003

Gbenebor et al: Proc. ICCEM (2012) 181 – 184

Effects of Pouring Temperature on Solidification Using Energy Profile Analysis on Aluminum Alloy

Gbenebor O.P, Aasa S.A. and Inegbenebor A.O

Department of Mechanical Engineering, Covenant University, Ogun state, Nigeria

Corresponding Author: Aasa, S.A. Samson.aasa@covenantuniversity.edu.ng

Abstract

This work covered the study of energy profiles as influenced by solidification on sand cast 6063 aluminum alloy. Temperature is an important parameter, most especially in foundry technology that influences properties and morphology of cast products. Different pouring temperatures of 680^{o}C, 740^{o}C and 780^{o}C were considered. Mechanical energy expended and the quantity of heat evolved was evaluated from results obtained from tensile test experiments carried on the three samples. Relationship between change in coefficient of thermal expansion and change in applied tensile load were derived; it was observed that the maximum energy expended before fracture for samples decreased with increasing pouring temperature. Increasing pouring temperature decreased the amount of energy to be expended during deformation. This also influenced the change in heat evolved per time.

Key words: *coefficient of thermal expansion, mechanical energy, pouring temperature, quantity of heat, tensile load*

1. Introduction

Products of the aluminum alloy foundry have increased over the years and this can be justified by the increasing number of applications of its products in the areas of aerospace, automobiles, mechanical manufacturing industries ,etc (Bonollo et al., 2005; Ding et al., 2001). The properties of these alloys - high specific strength, light weight, good mechanical behaviour, good corrosion resistance, low density etc., have led to the introduction of new applications and the development of new processing techniques to produce aluminum alloy castings of desired properties. The chemical, physical and mechanical properties of cast and wrought alloys are greatly influenced by their microstructures formed during solidification (Yanwei et al 2010, Bo et al., 2011; Groll,2004).These properties are sensitive to composition, process, shape, size and type of phases evolved during solidification, etc. Aluminum alloys containing silicon as the major alloying element, are majorly used in casting because of the significant effect of silicon on the casting properties, combined with other physical, chemical and mechanical properties such as good weldability, low coefficient of thermal expansion high wear and corrosion resistance (.Mudakappanavar and Radhakrishna, 2012; Kaya et al., 2007). Casting, as a process involves parameters such as charge melting, mould temperature, pouring speed, pouring temperature, composition, microstructure, size of casting, runner size, composition of the alloy and solidification time. The difference in the structure of the casting arises as a result of non-uniform cooling of the molten metal in the mould which later results to low mechanical properties. Studies have shown that the optimum pouring temperature for aluminum alloy is between 700_{o}C and 760^{o}C (.Raji and Khan, 2006; Ndaliman and Pius, 2007) because good quality casts and mechanical properties are produced; the rate of mechanical work and the heat generated as a result of this during tensile loading needs to be studied. In this research, one process parameter and mechanical test are employed. The parameter is pouring temperature while the mechanical test is tensile test from which results obtained were used in calculating mechanical work at deformation.

2. EXPERIMENTAL PROCEDURES

Sample preparation

A cylindrical steel pattern of 50mm diameter and 170mm high was placed in a wider cylindrical

steel container with both ends opened. Moulding sand was added to the container and rammed for easy compact and adherence to the pattern which was finally removed after the rammed mould had reached the required height (pattern's height). This was done for the three specimens needed for the experiment.

Table 1: Aluminum alloy AA 6063 spectrometer analysis

Element	Al	Si	Mg	Fe	Cu	Mn	Ti	Cr
Composition %	95	0.45	0.50	0.22	0.03	0.03	0.02	0.03

The billet was charged in an oil – fired crucible furnace which was initially preheated to 150^{o}C. On heating to the molten state, a pyrometer was brought close to the crucible to measure the melt's temperature. The melt was poured into one of the moulds until the cavity was filled. This was done for the other two samples while the pouring speed and the distance between the crucible and the mould were kept constant for each of the samples. Pouring temperatures recorded for each sample was 680^{o}C, 740^{o}C and 780^{o}C, designated as sample A, B and C respectively.

Mechanical test

Each sample was machined to a tensile test piece of geometry shown in Figure 1.

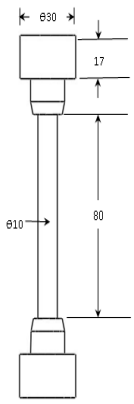

Figure 1: Tensile piece specimen (dimensions in mm)

Tensile test was carried out with the use of universal testing machine (TQSM 1000), which had digital load and displacement meters attached for the measurement of applied tensile loads (in kN) with corresponding specimen longitudinal displacements (mm). Also, the time to attain each elongation at corresponding load was recorded.

Sand casting

The material used 6063 aluminum alloy of composition shown in Table 1.

3. Evaluation equations

Energy expended during deformation

Energy performed during deformation was calculated from the equation

$$E = \frac{1}{2}kx^2 \qquad 1$$

Where k is the spring constant and x is the displacement. Knowing that F=kx, equation (1) becomes

$$E = \frac{1}{2}Fx \qquad 2$$

Quantity of heat given off during deformation

The mechanical equivalent of heat was calculated using the relationship (Kurtus', 2009) expressed as

$$Q = \frac{\text{Work done}}{C_p} \qquad 3$$

Where C_p is the specific heat capacity of 6063 aluminum at constant pressure. given as 0.9kJ/kg^{o}C.

Coefficient of thermal expansion and tensile load relationship

The relationship between coefficients of thermal expansion for the samples was derived resulting to:

$$\frac{d\alpha}{dF} = -\frac{Cp}{Lok^2}\left(\frac{dk}{dQ}\right)_F \qquad (4)$$

where α is the coefficient of thermal expansion, Cp is the specific heat capacity of the alloy, Lo,

the initial gauge length of the specimen, k, the spring constant and Q is the quantity of heat evolved during load application.

4. Results and Discussions

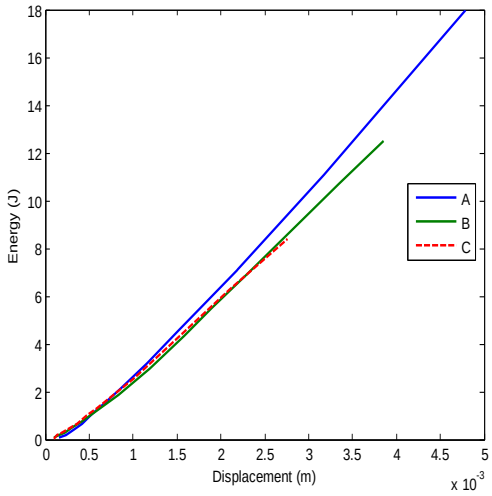

Figure 2: Graph of Energy against Displacement

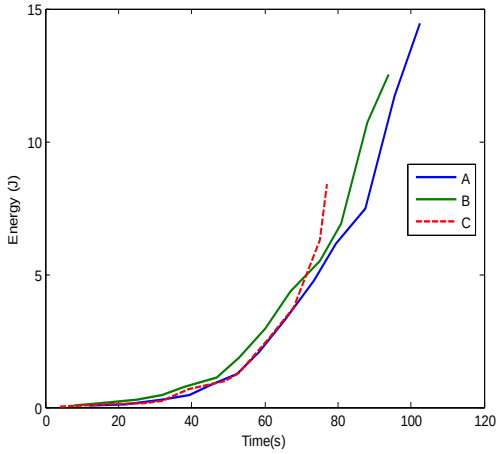

Figure 3: Graph of Energy against Time

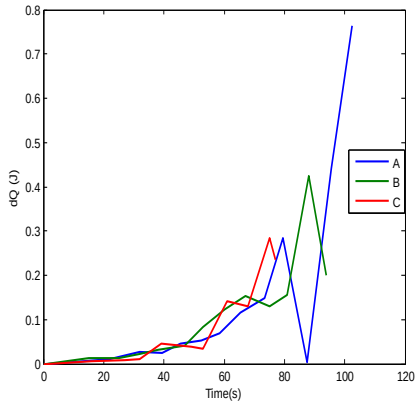

Figure 4: Graph of Heat change against Time

Figure 2 above shows a linear energy – displacement relationship for each specimen. More energy is required to displace each specimen from their instantaneous positions; this is a reflection of the fact that for a specimen to encounter further plastic deformation, higher magnitude of load is required to achieve this. The greatest work is done during deformation of sample A while that of B, though maintains almost similar energy magnitudes with C up to ≈ 2.6mm displacement, follows A. The Figure reveals that increasing pouring temperature lowers the extent to which a cast sample will deform. A non- linear relationship between energy expended and time for each sample is shown in Figure 3 with each curve showing almost similar pattern. A hundred and two seconds is needed for sample A to exhibit ≈4.8mm displacement before fracture. Sample C cannot expend much energy for a long time as compared with the rest.

Wavy curves are observed for the samples shown in Figure 4. The heat evolved during the deformation fluctuates with time. For samples B and C, the quantity dropped to 0.18J and 0.2J within 5s before fracture after attaining maximum values of 0.42J and 0.28J respectively. Minimum heat of ≈0.03J was evolved on the 80th second during deformation of sample A and after 20s, the heat evolved rose to 0.7J. These fluctuations could be as a result of anisotropic effects. The relationship $\left(\frac{d\alpha}{dF}\right)$ for each specimen at maximum load was calculated and values $26.3\mu(N^oC)^{-1}$, $12.2\mu(N^oC)^{-1}$ and

$1.27\mu(N^{0}C)^{-1}$ were recorded for samples A, B and C respectively.

5. Conclusion

Results of pouring temperatures on energy-displacement relationship, rate of energy dissipation and rate of heat evolved by the samples reveal the maximum energy expended before fracture for samples A, B and C are 17.9J, 12.5J and 8.4J respectively. Increasing pouring temperature decreases the amount of energy to be expended during deformation. This also influences the change in heat evolved per time which is seen to increase with decreasing pouring temperature. Furthermore, the maximum load for the system was estimated to be 7.5kN, 6.5kN and 6.1kN for samples A, B and C

Considering the results of this analysis, sample A possessed the highest energy to a maximum displacement of 17.9J at 4.9mm while sample C has the lowest values of 8.4J at 2.8mm. This also accounts for the heat change evolved. From this sudy,It can therefore be concluded that if certain numbers of pouring temperatures are to be considered, the one with the lowest temperature will possess the superlative energy absorbing capacity before fracture.

References

Bo X., Yuandong L., Ma Y. and.Yuan H (2011): Effects of novel self-inoculation method on the microstructure of AM60 alloy. *China Foundry*, vol.8(1), pp.121-126.

Bonollo F., Urban J., Bonatto B. and Botter, M (2005):.Gravity and low pressure die casting inaluminum alloys: a technical and economical bench mark. *Aluminio Eleghe; la metallurgia*

italiana, pp.23-32 .

Ding H.S., Gou J.J and Jia, J (2001).: Mould filling ability and microstructure of aluminum alloy
under electromagnetic casting.. *Trans. Nonferrous Met. Soc. China,* vol. 11(4), pp.540-546.

Groll A.T (2004): Effect of solidification rate on cast microstructure. *Laboratory module 5, Padnos College of Engineering and Computing Grand Valley State University*, pp.1-14..

Kaya H., Cadırlı, E. and. Gu¨ nduz M.(2007): Dendritic growth inaluminum – silicon alloy, *Journal of Materials Engineering and Performance,* vol. 16,(1) ,pp. 12-21.

Kurtus R (2009).: Thermodynamics is the connection between heat and work. *School for champions,http://www.school-for champions.com/science/thermodynamics.htm* (assessed on the 5th of November, 2012)

Mudakappanavar S. V and Radhakrishna. D.K: Effect of external parameters like mold material, mechanical mold vibration and pouring temperature on wear and hardness properties of Al - Si alloy casting. *B M S College of Engineering,* pp.1-22, (accessed on the 5th of November, 2012).

Ndaliman M.B and Pius A. (2007): Behavior of aluminum alloy castings under different pouring temperatures and speeds. *Leonardo Electronic Journal of Practices and Technologies*, no.11, pp. 71-80..

Raji A. and Khan R.H (2006): Effects of pouring temperature and squeeze pressure on Al-8%Si alloy squeeze cast parts. *A U J.T*, vol. 9(4) , 229-232 .

Yanwei S., Bangsheng L., Aihui L., Jingjie G. and Hengzhi F (2010).: Evolution of microstructure in centrifugal cast Al – Cu. *China Foundry*, Vol.7(1), , pages 43-46.

Potentials for generating alternative fuels from empty palm fruit bunches by pyrolysis

[1*]Ogunsina, B.S; [2]Ojolo S.J; [3]Ohunakin, O.S; [1]Oyedeji, O.A; [4]Matanmi, K.A and [5]Bamgboye, I.A

[1]Dept. of Agricultural & Environmental Engineering, Obafemi Awolowo University, Ile-Ife. Nigeria
[2]Dept. of Mechanical Engineering, University of Lagos. Nigeria
[3]Dept. of Mechanical Engineering, Covenant University, Ota, Nigeria
[4]Dept. of Mechanical Engineering, Obafemi Awolowo University, Ile-Ife. Nigeria
[5]Dept. of Agricultural & Environmental Engineering, Obafemi Awolowo University, Ile-Ife. Nigeria

Abstract

The threat that the disposal of empty palm fruit bunches constitute to communities in oil palm processing areas in Nigeria coupled with the current global focus on alternative energy is the trigger for this work. An existing pyrolytic reactor consisting of a reactor unit, condensate receiver, copper pipe connectors and gas receiver was modified and adapted for converting empty palm fruit bunches to alternative fuels. The average char yield was 44.9%, and the percentage of feedstock converted into pyrogas and tar oil was 55.1%. The char yield decreased gradually as temperature was increased from 300-700°C. Char yield was highest (39.78%) when the temperature was 300°C and the lowest char yield was 25.05% at 700°C The calorific values of char ranged between 21.12 and 23.76 MJ/kg. Apart from the potential of generating energy from pyrolysed EFB, it abates the disposal problem that EFB constitutes in the oil palm industry.

***Keywords**: Empty Palm Fruit Bunches, Thermo-Chemical conversion, Alternative Fuel, Char, Pyrogas, Tar Oil*

1. Introduction

With the continual depletion of fossil fuel reserves and increasing global concerns over climate change, Nigeria as a foremost country in sub-Sahara Africa (like other regions of the world) is faced with the need to explore alternative energy sources. One of the known approaches is the conversion of biomass into alternative fuels by pyrolysis. Pyrolytic conversion of organic wastes apart from generating alternative energy is an efficient way to eliminate emission of odour from disposed solid wastes. The biomass is converted into a black carbonaceous solid, a mixture of gases and tar oil; the proportion of which depends on composition of the biomass, temperature and duration of the process. Soltes (1986) documented that tar oil may be fractionated into gasoline and diesel fuels to run engines; and may also be processed as disinfectant, germicides and wood preservatives while the gasses may be used for powering internal combustion engines or processed into liquid fuels. Pyrolysis has received considerable attention as a method for waste disposal in an environmentally acceptable manner with remarkable resource recovery at the same time (Piechura, 1998). Several works have been documented regarding pyrolytic conversion of bulky agricultural wastes into alternative energy sources (Misson, 2009, Abdullah and Gerhauser, 2008; Ojolo, *et al.,* 2008; Bamgboye and Oniya, 2003; Ojolo and Bamgboye, 2005). Sukiran *et al.* (2009) documented a pyrolytic process for pulverised EFB under varied conditions in a fluidized fixed-bed reactor. Bamgboye and Oniya (2003) reported that pyrolytic conversion of corncobs to medium grade fuels and chemical preservatives yielded pyrogas, tar oil, pyroligenous acid and tar with about 91.49% conversion efficiency. The studies of Ojolo and Bamgboye (2005) on the thermo-chemical conversion of municipal solid wastes to produce fuel and reduce waste shows that municipal solid wastes when pyrolysed can be converted into useful fuel products such as tar oil, pyrogas and char. Barnerd and Gerald (1983) reported how pyrolytic systems are developed and used to power road vehicles during the second world war. The process is being used in Netherlands and USA to recycle plastic waste and shred rubbish (Westerhent *et al*., 1988). Ogunsina *et al.* (2008) investigated

the pyrolytic conversion of cashew nut shells into bio-fuels; the disposal of which has hitherto being a serious menace in the cashew nut processing industry.

In Africa and Asia, widespread cultivation of oil palm (*Elaeis guineensis*) is driven by the vegetable and industrial oils (*i.e* palm oil and palm kernel oil respectively) that its fruits provide. Presently, Nigeria ranks third among the largest producers of palm oil in the world after Malaysia and Indonesia; although the industry is largely concentrated in rural communities where processing is by manual or semi-manual methods (Salako *et al.*, 2009). The major unit operations include reception of the palm fruits bunch, sterilization, threshing, digestion, pulp pressing, oil clarification, nut recovery, oil and nut drying. Considerable amount of biomass such as the mesocarp fibre, shell, empty fruit bunches (EFB), frond, trunk and palm oil mill effluent are generated in each unit at different stages but EFB is usually the bulkiest. In Nigeria up till now, EFB is still being incinerated due to the dearth of information regarding its potentials as a source of alternative fuels.

In this work, an existing pyrolytic reactor by Ojolo and Bamgboye (2005) was modified and tested to investigate the potentials of converting EFB to alternative fuels.

2. MATERIALS AND METHODS

2.1 Materials

The following materials and equipment were used for this investigation: weighing machine, oven, pyrolytic reactor, stop watch, EFB, cutlass (for disintegrating the EFB bunches into smaller chunks) and attrition mill. About 20 kg of dried (18.8% moisture content) EFB were collected from Seldot palm oil mill, Gbongan, Osun State, Nigeria. The EFB were kept in polythene bags until when needed to prevent moisture loss.

2.2 Description and limitations of the existing pyrolytic reactor

The existing design is composed of a furnace which encloses a retort, a gas holder and condensate receiver (Fig. 1). The retort was connected to the condensing unit with copper pipes. The reactor was made of 1.6 mm thick mild steel into a cylinder of 5 dm^3 volume with a sealed bottom. A 3000 W capacity heating element connected to a 220 V single phase power source was placed at the bottom of the reactor. The reactor was fully lagged with fibre glass to prevent heat loss by radiation. A 1200 ^oC thermostat was installed inside the heating chamber for temperature control using a bimetallic material incorporated inside the heating chamber to monitor the resident time and heating rate of the feedstock. The condensate receiver was a mild steel container placed on a bed of ice; it condenses the tar oil from the mixture of gases conveyed from the reactor while the tar gas is further conveyed to the gases receiver through the lagged copper pipe. The gasses receiver is made of glass with a cork to prevent heat loss. The reactor had been tested with corn cobs and cashew nut shells; however with EFB, the system was unable to withstand the high pressure generated at temperatures above 650 ^oC and the backflow of pyrogas into the condensate receiver could not be prevented.

2.3 Design modifications

The functional elements of the modified unit are the reactor chamber, condensate receiver, copper pipes and gas receiver. A clip and a high heat resistance gasket were introduced to constitute an improved air tight cover that disallows leakage in and out of the container. A non-return flow valve controlled by gas pressure was in between the gas receiver and the condensate receiver. The valve poppet opens to allow gas passage to the receiver when the gas pressure rises above 35 kPa and does not allow a backward flow.

2.4 Machine testing

The EFB which had an average moisture content of 18.8 % (wb) were chopped into small particles and milled. The particle sizes used were between 100 -150 µm. The reactor was then loaded in batches with 300 g, 370 g, 360 g, 350 g and 400 g of EFB and allowed to operate for 9 h at an average temperature 550 ˚C each run in triplicates. The weight of the char after the thermo-chemical reaction was measured and recorded; the char yield was calculated as in eqn.1. The percentage of char produced was also calculated using eqn. 1. Tar oil produced was collected after distillation in the condensate receiver and the gas produced was collected in the gas receiver.

$$Y_c = \frac{W_c}{W_w} \times 100\% \quad (1)$$

where, Y_c = Char yield

W_c = Weight of char after pyrolysis

W_w = Weight of feedstock.

The percentage of empty fruit bunches used up during the investigation was calculated as follows:

$$\%\ of\ EFB\ used = \frac{W_w - W_c}{W_w} \times 100\% \quad (2)$$

2.4 Pyrolysis of EFB

The reactor was used to pyrolyse EFB at five different temperature levels: 300, 400, 400, 500, 600 and 700^{o}C selected based on review of literatures. With each temperature level, there were three replicates of the experiment. The calorific values of the char produced during each temperature trial were determined using Gallenkamp ballistic bomb calorimeter (Cambridge Instrument Co. Ltd., England) and ultimate analysis was carried out as documented by Ogunsina *et al.* (2009).

3. RESULTS AND DISCUSSIONS

The schematic drawing of the modified reactor is shown in Fig. 2. The performance test showed noticeable gaseous emission after the first 2 h into the experiment. After 4 h, some pyrogas were observed in the gas receiver and an insignificant amount of tar oil was observed in the tar oil receiver. At the end of each experimental run, there was reduction in the weight of the empty fruit bunch loaded at the start of the experiment. The resulting char yield during each run is presented in Table 1. With an average char yield of 44.9%, the percentage of EFB converted in pyrolytic products was 55.1%. Beside the potential for generating energy from EFB the reduction in the bulk offers solution to the problem that the disposal of EFB constitute in the oil palm industry.

Table 2 shows the average yield of pyrolytic products at different temperature. The char yield decreased gradually as temperature was increased from 300-700°C. Char yield was highest (39.78%) when the temperature was 300°C and the lowest char yield was 25.05% at 700°C. It was however observed that the yield of other pyrolytic products increased with temperature.

Table 3 shows the ultimate analysis and calorific value including the H/C and O/C molar ratios of pyrolysed EFB products at different temperatures. The values do not depict a definite trend but showed little differences. The calorific values of char based on the different temperatures considered in this work ranged between 21.12 and 23.76 MJ/kg. Although the calorific values also do not show a definite trend, the highest was 23.76 MJ/kg when pyrolysis temperature of 500°C. The H/C ratios of char changed between 0.50 and 0.65. The highest H/C ratio of char was 0.65 when the pyrolysis temperature was 400°C. The O/C ratios of the EFB char ranged between 0.37 and 0.55. The highest O/C ratio of char obtained was 0.55 when pyrolysis temperature was 700°C. The percentage range of hydrogen and nitrogen were 3.01 - 4.17% and 1.98 - 2.68% respectively. The highest hydrogen and nitrogen content obtained were 4.17% and 2.68% at pyrolytic temperatures of 400°C in both cases.

4. Conclusion

From the foregoing, it may be concluded that:

1) An existing pyrolytic reactor was modified and adapted for converting empty palm fruit bunches to alternative fuels. A clip and a high heat resistance gasket were introduced to constitute an improved air tight cover that disallows leakage in and out of the container. A non-return flow valve controlled by gas pressure was placed in between the gas receiver and the condensate receiver. The valve poppet opens to allow gas passage to the receiver when the gas pressure rises above 35 kPa and does not allow a backward flow.

2) Empty palm fruit bunches may be converted to char, tar oil and pyrogas by pyrolysis. The percentage of char produced was 44.9%; about 55.1% of the feedstock was converted to tar oil and pyrogas.

3) Char yield decreased gradually as temperature was increased from 300-700°C. Char yield was highest (39.78%)

when the temperature was 300°C and the lowest char yield was 25.05% at 700°C. The calorific values of char ranged between 21.12 and 23.76 MJ/kg.

4) Utilization of EFB as feedstock for energy generation by pyrolysis will help in abating EFB disposal problems in oil palm mills.

References

Abdullah, N. and Gerhauser, H. 2008. Bio-oil derived from empty fruit bunches. *Fuel* 87(12): 2606–2613.

Bamgboye, A.I. and Oniya, O. 2003. Pyrolytic Conversion of corncobs to medium grade fuels and chemical preservatives. *Journal of Environment and Engineering Technology*, Federal University of Technology, Akure, Nigeria. 3(2)50-53.

Barnerd, G. and Gerald, F. 1983. Biomass Gasification in Developing Countries. Earthscan International Institute for Environment and Development, London

Misson, M; Haron, R; Fadhzir, M; Kamaroddin, A; Aishah, N and Amin, S. 2009. Pretreatment of empty palm fruit bunch for production of chemicals via catalytic pyrolysis. *Bioresource Technology*, 100: 2867–2873

Ojolo, S.J and Bamgboye, A.I. 2005. Thermochemical conversion of municipal solid waste to produce fuel and reduce waste. *Agricultural Engineering International- The CIGR EJournal*. Vol. VII. Manuscript EE 05 006. September, 2005.

Ojolo, S.J; Bamgboye, A.I; Ogunsina, B.S and Oke, A. 2008. Analytical approach for predicting biogas generation in a municipal solid waste anaerobic digester. *Iranian Journal of Environmental Health Sciences and Engineering,* 5(3):179-186.

Ogunsina, B.S; Ojolo S.J.; Bamgboye A.I.; Muritala A.O.; Fasogbon S.K.; Femi-Falade O. and Imoudu D.E. 2009. Thermochemical Conversion of Cashew Nut (*Anacardium Occidentale*) Shells into Alternative Energy Sources. Proceedings of the 3rd International Conference of the West African Society for Agricultural Engineering & 9th Nigerian Institution of Agricultural Engineers Conference held at Obafemi Awolowo University, Ile Ife, NIGERIA. Jan. 25-29, 2009, pp 339-343

Piechura, H. 1998. *Pyrolytic Technology Applications. Hazardous Waste Detection, Control, Treatment.* Elsevier Science Publishers. B.V. Amsterdam, Netherlands. Pp 1335-1343

Soltes, E.I. 1986. Thermochemical Process for Bio-Energy Production*. Biomass Energy Development.* Plenum Press, New York

Sukiran, M.A; Kheang, L.S; Abu Bakar, N and May, C.Y. 2011. Production and characterization of Bio-Char from the Pyrolysis of Empty Fruit Bunches. *American Journal of Applied Sciences*, 8 (10): 984-988

Salako, Y.A; Owolarafe, O.K. and Anozie, A.N. 2009. Characterisation of sundried palm fruit waste biomass materials. *Ife Journal of Technology*, 18(2): 26-30.

Westerhent, R.W.; Wanders J. and Kuipers J.A.M. 1988. The development of a continuous rotation cone reactor pilot plant for the pyrolysis of polythene and polypropane. Industrial and Engineering Chemistry Research. *American Chemical Society*. U.S.A. 37(6): 2316-2327.

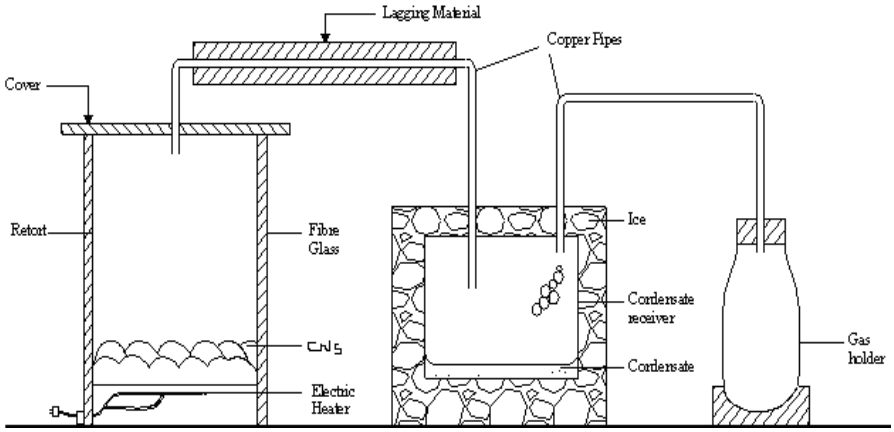

Fig. 1. Previous design of pyrolytic reactor
(Source: Ojolo and Bamgboye, 2005)

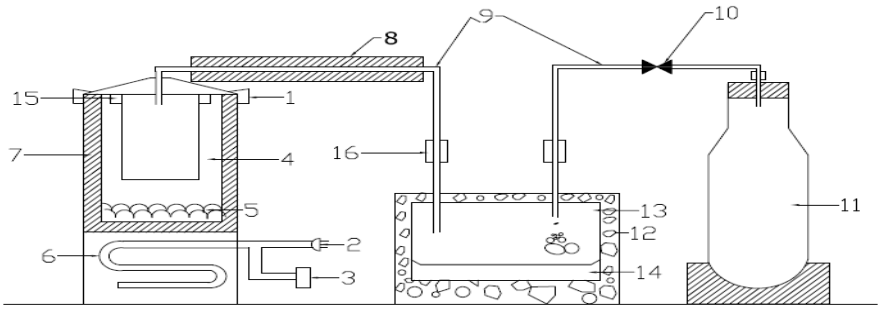

1 -Clip;2 -Power source;3 -Temperature control unit;4 -pyrolitic reactor; 5 -EFB;6 -Heating element;7 -Fibre glass;8-Lagging;9 -Copper pipes; 10 -Non-return valve;11 -Gas holder;12 -Ice block;13 -Condensate reclever; 14 -Tar oil; 15-Gasket; 16-Connector.

Fig. 2. The modified pyrolytic reactor design

Table 1: Char yield from the pyrolysed product

Replicates	Initial weight of EFB	Final weight of EFB	% Char yield
A	300	135	45.0
B	370	160	43.24
C	360	170	47.22
D	350	150	42.86
E	400	185	46.25
MEAN (SD)			44.9 (1.88)

Table 2. Average yield of pyrolytic products at different temperatures

	Yield (%)		
Temperature (^{o}C)	Tar-oil	Char	Gas

300	27.9	39.78	32.32
400	32.12	27.8	40.08
500	29.98	27.19	42.83
600	31.92	26.22	41.86
700	33.61	25.05	41.34

Table 3. Properties of EFB char produced at different temperature

Pyrolytic temperature (^{o}C)	Ultimate analysis						Calorific value (MJ/kg)
	C (wt. %)	H (wt. %)	N (wt. %)	O (wt. %) by diff.	O/C Molar ratio	H/C Molar ratio	
300	68.67	3.46	2.32	25.55	0.37	0.50	23.67
400	64.10	4.17	2.68	29.05	0.45	0.65	21.12
500	66.95	3.99	1.98	27.08	0.40	0.60	23.76
600	65.32	4.01	2.13	28.54	0.44	0.61	23.1
700	60.88	3.50	2.11	33.51	0.55	0.58	24.04

Root Locus-Based Magnetic Levitation System Stabilization: An Undergraduate Control System Design Approach

[1]Katende, J.; [2]Awelewa, A.A.; [3]Samuel, I.A.; and [4]Iyiola, S.O.

[1]College of Technology, Botswana International University of Science & Technology, Gaborone, Botswana.
[2,3,4]Department of Electrical and Information Engineering, College of Science & Technology, Covenant University, Ota, Ogun State, Nigeria

Abstract

The subject of control system design has evolved considerably over the years. Although several design techniques and strategies have been adopted to realize control systems that meet a predetermined set of performance criteria, the fundamental problem remains that of developing controllers to adjust the performance characteristics of a dynamic system in order to obtain a desired output behavior. The dynamic behavior of a magnetic levitation system (MLS) of a ferromagnetic ball is compensated in this paper. Consolidating the exposure of undergraduate students to the rudiments of control system design, the paper employs the classical root locus technique to stabilize the system. A combination of analytical and software-based methods is used to design proportional-derivative and phase-lead compensators based on the linearized model of the system. Complete details of the design approach, from modeling and analysis of the plant to computing the values of the controller parameters, are shown. MATLAB scripts for plotting root loci and simulating the system are provided.

***Key words**: compensators, magnetic levitation system, MATLAB® scripts, modeling, root-locus method, system stability*

1. Introduction

The magnetic levitation system has attracted a great deal of attention both in the industry and academia. In the industry, significant applications, such as passenger train levitation, magnetic bearing, metal sheet levitation, protection of sensitive machinery, etc., have been recorded, while in the academia, authors of books on control systems theory (Franklin et al., 1998; Nise, 2007) have used similar versions of the system to educate undergraduate students on the subject of control systems, with laboratories having prototypes and experimental models of the system handy for instructional purposes (Naumivic and Veselic, 2008; Green et al., 1995). The magnetic levitation system of a ferromagnetic ball has a complex nonlinear dynamic equation, and its characteristic response inherently unstable (Feedback Instrument, 2012). Successful efforts have been made to design nonlinear controllers (Al-Muthairi and Zribi, 2004) just as well as linear controllers (Naumivic and Veselic, 2008; Green et al., 1995; Feedback Instrument, 2012) to stabilize the system. This latter type, which is further considered in this paper, is based on the linearized version of the system operating in a small range around an operating point. The aim of the paper is to shed more light on the use of a classical technique in stabilizing a magnetic levitation system. The rest of the paper is arranged as follows. Section 2.0 considers the complete modeling of a magnetic levitation system, with both nonlinear and linearized models treated in detail. Section 3.0 focuses on the magnetic levitation system design and simulation, and also, shows graphical displays to buttress design results. And finally, Section 4.0 presents the conclusion. All the MATLAB scripts used for the design and simulation are separately given in the appendix.

2. Magnetic Levitation System Modelling

2.1 Layout of the System

The layout of a typical magnetic levitation system is illustrated in Fig. 1 (Al-Muthairi and Zribi, 2004). This arrangement involves the adjustment of magnetic energy or force in order to balance or counteract the gravitational pull exerted on an object (a small light ferromagnetic ball in this case).

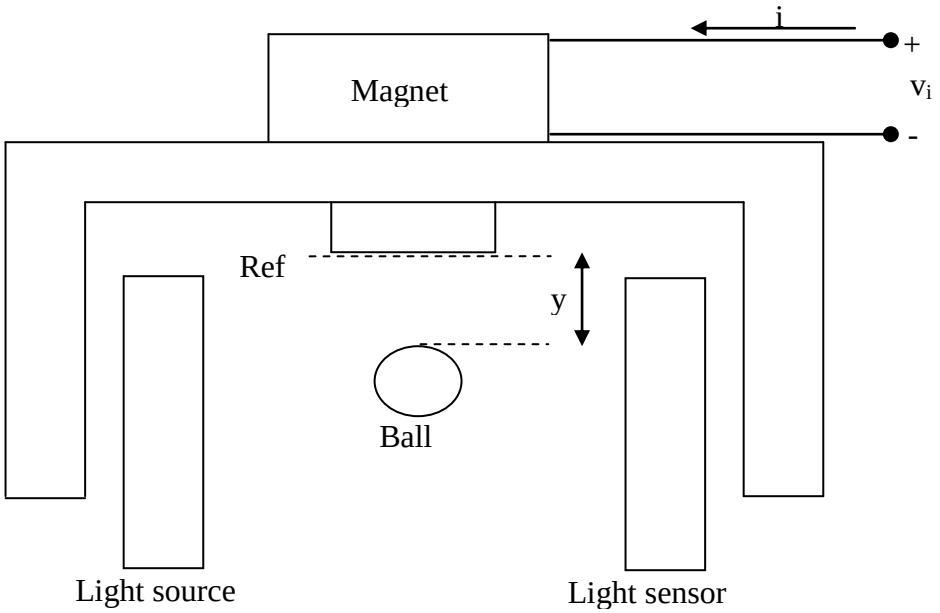

Fig. 1: Schematic of a magnetic levitation system

Restricted to the vertical direction only, the motion of the ball is monitored by a properly arranged pair of a light emitter and a light detector so that the instantaneous position of the ball can be fed back for the purpose of control computation. This control effort (generated by an electromagnetic circuit) is to ensure that the ball is brought to, and kept at, a desired position. As the ball's position deviates, due to an external disturbance, from the set point, the sensor output changes accordingly so that the right amount of control effort is computed and used to bring the ball back to the set point and keep it there.

Fig. 2 is the representation of the electric circuit subsystem of the magnetic levitation system. It is a series combination of a linear resistor, with resistance R, and a non-linear inductor, with inductance L(y).

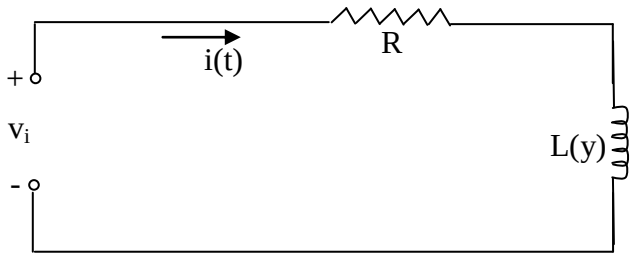

Fig. 2: An electric circuit subsystem of the maglev system.

The inductance is non-linear due to the variable reluctance of the magnetic circuit—the reluctance is directly proportional to the distance between the electromagnet and the ball, implying that as this distance decreases (i.e., ball's approaching the magnet), the inductance increases, and vice versa.

2.2 Non-linear Model of the System

To determine the complete model of this system, two important dynamic equations, one representing the variations of the magnetic flux with time (based on Fig. 2) and the other the Newtonian equation of

motion of the ball based on forces acting on it as shown in Fig. 3, are required.

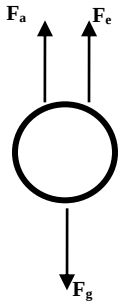

Fig. 3: A free-body diagram showing forces acting on the ball.

From Fig. 2, it can be written that

$$\frac{d\phi(t,y)}{dt} + Ri(t) = v_i \qquad 1$$

where $\phi(t, y)$ is the magnetic flux in webers, i(t) is the current in amperes, R is the resistance in ohms, v_i is the source voltage in volts, and t is time in seconds.

Since the magnetic flux around a coil is directly proportional to the current flow in the coil, with the coil inductance being a factor of proportionality, thus,

$$\phi(t,y) = L(y)i(t) \qquad 2$$

Differentiating (2) with respect to time and substituting the result into (1) yield

$$L(y)\frac{di(t)}{dt} + \frac{dL(y)}{dy}\cdot\frac{dy}{dt} + Ri(t) = v_i$$

or

$$L(y)\frac{di(t)}{dt} + \left(R + \frac{dL(y)}{dy}\frac{dy}{dt}\right)i(t) = v_i \qquad 3$$

where y(t) is the distance between the electromagnet and the ball, and L(y) is the total inductance of the circuit in henry.

Also, from Fig. 3,

$F_a + F_e = F_g \qquad 4$

where F_a is the accelerating force due to the mass of the ball, F_e is the magnetic force, and F_g is the gravitational force.

Since

$$F_a = m\frac{d^2y}{dt^2} \text{ and } F_g = mg,$$

therefore, (4) can be rewritten as

$$m\frac{d^2y}{dt^2} = mg - F_e$$

or

$$m\frac{dv}{dt} = mg - F_e \qquad 5$$

In (5), m is the mass of the ball in kg, v(= dy/dt) is the velocity of the ball in m/s, and g is the acceleration due to gravity in m/s^2.

Equations (3) and (5), which constitute the mathematical representation of the system, can be developed further by redefining L(y) and F_e and finding appropriate expressions for them, respectively, as shown by the following derivations.

L(y) represents the sum of two inductances, L_c and L_b, i.e.,

$L(y) = L_c + L_b \qquad 6$

L_c, which is fixed, is the inductance due to the electromagnet coil; L_b is the inductance due to the ball. Because L_b is inversely proportional to the distance between the electromagnet and the ball, it implies that if L_o is the inductance that corresponds to a set-point position, y_o, then the inductance, L_b, that corresponds to an instantaneous position, y, is expressed as

$$L_b = \frac{L_o y_o}{y} \qquad 7$$

Therefore, putting (7) in (6) gives

$$L(y) = L_c + \frac{L_o y_o}{y} \qquad (8)$$

Further, the magnetic force, F_e, is defined as the rate of change of work done with distance as the ball is moved from one position to the other by the force, and is given as

$$F_e = -\frac{dW}{dy} \qquad 9$$

Where

$W = \frac{1}{2} L(y) i^2$ (i.e., the energy stored in the magnetic field)

Hence, (9) gives

$$F_e = \frac{1}{2} L_o y_o \frac{i^2}{y^2} \qquad 10$$

which, with L_o and y_o fixed, can further be reduced to

$$F_e = K \frac{i^2}{y^2} \qquad 11$$

where K(called the magnetic force constant) = $\frac{1}{2} L_o y_o$

Now, substituting (8) into (3), and (11) into (5), we have

$$L(y) \frac{di(t)}{dt} + \left(R - \frac{L_o y_o}{y^2} \frac{dy}{dt} \right) i(t) = v_i \qquad 12$$

and

$$m \frac{dv}{dt} = mg - K \frac{i^2}{y^2} \qquad 13$$

The final non-linear equations are

$$\frac{di(t)}{dt} + \frac{1}{L(y)} \left(R - \frac{2K}{y^2} v \right) i(t) = \frac{1}{L(y)} v_i \qquad 14$$

$$\frac{dv}{dt} = g - \frac{K}{m} \frac{i^2}{y^2} \qquad 15$$

Let state variables and the input be defined as:

$$x_1 = y;\ x_2 = dy/dt = v;\ x_3 = i;\ u = v_i$$

The equivalent nonlinear state-space dynamic model of the system is:

$$\frac{dx_1}{dt} = x_2$$

$$\frac{dx_2}{dt} = g - \frac{K}{m} \left(\frac{x_3}{x_1} \right)^2$$

$$\frac{dx_3}{dt} = \frac{1}{L(y)} u - \left(\frac{R}{L(y)} - \frac{2K}{L(y)} \frac{x_2}{x_1^2} \right) x_3 . \qquad 16$$

2.3 Linearized Model of the System

As can be seen in the model just developed, the maglev system is non-linear. As mentioned earlier, several non-linear controllers have been designed for this system in the literature. But the focus here is on how to improve the system performance for small-range operation. Therefore, the above non-linear model is linearized about a nominal operating point, $\boldsymbol{x}_o(t)$, which corresponds to a nominal input, u_o, using a Taylor series (Kuo and Golnaraghi, 2003).

First, the model in (16) is rewritten as

$$\frac{dx_1}{dt} = f_1(x_1, x_2, x_3, u) = x_2$$

$$\frac{dx_2}{dt} = f_2(x_1, x_2, x_3, u) = g - \frac{K}{m} \left(\frac{x_3}{x_1} \right)^2 \qquad 17$$

$$\frac{dx_3}{dt} = f_3(x_1, x_2, x_3, u) = \frac{1}{L(y)} u - \left(\frac{R}{L(y)} - \frac{2K}{L(y)} \frac{x_2}{x_1^2} \right) x_3 .$$

Then expanding (17) into a Taylor series about $\boldsymbol{x}_o(t) = [x_{o1}, x_{o2}, x_{o3}]$ and ignoring terms of order higher than first result in

$$\frac{dx_i}{dt} = f_i(x_1, x_2, x_3, u)\Big|_{x_o(t),u_o} + \frac{\partial f_i(x_1, x_2, x_3, u)}{\partial x_1}\Big|_{x_o(t),u_o} (x_1 - x_{o1})$$

$$+ \frac{\partial f_i(x_1, x_2, x_3, u)}{\partial x_2}\Big|_{x_o(t),u_o} (x_2 - x_{o2}) + \frac{\partial f_i(x_1, x_2, x_3, u)}{\partial x_3}\Big|_{x_o(t),u_o} (x_3 - x_{o3})$$

$$+ \frac{\partial f_i(x_1, x_2, x_3, u)}{\partial u}\Big|_{x_o(t),u_o} (u - u_o)$$

18

where i = 1, 2, 3.

Hence,

$$\frac{dx_1}{dt} = \frac{dx_{o1}}{dt} + 0 + 1.(x_2 - x_{o2}) + 0 + 0$$

$$\frac{dx_2}{dt} = \frac{dx_{o2}}{dt} + \frac{2K}{m}\frac{{x_{o3}}^2}{{x_{o1}}^3}.(x_1 - x_{o1}) + 0 - \frac{2K}{m}\frac{x_{o3}}{{x_{o1}}^2}.(x_3 - x_{o3})$$

$$\frac{dx_3}{dt} = \frac{dx_{o3}}{dt} - \frac{4Kx_{o2}x_{o3}}{L{x_{o1}}^3}.(x_1 - x_{o1}) + \frac{2Kx_{o3}}{L{x_{o1}}^2}.(x_2 - x_{o2}) - \left(\frac{R}{L} - \frac{2Kx_{o2}}{L{x_{o1}}^2}\right)(x_3 - x_{o3})$$

$$+ \frac{1}{L}(u - u_o)$$

19

Noting that

$$\Delta x_i = x_i - x_{oi} \;;\; \frac{d\Delta x_i}{dt} = \frac{dx_i}{dt} - \frac{dx_{oi}}{dt} \qquad (i = 1, 2, 3),$$

then, (19) becomes

$$\frac{d\Delta x_1}{dt} = \Delta x_2$$

$$\frac{d\Delta x_2}{dt} = \frac{2K}{m}\frac{{x_{o3}}^2}{{x_{o1}}^3}\Delta x_1 - \frac{2K}{m}\frac{x_{o3}}{{x_{o1}}^2}\Delta x_3$$

$$\frac{d\Delta x_3}{dt} = -\frac{4Kx_{o2}x_{o3}}{L{x_{o1}}^3}\Delta x_1 + \frac{2Kx_{o3}}{L{x_{o1}}^2}\Delta x_2 - \left(\frac{R}{L} - \frac{2Kx_{o2}}{L{x_{o1}}^2}\right)\Delta x_3 + \frac{1}{L}\Delta u$$

20

The complete linearized state-space model in matrix notation, defining the output as

$$\Delta y = \Delta x_1$$

yields

$$\begin{pmatrix} \Delta\dot{x}_1 \\ \Delta\dot{x}_2 \\ \Delta\dot{x}_3 \end{pmatrix} = \begin{pmatrix} 0 & 1 & 0 \\ \frac{2Kx_{o3}^2}{m{x_{o1}}^3} & 0 & -\frac{2Kx_{o3}}{m{x_{o1}}^2} \\ \frac{4Kx_{o2}x_{o3}}{L{x_{o1}}^3} & \frac{2Kx_{o3}}{L{x_{o1}}^2} & -\frac{R}{L} + \frac{2Kx_{o2}}{L{x_{o1}}^2} \end{pmatrix} \begin{pmatrix} \Delta x_1 \\ \Delta x_2 \\ \Delta x_3 \end{pmatrix} + \begin{pmatrix} 0 \\ 0 \\ \frac{1}{L} \end{pmatrix} \Delta u$$

$$\Delta y = \begin{pmatrix} 1 & 0 & 0 \end{pmatrix} \begin{pmatrix} \Delta x_1 \\ \Delta x_2 \\ \Delta x_3 \end{pmatrix}$$

21

Now, the nominal operating point of the system can be deduced by considering the behavior of the system at an equilibrium point.

At an equilibrium point, and referring back to (16),

$$\left.\frac{dx_i}{dt}\right|_{x_1 = x_{o1}; x_2 = x_{o2}; x_3 = x_{o3}} \equiv 0 \qquad (i = 1, 2, 3).$$

Hence,

$$\frac{dx_{o1}}{dt} = x_{o2} = 0$$

$$\frac{dx_{o2}}{dt} = g - \frac{K}{m}\left(\frac{x_{o3}}{x_{o1}}\right)^2 = 0$$

$$\frac{dx_{o3}}{dt} = \frac{1}{L(y)}u - \left(\frac{R}{L(y)} - \frac{2K}{L(y)}\frac{x_{o2}}{x_{o1}^2}\right)x_{o3} = 0, \qquad (22)$$

which implies that, given an equilibrium position, x_{o1}, of the ball,

$$x_{o2} = 0 \;\; ; \;\; x_{o3} = \left(\sqrt{\frac{mg}{K}}\right)x_{o1}$$

By substituting $x_{o2} = 0$ into (21), a simplified linearized state-space model

$$\begin{pmatrix} \dot{x}_1 \\ \dot{x}_2 \\ \dot{x}_3 \end{pmatrix} = \begin{pmatrix} 0 & 1 & 0 \\ \frac{2KI^2}{my_o^3} & 0 & -\frac{2KI}{my_o^2} \\ 0 & 0 & -\frac{R}{L_c} \end{pmatrix}\begin{pmatrix} x_1 \\ x_2 \\ x_3 \end{pmatrix} + \begin{pmatrix} 0 \\ 0 \\ \frac{1}{L_c} \end{pmatrix}u$$

$$y = \begin{pmatrix} 1 & 0 & 0 \end{pmatrix}\begin{pmatrix} x_1 \\ x_2 \\ x_3 \end{pmatrix} \qquad (23)$$

results, where $I = x_{o3}$; $y_o = x_{o1}$.

Note that the incremental symbol, Δ, has been dropped in (23). While this makes the model appear more compact, however, it does not change the meaning and interpretation of the model. Also in the same equation, L has been assumed to be equivalent to L_c since $L_c >> L_o$, and, under a properly tuned compensator, $y = y_o$.

For system design, typical parameters values used are (Shahian and Hasul, 1993):

R = 31.1Ω; L_c = 0.109H; g = 9.81m/s^2; K = 0.0006590Nm^2/A^2;

m = 0.01058kg; I = 0.125A; y_0 = 0.01m;

The transfer function of the system can be determined from (23) as

3. Magnetic Levitation System Design and Simulation

$$\frac{Y(s)}{U(s)} = \frac{-1419.6}{s^3 + 283.50s^2 - 1946.5s - 551830}$$

(The MATLAB script for finding this transfer function is shown in the appendix.)

As can be seen from (24), this system is unstable—the Routh-Hurwitz stability criterion is clearly not met. Therefore, a compensating network is required to stabilize it. The overall block diagram of the system is shown in Fig. 4. Here G(s) is the gain (or transfer function) of the plant, $G_c(s)$ is the compensator gain, $G_s(s)$ is the gain of the sensor (156V/m) (Shahian and Hasul, 1993), $V_1(s)$ is the output voltage of the desired position transducer, $V_2(s)$ is the output voltage of the sensor, E(s) is the error signal, U(s) is the compensator output, and R(s) and Y(s) are the desired and actual positions of the maglev system, respectively.

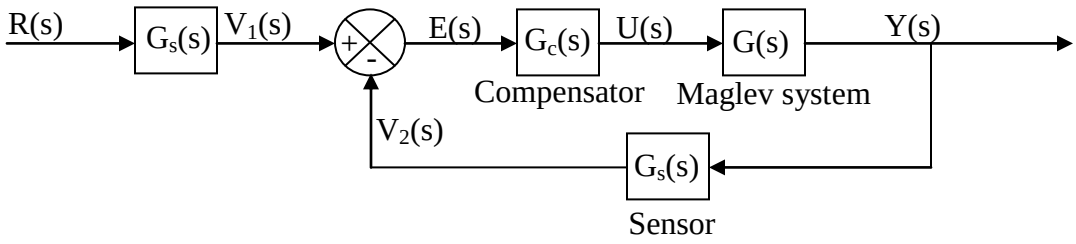

Fig. 4: Overall closed-loop representation of the maglev system

To verify whether simple gain adjustment will stabilize the system, a constant-gain compensator is used as shown in Fig. 5. The root locus for this situation is depicted in Fig. 6.

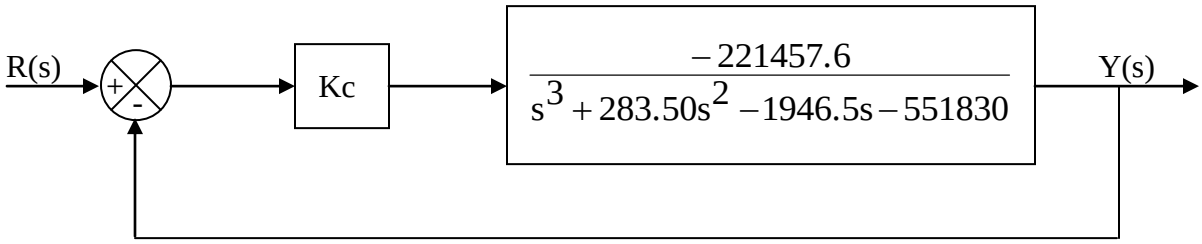

Fig. 5: Block diagram of a constant gain-compensated maglev system.

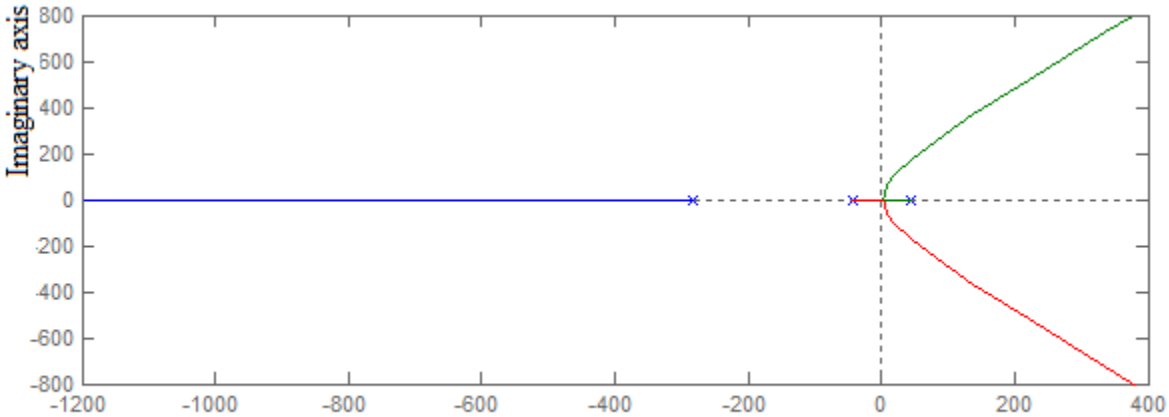

Fig. 6: The root locus of a constant gain-compensated maglev system

The root locus shows that no amount of increase in gain will result in system stability, as two of the system closed-loop poles always fall in the right-half s-plane. This is further supported by the Bode plot of the uncompensated system (shown in Fig. 7), which clearly reveals that for any value of the system gain, both the gain margin and the phase margin remain negative. (See the appendix for a MATLAB script to create these plots.) Therefore, the most important design challenge here reduces to that of stabilizing the magnetic levitation system.

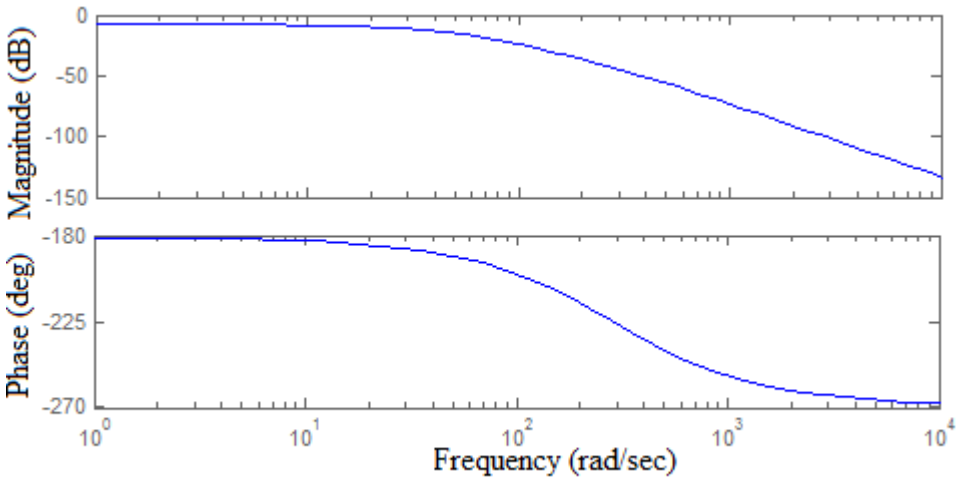

Fig. 7: The Bode plot of an uncompensated maglev system.

3.1 Root Locus Design

The maglev system can be stabilized if the uncompensated system root locus is reshaped such that a certain range of values of the system gain will make all the closed-loop poles fall in the right-half s-plane. And insightful leads from the locus show that this corrective reshaping can be effected if a zero or a combination of a zero and a pole is inserted at appropriate locations on the negative real-axis of this uncompensated root locus. This implies that a proportional-derivative (PD) or a phase-lead controller will be effective in stabilizing system. The design of these two compensators is considered here.

3.1.1 Proportional-Derivative Compensator

A general cascade proportional-derivative controller is described by the transfer function

$$G_C(s) = \frac{U(s)}{E(s)} = K_p + K_D s = K_p\left(1 + \frac{K_D}{K_p}s\right) \tag{25}$$

where K_p and K_D are the proportional and derivative constants of the controller, respectively.

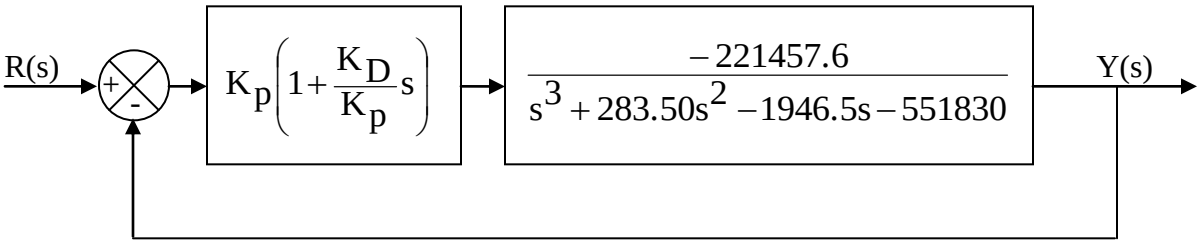

Fig. 8: Block diagram of a PD-compensated maglev system.

Combining this with the maglev system transfer function, as shown in Fig. 8, results in the open-loop transfer function

$$GH(s) = \frac{221457.6K_p\left(1+\frac{K_D}{K_p}s\right)}{s^3 + 283.50s^2 - 1946.5s - 551830} \quad 26$$

To determine the ranges of values of K_p and K_D that will ensure system stability, the popular Routh-Hurwitz criterion (Nise, 2007) is used. The analysis is shown in Table 1.

Table 1: The Routh array for PD-compensated system stability analysis

s^3	1	$221457.6K_D - 1946.5$	0
s^2	283.50	$221457.6Kp - 551830$	0
s^1	$\frac{283.50(221457.6K_D - 1946.5) - (221457.6K_p - 551830)}{283.50}$	0	0
s^0	$221457.6Kp - 551830$		

From this table, the system is stable if the condition

$$K_p > 2.4918; K_p/K_D < 283.50 \quad 27$$

is met. The information given in (27) is used to generate root loci for the system in (26) in order to obtain an appropriate combination of values of K_p and K_D that guarantees stability and gives good response. This is carried out by sweeping through various values for the ratio K_P/K_D and determining proper corresponding values for K_p. The resulting loci are displayed in Fig. 8.

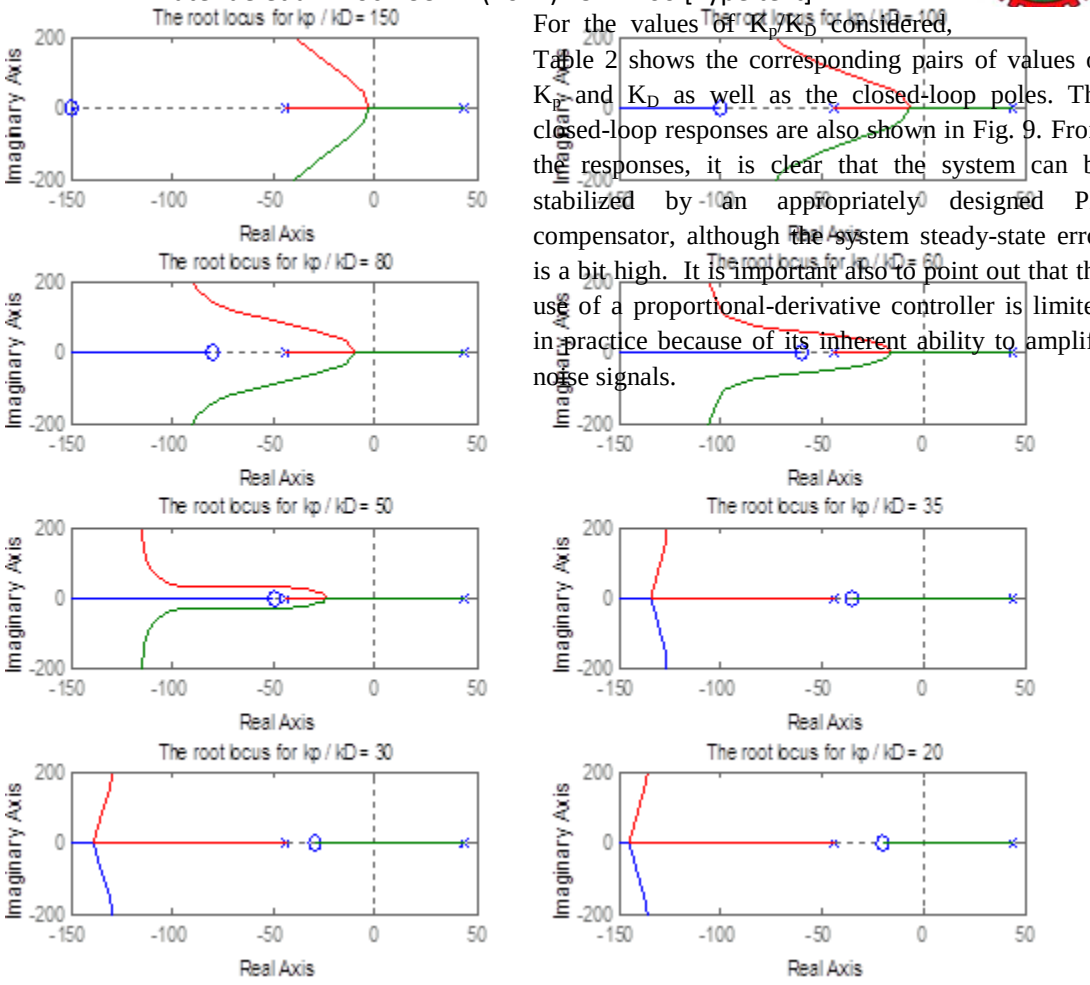

Fig. 8: Root loci for the pd-compensated maglev system for various values of Kp/KD.

For the values of K_P/K_D considered, Table 2 shows the corresponding pairs of values of K_P and K_D as well as the closed-loop poles. The closed-loop responses are also shown in Fig. 9. From the responses, it is clear that the system can be stabilized by an appropriately designed PD compensator, although the system steady-state error is a bit high. It is important also to point out that the use of a proportional-derivative controller is limited in practice because of its inherent ability to amplify noise signals.

Table 2: Selected pairs of values of K_p and K_D and corresponding closed-loop poles

K_p/K_D	K_p	K_D	Pole s_1	Poles s_1, s_2
150	22.2	0.1480	-231.74	-25.88+134.77j, -25.88-134.77j
100	16.8	0.1680	-185.51	-48.99+121.16j, -48.99-121.16j
80	14.3	0.1788	-148.64	-67.43+114.22j, -67.43-114.22j
60	8.66	0.1443	-137.38	-73.06+67.86j, -73.06-67.86j
50	5.85	0.1170	-166.28	-58.61+32.21j, -58.61-32.21j
35	10	0.2857	-31.09	-126.20+193.78j, -126.20-193.78j
30	13.1	0.4367	-26.73	-128.39+267.23j, -128.39-267.23j
20	9.14	0.4570	-15.48	-134.01+277.76j, -134.01-277.76j

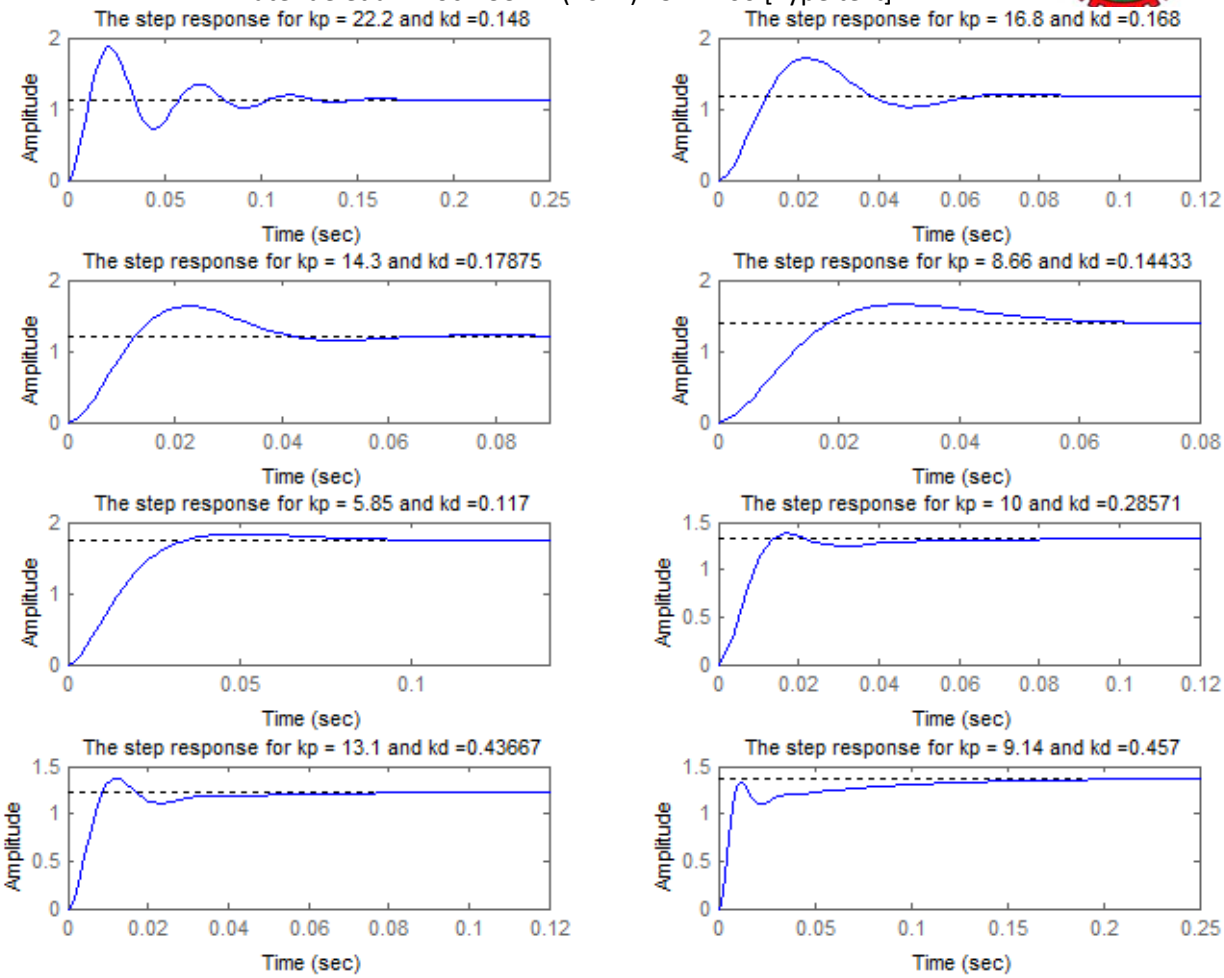

Fig. 9: Closed-loop responses for the pd-compensated maglev system.

3.1.2 Phase-Lead Compensator

As can be seen from the uncompensated maglev system root locus, a pair of a zero (located between s = 0 and s = - 44.1190) and a pole (located elsewhere in the right-half s-plane, but farther away to the left of the zero) can be used to augment the uncompensated open-loop transfer function of the maglev system in order to stabilize it. This gives rise to a phase-lead compensator. And a typical representation of a phase-lead compensator is given by

$$G_C(s) = K_C \frac{s+a}{s+b}; \quad a < b \qquad (28)$$

where K_c, a, and b are the compensator gain, zero, and pole, respectively.

If (28) is used to compensate the maglev system, the resulting open-loop transfer function becomes

$$GH(s) = \frac{221457.6K_C(s+a)}{(s+b)(s^3+283.50s^2-1946.5s-551830)} \qquad (29)$$

The root-contour approach can be employed to find the appropriate values of K_c, a, and b, or since an

approximate range of values of 'b' is known, and the value of 'a' can be deduced based on the reasoning that the farther 'a' is from the imaginary axis (but not too close to the system open-loop pole at s = -44.1190) the better the stability, then the compensator parameters can be determined from root loci generated for varying values of K_c. The latter approach is used here.

Fig. 10 shows root loci for values of b between 44.119 and 490, and a = 35. From this figure, it is apparent that the greater the value of 'b' the farther to the left the branches of the locus between s = -44.119 and s = -283.50 (or -b) are. And for a typical pair of a = 35 and b = 290, the range of values of K_c that guarantees system stability is $24 < K_c < 212$. For these values of a and b, and a selected set of values of K_c, the closed-loop poles are given in Table 3 while the closed-loop responses are displayed in Fig. 11.

Table 3: Selected values of K_c and the corresponding closed-loop poles for a = 35; b=290

K_c	Poles s_1, s_2, s_3, s_4			
30	-408.98;	-71.17 -68.99j;	-71.17 +68.99j;	-22.17
40	-425.34;	-59.37 - 101.15j;	-59.37 +101.15j	-29.42
50	-439.38;	-50.98 -124.34j;	-50.98 +124.34j;	-32.16
60	-451.79;	-44.09 -142.77j;	-44.09 +142.77j;	-33.53
70	-463.00;	-38.08 - 158.24j;	-38.08 +158.24j;	-34.35
80	-473.25;	-32.68 - 171.69j;	-32.68 +171.69j;	-34.89
90	-482.74;	-27.74 - 183.65j;	-27.74 +183.65j;	-35.27
100	-491.59;	-23.17 -194.47j;	-23.17 +194.47j;	-35.56
120	-507.77;	-14.89 - 213.54j;	-14.89 +213.54j;	-35.95
130	-515.23;	-11.09 - 222.09j;	-11.09 +222.09j;	-36.10

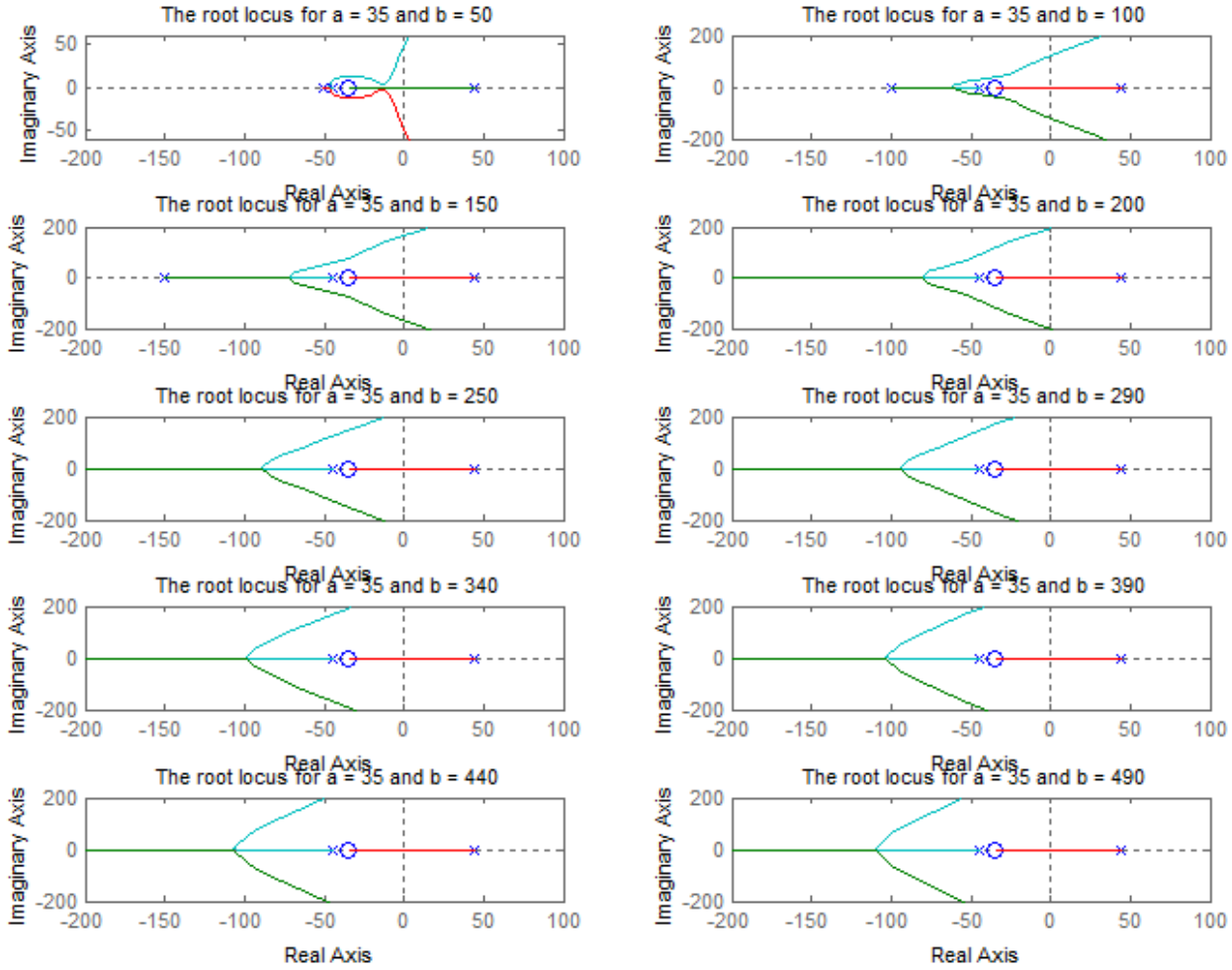

Fig. 10: Root loci for a = 35, and various values of b.

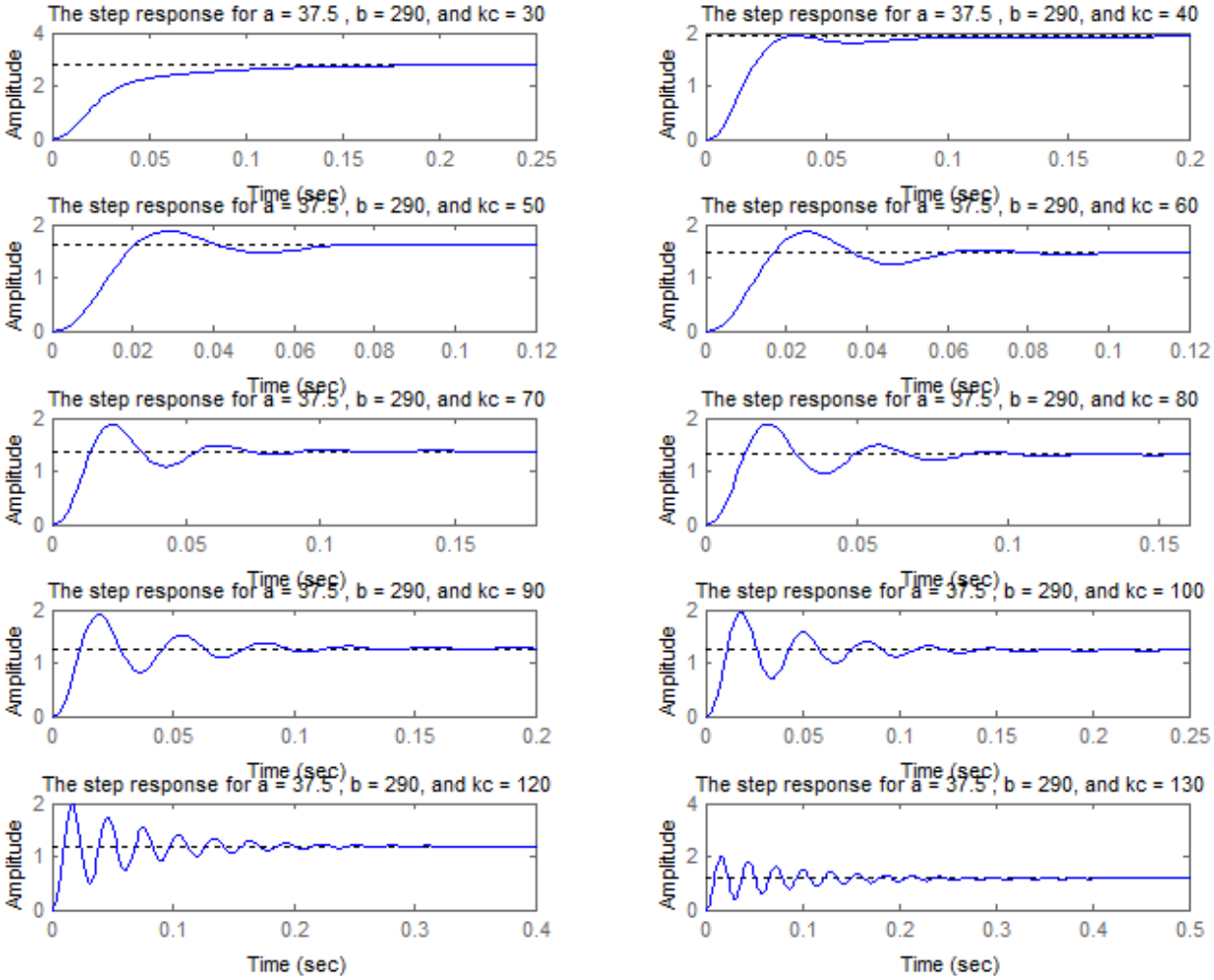

Fig. 11: Closed-loop step responses for a phase lead compensated maglev system.

4. Conclusion

Stabilization of a magnetic levitation system has been the focus of this paper. Although the system is an unstable nonlinear one, it is clear that a linear compensator can be designed to stabilize it if its operation is limited to a small range. We develop a complete nonlinear model of the system, and then form an approximate linearized equivalent from it. Based on this linearized model, we consider two linear compensators—proportional-derivative and phase lead—and show that the magnetic levitation system can be stabilized by an appropriate selection of the parameters of the compensators using a classical design approach aided by a computer software tool. We compute and present the closed-loop poles of each design and the corresponding step responses, and also show the system stability limits. This approach proves quite useful and effective, as several simulation runs can be performed quickly to expedite the design. However, for a large-range operation, a more robust controller will be required to effectively bring the system into a region of stability. And for this latter type of controllers, several strategies have been employed and are available in the literature, while the maglev system continues to attract more research attention.

Appendix

The various MATLAB scripts used in this tutorial are highlighted below.

A. Computation of the maglev system transfer function

```
% This script computes the
transfer function of a maglev
system using
% Y/U=C((SI-A)^-1)B.
syms s
% Define the parameters of the
model.
R = 31.1; Lc = 0.1097; g = 9.81; K
= 0.00065906;m = 0.01058;I =
0.125;
y0 = 0.01;
% Compute the values of A, B, and
C.
A=[0 1 0;(2*K*I^2)/(m*y0^3) 0 -
(2*K*I)/(m*y0^2);0 0 -R/Lc];B=[0 0
1/Lc]';
C=[1 0 0];
% Find the transfer function, Y/U.
id=eye(3,3);
disp('The transfer function is:')
Tfunction=C*(inv(s*id-A))*B
% Find the simplified transfer
function, Y/U.
[numTfunc,denTfunc]=numden(Tfuncti
on);numTfunc=sym2poly(numTfunc);
denTfunc=sym2poly(denTfunc);numTfu
nction=numTfunc/denTfunc(1);
denTfunction=denTfunc/denTfunc(1);
disp('While the simplified
transfer function is now')
tf(numTfunction,denTfunction)
```

B. The Root locus and bode plots of the uncompensated maglev system

```
% This script plots the root locus
and the bode diagram of the maglev
% system when compensated by a
constant gain.
fnum=1419.6*156;fden=[1 283.50 -
1946.55 -551830];
sys1=tf(fnum,fden);
figure(1)
rlocus(sys1)
figure(2)
bode(sys1)
```

C. The root loci for simulating the pd-compensated maglev system

```
% Script for simulating the root
locus-based pd-compensated design
kp_kd=[150 100 80 60 50 35 30 20];
L=length(kp_kd);
sysden=[1 283.50 -1946.5 -551830];
i=1;
while(i<=L)
    f=kp_kd(i);
    sysnum=221457.6*[0 0 1/f 1];
    subplot(4,2,i)
    rlocus(sysnum, sysden)
    str=['The root locus for kp /
kD = ' num2str(f)];
    title(str)
    axis([-150 50 -200 200]);
    i=i+1;
end
```

D. Closed-loop poles and step responses of the pd-compensated maglev system

```
% Script for generating the
closed-loop poles as well as the
responses of
% the pd-compensated maglev
system.
kp_kd=[150 100 80 60 50 35 30 20];
kp=[22.2 16.8 14.3 8.66 5.85 10
13.1 9.14];
kd=kp./kp_kd;
L=length(kp_kd);
sysden=[1 283.50 -1946.5 -551830];
sys2=1;syspoles=zeros(8,3);
i=1;
while(i<=L)
    f1=kp_kd(i);f2=kp(i);
    sysnum=f2*221457.6*[0 0 1/f1
1];
    sys1=tf(sysnum,sysden);
    sysfun=feedback(sys1,sys2);
    syspole=eig(ss(sysfun))';
    syspoles(i,1:3)=syspole;
    subplot(4,2,i)
    step(sysfun)
    str=['The step response for kp
= ' num2str(f2) ' and kd ='...
    num2str(f1)];
    title(str)
    i=i+1;
end
disp('The closed-loop poles are:')
syspoles;
```

E. The root loci for simulating the phase lead-compensated maglev system

```
% Script for simulating the root
locus-based phase lead-compensated
design.
a=35;
sysnum=221457.6*[0 0 0 1 a];
sysden1=[1 283.50 -1946.5 -
551830];
b=[50 100 150 200 250 290 340 390
440 490];
Lb=length(b);
i=1;clf;
while(i<=Lb)
```

```
    f1=b(i);
    sysden=conv([1 f1],sysden1);
    figure(3)
    subplot(5,2,i)
    rlocus(sysnum, sysden)
    str=['The root locus for a = '
num2str(a) ' and b = '
num2str(f1)];
    title(str)
    axis([-200 100 -200 200])
    i=i+1;
end
```

F. Closed-loop poles and step responses of the phase lead-compensated maglev system

```
% Script for generating the
closed-loop poles as well as the
responses of
% the pase lead-compensated maglev
system when b = 290.
a=37.5;
b=290;
kc=[30 40 50 60 70 80 90 100 120
130];
L=length(kc);
sys2=1;syspoles=zeros(10,4);
i=1;
while(i<=L)
    f1=kc(i);
    sysnum=f1*221457.6*[0 0 0 1
a];
    sysden=conv([1 b],[1 283.50 -
1946.5 -551830]);
    sys1=tf(sysnum,sysden);
    sysfun=feedback(sys1,sys2);
    syspole=eig(ss(sysfun))';
    syspoles(i,1:4)=syspole;
    figure(5)
    subplot(5,2,i)
    step(sysfun)
    str=['The step response for a
= ' num2str(a)' , b = '
num2str(b)',...
    and kc = ' num2str(f1)];
    title(str)
    i=i+1;
end
disp('The closed-loop poles are:')
syspoles
```

References

Al-Muthairi N. F., and Zribi M., "Sliding mode control of a magnetic levitation system," Mathematical Problems in Engineering 2004, vol. 2, 2004, pp. 93-107.

Feedback Instrument Limited, Magnetic levitation system—getting started, http://www.fdb.com, 18th September, 2012.

Franklin G.F., Powell J.D., and Workman M., Digital Control of Dynamic Systems, Addison Wesley Longman, Inc., 1998, pg. 273.

Green S.A., Hirsch R.S., and Craig K.C., "Magnetic levitation device as teaching aid for mechatronics at Rensselaer," Proc. ASME Dynamic Systems and Control Division, vol. 57-2, 1995, pp. 1047–1052.

Kuo B. C., and Golnaraghi F., Automatic Control Systems, John Wiley & Sons (Asia) Pte. Ltd., 2003, pp. 110-111.

Naumivic M. B., Veselic B. R., "Magnetic levitation system in control engineering education," Automatic Control and Robotics, vol. 7, no.1, 2008, pp. 151-160.

Nise N. S., Control Systems Engineering, Wiley India (P.) Ltd., Delhi, Third Reprint, 2007, pp. 329-352.

Shahian B., and Hassul M., Control System Design Using MATLAB. Englewood Cliffs: Prentice Hall, 1993, pp. 455–465.

Morphology and Properties of Zn-Al-TiO_2 Composite on Mild Steel

O.S.I Fayomi[1, 2*] A.P.I Popoola[1] C.A Loto[2] and O.M Popoola[1],
[1]Faculty of Engineering and the Built Environment, Tshwane University of Technology, Private Bag X680, Pretoria 0001, South Africa.
[2]College of Science and Technology, Covenant University, P.M.B 1023, Ota, Ogun State
*E-mail: ojosundayfayomi3@gmail.com, popoolaapi@tut.ac.za.

Abstract

The influence of TiO_2 composite and dispersed pure Al particle on zinc alloy electrodeposited on mild steel was studied from chloride bath solution.Microstructural and mechanical properties of the alloy were investigated. The structure, surface morphology, and surface topography of the deposited alloys were characterized by scanning electron microscopy (SEM) and atomic force microscope (AFM).In addition, hardness of the coated alloys was measured. It was found that the obtained Zn-Al-TiO_2 alloyexhibited more preferred surface morphology and mechanical strength compared tothe substrate. The result shows the existence of interaction between TiO_2 compounds and zinc alloy particulate. It also exhibited well bright dominate zinc coating on steel surface.

Keywords: *Morphology, Additive, TiO_2, Atomic force microscopy (AFM).*

1. Introduction

Deposited zinc coating is widely used method considered for corrosion resistance of steel [Shivakumara et al., 2009, Popoola et al., 2012]. However, the corrosion prevention and hardness properties are minimal compare to the huge expectation. Efforts have been directed toward improving the properties of zinc electrodeposition with other metal such as cadmium and nickel. Hence, some alloy formation such as Zn-Cd, Zn-Ni and Zn-Fe have gained successful access to the zinc industries as direct replacement for ordinary zinc coating [Praveen and Venkatesha, 2011, Popoola et al., 2012 and Basavanna and arthoba, 2009]

Recently focus is now shifting toward possessing a better hardness material and preferred corrosion resistance properties through the use of composite material [Rahman et al., 2009, Volinsky et al., 2001 and Fayomi et al., 2011]. In this paper Zn-Al-TiO_2 deposition on steel was prepared. The solution contains zinc, aluminum salt with TiO_2dispersed within the bath formation. The investigation also examined the mechanical property of composite.

2. Experimental

The deposition of Zn-Al-TiO_2 alloy was performed in an electrochemical cell of two electrodes in which mild steel (50mm x 25mm x 1mm) sheet was used as substrate and zinc sheets of mild steel size were used as anodes. Before electro-deposition thesubstrate was polished with successively finer grades of emery paper, cleaned with Na_2CO_3solution, pickled and activatedin 10% HCl solution at room temperature for 15 seconds and immediately followed by rinsing in distilled water. The working electrodes were connected to the rectifier. The baths were prepared by dissolving amounts of 150g/l ZnO, 35g/l Al, 9g/l TiO_2, 100g/l KCl and 10g/l H_3BO_3. Deposition was carried out at constant potential of 0.3Vat 0.8A/cm^2 with the bath pH of 4.5. All the depositions were performed in 20 minutes.
Surface morphology of the Zn-Al-TiO_2coatingwas investigated using Scanning Electron Microscope (SEM) and Atomic force microscope(AFM). Microhardness (VHN) of the coatings deposited was measured by using a Dura scanmicrohardness tester under an application of 100 g load.

3. Results and Discussion

Substrate Characterization

Chemical composition of mild steel substrate can be seen in Table1. The SEM spectrum in Figure 1 shows the morphology of mild steel. EDSanalysis established the essential elemental composition with Fe being the major constituent.

Table 1:Chemical composition of as-received mild steel

Elements	Composition (wt%)
Carbon	0.150
Silicon	0.180
Sulphur	0.031
Phosphorus	0.010
Iron	Balance

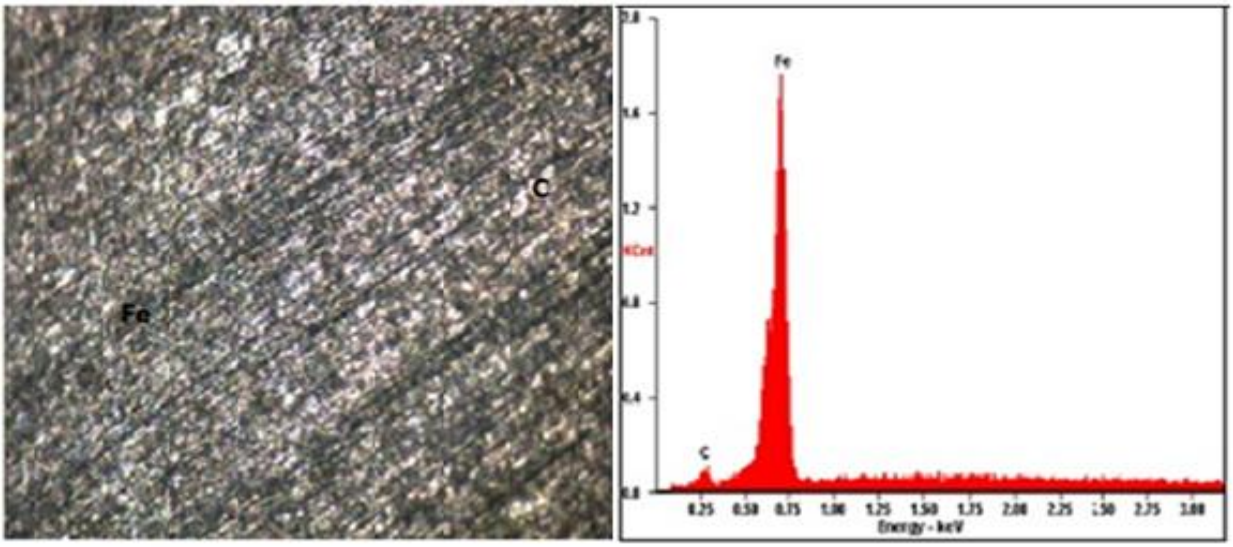

Figure 1:SEM/EDS spectra of as-received mild steel

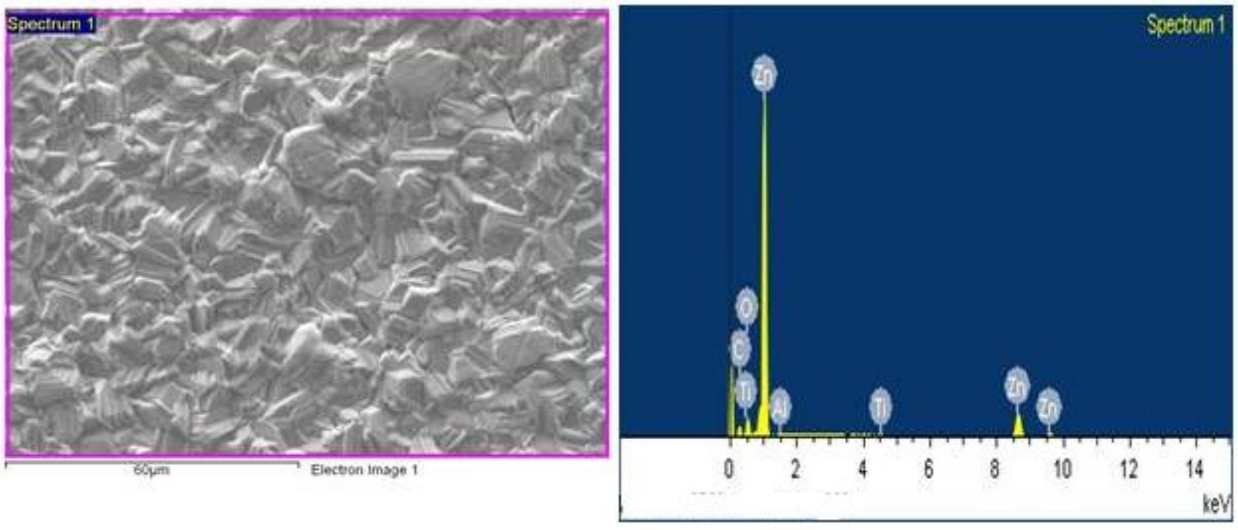

Figure 2.SEM/EDS spectra Zn-Al-TiO_2

SEM photomicrograph studies

Scanning electron microscope SEM, combined with energy dispersive spectroscopy, EDS, was used to investigate the surface morphology of the deposited coating. SEM photomicrograph of the deposited obtained from the ternary bath shows more finely grained and homogeneous surface appearance compare to the previous studies by (Fayomi et al., 2011) which has some porous and nonhomogeneous composition.

It is ideal to say that the porous free nature of the coating and the visible smaller grain size as seen in (Fig 2) is a direct influence of the composite which lead to the change in the structural modification and the tendency of crystal growth. The change in morphology and

the nature of crystal formation can be linked to a blocking influence of the titanium additive particulate which leads to an increased nuclei resulting into rapid nucleation surface formation, perfect crystal growth, and refinement in crystal size, bright deposit and arrangement of crystals.

AFM Studies

Scanning studies performed using AFM in Figure 3 also review the surface topography and the adhesion behavior of the coatings. In general, there are degrees of topography from the Zn-Al-TiO_2imaging indicating a homogeneous coating diffusion and perfect preferential sites.

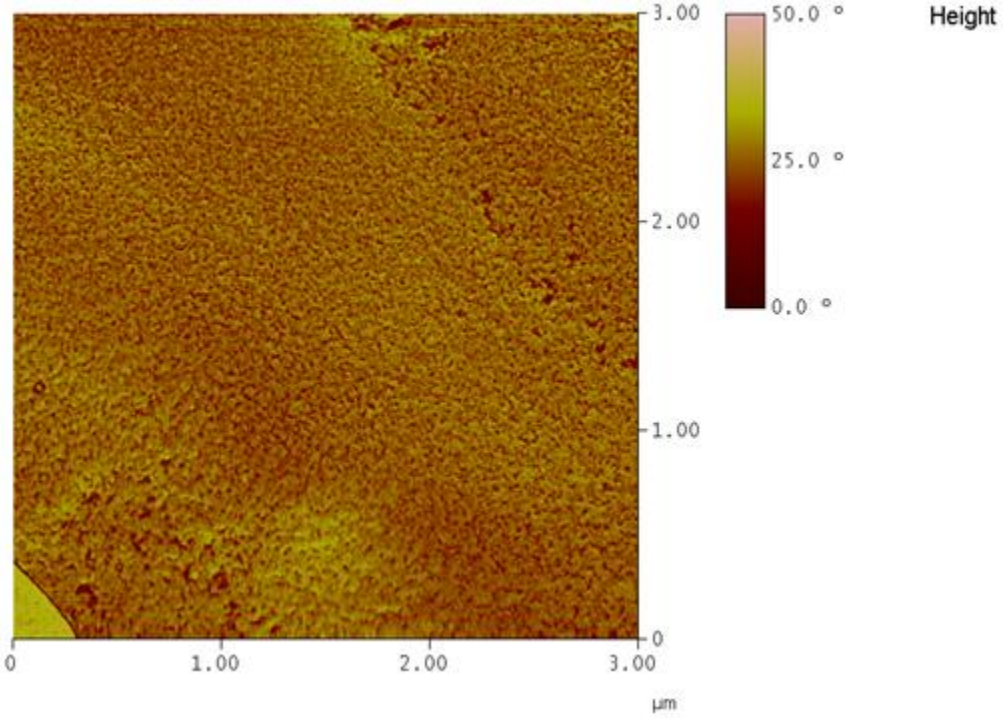

Figure 3: AFM Photograph of electrodeposited Zn-Al-TiO_2

The additive has a noticeable influence on the surface morphological topography of the coated sample with fine crystals around the surface which possesses fine grain size and good surface morphologies. Moreso, it has been reported that addition of composite to a bath resulted in microstructural changes leading to formation of complex intermetallic compounds [Praven and Venkatesha, 2011].

Microhardness Studies:

The microhardness value of Zn-Al-$TiO_2$and the substrate were measured. Figure 4 shows the influence of co-deposition of Zn-Al-$TiO_2$and the operating parameter on the hardness properties. Microhardness value for the coated sample and the substrate were 152 and 61 HVN, respectively.

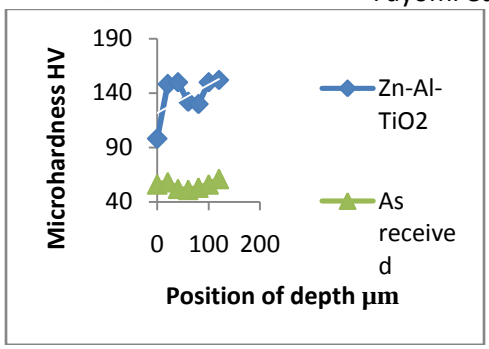

Figure 4.The microhardness/depth profile for mild steel and Zn-Al-TiO_2 coatings

This shows that a better grain size formation on the surface of the coated substrate occurs. It is obvious that there is resistance to dislocation as a result of the resultant bath formation matrix and the refinement of the grain size. Hence, the effect of Al andTiO_2can be said to significantly influence the tendency of highermicrohardness value which is in accordance to investigation by [Shivakumara et al, 2007Sundararaja et al., 2003, Rahman et al., 2009and Popoola et al., 2012]that fine-grained structure of the deposit or alloys and the dispersed particles in the fine-grained matrix may obstruct the easy movement of dislocations, to give a higher hardness value of deposited sample.Furthermore, it can also be noted by [Popoola et al., 2012] thatthe hardenability of the coating is determined to a large extent by the additive and the process parameter employed.

4. Conclusions

- A successful ternary co-deposition was achieved.
- Surface modification through the influence of Al andTiO_2 deposition has significantly enhanced surface adhesion property and improved the stability of mild steel.
- The hardness value increased 100% over the mild steel

Acknowledgments

This material is based upon work supported financially by the National Research Foundation (NRF) and Technology Innovation Agency (TIA), Pretoria, Republic of South Africa.

References

1. Basavanna,S. andArthobaNaik,Y. *J. of Appl. Electrochem*., 39 (2009) 1975
2. Fayomi,O.S. Tau,V.R. Popoola,A.P.I. Durodola,B.M. Ajayi,O.O. Loto,C.A. andInegbenebor,O.A. *J. of Mat. andEnv. Sci.,* 3, (2011) 271
3. Popoola,A.P.IFayomi,O.S. andPopoola,O.M *Int. J. of Electrochem. Sci.*, 6, (2012) 4860
4. Praveen,M and Venkatesha,T.V. *Int J. of Electrochem*, 261, (2011) 407
5. Popoola,A.P.IFayomi,O.S. andPopoola,O.M.*Int. J. of Electrochem. Sci.*, 6, (2012)4898
6. Rahman,M.J. Sen,S.R. Moniruzzaman,M. andShorowordi,K.M. *J. of Mech. Eng, Tran.*, 40, (2009) 9.
7. Shivakumara,S. Manohar,U. ArthobaNaik,Y. andVenkatesha,T. U. *Bull. Mat. Sci.* 30 (2007) 455
8. Sundararajan,G. andRama Krishna,L. *Surf. and Coat. Tech*, 167, (2003) 269.
9. Volinsky,A.A. Vella,J. Adhihetty,I.S. Sarihan,V.L. Mercado,L. Yeung,B.H. andGerberich,W.W. 2001. *Mat. Res. Soc.,* 649, 1-6

Oyebanji et al: Proc. ICCEM (2012) 211 - 223

Performance evaluation of two palm kernel nut cracker machines

Oyebanji J.A[*1], Oyedepo, S.O [1]and Adekeye, T[1]

[1]Department of Mechanical Engineering, Covenant University, Ota Nigeria

Correspondence: joseph.oyebanji@covenantuniversity.edu.ng

Abstract

In this study performance evaluation of centrifugal impact approach and vertical palm kernel nut cracker machine was carried out. The results of the study show that the vertical centrifugal palm kernel cracker is more efficient than the centrifugal impact approach palm kernel cracker. The efficiency of Vertical centrifugal palm kernel cracker is 71.3% and that of centrifugal impact approach is 50.38%. Apart from this, the vertical centrifugal machine though has low speed but it produces clean and neat nut cracked output.

Key words: *Palm nut, centrifugal nut cracker, vertical nut cracker machine, performance evaluation, racking efficiency, kernel breakage.*

1. Introduction

Palm kernel industry had remained very popular in third world because of the dependency of many companies on palm kernel oil as raw material, which is quite inadequate (Hartley, 1987). Nigeria is one of the world largest exporters of palm kernel product in early sixties, providing about 400,000 metric tons amounting to 65% of the world trade. Nigeria palm kernel nut export reduced drastically within seventies, from 65 to 15% when there was an oil boom (Ndegwe, 1987). Based on high dependent of many companies like soap, vegetable oil and body cream industries on palm kernel oil, an efficient palm kernel-processing machine is therefore not only necessary but also important to revitalize the production of palm kernel in other to meet up with ever increases industrial demand (Oke, 2007).

The processing of the palm kernels into palm kernel oil involves the cracking of the palm nut, separation of the shells from the kernels, washing, cleaning, kernel milling and kernel oil extraction. The separation of the kernels from the shells is a very difficult process and an issue which continues to be of great importance within the industry (Akubuo and Eje, 2002). Cracking palm nuts to release the kernels is a critical step that affects the quality of kernel oil. There are two widely methods commonly used for these processes: Manual (traditional) method and Mechanical method.

The manual method of palm nut processing is the traditional way of cracking and separating palm kernel. It is a method in which nuts are cracked using stone and kernel separated by hand picking from the shell at the same time. This method is labour intensive, time consuming, cumbersome and very slow to meet the demand of growing industry (Oke, 2007). Preserving the kernel embedded in the palm nut when cracking the nutshell is important in the subsequent palm kernel and shell separation and, in enhancing the quality of the palm kernel oil.

There are two basic mechanical methods that can be used to crack the shell of the nut. The shock caused by an impact against a hard object and the application of direct mechanical pressure to crush, cut or shear through the shell. Palm nut cracking machine are developed on the principle of hurling of the palm nuts at a fairly high speed against stationery hard surface (Okoli, 1997). Generally, two types of nutcrackers are used in palm oil mill; roller crackers and centrifugal impact crackers. In rollers cracker the nuts are cracked in between two fluted rollers revolving in opposite directions. The clearance between the rollers is invariable but the nuts are of different sizes, which make the machine to be operating at reduced efficiency. The other cracker is a centrifugal impact cracker that used principle of centrifugal force to flap the palm kernel nuts on the stationary hard surface. This method involves using a shock

caused by an impact against hard objects to shear, crush or cut through the shell.

Currently, locally manufactured centrifugal nutcrackers are used for the cracking step in the oil-mill in Nigeria. Although, this has high productivity, the process has quite a number of deficiencies which include; breaking of kernels in the course of cracking which may be due to insufficient drying of nut as well as high rotor speed. Inappropriate spacing of the impactors (blow bars) may also result in a number of uncracked nuts in the finished product as well as the feeding rate of the nut into the cracking chamber (Ofei, 2007). Kernel breakage also results partly because the kernel upon release from the nutshell rebound in the cracking chamber and is subjected to secondary impacts which induce breakage. Also the interaction between the adjacent nuts may obstruct the direct impingement of the individual nut to the cracking wall, so that some of the nuts are discharged uncracked (Koya, 2006). The level of Free Fatty Acids (FFA) is higher in broken kernels than in whole kernels, therefore breakage of kernels should be kept as low as possible according to Poku (2002).

Every unit operation in farm has specific objective and this calls for special machines. Attempts have been made worldwide to develop perfect machines for each operation. Unfortunately there is a widening gap between the developed world and developing world. This low performance of locally fabricated machines were compared with the foreign ones could be as a result of adoption impossibility of modern techniques and the high cost of machines involved (Kaul and Egbo 1985). Having critically examined this complicated problem, we acknowledge the needs to embark on comparison and performance evaluation of two existing indigenous palm kernel nut cracking machines to know the best of the machines for adequate agricultural yields at affordable price and one that gives better efficiency. These machines are electrically powered, parts are mechanically fabricated and assembled together to allow for necessary relative motion, feeding process, discharge operation as well as ease of maintenance. Electric motor is required to drive the cracker.

Having discussed the problems associated with local means of cracking palm kernels, this study aims at the followings: (i) to test and ascertain the performance of existing palm kernel cracking machines using common palm kernel species for the machines, (ii) to compare the efficiency of each palm kernel nut-cracking machines and which is to be adopted by farmers for easy operation, high maintainability and optional output and (iii) to know the time taken to crack a measured amount of palm kernel nut.

2. Materials and Method

2.1 D*esign consideration and material selection for the two palm kernel cracker machines*

2.1.1 Design of the Machine

In the design of a palm kernel cracker the following factors affect its design, material selection and manufacture (Badmus, 1990).

a. Velocity of the palm kernel nuts towards the hard wall.
b. Rotor speed
c. Varieties of the palm kernel nut (size, weight etc)
d. Clearance between the rotor and the cracking wall
e. Feed rate of the palm kernel nut.

In the existing cracking machine the different sizes of nut were not put into consideration experiments were carried out to determine the average size ,average mass ,Velocity require to crack the kernel nut and the average volume of the kernel nut to aid design and fabrication of the machine.

2.1.2 Mass of the Kernel Nut

Samples of palm kernel nuts were collected from various Ondo State, Nigeria. The nut's nominal diameter was measured using a venire caliper; the mass of each nut was measured using an electronic weighing balance.

Table1: Mass and diameter of palm kernel samples

S/NO	MASS (KG)	DIAMETER (M)
1.	0.0035	0.0135
2.	0.0028	0.0200
3.	0.0030	0.0200
4.	0.0038	0.0145
5.	0.0031	0.0145
6.	0.0037	0.0123
7.	0.0035	0.0130
8.	0.0036	0.0134

9.	0.0039	0.0135
10.	0.0040	0.0141

Cracking was done manually by placing each not at the center of a rig base. The rig consists of a 1.5kg weight (15N) that was moved along a wooden vertical scale. The weight was raised to a pre-determined height by means of a rope attached to it.

2.1.3 Determination of velocity required to crack a palm kernel nut

A rig apparatus was set up where a kernel nut was placed on a hand steel plate. The kernel nut was gently loaded with weights. It was observed that over 200N was not able to crack the nut.

A different method was then adopted, basing it on the Conservation of Energy Theory which states that energy is neither created nor destroyed but can be transformed from one form to another in this method, a small pre-determined height was placed between the kernel and the weight. It was observed that as little as 10N was able to crack the kernel nut satisfactorily. Different weights were tried, but by the time the weights reached 20N they started smashing up the kernels which was unacceptable.

The experiment employed analysis of potential and centrifugal force models. The potential energy model postulates that the kernel absorbs the potential energy of a falling hammer or weight (M) due to the height (h-d) through which it falls, making the nuts kinetic energy to be equal to the potential energy of the falling weight. While the centrifugal energy model postulates that, it is the force with which the nut is thrown that will aid its cracking and also the distance between the rotor and cracking.

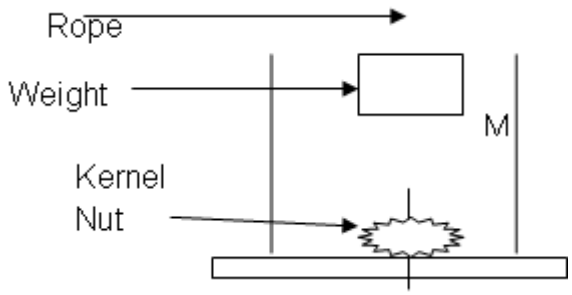

Figure 1: Determination of force to crack kernel nut

The mathematical Expression used is

P.E. = Mgh

= Mg(h-d) 1

Force = Work done W

F =Ma =Mwv=Mv(v/r)X 2

Where

P.E. = Potential energy (Joules)

W = Work done on kernel nut (Joules)

X = Distance between rotor and cracking wall (meter)

M = Mass of weight (kilogram)

m = Mass of kernel nut (kilogram)

h = Height between weight and base plate (meter)

d = Diameter of kernel (meter)

g = Acceleration due to gravity ($m/5^2$)

f = Velocity of the nut (M/S)

$$V = \frac{[Mgr(h-d)]^{½}}{(Mx)^{½}} \quad 3$$

Table 2: Parameter to determine velocity required to crack palm kernel nut

S/NO	MASS (M) (KG)	DIAMETER (D)	h-d(M)	Mx (M)	√Mgr(h-d)/mx(m/s)
1.	0.0035	0.0136	0.1365	0.00070	0.4841
2.	0.0028	0.0200	0.1481	0.00056	0.5042
3.	0.0030	0.0200	0.1300	0.00060	0.4727
4.	0.0038	0.0145	0.1358	0.00076	0.4828
5.	0.0031	0.0134	0.1366	0.00062	0.4843
6.	0.0037	0.0123	0.1377	0.00074	0.4862
7.	0.0035	0.0130	0.1370	0.00070	0.4717
8.	0.0036	0.0134	0.2366	0.00072	0.6378
9.	0.0039	0.0135	0.1365	0.00078	0.4841
10.	0.0040	0.0141	0.1359	0.00080	0.4830
TOTAL	0.0349	0.01478	1.6938	0.00698	4.9909

Using the data above velocity for each mass of kernel nut is obtained.

Velocity (V) = V/10 = 4.9909/10 = 0.4991 m/s

Mass (M) = M/10= 0.0349/10 = 0.00349 kg

Diameter (d)= D/10 =0.1478/10 = 0.01478m

2.1.4 Determination of average volume of a kernel nut

The volume of a dried palm kernel nut displaced using up-thrush method was investigated. The beaker was filled with water and reduced to an exact level; a kernel nut was then dropped into the beaker of water. The kernel nut displaces a particular volume of the water equal to its own volume. This volume was read directly from the graduate scale. The original volume of the water was then subtracted from the water volume after immersion to determine the volume of the kernel nut. The experiment was repeated for other kernel nut of different size and shapes.

The results of measurement of palm kernel volume are shown in the Table 3.

Table 3: Data to show Volume of average kernel nut

s/n	1	2	3	4	5	6	7
Volume of nut (ml)	10.0	5.0	6.9	8.6	4.0	6.2	4.5

Volume of kernel used =6.4 ml

1ml=1/10 x m^3

:. Volume=6.45/10^6 = 6.45 X $10^{-6}M^3$

2.2 Design Calculation of Centrifugal Impact Approach Cracker

2.2.1 Determination of the Force Required for Cracking the Nut and the Horse Power Rating of the Required Electric Motor

From the equation $V = \frac{wr}{4}$

$W = \frac{v/r}{5}$

Force $F = mw^2r$ 6

Where M = Mass of kernel

Power $P = FV$ 7

Horse power (hp) = 0.0015hp

2.2.2 Estimation of Time Taken to Crack Measured Mass (Kg) of Kernel Nut.

According to Newton's law of motion: impulse produces changes in motion and is equal to change in momentum

Ft = MV 8a

For 1kg 2.07sec. → 0.0349kg

T → 1kg

t = MV/F 8b

t=13.2 sec.

2.2.3 Estimation of Volume of Hopper for Kernel Nuts.

The geometrical shape of the hopper to be used is shown below

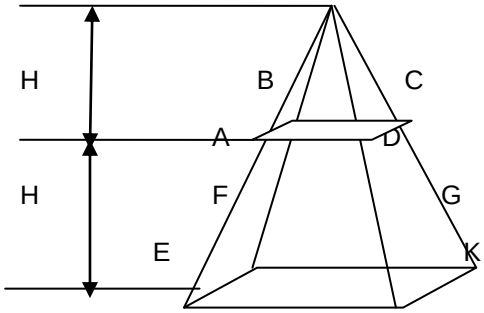

Figure 2: Geometrical shape of hopper

L = EF=FG =320mm= 0.33m

H = 305m= 0.305m

L = AD=DC=85mm=0.085m

H = 90mm = 0.09m

Volume of entire Pyramid $=1/3L^2 (H + h)$

Volume of imaginary Pyramid = $1/3 L^2h$

Volume of truncated part required $=V^1-V^2$ $=0.01328m^3$

Now considering the volume of the rectangular box bolted to the bottom of the hopper, we have

Rectangular box bottled to the bottom of the Hopper

Volume of cuboids=L x B x H 9

Total Volume = Vol. of Hopper + Vol. of cuboid

$=0.013422m^3$

Discharge Compartment

Area of discharge (small Opening) to the cracking section is given by:

Area = L x B 10

For an average size of kernel nut with diameter 14.78mm, the volume to be occupied by kernel nut in cracking compartment is given by:

Volume $=5.2764 \times 10^{-4} m^3$

2.2.4 Capacity of the Cracker

Average volume of kernel = 6.45ml

$= 6.45 \times 10^{-6} m^3$

If $6.45 \times 10^{-6} m^3$ is the volume occupied by 1 Kernel, then $1m^3$ will be occupied by $1/6.45 \times 10^{-6}$ kernel. Therefore, number of kernels entering cracking compartment is found by:

Number of kernels in cracking compartment =Volume of kernel X Volume occupied by kernels in cracking section i.e

$(1/6.45 \times 10^{-6}) \times (5.2764 \times 10^{-4}) = 81.8$ kernels.

That is 81 kernels will be in the cracking section at a time

Number of kernels to be occupied by the hopper is evaluated as:

Total Volume =(Vol. of hopper + Vol. of cuboids + Vol. of cracking compartment) x 1/6.45 x 10^{-6}

(V_1-V_2) +lbh +lbd= 2181.6 kernels

Total mass passing from hopper for cracking = Number of kernels in cracking sector x mass of kernel nut(in Table 2)

Capacity of the cracker =0.2855 X 3600

=1027.75 Kg/hr

2.2.5 Belt Selection

2.2.5.1 Determination of belt tension

Determination of the appropriate power that may be transmitted to nut cracking machine is a pre-requisite for belt selection and is a function of the belt tension and belt speed.

Power = $(T_1 - T_2)$ V 12

From the formula for V - belt in the grove, we have.

$(\sigma_1 - M_1V_2) / (\sigma_2 - M_1 V_2) = e^{(N \text{ Ø1/Sin } Q/2)}$ 13

Where

T_1 =Belt tension in tight side (N)=0.1063

T_2 =Belt tension in loose side (N)=0.0505

V =Belt speed m/s= D_1N_1 /60 =20.23 M/S

$Ø_1$ =angle of wrap of smaller puller=3.367rad

$Ø_2$ =angle of wrap of larger pulley=2.915rad

r =Radius of small pulley = 0.064

R =Radius of large pulley=0.07

C =Centre distance between pulleys =0.35m

B = Sin^{-1} (R-r/c)

σ_1 = Maximum allowable stress =12 MN/m^2

σ_2 =Stress on Black of the belt=0.563MN/m^2

M1=Density of 1m belt (1m Cross Section) - 1250 Kg/m^3

Q=Groove angle =38^0

N=Constant =0.25

It can be seen from above that the angle of wrap of the smaller pulley governs the design.

The required cross sectional area of the belt is given by:

Area = $(T_1 - T_2)/ (\sigma_1 - \sigma_2)$ =8.857 X 10^{-8} m^2

2.2.6 Shaft Design

Motor installed horizontally, so all the belt pull on shall is horizontal, for solid shaft having little or no axial loading, the equation reduces to

$d^3 = 16Ss (K_bM_b)^2 + (K_1m_1)^2$

For a belt drive, the torsion Moment is gotten by:

Torsion moment M_1 = 3.55 NM

Bending of moment M_b = 687.89NM

Shock and fatigue factor applied to bending moment M_b = 1.5

Shock and fatigue factor applied to Torsion Moment M_1 = 1.0

Allowable Stress for shaft with key way S_S = 40 x 10^6 MN/m^2 (Holowenko, 1980)

From above Formula Considering the factor of safety of 1.5

d=1.5 x 0.05096m =0.0764

=76.4mm

Therefore a shaft diameter of 76mm is recommended.

2.3 Design Calculation of Vertical Palm Kernel Cracker

2.3.1 Determination of the Force Requires for Cracking Kernel Nut and the Horse Power Rating of Electric Motor

V =wr (13)

W =v/r=38.74rev/min

Force $F = mw^2r$ =1.833N Ft = MV

Power P= FV =0.0009149 t = MV/F

Horse Power (hp) =0.00122hp For 1kg $t = \frac{0.00349 \times 0.4991}{1.833}$

=0.057 Sec.

2.3.2 Estimation of Time Taken to Crack Measured Mass (Kg) of Kernel Nut

2.3.3 Estimate of Volume of the Hopper for Kernel Nuts.

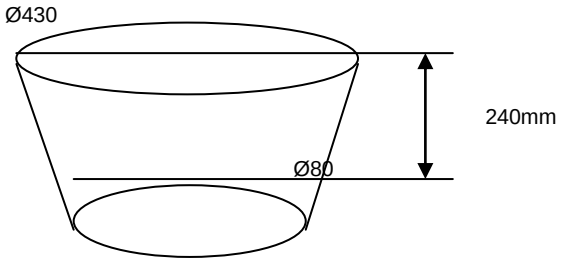

Figure3: Volume of Hopper

Height h=240mm

Inner diameter d_1= Ø80 =0.080mm

Radius r_1=0.04

Outside diameter d_2= Ø430=0.430

Radius r_2=0.215

Volume $V_1=1/3\pi r^2h=0.402 \times 10^{-3}$ m^3

Volume $V_2=1/3\pi r^2h=11.617 \times 10^{-3}$ m^3

Volume of truncated part required $=V_2-V_1$

$=11.22 \times 10^{-3}$ m^3

To determine the Volume of the rectangular box bolted to the bottom of the hopper, we have

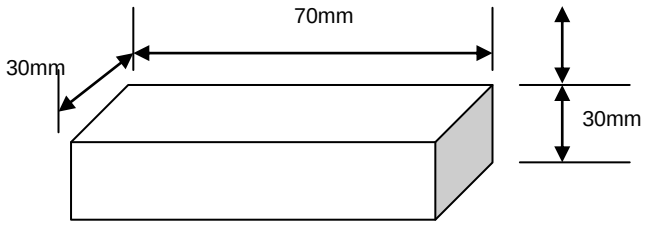

Figure 4: Rectangular box bolted to the bottom of the hopper

Volume of cuboids=LXBXH

L=0.070m, B=0.030m, H=0.030m

Volume=0.630 $\times 10^{-4}$ m^3

Discharge Compartment

Area =l x b=0.070 x 0.030 =0.00211m^2

For an average size of kernel nut with diameter 14.78 mm, the volume to be occupied by the kernel nut in cracking compartment is given by

Volume = area X 14.78 =3.10 $\times 10^{-5}m^3$

2.3.4 Capacity of the Cracker

Number of kernel going to cracking compartment is found by multiplying volume of kernel with volume occupied by kernel in cracking section, that is

Total Volume x 1/6.45 x 10^{-6} = (3.10 x 10^{-3}) 1/6.45 x 10^{-6} =4.812 kernels

That is 4 kernels will be in the cracking section at a time.

Number of kernels that will occupy the hopper is evaluated as:

Number of kernels in the hopper= total volume x Average Volume of kernel

(11.223 x10^{-3}) x 1/6.45 x 10^{-6}=1739.53 kernels

Total mass of kernel passing from hopper for cracking is estimated by multiplying the number of kernels in cracking section with the mass of kernel nut per unit time i.e 0.01396 Kg/s

The capacity of the cracker

= 0.01396 x 3600

= 50.25 Kg/hr

2.3.5 Belt Selection

Where r=Radius of small pulley=0.050m

R=Radius of large pulley=0.10m

C= Center distance between pulley= 0.38m

$Ø_1$ = 180 - 2B=3.205rad

$Ø_2$ = 180 + 2B=3.078rad

β = Sin-1 (R-r/C)=-1.8096

σ_1 = 1.2MN/m^2

σ_2 = 0.341MN/m^2

From the formula for V - belt in the grove, we have

$$(\sigma_1 - M_1V_2) / (\sigma_2 - M_1V_2) = e^{(NØ1/sinQ/2)}$$

The required cross sectional area of the belt is given by.

Area =(T_1 - T_2) / (∂_1 - ∂_2) 14

Where power to be transmitted by motor is given by

Power = (T_1 - T_2) V 15

$T_1 - T_2 = 0.063N$

From equation

Area =(T_1 - T_2) / (∂_1 - ∂_2) 16

= 7.537 x 10^{-8} m^2

T_1 = $\sigma_1 A$ =0.090444

T_2 = 0.090444 - 0.063 =0.027444

∴ $T_1 + T_2$ = 0.090444 +0.027444 =0.117888N

2.3.6 Shaft Design

From equation

$d^3=16/\prod Ss (K_bm_b)^2 + (k1m1)^2$

For a belt drive

Torsional moment M_1 =7.05Nm

Bending Moment M_b = 11.67Nm

Shock and fatigue factor s applied to bending moment M_b = 1.5

Shock and fatigue factor applied to Torsional moment M_1 = 1.0

Allowable stress=Ss =40 x 10^6 N/m^2

From above formula considering the factor of safety of 1.5

d=20.09mm

Hence, this is the minimum shaft diameter that can be used to transmit this drive. Therefore, 20 mm. shaft diameters used for the design is appropriate.

Table 4: Comparison of Calculated Parameters for Impact approach and Vertical Crackers

PARAMETERS	IMPACT APPROACH CRACKER	VERTICAL CRACKER
POWER	0.00113kw	0.0009149kw
HORSE POWER	0.0015hp	0.00122hp
CRACKING TIME	13.2sec.	16.33sec.
CAPACITY	100.5kg/hr	50.25kg/hr
SHAFT DIAMETER	76mm	20.09mm

From the calculated parameters, it is discovered that the centrifugal impact approach nut cracker is faster in operation than vertical nut cracking machine because of its high speed and high impact on the kernel nut .

3. Materials Selection

i. **Hopper:** The hopper of both machines is made of mild steel plate. The hopper serves as an inlet through which the kernels enter the spinning bow. The top is wide enough to take sufficient kernel at a time. The base of the hopper is bolted to the top of main hosing. This means that the hopper can easily be detached after use for easy transportation of the machine required shape.

ii. **Main Housing:** The main housing was constructed from medium carbon steel with reliable strength, toughness and good weld ability. This is to make the machine easier for servicing and repair when maintenance is necessary.

iii. **Rotor:** The rotor is a rotating part of the machine. The rotor receives palm kernel from the hopper at high speed against the cracking wall.

iv. **Mechanism bed:** The mechanism bed is directly mounted on the top of frame support to support the weight of the engine. Mechanism bed was constructed from 3mm angle iron cut into size and welded together. It has the ability to withstand shocks and vibration.

v. **Mainshaft:** Shaft is a rotating element made from a mild steel rode of which aid the racking of palm kernel nut. The reason for its elections based on its high torsion strength, resistance to wear and low cost.

vi. **Bearings:** Bearings are manufactured to take pure radial loads pure thrust loads or the combination of both bearing has the following advantages.

* It is a unit that has its own bearing housing
* It has self-alignment ability
* It has longer life than ball bearing
* It is easier to replace because bearing housing is not required.
* It is able to reduce friction to the minimum
* It is able to withstand weight of shaft and can be easily mounted.

vii. **V-belt:** The selected belt for the machine is a single v. belt. A ball provides convenient means of transmitting power from one shaft in another. This belt operates on V - groove pulley. The selection of V belt based on obtaining along and trouble free life and quiet running, the important part in absorbing shock loads and in damping out and isolate the effects of vibration.

vii. **Pulleys:** The recommended pulley for this machine is mild stead. The criterion for selecting mild steel materials is based on comparatively lighter weight than cast iron pulley, higher strength and durability, less tendency of failure or breakage. Both pulleys grooved and the belt runs on v-grooved pulley. The small and large pulleys have dimension of 75mm and 16mm respectively.

ix. **Supporting frame:** The stand was made of 2 inches angular iron cut into sizes and welded together to form a table0-like structure. The foundation was provided to prevent vibration of the machines. The machines are installed on the required stand through

the foundation bolts on the stand. The frame is designed to withstand shock and vibration, to prevent twisting and maintain firm stability.

x. **Electric motor:** The main purpose of the electric motor is to drive the rotor at a very high speed. The combined effect of centrifugal forces and kinetic energy of rotation are employed in palm kernel cracking machines that can be obtained from electric motor of 2 horsepower and revolution per minute. The motor is mounted to the angular bar bolted to the stand for the motor positioning.

3.1 Assembly of the Machine Parts

Parts of the machines were assembled as follows:

- Mounting of the rotor on the main shaft.
- Welding of the main housing to the mechanism bed
- Mounting of the rotor and shaft on the main housing.
- Mounting of the bearings on the shaft by force fit method.
- Mounting of the pulley on the shaft by force fit method.
- Bolting of the hopper on the main housing
- Lubrication of the bearing with grease.
- Mounting of the machine on the mild steel frame
- Mounting of the electrical motor on the base of machine platform.
- Mounting of the belt connecting the motor shaft and the main shaft
- Tightening of the motor belt on its seat to create necessary tension in the belt.
- The palm kernel-cracking machines were completed for testing and evaluation.

4.0 Operation and maintenance

4.1 Operation of the two Cracking Machines

The palm kernel cracking machines are guaranteed for high efficiency of kernel cracking. The machine is designed and constructed to operate in all weathers. It can be used on the farm, in the villages and hamlets.

4.2 Maintenance

The maintenance of the machine is minimal and does not require skilled labour to carry out maintenance exercise. In addition, the cost of maintenance is very minimal. the maintenance is carried out as follows:

-The machine must be clean after use.

- Periodic repainting is recommended for the surface of the bearing.
- The machine can be installed on reinforced concrete to reduce noise and vibration.

4.2.1 Lubrication

The machines has been designed to standard, that most of the components do not require lubrication but the two pillow bearing deserve grease lubrication. The choice of grease is based on the following reasons;

- Unusual protection is required from the entrance of foreign matters.
- Sample bearing enclosures are used.
- Operation of the machine for long periods without attention is desired.

The lubricant achieves the following purposes:

It provides film of lubricant between the sliding and tolling surfaces, it distributes and disputes heats; lubrication prevents corrosion on bearing surfaces and protects the parts from the entrance of foreign matters (Shigley, and Mischke, 1998).

5. Testing and evaluation

The aim of the performance test is to obtain the cracking efficiency of the two machines.

The palm kernel-cracking machines that were design and constructed were connected to the electric motor by V-belt drive and to the power supply which is run for some time, after which it was tested to crack weighted palm kernels to determine cracking efficiency of each machines. The standard set for the testing was the cracking of the kernel without damaging the seed of the kernel.

In performing the test to determine the efficiency, 1000g (1kg) were fed into the hopper for five consecutive times and the output obtained in each operation is tabulated below for each machine.

Table 5 : Computed Efficiency of Vertical centrifugal Palm Kernel nut Cracking Machine

S/N	MASS OF KERNEL FEED	NO. OF KERNEL	NO. OF KERNEL CRACKED	NO. OF KERNEL UNCRACKED	NO. OF BROKEN KERNEL	TIME (SEC.)	EFFIENCY (5)
1.	1KG	530	370	130	30	73	69.8
2.	1KG	531	390	116	25	81	73.5
3.	1KG	528	365	126	37	78	68.2
4.	1KG	526	395	96	35	75	75.1
5.	1KG	532	372	119	41	74	69.9

Efficiency of palm kernel cracking machine =(Output/Input) x100%

Aveη=(£N/5) %

(i.e. the number of cracked nut divided by total number of kernel nut)

Average efficiency = (69.8 + 73.5 + 68.2 + 75.1+ 69.9)/5

=356.5/5

=71.3%

Table 6 : Calculated Efficiency of Impact approach centrifugal Palm Kernel nut Cracking Machine

S/N	MASS OF KERNEL FEED	NO. OF KERNEL	NO. OF KERNEL CRACKED	NO. OF KERNEL UNCRACKED	NO. OF BROKEN KERNEL	TIME (SEC.)	EFFIENCY (5)
1.	1kg	532	270	51	211	76	50.8
2.	1kg	529	250	37	242	62	47.3
3.	1kg	528	265	52	211	70	50.2
4.	1kg	530	27	31	227	69	51.3
	1kg	533	279	38	216	72	52.3

Efficiency of palm kernel cracking machine = (Output/Input) x100%

Aveη=(£N/5) %

(i.e. the no. of cracked nut divided by total no. of kernel nut)

Average efficiency = (50.8+47.3+50.2+51.3+52.3)

= 251.9/5

= 50.38%

Efficiency of the palm kernel cracking machine = 50.38%

6. Results and discussion

The result evaluation of performance of the two palm kernel cracking machines show that the efficiency of the vertical centrifugal palm kernel cracking machine is 71.3% and 50.38% for impact approach centrifugal palm kernel cracking machine from this it can stated that the two machine are not as such efficient. This is due to many factors among which are error in design and construction.

The impact approach centrifugal palm kernel machine has the highest damage output of the kernel nut due to high impact of the rotor on the kernel nut. Critical examination of the few uncracked kernels reveals that the size of the uncracked kernel nut are smaller than the average mass and diameter of the kernel obtained for the design (refer to experiment 1). By increasing the speed of the motor would cause more damage to the shell of the kernels.

Table 7: Comparison of machine cracking output

S/N	*Vertical centrifugal Palm kernel nut cracker*	*Impact approach centrifugal* palm kernel nut cracker
1	The cracking seeds are very neat	The cracking seeds are damage and rough
2	Slightly slow in operation	Very fast in operation
3	Enough clearance in cracking Spinning bowl	Clearance between the rotor and cracking wall is too tight
4	It have good discharge outlet	Having truncated discharge Outlet.

7. Conclusion and recommendation

The performance test carried out on the two machines shows that both machines needed to be modified. Improvement on the design of the machines is important for higher cracking efficiency. From the result of evaluation, the vertical centrifugal palm kernel cracker has higher efficiency, hence, it is preferred to impact approach centrifugal cracker. Although the vertical centrifugal palm kernel cracker is very slow in operation, but the cracking output is very neat and clean compare to that of impact approach centrifugal cracker is very fast.

In order to boost the efficiency of the kernel nut crackers for the advantages of small - scale industries that use kernel oil, the two machines has to be worked upon to minimize damage to kernel nut and to increase the cracking efficiency. I n order to have relative comparison in term of performance to the imported cracking machine, these two existing machines should be worked upon so as to improve their performance. The following recommendations are made for the two machines.

7.1 Vertical Palm Kernel Nut Cracker

i. Palm kernel nut regulator at the opening of the hopper to cracking chamber has to be included in the design and be constructed to regulate the number of nut going to cracking chamber.
ii. Reducing the hopper discharge opening and position it in a slight form to minimize the number of palm kernel entering to the spinning bowl at a time.
iii. Feeding of kernel nut to the machines has to be gradually drop into the hopper which bring about good cracking output with increase in cracking time.

7.2.2 Impact Approach Centrifugal Cracker

i. Hopper cover with small opening on it must be constructed to avoid scattering of cracked kernel nut.
ii. The machine must be installed on reinforce concrete to reduce noise and vibration.
iii. Enough clearance must be between the rotor and cracking wall in order to allow

the free movement of rotor in cracking the palm kernel nut.

iv. Collector must be constructed to the discharge opening to limit the splashing of cracked nut.

Based on the evaluation of the output and performance of these machines, the vertical centrifugal palm kernel is recommended for small-scale industries that make use of kernel oil to increase their productivity.

References

Asiedu,J. J. (1989), processing tropical crops- A technological approach. Macmillan, London and basing stoke pp 167-185

Akubuo, C.O and Eje, B.E (2002), 'Palm Kernel and Shell Separator', *Biosystems Engineering* 81 (2), 193 - 199

Gbadam, E.K., Anthony, S and Asiam, E.K (2009), ' The Determination of Some Design Parameters for Palm Nut Crackers', European Journal of Scientific Research, Vol.38 No.2 , pp.315-327

Ofei, T. N., (2007), "Design of Palm Nut Cracker: Influence of Drying Time on Static Force Required to Crack Nut", *BSc Project Report, Unpublished*, UMaT, Tarkwa, Ghana, pp. 37.

Koya, O. A., (2006), "Palm Nut Cracking under Repeated Impact Load", *Journal of Applied Sciences,* Vol. 6, No. 11, pp. 2471-2475.

Poku, K., (2002), "Small-Scale Palm Oil Processing in Africa", FAO Agricultural Services Bulletin, No. 148, Publishing Management Service, Information Division, FAO, Rome, pp 56,

Oke, P.K (2007), 'Development and Performance Evaluation of Indigenous Palm Kernel Dual Processing Machine' Journal of Engineering and Applied Sciences 2 (4): 701-705

Hartley, C.W.S (1987), The Project of Oil Palm and The Extraction in the Oil Palm Published by Longman. London. pp: 40-48.

Ndegwe. N.A.(1987), The Oil Palm in Rivers State of Nigeria, pp: 103-104

Okoli. J.U (1997), Determination of Optimum Hurling Speed for Effective Palm Nut Cracking, Harrison Ayeesin,R.S Aad Opekere, K.(1999), Energy requirement for palm nut cracking, The Nigeria Society of engineer, Lagos Vol. 26 No.3 pp7-8.

Adamus, G. A(1990), design and Construction of vertical shaft centrifugal nut cracker, A paper presented at the 9th Annual Conference of Nigeria society of agricultural Engineering, NASE. PP 11-12

Davies,O.I (1971), The design and analysis of industrial experiment oliver and body, new york, pp12-14.

Egbo,C.O and Kaul, R.N. (1985), Introduction of Agricultural Mechanisation, London and oxford. (p. Ix).

Gerb- Stork (1963), Kernel recovery II. Stock Palm Oil Review Gerb-Stork And Co. Holland Vol.3 (4) Publishing Co. Port Harcourt Rivers State, Nigeria

Bolu et al: Proc. ICCEM (2012) 229 - 237

University Optical Fibre Network Access Optimisation: A Case Study

Christian A. Bolu[1], Ademisoye O. Tolulade[2] and Alimi Adeshina[3]

Department of Mechanical Engineering, Covenant University, Ota, Ogun State, Nigeria
[1]christian.bolu@covenantuniversity.edu.ng
[2]tolulade.ademisoye.6462@covenantuniversity.edu.ng
[3]adeshina.alimi.6469@covenantuniversity.edu.ng

Abstract

For network access, it is always desired that a fibre optic network connectivity be the major area of cost minimization, while keeping quality of service as high as possible. This is because overall cost of setting up a fibre optic cable route is usually very high in relation to other components of the network. In this study, three buildings clusters were mapped to the University Network Operating Center, and the network was developed as a fail-safe network, so that in the case of damage to a cable or connecting component, users are not cut out. The problem was formulated as a Mathematical Programming problem and solved the resulting transportation problem using MATLAB linear programming solution. Results from the mathematical model shows an optimized cost for which a fibre Optic network connectivity can be further developed.

***Key words**: Optimisation, Optical Fibre, Cabling, Access Network, Dynamic Programming, Linear Programming*

1. Introduction

The rapidly changing face of data communications and telecommunications has seen a continued growth in the need to transfer enormous amounts of information across large distances. Technologies such as coaxial cable, satellite and microwave radio are in use but optical fibre cabling is gaining ground as internet network backbone.

There is a growing requirement to provide a communications medium that is more suitable to the noisy industrial environment where the need for data integrity is paramount. Optical fibre is simply a very thin piece of glass which acts as a pipe, through which light can pass. The light that is passed down the glass fibre can be turned on and off to represent digital information or it can be gradually changed in amplitude, frequency, or phase to represent analog information. (David Bailey & Edwin Wright 2003)

1.1 Fibre Optics Basics

a. Fibre Optics is a branch of optics dealing with the transmission of light through hair-thin, transparent fibres. It is also known as the technology of using “waveguides” to transport information from one point to another in the form of light. It is characterized as follows:

- Optical Fibre: Thin strands of highly transparent glass or sometimes plastic that guide light.
- Core: The centre of the fibre where the light is transmitted.
- Cladding: The outside optical layer of the fibre that traps the light in the core and guides it along through curves.
- Buffer Coating or Primary Coating: A hard plastic coating on the outside of the fibre that protects the glass from moisture or physical damage.
- Mode: A single electromagnetic field pattern (think of a ray of light) that travels in fibre.

b. Optical Fibre Cabling can be classified as follows:
   - Multimode step and graded index fibres **-** The term ‘multimode’ generally applies to fibres with a diameter of 50 micrometers or greater. Because of the relatively wide diameter of the core, multiple modes of light are able to travel down the fibre core. The modal dispersion that occurs in a multimode fibre affects or is affected by a number of

operating parameters of the fibre. They are:

- Attenuation: Multimode fibres have a maximum operating distance of approximately 5km.
- Bandwidth: Multimode fibres have maximum operating data speed of approximately 2-300 Mbps
- Wavelength: They generally operate at wavelength of 850 nm or 1300 nm. The wide diameter of the multimode makes it suitable for LED light sources.

- Graded index: A graded multimode has a core that has a gradual changing cross-sectional refractive index. The center of the core has the highest refractive index that gradually reduces moving away to the edges of the core. Because of this smooth changing refractive index, the light ray refracts (rather than reflects as in step index fibres) as it moves through the core, and set up a set of sinusoidal wave patterns in the fibre.

- Single mode Fibres - A single mode fibre (or sometimes referred to as a single mode cable) is basically a step index fibre with a very small core diameter. In theory, because the cores are so small only a few modes of light can travel down the fibre. They have a very small core causing light to travel in a straight line and typically has a core size of **8 or 10 microns**. It has unlimited bandwidth that can go unrepeated for over 80km, depending on the type of transmitting equipment. Single mode fibre has enormous information capacity, more than multimode fibre.

2. Literature Review

Designing minimum-cost transport network for fibre optical network access has been in the literature on for over a decade now. Optical ring networks are widely regarded as essential to serve the unprecedented growth in demand for data transport capacity, largely driven by internet applications. Fibre optic cables are widely used in Access Networks. In other to determine a suitable 'ring route' a network planner must specify its logical type, capacity, topological layout.

Dynamic programming principle has been successfully used for Network Planning. Aside from a few specific case studies of optical ring-based networking, most of the relevant literature for ring network optimization is found in the form of mathematical formulations for multi-ring network design problem. Most methods routed the demands using a shortest-path algorithm and select rings using either a heuristic algorithm or integer programming [Morley, 1999, Krendzel, Pirmez, 2010]

(Krendzel, 2012), formulated a routing problem in an Access Network ring structure as a combinatorial-optimization problem and dynamic programming was used to solve it. The problem of cable-laying ring routing between a Local Exchange and its Remote Units is considered. Their objective was to determine the minimum-cost ring route that satisfies the specified constraints which are:

1. To pass over the Local Exchange and all Remote Units,
2. To pass over each Remote unit only once,
3. To begin and to end in the same point corresponding to the Local Exchange,
4. To have no splits.

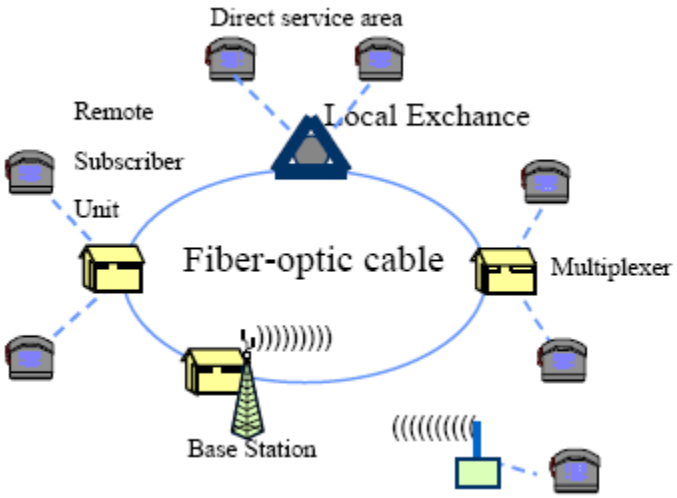

Figure 1: Model of a perspective Access Network (Krendzel, accessed 2012)

(Kulkarni S. and El-Sayed, M, 2010) discussed some economic, technical and business drivers that impact the selection of the right fibre to the home technology for an operator to deploy. Here they focused on an optimized total cost of ownership (TCO) network model to evaluate different technological choices for new deployment and redeployment for both incumbent telecommunications and cable operators.

(Ray, et al 2012), introduced the concept of a fibre aided wireless network architecture, which allows high-speed mobile connectivity by leveraging the speed of optical networks. As a first step towards designing such network architectures, they considered a single-input, single-output (SISO) wireless-optical channel and proposed a scheme in which the wireless signal at the radio-optical converter is sampled and quantized using a fixed-rate, memoryless, vector quantizer, before being sent over the fibre communication link.

3. Methodology

a. Network Representation- The first step in our methodology was to produce the **Network Representation** of the University showing the access network structure. Network representation provides a powerful visual and conceptual aid for portraying the relationship between the components of systems that is used.

The Access Network (AN) is based on a fibre-optic cable passing over a number of remotes units. The subscribers are connected to the Local Exchange (LE) and the remote units and subscriber lines. By a remote unit (RU) is meant a multiplexer, a remote subscriber unit, a base station (for wireless access) or a combination of these elements. (Krendzel, 2012).

Local Exchange: The University Network Operating Center
Subscribers: In this case they are the Halls of Residence, Academic buildings, Cafeterias, Workshops, University Chapel, University Library, and Post-Graduate Quarters.
Base Station: Located in each of the subscriber unit, for ease of wireless access in each building and surrounding area.
Multiplexer: For distributing signals usually located in each of the base station.
Subscriber Lines (Individual): Staff and Students.

Figure 2: Google Earth of University Campus accessed January

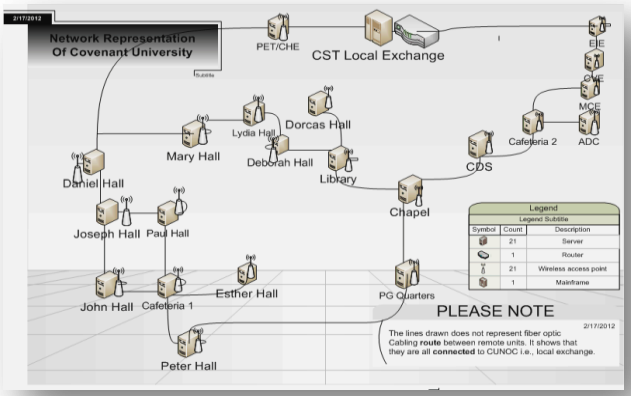

Figure 3: Network Representation of the University Network, using Microsoft Visio 2007

b. The Transportation Problem.

1. Known Capacity of Internet Bandwidth is available from three Bandwidth Supply Companies.
2. In the University, Known quantity of Bandwidth is distributed to a number of users in Academic, Administrative and Residential Buildings for use by staff and students.
3. The academic, administrative and residential buildings are interconnected to each other using Optical Fibre Cabling (OFC) with associated costs with respect to material, technology and logistics.

The transportation problem is to determine the **Bandwidth size** to move from each Bandwidth Supply source to the various academic, administrative and residential buildings to **minimise the overall cost** while satisfying the constraint of demand from staff and students in the University over a given period of time.

c. Supply Side (Internet Service Providers)

There are three supply companies which are:

- ISP-1 provides the University with 25 Mbps (Megabyte) of internet data.
- ISP-2 provides the University with 30 Mbps (Megabyte) of internet data.
- ISP-3 supplies the University 30 Mbps (Megabyte) of internet data.

d. Formulation of the Problem

Here we will be formulating the transportation problem as linear programming problem.

Let x_{ij} = amount of bandwidth routed from ISP i to cluster $j; i = 1,2 \ldots\ldots, m; j = 1,2, \ldots \ldots, n$
Let c_{ij} = cost to route bandwidth 1 from ISP i to user cluster $j; i = 1,2, \ldots\ldots m; j = 1,2, \ldots \ldots, n$
Let d_j = required number of units at user cluster $j; j = 1,2, \ldots \ldots\ldots, n$
Let s_i = capacity of ISP $i; i = 1,2, \ldots \ldots, m$

The problem can be formulated as a linear model, namely (Gillett, 1979).

Minimize: $z = \sum_{i=1}^{m} \sum_{j=1}^{n} c_{ij}\, x_{ij}$

Subject to: $\sum_{j=1}^{n} x_{ij} \leq s_i \quad i = 1, 2, \ldots \ldots, m$

Equation 1: Supply Capacity Constraint

$\sum_{i=1}^{m} x_{ij} \geq d_j \quad j = 1, 2, \ldots \ldots, n$

Equation 2: Bandwidth Demand Constraint

all $x_{ij} \geq 0$

Equation 3: Bandwidth Non negativity Constraint

If al least one feasible solution exists, then there exists an optimal solution where all the

x_{ij} values are integer or zero. The simplex method will produce this integer optimal solution

If equation 1 is summed up over all i, then

$$\sum_{i=1}^{m}\sum_{i=1}^{n} x_{ij} \leq \sum_{i=1}^{m} s_i$$

Likewise if equation 2is summed over all j, then

$$\sum_{j=1}^{n}\sum_{i=1}^{m} x_{ij} \geq \sum_{j=1}^{n} d_j$$

Thus from equations 1 and 2,

$$\sum_{i=1}^{m} s_i \geq \sum_{j=1}^{n} d_j$$

Suppose

$$\sum_{i=1}^{m} s_i = \sum_{j=1}^{n} d_j$$

Thus constraints equation 1 and 2 can be rewritten as equalities so that the model becomes (Gillett, 1979):

Minimize: $z = \sum_{i=1}^{m}\sum_{j=1}^{n} c_{ij}\, x_{ij}$

Subject to: $\sum_{j=1}^{n} x_{ij} = s_i \quad i = 1, 2, \ldots\ldots, m$

$\sum_{i=1}^{m} x_{ij} = d_j \quad j = 1, 2, \ldots\ldots, n$

all $x_{ij} \geq 0$

Where $\sum_{i=1}^{m} s_i = \sum_{j=1}^{n} d_j$

Assumptions

a. Objective function will be: [(The cost of fibre per metre) x (the distance to run through) + (cost of mbps/annum) x (amount of mbps)]
b. 48 core single mode fibre optic cable at N450/m
c. Taking 1mbps/month = $350
d. Exchange rate is NGN/US$ 170
e. Demand Nodes:
   - Academic Building/Administrative (**A**) using College of Development studies CDS as our point of reference.
   - Non Academic (**B**) using the University Chapel as our reference point
   - Residential/Non-Academic (**C**) using Cafeteria 2 as our reference point.
f. Based on preliminary demand analysis done (Bolu, 2010) we assume the following:
   - Point A needs 40Mbps due to:
     - The high degree of work being done in the Building by the lecturers, Administrative staff, students in class who also use the e-learning portal and other internet activities.
     - Population will be averagely highest here during the day except for lecture free day or public holidays.
   - Point B needs 25Mbps due to:
     - Being a non-academic area, less work will be done here compared to the college/department buildings and student population will be randomly high.
   - Point C needs 20Mbps due to:
     - Being residential - activities that will be done here will not be as intensive as at Point A. Activities like; Webinar (occasionally), Online conference meeting (occasionally), checking of mails, watching of academic videos online, and other social and academic download.
     - Students/Staffs will only be at their residence in the evening or lecture free day or a general public holiday. During the day not many activities will take place.

The transportation matrix is shown below:

Table 1: Transportation matrix

Buildings	User Demand (Mbps)	ISP

	Academic	Administration	Residential	Capacity (Mbps)
ISP 1 Google	x_{11}	x_{12}	x_{13}	25
ISP 2 Glo	x_{21}	x_{22}	x_{23}	30
ISP 3 Etranzact	x_{31}	x_{32}	x_{33}	30
User Demand (Mbps)	40	25	20	85

4. Results and Analysis

Note 1: ISP *Globacom, Etranzact and Google* are all in the **same point** (Network Operating Center, CUNOC). That means they have the **same distance** to the demand points.

Note 2: Representations are:

- 'E' represents Etranzact
- 'Gl' represents Globacom
- 'Gg' represents Google

Note 3: Distance from points obtained from Google Earth and some confirmed by physical measurement (Bolu, 2011).

Note 4: Drawing made using Microsoft Visio 2007.

Figures 4, 5, and 6 shows some feasible solutions.

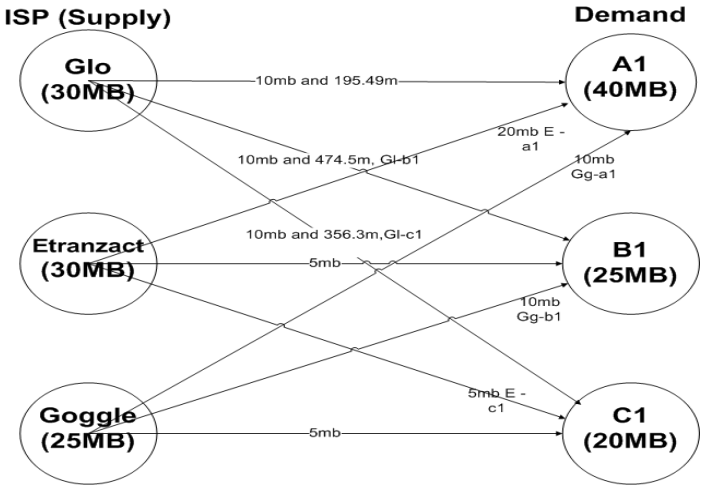

Figure 4: Feasible Solution 1

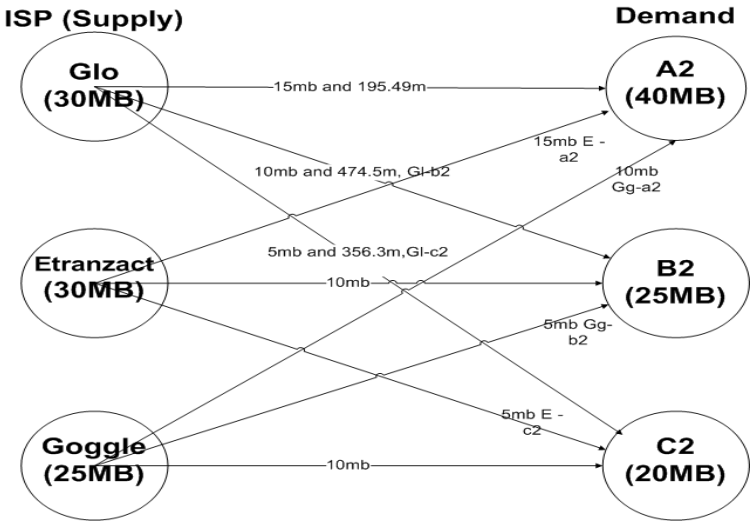

Figure 5: Feasible Solution 2

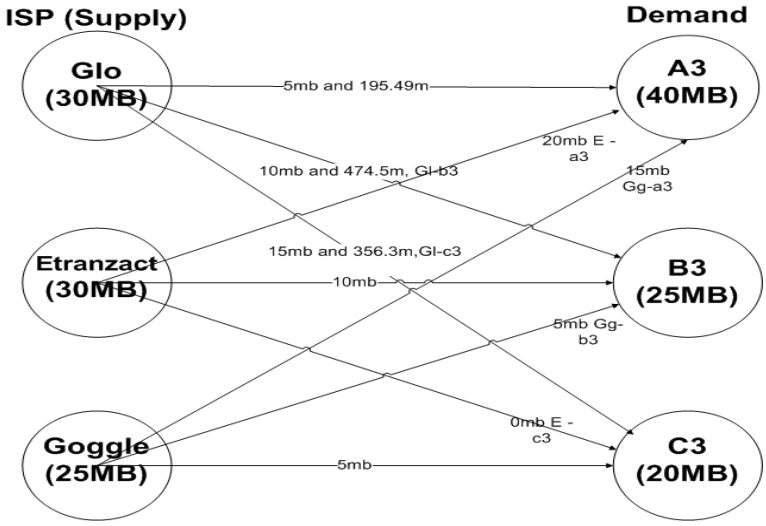

Figure 6: Feasible Solution 3

Solution

Minimise z = $2643900\mathcal{X}_{11} + 2643900\mathcal{X}_{12} + 2643900\mathcal{X}_{13} + 2128075\mathcal{X}_{21} + 2128075\ \mathcal{X}_{22} + 2128075\mathcal{X}_{23} + 1671005\mathcal{X}_{31} + 1671005\mathcal{X}_{32} + 1671005\mathcal{X}_{33}$

Subject to:

$$\sum_{i=1}^{3} x_{i1} = 30 \text{ Glo}$$

$$\sum_{i=1}^{3} x_{i2} = 30 \text{ Etranzact}$$

$$\sum_{i=1}^{3} x_{i3} = 25 \text{ Goggle, all } x_{ij} \geq 0$$

$\sum_{j=1}^{3} x_{1j} = 40$ Academic/Administrative Building

$\sum_{j=1}^{3} x_{2j} = 25$ Non-Academic Building

$\sum_{j=1}^{3} x_{3j} = 20$ Residential Building

And

$$\text{all } x_{ij} \geq 0 \begin{bmatrix} 1\,1\,1\,0\,0\,0\,0\,0\,0 \\ 0\,0\,0\,1\,1\,1\,0\,0\,0 \\ 0\,0\,0\,0\,0\,0\,1\,1\,1 \end{bmatrix} \begin{bmatrix} x_{11} \\ x_{12} \\ x_{13} \\ x_{21} \\ x_{22} \\ x_{23} \\ x_{31} \\ x_{32} \\ x_{33} \end{bmatrix} = \begin{bmatrix} 40 \\ 25 \\ 20 \\ 30 \\ 30 \\ 25 \end{bmatrix}$$

Using the MATLAB Linear Programming module, the following solution diagrammatically shown below was obtained.

Through linear programming we have optimized the cost. The resulting objective function is ₦184, 930,000.00k

5. Conclusion

We have been to determine the bandwidth size to be supplied and the minimised cost of distribution using linear programming.

The final outcome of using a linear program in generating a model to solve the access network problem of connecting buildings across the University is one that can be deployed for use in other models. Though other forms of costs might arise during the process of construction and laying the cables, the final cost used is accurate and would be very close to the actual cost to be spent depending on the amount of miscellaneous expenses that arise during actual cable laying.

Also, though this model has been developed for a specific location, the steps followed can be useful as a guideline for modeling another Access Network for a different location having Network (communications) problems.

Since the objective function of a system is the measure of the effectiveness of the system thus, we have been able to determine the cost of meeting the demand of the three main locations with a supply of 85 Mbps.

6. Recommendations

In line with all that has been done, there are still some improvements that can be made to the model and this can model can serve as a guideline for whatsoever would be done. Such additions and/or improvements could be:

- Use of Integer or Dynamic Programming for a better bandwidth allocation and adequate Network Planning.
- Expansion of this model to encompass other buildings being in Covenant University Network.
- It should be noted that this model was simplified by clustering the users. This should be un-clustered for future work.

Acknowledgement

The authors acknowledge the laboratory investigation contribution of the Innovation Centre, University of Nigeria, Nsukka and the Department of Mechanical Engineering, Covenant University, Ota for the provision of computing facilities for this work.

References

Ab-Rahman, M. S., (2011), The Extension of OXADM Survivability Scheme to Fibre-to-the Home Wavelength Division Multiplexing (FTTH-WDM) Network. *Journal of Applied Sciences Research*, 8(6): 880-884

Ab-Rahman, M. S., et al, (2009), Transmission surveillance and self-restoration against fibre fault for time division multiplexing using passive optical network by ISSN 1751-8628, 2nd April 2009.

Bailey, D., and Wright, E., (2003), Practical Fibre Optics - ISBN: 0750658002.

Bolu, C. A, (2011), *Modeling and Simulation in Mechanical Engineering* in Principles of Mathematical Modeling, Lecture note (MCE 414), Covenant University, Ota, Ogun State. Nigeria. 2011, pp 3-7

Bolu, C. A., (2011), *Fibre Optics Network Optimisation as a Transportation Problem*, [Lecture Note in Engineering Mathematics], Department of

Mechanical Engineering Covenant University, Nigeria.

Gillett, B. E.,(1979), Introduction to Operations Research: A Computer Oriented Algorithmic Approach, New Delhi: Tata McGraw-Hill Publishing Company Ltd

Krendzel, A. V., *Access Network Planning: Minimisation of Construction Cost*, Dept., of Network Planning, St. Petersburg Research Institute of Telecommunications (LONIIS) 11, Warshawskya Str.196128

Kulkarni, S. and El-Sayed, M., (2010), *FTTH-Based Broadband Access Technologies: Key Parameters for Cost Optimized Network Planning by.* Bell Labs Technical Journal 14(4), pp 297–310 Alcatel-Lucent, Wiley Inc.

Morley, G.D, Grover, W.D, (1999), *Comparison of Mathematical Programming Approaches to Optical Ring Network Design* TR Labs and University of Alberta, Dept., of Electrical and Computer Engineering, Edmonton, T6G2EI, Canada.

Pfarrhofer, R.,et al, (2012), *Distributed Optimization of Fibre Optic Network Layout Using MATLAB*, uhl@cosy.sbg.ac.at – http://www.cti.ac.at/ accessed January 28, 2012

Pirmez L., et al, (2010, September 15), Network Selection Based On Utility Function and Integer Linear Programming*, Journal of Computer Networks*, Volume 54 (13), ISSN 1389-1286.

Ray, S., et al, (2012), *Fibre Aided Wireless Network Architecture: A SISO wireless -optical channel*, Laboratory for Information and Decision Systems, MIT, Cambridge

Anake: *Lead Paper* Proc. ICCEM (2012) 224 - 228

Developing Clean Technology through Approximate Solutions of Mathematical Models

Timothy A. Anake
Department of Mathematics, School of Natural and Applied Sciences, College of Science and Technology, Covenant University, Canaanland, Ota, Ogun State, Nigeria

Abstract

In this paper, the role of mathematical modeling in the development of clean technology has been considered. One method each for obtaining approximate solutions of mathematical models by ordinary differential equations and partial differential equations respectively arising from the modeling of systems and physical phenomena has been considered. The construction of continuous hybrid methods for the numerical approximation of the solutions of initial value problems of ordinary differential equations as well as homotopy analysis method, an approximate analytical method, for the solution of nonlinear partial differential equations are discussed.

Key words: *Mathematical models, simulation, continuous hybrid methods, homotopy analysis method*

1. Introduction

The term “clean technologies” refer to production systems developed and adopted for the primary purpose of improving environmental performance, (Koltuniewicz, 2008). The development of these environmentally friendly technologies is of great interest to scientists and governments all over the world as a result of the effects of global warming. In Nigeria for instance, a Science and Technology Policy, which advocates the use of clean technologies in production systems, was launched in 2011 by her federal government to underscore the importance it accords the development of clean technologies (Federal Republic of Nigeria Science Technology and Innovation Policy, September, 2011).

The reality is that this advancement in technology has modified in many ways the expectations facing mathematicians and the practice of applied research. With industries becoming typically “high-tech”, computationally intensive methods are employed at all levels. The increased supply in computing power has also made it possible to implement and apply computational methods no matter how sophisticated. This interplay of mathematics, computing and technology could best be described as the art of mathematical modeling and simulation (Heilio, 2009).

According to the report of the 2012 Workshop on mathematical modeling and simulation of power plant and CO_2 capture held at the University of Warwick, mathematical modeling and simulation play important roles in proof of concept, feasibility study, reliability and performance analysis for the designs and development of new systems to be cost effective and robust. This is especially relevant where experiments with real objects are difficult or completely not feasible.

The design and development of any new system, typically begins with a mathematical model which is assumed to represent the structure and the laws governing the system or phenomenon. The model represents the key relationships among system components by means of equations. The equations can be derived in a number of ways. Many of them come from extensive scientific studies that have formulated and tested mathematical relationship against real data. Some come from laboratory testing of relationships where that is feasible. Sometimes real data are used to derive relationships using statistical techniques to fit a particular relationship to the data and to measure the level of error associated with that representation.

The aim of this paper is not to build mathematical models but to discuss the numerical approximation to the solutions of the mathematical models of systems that lead to differential equations.

The paper is arranged as follows: in section two mathematical models by ordinary differential equations and the methods of obtaining approximate solutions are considered; models by partial differential equations and the methods of approximating their solutions are described as well in section three; and section four is the conclusion

2. Models by Ordinary Differential Equations (ODE)

Many mathematical problems in applied mathematics lead to ordinary differential equations. In the simplest case, to solve ODE one seeks a differentiable function, say $x=x(t)$ of one real variable t, whose n^{th} derivative, $x^n(t)$, $n=1,2,\ldots,n-1$, is to satisfy an equation of the form

$$\frac{d^n x}{dt^n}=f\left(t,x(t),x^1(t),x^2(t),\ldots x^{n-1}(t)\right), \qquad 1$$

describing systems with dissipation, where n represents order of the problem, or the special case,

$$\frac{d^n x}{dt^n}=f\left(t,x(t)\right), \qquad 2$$

for systems without dissipation. Generally, for an initial value problem (IVP), one seeks a solution, say $x(t)$, which satisfies n initial condition of the form

$$x^{(n)}(t_0)=x_0, \qquad 3$$

where $n=0,1,2,\ldots n-1$.

For the boundary value problems (BVP), the desired solution of (1) and (2) has to satisfy a boundary condition

$$r\left(x(a),x(b)\right)=0, \qquad 4$$

where $a\neq b$ are two different numbers and $r(u,v)=\begin{bmatrix} r_1(u_1,u_2,\ldots,u_n,v_1,v_2,\ldots,v_n) \\ r_n(u_1,u_2,\ldots,u_n,v_1,v_2,\ldots,v_n) \end{bmatrix}$ is a vector of n given functions r_i of $2n$ variables.

In what follows, the numerical approximation of solutions of IVP of ODE is discussed

2.1 Numerical Approximation of the Solutions of IVP of ODE

The numerical solution of mathematical models by ordinary differential equations, in particular initial value problems, has been widely studied. The most widely used numerical method for this class of problems is the finite difference methods. For BVP, any of the following methods can be employed: finite element methods and the semi-analytic methods such as homotopy perturbation method (He, 2008, 2009a; Jin, 2008; Liang and Jeffrey, 2009), the adomian decomposition method (Adomian, 1994), homotopy analysis methods (Kumar and Gupta, 2010; Liang and Jeffrey, 2009; liao, 1992; Yuen et. al., 2010; Zhu et. al., 2010), variational iterative method (He, 1999a, 2000; Nikkar, 2012), regular perturbation methods (Cole, 1968), etc. In the sequel, only finite difference methods for IVP of ODE shall be considered.

2.1.1 Finite Difference Methods

This is the most widely used numerical method to solve ordinary differential equations of the form (1), (or the special case (2), with either of the conditions (3) or (4). This method uses difference equations to approximate the solution of the problem. They include first order methods such as Euler's method, the family of Runge-Kutta methods, and higher order methods such as Runge-Kutta Nystrom method, the backward difference methods, and the continuous linear multistep methods (Lambert, 1973). The focus here shall be on the integration of the initial value problem (1) and (3) directly by continuous hybrid one step methods. For the purpose of this paper, second order problems, that is when $n=2$, which arise from the modeling in the domains of celestial and mechanical systems are considered (Hindamarsh, 1986).

Conventionally, to solve the initial value problem (1) and (3), one can either choose to reduce the problem to an equivalent system of first order equations and then use any of the first order methods or solve the problem directly using higher order methods. It has been reported in (Anake, 2012a, 2012b) however, that it is more convenient to solve the initial value problem (1) and (3) directly.

The continuous one step hybrid method uses the power series polynomial of the form

$$P(t)=\sum_{j=0}^{d} u_j t^j, \qquad 5$$

as the approximating polynomial on the partition $\pi_{[a,b]}: a=t_0<t_1<t_2<\cdots<t_{j-1}<t_j=b$ of the interval of integration $[a,b]$. The numerical scheme is developed by the combined techniques of interpolation and collocation. The approximating polynomial, expected to satisfy (1) and (3), takes the form

$$P(t)=\sum_{j=0}^{r+s-1} u_j t^j, \qquad 6$$

where r and s represent the number of interpolation and collocation points respectively. In particular, let us interpolate (5) at the origin and the fifth point, that is $r=2$ and collocate the differential system at nine points, that is $s=9$, in the one step hybrid design. It is worth mentioning, that this one step hybrid design incorporates

seven non-step points between the origin and the next step point. Thus, these eleven conditions imposed by the IVP (1) and (3) on (6) given as

$$P(t)=\sum_{j=0}^{10} u_j t^j = x_{n+r},\ r=0,5 \qquad 7$$

and

$$P''(t)=\sum_{j=0}^{10} j(j-1)u_j t^{(j-1)} = f_{n+s},\ s=0,1,2,...,8, \qquad 8$$

Leads to a system of eleven equations in eleven unknowns to be determined using any convenient method in the literatures.

By putting the unknowns obtained in the system (7) and (8) into (6), a one step numerical scheme is obtained in the form

$$x_{n+1}=\alpha_1(z)x_n+\alpha_2(z)x_{n+\nu_4}+h^2\left[\sum_{j=0}^{1}\beta_j(z)f_{n+j}+\sum_{i=1}^{7}\beta_{\nu_i}(z)f_{n+\nu_i}\right], \qquad 9$$

where, ν_i indicates the non-step points, $h=t_{n+j}-t_{n+j-1}$ is a fixed step size, $t_{n+j}=t_n+jh$, $x_{n+j}=x(t_{n+j})$ approximates the exact solution at t_{n+j} and $f_{n+j}=f(t_{n+j},x_{n+j},x'_{n+j})$. The coefficients $\alpha_r(z)$ and $\beta_s(z)$ are obtained from the transformation of the unknowns obtained earlier using a scaling factor, $z=\frac{t-t_n}{h}$. For emphasis, note that (9) is completely determined by the coefficients $\{\alpha_r(z),\beta_s(z)\}$ for all values of $z\in[0,1]$.

Error issues concerning the scheme, (9) are considered by the concept of local truncation error. The local truncation error (*l.t.e*) is a simple concept that determines the difference between the approximate solution x_{n+j} and the exact solution $x(t_{n+j})$ when the step is taken with all earlier data exact. Typically, (9) satisfies *l.t.e* if

$$l.t.e=O(h^{p+2}) \text{ as } h\to 0,$$

where p, determined by relations among the schemes coefficients, is the order of accuracy of the scheme. Apart from analyzing error issues, for (9) to be valid, the nature of its convergence has to be established. To do this, it suffices to show that the method is consistent and zero stable according to (Henrici, 1962). Further more, the absolute stability of the scheme is investigated using either, boundary locus methods, Schurz criterion method or the Rout Hurwitz method (Lambert, 1973). This property guarantees that if the solution of the IVP (1) and (3) is bounded then, the numerical solution (9) is also bounded.

3. Models by Partial Differential Equations

Partial Differential Equations (PDE) are equations that involve rates of change with respect to two or more continuous variables. The distinction in the configuration of PDE problems unlike ODE problems makes it usually much harder to solve. However, simpler solutions exist for linear problems. Basically, PDE may arise from phenomena such as acoustics, fluid flow, electrodynamics, and heat transfer.

For a function F, the PDE is of the form

$$F\left(x_1,x_2,...,x_n,u,\frac{\partial u}{\partial x_1},...,\frac{\partial u}{\partial x_n},\frac{\partial^2 u}{\partial x_1\partial x_1},...,\frac{\partial^2 u}{\partial x_1\partial x_n},...\right)=0 \qquad 10$$

A solution of a PDE is generally not unique; additional conditions must generally be specified on the boundary of the region where the solution is defined. Basically, PDE are classified as parabolic, hyperbolic and elliptic. The classification provides a guide to appropriate initial and boundary conditions, and to smoothness of the solutions.

Several methods have been studied for the solution of PDE; this range from analytical through approximate analytical methods (He, 1998, 1999a, 1999b, 2000; Jin, 2008; Kumar and Gupta, 2010; Liang and Jeffrey, 2009; Liao, 1992; Nikkar, 2012; Yuen et. al., 2010; Zhu et. al., 2010) to numerical methods.

In this paper, only approximate analytical will be discussed.

3.1 Approximate Analytical Methods

By approximate analytical methods we refer to series expansion methods. These include the Adomian decomposition method (Adomian, 1994), the homotopy perturbation method (He, 1998, 1999a; Jin, 2008;Liang and Jeffrey, 2009), variational iteration methods (He,1999b, 2000; Nikkar, 2012), homotopy analysis methods (Kumar and Gupta, 2010; Liao, 1992; Yuen et. al., 2010; Zhu et. al., 2010), regular perturbation (Cole,1968), etc. They are especially suitable for non linear PDE. Note that, the Adomian decomposition method, the Lyapunov artificial small parameter method, and He's homotopy perturbation method are all special cases of the more general homotopy analysis method

(Liao, 1992). Except for the Lyapunov method, these methods are independent of small physical parameters as compared to the well known perturbation theory, which means greater flexibility and solution generality. In what follows, the Homotopy analysis method is discussed for the solution of nonlinear PDE arising from the mathematical modeling of physical phenomena.

3.1.1 The Homotopy Analysis Method (HAM)

The homotopy analysis method was first developed in 1992 by S. J. Liao, (Liao, 1992). The simple manner in which this method ensures the convergence of the solution series does not remove the fact that the method is a powerful mathematical tool for obtaining accurate enough approximations.

To describe the basic idea of HAM, consider the following nonlinear differential equation:

$$N\left[u\left(x,t\right)\right]=0, \qquad 11$$

where N is a nonlinear operator and the unknown function $u\left(x,t\right)$ is specified by the independent variables x and t. The zeroth-order deformation equation is derived by means of HAM as follows:

$$\left(1-p\right)L\left[\phi\left(x,t;p\right)-u_0\left(x,t\right)\right]=\hbar H\left(x,t\right)N\left[\phi\left(x,t;p\right)\right], \qquad 12$$

where $p\in\left[0,1\right]$ is the embedding parameter, $\hbar\neq0$, is a nonzero auxiliary parameter, $H\left(x,t\right)\neq0$, is an auxiliary function, L is an auxiliary linear operator, $u_0\left(x,t\right)$ is the initial guess of $u\left(x,t\right)$. We can see that when the embedding parameter changes from $p=0$ to $p=1$, the function $\phi\left(x,t;p\right)$ varies from the initial guess $u_0\left(x,t\right)$ to the exact solution $u\left(x,t\right)$. Now, expanding $\phi\left(x,t;p\right)$ in Taylor series with respect to p gives

$$\phi\left(x,t;p\right)=u_0\left(x,t\right)+\sum_{k=1}^{\infty}p^k u_k\left(x,t\right), \qquad 13$$

where

$$u_k\left(x,t\right)=\frac{1}{k!}\frac{\partial^k\phi}{\partial p^k}\bigg|_{p=0} \qquad 14$$

The parameter $\hbar$ controls the convergence of the series (13) such that if it is convergent at $p=1$, we have

$$\phi\left(x,t;p\right)=u_0\left(x,t\right)+\sum_{k=1}^{\infty}u_k\left(x,t\right).$$

As proven earlier in [19], this must be one of the solutions of (11).

Substituting (13) into (11) and equating the coefficients of like powers of p, the m^{th}-order deformation equation is obtained as follows:

$$L\left[u_m\left(x,t\right)-\chi_m u_{m-1}\left(x,t\right)\right]=\hbar R_m\left(\bar{u}_{m-1}\left(x,t\right)\right), \qquad 15$$

subject to the initial conditions

$$u_i\left(x,0\right)=0 \qquad 16$$

where the vector $\bar{u}_n\left(x,t\right)=\left\{u_0\left(x,t\right),u_1\left(x,t\right),...,u_n\left(x,t\right)\right\}$,

$$R_m\left(\bar{u}_{m-1}\left(x,t\right)\right)=\frac{1}{\left(m-1\right)!}\frac{\partial^{m-1}N\left[\phi\left(x,t;p\right)\right]}{\partial p^{m-1}}\bigg|_{p=0}$$

and

$$\chi_m=\begin{cases}0, & m\leq1,\\ 1, & m>1.\end{cases}$$

Thus, the solution of the m^{th}-order deformation equation (15) for $m\geq1$ becomes

$$u_m\left(x,t\right)=\chi_m u_{m-1}\left(x,t\right)+\hbar\int_1^t R_m\left(u_{m-1}\left(x,t\right)\right)d\tau+c, \qquad 17$$

where c is the integration constant determined by the initial condition (16). This way, we obtain the solution of (11) as

$$u\left(x,t\right)=\lim_{N\to\infty}\Phi_N\left(x,t\right) \qquad 18$$

where

$$\Phi_N\left(x,t\right)=\sum_{m=0}^{N-1}u_m\left(x,t\right).$$

The main advantage of the HAM is that it always provides one with a simple way to adjust and control the convergence radius of solution series (Liao, 1992). Different from perturbation techniques, the HAM is valid no matter if a nonlinear problem contains small/large physical parameters; be it a strongly nonlinear system or a weakly nonlinear cases.

4. Simulations

It is a well known fact that even though mathematical equations can be formulated to model systems, these equations are many times analytically intractable. In these situations, a computer can implement the mathematics literally and repeatedly to very extreme advantages. Both methods discussed above for instance, lend themselves easily to computer simulations. Infact, the implementation of the scheme (9) is only realistic when a computer program is written to simulate the result at the respective grid points. Similarly, symbolic computation programs such as maple, mathematica or matlab are employed to obtain the solutions in (17).

5. Conclusion

The role of mathematical models and simulation in the development of clean technology is revealed in the methods discussed for the solutions of ordinary and partial differential equations. Systems and phenomena that lead to IVP of ordinary differential equations and nonlinear partial differential equations are clearly understood and can be interpreted from the solutions of these mathematical models. In this paper, one method each for the solutions of models by ODE and models by PDE respectively has been discussed. These methods are by no means the only methods available as earlier mentioned, but they seemed the most convenient for this discussion.

References

Adomian, G., Solving frontier problems of Physics*. The decomposition method,* Kluwer Academic, Dordrecht. 1994.

Anake, T.A., Awoyemi, D. O., Adesanya, A. O, Famewo, M. O. Solving general second order ordinary equations by a one step hybrid collocation method. International Journal of Science and Technology. **2**(4), 164-168. 2012a.

Anake, T.A.**,** Awoyemi, D. O., Adesanya, A. O. A one step method for the solution of general second order ordinary differential equations. International Journal of Science and Technology. 2(5), 159-163. 2012b.

Cole, J. D. Perturbation Methods in Applied Mathematics*,* Blaisdel, Waltham, MA, 1968.

Dangelmayr, G and Kirby, M. Mathematical modeling: A comprehensive introduction, Prentice-Hall, New Jersey. 2005.

Federal Republic of Nigeria Science, Technology and Innovation Policy. September, 2011, available online[http://www.fmst.gov.ng/uploadfil/sti_policy2011.pdf], assessed(October, 2012).

He, J. H. An approximate solution technique depending upon an artificial parameter, Commun. Nonlinear Sci. Numer. Simul **3,** 92 – 97. 1998.

He, J. H. Homotopy perturbation technique, Comput. Methods Appl. Mech. Eng.*,* **178**, 257 – 262. 1999a.

He, J. H. Variational iteration method – a kind of nonlinear analytical technique: some examples, *Int. J. Non Linear Mech,* **34,** 699 – 708. 1999b.

He, J. H. (2000). Variational iterative methods for autonomous ordinary differential systems, *Appl. Math. Comput.,* **114,** 115 – 123.

Heilio, M. (2009). Mathematics for Society, Industry and Innovation. *J. of Math. Modeling and Appl.* **1**(1), 77-88.

Henrici P., *Discrete Variable Methods in ODE*. John Wiley and Sons, New York. 1962.

Hindamarsh, A. C. Numerical techniques for ordinary differential equations *Particle Accelerators*, **19**, 67 – 71. 1986.

Jin, L. Homotopy Perturbation Method for solving partial differential equations with variable coefficients, Int. J. Contemp. Math. Sci.*,* **3**(28), 1395 – 1407. 2008.

Koltuniewicz, A. B. and Drioli, E.. Membranes in clean technologies. Theory and practice, Wiley – VCH Verlag GmbH & Co. KGaA, Weinheim. 2008

Kumar, S. D. and Gupta, P. K. Approximate analytical solutions for fractional space- and time- partial differential equations using homotopy analysis method. *Appl. Appl. Math.:* An international Journal, **5**(2), 544 – 562. 2010.

Lambert, J. D. Computational Methods in ODEs. New York: John Wiley, 1973.

Liang, S and Jeffrey, D. J.Comparison of homotopy analysis method and homotopy perturbation method through evolution equations, Commun. Nonlinear Sci. Numer. Simul *14(12)***,** 4057 – 4064. 2009.

Liao, S. J. On the Proposed Homotopy Analysis Technique for Nonlinear Problems and its Applications, Ph.D. Dissertation, Shanghai Jio Tong University. 1992.;

Nikkar, A. A new approach for solving gas dynamic equations. Acta Technica Conviniensis - Bulettin of Engineering, **4,** 113-116. 2012.

Report of the 2012 workshop on mathematical modeling and simulation of power plant and CO_2 capture held at the University of Warwick, available online [http://www.geos.ed.ac.uk/ccs/Meetings/Mathematic_Modelling_Simulation_WORKSHOP_2012.pdf], assessed (October, 2012)

Yuen, C. F., Hong, L. K. and Seng, C. F.Solving nonlinear algebraic equations by homotopy analysis method. Proceedings of the 6th IMT-GT conference on mathematics, statistics and its applications, at Universiti Tunku Abdul, Kuala Lumpur, Malaysia, 712 – 720. 2010.

Zhu, H., Shu, H. and Ding, M. Numerical solutions of partial differential equations by discrete homotopy analysis method, *Appl. Math. Comput.* **216,** 3592 – 3605. 2010.

Design and development of vapor absorption refrigeration system for rural dwellers

Adekeye, T. Oyedepo, S.O and Oyebanji, J.A

Mechanical Engineering Department, Covenant University, Ota Nigeria

Correspondence: tunde.adekeye@covenantuniversity.edu.ng

Abstract

In this study, the experimental analysis of the performance of vapor absorption system was developed and developed. The influence of generator, evaporator and condenser's temperatures on the system performance was studied using gas burner as source of energy, ammonia-water combination as working fluid and energy equations as governing equations for the work. There was variation in the results when compared with the earlier worker who used kerosene burner as source of energy and ammonia-water combination. Result of this study shows that if higher cooling capacity and also lower evaporator`s temperature are desired from the system, generator`s temperature should be increased considerably. Also the combination of an analyzer, rectifier and heat exchanger would produce better COP of the System.

***Key words**: Refrigeration, Vapour absorption, cooling load, COP*

1. Introduction

The role of energy to human being on the earth cannot be overemphasized; its application for basic human needs is inevitable.

But, a large population of people resides in rural areas where access to conventional electricity as source of energy for human use mainly for operation such as refrigeration which includes the processing and preservation of foods, mixed vegetables and other uses in the area is grossly unavoidable and an alternative source of energy is required (Omoniyi,2003).

In hot climates, the heating and the cooling demand of domestic dwellings can be reduced substantially with various measures such as good insulation, double glazing, use of thermal mass and ventilation.

However, due to the high summer temperatures, the cooling demand cannot be reduced to the level of thermal comfort with passive and low energy cooling techniques, and therefore ,an active cooling system is required .It is preferable that such a system is not powered by electricity.

During the last few decades, an increasing interest ,based on research and development, has been concentrated on utilization of non-conventional energy sources, namely solar energy ,wind energy ,tidal waves ,biogas ,geothermal energy ,gas burner, kerosene burner, hydropower ,exhaust from furnace ,biogas etc.

Among these sources, gas burner, this is available and could be used to power an active cooling system based on the absorption cycle.

Ammonia-water and lithium bromide-water absorption combinations are the most suitable for gas burner applications. Research has been performed for ammonia-water absorption system theoretically and experimentally.

The first purpose of the study is to design and construct an absorption refrigeration system powered by gas burner and ammonia-water as working fluid. The second purpose of the study is to investigate experimentally the effects of the operating temperatures on the coefficient of performance of the system (Adekeye, 2006).

Most essentially, a refrigerating system must incorporate a condenser, an evaporator, a generator and an absorber that serve to

increase and decrease the pressure of the working fluid called the refrigerant which circulates between these components through connecting tubes. The energy required might be supplied through a gas burner in form of heat to replace the conventional electricity that is readily available (Williams,1955).

Refrigeration means the cooling or removal of heat from a system. The equipment employed to maintain the system at a low temperature is termed refrigerating system and the system which is kept at lower temperature is called refrigerant. Refrigeration is generally produced in one of the following three ways:

(i) By melting a solid

(ii) By sublimation of solid and

(iii) By evaporation of liquid (Williams, 1955)

The refrigeration system can be classified into two main groups

(i) Vapor compression refrigeration system

(ii) Vapor absorption refrigeration system

1.1 Vapor compression system

The vapor compression refrigeration system cycle operates ideally on four processed as indicated in the diagram shown below.

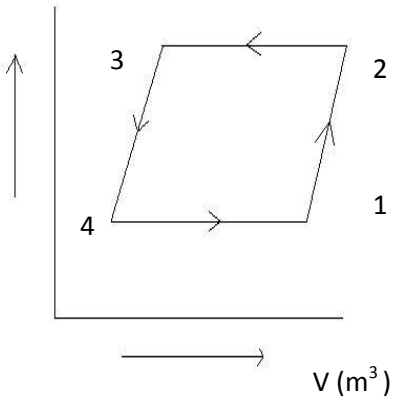

Pressure – volume diagram

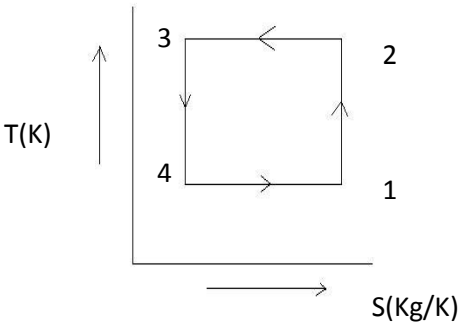

Temperature Entropy diagram

Fig 1-vapor-compression refrigeration cycle. 1-2-Adiabatic compression at constant entropy; 2-3-Isohermal heat rejection

3-4-Adiabatic expansions at constant entropy; 4-1 –Isothermal heat absorption (Bacom and Stephen,1991).

The compression process is affected by the vapor compression incorporated in the system, which compressed the vapor compression from the evaporator and raised its temperature and pressure to a certain value to allow the condensation of the vapor in the condenser. The condenser fluid then expands into evaporator through the expansion device .In the evaporator, the low pressure refrigerant vaporizes, taking heat of vaporization from the conditioned space surrounding it thus producing the cooling effect. The vaporized refrigerant flows to the compressor via the suction line and the cycle continues (Bacom and Stephen, 1991).

1.2 Vapor absorption refrigeration system

The absorption refrigeration system cycle is similar to the vapor compression cycle in that it

employs a volatile refrigerant usually either ammonia-water, which alternatively vaporizes under low pressure in the evaporator by absorbing latent heat from the material being cooled and condenses under high temperature in the condenser by releasing the latent heat of the condensing medium.

The principal difference in the absorption and compression cycles is the motivating force that circulates the refrigerant through the system and provides the necessary pressure differential between the vaporizing and condensing processes.

In the absorption cycle, the vapor compressor employed in the vapor compression cycle is replaced by an absorber and generator, which perform all the functions performed by the compressor in the vapor compression cycle. In addition, the energy input required by the vapor compression cycle supplied by the mechanical work of the compressor, the energy input in the absorption cycle in the form of heat supplied to the generator is usually low pressure steam or hot water, although in smaller systems the heat usually supplied to the combustion of an appropriate fuel such as natural gas, propane or kerosene, directly in the generator.

The system consists of four basic components, an evaporator, an absorber which are located on the low pressure side of the system generator and a condenser which are located on the high pressure side of the system. Two working fluids are employed as refrigerant and absorbent.

The flow cycle for the refrigerant is from the condenser to the evaporator to the absorber to the generator and back to the condenser, while the absorbent passes from the absorber to the generator and back to the absorber .High pressure liquid refrigerant from the condenser passes into the evaporator through an expansion valve that reduces the pressure of the refrigerant to the low pressure existing in the evaporator. The liquid refrigerant vaporizes in the evaporator by absorbing latent heat from the material being cooled, and the resulting low pressure vapor then passes from the evaporator through an unrestricted passage to the absorber when it is absorbed and goes back into solution in the absorber.

The refrigerant flows from the evaporator to the absorber because the vapor pressure of the absorbent –refrigerant solution in the absorber that determines the pressure on the low pressure side of the system and consequently the vaporizing temperature of the refrigerant in the evaporator.

As the refrigerant vapor from the evaporator is dissolved into the absorbent solution, the volume of the refrigerant is decreased (compression occurs) and the heat of absorption is released. In order to maintain the temperature and vapor pressure of the absorbent solution at the required level, the heat released in the absorber which is equal to the sum of the latent heat of condensation of the refrigerant vapor and the heat of dilution of the absorbent, must be discarded to the surroundings(Bacom and Stephen,1991.)

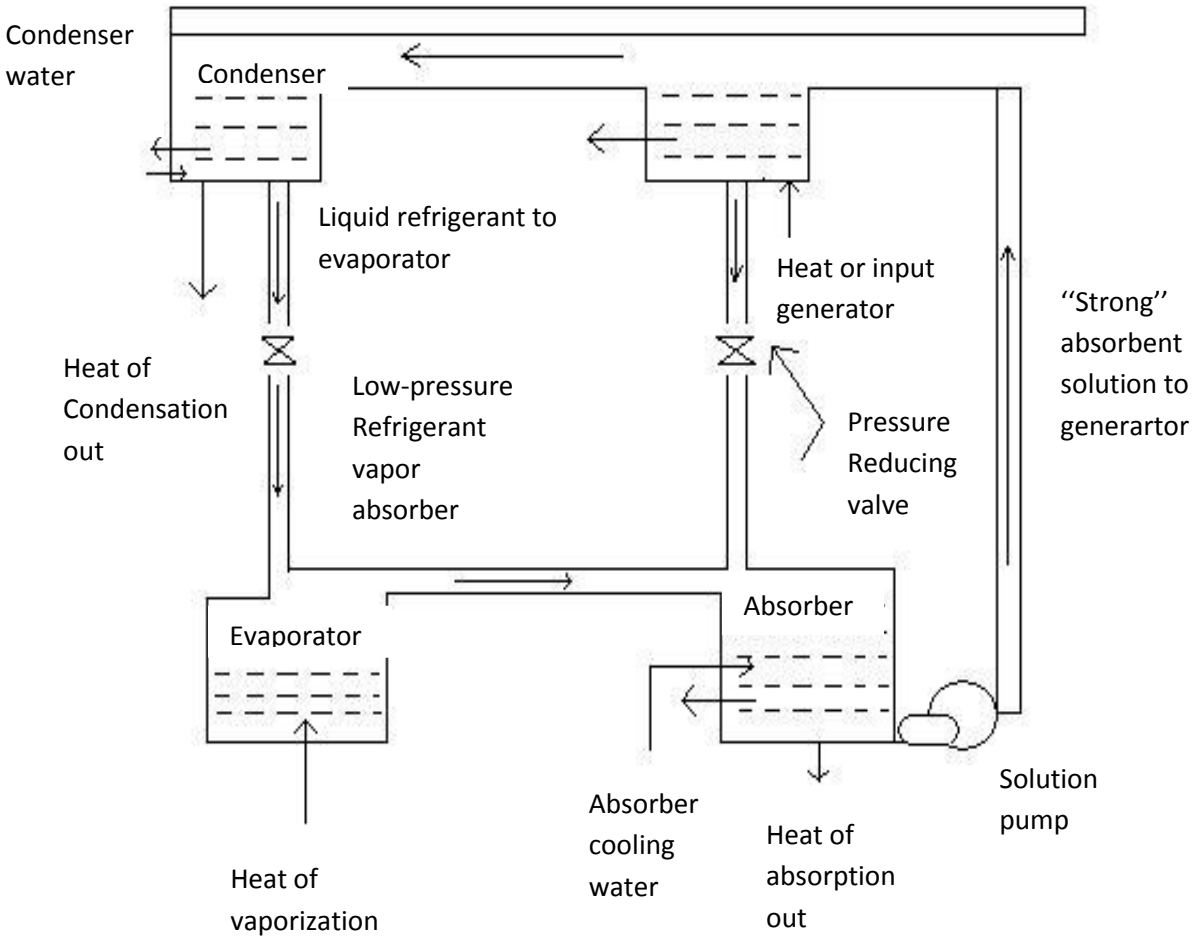

Fig.2-Basic Absorption Refrigeration Cycle (5)

1.2.1 Refrigerant-absorbent solution

To be suitable in an absorption system, there are certain criteria that the refrigerant- absorbent combination should meet, at least to some degree.

Obviously, the absorbent must have a strong affinity for the refrigerant vapor, and the two must be mutually soluble over the desired range of operating conditions. The two fluids should be safe, stable and non-corrosive both individually and in combination. Ideally, the absorbent should have a low volatile so that the refrigerant vapor leaving the generator will contain little or no absorbent and working pressure should be reasonably low are preferably near atmospheric pressure to minimize equipment weight and leakage into and out of the system. The refrigerant should have a reasonably high latent heat value so that the required refrigerant flow rate is not excessive.

For this project, ammonia-water combination was selected because of the following advantages:

Ammonia-water combination is widely used in domestic refrigerator and in commercial and industrial systems where the evaporator temperature is maintained close to or below 32˚F.

The water (absorbent) has a very strong affinity for ammonia vapor and the two are mutually soluble over a wide range of operating condition.

Both fluids are highly stable and are compatible with most materials found in refrigeration system.

The major disadvantage of the ammonia water system is the fact that the absorbent (water) is reasonably volatile so that the refrigerant (ammonia) vapor leaving the generator will usually contain appreciable amount of water vapor which is allowed to pass through the condenser and go into the evaporator will raise the evaporator temperature and reduce the refrigerating effect by carrying on vaporized refrigerant out of the evaporator.

For this reason, the efficiency of the ammonia-water system can be improved by the use of an analyzer and rectifier which function to remove the water vapor from the mixture leaving the generator before it reaches the condenser (Arora,2004).

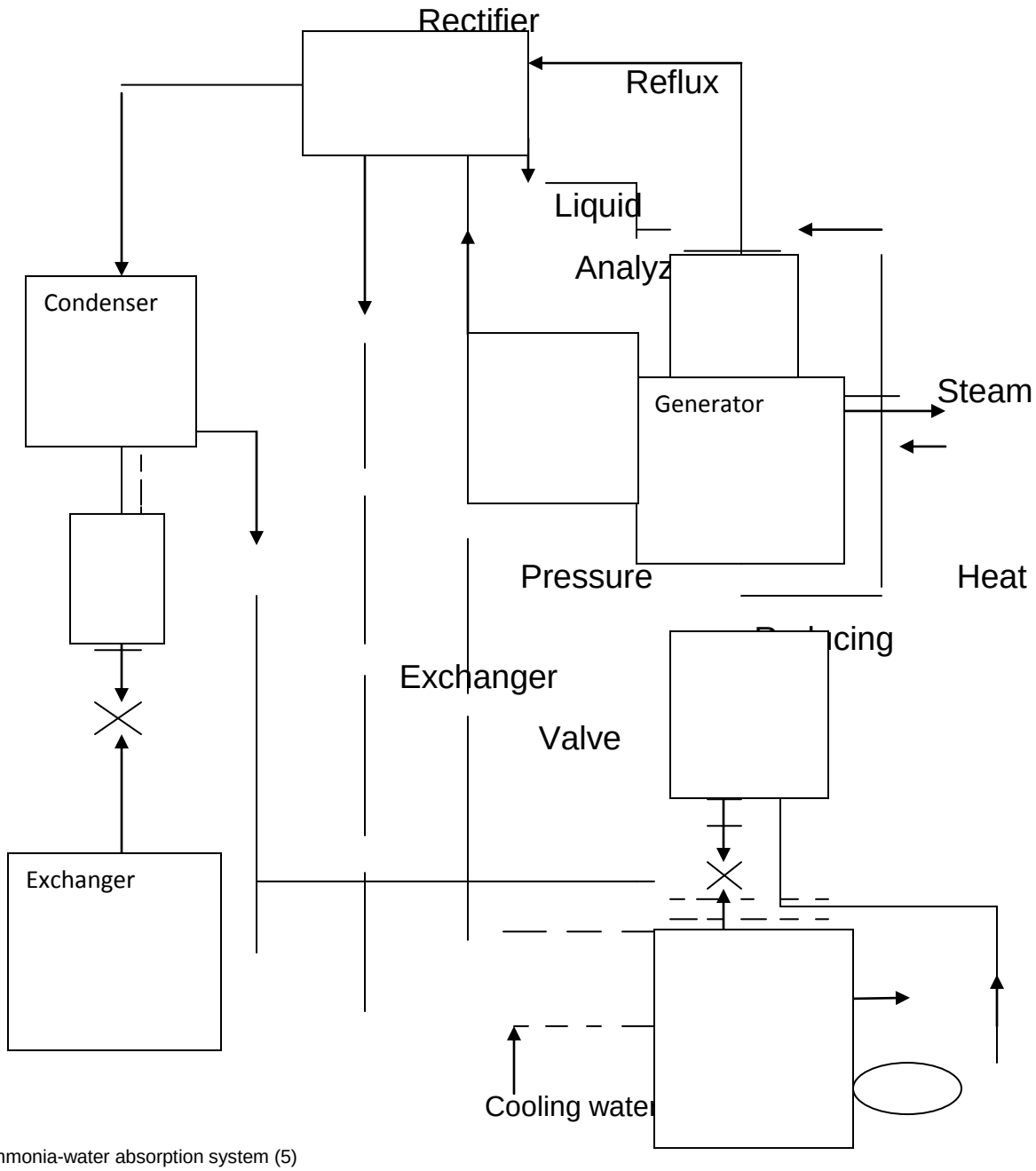

Fig.3 Ammonia-water absorption system (5)

In comparison, the followings are the advantages of vapor absorption refrigeration over compression system:

1) There is no moving part in the system except the aqua-pump motor. The pump motor is quite small as compared to the compressor motor in compression system.

2) Absorption system is quite in operation, very little wear and it has low maintenance cost

3) It can use processed steam, hot exhaust from the furnace, burner (kerosene or gas) solar energy as source of thermal energy in the generator.

4) The capacitor of the absorption system is controlled and maintained by adjusting the steam generator`s temperature even if the evaporator pressure falls.
5) The absorption system can be operated at the designed COP (Coefficient of performance) by the appropriate control of generator`s temperature.

6) It is much more compact and less bulky than the compression (Arora,2004).

2.0 Design specifications and assumptions

The design was based mainly on household refrigeration for both rural and urban Dwellers. The following assumptions were made:

APPLICATION: The system was designed for food preservation, mixed vegetables

AMBIENT TEMPERATURE: The maximum dry bulb and minimum wet bulb temperatures were taken to be 30˚C and 26˚C respectively. The temperature of the evaporator is assumed to be 0˚C while the product freezing temperature was considered to be 2˚C and the generator`s temperature was 100˚C.

2.1 Dimension of the Refrigerator

The unit consists of condenser, evaporator, expansion device, absorber and generator. The compartment formed serves as storage area for the products meant for freezing, therefore the following dimensions were considered

i) External Dimension of the Refrigeration

Length=breadth=800mm=0.8m each

Height=1200mm=1.2m high

ii) Internal Dimensions

Length=breadth=600mm=0.6

Height=1000mm=1m high

2.2 Insulation and Thickness

The insulation of the refrigerator prevents heat loses from compartment. The contents could thus be adequately preserved. Polyurethane was selected as the insulating material because of the following properties:

(i)High insulating strength

(ii)It has very low thermal conductivity when compared with other insulating materials

(iii)Water absorption rate is 0

For the thermal insulating material, polyurethane of 100mm thick was selected and used (Boast,1992).

2.3 Cooling Load Calculation

Cooling loads is the amount of heat that must be removed from the refrigerator space to provide and maintain the desired temperature. The total cooling loads of the refrigerator was determined by all the heat gained from various sources that must be removed from the refrigerated space. These include:

I. Wall, floor and cooling heat gained due to conduction

II. Air change load due to ingress outside, and the air from infiltration and door opening.

III. Product load from incoming goods to be reduced to storage temperature including freezing duties.
IV. Heat of respiration from stored product for food, drugs and farm produces.
V. Miscellaneous loads.

2.3.1 Wall, Floor and Ceiling Conduction Heat Gained

$Q_{gained} = AU\Delta T$

Where:

A = total external surface area of the refrigerated area in squared meters, obtained from:

[(length + width) x 2 x height] + [(change x width) x 2]

U = Overall rate of heat transfer for the well panel in W/m^2°C

ΔT = the temperature difference between the internal temperature and ambient temperature.

2.3.2 Infiltration Load

This occur when the warmth air from outside enters the refrigerated space to replace the more dense cold air while opening and closing the door of the unit.

The warmth air load becomes part of the total of the experiment that must be removed along with other sources of load. It is calculated thus,

I. Air change load (w) = (room volume x heat to be removed x number of air change per day i.e. 86,400)
II. Number of seconds in a day = 60 x 60 x 24

=

86,400secs

III. The room volume (m^3) is the internal volume of the refrigerated space, obtained by multiplying the internal length by the width and height dimensions of the room.
IV. The heat to be removed (j) is that of the infiltration air.
V. The number of air change depends on the temperature i.e. above or below 0°C

2.3.3 Product Load

This is the load that is required to be removed from the contents of the refrigerator in other to reduce their temperature

2.3.3.1 Product Cooling above Freezing

Product load (w) = weight of product x specific heat x temperature difference/86,400. The weight product (kg) loaded per day (24 hours)

Freezing

Product load (w) = (weight of product x latent heat/86,400)

The height of the product is the weight load per day. The freezing process of the product starts from outside when the outside surface has frozen a barrier is formed to the transfer of heat from the outside of the product which will prolong the freezing time.

2.3.3.2 Product Cooling below Freezing

Product load (w) = (weight of product x specific heat/86,400). The parameters are for cooling above freezing because the application is a continuous freezing process; it is normally calculated on the basis of 16 to 18 hours running time per 24hours.

Respiration

Product load (w) = (weight of product x heat of respiration/86,400). The weight of product is the total height in store (not that it was brought into the store par day) (Boast,1992).

2.4 Adopted Specifications

Cold room temperature = 0°C

Ambient temperature = 35°C

Room diameter (internal) = 0.6m long x 0.6m wide

Insulation – polyurethane foamed panel insulation thickness = 100mm

External diameter = 0.8 x 0.8 x 1.2

Product load = 40kg per day entering at 25°C and reduce to 0°C

Product specific heat = 3.97 x 10^3 kJ/kg above freezing and 2.03kJ/kg below freezing

Product latent heat = 31.4kJ/kg

Product freezing temperature = 0°C

2.4.1 Wall Load

Surface area = [(0.8 x 0.8) x 2 x1.2] x [(0.8 x 0.8) x 2]

= 3.84 + 1.28

= 5.12

≈ $5m^2$

Heat gained = Surface area x thermal transmittance x temperature difference

= 5 x 0.14 x (25-0)

= 5 x 0.14 x 25

= 17.5W

2.4.2 Air Infiltration Load

Load = volume x heat factor x air change/86,400

$$= (0.36 \; x \; 109{,}000 \; x \; 0.8)/86{,}400$$

$$= 31{,}392/86{,}400$$

= 0.36W

2.4.3 Product Load

Load = product height x specific heat x temperature difference/86,400

$$= 40 \; x \; 39{,}700 \; x \; (25 - 0)/86{,}400$$

$$= 39{,}700{,}000 \; /86{,}400$$

= 459.5W

2.4.4 Heat of Respiration

Load = product height x heat of respiration/86,400

$$= 1200 \; x \; 3200/86{,}400$$

= 44.6W

Total Load = 16.1 + 0.36 + 459.5 + 44.6

= 520.4W

Allowing 16 hours running time per day, then:

Load = 520.4 x (24/16)

= 780.6W or 0.781KW

Total load = wall load + infiltration load + product load + respiration

= 780.6W

Q_E = 0.781KW

2.5 Determination of Mass Flow Rate

The flow of the refrigerant through the generator, the condenser is assumed to be in continuous system. For analytical evaluation of the ammonia- water cycle, the following simplifying assumptions were made.

The refrigerant and absorbent phases at evaporator inlet, absorbent outlet, bottom of the generator, the condenser inlet and vapor from the rectifier are all in equilibrium.

The total pressure of the fluid solution is constant through the system except in the expansion device.

From energy flow equation, the mass flow rate of refrigeration in the equation (m) is given as:

$Q_E = m\Delta H \quad (m = m_i)$

Where:

Q_E = cooling load capacity in kJ/s or kW

M = mass flow rate of the evaporator in kg/s

ΔH = change in enthalpy (refrigerating effect (RE))

M = Q / ΔH (RE) kg/s

2.5.1 Determination of Mass Flow Rate of Weak Solution

To determine the mass flow rate of weak solution, the following equations were employed.

From overall mass balance equation

=

$$m + m_2^1 = m_1^1 \ldots\ldots\ldots\

$= m_2^1 h_2^1 + m_1 h_2 - m_1 h_1$ 7

Where:

($m_2 = m_1 = m$)

2.5.5 Determination of Condenser Heat Ejection (Q_c)

$Q_C = m (h_2 – h_3)$ 8

Where:

Q_C = condenser heat ejection

m = mass of flow rate

$h_2 - h_3$ = change in enthalpy refrigerating effect

2.5.6 Determination of Overall Energy

Overall energy balance = $Q_G + Q_E - Q_A - Q_C$

2.6 Coefficient of Overall Energy Balance by Coefficient of Performance

C.O.P = $\frac{Q_E}{Q_A}$ 9

2.7 Determination Of Coefficient Of Performance Of An Ideal Vapour Absorption System

From the first law of thermodynamics neglecting Q_P, we have;

$Q_C = Q_G + Q_E$ 10

As the vapour absorption system can be considered as a perfectly reversible systems, therefore the initial enthalpy of the system = enthalpy of the system after the change of its condition.

i.e.

$$\frac{Q_G}{T_G} + \frac{Q_E}{T_E} + \frac{Q_C}{T_C} \quad \text{.....} \quad 11$$

From equation (2)

$$\frac{Q_G + Q_E}{T_C} = \frac{Q_G}{T_C} = \frac{Q_E}{T_C}$$

Or

$$\frac{Q_G}{T_G} - \frac{Q_G}{T_C} = \frac{Q_E}{T_C} - \frac{Q_E}{T_C}$$

Or

$$Q_G \left(\frac{T_C - T_G}{T_G \, X \, T_C}\right) = Q_E \left(\frac{T_E - T_C}{T_C \, X \, T_E}\right)$$

Or

$$Q_G = Q_E \left(\frac{T_E - T_C}{T_C \, X \, T_E}\right)\left(\frac{T_C - T_G}{T_G \, X \, T_C}\right)$$

$$= Q_E \left(\frac{T_C - T_E}{T_C \, X \, T_E}\right)\left(\frac{T_G - T_C}{T_G \, X \, T_C}\right) = Q_E \left(\frac{T_E - T_C}{T_E}\right)\left(\frac{T_G}{T_C - T_G}\right)$$

..... 12

Maximum coefficient of performance of the system

$$C.O.P_{max} = \frac{Q_E}{Q_G} = \frac{Q_E}{\left(\frac{T_E - T_C}{T_E}\right)\left(\frac{T_G}{T_C - T_G}\right)} = \left(\frac{T_E}{T_C \, X \, T_E}\right)\left(\frac{T_G - T_C}{T_G}\right)$$

…… (13)

3.0 RESULTS AND DISCUSSION

In this study, mass flow rate and heat transfer in the evaporator, absorber, generator and condenser of designed and developed vapour absorption refrigeration system for rural dwellers were determined. The following specifications were used to determine the mass flow rate and heat transfer in the above components.

Generator temperature = 100°C

Condenser temperature = 45°C

Evaporator temperature = 0°C

Absorber temperature = 30°C

Evaporator - the main aim of refrigeration is achieved in the evaporator, so in designing the system, care was taken to ensure enough surface area so as to enhance the design refrigeration capacity.

Determination of Refrigerating Effect

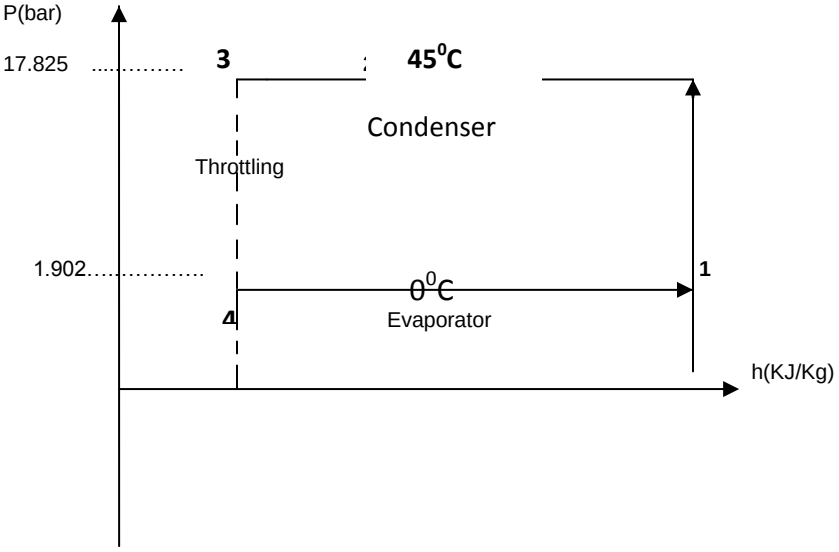

Fig 4: Vapour Absorption Cycle

From Ammonia (NH_3) tables, T_2= 45°C

P (cond) = 17.85 bar from steam table

At 0°C, P_{evap} = 1.902 bar (steam table)

From steam table,

$h_1 = h_g$ = 1444.4kJ/kg (saturated vapor 0°C)

$h_2 = h_g$ = 1474.4kJ/kg (saturated vapor 40°C)

$h_3 = h_g$ = 396.8kJ/kg (saturated vapor -45°C)

But $h_3 = h_4$ (throttling process)

Refrigerating effect (RE) = $h_1 - h_4$

= 1444.4 – 396.8

= 1047.6kJ/kg

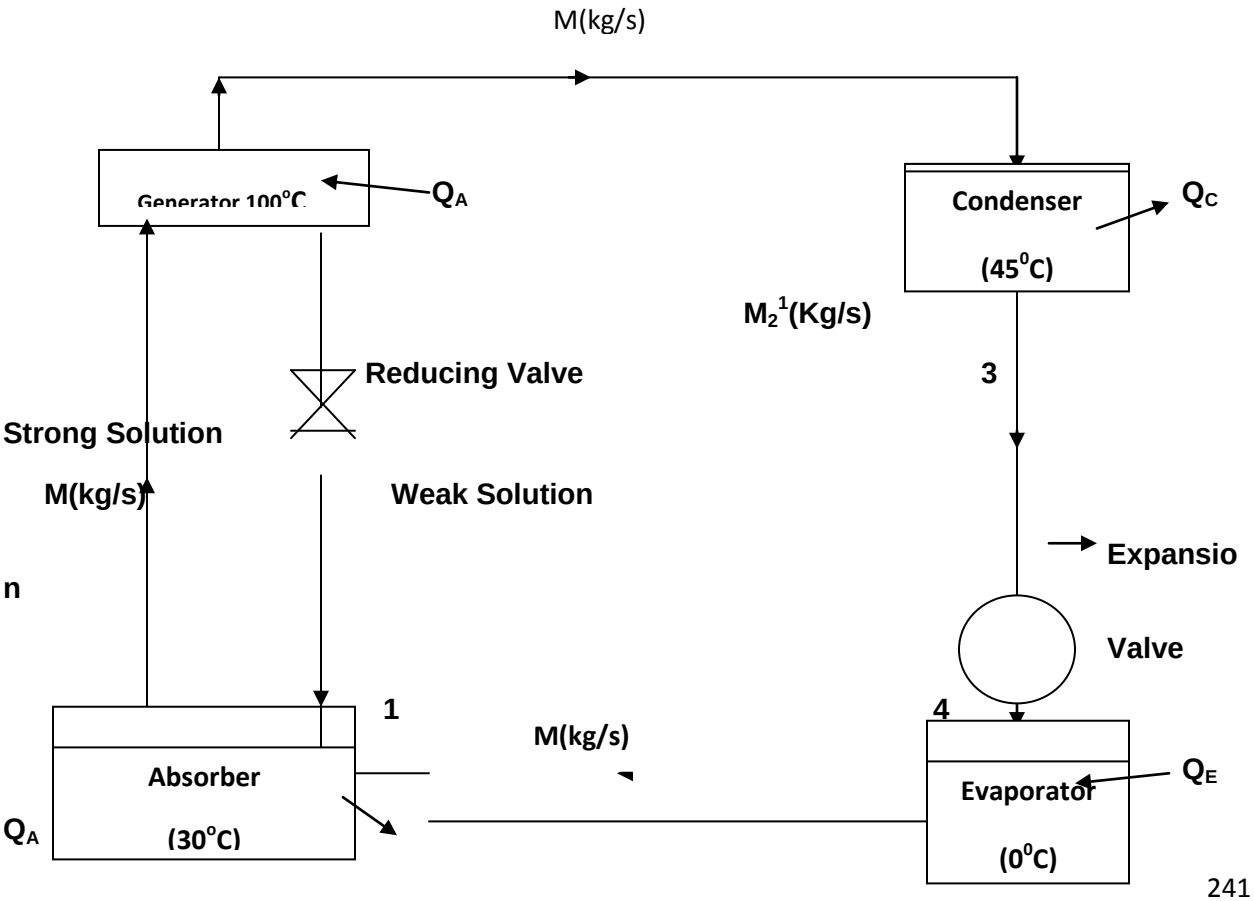
M(kg/s)
Generator 100°C
Q_A
Condenser
(45°C)
Q_C
M_2^1(Kg/s)
Reducing Valve
3
Strong Solution
M(kg/s)
Weak Solution
Expansio
n
Valve
1
4
M(kg/s)
Absorber
(30°C)
Q_A
Evaporator
(0°C)
Q_E

Assumed Saturated Vapour

Fig 5 Schematic arrangement of vapour absorption System

Table 1 : showing the enthalpy, ammonic concentration x weight fraction at some selected points along the flow above.

Point in the figure	Ammonic concentration	Enthalpy h (kJ/kg)
1^1	0.35	22
2^1	0.1	695
1	0.945	1420
2	0.945	1474.45
3,4	0.945	396.8

Based on the specifications given above, mass flow rate of refrigerant through the generator and absorber is 0.000745kg/s, mass flow rate of weak solution from generator is 0,00193kg/s and mass flow rate of strong solution from the absorber is 0,002682kg/s. the heat supplied to the generator is 2.39kJ/s, heat rejected in the condenser is 0.8028kJ/s, while heat rejected from the absorber is 2.345kJ/s. the coefficient of performance (COP) of the designed and developed vapour absorption system is 0.32.

4.0 CONCLUSION

In this work, an experimental absorption refrigeration system powered by a gas burner was designed and developed and the system was tested successfully.

A lot has been reviewed and analyzed about vapor Absorption Refrigeration System in this work such as its applications, material selection with their properties, various components used and their sizes, their functions, selection of suitable refrigeration-absorbent combinations with their characteristics, cooling loads and other mathematical analysis.

It was seen that if higher cooling capacity and also lower evaporator temperatures are desired from the system, the generator `s temperature should be increased considerably. In order to improve the COP of the system, combination of analyzer, rectifier and heat exchanger should be incorporated to the system and a better source of energy should be employed.

References

Adekeye, T (2006), Design and Construction of Vapor Absorption Refrigeration System, (Unpublished PGD Project) LAUTECH, Ogbomosho, Nigeria

Althouse,T.B (1935), Modern Refrigeration and Air Conditioning, Good-Heart Wilcox Company, USA

Arora, C.P (2004), Refrigeration and Air Conditioning, McGrawhill, New Delhi (India)

Bacon,D.H and Stephen,R.C (1991), Basic Thermodynamic and Heat transfer, Butter Worth and Co. Ltd ,London.

Boast, M.F.G (1992), Cooling Loads Capacity, 2nd Edition, CBS, Delhi (India)

Eastop, T.D and Conkey,M.C (1993), Applied Thermodynamic, 5th edition, Longman, London.

Enibe, S.O (1997),"Solar Refrigeration for Rural Application energy" Elselver Science Ltd., Britain, Vol 12, No2, Page 157-158.

Omoniyi E B (2003), Design and Construction of Vapor Absorption System for Rural Dwellers,(Unpublished B.Tech Project), LAUTECH, Ogbomosho, Nigeria

Rajput, R. K (2006), Refrigeration and Air Conditioning, Kateria and Son, Delhi(India),page 438-446.

Williams, D.A (1955), "Intermittent Absorption Cooling System", General Refrigeration, Engineering Journal, pg 132.

Sobamowo et al: Proc. ICCEM (2012) 243 - 259

Experimental and numerical investigations of free convection heat transfer in solar oven

Sobamowo M.G., Ogunmola B.Y., Ismail S.O.

Department of Mechanical Engineering, University of Lagos, Akoka, Lagos, Nigeria.

Phone: +2348055444285, +2347034717417 ; **E-mail**- mikegbeminiyiprof@yahoo.com

Abstract

The use of solar energy for baking, heating or drying represents a sustainable way of solar energy applications with negligible negative effects. Solar oven is an alternative to conventional oven that rely heavily on coal and wood or Electric oven that uses the power from the National grid of which the end users have little or no control. Since the Solar oven uses no fuel and it cost nothing to run, it use are widely promoted especially in situations where minimum fuel consumption or fire risks are considered highly important. As useful as the Solar Oven proved, it major setback in the area of applications has been its future sustainability. For the use of Solar Oven/Cookers to be sustained in the future, the design and development of solar oven must rely on sound analytical tools. Therefore, this work focused on the design and development of the solar oven. To test the performance of the Small Solar Oven a 5000cm^3 beaker of water was put into the Oven and the temperature of the water was found to reach 81^{0}C after about 3hrs under an average ambient temperature of 30^{0}C. On no load test, the oven reached a maximum temperature of 112^{o}C in 6hrs. In order to carry out the parametric studies and improve the performance of the Solar Oven, Mathematical models were developed and solved by using Characteristics-Based Split (CBS) Finite Element Method. The Model results were compared with the Experimental results and a good agreement ware found between the two results.

Key words: *Solar Oven; Free Convection; Heat Transfer; CBS Finite Element Method*

1. Introduction

The world rapidly growing population and exploding energy demands coupled with the climatic profile, socio-economic development, energy supply infrastructures and the threats on health and environment accompanying the utilization of fossil fuels strongly suggest the use of renewable energy powered systems. In fact, the strategies for attaining balance between energy demands and effects in various countries has provoked vast majority in considering the alternative sources. Furthermore, the convergence of rapidly rising costs, dwindling and threatened supply of fossil fuel are stimulating renewed efforts to find viable energy alternatives. Some of the proposed alternatives such as large scale use of bio-fuels may not be achievable or sustainable-or, eventually practical. Some other interesting possibilities such as geothermal energy may be viable but are local and limited. Solar energy that is virtually an inexhaustible natural source produces little or no greenhouse gases. It is known as a clean and environmental friendly energy source. Aside from the indisputable advantages of solar energy mentioned above, the consideration of harnessing solar energy among all other alternative sources of energy sources to meet the needs especially in developing countries is based on well established visibility studies. Firstly, most of the countries called developing, like Nigeria, are in or adjacent to the tropics and have good solar radiation available as shown in Fig.1. Secondly, energy is a critical need of these countries but they do not have widely distributed readily available supplies of conventional energy resources. Thirdly, most of the developing countries are characterized by arid climates, dispersed and inaccessible populations and a lack of investment capital and are thus faced with practically insuperable obstacles to the provision of energy by conventional means, for example, by electrification. In contrast to this, solar energy is readily available and is already distributed to the potential users. Fourthly, because of the diffuse nature of solar energy the developments all over the world, the energy source has been in smaller units which fit well into the pattern of rural economics.

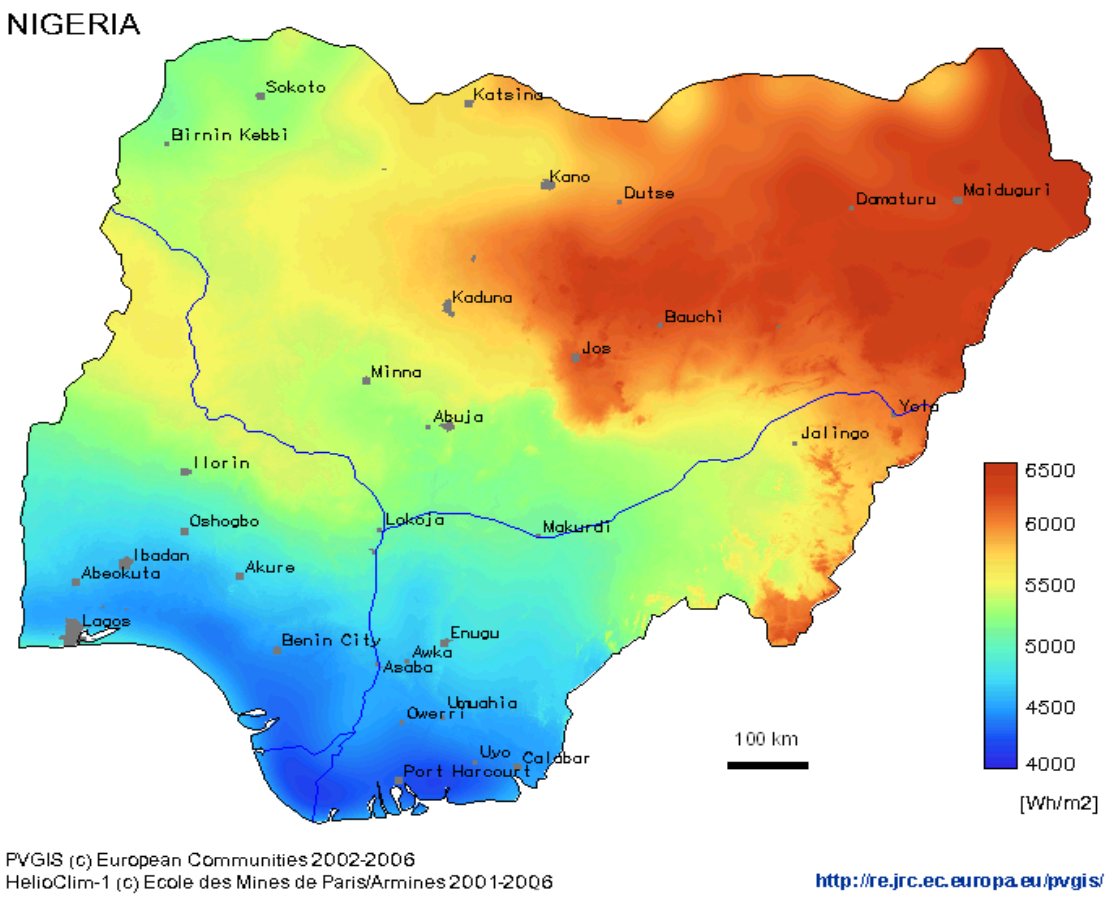

Fig.1 Solar insolation in different States in Nigeria

The abundant solar radiation in the tropical and subtropical regions proved solar energy as the most attractive a1ternative energy source for baking, cooking, drying and heating. A number of government, non-government and private organizations along with a few research institutions and other individual researchers (Reddy et al, 1979; Mumba, 1995; Oosthuizen, 1995; Wisniewski and Pietruszko, 1997, Adelaja et al, 2009, Muhammad *et al*, 2011) have applied the knowledge of solar radiation on the earth surface for the fabrication, promotion and dissemination of different types of solar dryer (direct, indirect and mixed-mode types) in developing countries. In meeting the essential and basic need of human being, wood and fossil fuel as sources of energy for cooking food have played tremendous and invaluable roles. However, the direct combustion of wood and fossil fuel as the major sources of cooking has immensely contributed to global warming and acid rains. Aside from these adverse effects, the inhalation of these gases irritates the lungs and the eyes and can cause diseases such as pneumonia. In order to obviate or eliminate this problem, a lot of researchers have developed different solar ovens/cookers over the years (Lof, 1965; Duffie *et al,* 1974; Daniel, 1990; Halacy *et al*; 1992, Wary, 1992, Warren, 1994, Barbara, 1994, Malik et al, 1996, Frederick, *et al*, 1997, Kulkarni *et al*, 1997, Adegoke, *et al*, 1998; Patel *et al*, 2000, Felix, *et al*, 2002, Amer, 2003; Ekechukwu *et al*, 2003; Folmer *et al,* 2003, Volker, 2003, 2004, Fronco et al, 2004, Negi *et al*, 2005; Hussein *et al*, 2008; Uhuegbu, 2011; Tuara and Musa, 2012). The range of temperature achieved in most of these ovens/cookers (80^{o}C-100^{o}C) is most suitable for cooking by boiling. Talking about the advantages, this application of solar energy has been assisting in preventing deforestation, saving of fossil fuel and reduction in

utility bills in most countries. Also, since the solar oven uses no fuel, it cost nothing to run and therefore, it use are widely promoted especially in situations where minimum fuel consumption or fire risks are considered highly important. However, as useful as the Solar Oven proved, it major setback in the area of applications has been its future sustainability. For the use of Solar Oven/Cookers to be sustained in the future, the design and development of solar oven must rely on sound analytical tools. Also, to understand the physical phenomena of solar oven and to optimize the performance of the forced convection solar dryer, theoretical investigation is essential. An adventure into the analytical methods in solving the resulting conservation equations for the theoretical investigations of the performance and optimisation of the Oven has proven abortive and over the years, recourse has been made to numerical methods such as Finite difference or Finite volume methods in analysing such class of problems involving conduction, convection and sometimes diffusion. The finite element method has been somehow stated to be limited to Computational Solid Mechanic or at its best in Thermo-Fluid problems, conductive heat transfer. Actually, for most conduction equations in heat transfer problems, the finite element method especially Galerkin Method is straight forward. However, if similar Garlerkin type approximation is applied in the solution of convection equations, the results will be marked with spurious oscillations in space if certain parameters exceed a critical value, element peclet number. This method is not unique to finite elements as all other spatial discretization techniques techniques have difficulties (Lewis et al, 2009). Direct application of the Characteristic Galerkin scheme to solve the momentum equation is difficult. Therefore, In this work, a Characteristic Based Split (CBS) scheme which satisfies the well-known Babuska-Brezzi condition (21, 22) as proposed by Lewis et al (20) is used to analysis and simulate the heat transfer in a photovoltaic-powered forced convection solar dryer. In order to optimize the performance of the solar dryer, the developed finite element models were used to investigate the effects of the blower speeds and the solar dryer chamber aspect ratios on the temperature distribution, velocity distribution and the pressure drop in the drying chamber.

2. The Working Principle of Solar Oven and Experimental Set up

When solar energy is radiated on the solar collector of the solar oven, some of energy is reflected, some is absorbed; or some of it passes right through. But only the absorbed energy is converted heat energy in the enclosure of the solar oven. When food is placed in this solar oven enclosure, moisture at the surface is evaporated and removed by the hot air and the low humidity of air in the oven. This establishes moisture vapour pressure gradient, which causes movement of moisture form the interior of the food to the surface. Depending on the nature of the food and the rate of heating when the extent of moisture loss exceeds the rate of movement from the interior, the zone of evaporation moves inside the food, the surface dried out, the temperature rise to the temperature of the hot air (119°-240°C) and a crust is formed (Halacy, 1978) but the internal temperature of the food does not exceed 100°C cause baking takes place at atmospheric pressure and moisture escape freely from the food.

Fig. 2 Physical model of the solar oven

Since the food does not reach too high temperature in the oven, it can safely be left in the cooker all day without burning. Depending on the latitude and The two test carried above was conducted on solar oven. The results obtained are shown in the Fig.13 and Fig .14. The test at load which involved placing of 500cm^3 beaker of water.

3. Model development for the solar oven

The numerical investigations of the solar oven involve setting up mathematical models. In order to achieve this, a set of conservation equations were set up for the numerical analysis

weather, food can be cooked or baked either early or later in the day. The cooker can also be used to warm food, drinks and pasteurize water or milk.

3.1 Conservation Equations for the Analysis of Solar Oven

The following set of conservation equations were used for the finite element analysis.

Continuity Equation.

$$\frac{\partial u}{\partial x} + \frac{\partial v}{\partial y} = 0 \qquad (1)$$

x-momentum equation.

$$\frac{\partial u}{\partial t} + u\frac{\partial u}{\partial x} + v\frac{\partial u}{\partial y} = -\frac{1}{\rho}\frac{\partial p}{\partial x} + v\left[\frac{\partial^2 u}{\partial x^2} + \frac{\partial^2 u}{\partial y}\right] \qquad (2)$$

y-momentum equation.

$$\frac{\partial v}{\partial t} + u\frac{\partial v}{\partial x} + v\frac{\partial v}{\partial y} = -\frac{1}{\rho}\frac{\partial p}{\partial y} + v\left[\frac{\partial^2 v}{\partial x^2} + \frac{\partial^2 v}{\partial y^2}\right] + \beta g(T - T_o) \qquad (3)$$

Energy Equation.

$$\frac{\partial T}{\partial t} + u\frac{\partial T}{\partial x} + v\frac{\partial T}{\partial y} = \alpha\left[\frac{\partial^2 T}{\partial x^2} + \frac{\partial^2 T}{\partial y^2}\right] \qquad (4)$$

The initial conditions used in this model are:

$$t = 0, \quad u = 0, \quad v = 0, \quad T = T_\infty, \quad p = p_\infty \quad for\ 0 < x < L, 0 < y < L$$

The boundary conditions used in this model are:

$$t > 0, \quad y = 0, \quad u = v = 0, \quad \frac{\partial T}{\partial y} = 0, \quad \frac{\partial p}{\partial y} = 0 \quad for\ 0 < x < L$$

$$t > 0, \quad y = L, \quad u = v = 0, \quad T = T_w, \quad p = p_m \quad for\ 0 < x < L$$

$$t > 0, \quad x = 0 \quad u = v = 0, \quad \frac{\partial T}{\partial x} = 0, \quad \frac{\partial p}{\partial x} = 0 \quad for\ 0 < y < L$$

$$t > 0, \quad x = L \quad u = v = 0, \quad \frac{\partial T}{\partial x} = 0, \quad \frac{\partial p}{\partial x} = 0 \quad for\ 0 < y < L$$

5a

To obtain the non-dimensional form of the equation, the following non-dimentional scales are used.

$$X = \frac{x}{L}, \ Y = \frac{y}{L}, \ \tau = \frac{tu_\infty}{L}, \ U = \frac{u}{U_\infty}, \ V = \frac{v}{U_\infty}, \ P = \frac{p}{\rho U^2{}_\infty}, \ \theta = \frac{T - T_\infty}{T_W - T_\infty}$$

5b

Where L is the characteristics dimention, T_w is the wall temperature (reference temperature) and U_∞ is the free stream velocity.

On substituting the above scales into the equations(1-4), we have:

Continuity equation.

$$\frac{\partial U}{\partial X} + \frac{\partial V}{\partial Y} = 0 \qquad 6$$

X-momentum equation.

$$\frac{\partial V}{\partial \tau} + U\frac{\partial U}{\partial X} + V\frac{\partial U}{\partial Y} = -\frac{\partial P}{\partial Y} + \frac{1}{Re}\left(\frac{\partial^2 U}{\partial X^2} + \frac{\partial^2 U}{\partial X^2}\right) \qquad 7$$

Y-momentum equation.

$$\frac{\partial V}{\partial \tau} + U\frac{\partial V}{\partial X} + V\frac{\partial V}{\partial Y} = -\frac{\partial P}{\partial Y} + \frac{1}{Re}\left(\frac{\partial^2 V}{\partial X^2} + \frac{\partial^2 V}{\partial X^2}\right) + \frac{Gr}{Re^2}\theta \qquad 8$$

Energy Equation.

$$\frac{\partial \theta}{\partial \tau} + U\frac{\partial \theta}{\partial X} + V\frac{\partial \theta}{\partial Y} = \frac{1}{RePr}\left(\frac{\partial^2 \theta}{\partial X^2} + \frac{\partial^2 \theta}{\partial X^2}\right) \qquad 9$$

or

$$\frac{\partial \theta}{\partial \tau} + U\frac{\partial \theta}{\partial X} + V\frac{\partial \theta}{\partial Y} = \frac{1}{Pe}\left(\frac{\partial^2 \theta}{\partial X^2} + \frac{\partial^2 \theta}{\partial X^2}\right) \quad (10)$$

The initial and Boundary conditions in dimensionless form are:

$$\tau > 0, \quad Y = 0, \quad U = V = 0, \quad \frac{\partial \theta}{\partial Y} = 0, \quad \frac{\partial P}{\partial Y} = 0 \quad for\ 0 < X < 1$$

$$\tau > 0, \quad Y = 1, \quad U = V = 0, \quad T = 1, \quad P = p_m/\rho U^2 \quad for\ 0 < X < 1$$

$$\tau > 0, \quad X = 0 \quad U = V = 0, \quad \frac{\partial \theta}{\partial X} = 0, \quad \frac{\partial P}{\partial X} = 0 \quad for\ 0 < y < 1$$

$$\tau > 0,\ X = 1 \quad U = V = 0,\ \frac{\partial \theta}{\partial X} = 0,\ \frac{\partial P}{\partial X} = 0 \quad for\ 0 < y < 1 \quad (11)$$

3.2 Characteristics-Based Split (CBS) Finite Element Analysis of the Conservation Equations

For the continuity equation

$$\frac{U^n_{i+1,j} - U^n_{i,j}}{\Delta X} + \frac{V^n_{i+1,j} - V^n_{i,j}}{\Delta Y} = 0 \quad \text{or} \quad \frac{\partial U^n_{ij}}{\partial X} + \frac{\partial V^n_{ij}}{\partial X} \quad (12)$$

For the x momentum equation, the semi-discrete form is:

$$\frac{U^{n+1}_{ij} - U^n_{ij}}{\Delta \tau} = U^n_{ij}\frac{\partial U^n_{ij}}{\partial X} - V^n_{ij}\frac{\partial U^n_{ij}}{\partial Y} + \frac{1}{Re}\left(\frac{\partial^2 U_{ij}}{\partial X^2} + \frac{\partial^2 V_{ij}}{\partial Y^2}\right)^n - \frac{\partial P_{ij}}{\partial X} + U_{ij}\frac{\Delta \tau}{2}\frac{\partial}{\partial X}\left[U^n_{ij}\frac{\partial U^n_{ij}}{\partial X} + V^n_{ij}\frac{\partial U^n_{ij}}{\partial Y} + \frac{\partial P^n_{ij}}{\partial X}\right] + V_{ij}\frac{\Delta \tau}{2}\frac{\partial}{\partial Y}\left[U^n_{ij}\frac{\partial U^n_{ij}}{\partial X} + V^n_{ij}\frac{\partial U^n_{ij}}{\partial Y} + \frac{\partial P^n_{ij}}{\partial X}\right] \quad (13a)$$

For y momentum equation, the semi-discrete form is:

$$\frac{V^{n+1}_{ij} - V^n_{ij}}{\Delta \tau} = U^n_{ij}\frac{\partial V^n_{ij}}{\partial X} - V^n_{ij}\frac{\partial V^n_{ij}}{\partial Y} + \frac{1}{Re}\left(\frac{\partial^2 V_{ij}}{\partial X^2} + \frac{\partial^2 V_{ij}}{\partial Y^2}\right)^n - \frac{\partial P_{ij}}{\partial X} + U_{ij}{}^n\frac{\Delta \tau}{2}\frac{\partial}{\partial X}\left[U^n_{ij}\frac{\partial U^n_{ij}}{\partial X} + V^n_{ij}\frac{\partial}{\partial} \right.$$

$$\left.\frac{\partial P^n_{ij}}{\partial X}\right] + V_{ij}{}^n\frac{\Delta \tau}{2}\frac{\partial}{\partial Y}\left[U^n_{ij}\frac{\partial V^n_{ij}}{\partial X} + V^n_{ij}\frac{\partial V^n_{ij}}{\partial Y} + \frac{\partial P^n_{ij}}{\partial X}\right] + \frac{Gr}{Re^2}\theta^n_{ij} \quad (13b)$$

On removing the pressure from equations 13a and 13b, we arrived equation 14-15

$$\frac{U_{ij} - U^n_{ij}}{\Delta \tau} = U^n_{ij}\frac{\partial U^n_{ij}}{\partial X} - V^n_{ij}\frac{\partial U^n_{ij}}{\partial Y} + \frac{1}{Re}\left(\frac{\partial^2 U_{ij}}{\partial X^2} + \frac{\partial^2 U_{ij}}{\partial Y^2}\right)^n + U_{ij}{}^n\frac{\Delta \tau}{2}\frac{\partial}{\partial X}\left(U^n_{ij}\frac{\partial U^n_{ij}}{\partial X} + V^n_{ij}\frac{\partial U^n_{ij}}{\partial Y}\right)$$

$$+V^n_{ij}\frac{\Delta \tau}{2}\frac{\partial}{\partial Y}\left(U^n_{ij}\frac{\partial U^n_{ij}}{\partial X} + V^n_{ij}\frac{\partial U^n_{ij}}{\partial Y}\right) \quad (14)$$

$$\frac{V_{ij}-V_{ij}^{n}}{\Delta\tau}=U_{ij}^{n}\frac{\partial V_{ij}^{n}}{\partial X}-V_{ij}^{n}\frac{\partial V_{ij}^{n}}{\partial Y}+\frac{1}{Re}\left(\frac{\partial^{2}V_{ij}}{\partial X^{2}}+\frac{\partial^{2}V_{ij}}{\partial Y^{2}}\right)^{n}+U_{ij}^{n}\frac{\Delta\tau}{2}\frac{\partial}{\partial X}\left(U_{ij}^{n}\frac{\partial U_{ij}^{n}}{\partial X}+V_{ij}^{n}\frac{\partial U_{ij}^{n}}{\partial Y}\right)+$$
$$V_{ij}^{n}\frac{\Delta\tau}{2}\frac{\partial}{\partial Y}\left(U_{ij}^{n}\frac{\partial V_{ij}^{n}}{\partial X}+V_{ij}^{n}\frac{\partial V_{ij}^{n}}{\partial Y}\right)+\frac{Gr}{Re^{2}}\theta_{ij}^{n}$$

15

On substracting equation 14 and 15 from equations 13a and 13b respectively, we obtained the real velocity field equations(velocity or momentum correction equations) as:

$$\frac{U_{ij}^{n+1}-\breve{U}_{ij}}{\Delta\tau}=-\frac{\partial P^{n}}{\partial X}+U\frac{\Delta\tau}{2}\frac{\partial}{\partial X}\left(\frac{\partial P}{\partial X}\right)^{n}+V\frac{\Delta\tau}{2}\frac{\partial}{\partial X}\left(\frac{\partial P}{\partial X}\right)^{n}$$

16

$$\frac{V_{ij}^{n+1}-\breve{V}_{ij}}{\Delta\tau}=-\frac{\partial P^{n}}{\partial Y}+U\frac{\Delta\tau}{2}\frac{\partial}{\partial X}\left(\frac{\partial P}{\partial X}\right)^{n}+V\frac{\Delta\tau}{2}\frac{\partial}{\partial Y}\left(\frac{\partial P}{\partial Y}\right)^{n}$$

17

On differentiating equation 17 with respect to X and also with respect to Y and adding the resulting equations together neglecting third-order terms gives.

$$\frac{\partial U_{ij}^{n+1}}{\partial X}+\frac{\partial V_{ij}^{n+1}}{\partial Y}-\frac{\partial \breve{U}_{ij}}{\partial X}-\frac{\partial \breve{V}_{ij}}{\partial Y}=-\Delta\tau\left(\frac{\partial^{2}P_{ij}}{\partial X^{2}}+\frac{\partial^{2}P_{ij}}{\partial Y^{2}}\right)^{n}$$

18

Which gives the pressure caculation

$$\left(\frac{\partial^{2}P_{ij}}{\partial X^{2}}+\frac{\partial^{2}P_{ij}}{\partial Y^{2}}\right)^{n}=\frac{1}{\Delta\tau}\left(\frac{\partial \breve{U}_{ij}{}^{n}}{\partial X}+\frac{\partial \breve{V}_{ij}{}^{n}}{\partial Y}\right)$$

19

Since (continuity equation);

$$\frac{\partial U_{ij}^{n+1}}{\partial X}+\frac{\partial V_{ij}^{n+1}}{\partial Y}=0$$

20

Temperature Calculation

On applying the characteristic Galerkin procedure to the temperature equation (11), it gives:

$$\frac{\theta_{ij}^{n+1}-\theta_{ij}^{n}}{\Delta t} = U_{ij}^{n}\frac{\partial \theta^{n}}{\partial X} - V_{ij}^{n}\frac{\partial \theta_{ij}^{n}}{\partial Y} + \frac{1}{RePr}\left(\frac{\partial^2 \theta_{ij}}{\partial X^2} + \frac{\partial^2 \theta_{ij}}{\partial Y^2}\right)^{n} + U\frac{\Delta\tau}{2}\frac{\partial}{\partial X}\left(U\frac{\partial \theta}{\partial X} + V\frac{\partial \theta}{\partial Y}\right) + V\frac{\Delta\tau}{2}\frac{\partial}{\partial Y}\left(U\frac{\partial \theta}{\partial X} + V\frac{\partial \theta}{\partial Y}\right)^{n}$$

21

In summary, we have the intermediate X-momentum equation is:

$$\frac{\tilde{U}_{ij}-\tilde{U}_{ij}^{n}}{\Delta t} = U\frac{\partial u_{ij}^{n}}{\partial X} - V\frac{\partial u_{ij}^{n}}{\partial X} + \frac{1}{Re}\left(\frac{\partial^2 U_{ij}}{\partial X^2} + \frac{\partial^2 U_{ij}}{\partial Y^2}\right)^{n} + U_{ij}^{n}\frac{\Delta\tau}{2}\frac{\partial}{\partial X}\left(U_{ij}^{n}\frac{\partial V_{ij}}{\partial X} + V\frac{\partial V_{ij}}{\partial Y}\right)^{n} + V_{ij}^{n}\frac{\Delta\tau}{2}\frac{\partial}{\partial Y}\left(U_{ij}^{n}\frac{\partial U_{ij}}{\partial X} + V\frac{\partial U_{ij}}{\partial Y}\right)$$

22

And the intermediate Y-momentum equation is:

$$\frac{\tilde{V}_{ij}-\tilde{V}_{ij}^{n}}{\Delta t} = U_{ij}\frac{\partial V_{ij}^{n}}{\partial X} - V\frac{\partial V_{ij}^{n}}{\partial Y} + \frac{1}{Re}\left(\frac{\partial^2 V_{ij}}{\partial X^2} + \frac{\partial^2 V_{ij}}{\partial Y^2}\right)^{n} + U_{ij}^{n}\frac{\Delta\tau}{2}\frac{\partial}{\partial X}\left(U_{ij}^{n}\frac{\partial V_{ij}}{\partial X} + V\frac{\partial V_{ij}}{\partial Y}\right)^{n} + V_{ij}^{n}\frac{\Delta\tau}{2}\frac{\partial}{\partial Y}\left(U\frac{\partial U_{ij}}{\partial X} + V\frac{\partial U_{ij}}{\partial Y}\right)$$

23

Pressure Calculation

$$\left(\frac{\partial^2 P_{ij}}{\partial X^2} + \frac{\partial^2 P_{ij}}{\partial Y^2}\right)^{n} = \frac{1}{\Delta\tau}\left(\frac{\partial \tilde{U}_1}{\partial X} + \frac{\partial \tilde{V}}{\partial Y}\right)$$

24

Temperature equation

$$\frac{\theta_{ij}^{n+1}-\theta_{ij}^{n}}{\Delta t} = U_{ij}^{n}\frac{\partial \theta^{n}}{\partial X} - V_{ij}^{n}\frac{\partial \theta_{ij}^{n}}{\partial Y} + \frac{1}{RePr}\left(\frac{\partial^2 \theta_{ij}}{\partial X^2} + \frac{\partial^2 \theta_{ij}}{\partial Y^2}\right)^{n} + U\frac{\Delta\tau}{2}\frac{\partial}{\partial X}\left(U\frac{\partial \theta}{\partial X} + V\frac{\partial \theta}{\partial Y}\right) + V\frac{\Delta\tau}{2}\frac{\partial}{\partial Y}\left(U\frac{\partial \theta}{\partial X} + V\frac{\partial \theta}{\partial Y}\right)^{n}$$

25

Spatial Discretization

Applying the standard Galerkin approximation for solving equations 20-25, assuming linear interpolation functions for all variables, the spatial variation for a linear triangular element may be written as :

$$U = N_i U_i + N_j U_j + N_k U_k = [N][U]$$

26

$$V = N_i V_i + N_j V_j + N_k V_k = [N][V] \quad 27$$

$$P = N_i P_i + N_j P_j + N_k P_k = [N][P] \quad 28$$

$$\theta = N_i\theta_i + N_j\theta_j + N_k\theta_k = [N][\theta] \quad 29$$

After performing spatial discretization, the Element Mass Matrix from the Characteristics-Based Split scheme is

$$[M_e] = \frac{A}{12}\begin{bmatrix} 2 & 1 & 1 \\ 1 & 2 & 1 \\ 1 & 1 & 2 \end{bmatrix}$$

30

And the Element Convection Matrix

$$[C_e] = \frac{1}{24}\begin{bmatrix} (wsw+u_i)b_i & (wsw+u_i)b_j & (wsw+u_i)b_k \\ (wsw+u_j)b_i & (wsw+u_j)b_j & (wsw+u_j)b_k \\ (wsw+u_k)b_i & (wsw+u_k)b_j & (wsw+u_k)b_k \end{bmatrix} + \frac{1}{24}\begin{bmatrix} (wrw+u_i)c_i & (wrw+u_i)c_j & (wrw+u_i)c_k \\ (wrw+u_j)c_i & (wrw+u_j)c_j & (wrw+u_j)c_k \\ (wrw+u_k)c_i & (wrw+u_k)c_j & (wrw+u_k)c_k \end{bmatrix}$$

31

Where

$$wsw = u_i + u_j + u_k$$

$$wrw = v_i + v_j + v_k$$

$$[K_e] = \frac{Re}{4A}\begin{bmatrix} b_i^2 & b_ib_j & b_ib_k \\ b_jb_i & b_j^2 & b_jb_k \\ b_kb_i & b_kb_j & b_k^2 \end{bmatrix} + \frac{Re}{4A}\begin{bmatrix} c_i^2 & c_ic_j & c_ic_k \\ c_jc_i & c_j^2 & c_jc_k \\ c_kc_i & c_kc_j & c_k^2 \end{bmatrix}$$

32

For the momentum diffussion, we have;

$$[K_{te}] = \frac{P_r}{4A}\begin{bmatrix} b_i^2 & b_ib_j & b_ib_k \\ b_jb_i & b_j^2 & b_jb_k \\ b_kb_i & b_kb_j & b_k^2 \end{bmatrix} + \frac{P_r}{4A}\begin{bmatrix} c_i^2 & c_ic_j & c_ic_k \\ c_jc_i & c_j^2 & c_jc_k \\ c_kc_i & c_kc_j & c_k^2 \end{bmatrix}$$

33

And for the Heat diffusion and Stabilization Matrix

$$[K_{se}] = \frac{U_{av}}{12}\begin{bmatrix} b_i^2 & b_i b_j & b_i b_k \\ b_j b_i & b_j^2 & b_j b_k \\ b_k b_i & b_k b_j & b_k^2 \end{bmatrix} + \frac{U_{av}}{12}\begin{bmatrix} b_i c_i & b_i c_j & b_i c_k \\ b_j c_i & b_j c_j & b_j c_k \\ b_k c_i & b_k c_j & b_k c_k \end{bmatrix} + \frac{V_{av}}{12A}\begin{bmatrix} c_i b_i & c_i b_j & c_i b \\ c_j b_i & c_j b_j & c_j b \\ c_k b_i & c_k b_j & c_k b \end{bmatrix}$$

$$\frac{V_{av}}{12A}\begin{bmatrix} c_i^2 & c_i c_j & c_i c_k \\ c_j c_i & c_j^2 & c_j c_k \\ c_k c_i & c_k c_j & c_k^2 \end{bmatrix}$$

34

Where $U_{av}$and V_{av} are the average values of U and V over the element. The discretization of the CBS steps requires three more matrices and four forcing vectors to complete the process. The matrix from the discretized second-order terms for pressure calculations is:

$$K = \frac{1}{4A}\begin{bmatrix} b_i^2 & b_i b_j & b_i b_k \\ b_j b_i & b_j^2 & b_j b_k \\ b_k b_i & b_k b_j & b_k^2 \end{bmatrix} + \frac{1}{4A}\begin{bmatrix} c_i^2 & c_i c_j & c_i c_k \\ c_j c_i & c_j^2 & c_j c_k \\ c_k c_i & c_k c_j & c_k^2 \end{bmatrix}$$

35

The first gradient matrix in the X-direction is:

$$[G_u] = \frac{1}{6}\begin{bmatrix} b_i & b_j & b_k \\ b_i & b_j & b_k \\ b_i & b_j & b_k \end{bmatrix}$$

36

And the second-gradient matrix in the Y-direction is

$$[G_v] = \frac{1}{6}\begin{bmatrix} c_i & c_j & c_k \\ c_i & c_j & c_k \\ c_i & c_j & c_k \end{bmatrix}$$

37

The forcing vectors of the X-component of the momentum equation is:

$$[f_1] = \frac{\Gamma}{4A} Re \begin{bmatrix} b_i u_i & b_j u_j & b_k u_k \\ b_i u_i & b_j u_j & b_k u_k \\ 0 & 0 & 0 \end{bmatrix}^n n_u + \frac{\Gamma}{4A} Re \begin{bmatrix} c_i u_i & c_j u_j & c_k u_k \\ c_i u_i & c_j u_j & cb_k u_k \\ 0 & 0 & 0 \end{bmatrix}^n n_v$$

38

Where $i\ j$ is the boundary edge of an element.

The forcing vector of the Y- component momentum equation is:

$$[f_2] = \frac{\Gamma}{4A} Re \begin{bmatrix} b_i v_i & b_j v_j & b_k v_k \\ b_i v_i & b_j v_j & b_k v_k \\ 0 & 0 & 0 \end{bmatrix}^n n_u + \frac{\Gamma}{4A} Re \begin{bmatrix} c_i v_i & c_j v_j & c_k v_k \\ c_i v_i & c_j v_j & c_k v_k \\ 0 & 0 & 0 \end{bmatrix}^n n_v \quad 39$$

The forcing vector from the discretion of the second-order pressure terms in pressure calculations is:

$$[f_3] = \frac{\Gamma}{4A} \begin{bmatrix} b_i P_i & b_j P_j & b_k P_k \\ b_i P_i & b_j P_j & b_k P_k \\ 0 & 0 & 0 \end{bmatrix}^n n_u + \frac{\Gamma}{4A} \begin{bmatrix} c_i P_i & c_j P_j & c_k P_k \\ c_i P_i & c_j P_j & c_k P_k \\ 0 & 0 & 0 \end{bmatrix}^n n_v \quad 40$$

Finally, the forcing term due to the discretization of the second-order terms in the equation is:

$$[f_4] = \frac{\Gamma}{4A} Pr \begin{bmatrix} b_i \theta_i & b_j \theta_j & b_k \theta_k \\ b_i \theta_i & b_j \theta_j & b_k \theta_k \\ 0 & 0 & 0 \end{bmatrix}^n n_u + \frac{\Gamma}{4A} P_r \begin{bmatrix} c_i \theta_i & c_j \theta_j & c_k \theta_k \\ c_i \theta_i & c_j \theta_j & c_k \theta_k \\ 0 & 0 & 0 \end{bmatrix}^n n_v \quad 41$$

The four steps of the characteristic based split scheme may now be written in matrix form.

Step 1: Intermediate Velocity Calculation X-Component

$$\left[\boldsymbol{M} \frac{\Delta[\tilde{U}]}{\Delta t}\right] = -[\boldsymbol{C}][\boldsymbol{U}]^n - [\boldsymbol{K_m}][\boldsymbol{U}]^n - [\boldsymbol{K_b}][\boldsymbol{U}]^n + [\boldsymbol{f_1}] \quad 42$$

Intermediate Velocity Calculation Y-Component

$$\left[M\frac{\Delta[\tilde{U}]}{\Delta t}\right] = -[C][V]^n - [K_m][V]^n - [K_s][V]^n + [f_2] \quad (43)$$

Step 2: Pressure Calculation

$$[K][P]^n = -\frac{1}{\Delta t}[G_u]\left[\tilde{U}\right] + [G_u]\left[\tilde{V}\right] + [f_3] \quad (44)$$

Step 3: Velocity Correction

$$[M][U]^{n+1} = [M]\left[\tilde{U}\right] - \Delta\tau[G_v][P]^n \quad (45a)$$

$$[M][V]^{[n+1} = [M]\left[\tilde{V}\right] - \Delta\tau[G_v][P]^n \quad (45b)$$

Step 4: Temperature Computation

$$\left[M\frac{\Delta[\theta]}{\Delta t}\right] = -[C][\theta]^n - \left[K_f\right][\theta]^n - [K_s][\theta]^n + [f_4] \quad (46)$$

4. Results and Discussion

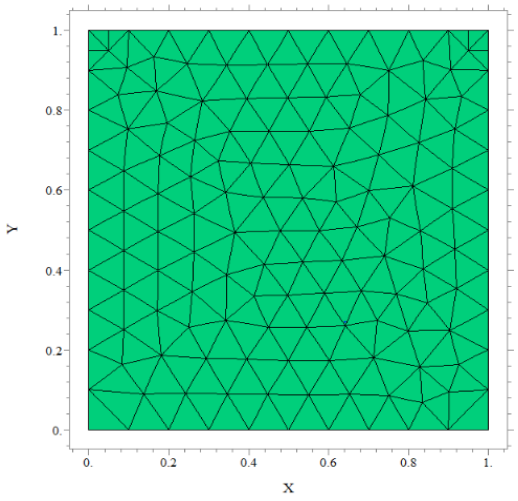

Fig.3 The Finite Element discretization of the solar oven enclosure

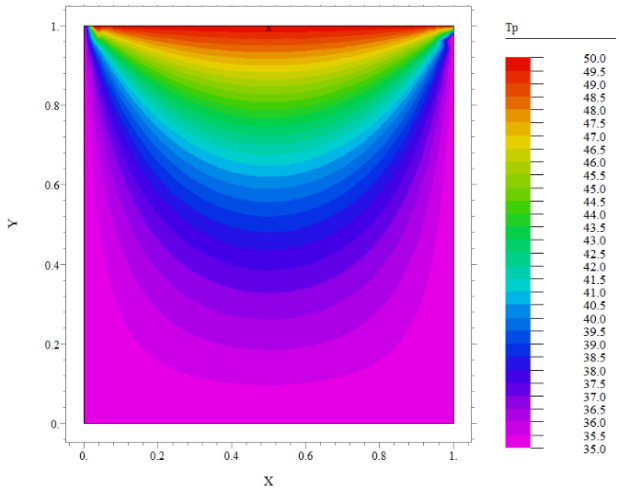

Fig.4 Temperature distribution in the oven after 30mins

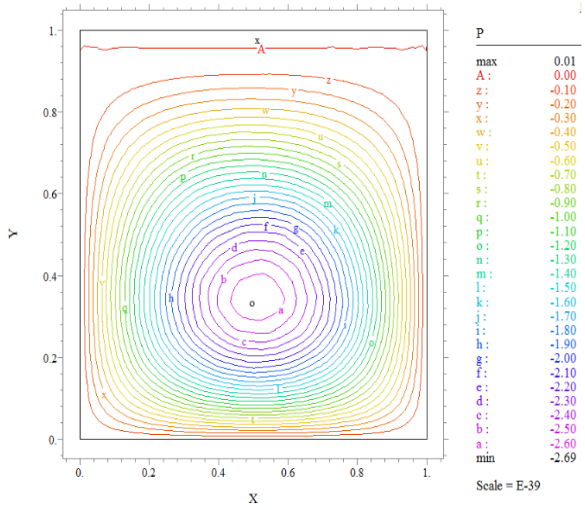

Fig.5 Pressure distribution in the oven after 30mins 30mins

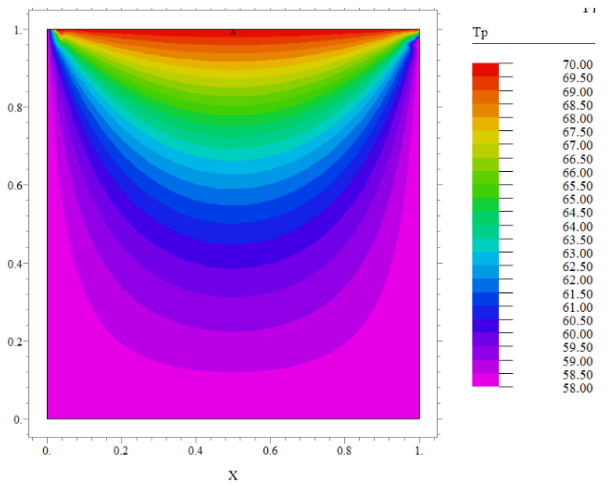

Fig.6 Temperature distribution in the oven after 2hrs 30mins

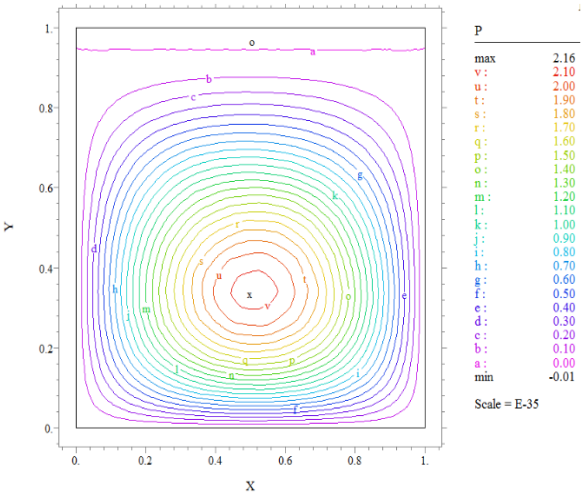

Fig.7 Pressure distribution in the oven after 2hrs 30mins 30mins

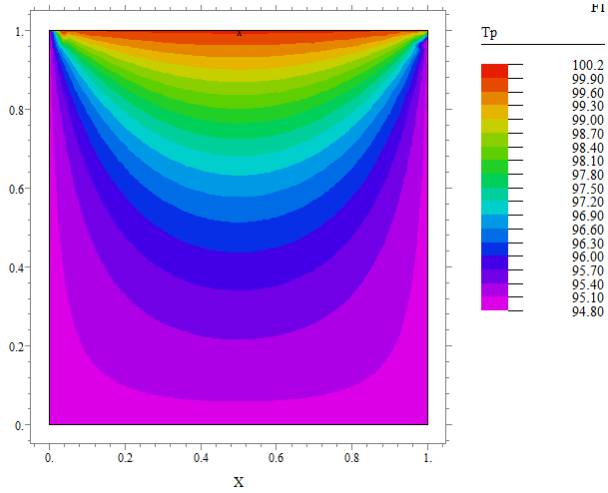

Fig.8 Temperature distribution in the oven after 4hrs 30mins

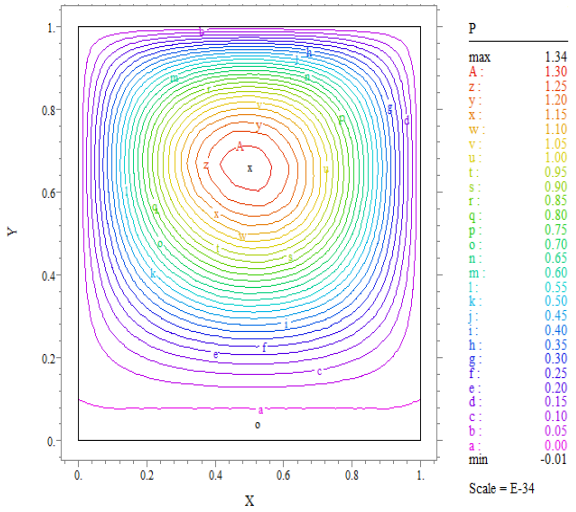

Fig.9 Pressure distribution in the oven after 4hrs 30mins

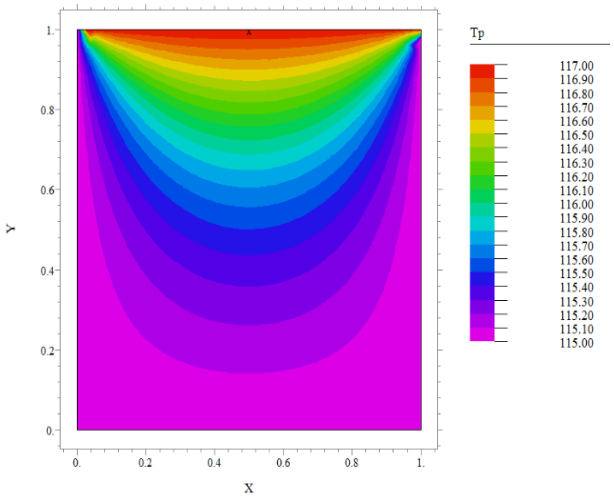

Fig.10 Temperature distribution in the oven after 6hrs

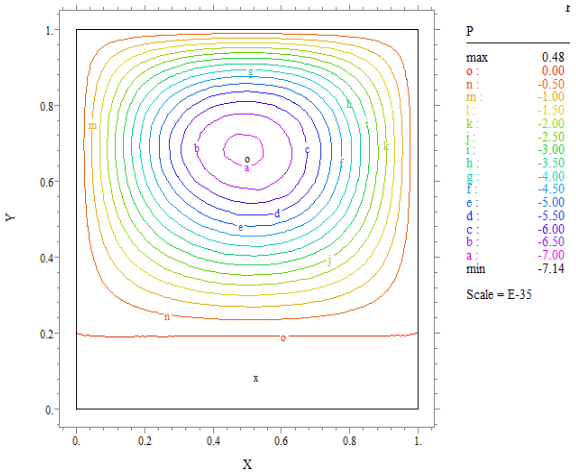

Fig.11 Pressure distribution in the oven after 6hrs

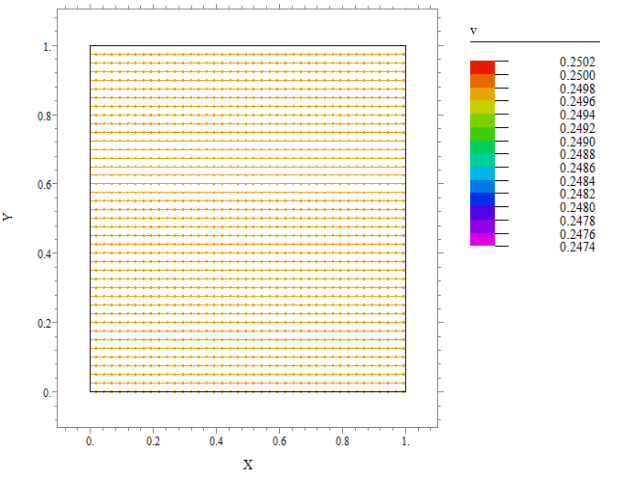

Fig.12 Velocity distribution in the oven after 6hrs

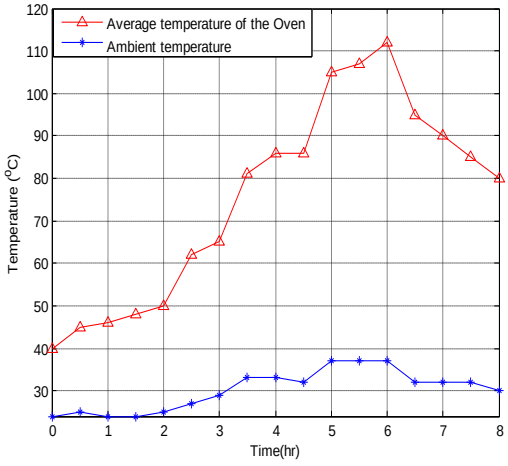

Fig.13 Experimental results of the solar oven

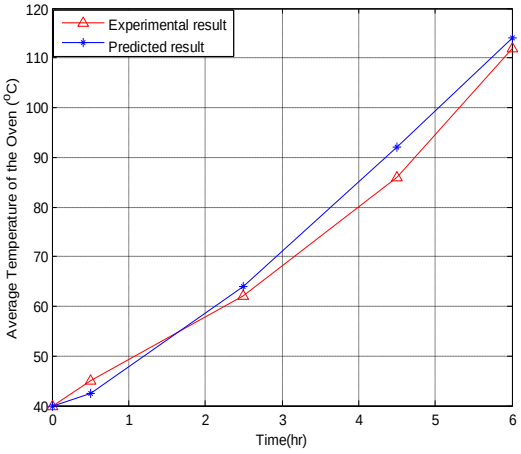

Fig.14 Comparison of Experimental results with model results

Fig. 3-12 show the temperature pressure, and velocity distributions as predicted from the numerical analysis of the solar oven. The figures display the variation and the distributions in colours and contours. The simulated results shown above are the results of what happened in the Solar oven chamber during a period of 6hours of maximum insolation.

Fig.13 shows the experimental results of the average temperature of the solar oven and the ambient. The test was set out around 8am of 8th October, 2005. From the results, it was discovered that the time taken for the oven to attain a maximum temperature of 112°C was 6hours without the average insolation on no load. Fig. 14 shows the comparison of the predicted results with the experimental results. As it could be seen from the figure, a good agreement was achieved between the predicted results of the numerical analysis and the experimental results.

5. CONCLUSION

In this work, mathematical models were developed and solved by using Characteristics-Based Split (CBS) Finite Element Method to numerically investigate the temperature, velocity and pressure distributions in solar oven. The numerical results were compared with the Experimental results and a good agreement ware found between the two results. The work will greatly assist in developing and optimising the design solar oven especially for the developing countries.

Nomenclature

Gr Grashof number
Pr Prandtl number
Re Reynold Number
Pe Peclet number
t time, s
T temperature, ^{o}C
T_w Wall Temperature, ^{o}C
T_∞ Atmospheric temperature, ^{o}C
U dimensionless velocity along x-axis
u_∞ Free stream velocity, m/s
V dimensionless velocity along x-axis
x length of the drying chamber, m
X dimensionless length of the drying chamber
y breadth of the drying chamber, m
Y dimensionless breadth of the drying chamber

Symbol

α thermal diffusivity, m^2/s
θ dimensionless temperature
τ dimensionless time
ρ density, kg/m^3
μ Coefficient of dynamic viscosity, kg/ms
β Volumetric expansion coefficient

References

Adegoke, C. O. and Fasheun, T. A (1998): Performance evaluation of a solar cooker under a tropical humid climate, Nigeria Journal of Renewable Energy vol. 6, nos. 1&2 Pp 71-74

Amer, E. H (2003): Theoretical and experimental assessment of a double exposure solar cooker, Energy Conversion and Management vol. 44 Pp 2651-2663

ASAE Standards. Testing and Reporting Solar Cooker Performance. *ASAE S580* Jan 2003

Babuska."The finite element method with Lagrangian multipliers," Numer. Math., v. 20, 1973, pp. 179-192.

Barabara, P. K (1994): Solar panel cookers, a new low technology design line proceeding of the second world conference on solar cookers held between July 12 -15 Heredia Costa Rica

Bello, A.M.A., Makinde, V., Sulu, H.T., (2010), performance, tests and thermal efficiency of a constructed solar Box Cooker at aGuinea Savannah Station (Nigeria). Journal of American Science**Vol**.6 pp32

Beth, Halacy and Dan, Halacy (1992): Cooking with the sun, how to build and use solar cookers Pp. 3-6

Brezzi F. "On the existence, uniqueness and approximation of saddle-point problems arising from Lagrangian multipliers." RAIRO Ser. Rouge, v. 8. 1974, pp. 129-151

Daniel, M. K (1990): Comparative study of box type solar in Nicaragua solar and wind technology vol. 7, no. 4 Pp. 463-471

Devadas, R. P. (1992): Solar cooking experiments with different foods, Proceedings of the first world conference on solar cooking held between June

19=20 at University of the Pacific Stickton, California U.S.A Pp. 77-84
Devadas, R. P (1997): An option for cooking solar energy, proceedings of the third international conference on solar cooker use and technology, Jan. 6-10, Coimbatore 641043 Tamil Nadu India Pp. 15-17

Diso D.G, Chiromawa, N.L, Hotoro, M.A.Y. and Ali M.H., (2008), A comparative study of Solar cooker with array of reflectors and single reflector.Techno Science Africana Journal

Duffie, J. A and William, A. B (1974): Solar energy thermal processes, John Wiley Interscience, New York Pp. 20

Ekechukwu, O. V and Ugwuoke, N. T (2003): Design and measured performance of a plane reflector augmented box type solar energy cooker, Renewable Energy vol. 28 Pp. 1935-1952

Felix, A. P, Karl-Heinz, R and Martin, S (2002): Solar thermal system, successful planning and construction, Solar praxis Berling, Pp. 15-17, 101-105

Folmer, J. C and Franzen, w (2003): Study of polymer glasses by modulated differential scanning calorimetry, Stefan Journal of Chemical Education 80(7) Pp. 813-818

Franco, J., Cadena, C. and Saravia, L.: "Multiple use communal solar cookers". Solar Energy 77, pp. 217–223, 2004

Frederick, J. B and Eugene, H (1997): College Physics, Schaum's outline McGraw-Hill Pp. 346

Gary, H. P (1994): Solar cooking technology and promotional programme in India, proceedings of the second world conference on solar cookers use and technology held at Universidad National, Heredia Costa Rica

Hussein, H. M. S, El-Ghetang, H. H and Nada, S.a (2008): Experimental investigation of novel indirect solar cooker with indoor PCM thermal storage and cooking unit, Energy Conversion and Management vol. 49, Pp. 2237-2246

Kimambo, C. Z. M, (2007) Development and Performance testing of Solar cooker. Journal of Energy in South Africa. Vol. 18, No 3

Kulkarni, S. S, Joshi, J. B., Pandit, A. B and Patel, S. b (1997): Development of high efficiency concentrating solar cookers, Proceedings of the third International conference on solar cookers use and technology held between Jan 6-10 in Coimbatore, Tamil Nadu, India Pp. 244-249

Kumar, S. (2005), Estimation of Design parameters for thermal of box-type Solar cooker. Renewable Energy Journal **Vol.**30, 1117 - 1126

Lewis R.W., Nithiarasu P. and SeetharamuK.N. Fundamental of the Finite Element Method for Heat and Fluid Flow John Wiley and Sons, Ltd, 2004.
Lof, G. O. G (1963): Recent investigations in the use of solar energy for cooking, SolarEnergy vol. 7 Pp. 125

Malik, A. Q and Hamid Bin Hussen (1996): Development of a solar cooker in Brunces Darussalam, Renewable Energy vol. 7 no. 4 Pp. 419-425

Mark, A. (2009) Principles of solar cooker design. www.sciencedirect.com (15/04/2009.
Mazen, M. A., Mohammed, A. H., Salah, A. and Badran, O. (2009) Evaluation Thermal

Melanic, S (2006): Field test of the hot pot, a new solar cooker in West Africa, solar household energy Incorporated.Solar cooking for Human Development and Environment Relief

Nahar,. N. M. (1988), Performance and testing of a low cost solar water heater cum solar

Nandwani, S. S (1992): Twelve years experience with solar cookers, necessary tools for a cleaner environment, Proceedings of the first world conference on solar cooking held between June 19-20 in University of the Pacific Stockton California U.S.A, Pp. 4-11

Negi, B. S and Purohit, I (2005): Experimental investigation of a box type solar cooker employing a non-tracking concentrator, Energy Conversion and Management, vol. 46, Pp. 577-605

Olusegun, H. D (2006): Design construction and testing of a solar box cooker using locally sourced material, Journal of Research Information in civil energineering, vol. 3 no. 1 Pp. 102-125

Passamai, V.: "Laboratory and field experiments with a solar oven" (Experiencias de laboratorio y de

campo con un horno solar). Avances en Energies Renovables y Medio Ambiente, Vol. 2, No. 1, pp. 02.29-02.03,1998.

Patel, N. V. and Philip, S. K (2000): Performance evaluation of three solar concentrating cookers, Renewable Energy vol. 20, Pp. 347-354

Performance of solar cookers under Jordan climate. salahabdalah@asu.edu.jo
Rai, G.D. (2008), Solar Energy Utilization, 5th edition. Khano Publishers New Delhi, India (pp 522 - 528)

Ramon, C (2004): Solar cooker review, vol. 10, no. 2, http//:solarcooking.org

Renewable Energy Journal **Vol.**30

Shaw, Shaw (2005): Development of a comparative frame work for evaluating the performance of solar cooking devices, Dept of Physics, Appied Physics and Astronomy, Renseselaes Polytechnic Institute 1108th St Troy NY 12130

Sukhatme, S. P., (2005) Solar Energy, Principles of thermal collection and storage, 2nd Edition, 10, Tata McGraw-Hill Publishing Company Limited, New Delhi, India (pp102).

Volker, Q (2003): The sun as an energy source, Renewable Energy World, vol. 6, no. 5, Pp. 90-92

Volker, Q (2004): Solar thermal water heating, Renewable Enegry World, vol. 7 no. 2 Pp95-96

Warren, R. C (1994): Solar cooking the history problems parameters and goals, Proceedings of the second world conference on solar cookers use and technology held between July 13-15 in Heredia Costa Rica

Wary, Xiping (1992): Solar cooking in China, Proceedings of the first World conference on solar cooking held between June 19-20 at University of the Pacific Stockton California U.S.A

Babalola et al: Proc. ICCEM (2012) 260 – 271

Design and construction of tilting furnace for producing aluminium matrix composites

Babalola P.O., Inegbenebor, A.O and Bolu, C.A
Mechanical Engineering Department, College of Science and Technology
Covenant University, Ota
phillip.babalola@covenantuniversity.edu.ng; phillgail@yahoo.com

Abstract
Aluminium matrix composites (AMCs) are a range of advanced engineering materials that can be used for a wide range of applications within the aerospace, automotive, biotechnology, electronic and sporting goods industries. AMCs consist of a non-metallic reinforcement (SiC) incorporated into Aluminium matrix which provides advantageous properties over base metal (Al) alloys. These include improved thermal conductivity, abrasion resistance, creep resistance, dimensional stability, exceptionally good stiffness-to-weight and strength-to-weight ratios and better high temperature performance. Oil fired 20 kG tilting furnace with integral mixing mechanism was designed and constructed for the production of AMC. This cost effective furnace can be used in cottage industries without electric power.
Key words: Tilting furnace, Aluminium, SiC, Composite

1. Introduction
Metal matrix composites (MMCs) are a range of advanced materials that can be used for a wide range of applications within the aerospace, automotive, nuclear, biotechnology, electronic and sporting goods industries. MMCs consist of a non-metallic reinforcement incorporated into a metallic matrix which can provide advantageous properties over base metal alloys. These include improved thermal conductivity, abrasion resistance, creep resistance, dimensional stability, exceptionally good stiffness-to-weight and strength-to-weight ratios and better high temperature performance. Hard and strong particles in the form of particulates or fibers are added to improve the thermo-mechanical properties and performance of the lightweight but comparatively soft host metal. Common reinforcement particles include ceramics such as silicon carbide and alumina, B_4C, Si_3N_4, AlN, TiC, TiB_2, TiO_2 and hard metals such as titanium and tungsten (Tjong, 2008; Law et al.,2011; Senthilkumar et al.,2011).

There are two basic processing routes for producing Metal Matrix Composites; Liquid state and solid state routes. Liquid fabrication of Metal Matrix Composites involves incorporation of dispersed phase into a molten matrix metal, followed by its Solidification.

The methods of liquid state fabrication of Metal Matrix Composites:

- Stir Casting
- Infiltration
- Gas Pressure Infiltration
- Squeeze Casting Infiltration
- Pressure Die Infiltration

Solid state fabrication of Metal Matrix Composites is the process, in which Metal Matrix Composites are formed as a result of bonding matrix metal and dispersed phase due to mutual diffusion occurring between them in solid states at elevated temperature and under pressure.

There are two principal groups of solid state fabrication of Metal Matrix Composites:

- Diffusion bonding
- Sintering

This work is an example of liquid state fabrication of Metal Matrix Composites using stir casting method.

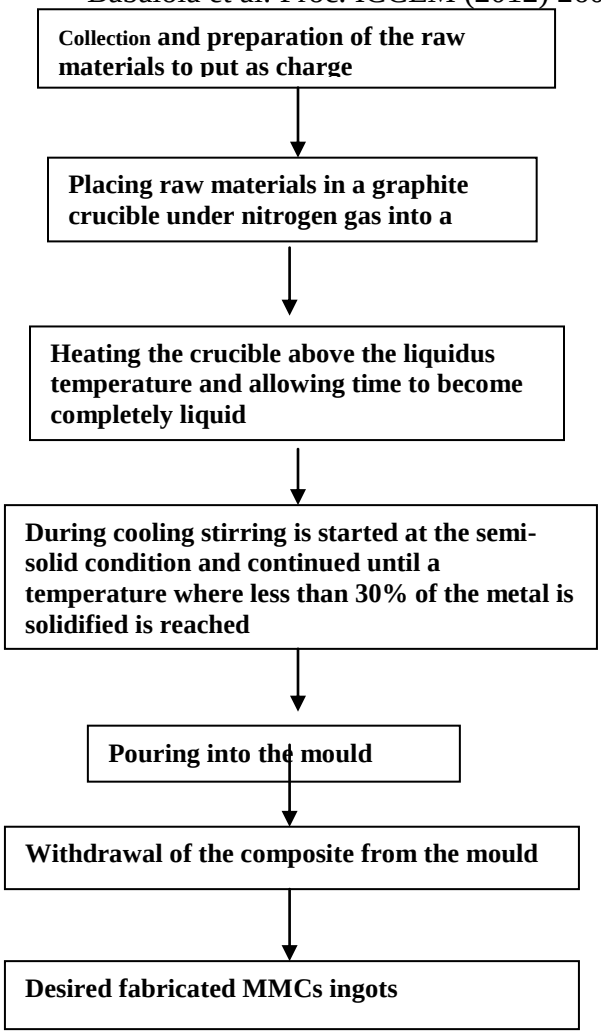

Figure 1. Composites Product Fabrication

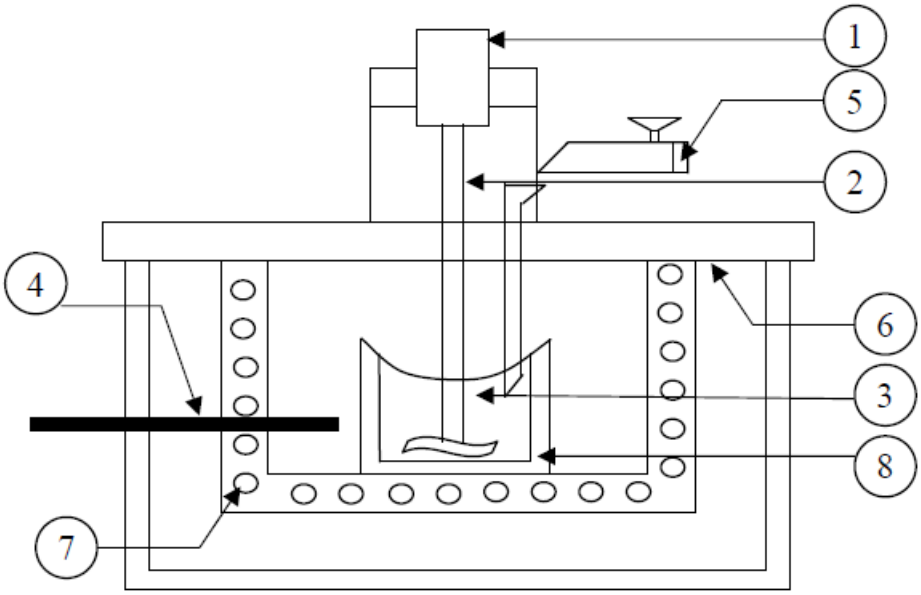

1. Motor
2. Shaft
3. Molten aluminium
4. Thermocouple
5. Particle injection chamber
6. Insulation hard board
7. Furnace
8. Graphite crucible

Fig. 2. Schematic view of setup for Fabrication of composite (Singla et al. 2009)

2. Materials and Methodology

2.1 The furnace

2.1.1 Parts functions

The crucible

The crucible is used for holding the molten aluminium which is to be melted.

The shell

The shell is the housing, which holds refractory bricks around the crucible inside of which the heating process takes place.

The shaft and rotating handle

The shaft holds the shell in place while the rotating handle, is used in turning the shaft, so as to turn the shell when pouring out the molten aluminium. The rotary assembly comprises of the shafts, the bearings and the rotary handle.

The shafts, which are being held in place by pillow bearings, are connected to opposite sides of the shell from the stands. They are made of stainless steel, and transmit rotary motion from the rotor to the shell, in order to enable tilting of the furnace for easy pouring of the molten aluminium.

The stand

The stand is holds the whole assembly in place and gives support to the assembly

.

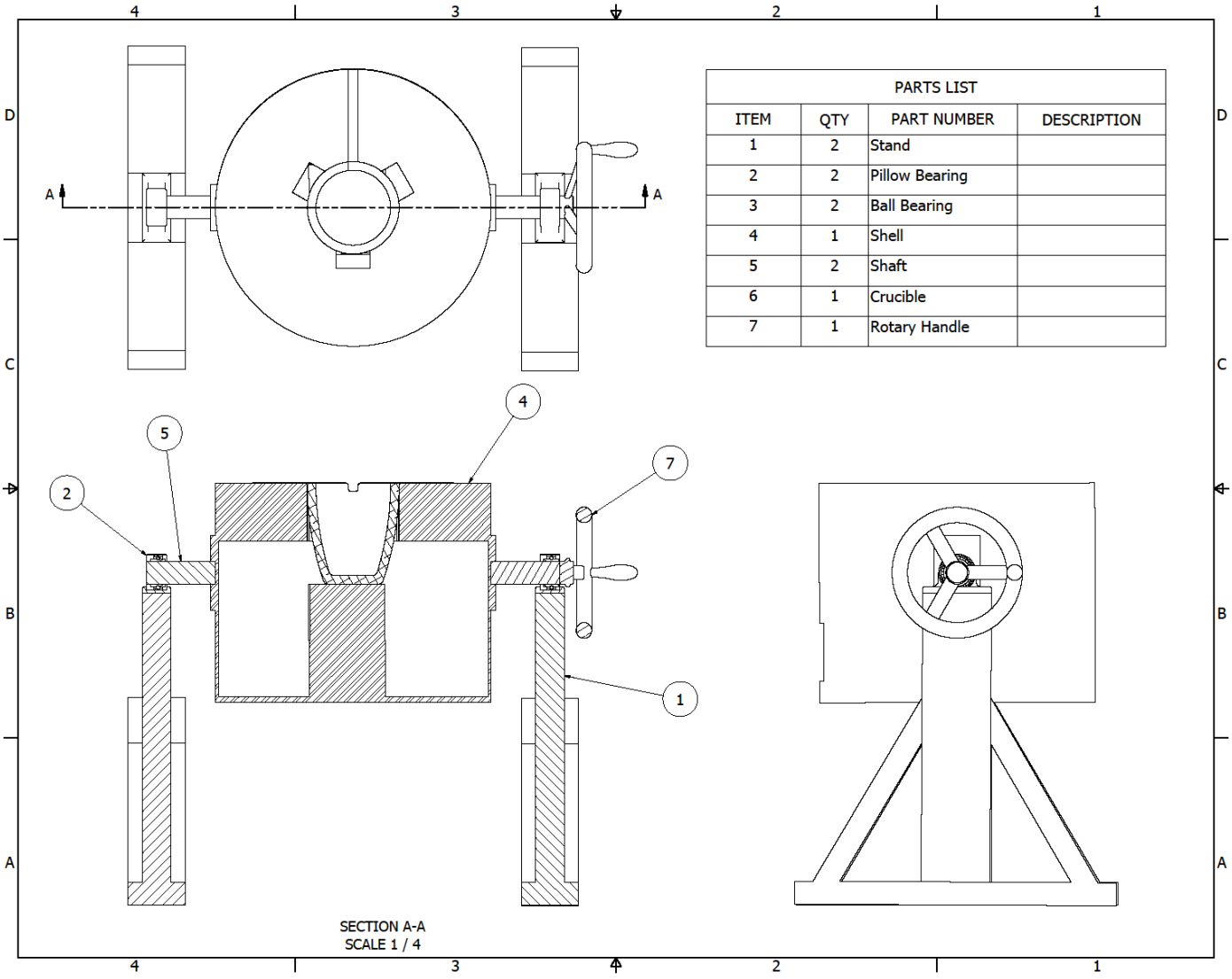

Figure 3 - Orthographic projection of the furnace assembly, showing the various parts.

2.1.2 Materials selection

The crucible

The crucible is made from graphite. This is because graphite has the following suitable properties

1. It is a good conductor of heat.
2. It has a higher temperature than aluminium.
3. It doesn't react with the molten metal at high temperatures.

This therefore sees to it that the heat is being conducted properly and that crucible is still stable, even at the melting temperature of aluminium (about 660^0C).

The shell

The shell serves as the housing for the crucible and the refractory materials. The shell is made of iron steel and assumes a drum shape, with a base. It has an opening, in order to allow for heating up of the furnace, through the firing method. The reason for choosing iron is because:

1. It has a high strength, and so will be able to carry the load (crucible, refractory bricks and binder) required.
2. It is easily worked on and so can be cut and shaped easily.
3. It is still very stable at high temperatures and so can withstand the heat (flames) needed to melt the aluminium

The rotary assembly (the shaft/bearings/rotor)

Stainless steel is chosen as the shaft material. This is because it has high strength and can support heavy load. It can be easily machined and has a very high level of corrosion resistance and also does not wear easily.

The stand

The stand was fabricated from hollow rectangular iron beams. The hollow beams were chosen in order to reduce the weight of the assembly. Iron was chosen as the material, because of much attention to details such as corrosion. Iron on the other hand apart from being cheaper, has the ability to support the assembly due to its high strength.

2.1.3 Constructing the furnace

The stand was fabricated from hollow rectangular iron beams cut to size and then joined together in such a way as to support the weight of the shell, refractory bricks, shafts, refractory binder and crucible. The shell was fabricated by first cutting out a section out of a large cylindrical iron pipe. The bottom of the shell was covered. The cut out, where the flame source would pass, was then cut out. The mounts on which the shafts were to be connected were welded onto the body of the shell at opposite sides of the shell. The refractory bricks were put in the shell to support the crucible as a base from the bottom. The crucible was placed on the bricks, and then held in place by the use of a refractory binder, with hot gas exhaust routes from the sides of the crucible, through spaces made between the crucible and the refractory binder in some sections of the circumference around the crucible. The shell was mounted in the pillow block bearings on the stand. The revolving handle is then connected to the shaft end to allow for rotating of the shaft, in order to rotate the shell for ease of pouring. The whole assembled was mounted on the floor through the legs of the stand.

2.1.4 Part analysis

Here are the parts used for the furnace construction and why they were used.

Table 1 - Part description for the furnace

Parts	**Material**	**Characteristic**
Crucible	Graphite	It is a good conductor of heat and electricity, is resistant to acids and alkalies, and is readily molded. It is infusible, subliming at 3704°C (6700°F) Brady et al
Shell	Cast Iron	High melting(1525^{0}C)temperature and tensile strength (~400 MPa)
Pillow Block Bearing	Mild Steel	High melting temperature and tensile strength
Shafts	Stainless Steel	High melting temperature and tensile strength
Revolving handle	Cast Iron	High melting(1525^{0}C)temperature and tensile strength (~400 MPa)
Stand	Cast Iron	High melting(1525^{0}C)temperature and tensile strength (~400 MPa)
Refractory Brick	Refractory materials (Ceramic)	Ceramic material with resistance to very high temperature, used for furnace linings and metal-melting pots

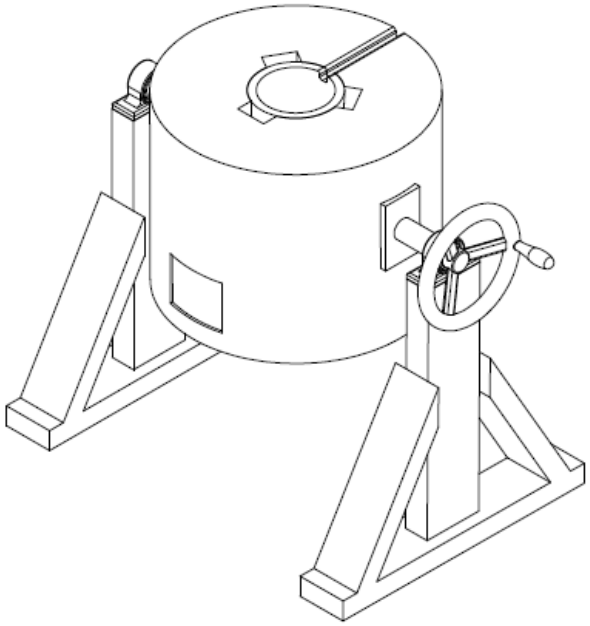

Figure 4 Isometric view of the furnace

2.1.5 Heating the furnace

The furnace is heated up from flames resulting from the combustion of a fuel (diesel or used engine oil) in the presence of air. The burner is a nozzle with 50mmθ air pipe from the blower and 8mmθ pipe conveying the fuel (Fig.7). The air line is directed into the furnace, through the opening located in the shell. The air pump is first of all started in order to pump air into the line. The fuel valve is then adjusted to allow for flow of the fuel down the pipe into the air line in order to create a combustible mixture. This mixture is then ignited to generate the flame needed for heating.

Figure 5. The furnace

Figure 6. The fuel reservoir

Figure 7. The air-fuel supply connection, showing how air and fuel pipes are connected

2.2 The mixer

The purpose of the mixer is to mix (using stirring action) the reinforcement and the molten metal together. This is achieved by transferring the molten aluminium from the furnace to the mixing container where the aluminium is stirred while adding the reinforcement materials.

2.2.1 Parts

The mixing assembly comprises of

1. The platform
2. Stands
3. Base
4. Motor
5. Shaft and agitator

The platform

The platform acts as the support for the motor. It is mounted on the stands and then the motor is fixed on it with the shaft and agitator extending downwards from it.

The stands

The stands act as supports for the platform. They are made from iron and have a square hollow shape.

Motor

The motor is used to drive the shaft and agitator, which stir the molten aluminium and the reinforcements together. The motor has a speed of 800 rpm however we introduced external variable rheostat to vary the rotation as desired and measure the speed with handheld tachometer. The shaft and the agitator are made from mild steel and iron respectively.

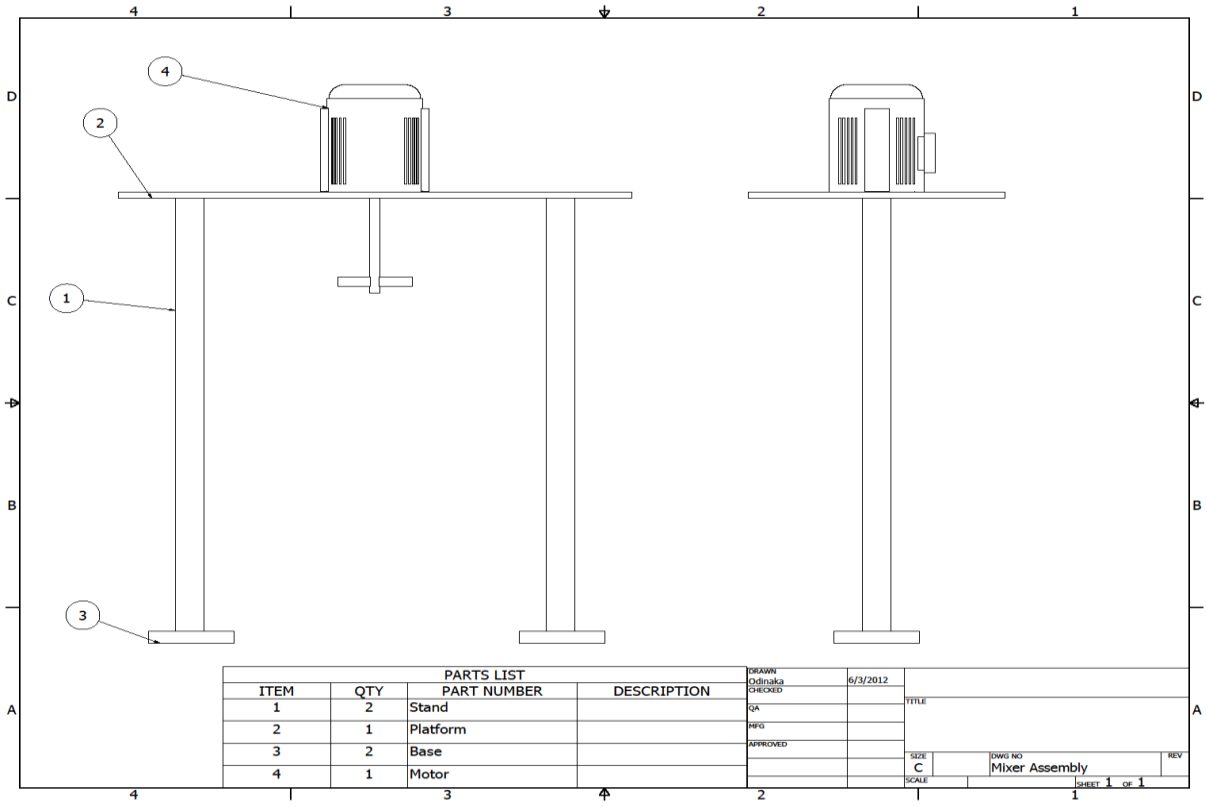

Figure 8. - Front and side views of the mixer

2.2.2 Fabricating the mixer

The mixer was constructed by cutting out the stands from 3x3 inches hollow iron bars and welding them onto bases as shown in fig. 3. Welded on the stands is a platform made from flat rolled iron. This platform holds the motor in place. The motor which is fixed on the platform has a shaft extending downwards through a hole in the platform. This shaft also holds the agitator needed to carry out the mixing.

2.2.3 Designing the shaft

The shaft is made from mild steel and was chosen, because of its characteristics which suit the desired operation and also because it is cheaper than stainless steel. The shaft was designed to be able to transfer a speed of 500 rpm directly from the motor to the agitator for mixing the molten aluminium and the reinforcements. The design was based on the following considerations

1. The speed of the shaft is to be 500 rpm.
2. The diameter of the agitator (d) is one-half the mixing ladle (D).
3. The agitator blade is a vertical one.

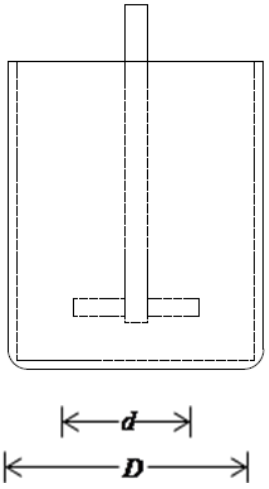

n = Speed (rpm)

R_e = Reynolds number

d = Impeller diameter (0.5D)

D = Viscosity of molten aluminium (pa.s)

P = Power (W)

T = Torque (Nm)

N_p = Power Number

The Reynolds number for the flow is gotten from the equation

$$R_e = \frac{\rho n d^2}{\mu}$$

The power number is obtained from a power number vs Reynold's number chart.

$$P = N_p \rho n^3 d^5$$

$$P = Tn$$

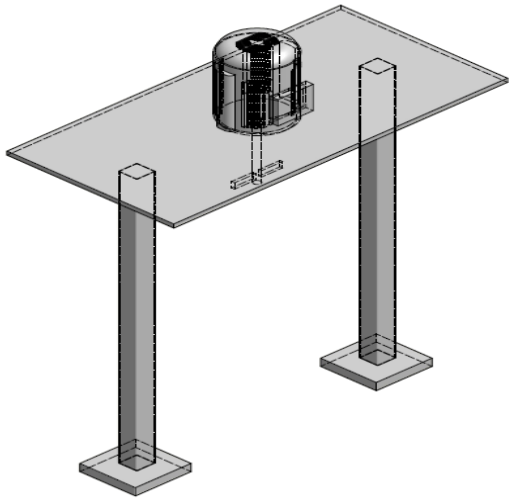

Figure 9. Isometric view of the mixer

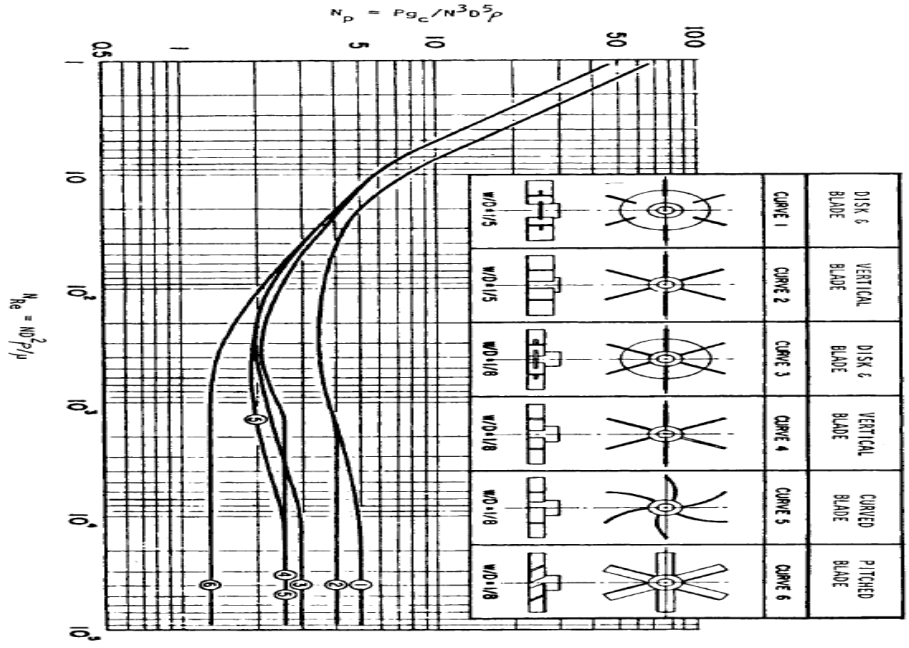

Figure 10 - Graph showing the relationship between the power number and reynold's number for various agitator blade arrangement

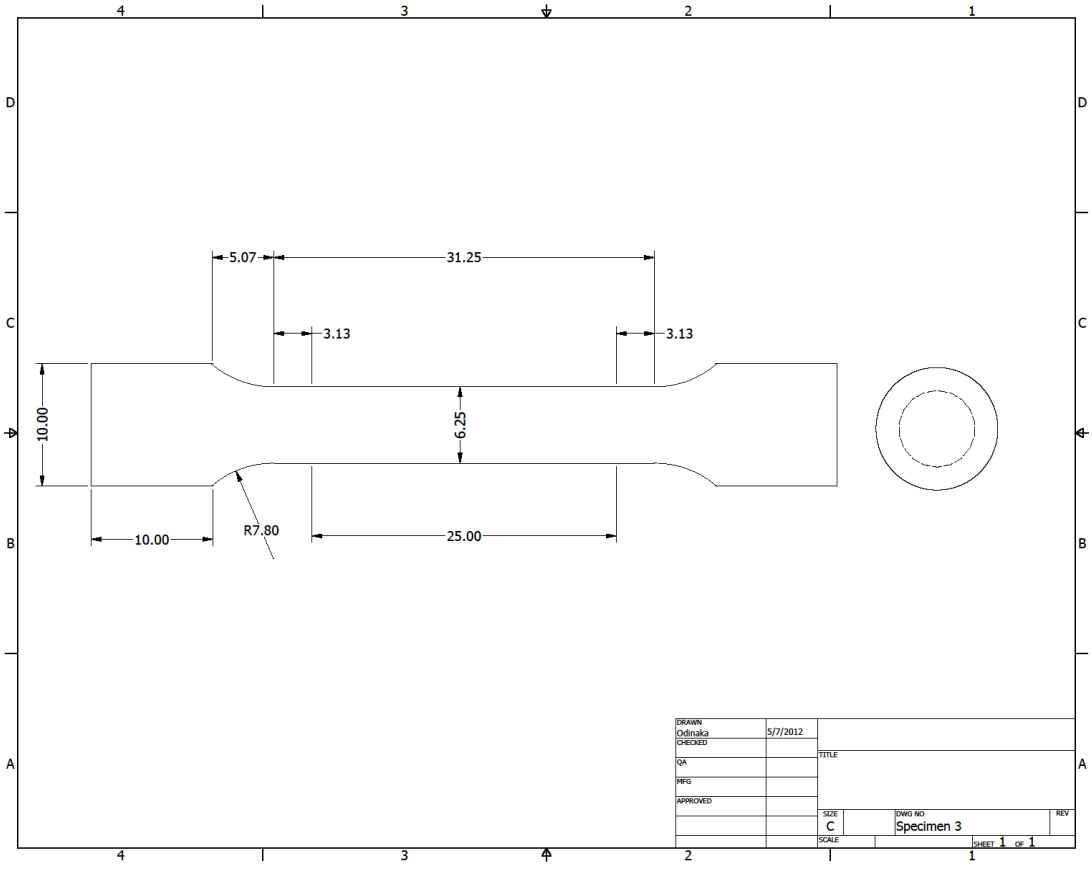

Figure 10 - Tensile specimen (based on asme standards)

3. Testing the furnace

The furnace was tested for functionality and was found to melt 10kG of Aluminium within 20minutes. The furnace diesel fuel consumption rate was found to be 0.15 L/min. The mixer was also used to mix the aluminium and the reinforcements. It was found to be suitable and was able to carry out the mixing properly.

4. Conclusion

The aluminium furnace melts the aluminium to a liquid state, from which it is then transferred to the mixer for reinforcing and then casting to obtain specimens for testing.

The aluminium furnace heats to a temperature higher than the liquidus temperature of aluminium and so melts aluminium. The graphite crucible has the ability to conduct heat and so transfers heat without much loss to the aluminium. Molten metal is easily poured out from the furnace due to its design which permits it to swivel. Mixing the molten aluminium and the reinforcements are mixed in the mixer.

References

Balasivanandha, S., Kaarunamoorthy, L., Kaithiresan, S. and Mohan, B. (2006), "Influence of stirring speed and stirring time on distribution of particles in cast metal matrix composite". Journal of Material Processing Technology, Vol. 171, pp. 268-273.

Brady S. Georges, Henry R. Clauser, John A. Vaccari. Materials, Their Properties and Uses, Materials Handbook, Fifteenth Edition, McGraw-Hill Handbooks, pp. 258-268

Hashim, J., L. Looney, and M. S. J. Hashmi. 1998. Particles Distribution in Cast MMC, Part II, Proceeding.of Advances Materials Processing Technology. 1999, K. Lumpur, pp 349–358.

Law E., Pang S.D., Quek S.T., 2011. Discrete dislocation analysis of the mechanical response of

silicon carbide reinforced aluminum nanocomposites. Composites: Part B 42 , 92–98

Senthilkumar V., Omprakash B.U.,2011. Effect of Titanium Carbide particle addition in the aluminium composite on EDM process parameters. Journal of Manufacturing Processes 13, 60–66

Singla M., Dwivedi D.D., Singh L., Chawla V., 2009. Development of Aluminium Based Silicon Carbide Particulate Metal Matrix Composite. *Journal of Minerals & Materials Characterization & Engineering*, Vol. 8, No.6, pp 455-467

Tjong S.C.,2008, Recent Advances in Discontinuously Reinforced Aluminum Based Metal Matrix Nanocomposites, Composite Materials Research Progress (ISBN: 1-60021-994-2), Editor: Lucas P. Durand, Nova Science Publishers, Inc., pp. 275-296

Statistical approach to optimization of the transesterification reaction from sorrel (*hibiscus sabdariffa*) oil

Tunde F. Adepoju[a]*, Eriola Betiku[b], Bamidele O. Solomon[b,c] , Bello J. Olatunde[a], Emmanuel M. A. Olatunji[a]
aChemical Engineering Department, Landmark University, Omu-aran, P.M.B. 1001, Kwara State, Nigeria.
[b]Biochemical Engineering Laboratory, Department of Chemical Engineering, Obafemi Awolowo University, Ile-Ife 220005, Osun State, Nigeria.
[c]National Biotechnology Development Agency, 16, Dunukofia Street, Area 11, Garki, P. M. B. 5118 Wuse, Abuja, Nigeria.
* Corresponding Author: Chemical Engineering Department, Landmark University, Omu-aran, P.M.B. 1001, Kwara State, Nigeria.
Email Address: avogadros2002@yah.com, Tel: +234-803-39404673.

Abstract

In an effort to optimize the reaction conditions of biodiesel production from Sorrel seed oil, Response Surface Methodology (RSM) was applied and the effects of reaction temperature, catalyst amount, reaction time and methanol/oil molar ratio, and their reciprocal interactions were ascertained. A total of 30 experimental runs were designed by Central Composite Rotatable Design (CCRD) and carried out. A quadratic polynomial was obtained for predicting the Transesterification process and the ANOVA test showed the model to be significant ($p<0.05$). The validity of the predicted model was confirmed by carrying out three independent replicates experiments. The actual maximum biodiesel yield obtained was 99.23% (w/w) at methanol/oil molar ratio 6.21, catalyst amount 1.03 (% wt.), reaction temperature 51 ^{o}C, and reaction time 63 min. The fuel properties of Hibiscus sabdariffa methylester (HSME) produced were found to be within the ASTM D6751 and DIN EN 14214 biodiesel standards. The fatty acid profile of the HSME revealed that the dominant fatty acids were oleic (58.34%), arachidic (1.55%), palmitic (18.28%) and linoleic (21.19%). Emission assessment revealed 70% reduction of CO at B80, 80% reduction of NO concentration at B40.

Key words: Biodiesel, Sorrel oil, Transesterification, Optimization, Response surface methodology

1. Introduction

Biodiesel, which is considered as an substitute of convectional diesel is gaining ground as a biodegradable, non-toxic and environment-friendly fuel to neat diesel (Knothe et al., 2005; Demirbas, 2008). It is produced through a chemical process known as “transesterification or alcoholysis” in which there is displacement of alcohol from an ester under acidic or basic catalytic conditions producing free glycerol and the fatty acid esters of the respective alcohol (Knothe et al., 2007). Biodiesel is derived from renewable feedstock like vegetable oils or animal fats. Both edible and non-edible oils have been successfully employed in biodiesel production. In Nigeria, convectional diesel is produced mainly from crude oil; however, there are alternative oil-yielding crops which can be utilized as feedstocks, such as Palm oil, *Moringa* oil, Shea butter, *Jatropha* and Coconut. Sorrel seed oil, a new competitor is emerging as a promising feedstock.

In Africa, the Sorrel seeds are hard-pressed for oil and the residual cake is cooked, seasoned with *kambo*, a local condiment. The seeds are also used for their oil in china and eaten in West Africa. In Malaysia, the seeds are used to produce scrubs and soaps. However, most of the seeds are merely discarded as by-products by the manufacturers. In Africa, the bitter seeds are roasted and grounded into powder and is used in oily soup and sauces as a meal for human consumption. Roasted seeds have been used as coffee replacement that is said to have aphrodisiac properties (Duke, 1984). According to Omobuwajo *et al*. (2000), in northern Nigeria, the seeds are fermented into a condiment known as *Mungza ntusa*. In Sudan, the seeds are used for edible oil

manufacture and the by-products of this process were used for poultry feeding Al-Wandawi *et al*. (1984). However, in a commercial sense, this oil is not in current widespread use in Nigeria, having relatively few competing medicinal and food uses.

Response surface methodology (RSM) is a useful statistical tool, which has been applied in research for optimizing various processes including transesterification reaction of vegetable oils: *Moringa oleifera* (Rashid et al., 2011), *Jatropha* oil (Tiwari et al., 2007) and cottonseed oil (Zhang et al., 2011). The main advantage of RSM is the ability to reduced number of experimental runs needed to provide sufficient information for statistically acceptable results. In this present study, an effort was made to optimize the process conditions for the transesterification step of Sorrel oil.

2.0 METHODOLOGY

2.1 *Extraction of Sorrel seed oil*

Sorrel seeds were collected from Adamawa State, Nigeria. Chaff was separated from the oilseeds by winnowing. The cleaned oilseeds were milled into powder by grinding with plate machine. A 5-liter Soxhlet apparatus and ethanol as solvent were used for the oil extraction.

2.2 *Experimental design of HSME production*

In this study, the central composite rotatable design (CCRD) was employed to optimize the HSME production. Five-level-four-factors design was applied, which generated 30 experimental runs. This included 16 factorial points, 8 axial points, and 6 central points to provide information regarding the interior of the experimental region, making it possible to evaluate the curvature effect. Selected factors for the transesterification process from the Sorrel seed oil were reaction temperature (X_1), catalyst amount (X_2), reaction time (X_3) and methanol/oil molar ratio (X_4). The coded levels of the independent factors are given in Table 1. The experiments were randomizes to minimize the effects of unexplained variability in the observed response due to extraneous factors.

2.3 *Experimental procedure*

Base catalyst transesterification reaction was applied for the HSME production, due to the low FFA value of the seed oil. A known weight of NaOH pellet was dissolved in a known volume of anhydrous methanol and was quickly transferred into the seed oil in the reactor and the reaction was monitored according to the design variables. At the completion of the reaction, the product was transferred to a separating funnel for glycerol and HSME separation. Glycerol was tapped off and the HSME left was washed with distilled water to remove residual catalyst, glycerol, methanol and soap. The washed HSME was further dried over heated $CaCl_2$ powder. The HSME yield was determined gravimetrically as described in Eqn.1

$$AIME\ yield = \frac{weight\ of\ HSME\ produced}{weight\ of\ Sorrel\ oil\ used} \quad (1)$$

2.4 *Statistical Data Analysis*

HSME production data was analyzed statistically using RSM, so as to fit the quadratic polynomial equation generated by the Design-Expert software version 8.0.3.1 (Stat-Ease Inc., Minneapolis, USA). To correlate the response variable to the independent factors, multiple regressions was used to fit the coefficient of the polynomial model of the response. The quality of the fit of the model was evaluated using test of significance and analysis of variance (ANOVA). The fitted quadratic response model is given by Eqn. 2.

$$Y = b_0 + \sum_{i=1}^{k} b_i X_i + \sum_{i=1}^{k} b_{ii} X_i^2 + \sum_{i<j}^{k} b_{ij} X_i X_j + e \quad (2)$$

Where, Y is response factor (HSME), b_o is the intercept value, b_i (i= 1, 2, …, k) is the first order model coefficient, b_{ij} is the interaction effect, and b_{ii} represents the quadratic coefficients of X_i, and e is the random error.

2.5 *Oil and fuel properties*

Fuel properties namely, moisture content, specific gravity, kinematic viscosity at 40 ^oC, iodine value, acid value, saponification value, higher heating value, flash point, cloud point and cetane number of both Sorrel seed oil and HSME were determined following standard methods and compared with American and European standards (ASTM and DIN EN 14214).

2.6 *Emissions Assesment*

In order to test the suitability of the HSME produced in I.C engine as well as compare the emissions with that of neat diesel (AGO), B10, B20, B30..... B90 blends of pure HSME with AGO at different loads (0-2.7 kW) was used, 100% AGO and 100% HSME were burnt in succession and emissions such as CO and NO were measured with with the aid of TORIX gas analyzer.

3.0 RESULTS AND DISCUSSION

3.1 *Properties of the extracted Sorrel seed oil*

The analysis of the oil showed that it has a moisture content of 0. 065%%, specific gravity of 0.886 and viscosity of 15.40 cP. The acid value of the oil was 0.80 mg KOH/g oil while the iodine value was 97.77 g I2/100g oil. Whereas the saponification value of the oil was 197.75 mg KOH/g oil, its higher heating value and cetane number were 39.86 MJ/kg and 51.90, respectively. These results are within the ranges earlier reported in the literature (Nakpong and Wootthikanokkhan, 2010; Bouanga-Kalou *et al.*, 2011).

3.2 *Optimization of the transesterification step*

Table 2 depicts the coded factors considered in this study with experimental results, predicted values as well as the residual values obtained. The highest HSME yield obtained was 99.30 % (w/w) at reaction temperature 60 ^{o}C, catalyst amount 0.90% (w/w), reaction time 50 min and methanol/oil molar ratio 6:1, while the lowest HSME yield of 89.29% (w/w) was observed at reaction temperature 60 ^{o}C, catalyst amount 0.70% (w/w), reaction time 50 min and methanol/oil molar ratio 6:1. Design Expert 8.0.3.1 software was employed to evaluate and determine the coefficients of the full regression model equation and their statistical significance. Table 3a shows the results of test of significance for every regression coefficient. The results showed that the p-value of the model terms were significant, i.e. $p < 0.05$. In this case, the four linear terms (X_1, X_2, X_3, X_4), five cross-products (X_1X_2, X_1X_3, X_1X_4, X_2X_3, X_3X_4) and the four quadratic terms (X_1^2, X_2^2, X_3^2 and X_4^2) were all remarkably significant model terms at 95% confidence level except X_2X_4. However, all other model terms were more significant than both X_4 and X_1X_2. In order to minimize error, all the coefficients were considered in the design. Table 3b shows the analysis of variance (ANOVA) of the regression equation. The model F-value of 361.87 implied a high significant for the regression model (Yuan et al., 2008). The goodness of the fit of a model was checked by the coefficient of determination (R^2). R^2 should be at least 0.80 for the good fit of a model (Guan and Yao, 2008). The R^2 of 0.9941 in this case indicated that the sample variation of 99.41% for HSME yield was attributed to the independent factors and only 0.59% of the total variation are not explained by the model. The value of adjusted determination coefficient (Adj. R^2 = 0.9962) was also very high, supporting a high significant of the model (Khuri and Cornell, 1987) and all p-value coefficients were less than 0.0001, which implied that the model proved suitable for the adequate representation of the actual relationship among the selected variables. The lack-of-fit term of 0.9589 was not significant relative to the pure error. The final equation in terms of coded factors for the response surface quadratic model is expressed in Eqn. (3).

$$Y(w/w\ \%) = 98.91 + 0.95X_1 + 1.88X_2 + 0.60X_3 + 0.13X_4 + 0.14X_1X_2 - 0.27X_1X_3 + 0.87X_1X_4 - 0.45X_2X_3 - 0.061X_2X_4 + 0.56X_3X_4 - 1.70X_1^2 - 1.44X_2^2 - 1.75X_3^2 - 1.90X_4^2 \quad (3)$$

All the X_1, X_2, X_3, X_4, X_1X_2, X_1X_4 and X_3X_4 had positive effect on the HSME yield while the rest had negative influence on the yield (Table 4).

In general, the 3D response surface plot is a graphical representation of the regression equation for the optimization of the reaction variables. Figure 1(a-f) described the 3D surfaces linked to the effect of two variables on the yield of HSME (biodiesel). The curvatures nature of 3D surfaces in Fig. 1b, c and f indicated the mutual interaction of the reaction time with reaction temperature, methanol/oil molar ratio with reaction temperature and methanol/oil molar ratio with reaction time, respectively. Meanwhile, there was a moderate interaction examined between methanol/oil molar ratio with catalyst amount and catalyst amount with reaction temperature, (Fig.1a and e), but no interaction was observed between reaction time and catalyst amount as represented in Fig.1d. The optimal condition predicted by the model were

methanol/oil molar ratio 6.21, catalyst amount 1.03 (%wt.), reaction temperature 51 ^{o}C, and reaction time 63 min, which gave 99.71% (w/w). Using these optimal condition values for three independent experimental replicates, an average HSME yield of 99.23% (w/w) was achieved, which was within the range predicted by the model.

3.3 *Quality and fuel properties of HSME*

Table 5 shows the properties of the HSME in comparison with ASTM biodiesel and DIN EN 14214 standards. All the tested characteristics and fuel properties of the HSME satisfied both the ASTM D 6751 and DIN EN 1424 standards. Gas chromatography analysis of fatty acids present in the HSME is shown in Table 6. The results indicated HSME was highly unsaturated. The dominant fatty acids were oleic (58.34%), arachidic (1.55%), palmitic (18.28%) and linoleic (21.19%).The total unsaturated fatty acid composition of the HSME was 79.53%.

3.4 *Engine Performance at Various Blends*

The performance characteristics of HSME and diesel blends are shown in Fig. 2(a-b). It was observed that from 20% up to 90% blends of HSME with AGO gives quite satisfactory performance related to CO and NO. The cetane number and viscosity of the blends lower than 10% or higher than 90% are not effective to give good performance.

4. Conclusions

In this study, experiments were conducted using RSM to determine the effects of four reaction factors namely methanol/oil molar ratio, reaction temperature, catalyst concentration and reaction time on HSME yield in the transesterification of the Sorrel seed oil. The maximum HSME conversion yield was validated as 99.23% (w/w) at the reaction temperature of 63 ^{o}C, a catalyst amount of 1.03 wt. %, methanol/oil molar ratio of 6.21 and reaction time of 51 min. The fuel properties of the HSME were within the ASTM D6751 and DIN EN 14214 specifications. Emission assessment revealed 70% reduction of CO at B80, 80% reduction of NO concentration at B40.

ACKNOWLEDGEMENTS

E. Betiku gratefully acknowledged equipment donation by the World University Service, Germany and provision of relevant literature by the DAAD.

References

Al- Wandawi, H., Al-Shaikhaly, K. and Abdu-Rahman, M., Roselles seeds: a source of protein. *J Agr Food Chem*. 32: 510-512, 1984.

Bouanga-Kalou, G., Kimbongila, A., Nzikou, M., Ganongo-Po, F.B., Moutoula, F.B., Tchicaillat-Landou, M., Bitsangou, R.M., Silou, T.H. and Desobry, S., Chemical Composition of Seed Oil from Roselle (*Hibiscus sabdariffa* L.) and the kinetics of Degradation of the Oil during Heating. *JASET.* 3(2): 117-122, 2011.

Demirbas, A., Comparison of transesterification methods for production of biodiesel from vegetable oils and fats. *Energ. Convers. Manage*. 49: 125–30, 2008.

Duke and Atchley, Properties of Sorrel seeds and its compositions. *J AGR FOOD CHEM.* 23: 136-140, 1984.

Guan, X. and Yao, H., Optimization of viscozyme L-assisted extraction of oat bran protein using response surface methodology. *Food Chem.* 106:345-351, 2008.

Khuri, A. I., and Cornell, J. A., *Response surfaces: design and analysis*. Marcel Dekker: New York, 1987.

Knothe, G., Krahl, J., and Gerpen, J.V., *The biodiesel handbook*. Champaign, IL: AOCS Press, 2007.

Nakpong, P. and Wootthikanokkhan, S., Roselle (*Hibiscus sabdariffa* L.) oil as an alternative feedstock for biodiesel production in Thailand. *Fuel.* 89: 1806–1811, 2010.

Omobuwajo, T.O., Sanni, L.A. and Balami, Y.A., Physical properties of sorrel (*Hibiscus sabdariffa*) seeds. *J. Food Eng.* 45: 37-41, 2000.

Rashid, U., Anwar, F., Ashraf, M., Saleem, M., and Yusup, S., Application of response surface methodology for optimizing transesterification of *Moringa oleifera* oil: Biodiesel production. *Energ. Convers. Manage*. 52:3034–3042, 2011.

Tiwari, A. K., Kumar, A., and Raheman, H., Biodiesel production from jatropha oil (*Jatropha curcas*) with high free fatty acids: An optimized process. *Biomass Bioenerg*. 31:569-575, 2007.

Yuan, X., Liu, J., Zeng, G., Shi, J. and Huang, G., Optimization of conversion of waste rapeseed oil with high FFA to biodiesel using response surface methodology. *Renew. Energ.* 33:1678-1684, 2008.

Zhang, X. W. and Huang, W., Optimization of the transesterification reaction from cottenseed oil using a statistical approach. *Energ. Sources.* 33:1107-1116, 2011.

Table 1: Factors and Their Levels for Composite Central Design

Variable	Symbol	Coded factor levels				
		-2	-1	0	1	2
Reaction temperature (^oC)	X_1	50	55	60	65	70
Catalyst amount (wt %)	X_2	0.7	0.8	0.9	1.0	1.1
Reaction time (min)	X_3	40	45	50	55	60
Methanol/oil ratio	X_4	4	5	6	7	8

Table 2: Central Composite Design, Experimental, Predicted and Residual Values for Five – Level-Four Factors Response Surface Analysis

Std order	X_1 (^oC)	X_2 (wt %)	X_3 (min)	X_4	Experimental value (w/w %)	Predicted value (w/w %)	Residual values (w/w%)
1	-1	-1	-1	-1	89.30	89.35	-0.050
2	1	-1	-1	-1	90.00	89.79	0.210
3	-1	1	-1	-1	93.92	93.87	0.050
4	1	1	-1	-1	94.79	94.86	-0.066
5	-1	-1	1	-1	90.90	90.87	0.031
6	1	-1	1	-1	90.17	90.21	-0.039
7	-1	1	1	-1	93.67	93.57	0.096
8	1	1	1	-1	93.56	93.47	0.091
9	-1	-1	-1	1	86.99	86.88	0.110
10	1	-1	-1	1	90.70	90.78	-0.084
11	-1	1	-1	1	91.20	91.15	0.051
12	1	1	-1	1	95.78	95.61	0.170
13	-1	-1	1	1	90.73	90.65	0.077
14	1	-1	1	1	93.61	93.46	0.150
15	-1	1	1	1	93.10	93.11	-0.013
16	1	1	1	1	96.54	96.48	0.062
17	-2	0	0	0	90.15	90.22	-0.072
18	2	0	0	0	93.88	94.02	-0.140
19	0	-2	0	0	89.29	89.39	-0.097
20	0	2	0	0	96.80	96.92	-0.120
21	0	0	-2	0	90.64	90.73	-0.093
22	0	0	2	0	93.00	93.12	-0.120
23	0	0	0	-2	91.00	91.06	-0.058
24	0	0	0	2	91.44	91.60	-0.160
25	0	0	0	0	98.49	98.91	-0.420
26	0	0	0	0	99.30	98.91	0.390
27	0	0	0	0	99.10	98.91	0.190
28	0	0	0	0	98.65	98.91	-0.260
29	0	0	0	0	99.07	98.91	0.160
30	0	0	0	0	98.87	98.91	-0.043

Table 3a: Test of Significance for Every Regression Coefficient CCD

Source	Sum of Squares	df	Mean Square	F-Value	p-value
X_1	21.66	1	21.66	453.37	< 0.0001
X_2	85.05	1	85.05	1780.23	< 0.0001
X_3	8.54	1	8.54	178.84	< 0.0001
X_4	0.43	1	0.43	9.04	0.0088
X_1X_2	0.31	1	0.31	6.45	0.0227
X_1X_3	1.20	1	1.20	25.10	0.0002
X_1X_4	12.04	1	12.04	252.03	< 0.0001

X_2X_3	3.28	1	3.28	68.57	< 0.0001
X_2X_4	0.060	1	0.060	1.26	0.2800
X_3X_4	5.09	1	5.09	106.44	< 0.0001
X_1^2	79.07	1	79.07	1655.12	< 0.0001
X_2^2	56.91	1	56.91	1191.17	< 0.0001
X_3^2	83.68	1	83.68	1751.53	< 0.0001
X_4^2	98.67	1	98.67	2065.28	< 0.0001

Table 3b: Analysis of Variance of Regression Equation

Source	Sum of squares	df	Mean Square	F-value	p-value
Model	361.87	14	25.85	541.03	< 0.0001
Residual	0.72	15	0.048		
Lack of Fit	0.26	10	0.026	0.28	0.9589
Pure Error	0.46	5	0.092		
Cor Total	362.59	29			
			R-Sq = 99.40%,	R-Sq(adj) = 99.62%	

Table 4: ANOVA for Response Surface Quadratic Model for Intercept.

Factors	Coefficient Estimate	df	Standard Error	95%CI Low	95%CI High	VIF
Intercept	98.91	1	0.089	98.72	99.10	-
X_1	0.95	1	0.045	0.85	1.05	1.00
X_2	1.88	1	0.045	1.79	1.98	1.00
X_3	0.60	1	0.045	0.50	0.69	1.00
X_4	0.13	1	0.045	0.039	0.23	1.00
X_1X_2	0.14	1	0.055	0.022	0.26	1.00
X_1X_3	-0.27	1	0.055	-0.39	-0.16	1.00
X_1X_4	0.87	1	0.055	0.75	0.98	1.00
X_2X_3	-0.061	1	0.055	-0.57	-0.34	1.00
X_2X_4	0.56	1	0.055	-0.18	0.55	1.00
X_3X_4	-1.70	1	0.055	0.45	0.68	1.00
X_1^2	-1.44	1	0.042	-1.79	-1.61	1.05
X_2^2	1.75	1	0.042	-1.53	-1.35	1.05
X_3^2	-1.90	1	0.042	-1.84	-1.66	1.05
X_4^2	98.67	1	0.042	-1.99	-1.81	1.05

Table 5: Properties of HSME in Comparison with Biodiesel Standards

Parameters	HSME	ASTM D6751	DIN EN 14214
Moisture content %	<<<1ppm	< 0.03	0.02
Specific gravity@15 ^oC	0.882	0.86-0.90	0.85
Viscosity at 40 ^oC (cP)	5.80	1.9-6.0	3.5-5.0
Iodine Value (g I_2/100g)	64.47	-	120 max
Acid Value	0.24	< 0.80	0.5 max
Density (kg/m^3) at 25 ^oC	0.92	0.84	0.86-0.90
Saponification value (mg KOH/g oil)	148.49	-	-
Higher heating value (MJ/kg)	42.48	-	-
Diesel index	81.94	50.40	-
API	32.65	36.95	-
Cetane number	69.0	47 min	51 min
Aniline point	250.96	331.00	-

Pour Point ^{o}C	-15	Not specific	Not specific.
Cloud Point ^{o}C	+5	Report	Not specific.
Flash Point ^{o}C	186	93 min	120 min

Table 6: Fatty Acids Compositions of the HSME Produced

Fatty acid	Compositions %
Palmitic acid (C16:0)	18.280
Palmitoleic acids (C16:1)	0.055
Stearic acids (C18:0)	0.213
Oleic acids (C18:1)	58.337
Linoleic acids (C18:2)	21.194
Linolenic acid (C18:3)	0.165
Myristic acid (C14:0)	0.0943
Arachidonic acid (C20:4)	1.548
Other	0.114
Total	100

(a)

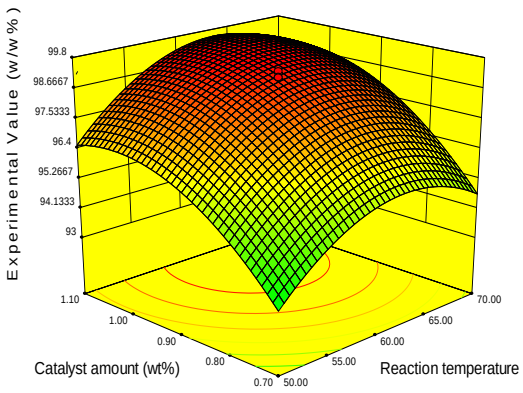

(b)

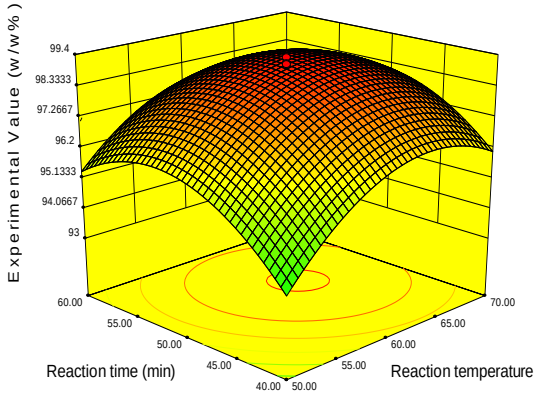

(c)

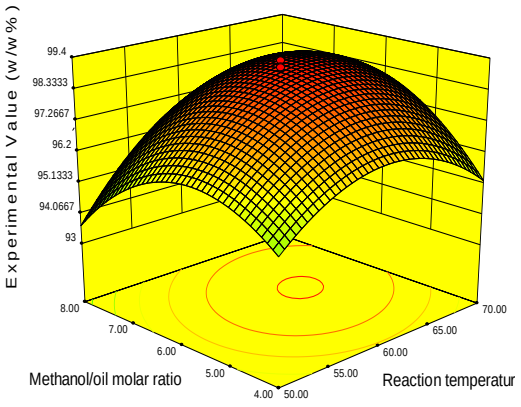

(d)

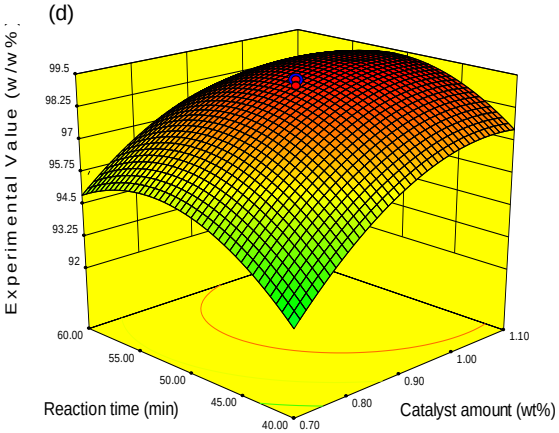

(e)

(f)

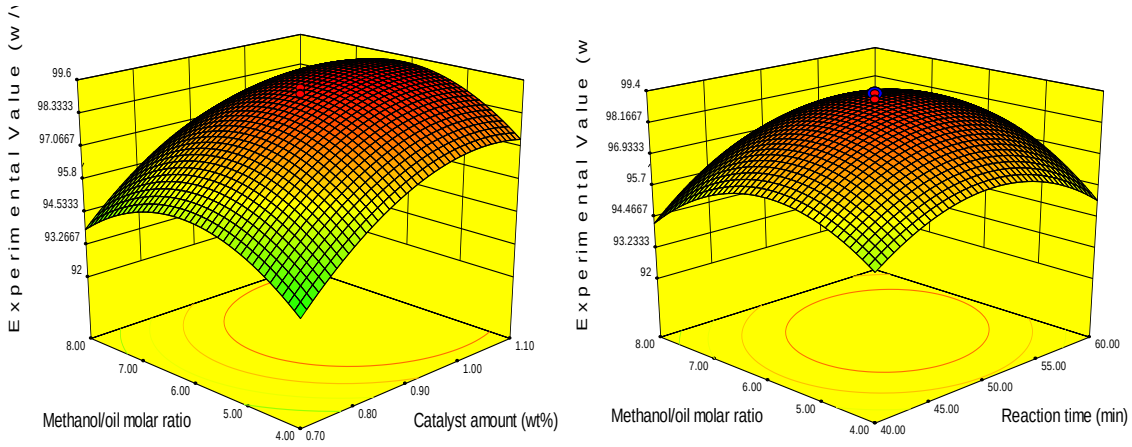

Figure 1: Response surface plots for HSME production

(a)

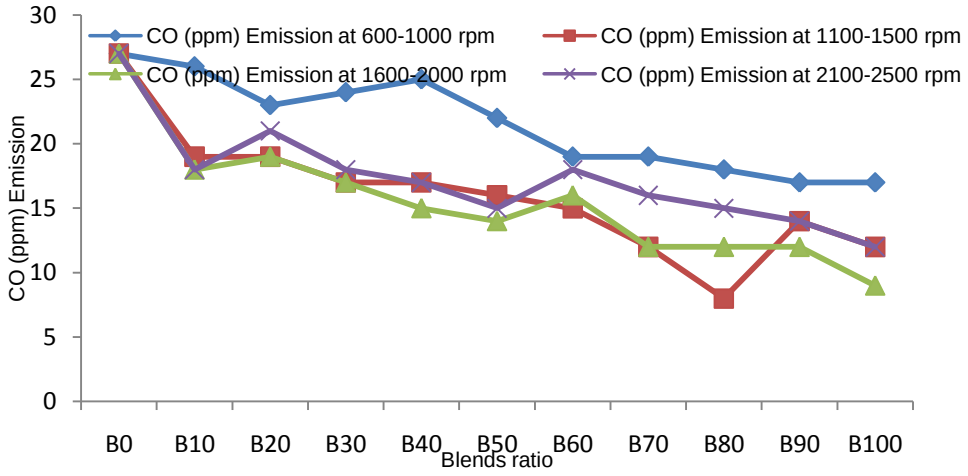

(b)

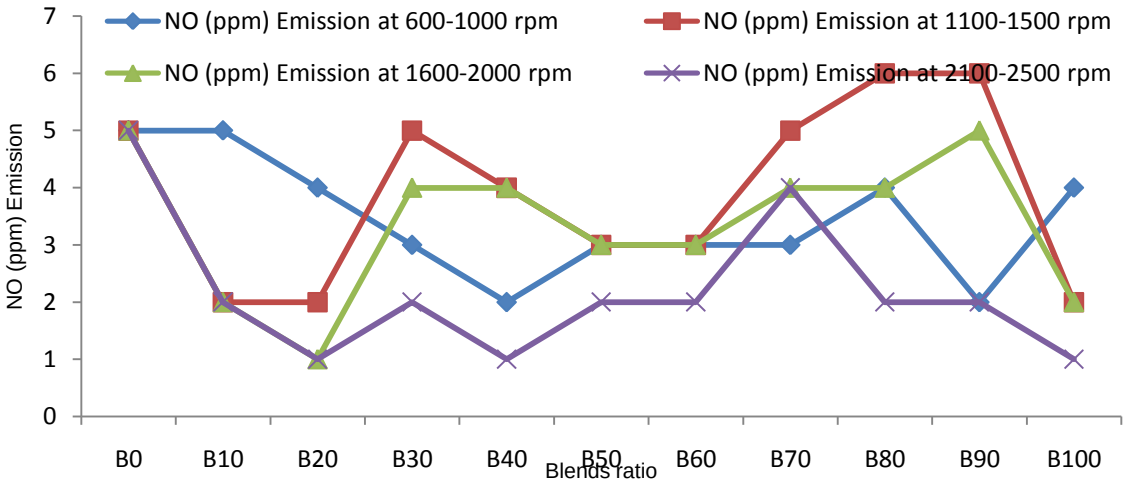

Figure 2 : Plots of performance characteristics of HSME and diesel blends

Bolu et al: Proc. ICCEM (2012) 280 - 288

University Optical Fibre Network Access Optimisation: A Case Study

Christian A. Bolu[1], Ademisoye O. Tolulade[2] and Alimi Adeshina[3]

Department of Mechanical Engineering, Covenant University, Ota, Ogun State, Nigeria
[1]christian.bolu@covenantuniversity.edu.ng
[2]tolulade.ademisoye.6462@covenantuniversity.edu.ng
[3]adeshina.alimi.6469@covenantuniversity.edu.ng

Abstract

For network access, it is always desired that a fibre optic network connectivity be the major area of cost minimization, while keeping quality of service as high as possible. This is because overall cost of setting up a fibre optic cable route is usually very high in relation to other components of the network. In this study, three buildings clusters were mapped to the University Network Operating Center, and the network was developed as a fail-safe network, so that in the case of damage to a cable or connecting component, users are not cut out. The problem was formulated as a Mathematical Programming problem and solved the resulting transportation problem using MATLAB linear programming solution. Results from the mathematical model shows an optimized cost for which a fibre Optic network connectivity can be further developed.

Key words*: Optimisation, Optical Fibre, Cabling, Access Network, Dynamic Programming, Linear Programming*

1. Introduction

The rapidly changing face of data communications and telecommunications has seen a continued growth in the need to transfer enormous amounts of information across large distances. Technologies such as coaxial cable, satellite and microwave radio are in use but optical fibre cabling is gaining ground as internet network backbone.

There is a growing requirement to provide a communications medium that is more suitable to the noisy industrial environment where the need for data integrity is paramount. Optical fibre is simply a very thin piece of glass which acts as a pipe, through which light can pass. The light that is passed down the glass fibre can be turned on and off to represent digital information or it can be gradually changed in amplitude, frequency, or phase to represent analog information. (David Bailey & Edwin Wright 2003)

1.1 Fibre Optics Basics

a. Fibre Optics is a branch of optics dealing with the transmission of light through hair-thin, transparent fibres. It is also known as the technology of using “waveguides” to transport information from one point to another in the form of light. It is characterized as follows:

- Optical Fibre: Thin strands of highly transparent glass or sometimes plastic that guide light.
- Core: The centre of the fibre where the light is transmitted.
- Cladding: The outside optical layer of the fibre that traps the light in the core and guides it along through curves.
- Buffer Coating or Primary Coating: A hard plastic coating on the outside of the fibre that protects the glass from moisture or physical damage.
- Mode: A single electromagnetic field pattern (think of a ray of light) that travels in fibre.

b. Optical Fibre Cabling can be classified as follows:

- Multimode step and graded index fibres **-** The term 'multimode' generally applies to fibres with a diameter of 50 micrometers or greater. Because of the relatively wide diameter of the core, multiple modes of light are able to travel down the fibre core. The modal dispersion that occurs in a multimode fibre affects or is affected by a number of operating parameters of the fibre. They are:
    - Attenuation: Multimode fibres have a maximum operating distance of approximately 5km.
    - Bandwidth: Multimode fibres have maximum operating data speed of approximately 2-300 Mbps
    - Wavelength: They generally operate at wavelength of 850 nm or 1300 nm. The wide diameter of the multimode makes it suitable for LED light sources.
- Graded index: A graded multimode has a core that has a gradual changing cross-sectional refractive index. The center of the core has the highest refractive index that gradually reduces moving away to the edges of the core. Because of this smooth changing refractive index, the light ray refracts (rather than reflects as in step index fibres) as it moves through the core, and set up a set of sinusoidal wave patterns in the fibre.
- Single mode Fibres - A single mode fibre (or sometimes referred to as a single mode cable) is basically a step index fibre with a very small core diameter. In theory, because the cores are so small only a few modes of light can travel down the fibre. They have a very small core causing light to travel in a straight line and typically has a core size of **8 or 10 microns**. It has unlimited bandwidth that can go unrepeated for over 80km, depending on the type of transmitting equipment. Single mode fibre has enormous information capacity, more than multimode fibre.

2. Literature review

Designing minimum-cost transport network for fibre optical network access has been in the literature on for over a decade now. Optical ring networks are widely regarded as essential to serve the unprecedented growth in demand for data transport capacity, largely driven by internet applications. Fibre optic cables are widely used in Access Networks. In other to determine a suitable 'ring route' a network planner must specify its logical type, capacity, topological layout.

Dynamic programming principle has been successfully used for Network Planning. Aside from a few specific case studies of optical ring-based networking, most of the relevant literature for ring network optimization is found in the form of mathematical formulations for multi-ring network design problem. Most methods routed the demands using a shortest-path algorithm and select rings using either a heuristic algorithm or integer programming [Morley, 1999, Krendzel, Pirmez, 2010]

(Krendzel, 2012), formulated a routing problem in an Access Network ring structure as a combinatorial-optimization problem and dynamic programming was used to solve it. The problem of cable-laying ring routing between a Local Exchange and its Remote Units is considered. Their objective was to determine the minimum-cost ring route that satisfies the specified constraints which are:

1. To pass over the Local Exchange and all Remote Units,
2. To pass over each Remote unit only once,

3. To begin and to end in the same point corresponding to the Local Exchange,
4. To have no splits.

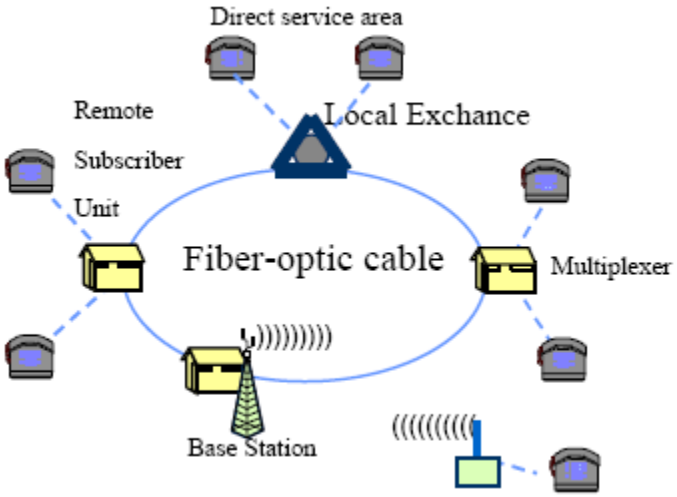

Figure 1: Model of a perspective Access Network (Krendzel, accessed 2012)

(Kulkarni S. and El-Sayed, M, 2010) discussed some economic, technical and business drivers that impact the selection of the right fibre to the home technology for an operator to deploy. Here they focused on an optimized total cost of ownership (TCO) network model to evaluate different technological choices for new deployment and redeployment for both incumbent telecommunications and cable operators.

(Ray, et al 2012), introduced the concept of a fibre aided wireless network architecture, which allows high-speed mobile connectivity by leveraging the speed of optical networks. As a first step towards designing such network architectures, they considered a single-input, single-output (SISO) wireless-optical channel and proposed a scheme in which the wireless signal at the radio-optical converter is sampled and quantized using a fixed-rate, memoryless, vector quantizer, before being sent over the fibre communication link.

3. Methodology

a. Network Representation- The first step in our methodology was to produce the **Network Representation** of the University showing the access network structure. Network representation provides a powerful visual and conceptual aid for portraying the relationship between the components of systems that is used.

The Access Network (AN) is based on a fibre-optic cable passing over a number of remotes units. The subscribers are connected to the Local Exchange (LE) and the remote units and subscriber lines. By a remote unit (RU) is meant a multiplexer, a remote subscriber unit, a base station (for wireless access) or a combination of these elements. (Krendzel, 2012).

Local Exchange: The University Network Operating Center
Subscribers: In this case they are the Halls of Residence, Academic buildings, Cafeterias, Workshops, University Chapel, University Library, and Post-Graduate Quarters.
Base Station: Located in each of the subscriber unit, for ease of wireless access in each building and surrounding area.
Multiplexer: For distributing signals usually located in each of the base station.
Subscriber Lines (Individual): Staff and Students.

Figure 2: Google Earth of University Campus accessed January

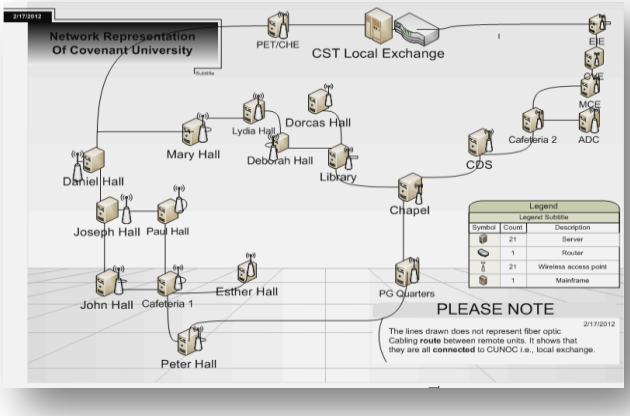

Figure 3: Network Representation of the University Network, using Microsoft Visio 2007

b. The Transportation Problem.

1. Known Capacity of Internet Bandwidth is available from three Bandwidth Supply Companies.
2. In the University, Known quantity of Bandwidth is distributed to a number of users in Academic, Administrative and Residential Buildings for use by staff and students.
3. The academic, administrative and residential buildings are interconnected to each other using Optical Fibre Cabling (OFC) with associated costs with respect to material, technology and logistics.

The transportation problem is to determine the **Bandwidth size** to move from each Bandwidth Supply source to the various academic, administrative and residential buildings to **minimise the overall cost** while satisfying the constraint of demand from staff and students in the University over a given period of time.

c. Supply Side (Internet Service Providers)

There are three supply companies which are:

- ISP-1 provides the University with 25 Mbps (Megabyte) of internet data.
- ISP-2 provides the University with 30 Mbps (Megabyte) of internet data.
- ISP-3 supplies the University 30 Mbps (Megabyte) of internet data.

d. Formulation of the Problem

Here we will be formulating the transportation problem as linear programming problem.

Let x_{ij} = amount of bandwidth routed from ISP i to cluster $j; i = 1,2 \ldots\ldots, m; j = 1,2, \ldots\ldots, n$
Let c_{ij} = cost to route bandwidth 1 from ISP i to user cluster $j; i = 1,2, \ldots\ldots m; j = 1,2, \ldots\ldots, n$
Let d_j = required number of units at user cluster $j; j = 1,2, \ldots\ldots\ldots, n$
Let s_i = capacity of ISP $i; i = 1,2, \ldots\ldots, m$

The problem can be formulated as a linear model, namely (Gillett, 1979).

Minimize: $z = \sum_{i=1}^{m} \sum_{j=1}^{n} c_{ij}\, x_{ij}$

Subject to: $\sum_{j=1}^{n} \boldsymbol{x_{ij}} \leq \boldsymbol{s_i} \quad \boldsymbol{i = 1, 2, \ldots\ldots, m}$

Equation 1: Supply Capacity Constraint

$$\sum_{i=1}^{m} \boldsymbol{x_{ij}} \geq \boldsymbol{d_j} \quad \boldsymbol{j = 1, 2, \ldots\ldots, n}$$

Equation 2: Bandwidth Demand Constraint

all $\boldsymbol{x_{ij} \geq 0}$

Equation 3: Bandwidth Non negativity Constraint

If al least one feasible solution exists, then there exists an optimal solution where all the

x_{ij} values are integer or zero. The simplex method will produce this integer optimal solution

If equation 1 is summed up over all i, then

$$\sum_{i=1}^{m}\sum_{i=1}^{n} x_{ij} \leq \sum_{i=1}^{m} s_i$$

Likewise if equation 2is summed over all j, then

$$\sum_{j=1}^{n}\sum_{i=1}^{m} x_{ij} \geq \sum_{j=1}^{n} d_j$$

Thus from equations 1 and 2,

$$\sum_{i=1}^{m} s_i \geq \sum_{j=1}^{n} d_j$$

Suppose

$$\sum_{i=1}^{m} s_i = \sum_{j=1}^{n} d_j$$

Thus constraints equation 1 and 2 can be rewritten as equalities so that the model becomes (Gillett, 1979):

Minimize: $z = \sum_{i=1}^{m}\sum_{j=1}^{n} c_{ij}\, x_{ij}$

Subject to: $\sum_{j=1}^{n} x_{ij} = s_i \quad i = 1, 2, \ldots\ldots, m$

$\sum_{i=1}^{m} x_{ij} = d_j \quad j = 1, 2, \ldots\ldots, n$

all $x_{ij} \geq 0$

Where $\sum_{i=1}^{m} s_i = \sum_{j=1}^{n} d_j$

Assumptions

a. Objective function will be: [(The cost of fibre per metre) x (the distance to run through) + (cost of mbps/annum) x (amount of mbps)]
b. 48 core single mode fibre optic cable at N450/m
c. Taking 1mbps/month = $350
d. Exchange rate is NGN/US$ 170
e. Demand Nodes:
   - Academic Building/Administrative (**A**) using College of Development studies CDS as our point of reference.
   - Non Academic (**B**) using the University Chapel as our reference point
   - Residential/Non-Academic (**C**) using Cafeteria 2 as our reference point.

f. Based on preliminary demand analysis done (Bolu, 2010) we assume the following:
   - Point A needs 40Mbps due to:
     - The high degree of work being done in the Building by the lecturers, Administrative staff, students in class who also use the e-learning portal and other internet activities.
     - Population will be averagely highest here during the day except for lecture free day or public holidays.
   - Point B needs 25Mbps due to:
     - Being a non-academic area, less work will be done here compared to the college/department buildings and student population will be randomly high.
   - Point C needs 20Mbps due to:
     - Being residential - activities that will be done here will not be as intensive as at Point A. Activities like; Webinar (occasionally), Online conference meeting (occasionally), checking of mails, watching of academic videos online, and other social and academic download.
     - Students/Staffs will only be at their residence in the evening or lecture free day or a general public holiday. During the day not many activities will take place.

The transportation matrix is shown below:

Table 1: Transportation matrix

Buildings	User Demand (Mbps)	ISP

	Academic	Administration	Residential	Capacity (Mbps)
ISP 1 Google	x_{11}	x_{12}	x_{13}	25
ISP 2 Glo	x_{21}	x_{22}	x_{23}	30
ISP 3 Etranzact	x_{31}	x_{32}	x_{33}	30
User Demand (Mbps)	40	25	20	85

4. Results and analysis

Note 1: ISP *Globacom, Etranzact and Google* are all in the **same point** (Network Operating Center, CUNOC). That means they have the **same distance** to the demand points.

Note 2: Representations are:

- 'E' represents Etranzact
- 'Gl' represents Globacom
- 'Gg' represents Google

Note 3: Distance from points obtained from Google Earth and some confirmed by physical measurement (Bolu, 2011).

Note 4: Drawing made using Microsoft Visio 2007.

Figures 4, 5, and 6 shows some feasible solutions.

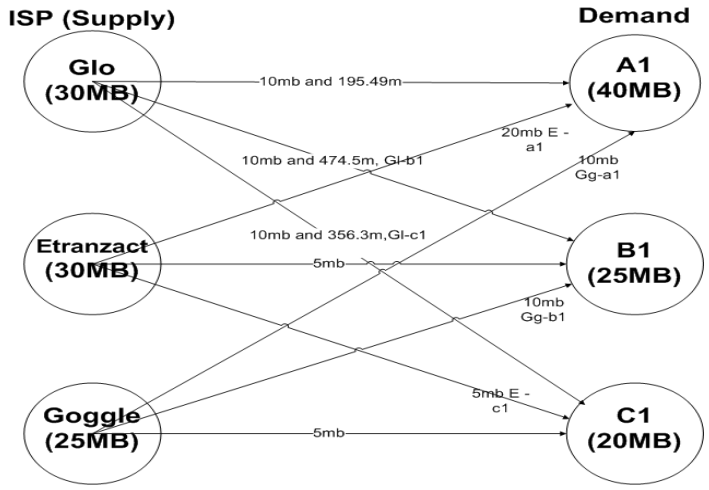

Figure 4: Feasible Solution 1

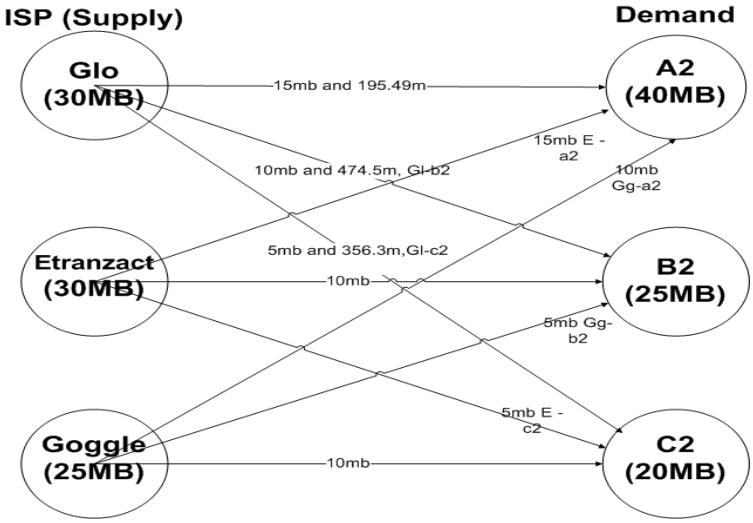

Figure 5: Feasible Solution 2

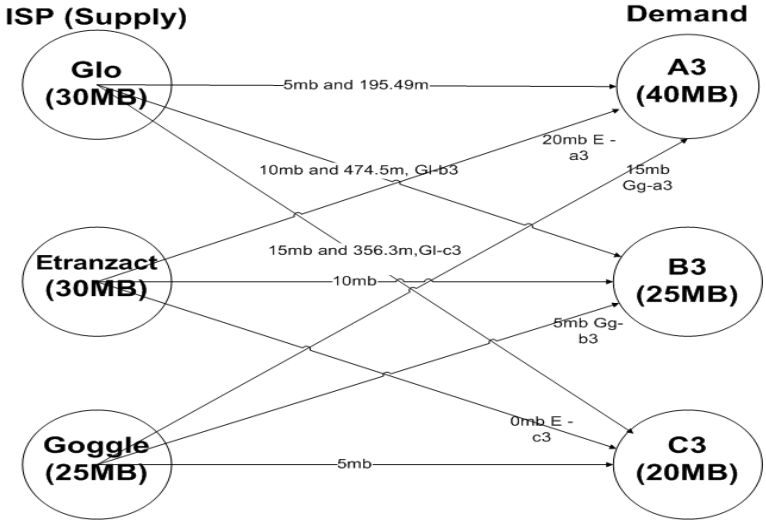

Figure 6: Feasible Solution 3

Solution

Minimise z = $2643900\mathcal{X}_{11} + 2643900\mathcal{X}_{12} + 2643900\mathcal{X}_{13} + 2128075\mathcal{X}_{21} + 2128075\ \mathcal{X}_{22} + 2128075\mathcal{X}_{23} + 1671005\mathcal{X}_{31} + 1671005\mathcal{X}_{32} + 1671005\mathcal{X}_{33}$

Subject to:

$$\sum_{i=1}^{3} x_{i1} = 30 \text{ Glo}$$

$$\sum_{i=1}^{3} x_{i2} = 30 \text{ Etranzact}$$

$$\sum_{i=1}^{3} x_{i3} = 25 \text{ Goggle, all } x_{ij} \geq 0$$

$\sum_{j=1}^{3} x_{1j} = 40$ Academic/Administrative Building

$\sum_{j=1}^{3} x_{2j} = 25$ Non-Academic Building

$\sum_{j=1}^{3} x_{3j} = 20$ Residential Building

And

$$\text{all } x_{ij} \geq 0 \begin{bmatrix} 1\,1\,1\,0\,0\,0\,0\,0\,0 \\ 0\,0\,0\,1\,1\,1\,0\,0\,0 \\ 0\,0\,0\,0\,0\,0\,1\,1\,1 \end{bmatrix} \begin{bmatrix} x_{11} \\ x_{12} \\ x_{13} \\ x_{21} \\ x_{22} \\ x_{23} \\ x_{31} \\ x_{32} \\ x_{33} \end{bmatrix} = \begin{bmatrix} 40 \\ 25 \\ 20 \\ 30 \\ 30 \\ 25 \end{bmatrix}$$

Using the MATLAB Linear Programming module, the following solution diagrammatically shown below was obtained.

Through linear programming we have optimized the cost. The resulting objective function is ₦184, 930,000.00k

5. Conclusion

We have been to determine the bandwidth size to be supplied and the minimised cost of distribution using linear programming.

The final outcome of using a linear program in generating a model to solve the access network problem of connecting buildings across the University is one that can be deployed for use in other models. Though other forms of costs might arise during the process of construction and laying the cables, the final cost used is accurate and would be very close to the actual cost to be spent depending on the amount of miscellaneous expenses that arise during actual cable laying.

Also, though this model has been developed for a specific location, the steps followed can be useful as a guideline for modeling another Access Network for a different location having Network (communications) problems.

Since the objective function of a system is the measure of the effectiveness of the system thus, we have been able to determine the cost of meeting the demand of the three main locations with a supply of 85 Mbps.

6. Recommendations

In line with all that has been done, there are still some improvements that can be made to the model and this can model can serve as a guideline for whatsoever would be done. Such additions and/or improvements could be:

- Use of Integer or Dynamic Programming for a better bandwidth allocation and adequate Network Planning.
- Expansion of this model to encompass other buildings being in Covenant University Network.
- It should be noted that this model was simplified by clustering the users. This should be un-clustered for future work.

Acknowledgement

The authors acknowledge the laboratory investigation contribution of the Innovation Centre, University of Nigeria, Nsukka and the Department of Mechanical Engineering, Covenant University, Ota for the provision of computing facilities for this work.

References

Ab-Rahman, M. S., (2011), The Extension of OXADM Survivability Scheme to Fibre-to-the Home Wavelength Division Multiplexing (FTTH-WDM) Network. *Journal of Applied Sciences Research*, 8(6): 880-884

Ab-Rahman, M. S., et al, (2009), Transmission surveillance and self-restoration against fibre fault for time division multiplexing using passive optical network by ISSN 1751-8628, 2nd April 2009.

Bailey, D., and Wright, E., (2003), Practical Fibre Optics - ISBN: 0750658002.

Bolu, C. A, (2011), *Modeling and Simulation in Mechanical Engineering* in Principles of Mathematical Modeling, Lecture note (MCE 414), Covenant University, Ota, Ogun State. Nigeria. 2011, pp 3-7

Bolu, C. A., (2011), *Fibre Optics Network Optimisation as a Transportation Problem*, [Lecture Note in Engineering Mathematics], Department of

Mechanical Engineering Covenant University, Nigeria.

Gillett, B. E.,(1979), Introduction to Operations Research: A Computer Oriented Algorithmic Approach, New Delhi: Tata McGraw-Hill Publishing Company Ltd

Krendzel, A. V., *Access Network Planning: Minimisation of Construction Cost*, Dept., of Network Planning, St. Petersburg Research Institute of Telecommunications (LONIIS) 11, Warshawskya Str.196128

Kulkarni, S. and El-Sayed, M., (2010), *FTTH-Based Broadband Access Technologies: Key Parameters for Cost Optimized Network Planning by.* Bell Labs Technical Journal 14(4), pp 297–310 Alcatel-Lucent, Wiley Inc.

Morley, G.D, Grover, W.D, (1999), *Comparison of Mathematical Programming Approaches to Optical Ring Network Design* TR Labs and University of Alberta, Dept., of Electrical and Computer Engineering, Edmonton, T6G2El, Canada.

Pfarrhofer, R.,et al, (2012), *Distributed Optimization of Fibre Optic Network Layout Using MATLAB*, uhl@cosy.sbg.ac.at – http://www.cti.ac.at/ accessed January 28, 2012

Pirmez L., et al, (2010, September 15), Network Selection Based On Utility Function and Integer Linear Programming*, Journal of Computer Networks*, Volume 54 (13), ISSN 1389-1286.

Ray, S., et al, (2012), *Fibre Aided Wireless Network Architecture: A SISO wireless -optical channel*, Laboratory for Information and Decision Systems, MIT, Cambridge

Occupational mobility in engineering profession (craftman and artisan) in Oyo State, Nigeria.

[1] Ilori, T.A., [2]Dauda.,T.O., [3]Raji.A.O, and [4]Kilanko,. O. O

[1]Dept. of Agric. Engineering Programme, Federal College of Agric., Ibadan.
[2]Obafemi Awolowo University, Institute of Agricultural Research & Training, PMB 5029, Moor Plantation, Ibadan, Nigeria.
[3]Dept. of Agric. and Environmental Engineering, University of Ibadan, Ibadan.
[4]Dept of Mechanical Engineering, Covenant university Ota.
Corresponding author: iloritaa@yahoo.com

Abstract

This paper evaluate occupational mobility in engineering professional in Oyo State of Nigeria with the goal assessing causes and readiness of the professionals to return to the profession when the hindering factors are removed as well as sufficiency of the survey instrument in addressing the research problems. The study was conducted using a well structured questionnaire administered in 20 local government of Oyo State, Nigeria representing the sample space of 0.424. The Cronbach's alpha of the reliability test of 0.453 was returned for the scale mean statistics of 11516.83 and variance of 0.0000007 showing that the survey instrument was sufficient and could be relied upon. The result of the socio economic analysis showed that 80% of the respondents were married while (15%) were single and the rest (5%) were divorced. The age distribution of the respondents ranged between greater than 50 years groups (12%) and 30 -39 years group (39%).The result of the analysis of job characteristics of the respondents showed that the longer the year of graduation, the lesser the number of graduates still in the business. The cross table analysis of the socio-economic indices with the job status of the respondents showed that marital status and level of education does not have significant effects on the job status of the respondents (whether still practicing or not) because 1.454 and 5.223 returned for both marital status and level of education are not significant ($P<0.05$). Also, the contingency table analysis of the effects of the skill acquisition methods showed that more of the respondents who acquired their skill via Technical School (70%) are willing to go back to the professions. However, for those who acquired their skill through Learning/artisanship, less than average (32%) of the respondents are ready to return to the profession. Lastly, the establishment of the regression model for the relationship between the proportion of the people wishing to go back to the profession and year of practicing the profession provide a necessary impetus for addressing the Job mobility problem faced by the profession.

***Key words**: Mobility, artisan, craftsman, okada, occupation.*

1. Introduction

Occupational mobility different from labour mobility refers to voluntary resignation (partially or totally) of an employee from an occupation. Labour mobility on the other hand refers to voluntary resignation or loss of Jobs (Izamoje, 2011). The two terms are though distinct but are governed by almost the same factors. Engineering is one of the several occupation that have attracted several factors of mobility hence, occupational mobility have been in the increase in the profession in the region of the country. Engineering is a broad discipline which is often broken down into several sub disciplines. Basically, engineering fields can be categorized among others as, Agricultural Engineering, Chemical Engineering, Civil Engineering, Electrical Engineering, and Mechanical Engineering (Adesina 1999; Ademousun 1997). Designs are made by engineers based on sound

theoretical knowledge of basic and advanced engineering principles. These designs are translated into real products by the combined efforts of technologist, technician and craftsman who actually execute the design and thus, engineers are of different shades.

Motorcycle transportation (also known as *Okada*, *achaba*) refers to commercial motorcycle in Nigeria, where motorcycle riders carry passengers for commercial purposes. It is one of the chief modes of transportation in Nigeria and the most common form of formal transport system in Nigeria under a registered association called Amalgamated Commercial Motorcycle Owners Rider Association (ACOMORAN). The popularity and widespread acceptance of motorcycle transportation has rapidly risen in recent years. It has been adopted easily due to the prevailing economic climate in contemporary Nigeria society plagued by a dearth of taxi and bus services, hyper congestion and poor state of roads. Also, they have become a ubiquitous future of Nigerian cities because of their low cost of purchase and maintenance for consumers than other forms of road transportation. Motorcycle transportation provide the cheapest, accessible and fast to overcome traffic congestion even short distance travel and likewise the money earn is on daily basis with little stress. Unfortunately, the rise in number of motorcycle for commercial purpose has led to mobility of people from other occupation (particularly engineering).

Theoretical Frame work.

The theoretical framework for this work is based on Rational Action theory (RAT) and Work adjustment theory (WAT). RAT according to Izamoje (2011) provides the basis for the explanation of individual's ability to make informed decision in a given situation. It (RAT) assumes that individuals are independent in any decision – making process. The decision of labour to move from one occupation to other is an independent action. WAT on the other hand focuses on issues associated with work or occupation including choice of career, job stability and others.

Mamoured of works have been conducted on labour and however, despite the importance of motorcycle transportation mention above, it has been attracting interest as more people are now engage in commercial motorcycle transportation. The objective of this research work is therefore to assess morbility of labour in engineering profession (Craftsman and Artisan) in the study area and to evaluate the effects of the socio economic characteristics of the respondent on their mobility. Also, this study was carried out to evaluate the reliability of the survey instrument.

2. Materials and methods

The study was carried out using a purposive sampling via a well structured questionnaire in fourteen local government areas of Oyo State. The sample space, which is the local governments including Akinyele, Ibadan South-East, Atisbo, Itesiwaju, Ibarapa East, Saki East, Egbeda, Ogbomosho North, Ajaawa, Iseyin, Oyo West, Ibadan South West, Ido, Ibadan North-East local government areas were randomly selected among the 33 local Government of the state. This represents the sampling frame of 0.424 which is quite sufficient for the study area. The survey was conducted by means of structured questionnaires administered through participatory learning techniques. A total of four hundreds questionnaires were administered with at least 20 sample information obtained in each local government area. Some of the issues addressed by the questionnaire include; Year of graduation from training, Engineering Skill Acquisition, amount earned per week while practicing engineering as a profession, amount earned per week on motorcycle transportation, problems faced while practicing engineering job, year motorcycle transportation business was started, motorcycle operation competence, willingness to go back to engineering profession if constraints were removed. All the distributed sampling tools (questionnaires) were retrieved and analyzed.
Reliability analysis was computed for 3 randomly selected items of the questionnaire using Cronbach's alpha (α). These items are amount earned while practicing the profession, year of commencement of motorcycle business and amount earned from motor cycle transportation.

$$Cronbach's\alpha = \frac{N - \overline{C}}{\overline{V} + (N-1).\overline{C}}$$

Where N = No of items (3), $\overline{C}$ = average inter – item covariance among the items and $\overline{V}$ = average variance.

The data was further subjected to descriptive statistical analysis (frequency and graphs) and cross tabulation analysis using chi square statistics. Chi square statistics test for the significant difference(s) between the observed and the expected frequency of respondents for related items of the study tools (questionnaire). The resultant statistics were compared with the critical $\chi_{149,0.05}^{2}$ for appropriate decision. Box plot of the two response categories was done for amount earned from the profession per week as well as amount earned from commercial motorcycle par week. The proportion of the respondent according to the year of graduation was subjected to the third order polynomial regression to determine the relationships between the year of graduation and the proportion of the frequency of the respondents still on the job. The model estimate as well as the coefficient of the determination (R^2) were determined.

3. Results and discussions

Survey Instrument Sufficiency Study (SISS). The results of the SISS showed that the items of the instruments were sufficient in the analysis of the problem under study. The Cronbach's alpha of the reliability test of 0.453 was returned for the scale mean statistics of 11516.83 and variance of 0.0000007. The low value of the Cronbach's α could be hinged on the fewness of the items included in the reliability study.

Socioeconomic Characteristic of the respondents.

The result of the survey, (table1), showed that 80% of the respondents were married while (15%) were single and the rest (5%) were divorced. The age distribution of the respondents ranged between greater than 50years groups (12%) and 30 -39 years group (39%). Other age groups are 20 -29 yrs (29%) and 40 – 49 yrs (20%). It could be observed that as the age increases, the frequency of people involved in the profession increases (Figure 1). However, at the peak of 30 - 39 years age group, it started to decline. This can be linked to 2 prime factors of strength and responsibilities that can be a driving for engaging in such venture. Majority of the respondent (69%) of population sampled has formal education, (26% has primary school education, 27% has secondary school education, 10% has adult education and 6.0% have Grade II/ OND / NCE) and 31% has no formal education. Most of the respondent (91%) acquired engineering skill through learning (Artisan) while others (9%) acquired engineering skill through technical school (craftsman). With the level of education, the respondents' technical experience while on the professional job can withstand the test of time to acquired new engineering skill and or innovation in technology whereby some machines are designed made with some electrical/electronic devices to operate it.

Job characteristics of respondents.

The result of the analysis of job characteristics of the respondents showed that the longer the year of graduation, the lesser the number of graduates still in the business. Indeed, most of the respondents can be tagged as fresh or nearly fresh graduates because they graduated in the range of 1990 – 1999 (37%) and 2000-2009 (31%). There were also old graduates of 1970-1979 (12%) and 1980-1989 (20%). This could be linked to the fact that the engineering profession is not feasibly practicable at the said ages due to the energy requirements. The box plot analysis of the amount earned while still practicing the engineering job for those still on the job was appreciably higher than those who quitted the job. Even the mean of those still on the job was appreciably higher than those who quitted the job. Even the mean of each of the group (that is those still practicing and those not practicing) are almost the same (Figure 2). The result of the job characteristics analysis showed that majority of

the respondents (330) have come of age spending above 5 years practicing the profession. Most of the respondents acquired their skill learning (artisanship – 365) while other skill acquisition methods include, Technical school and others 1). The result of job characteristic analysis showed that majority (78%) of the respondents owned the motorcycle by themselves while some (17%) acquired their motorcycles through hiring (Table 2).

Contingency Table analysis. The cross table analysis of the socio-economic indices with the job status of the respondents showed that marital status and level of education does not have significant effects on the job status of the respondents (whether still practicing or not). This is because 1.454 and 5.223 (Table 3) returned for both marital status and level of education are not significant (P<0.05). The implications of these are;

1 – Marital status could not have influenced people's quiting the job temporarily or permanently

2 – The level of education has not had significant effects on their job status.

Also, the cross table analysis of the effects of age on job status of the respondents indicated that greater percentage (49%) of people in the age group 40 – 49 years are still on the job while the least percentage (21%) of respondents in the age group 30 – 39 years are still practicing. This is significant (P < 0.01) because 11.633 < $\chi_{4,\ 0.05}$ = 9.488 and thus wise to hinge job mobility on age factor. This may be due to the fact that motorcycle transportation though is lucrative but require enormous energy which is found in the age group 30 – 39 years. Similarly, the longer the length of graduation, the higher the proportion of the respondents still found in the profession (Table 3). However, this trend was irregular because, it changes with the changes in the age group. Majority of the respondents (382) are ready to move back to the profession if their constraints are removed and this is significant (P<0.05) because 6.157 was significant (Table 4). Also, the contingency table analysis of the effects of the skill acquisition methods showed that more of the respondents who acquired their skill via Technical School (70%) are willing to go back to the professions. However, for those who acquired their skill through Learning/artisanship, less than average (32%) of the respondents are ready to return to the profession (Table 4). This result is significant ($\chi^2_{4,\ 0.05}$ = 5.175) at 0.05 level of significant. The implication of this is that skill acquisition method could be said to be a factor of respondents' readiness to go back to the profession. The results of regression analysis of the proportion of the respondents that are ready to go back to the profession showed that 3rd order polynomial gives the best model estimates. The proportion can be estimated using;

$$Y = 0.079x^3 - 0.594x^2 + 1.321x - 0.556$$

The coefficient of determination, R^2 for this model is 1.00 signifying a high level of predictability. The implication of this is that the model estimates can be adopted for the prediction of the proportion of the frequency of the respondents when the year of graduation group of the respondents (x) is known.

Conclusion

The goal of this study is the assessment of morbility of labour in engineering profession (Craftsman and Artisan) in the study area as well as evaluation of the effects of the socio economic characteristics of the respondent on their mobility. The sufficiency of the survey instrument despite the fact that the data were not collected overtime indicated that labour mobility study do not necessarily have to be overtime as posited by Giuseppe and Kaj (2007). However, if the goal of the study emphasizes the effects of period, then, time factor must be inclusive. This study have provided evident of job mobility in the engineering sector which represent further advance from Izamoje (2011). Izamoje (2011) established that 74.7% of the respondents have tendency to move from one job to another while the present study established that more than average of the respondents have moved form their job. Also worthy of note is that while some socio economic characters have no significant effects on the respondents' job mobility some others (socio economic characteristics) do have (and may be negative or positive). In addition, job mobility in this study has be linked to a number of factors including, poor working environment/facilities,

lower income compare to other jobs and dying interest of the professionals. This is in line with Izamoje (2011) Gueorgui and Lourii (2004) and Ogege (2011). The establishment of the regression model for the relationship between the proportion of the people wishing to go back to the profession and year of practicing the profession provide a necessary impetus for addressing the problem faced by the profession and it is in line with Izamoje (2011). This study therefore recommends that the model can be adopted for investigating the proportion of people wishing to go back to the profession in any other region of the Country. Similarly, the model as well as other findings of this study would be found useful by stake holders in addressing the problem of job mobility.

References

Adesina 1999.

Ademousun 1997.

Giusepe, M. and Kaj, T. 2007. Occupational and Job Mobility in the US. Scandinavian Journal of Economics. 109 (4), 807 – 836.

Gueorgui K. and Lourii M. 2004. Occupational Mobility and Wage Inequality. IZA DP No 1189, 65pp.

Izamoje, L. 2011. Reactions to Labour Mobility in Small and Medium Organisations in Nigeria. European Journal of Social Sciences. 25 (3) 291 – 304.

Ogege S.O. 2011. Gender Role Differentiation and Social Mobility of Women in Nigeria. Journal of Social Science. 27 (1) 67 – 74.

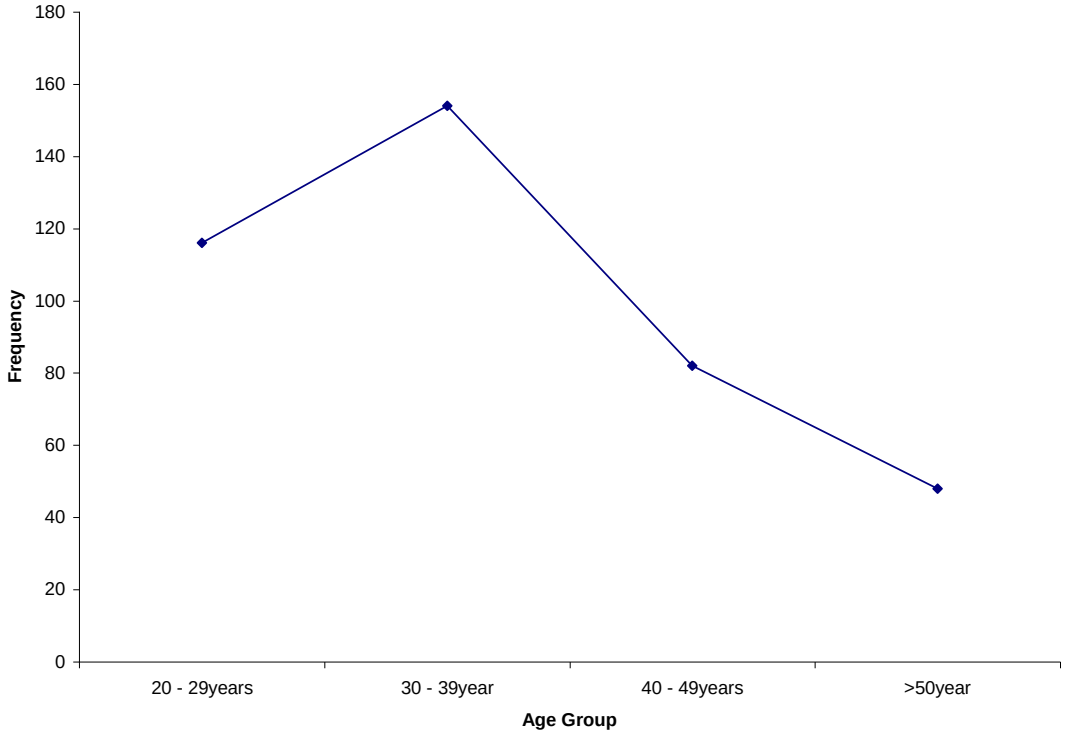

Figure 1. Distribution of Respondents according to age Group

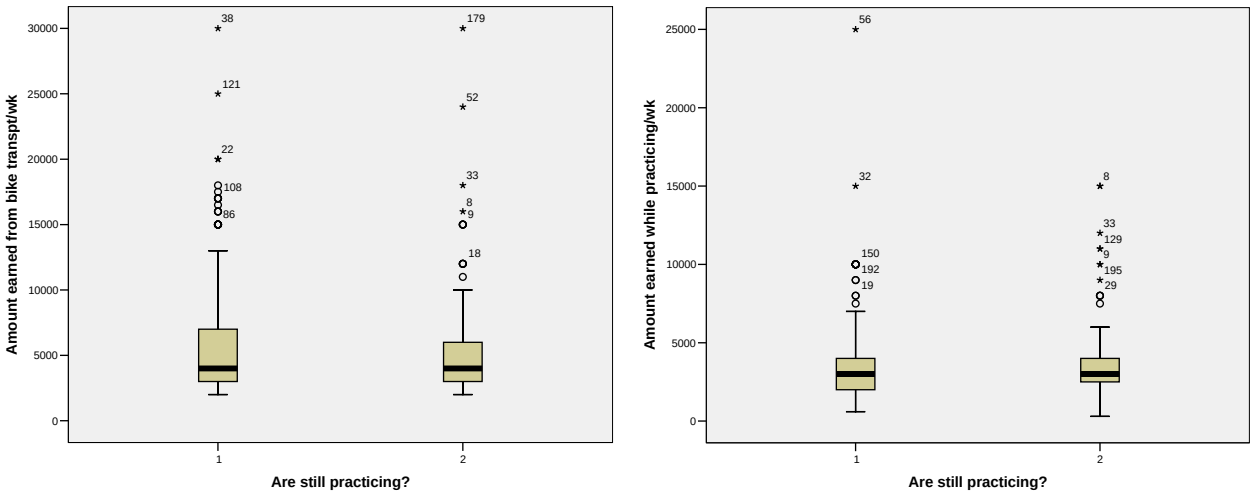

Figure 2. Box Plot of the amount earned while still Practicing and/or from Bike against their Job Status (whelther on Job or not).

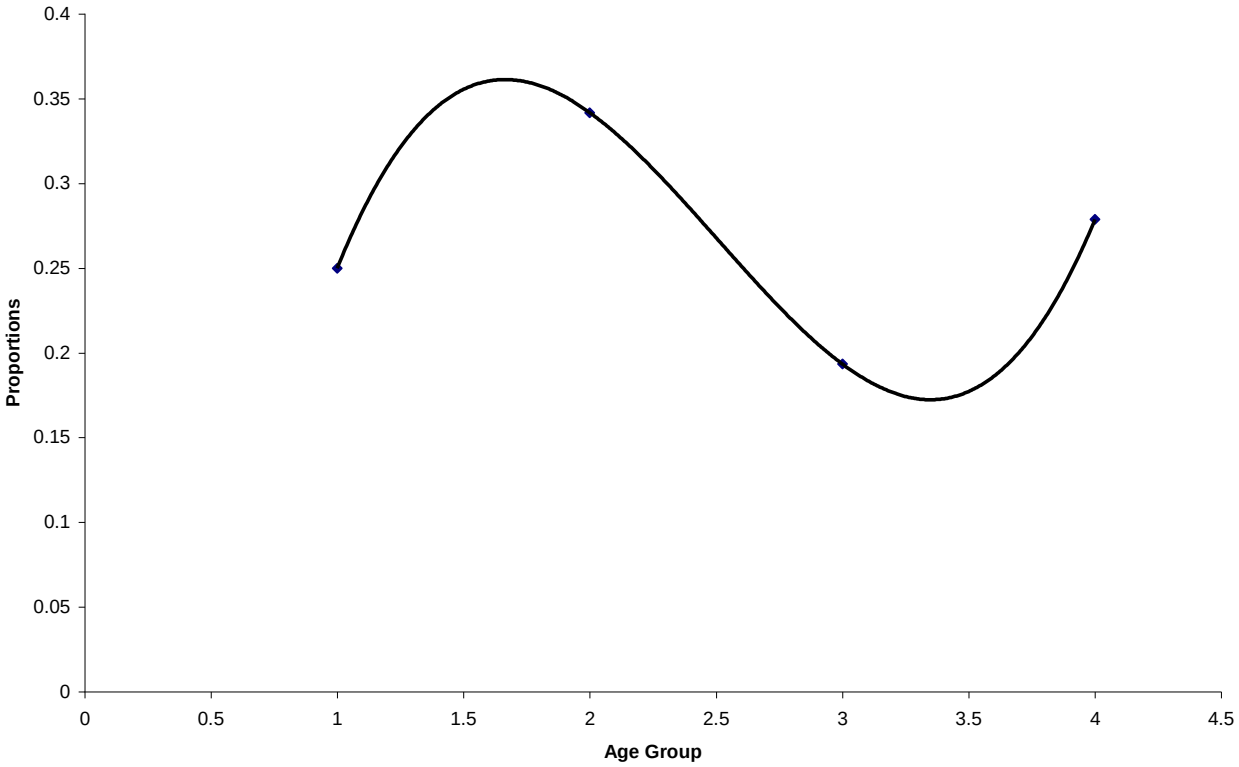

Figure 3. Proportion of the respondents still in the profession by their year of graduation
NB 1 = 30-39years; 2= 20 -29years; 3=10-19years and 4 = < 10years.

Table 1: Socio-Economic Characteristics of the Respondents

Variables	Options (years)	Frequency	Percentages (%)
Marital Status	Divorced	21	5.3
	Married	320	80
	Single	59	14.8
Education	Adult Education	40	10
	GII/OND/NCE	24	6
	Sec. Education	107	26.8
	Primary School	105	26.3
	No formal Education	124	31
Method of Skill Acquisition	Learning	365	91.3
	Technical school	34	8.5
	Others	1	0.3
Still Practicing	Yes	102	25.5
	No	297	74.3
	NA	1	0.3

Table 2: Job Characteristics of Respondents

Variables	Options (years)	Frequency	Percentages (%)	C%
Year of Graduation	1970 – 1979	49	12	12
	1980 – 1989	79	20	32
	1990 – 1999	150	37	69
	2000 – 2009	122	31	100
Years of Practice	1 – 2 years	11	3	3
	3 – 4	59	15	18
	5 – 6	85	21	49
	7 – 8	83	20	69
	9 – 10	112	28	87
	> 10	50	13	100
Skill Acquisition Method	Learning	365	91	91
	Technical School	34	9	100
	Others	1	0	100
Motorcycle Ownership	Company	2	0.5	0.5
	Group of people	18	4.5	5.0
	Hire	68	17	22
	Personal	312	78	100

Table 3: Effect of Socio-Economic Status on Job Status of the Respondents

Variables	Options (years)	Job Status		Remarks
		Yes	No	
Age	20 – 29	31	85	11.633**
	30 – 39	32	122	
	40 – 49	27	55	
	50 and above	12	35	
Marital Status	Divorced	7	14	1.454
	Married	78	241	
	Single	17	42	
Level of Education	Adult Education	8	32	5.223
	Grade II/NCE	9	15	
	NFE	34	89	
	Primary Education	25	80	
	Secondary Education	26	81	
Year of Graduation	1970 – 1979	12	36	13.686**

1980 – 1989	27	52
1990 – 1999	29	121
2000 – 2009	34	88

Table 4. Occupational Status and Readiness to be back to the occupation on Constraint Removal as well as skill acquisition Methods.

		Occupational Status		χ^2- statistics
		Yes	No	
Readiness to be back to the Occupation on Constraint Removal	Still on Job	102	0	6.157*
	Not on Job	280	17	
	Technical Schools	14	20	
Skill Acquisition methods	Learning	88	276	5.175*
	Others	0	1	

Babalola: Proc. ICCEM (2012) 298 - 314

Design and construction of parabolic solar heater using polymer matrix composite

Babalola P.O.
Department of Mechanical Engineering, College of Science and Technology, Covenant University, Canaan Land, Km 10, Idiroko Road, PMB 1023, Ota, Ogun State.

phillip.babalola@covenantuniversity.edu.ng; phillgail@yahoo.com

Abstract

A parabolic dish is a type of concentrating reflective device that uses the shape of a circular paraboloid to collect or project energy such as light, sound, or radio waves. The parabolic reflector transforms an incoming plane wave traveling along the axis into a spherical wave converging toward the focus. In this work concentrating dish was moulded from polyester resin reinforced with fiber glass mat and inner surface lined with Aluminum foil to increase the reflectivity. The design was made up of a moulded dish of 246cm diameter with a height of 58.2cm which has a concentration factor of 54.9. The collector was mounted on a site with latitude 6°40′22.19″ and longitude 3°09′47.12″ and water at 27^{0}C was heated to a temperature of 85^{0}C within 20 minutes.

***Key words**: Solar energy, aluminium foil, polymer matrix composite (PMC), parabolic dish, polyester*

1. Introduction

World energy use increased more than tenfold over the 20th century, predominantly from fossil fuels (i.e. coal, oil and gas) and with the addition of electricity from nuclear power. In the 21st century, further increases in world energy consumption can be expected, much for rising industrialisation and demand in previously less developed countries, aggravated by gross inefficiencies in all countries. Whatever the energy source, there is an overriding need for efficient generation and use of energy (John Twidell et al, 2006).

The Sun is the largest energy source, annually producing $3.9x10^{24}$J = $1.08x10^{18}$KWh of solar energy which reaches the surface of the Earth. This is about 10,000 times more than the annual global primary energy demand and much more than all available energy reserves on earth; therefore using one ten-thousandth part of the incoming sunlight would cover the whole energy demand of mankind**.** Nigeria receives about 5.08 x 10^{12} kWh of free energy per day from the sun, if solar devices with just 5% efficiency are used to cover only 1% of the country's surface area then 2.54 x 10^6 kWh of electrical energy can be obtained from solar energy; this amount of electrical energy is equivalent to 4.66million barrels of oil per day (Sambo and Doyle, 1986).

This energy is expected to be the foundation of a sustainable energy economy, because sunlight is the most abundant renewable energy resource; additionally, solar energy is harmless to the environment in terms of pollution and ecological stability.

There is a distinction between direct and indirect solar energy. Technical systems using direct solar energy convert incoming solar radiation directly to useful energy, for instance electricity or heat. Wind, river water and plant growth are indirect forms of solar energy. Here natural processes convert solar energy into other types of energy. Technical systems can use these indirect types of solar energy as well.

Solar thermal energy derived from the sun's heat has been used for centuries by ancient people for heating and drying. More recently, in a wide variety of thermal processes solar energy has been developed for power generation, water heating, mechanical crop dying, and water purification, among others.

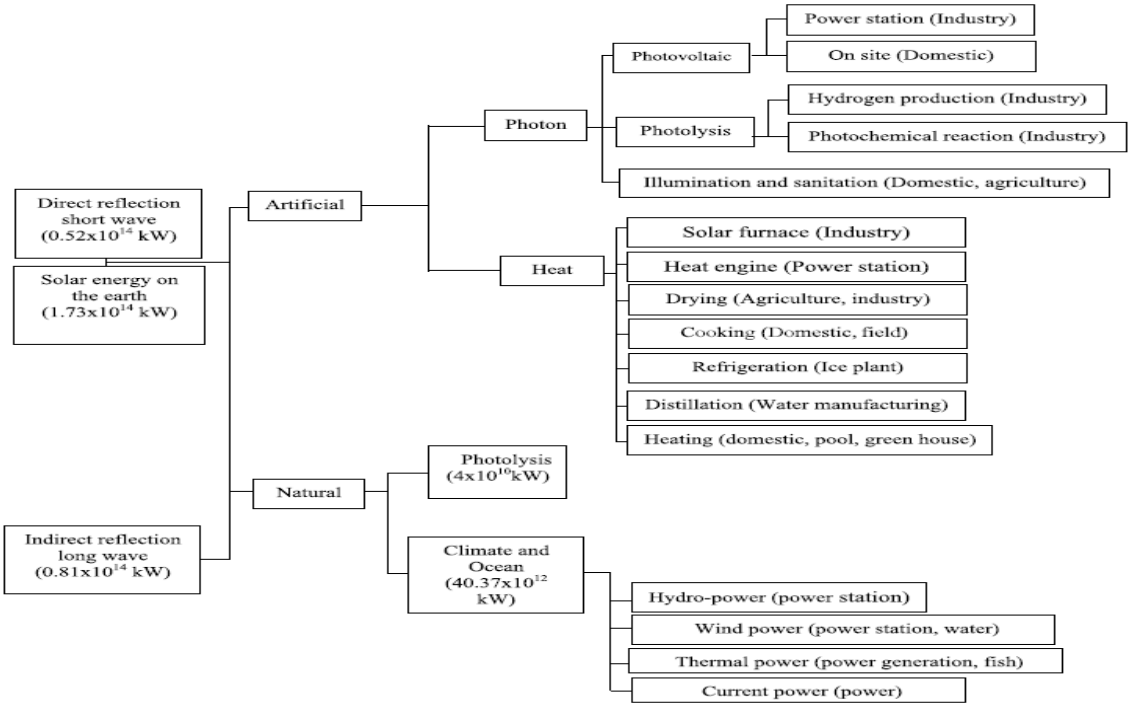

Figure 1: Solar energy distribution and utilization (Ohta 1979)

In our world today, a common use of solar energy is for heating air and water; dwellings in cold climates need heated air for comfort, and in all countries hot water is used for washing and other domestic purposes. For example, about 30% of the UK's energy consumption is beneficial for heat in buildings and of Australia's energy consumption, about 20% is used for heating fluids to 'low' temperatures *(*100^{o}C*)*. Because of this, the manufacture of solar water heaters has become an established industry in several countries, especially Australia, Greece, Israel, USA, Japan and China. The great majority of solar water heaters are for domestic properties, despite large volumes of hot water being used for process heat in industry (John Twidell et al, 2006).

Given the range of working temperatures of solar thermal processes, the most common applications are:

- For less than 100^{o}C: water heating for domestic use and swimming pools, heating of buildings, and evaporative systems such as distillation and dryers;
- For less than 150^{o}C: air conditioning, and heating of water, oil, or air for industrial use;
- For temperatures between 200^{o}C and 2000^{o}C: generation of electrical and mechanical power; and
- For less than 5000^{o}C: Solar furnace for the treatment of materials.

Solar powered devices are the most direct way of capturing the sun's energy, harnessing it, and turning it into something useful. These devices capture the sun's energy and directly transform it into a useful energy source. A solar powered device is said to be **passive** if the solar heat is absorbed and utilized without significant mechanical pumping and blowing; but if the solar heat is collected in a fluid, usually water or air, which is then moved by pumps or fans for use, the solar system is said to be **active**. The general principles and analysis that apply to solar water heaters apply also to many other systems which use active and passive mechanisms to absorb the Sun's energy as heat, e.g. air heaters, crop driers, solar 'power towers', solar stills for distilling water, solar buildings; (John Twidell et al, 2006)

The following technologies can utilize direct solar energy:

- Solar thermal power plants
- Photolysis systems for fuel production
- Solar collectors for water heating
- Passive solar heating systems
- Photovoltaic, solar cells for electricity generation.

1.0. AIM

The overall aim of this project is to harness part of the sun's energy to heat up water for domestic purposes.

1.1. Objective

The objective of this project is to design and build a parabolic solar dish of 2.46m diameter that takes the sun's energy by concentrating its rays to the parabola's focal point so as to heat up water to temperatures between 82-121ºC (180-250ºF).

1.2. Scope and de-limitation of work

This project would only cover the design and construction of a parabolic solar dish that would serve as a collector and concentrator of the sun's energy, choice of materials for better performance, calculations as relating to the designed system such as the amount of heat energy that can be generated by this system, and the amount of time it would take to achieve the amount of heat energy needed. The obtained temperatures can be applied as follow:

- For less than 100^{o}C: water heating for domestic use and swimming pools, heating of buildings, and evaporative systems such as distillation and dryers;
- For less than 150^{o}C: air conditioning, and heating of water, oil, or air for industrial use;

1.3. Importance

The importance of this project is harnessing the sun's thermal energy for heating of water and other fluids for domestic and industrial purposes.

2. Literature review

This project required a general research, to discover and utilize the past findings of others, this revealed articles discuss solar technologies and their construction. This served as a great starting point for understanding some of the components of designing any type of solar system; this included reviews on the design elements and materials needed for the reflector and absorber for optimal performance. The research also revealed in-depth consideration on several variation of solar heating systems and clear explanations on some underlying principles of how these systems work. A bibliography of the research resources used for this project is located at the end of this report.

2.1. Solar energy collectors

Solar collectors are devices which take the solar energy from over a wide area, and concentrate it into a smaller area. These devices are said to be **passive** if the solar heat is absorbed and utilized without significant mechanical pumping and blowing; but if the solar heat is collected in a fluid, usually water or air, which is then moved by pumps or fans for use, the solar system is said to be **active**. These devices can collect solar energy for the production of either heat or electricity.

The Design methods of solar energy collectors include:

- flat collectors,
- evacuated tubes, and
- Concentrators.

2.1.1. Flat collectors

Flat collectors work with both direct and diffused light. They provide low temperature heat (less than 70^{0}C) useful for ambient heating, domestic hot water systems, and swimming pools. This type of collector is affected by weather, and its efficiency decreases if large temperature rises are demanded.

Simple collectors are black plastic hoses exposed to the sun. More elaborate collectors use both front and back insulation to reduce heat losses. Collectors may heat water directly or may use an intermediate heat transfer fluid.

The figure below shows a cross section through a typical flat collector. Light and inexpensive aluminum is used extensively; however, it tends to be corroded by water. Copper is best suited for pipes. If an intermediate heat exchange fluid is employed, aluminum extrusions that include the channels for the liquid are preferred. Some panels use a thin copper sleeve inserted into the aluminum tubing; panels can be black-anodized or painted.

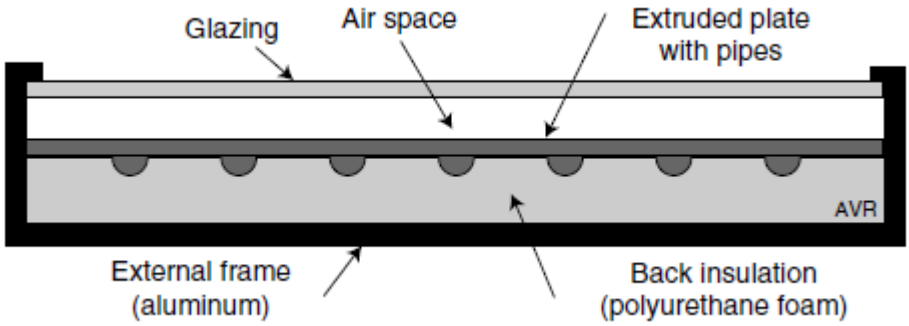

Figure 2.1: Cross section through a typical flat collector (DOE-EREC, 1996)

Flat-plate collectors fall into two basic categories: liquid and air. And both types can be either glazed or unglazed. Unglazed collectors are commonly used to heat swimming pool water. No glazing is needed because the system is used when both outdoor temperatures and solar radiation levels are high (DOE-EREC, 1996).

2.1.2. Evacuated tubes

This type of collector consists of two concentric cylinders, the outer one of glass and the inner, a pipe through which the liquid flows. They bear an exterior likeness to fluorescent lamps. A vacuum is established between the two cylinders therefore conductive and convective heat losses are eliminated because there is no air to conduct heat or to circulate and cause convective losses. There can still be some radiant heat loss (heat energy will move through space or vacuum from a warmer to a cooler surface). However, this loss is small and of little effect compared with the amount of heat transferred to the liquid in the absorber tube reducing the convection heat losses.

Evacuated tubes are non-directional and can heat liquids to some 80^0C. Reflectors placed behind the evacuated tubes can help to focus additional sunlight on the collector.

These collectors are more efficient than flat-plate collectors for two main reasons. First, they perform well in both direct and diffuse solar radiation; also due to the minimal heat losses to the outdoors due to the vacuum, makes these collectors particularly useful in areas with cold, cloudy winters. Second, because of the circular shape of the evacuated tube, sunlight is perpendicular to the absorber for most of the day. (DOE-EREC, 1996)

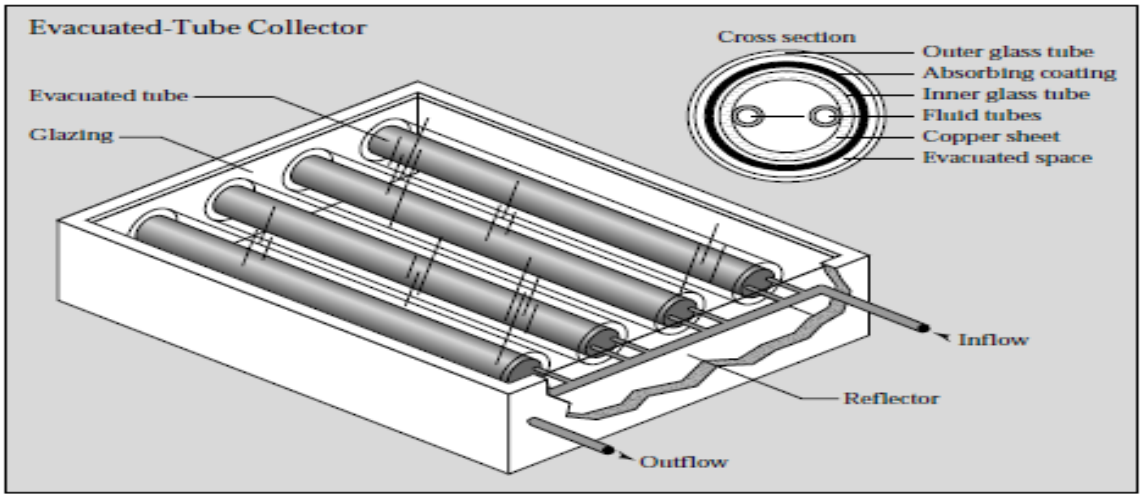

Figure 2.2: An Evacuated Tube Collector (DOE-EREC, 1996)

2.1.3. Concentrators

Concentrating collectors use mirrored surfaces to concentrate the sun's energy on an absorber called a receiver. Concentrating collectors also achieve high temperatures, but unlike evacuated-tube collectors and flat plate collectors, they can do so only when direct sunlight is available, with the result being that their performance is poor on hazy or cloudy days.

Some designs called a point focusing concentrators (3-D) concentrate solar energy onto a focal point, while others called a line focusing concentrator (2-D) concentrate the sun's rays along a thin line called the focal line. The receiver is located at the focal point or along the focal line. A heat-transfer fluid flows through the receiver and absorbs heat.

Concentrators are most practical in areas of high insolation (exposure to the sun's rays), such as those close to the equator and in the desert areas; and they perform best when pointed directly at the sun. To do this, these systems use tracking mechanisms to move the collectors during the day to keep them focused on the sun. Single-axis trackers move east to west; dual-axis trackers move east and west and north and south (to follow the sun throughout the year).

Concentrators are used mostly in commercial applications because they are expensive and because the trackers need frequent maintenance. Some residential solar energy systems use parabolic-trough concentrating systems. These installations can provide hot water, space heating, and water purification. Most residential systems use single-axis trackers, which are less expensive and simpler than dual-axis trackers. (Doe-Erec, 1996)

Two important parameters describe the collector performance:

- Concentration, *C*, and
- Acceptance angle, θ.

Concentration (C): can be defined as either the ratio of the aperture area to the receiver area or as the ratio of the power density at the receiver to that at the aperture.

$C_a = \frac{areaofaperture}{areaofreceiver}$ OR $C_d = \frac{powerdensityatreceiver}{powerdensityataperture}$; $C_a \neq C_d$

These definitions are not equivalent; the latter concentration is preferable.

Acceptance angle(θ): is the angle through which the system can be misaimed without (greatly) affecting the power at the receiver.

There is a theoretical relationship between the concentration and the acceptance angle for the ideal case:

- $C_{ideal} = (\sin\theta)^{-1}$ for a 2-D concentrator……2.1
- $C_{ideal} = (\sin\theta)^{-2}$ for a 3-D concentrator……2.2

It is instructive to calculate the maximum temperature that a receiver can attain as a function of concentration. An ideal receiver will work in a vacuum (no convection losses) and will be perfectly insulated (no conduction losses). Nevertheless, radiation losses are unavoidable. They will amount to

$Pr = \sigma\varepsilon T^4$ Wm^{-2}……2.3

where ε is the emissivity (taken as unity)and σ is the Stefan–Boltzmann constant (5.67×10^{-8} W $m^{-2}K^{-4}$).

The power density at the receiver (assuming no atmospheric losses) is

$P_{in} = 1360C$ Wm^{-2}……2.4

In equilibrium, $P_r = P_{in}$,

$\sigma T^4 = 1360C$ ……2.5

or,

$T = (2.4 \times 10^{10}C)^{1/4} = 394\ C^{1/4}$……2.6

With unity concentration (flat plate collector), T = 393K or 120 C.

When the concentration is raised to 1000, the maximum temperature theoretically attainable is 2200 K. Were it possible to construct a collector with a concentration of 1 million, the formula would predict a receiver temperature of 12,400 K. This would violate the second law of thermodynamics because heat would be flowing unaided from the cooler sun (6000 K) to the hotter receiver. Clearly, the upper bound of the receiver temperature must be 6000 K.

One can arrive at the same conclusion by considering the expression for C_{ideal}. The solar angular radius, as seen from Earth, is 0.25^o. Thus, the minimum acceptance angle that allows collection of light from the whole sun is 0.25^o, and this leads to a C_{max} = 52,000 for a 3-D collector and 230 for a 2-D collector as calculated from Equations 2.1 and 2.2. A concentration of 52,000 corresponds to a T_{max} of 5900K (Equation 2.6), just about right.

Numerous reasons cause the concentration (in terms of power densities) to be less than ideal:

1. Reflector shape and alignment errors
2. Less than perfect reflector surface reflectivity
3. Tracking errors
4. Atmospheric scatter
5. Atmospheric absorption

(Aldo V. Da Rosa, 2009)

2.2. Parabolic solar collector

A parabolic reflector (or dish or mirror) is a type of concentrating reflective device that uses the shape of a circular paraboloid (i.e. surface generated by a parabola revolving around its axis) to collect or project energy such as light, sound, or radio waves. The parabolic reflector transforms an incoming plane wave traveling along the axis into a spherical wave converging toward the focus. Conversely, a spherical wave generated by a point source placed in the focus is transformed into a plane wave propagating as a collimated beam along the axis. [Wikipedia, 2010]

Satellite dishes are used to concentrating waves emitted from satellites far above the earth surface into a focal point to strengthen the signal. Radio and television telescopes perched up high on hillsides also take signals from a wide area, focusing it down to a small point. These technologies are taking weak signals from outer space to a fine point where they can be processed. Solar concentrators using parabolic dishes are exactly the same with these technologies, the difference being the medium used to coat the dishes. Rather than being reflective to radio waves, the coatings used to coat a parabolic solar reflector are mirrors.

2.2.1. Historical background of parabolic reflectors

The principle of parabolic reflectors has been known since classical antiquity, when the mathematician Diocles described them in his book 'On Burning Mirrors' and proved that they focus a parallel beam to a point. Archimedes in the third century BC studied paraboloids as part of his study of hydrostatic equilibrium, and it has been claimed that he used reflectors to set the Roman fleet alight during the Siege of Syracuse. This seems unlikely to be true, however, as the claim does not appear in sources before the 2nd century AD, and Diocles does not mention it in his book. Parabolic mirrors were also studied by the physicist Ibn Sahl in the 10th century. James Gregory, in his 1663 book Optica Promota (1663), pointed out that a reflecting telescope with a mirror that was parabolic would correct spherical aberration as well as the chromatic aberration seen in refracting telescopes. The design he came up with bears his name: the "Gregorian telescope"; but according to his own confession, Gregory had no practical skill and he could find no optician capable of actually constructing one. Isaac Newton knew about the properties of parabolic mirrors but chose a spherical shape for his Newtonian telescope mirror to simplify construction. Lighthouses also commonly used parabolic mirrors to collimate a point of light from a lantern into a beam, before being replaced by more efficient Fresnel lenses in the 19th century (Wikipedia, 2010).

Back in the 1800s a Frenchman named Augustin Mouchot was actively experimenting with solar dishes to concentrate the sun's energy. Mouchot was concerned that coal was all going to be used up and that "Peak coal" was approaching. He said at that time "Eventually industry will no longer find in Europe the resources to satisfy its prodigious expansion, Coal will undoubtedly be used up." A little later in 1882, Abel Pifre, Mouchot's assistant, demonstrated a printing press in the Tuilleries Garden, Paris, powered by the sun, using a 3.5m diameter concave concentrating dish. At the focus of this concentrating furnace, was a steam boiler which provided steam for the printing press (Gavin, 2007).

Parabolic mirror surfaces are used to focus energy efficiently and accurately; the most common modern applications of the parabolic reflector are in satellite dishes, car headlights, astronomical telescopes, spotlights, parabolic solar heater, reflecting telescopes, radio telescopes, parabolic microphones, and many lighting devices such as spotlights, car headlights and LED housings. The Olympic Flame has been lit using a parabolic reflector concentrating sunlight. (Wikipedia, 2010)

2.2.2. The principle of the parabola

The parabolic reflector functions due to the geometric properties of the paraboloidal shape: if the angle of incidence to the inner surface of the collector equals the angle of reflection, then any incoming ray that is parallel to the axis of the dish will be reflected to a central point, or "focus". Because many types of energy can be reflected in this way, parabolic reflectors can be used to collect and concentrate energy entering the reflector at a particular angle. Similarly, energy radiating from the "focus" to the dish can be transmitted outward in a beam that is parallel to the axis of the dish**.** **(**Wikipedia,2010)

When Sun light (parallel rays) falls onto a correctly aligned parabolic mirror it will be reflected back towards a single point known as the focus. The parabolic mirror therefore directs the energy arriving over its surface to a 'hot spot' at the focus, so as to heat something.

The basic shape of a parabola is derived from the equation:

$Y = X^2/4p$

Where **X,** represents the distance away from the mirror centre and **Y**, represents the 'height above' the centre, see figure 1 and 2. The constant **p** is known as the focal length - the distance from the origin to the focus point.

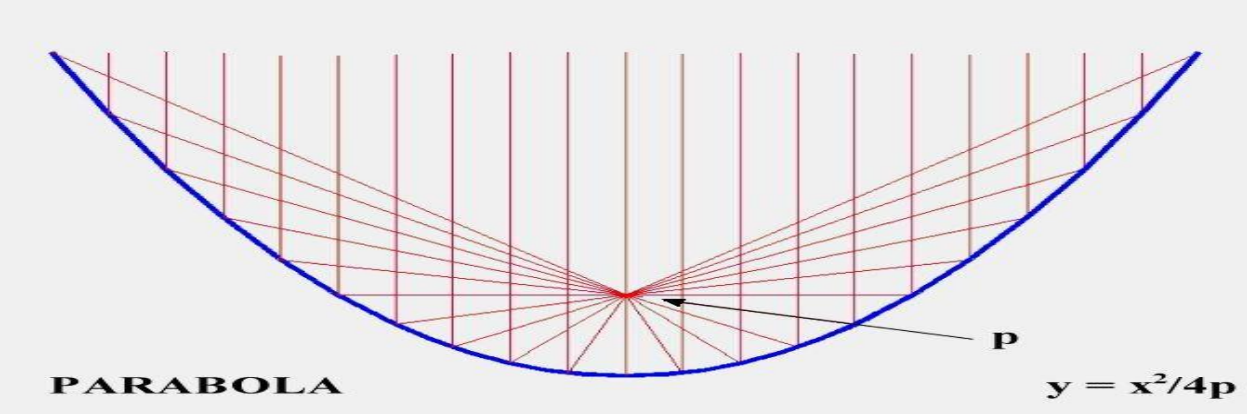

Figure 2.3: The basic geometry of a parabola mirror

Light rays coming from infinity will tend to be reflected towards a point called the focus.

To make a parabolic reflector in terms of its Diameter D, (i.e. having maximum X = D/2), height above origin **Y**, and focal length **p**, then equation above becomes: $p = D^2/16Y$

A focal length **p** is chosen; variables of X are chosen (i.e. from 0, 5, 10, 15...); then the corresponding values of Y are obtained from the equation above. The parabolic shape is then obtained from the X and Y values.

2.2.3. Types of parabolic collectors

There are 2 main designs of parabolic solar collectors these are:

2.2.3.1. Parabolic Dish:

This is also known as a point focus type collector; a practical application of a parabolic dish is a flashlight lens, which is used to transform a point source of light into a parallel beam. Since sunlight radiation is essentially parallel it may be concentrated at the focal point of the lens. As a matter of fact a tiny flashlight lens may be used as a cigarette lighter by substituting a cigarette for the bulb and by pointing the lens in the direction of the sun. A type of solar reflector dish concentrator may also be made by lining the inside of a cardboard box with aluminum foil.

Higher temperatures can be achieved with a parabolic dish as they focus the entire solar capture area to a point i.e. 1500^0C. Microwave radio antennas also use a parabolic dish to concentrate the incoming radio beam to a point to recover the diffused signal. The dish itself is not frequency selective but the "pick-up" at the focus is. Parabolic dishes develop solar concentrating factor of around 600 – 2000, depending on its size and focus. A parabolic dish with receiver for Stirling engine is the Plataforma Solar de Almeria – distal I and II.

Figure 2.4: Parabolic dish (Plataforma Solar de Almeria – distal I and II)

2.2.3.2. Heliostat

A field of heliostats tracks the sun using flat or slightly curved mirrors and focuses energy on to a stationary parabolic concentrator which refocuses energy to the central receiving tower; they are used with solar furnaces and power towers. Very high temperatures are achieved and as there are usually many collectors, the power level is enormous. The receiving target transfers the power away through a "working" fluid" to drive a turbine to generate electricity. A number of pilot plants have been built and have operated successfully for many years. 'Solar one" and "Solar two" are examples of the biggest solar power stations around; solar two is located in California near Barstowit incorporates thousands of tracking mirrors (heliostats) and has a system capacity of 10 MW. The working fluid (molten nitrate salt) is raised to 565^0C and stored in tanks for later use to generate electricity (up to 3 hrs after sundown). This system is an integrated power station utilizing fossil fuels as well so it can run continuously. Other pilot plants proving successful use a cluster of parabolic dishes to focus the energy to a special sterling engine. The entire system is mounted from a single tower and is designed this way to avoid the difficulties of the construction of a single large dish. Single pilot plants of 25 kW have been in service for some time and 10 plants to the acre is soon envisaged.

Figure 2.5: Heliostat (solar two)

2.2.3.3. Parabolic Trough

Also known as a line focus type collector; the sun's rays are focused to a central line or focal line along the trough. This "line" could be a "collector pipe" which could transfer the energy away to produce some "work". The "collector pipe" temperature is also high enough to cause water to vaporize to steam, so this could be used as a continuous "flash" boiler to drive a turbine or steam engine if scaled correctly. Solar power plants use parabolic troughs to make super heated steam and generate electricity because their fabrication and tracking equipment is less expensive than the dish.

This system could also be used to form an intermittent absorption refrigeration system if the pipe contained ammonia, it would boil off the ammonia with the condensate used to provide cooling in an evaporation box. With a bit more work a continuous cycle absorption refrigerator may be possible, (or possibly a heat exchange system could drive an existing gas fridge.) It could be used for air conditioning, or passive heating, desalination plants, water de-mineralization or purification. Solar trough systems as big as 80MW are in operation with a large number of troughs aligned "north-south" to track the sun. These are hybrid plants that also use natural gas etc. to enable continuous operation through the night. The solar concentrating factor of a parabolic trough is relatively low (10 – 100) depending on its size when compared to the other two types; they give concentration only in one dimension, so that the concentration factor is less than for a parabolic dish.

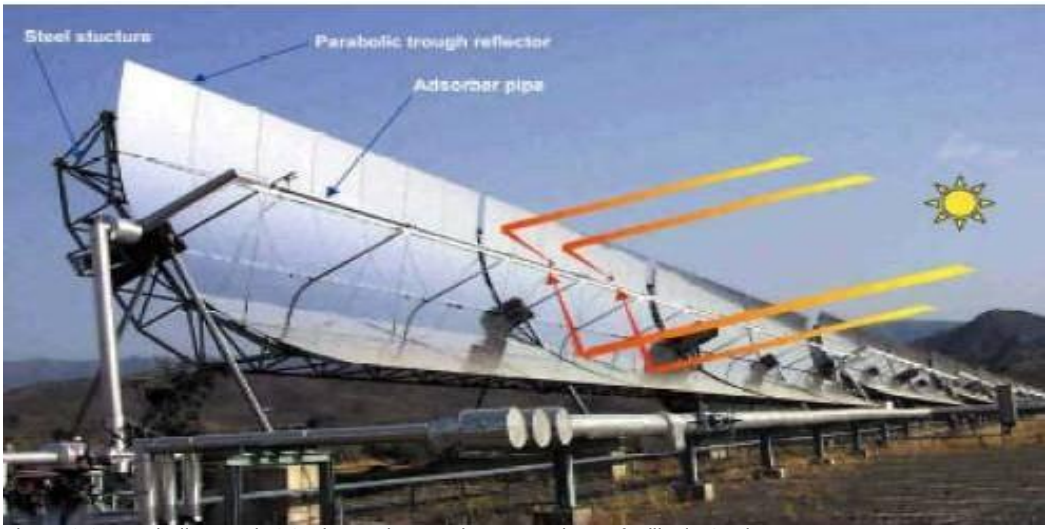

Figure 2.6: Parabolic trough SCA located at a solar research test facility in Spain
(Source: Plataforma Solar de Almeria)

The Saguaro Solar Generating Station north of Tucson, is the first solar thermal parabolic trough power plant built in The US; has a capacity of 1MW compared to 395MW in natural gas fired generating capacity at same site. Broke ground March 24, 2004 and started generating power December 2005.

Figure 2.7: Trough field located at Saguaro Power station in USA

2.3. Solar collector by MIT students

On Jan 28 2008, a team led by MIT students successfully tested a prototype of what may be the most cost-efficient solar power system in the world, as one team member believes has the potential to revolutionize global energy production.

The construction used can be likened to that of the satellite dishes used for services such as **Sky**; and can be called a parabolic collector. The difference being that it is a 12-foot wide dish consisting of an aluminium frame and rows of mirrors making up the surface. The mirrors focus the sunlight by a factor of 1,000 to a single point, therefore creating an immense amount of heat that can then be used for power generation or to melt a bar of steel.

Figure 2.9: Parabolic solar collector by MIT students (Source: MIT news)

Attached to the end of a 12-foot-long aluminum tube rising from the center of the dish is a black-painted coil of tubing that has water running through it; when the dish is pointing directly at the sun; the water in the coil flashes immediately into steam. They could be set up in huge arrays to provide steam for industrial processing, or for heating or cooling buildings, as well as to hook up to steam turbines and generate electricity. The team, led by Ahrens, also includes Micah Sze (Sloan MBA '08), UC Berkeley graduate and Broad Institute engineer Eva Markiewicz, Olin College student Matt Ritter and MIT materials science student Anna Bershteyn; with help from other students over the course of the semester. (David Chandler, 2008)

2.4. Parabolic solar concentrator for industrial heating created by Prof. Ajay Chandak

Figure 2.10: Parabolic solar concentrator by Prof. Ajay Chandak

Features of the system are:

i. Multiple reflectors with square shape in plan.
ii. Compact design as the shape is switched over to square than round.
iii. 100% aperture area available round the year. (Established Scheffler technology gives approximately 60% average aperture area.)
iv. Single axis fixed speed daily automatic tracking eliminates need of sensors and complicated hardware. Tracking system is easy to operate and maintain. Seasonal tracking is manual to be set once in 3-4 days.
v. Photograph shows two reflectors of 6.25m^2 each delivering 2000 to 2500 Watts per reflector. Trials on higher sizes of 10m^2 and 15m^2 square and rectangular dishes are to be conducted before standardization.
vi. Expected cost of this system installation after commercialization is around Rs. 15000/- per kW installation with payback period of less than 30 months without subsidies. This is very comfortable for Industries.
vii. Performance: For air working temp. of 250° C is comfortably achieved. Max. temp. attained for air is about 400° C. Thermic fluid can be comfortably used with second stage heat exchanger for steam generation.

2.5. Solar systems installed in Nigeria

Table 2.1. Solar Thermal systems installed in Nigeria(Source: Sokoto Energy Research centre)

S/N	Type of Project	Location & Date	Size of Project	Sponsor
1	Multi-booster Forage solar Dryer	NAPRI (Zaria) 1996	2 tonne/day	Energy Commission
2	Multi-booster Forage solar Dryer	New-Bussa and Yauri, 1997	1 tonne/day	Energy Commission
3	Solar water Heater	UDUTH (sokoto) 1997	1000 litres	Energy Commission

Figure 2.11.Community based solar water heater by SERC in Sokoto state

2.6. Advantages of solar heating

The following are reasons why solar heating has been used by people

i. **Solar heating saves money and time**

- Sunshine is free. Solar heating saves precious fuel for evenings, cloudy days and cold weather.
- System can be left for continuous heating without checking
- A solar heater is easy to make from a variety of materials.

ii. **Solar heaters are safe, healthy and convenient for cooking**

- There is no fire to cause burns or blow out of control.
- There is no smoke to either injure the eyes or cause lung problems.
- Most solar cookers cook at 82-121ºC (180-250ºF), ideal for retaining nutrients, moisture and flavor and not burning foods. Wood and gas fire temperatures, by contrast, exceed 260ºC (500ºF).
- You can bake, boil and lightly fry foods in their own juices. Meats get very tender.

iii. **Solar heaters help air quality**

- Burning traditional fuels such as wood and gas pollutes the air and contributes to global warming. Solar heaters provide a pollution-free alternative.

2.7. Why solar tracking?

Outside the earth's atmosphere, at any given point space, the energy given off by the sun (Insolation) is nearly constant. On earth, however, that situation changes as a result:

- The earth changing position in space: This makes some parts of the earth to be nearer to the sun on average over the period of a day; from hour to hour, day to day, and year to year. This is the reason for seasons, night and day.
- The earth rotation upon its axis: this makes the earth slightly inclined in relation to the sun. As the earth rotates at a constant speed, there will be certain points in the earth's orbit when the

sun shines for longer on a certain part of the earth.

- The earth's atmosphere (gases, clouds, and dust): The gases in the atmosphere remain relatively stable but due to pollution of the air in recent years due to a phenomenon known as global dimming, particulate matter resulting from fossil fuels, prevents a small fraction of the sun's energy reaching the earth. Clouds are largely transient, and pass from place to place casting shadows on the earth.

Therefore we need to move the solar device to account for the change in the sun's position so as to harness energy efficiently (Gavin D.J. Harper, 2007).

2.8. Losses in heating

Heat losses while solar heating fall into two main categories:

- Reflective losses i.e. the collector reflecting away some of the radiation supposed to be absorbed by it
- Absorption Losses i.e. the reflector absorbing part of the solar radiation incident on it.

2.9. Modes of heat transfer

Solar heat is transferred into the food by three mechanisms.

i) By radiation through direct solar rays, that is sunlight striking the heated material.

ii) By convection, that is by the hot air surrounding the heated material inside the chamber.

iii) By conduction; heat is conducted from the tray upon which the material rests.

If the tray is a heavy metal conductor such as steel or aluminum the sun's rays will heat the tray and conduct the heat under the material. All three mechanisms combine to make the heating process very efficient.

3. Methodology

The objective is to use a mould pattern to cast the dish form. This has to have an accurate shape and no imperfections upon the surface. A steel former with a top and bottom axle is used to "form" the concrete mould to the shape of your parabola. Concrete is readily workable to a smooth surface and it's relatively cheap, and any imperfections can be repaired with filler afterwards, (It is easier to fill than grind off.) The various materials to design components were locally sourced and manufactured by molding and fabrication as the need demanded.

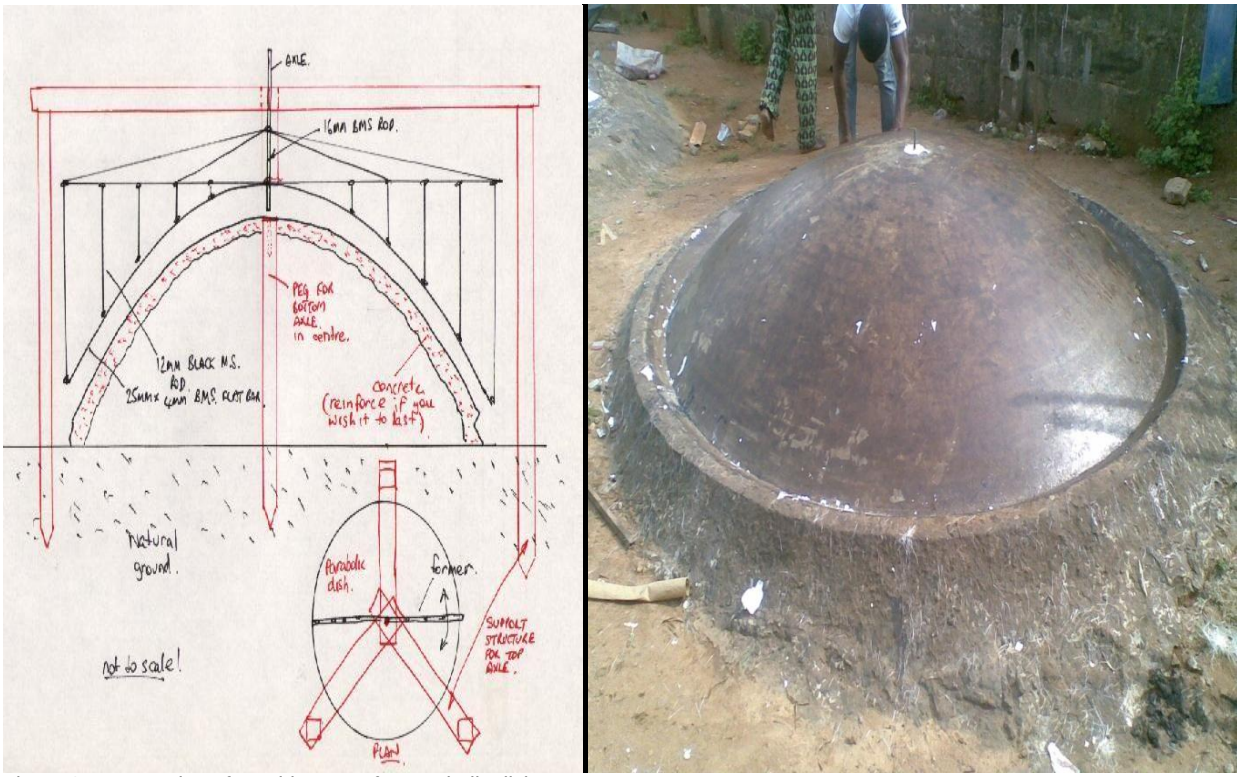

Figure 3.1: Formation of mould pattern for parabolic dish

Once the mould is finished the dish can be cast from it with whatever you wish to use, - i.e. more concrete, fiberglass, reinforced fiber polymer, clay, paper mache etc. If you wish to use the dish as a microwave antenna then construction should be made with fiberglass and "bird" wire netting or "aluminium foil" should be incorporated within the layers of fiber-glassing; or perhaps coat the parabolic surface with a heavy copper based paint (many coats) This will provide the necessary reflective surface for the microwave energy. If using fiber-glassing, a "chrome" paint, or highly silvered paint could be applied before applying the finish top clear gel coat, this may provide a satisfactory mirrored surface. Shinny aluminium foil could also be "laid and rolled" before the top gel coat and might provide a good reflector. Thin polished stainless steel sections cut to fit in together could be laid onto the surface and held into position from the rim and centre, and would provide a good mirrored surface for any use. Silicon sealant applied sparingly might "hold" any stubborn pieces down.

3.1. Materials

- Four packs of aluminium foil (each 8m long)
- Fiber (mat pattern)
- Catalyst (colorless)
- Accelerator (purple)
- Polyester resin
- Metals preferably iron (for the dish stand, dish frame, and pot holder).
- Pot (with a painted black); Dark surfaces get very hot in sunlight, whereas light surfaces don't. Heat is best transferred in dark, shallow, thin metal container with dark, tight-fitting lids to hold in heat and moisture.

3.2. Parabolic dish pattern profile

The parabolic dish to be designed is assumed to have a focal length of 65cm.Using this focal length and variable of x, the y variables can be determined, so that the profile can be traced out.
Using the formula: $y = x^2/4f$ (where f = 65cm and x = 20, 40, 60, 80 ……..cm)

X	Y
20	1.538
40	6.154
60	13.846
80	24.615
100	38.463
120	55.385
140	75.385
160	98.462
180	124.615
200	153.846

3.3. The moulding of the dish

The parabolic dish to be used in the design is a composite (fiber reinforced polymer) made up of fiber and pure polyester resin. Steps involved in the dish moulding process:

1. Clean the parabolic concrete moulded pattern surface, washing with soap and water.
2. Apply pure polyester resin to the surface of the mould to act as releasing agent for easy removal of the moulded dish from the pattern.
3. Use wet foam to line the pattern surface with aluminum foil, ensure that the more reflective part of the aluminum foil be put to the surface of the mould pattern, for better reflectivity of the surface.
4. Use polyester resin to attach the lapping aluminum foils together.
5. The entire surface of the mould pattern should now be covered with aluminum foil.
6. Next; cover the surface with fiber, just laying it over the surface of the aluminum.
7. Pour the polyester resin into a bowl, after which you add the accelerator, then catalyst (note: do not mix both catalyst and accelerator directly to avoid producing smoke or burning the fiber); this ensures forming of the polymer around the fiber, acting as hardener to the resin, which is characteristic of the polymer.
8. Leave for about 2 hours for the forming together of the fiber and polymer.
9. Place the Iron frame structure that has been fabricated in the workshop for the support of the composite structure.
10. Lay fiber on the iron frame place on the moulded structure, then apply the (pure polyester resin + accelerator +catalyst) combination to the fiber and frame structure.
11. Then leave for a day (24hours) for final setting.
12. After final setting, the parabolic dish is removed then re-foiled using shinny aluminium foil to act as a reflector.

The major problem faced during the production of the parabolic dish was the error associated with moulding and aligning the parabolic dish shape.

4. **Result and discussion**

The moulded dish diameter is 2.46m or 246cm (i.e. x = 123cm); with a height of 58.188cm.

While testing the device the absorber's position for optimal performance is at 60cm which is close to the theoretically value of 65cm.

Four (4) tests were carried out in the month of March to determine the temperature rise within a time frame, on the average the water placed within the collector increased from a temperature of 27-85ºC within 20 minutes.

4.1. Calculation

Data

Area of parabolic dish = 2/3 bh = 2/3 x 2.46 x 0.5818= 0.95m^2

Area of absorber = 0.0173m^2

Volume of water used= 75cL = 0.00075m^3 =750cm^3

Density of water is approximated to be 1g/cm^3

Specific heat capacity of water (c_w)= 4.186J/g^{0}C

Time of heat transfer(t)= 20min = 20 x 60 = 1200sec

Mass (m) = Density X Volume = 750 X 1 = 750g

i. Quantity of heat absorbed (Q) = m x c_w x(T_2 – T_1) = 750 x 4.186 x (85-27) = 182091J or 182.09KJ
ii. Power/Heat transfer rate = Q/t =182091/1200= 151.74W
iii. Concentration factor = area of reflector/ area of absorber = 0.95/0.0173 = 54.9
iv. *Since* C_{ideal}= (sin θ)$^{-2}$ for a 3-D concentrator (point – focus)
54.9 = (sin θ)$^{-2}$
Therefore acceptance angle (θ) = arc sin (0.13496) = 7.76^0

With a Concentration factor of 55 and with a power rating of 151.74W the designed dish can be used as follows:

i. For less than 100^{o}C: heated water can be used for domestic purposes and swimming pools, heating of buildings, and evaporative systems such as distillation and dryers;
ii. For less than 150^{o}C: air conditioning, and heating of water, oil, or air for industrial use.

4.2. Performance prediction

The test location for the parabolic dish solar heater is Covenant University situated in Ota (alternatively spelled Otta) a town in Ogun State, Nigeria, with an estimate of 163,783 residents living in or around it. Ota has the third largest concentration of industries in Nigeria. Ota in Ogun state is located on latitude 7^o 57'N and longitude 4^o 47'E.

Ideally, the data required to predict the solar input are several years of measurements of irradiance on the proposed collector plane. These are very rarely available, so the required (statistical) measures have to be estimated from meteorological data available either (i) from the site, or (ii) (more likely) from some 'nearby' site having similar irradiance, or (iii) (most likely) from an official solar atlas or database. All such data have systematic error and uncertainty, and natural climatic variability. Since there is no meteorological data for Ota having being to NIMET (Nigerian metrological Center), and there are no readily available solar radiation measuring instruments in this institution metrological data for a nearby site having similar solar irradiance shall be used. meteorological data for Abeokuta which is a located in Ogun state would be used.

Metrological data are available for Abeokuta and Ikeja; Abeokuta the capital of Ogun state is located on latitude 7.15^{0}N and Longitude 3.35^{0}E while Ikeja which is also close to ota is located on latitude 6.583^{0}N Longitude 3.333^{0}E. Due to the closeness in the latitude and longitudes of Otta with those of abeokuta the meteorogical data of abeokuta shall be used.

Table 4.1.Showing monthly mean daily global solar radiation on a horizontal surface (KWh/m^2 -day) for Abeokuta station in Ogun state, Nigeria

Month	Solar radiation (KWh/m^2 -day)
January	4.107
February	4.764
March	4.742
April	4.951
May	4.703
June	3.878
July	3.51
August	3.438
September	3.952
October	4.423
November	4.449
December	4.114
Annual mean	4.253

Based on the solar radiation data obtained, the operational power and capacity of the solar dish for each given month can be approximated, for the same period of time (20 minutes).

Table 4.2.Showing monthly mean daily global solar radiation on a horizontal surface (KWh/m^2 -day) and power rating of solar dish for Abeokuta station in Ogun state, Nigeria

Month	Solar radiation (KWh/m2 -day)	Power (W)
January	4.107	131.42
February	4.764	152.44
March	4.742	151.74
April	4.951	158.43
May	4.703	150.49
June	3.878	124.1
July	3.51	112.32
August	3.438	110.01
September	3.952	126.46
October	4.423	141.53
November	4.449	142.36
December	4.114	131.64
Annual mean	4.253	136.09

4.3. Limitation of the project

While carrying out the test on the parabolic solar dish the following drawbacks which we encountered include:

- Due to the intermittency of sunlight, the expected time for heating can vary.
- Less than perfect reflector surface reflectivity i.e. the reflectivity of the aluminium foil used is less than 1, hence there would be losses especially by surface absorption.
- Problem of Tracking the sun's position and angle of incidence.
- Drawbacks such as burns, alignment of collector, glare and reflections from surface
- Heat Losses associated with the heated water by convection and radiation i.e. the water contained in the absorber would lose part of its heat simultaneous to the atmosphere as it is being heated.

5. **Conclusion and recommendation**

5.1. Conclusion

The task of designing and constructing a parabolic solar dish that is efficient, functional and economically viable requires good technical knowledge of how the various components work. Also, material selection for optimal performance at lowest possible cost, engineering principles involving heat transfer, the concept of solar energy and how it can be effectively harnessed were used to design and produce this parabolic solar heater.

Application of this developed technology to provide energy for heating would supplement the heat energy provision for domestic uses otherwise derived from burning of fossil fuel energy resources and hydro-plants.

5.2 Recommendation

1. The heated water with the use of a properly designed piping system can be used to take heated water into buildings for various purposes: because most water heating systems use flat collectors (less than 70^{o}C) but this system provides a higher temperature above 80^{o}C.
2. This system can be used in heating air and water; dwellings in cold climates need heated air for comfort, and in all countries hot water is used for washing and other domestic purposes.

References

Aldo Vieira Da Rosa (2009), Fundamentals of Renewable processes; Second Edition published by Academic Press an imprint of Elsevier Inc. 525 corporate Drive, Suite 400, Burlington, MA 01803, USA.

Carolyn Roos, Ph.D. (2008), Portland State University - Solar Engineering: Concentrating solar collectors; Washington State University Extension Energy Program.

David Chandler (2008), published by the Massachusetts Institute of Technology (MIT) news office on Jan 18 2008.MIT news, 77 Massachusetts Avenue, Room 11- 400; Cambridge, MA 02139-4307, Tel: 617.253.2700, TTY 617.258.9344

Gavin .D.J. Harper (2007) solar energy – project for the evil genius; Printed by McGraw-Hill Companies, Two Penn Plaza-New York.

John Twidell and Tony weir (2006), Renewable energy resources; Second edition published by Taylor & Francis group 2 Park Square, Milton Park, Abingdon, Oxon OX14 4RN

Leng G (2000) RET Screen International: a decision-support and capacity-building tool for assessing potential renewable energy projects. UNEP Ind. Environ 3, 22–23 July–September

Ohta T. (1979), Solar–Hydrogen Energy System, Pergamon-New York.

P.A. Ilenikhena (2010) Solar Energy Applications in Nigeria - WEC Montreal 2010: Paper No. 135

Prof. Ajay Chandak (2010) parabolic solar Concentrator for Industrial heating. http://solarcooking.wikia.com/wiki/Parabolic_solar_concentrator_for_industrial_heating

Sambo A.S. and Doyle M.D.C (1986); Estimation of the global and diffuse components of the solar radiation for some Nigerian cities, Nigerian Journal of solar energy, Vol.5, Pg.16-24

SERC (Sokoto Energy Research Centre); www.sercng.org.

Solar heaters and other parabolic devices by Dr Jonathan Hare, The Creative Science Centre - Sussex University; published: J. P. Hare, Phys. Educ. 42 (2007) 267-270.

US department of Energy (DOE), The Energy Efficiency and Renewable Energy Clearinghouse (EREC) –Residential Solar heating Collectors *published by the Information Services Program, under the DOE Office of Energy Efficiency and Renewable Energy* on March 1996, DOE/GO-10096-051; FS 112. P.O. Box 3048 Merrifield, VA 22116 (800) DOE-EREC (363-3732); Fax: (703) 893-0400; Email: doe.erec@nciinc.com

Wikipedia, the free encyclopedia (2010) – Ota, Nigeria.

Wikipedia, the free encyclopedia (2010) – Parabolic reflector.

Abidakun et al: Proc. ICCEM (2012) 315 – 320

Effect of expression conditions on the yield of Dika Nut (*Irvingia Gabonesis*) oil under uniaxial compression

[1]Abidakun, O.A., [2]Koya O.A and. [1]Ajayi O.O.
[1]Department of Mechanical Engineering, Covenant University, Ota, Nigeria
[2]Department of Mechanical Engineering, Obafemi Awolowo University, Ile-Ife, Nigeria

Abstract

Efficient expression of Dika nut oil from the kernel is required for its subsequent use in producing comparatively cheap lubricant. Various factors responsible for proper oil expression include particle size, moisture content, heating temperature, heating time, pressing pressure and pressing time. Sundried Dika kernel ground to two particle sizes (fine: ≤ 1.4 mm and coarse: between 1.4 and 2.8 mm) were conditioned to moisture content of 3, 6 and 9 wt%. Considered in the study, are heating temperature ranging from 50 to 150^{o}C in steps of 25 degrees Celsius and heating time of 5 to 25 minutes in steps of 5 minutes. Pressing pressure of 5 to 25 MPa in steps of 5 MPa and pressing time of 2 minutes interval were also considered. The maximum oil yield was then correlated with the processing conditions. Test results showed that coarse particle gave higher oil yield. Maximum oil yield of 72.2% of the available oil was obtained at 6% moisture content, heating temperature of 100^{o}C and heating time of 10 minutes. Regression analyses of the oil yield with heating temperature, heating time, and pressing gave r^2 values of 0.9678, 0.999 and 0.9128. The processing conditions therefore has significantly influence the quantity of oil obtained from Dika kernel.

***Key words**:* Dika nut, oil expression, oil yield, regression analysis, heating temperature.

1. Introduction

The drive towards clean technology stirred up stronger environmental concerns and growing regulations over contamination and pollution of the environment. As a result, use of renewable and biodegradable lubricants which have little or no environmental foot print are being encouraged (Erhan et al., 2006; Nagendramma and Kaul, 2012). Presently, mineral oil based lubricant has the largest share in the lubrication industry, as more than 95% of lubricants are mineral oil based (Gaikwad and Paramjyothi, 2008). Mineral oil based lubricants has been found to contribute immensely to polluting the environment as over 60% of used lubricants are lost to the environment (Mann, 2007). This is further compounded by the non-biodegradability and ecotoxicity of this class of lubricant. Vegetable oils have so far been found a viable alternative to mineral oil as it tends to eliminate the environmental problems associated with mineral oil lubricants (Abidakun and Koya, 2012). In addition to this, they also possess excellent tribological properties such as high viscosity index, high lubricity, high flash point (Balamurugan et al., 2010; Abidakun and Koya, 2009, 2012)

Various vegetable oils have been tested for use as lubricant in place of mineral oil. Among oils that have shown potential for use as lubricants are rape seed oil, soy bean oil, palm kernel oil, palm oil (Sraj et al., 2000; Petlyuk and Adams, 2004; Abidakun and Koya, 2009). Dika nut oil has also been found to possess the qualities of being used as lubricant as it possesses good viscosity index, flash point and moderate pour point (Abidakun and Koya, 2009). However the cost of vegetable oil based lubricants as compared to that of mineral oil has been one of the major factors militating against its widespread use (Mann, 2007).

Proper expression of the oil can serve as a means of reducing the processing cost associated with biodegradable oil. Efficient expression of vegetable oils from oil bearing seeds by mechanical method requires optimum preliminary processing before the expression (Ibrahim and Onwualu, 2005; Mwthiga and Moriasi, 2007). These processing conditions

include particle size, moisture content, heating temperature, heating time, pressing pressure and pressing time. Just as processing conditions have shown effect on the thermo-physical properties of expressed dika nut oil (Abidakun and Koya, 2012), processing conditions have also shown effect on the oil yield from many oil bearing materials (Suganya *et al*., 2000; Akinoso *et al*., 2006; Willem *et al*., 2008; Ibrahim and Onwualu, 2005; Mwthiga and Moriasi, 2007).

From the aforementioned, efficient processing of the oil bearing materials prior to expression is necessary in order to achieve higher yield and subsequently cheaper end product. Adequate knowledge of oil yield from the kernel is also required for design and construction of the oil expeller to handle the expression on a large scale. Hence, the objectives of this study is to investigate the influence of particle size, moisture content, heating temperature and heating time, pressing pressure and pressing time on the quantity of oil expressed from Dika nut.

2.0 Materials and Methods

Dika kernel ground to average particle sizes less than 1.4 mm (fine) and between 1.4 and 2.8 mm (coarse) were conditioned to moisture contents of 3, 6 and 9% wt%. Fifty grammes of the sample with fine and coarse particles conditioned to 3% moisture content were heated at 50^{o}C for 5 minutes. The heated samples were subsequently pressed by applying uniaxial compression load via an experimental pressing rig. Based on the result of the pressing, subsequent experiments were performed on the sample with coarse particles. At 3% moisture content, the samples were further heated at 75, 100, 125 and 150^{o}C for 5, 10, 15, 20 and 25 minutes. The same combinations of heating temperatures and heating times were considered for moisture contents of 6 and 9%. In each case, pressing pressure of 5 MPa and pressing time of 5 minutes was applied. Pressing pressure of 10, 15, 20 and 25 MPa were also applied at a selected combination of moisture content, heating temperature and heating time. Quantity of oil expressed was measured at intervals of two minutes until there was no considerable increase in oil expressed. Weighing was by the use of electronic weighing balance with 0.01g accuracy. Each of the experimental runs was replicated three times. A summary of the experimental design is as shown in Table 1.

Table 1: Experimental design for the study

S/N	Processing Conditions	Levels
1	Moisture Content, wt%	3, 6, 9
2	Heating Temperature, ^{o}C	50, 75, 100, 125, 150
3	Heating Time, minutes	5, 10, 15, 20, 25
4	Pressing pressure, MPa	5, 10, 15, 20, 25
5	Pressing time	2 minutes interval
6	Replications	3

3.0 Results and Discussion

3.1 Effect of Particle Size on Oil Yield

Variation in oil yield with particle size at different moisture contents is shown in Fig. 1. Sample with coarse particles (between moisture content of 1.4 and 2.8 mm) yields higher quantity of oil than the sample with fine particles (≤ 1.4). The difference in the yield could be due to the larger surface area which permitted rapid loss of moisture than it was required for sufficient oil extraction in the sample with fine particles. Lower oil yield from samples with fine particles may also be attributed to the ease with which the ducts for oil flow were sealed up by the applied pressure. In both cases of fine and coarse particles, the oil yield reached the maximum value at a moisture content of 6 wt%.

This may be an indication that moisture content and particle size may not really have an interdependent effect on oil yield in mechanical pressing of Dika meal.

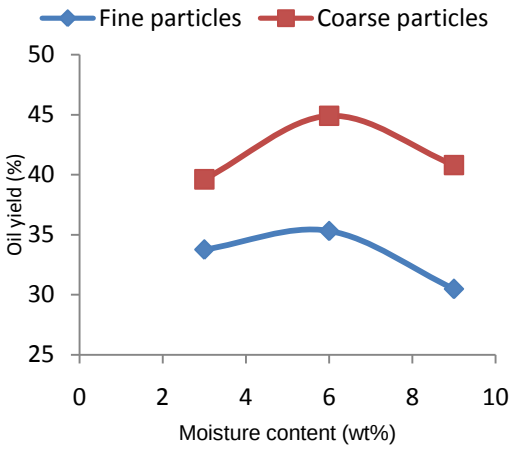

Figure 1: Variation of oil yield with moisture content at different particle sizes

3.2 Effect of Moisture Content, Heating Temperature and Heating Time on Oil Yield

Figures 2, 3 and 4 show the variation of oil yield with heating time and heating temperature at various moisture contents. Continuous decrease in oil yield was noticed as heating temperature increased for samples at 3% moisture content. For samples at moisture contents of 6 and 9%, the oil yield increased with heating temperature, up to 100 and 125^{o}C, respectively before it declined. At moisture content of 3 wt% and heating temperature of 50^{o}C (Fig. 2), the oil yield increased continuously as heating time increased from 5 to 20 minutes. A decline was however noticed at 25 minutes heating time. At higher heating temperatures, the oil yield decreased continuously with increase in heating time. The continuous decrease in oil yield at higher heating temperatures could be due to the fact that the moisture content decreased further as the heating increased (Mwthiga and Moriasi, 2007).

For all other heating times, the oil yield increased continuously for both 6% and 9% moisture contents when heated at 50^{o}C (Figs 3 and 4). The highest oil yield for 50^{o}C heating temperature was obtained at heating time of 25 minutes for sample conditioned to 9 wt% moisture content. There was no oil yield for samples heated at 50^{o}C and 75^{o}C for 5 minutes at both 6 and 9% moisture contents. This was probably due to the low oil temperature attained during these conditions. However, once sufficient heat treatment was accomplished, oil yield was higher at the higher moisture levels of 6 and 9 wt%. This also further confirms the need for adequate preheating of oil seeds in mechanical oil expression.

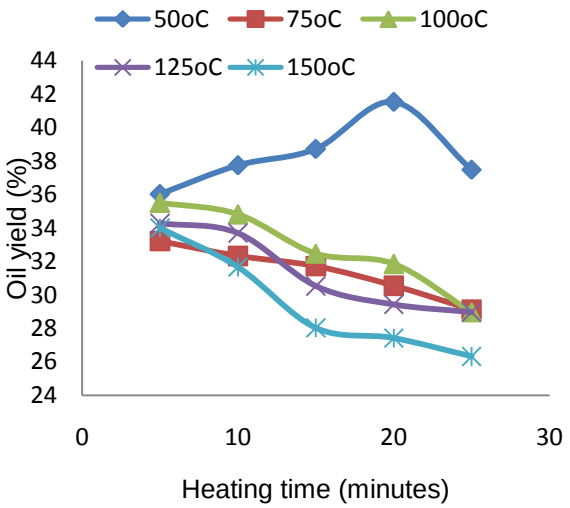

Figure 2: Variation of oil yield with heating time for different heating temperature at 3% moisture content.

Consequently, the combination of heating temperature and heating time is an integrated factor affecting oil yield. This is explicable as it represented the quantity of heat energy added to the sample. Therefore, if the heat energy exceeded the latent heat of vaporisation, the moisture content of the meal is readjusted and if it falls below a threshold, the oil expression is obstructed. Figure 3 shows the oil yield at 75^{o}C; oil yield reached the highest at heating time of 10 minutes and declined thereafter for samples at 6 wt% moisture content. The yield increased till 15 minutes heating time before it declined for samples at 9% moisture content (Figure 4). Samples at 6% moisture content heated for 15 minutes gave the highest yield among the samples heated at 75^{o}C. Samples at 6% moisture content heated at 100 and 125^{o}C gave their maximum yield at heating time of 10 minutes (Fig 3). Oil yield reached the maximum at 5 minutes when it was heated at 150^{o}C and declined continuously thereafter.

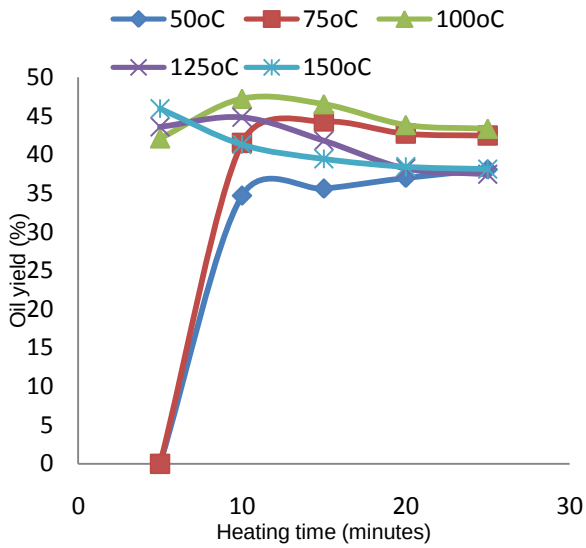

Figure 3 Variation of oil yield with heating time for different heating temperature at 6% moisture content.

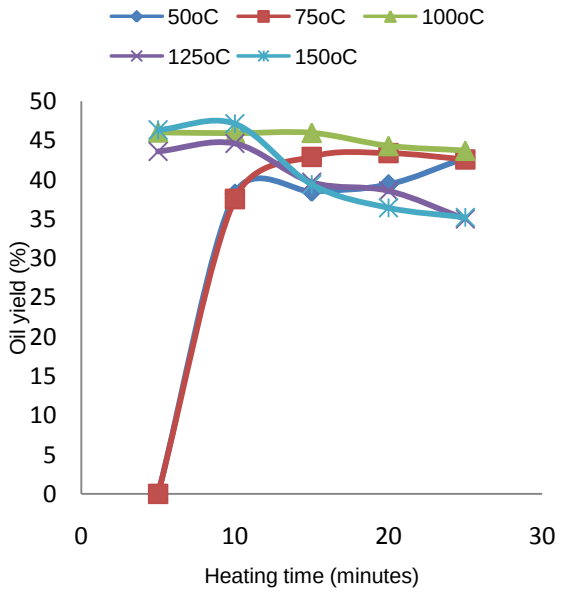

Figure 4: Variation of oil yield with heating time for different heating temperature at 9% moisture content.

Analysis of variance on the significance of the effect of the factors: moisture content, heating temperature and heating time considered showed that all the factors have significant effect ($p \leq 0.05$) on the quantity of oil expressed. Moisture content appeared to be the most significant of the three factors, followed by

heating time and thereafter heating temperature. The significance of the interactions among the factors indicates that the factors have interdependent effect on the quantity of oil expressed. This is similar to the case of palm kernel and sesame seed oil expression, where all the factors have significant effect on oil yield (Akinoso, 2006).

3.3 Effect of Pressing Pressure and Pressing Time on Oil Yield

Figure 5 shows the variation of oil yield with pressing time at various levels of pressing pressure when the sample pre-processed at optimum conditions of 6 wt% moisture content, 100^{o}C heating temperature and 10 minutes heating time. It was observed that oil yield increased for all pressure levels considered with the highest oil yield at 25 MPa. The oil yield increased as the pressing time increased for all pressure levels which is in accordance with what was reported for soybean (Mwthiga and Moriasi, 2007).

Furthermore, for all the pressing pressure, almost 80% of the maximum oil yield possible was expressed within the first two minutes of pressing time. Although, the pressing continued up to 24 minutes, only slight increase was noticed in oil yield. Over 92% and 95% of the maximum oil expressed had been expressed at pressing time of 4 minutes and 6 minutes, respectively. At 8 minutes of pressing time, oil yield increased from 44% to 54% with increase in pressing pressure from 5 to 25 MPa.

3.4 Relationship of Oil Yield, Heating Temperature, Heating Time and Pressing Pressure

Oil obtained at 6 wt% moisture content, heating temperature of 100^{o}C, pressure of 5 MPa and pressing time of 10 minutes related with heating time gave a second order polynomial equation (Equation 1). The yield obtained at heating time of 10 minutes also gave polynomial equation of the third order (Equation 2) when related with heating temperature. Correlation with heating temperature and heating time gave r^2 values of 0.9678 and 0.999 respectively. Oil yield obtained at pressing time of 8 minutes was related with pressing pressure by a logarithmic equation with r^2 value of 0.9128.

$$Y = -0.0033T^2 + 0.725T + 6.4692 \quad \ldots \quad \ldots \quad \ldots \quad 1$$

$$Y = 0.0054t^3 - 0.2803t^2 + 4.2983t + 26.936 \quad \ldots \quad \ldots \quad 2$$

$$Y = 5.69\ln P + 36.105 \quad \ldots \quad \ldots \quad \ldots \quad \ldots \quad 3$$

where Y in % is the oil yield, T in ^{o}C is the heating temperature, t in minutes is the heating time and P in MPa is the pressing pressure.

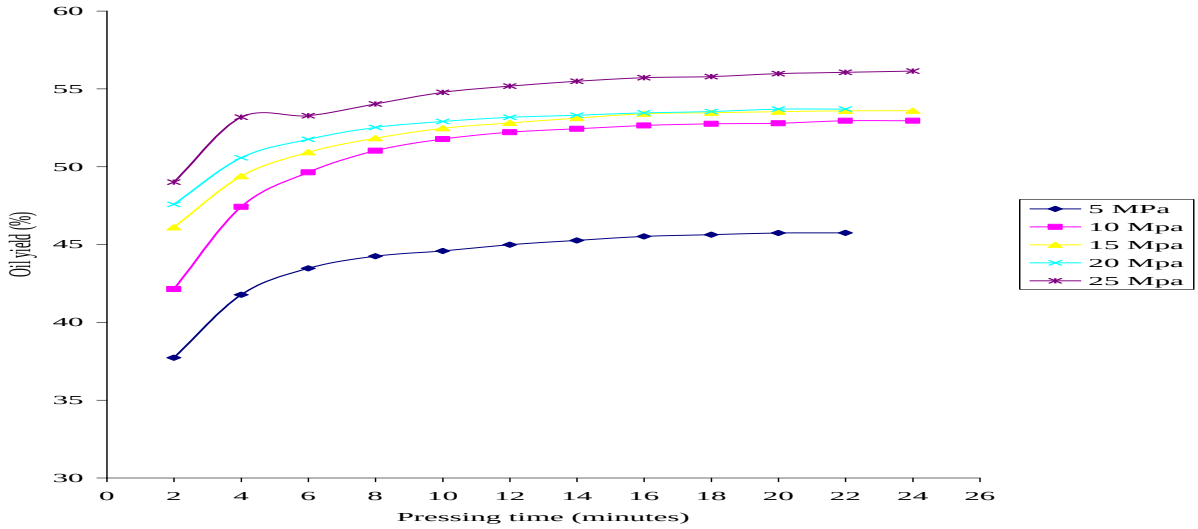

Figure 5: Variation of oil yield with pressing time for different pressing pressure

4. Conclusion

The highest oil yield was obtained from sample with coarse particles conditioned to 6% moisture content on wet basis, heated at 100^{o}C for 10 minutes. It was found that all the three factors: moisture content, heating temperature and heating time; have significant effect on the quantity of oil expressed. Pre-processing moisture content was the most significant. The oil yield increased with increase in pressure within the pressure range of 5 to 25 MPa considered in the study.

References

Abidakun, O.A. and Koya, O.A. Potential of Dika nut oil as lubricant for sustainable technological growth. Ife Journal of Technology, 18(2), 15–18, 2009.

Abidakun, O.A. and Koya, O.A. 2012, Dika nut oil as base oil for lubricants—effect of processing conditions on physicochemical properties. Lubrication Science, DOI: 10.1002/ls.1201, 2012.

Akinoso, R.; Igbeka, J. and Olayanju, T. Process optimization of oil expression from sesame seed (Sesamum indicum Linn.). Agricultural Engineering International: the CIGR Ejournal, Manuscript FP 06 011. Vol. VIII, 2006.

Balamurugan, K.; Kanagasabapathy, N. and Mayilsamy, K. Studies on soya bean oil based lubricant for diesel engines. Journal of Scientific and Industrial Research, 69, 794-797, 2010.

Erhan, S.Z.; Sharma, B.K. and Perez J.M. Oxidation and low temperature stability of vegetable oil-based lubricants. Industrial Crops and Products, 24, 292–299, 2006.

Gaikwad, R.D. and Paramjyothi, S. Physico-chemical and viscosity studies in some seed oils from wild and cultivated plants. Acta Chimica Slovenia, 55, 683–688, 2008.

Ibrahim, A. and Onwualu, A.P. Technologies for extraction of oil from oil-bearing agricultural products: A review. Journal of Agricultural Engineering and Technology, 13, 58-70, 2005.

Mann, S. Ranking without valuing in the face of major uncertainty—The case of the promotion of biodegradable lubricants. Journal of Environmental Management, 85, 198–203, 2007.

Mwthiga, G. and Moriasi, L.A. Study of yield characteristics during mechanical oil extraction of preheated and ground soybeans. Journal of Applied Sciences Research, 3(10), 1146-1151, 2007.

Nagendramma, P. and Kaul, S. Development of ecofriendly/biodegradable lubricants: An overview. Renewable and Sustainable Energy Reviews, 16 764–774, 2012.

Petlyuk, A.M. and Adams, R.J. Oxidation stability and tribological behaviour of vegetable oil hydraulic Fluids. Tribology Transactions, 47(2), 182-187, 2004.

Sraj, R.; Vizintin, J.; Svoljsak, M. and Petrol, M.F. Rapidly biodegradable hydraulic fluids on the basis of rapeseed oil. Lubrication Engineering, 56(2), 115-120, 2000.

Suganya, C.; Soottawat, B. and Nisit, S. Separation and quality of fish oil from precooked and non-precooked tuna heads. Food Chemistry, 69: 289–294, 2000.

Willem, P.; Kuipers, N.J.M. and de Haan, A.B. Gas assisted mechanical expression of oil seeds: Influence of process parameters on oil yield. The Journal of Supercritical Fluids, 45(3), 298-305, 2008.

Effect of using vegetable oils as quenching media for pure commercial aluminium

[1]Adekunle, A.S; [1*]Odusote J.K. and [1]Rabiu, A.B.

Department of Mechanical Engineering,
Faculty of Engineering and Technology, University of Ilorin, Ilorin, Nigeria
[*] jamiukolawole@gmail.com/odusote.jk@unilorin.edu.ng

Abstract

This paper presents the effects of rate of heat extraction by groundnut, melon, palm kernel, shea butter and palm oils on the mechanical properties of various samples of pure commercial aluminium heat treated at 200°C, 250°C, 300°C and 350°C. Muffle furnace equipped with digital thermometer and thermocouple was used for the heat treatment. Tensile strength and hardness tests were carried out using Instron Universal Tester and Vickers hardness methods, respectively. Results obtained from the experiment were presented graphically. The results showed that palm kernel oil cools faster at 200°C and 250°C, while palm oil and shea butter oil quench faster at 300°C and 350°C, respectively. Palm kernel oil offers the highest elongation at 200°C, while at 350°C shea butter oil gave the best result. The best among the bio-quenching oils in providing good ductility is shea butter oil at 200°C, while at 300°C and 350°C groundnut oil give the best result. Highest hardness values were obtained from samples quenched in melon oil between 200°C-300°C. However, these values decreased with increased heating temperature probably due to density and viscosity variation with temperature rise. Similar observations were made on most of other samples quenched in other bio-quenching oils used in this experiment. This study shows that these locally available vegetable oils have promising potentials to serve as a possible replacement for non-biodegradable mineral oils in many applications.

Key words: Mineral oils, Vegetable/biodegrable oils, heat treatment, Quenching media, Aluminium, Mechanical Properties.

1. Introduction

Aluminium is widely used in electrical, chemical, food packaging, petrochemical and construction industries on account of its excellent corrosion resistance, high thermal and electrical conductivities and good formability (John, 2007). One major drawback to the use of pure commercial aluminium is its low strength. It has been established that mechanical properties of metals and alloys can be effectively improved through alloying and heat treatment (Krauss, 1990). However, the choice of effective quenching medium after heat treatment is very critical in ensuring the achievement of desired mechanical properties (Feng and Khan, 2008). The most common quenching medium for metals and alloys is mineral oil, and it possesses excellent cooling capacity (Grishin and Churyukin, 1986). However, but they are relatively expensive, toxic and non-biodegradable. There have been considerable studies focused on possibility of reducing or replacing mineral oil with less expensive water-based or polymer-based quenching media (Tolstousov and Bannykh, 1981). Cooling capacity of aqueous solutions of different substances was examined in order to determine their suitability as quenching media, and it was observed that aqueous 6-7 % monosulfite liquor (MSL) with 1 % phenol could serve as a possible replacement for mineral oils (Grishin and Churyukin, 1986). Protsidium et al. 1988) studied the quenching capacity of spent and regenerated minerals oils, and observed that addition of 0.3 % antioxidant Ionol to regenerated oils improved their quenching capacity. The effectiveness of polymer based quenching medium, UZSP-1, was examined, and it was found that UZSP-1 of varying

concentrations was effective as a quenching medium for only low-carbon ball-bearing steels (Goryushin, et al., 1991) but not well suitable for high-carbon ball-bearing steels. The present study was undertaken with the objective of replacing mineral oils with local biodegradable oils, which are more readily available, relatively cheaper and environmental friendly. These oils also have many other good natural properties, which made them attractive as lubricants and other applications (Xia and Larock, 2010). This was done by examining the mechanical properties of heat-treated pure commercial Al after quenching with several locally available biodegradable oils.

2. Experimental Procedure

Samples of pure commercial Al were obtained from a local aluminium smelting company based in Lagos. The as-received samples were cut into experimental work pieces prior to heat treatment. Heat treatment of the samples was performed at 200ºC, 250ºC, 300ºC and 350ºC, using a muffle furnace. After heat treatment, the samples were soaked for 60 minutes inside the furnace and then quickly transferred into a quenching bath equipped with a digital thermometer and thermocouple. The quenching bath was filled separately with 50 cm^3 of groundnut oil, melon oil, palm oil, palm kernel oil and shea butter oil as quenchants. The heat losses by the heat treated pure commercial aluminium were recorded by the digital thermocouple at various time intervals from 30 s to 300 s.

After quenching, approximately 10 mm long and 9 mm in diameter specimens were cut from the quenched samples. The specimens were ground and polished down to 4000-grit SiC paper and 1 µm diamond paste finish. After polishing, the specimens were cleaned ultrasonically in acetone, followed by alcohol and immediately dried before hardness and other mechanical tests.

2.1 Mechanical Test

2.1.1 Tensile Testing

Tensile test were carried out on the quenched specimens using Instron Universal Tester. Each of the specimens was loaded till fractured, and the fracture load for each sample was recorded as well as the diameter at the point of fracture and the final gauge length. The initial diameter and initial gauge length for each sample was noted before the application of the uniaxial load. The percentage elongation of each test sample was determined, as well as the tensile strength.

2.1.2 Hardness Test

Vickers hardness method was used for the determination of the hardness of the quenched samples. Each of the test specimens were prepared metallographically after different heating and quenching regimes, and then mounted on the anvil. The specimens were brought in contact with the pyramid indenter and allowed to rest for a dwell time. The hardness of the specimens were indicated by the penetration of the indenter on the test specimens, and displayed by the machine. Average values were recorded after repeating the test for each of the test specimens.

3.0 Results and Discussion

3.1 Cooling Rate

Figures 1-4 show the rate of heat extraction by each of the quenching medium namely; groundnut oil, melon oil, palm oil, palm kernel oil and shea butter oil, from the heat-treated pure aluminium samples after heating at 200°C, 250°C, 300°C and 350°C, respectively. Figure 1 shows that at 200°C, palm kernel oil extracted heat to an elevated temperature of 31.9°C at 160s, while groundnut oil, melon oil, shea butter oil and palm oil extracted heat to 31.6°C at 185s, 31.8°C at 245s, 31.8°C at 205s, and 31.6°C at 265s, respectively. This indicates that palm kernel oil extracted heat and reached equilibrium with the samples faster than the other oils at this heating temperature, while the least heat was extracted by palm oil at this heating temperature. However, the temperature of each of the quenchants remained constant after getting to their elevated temperature during the quenching process. As shown in Figure 2, the temperatures of both palm kernel and melon oils were raised to 32.5°C from 30.8°C at 175s and 250s respectively, during quenching of aluminium samples heated to 250°C, while those of groundnut, shea butter and palm oils were raised to 32.4°C at 165s, 32.2°C at 145s

and 31.7°C at 280s, respectively. Thus, showing that palm kernel oil extracted faster than other oils, while palm oil extract least heat at 250°C. However, at 300°C, palm oil cools the heated aluminium faster, as more heat were extracted as shown in Figure 3. Similarly, at 350°C, shea butter oil removed heat and cooled the heated aluminium faster compared with other oils, as shown in Figure 4.

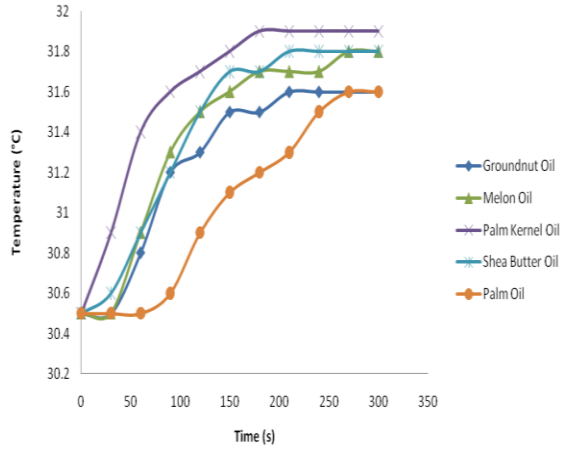

Figure 1. The rate of heat extraction of different bio-quenching oils at 200°C.

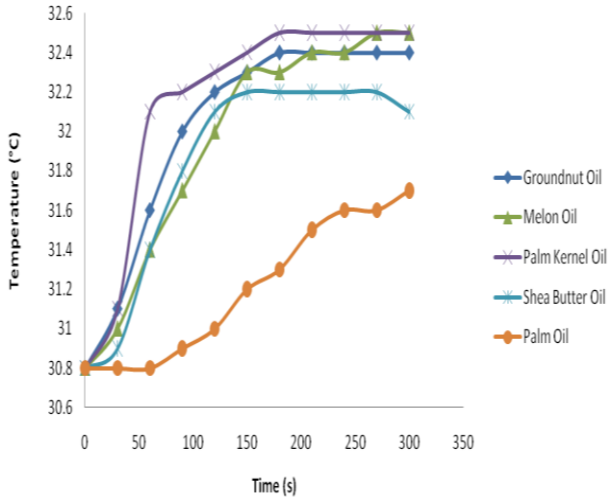

Figure 2. The rate of heat extraction of different bio-quenching oils at 250°C.

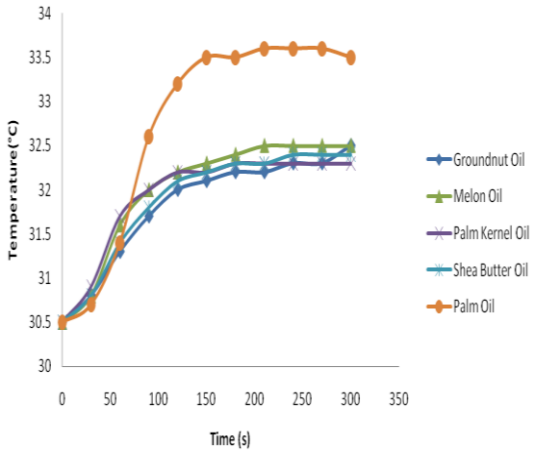

Figure 3: The rate of heat extraction of different bio-quenching oils at 300°C.

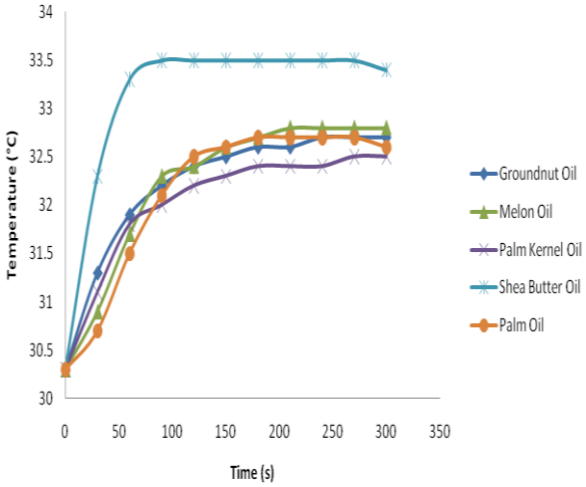

Figure 4: The rate of heat extraction of different bio-quenching oils at 350°C.

3.2 Mechanical Properties

3.2.1 Elongation of the quenched samples

Figure 5 shows the elongation of the investigated samples after quenching in various bio-quenching oils at different exposure temperatures. Comparing the value of elongation of the quenched samples at different heating temperatures with the as-received sample of 14.09 mm, it was evident that in most cases the elongation of the quenched samples increased with increasing heating temperature, as shown in Figure 5. This indicates possible improvement in the ductility of the quenched

samples at higher heating temperatures. The least elongation value of 6.92 mm was obtained after quenching in groundnut oil at 250°C, while shea butter oil produces samples with highest ductility at 350°C. As shown in the Figure, all the samples heated at 200°C and 250°C and quenched in the various oils are brittle, except those quenched in shea butter oil at 200°C, which are slightly ductile. Samples heated at 300°C and quenched in groundnut and shea butter oils are also ductile, while those quenched in other oils are brittle. However, at 350°C, all the quenched samples exhibited ductility, with highest elongation of 22.25 mm was displayed by those quenched in shea butter oil.

3.2.2 Tensile strength of the quenched samples

The tensile strength of the as-received commercial Al sample is 60.04 MPa, which is higher than those obtained from the quenched samples at some of the heating temperatures (Figure 6). At 200°C, samples quenched quenched in groundnut and melon oils displayed lower tensile strenght

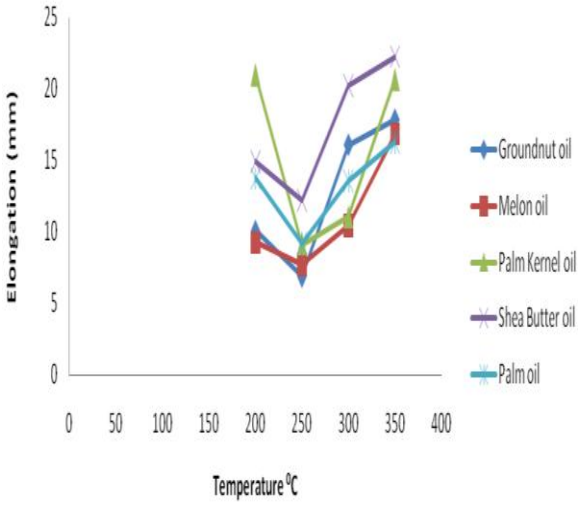

Figure 5. Elongation of Pure Commercial Aluminium in Different Bio-Quenching Oils at Different Heating Temperatures.

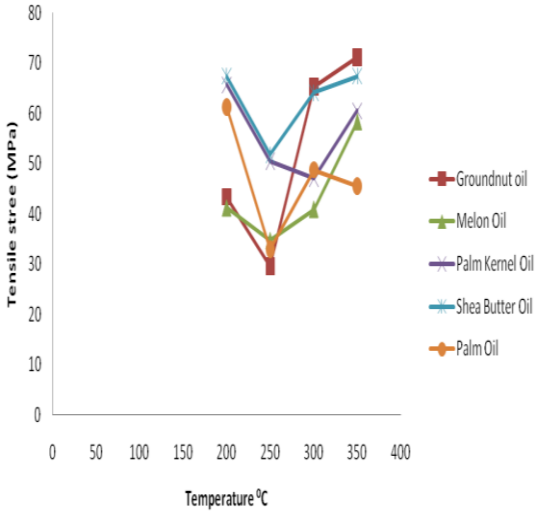

Figure 6. Tensile Strength of Pure Commercial Aluminium in Different Bio-Quenching Oils at Different Heating Temperatures.

compared with that of the as-received sample, while shea butter oil exhibited highest tensile strength value of 67.38 MPa. This value is higher than 65.62 MPa and 61.21MPa of palm kernel and palm oils, respectively. At 250°C, all the quenched samples gave lower tensile strength value compared with that of as-received sample, with sample quenched in groundnut oil showing lowest tensile strength value. However, at 300°C and 350°C, heat treated samples quenched in groundnut oil displayed highest tensile strength value, followed by those quenched in shea butter oil, with the least value obtained from samples quenched in melon oil at 300°C, and in palm oil at 350°C. Thus, quenching in groundnut oil after heating at 350°C, resulted in sample with best tensile strength.

3.2.3 Variation of the hardness of the quenched samples

The highest Vickers hardness value of the samples quenched in the various quenching oils were obtained at 200°C, with peak value from the sample quenched in melon oil, as shown in Figure 7. However, at 250°C, the hardness values of all the quenched samples decreased, with those quenched in melon, palm kernel and shea butter oils became lower than that of the as-received sample, which is 30.9 Hv. The hardness values of all the samples increased at

300°C above that of the as-received, but later decreased when quenched after heating up to 350°C, except that of the sample quenched in melon oil. This indicates that the best heating temperature to obtain highest hardness value will be 200°C, with melon oil as the quenching medium.

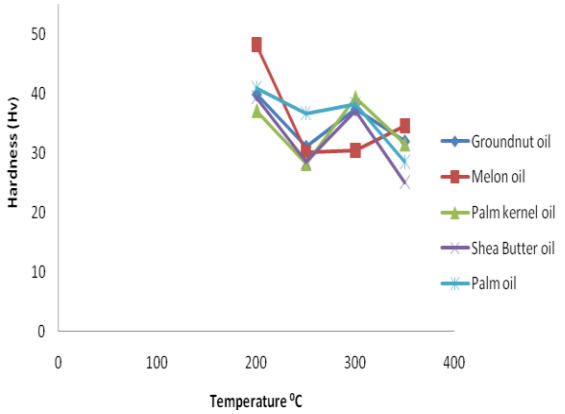

Figure 7. Vickers Hardness of Pure Commercial Aluminium in Different Bio-Quenching Oils at Different Heating Temperatures.

4. Conclusions

We established the possibility of using some of the bio-quenching oils for quenching pure commercial aluminium, in order to improve its mechanical properties. Quenching with Shea butter oil was found to produce pure commercial aluminium with best ductility after heating at 350°C, while groundnut oil can be used for quenching to improve the tensile strength at 350°C. The best bio-quenching oil in providing a high hardness value for the aluminium sample after quenching at 200°C is melon oil. However, use of any of the bio-quenching oils to quench the aluminium samples heating up to 250°C was found to be detrimental to both the hardness and tensile strength properties of the samples.

References

1. Feng, C. and Khan, Tahir I. (2008), “The Effect of Quenching Medium on the Wear Resistance of a Ti-6Al-4V alloy”, J. Mater. Sci., 43, 788-792.
2. Goryushin, V.V., Istomin, N.N., Ksenofontov, A.G., Marsel, A.V. and Shevchenko, S. Yu (1991), Metal Science and Heat Treatment, Vol. 41, Nos 1-2, 3-7.
3. Grishin, S.A. and Churyukin, Yu. N. (1986),”Evaluation of the Cooling Capacity of Quenching Media Based on Water”, Metal Science and Heat Treatment, Vol. 30, No.5, pp 86-88.
4. John, A.S.G. (2007), “Aluminium Recycling and Processing for Energy Conservation and Sustainabilty”, Material Park, Ohio, ASM International Publishers, ISBN 0871708590.
5. Krauss, G. (1990), “Steels: Heat treatment and Processing Principles”, ASM Int. pp 125-345.
6. Kulikov, A.I. (1997), “A New Quenching Medium for Metals and Alloys”, Metal Science and Heat Treatment, Vol. 39, Nos. 11-12, 528-530.
7. Protsidim, P.S., Rudakova, N.Ya and Shevemeta, B.K. (1988), Metal Science and Heat Treatment, Vol. 41, Nos 1-2, 3-7.
8. Tolstousov, A.V. and Bannykh, O.A. (1981), “New Quenching Media Based on Water-Soluble Polymers”, Metal Science and Heat Treatment, Vol. 23, No. 2, 104-106.
9. Xia, Y and Larock, R. C. (2010),”Vegetable oil-based polymeric materials: synthesis, properties, and applications”, Green Chemistry, Vol.12, 1893-1909.

Engineering innovation and industrial development

Oyawale Festus A.
Mechanical Engineering Department, Covenant University, Ota

Abstract

Nigeria remains underdeveloped fifty two years after colonial rule exporting primary raw materials and depending on imports of everything including even the debasing second hand goods. This paper examines the capacity of engineering innovation to transform the economy. Approach of successive governments was analysed. A linkage was traced between engineering innovation industrialisation and the nation's wellbeing. We conclude that power and the attitude of the people affect engineering innovation and industrial development.

1. Introduction

The primary purpose of engineering innovation is to provide product design and engineering to manufacturers of consumer goods. During the past one hundred years society has been transformed by the efforts and magnificent accomplishments of engineers. We presently celebrate feats like the locomotive, the automobile, the aeroplane, electricity, refrigeration and air-conditioning, radio and television, supercomputers and internet to mention a few. Topping the list is electricity which is perhaps the greatest invention without which other innovations would have been impossible. Abundant and available electric power helped the developed economies to achieve the great economic feats.

Refrigeration and air-conditioning have greatly improved the quality of life and have helped us sto preserve and distribute food that would have perished. Radio and television and lately, cable television have reduced the world to a small village readily accessed with the touch of a button. We have witnessed a tremendous achievement in satellite technology making telephony common place and further reducing the world to an electronic village. It is taken for granted as viewers all over the world watched the American elections in real time. Where in Nigeria is the present march to innovation revolution? Nigerians are conspicuous consumers unperturbed by the fact that the country has not contributed in anyway to transform the lives of people positively. Today, Nigeria exports only primary raw materials – an index of underdevelopment. How can Nigeria defend her unusually cold response to a world that is in a hurry? My Russian teacher once said "Nigeria, plenty talk no do". Forty years after, this has remained terribly true. Whither Nigeria?

Engineering is the profession in which a knowledge of the mathematical and natural sciences, gained by study, experience, and practice, is applied with judgment to develop ways to economically utilize, the materials and forces of nature for the benefit of mankind (ABET, 1993). Dahlman (1980) defined technology as the inherent or acquired capability possessed by people and/or institutions which enables them to convert available inputs into desired outputs at maximum efficiency level. We therefore articulate that engineering technology has three components – skills, knowledge and tools. In the Nigerian context, we ask if these three components are present. If we are in the affirmative, where did things go wrong that the entire system is suffering serious decay? The objective of this paper is to outline the issues that took us to the present level and to proffer solutions

Human development requires expanding people's capabilities for living decent lives and enhancing their opportunities for economic, social and political empowerment. Human capabilities are enhanced through education, skills development, and socio-cultural changes to innovate products that are required for health and other human needs to improve their quality of life.

In the words of the Lagos Plan of Action (LPA 1980), industrialisation constitutes "a fundamental option in the total range of activities aimed at freeing Africa from underdevelopment and economic dependency''. The industrial development policy pursued in most African countries after their decolonisation was billed as catch-up industrialisation. By that they did not

mean catching up on the industrialised nation's route to development, but rather emulating their level of development. The long and laborious path that had led to this level was to be leapfrogged at one bound. This strategy has failed.

With minimal capital and maximum labour input, limited and mostly handed-down commercial and technical knowledge, using easily procurable tools and locally available raw materials, local innovators produced goods and provided services for the local people. Local experiences existed in Awka, Bida and some parts of Yoruba land where blacksmiths provided for the needs of local farmers. However, most of the new governments did not recognise and promote these activities as the starting point for development. Instead, they saw them as being backward and crude and subjected them to discrimination and marginalisation.

The governments, their advisors and financiers pursued a different strategy. In the expectation that leapfrogging development by introducing state-of-the-art technology would have greater impacts than replicating the European path to it, they ensured that the most up-to-date production technologies were transferred to Africa from the industrialised nations. At the same time, the African governments created rules and regulations and promotion instruments which favoured and subsidised the import of everything while discriminating, criminalising, and persecuting the local efforts which they claim are illicit. The protagonists of this model of modernisation strategy, however, were disappointed. Importing state-of-the-art production plants merely created islands of modernity in a sea of handed-down imperfection.

Modern installations depend on the reliable provision of power, communications and other infrastructural services, and in the Nigerian environment there were too many supply bottlenecks. Their technology is so sensitive that it required only raw materials, fuels, spare parts, maintenance and repair services that meet the highest technical demands, which were not available in-country.

2. Local content

The Federal Government's aspiration to achieve 70 per cent local content in the oil and gas sector by 2010 was not feasible, due to poor compliance with the guidelines governing the Local Content policy by most International Oil Companies (IOCs) operating in the country. The Nigerian Content policy was initiated in 2006 by the Olusegun Obasanjo administration to help develop local capacity building in the Nigerian oil and gas sector, with a view to ensuring that Nigerians participated actively in the operations in the sector.

The government had directed oil companies operating in the country to commence in-country fabrication of equipment as well as other major components used in oil exploration. The government had reasoned that the implementation of the content policy would serve as a means of dissuading capital flight - and thus aspired that 45 per cent of total contractual jobs in the industry had to be done in Nigeria and 70 per cent of the jobs done in-country by 2010.

However, we are all witnesses to the serious hiccups resulting from lack of local content in the sector. To date, most of the contractual works involving engineering services, such as Front End Engineering Design, Detailed Engineering works, as well as materials procurement are still being done outside the country, contrary to the domiciliation guidelines issued by the Local Content Department (LCD) of the NNPC (Thisday on-line).

The government had hoped that local content development would ensure that the quantum or percentage of locally produced materials, personnel, goods and services rendered to the industry are increased, thereby generating more employment and economic empowerment. But this was not to be, as these multi-nationals preferred establishing Nigerian offices, which they used as cover-up, when the real services were rendered by foreign companies in Nigeria or off the shores of the country.

3. Power

Over 75% of the country still experiences constant power failure, which ranges from 4 to 5 days weekly. Reliable Electric Power supply continues to be one of the most essential factors in keeping an advantageous economy; especially for the small businesses all around the country to survive. Most of the economy problems in Nigeria rest on the inadequacy of the power sector. The attainment of a reliable Electric Power Supply in Nigeria

could immediately disentangle 60% of our poor economy issues. It is clear and simple that Nigeria as a nation will forever continue to struggle at very low standard unless something drastic was done right away to correct this deficiency. One of the possible solutions could be renewable energy instead of the continuous heavy investment on thermal generators.

4. Handling of waste

Accompanying population growth and the expansion of socio-economic activities, around the globe the demand for resources has increased, resulting in increases in the volume of waste as well as increasing diversity in the types of waste. Recycling is becoming a national habit, practiced by millions of people every day. However, recycling alone cannot end our dependency on landfills and incinerators, nor reverse the rapid depletion of our natural resources. As world population and consumption continue to rise, it is clear that our one-way system of extracting virgin resources to make packaging and products that will later be buried or burned is not sustainable. Zero Waste is a new way of looking at our waste stream. Instead of seeing used materials as garbage in need of disposal, discards are seen as valuable resources. A pile of "trash" represents jobs, financial opportunity, and raw material for new products. There is need to redesign products and manufacturing processes to meet the Zero Waste standards adopted by various countries.

"Each recycling step a community takes locally means more jobs, more business expenditures on supplies and services, and more money circulating in the local economy through spending and tax payments." In addition Zero Waste puts the responsibility for materials entering the waste stream on the front-end with the manufacturer, not on the consumer at the back-end of the product's life. The end result is that manufacturers redesign products to reduce material consumption and facilitate reuse, recycling and recovery.

5. Technology development

India has made commendable progress in terms of the growth of scientific and technological culture. Today, India has a vast pool of S&T infrastructure with over 800 technical institutions including around 200 universities. In addition, it already has a critical mass of cutting edge research through 400 national laboratories, over 1,300 in house R&D units in the corporate and other sectors. However, the environment and support system are not congenial for the faster commercialization of R&D outputs. There exists lot of delay in commercialization of R&D outputs and in majority of cases the R&D outputs do not get commercialized for want of initial investment, the needed environment and the networking. In the recent past, the Ministry of Science and Technology, Government of India has been focusing its attention towards this and initiated a number of programmes in order to plug the gaps cited above.

By training engineers and technologists and encouraging them to innovate by rewarding them generously with both real and psychic income, India has been able to compete in the world economy and thrive by trading high quality, high-tech products over international boundaries.

6. Entrepreneurial initiatives

The Science Park and similar initiatives in the developed countries are the latest in the evolutionary line to create an atmosphere for innovation and entrepreneurship; for active interaction between academics and industries; for sharing ideas, knowledge, experience and facilities for the development of new technologies and their rapid transfer to the end user.

The objectives of the initiative:

- To forge a close linkage between universities, academic and R&D institutions on the one hand and industry on the other
- To promote entrepreneurship among science and technology persons, many of whom were otherwise seeking jobs soon after their graduation
- To provide R&D support to the small-scale industry mostly through interaction with research institutions
- To promote innovation based enterprises

Facilities and services provided by the initiative:

- Offers facilities such as nursery sheds, testing and calibration facilities, precision tool room/central workshop, prototype development, business facilitation, computing, data bank, library and documentation, communication, seminar hall/conference room, common facilities such as phone, telex, fax, photocopying;
- Offers services like testing and calibration, consultancy; training, research, prototype development/process development, human resource development (short-term courses), technical support services, business facilitation services, database and documentation services, quality assurance services and common utility services.
- At present, there are around 3,000 incubators of various types operational in the world. In the United States, there are over 800 incubators including about 200 Internet incubators. Europe has about 1,000 incubators including 300 incubators in Germany. Among the developing countries, China leads with about 100 incubators.

Among the industrializing countries, Republic of Korea is reported to have about 300 incubators. Currently, infrastructure for Prototype Development and business incubation services in Nigeria is weak. The concept of Business incubation is just picking up.

We conclude that lack of infrastructure and the attitude of the populace are necessary for engineering innovation and possible linkage to industrialization through technology business incubation.

7. Conclusions

- Industries should be cited in rural communities to halt the rural-urban drift.
- More emphasis should be placed on engineering design and fabrication
- Present day engineering should be geared towards solving current problems. While India is replacing two wheelers with affordable four wheelers, Nigerians should be saved from the harrowing experience of carrying four or even five passengers on motorcycles with the attendant carnage.
- Engineers and technologists should be adequately compensated. The Nigerian Society of Engineers has some job to do in this regard.
- Universities and polytechnics should be centres of excellence and adequate linkage should be maintained with government and industries.
- Engineering and technology students should be made to solve live national problems in their class assignments and projects.
- Economic crimes that enslave Nigerians should be seriously tackled.
- The country should adopt appropriate mechanisms for technology business incubation in order to nurture new enterprises and provide technical advisory services to SMEs.
- Some external assistance from agencies like UNDP, UNIDO, should be sought under a broad framework.
- Efforts should be made to initiate country exchange programmes with other developing countries to understand and complement mutual efforts in carrying out studies, assessment surveys, training and setting up of incubation mechanisms.

This kind of conference should take the bull by the horn. It should not be a talk shop. Meaningful and workable solutions to our problems must emerge. Covenant University should blaze the trail as the Nigerian foremost private engineering university. A situation where everything from toys to air conditioners and passenger cars and trucks are imported from Asia is disturbing not to even talk of the dehumanizing “Tokunbo” and “Belgium” products. Pardon me for being so passionate and emotional but we have no choice if we are to refocus our national innovative ingenuity.

Thank you for giving me this opportunity to scrape the tip of the iceberg. I rest my case by saying that our problem though enormous is not insurmountable.

References

Paul Andre de la Porte, (2005) Resident Representative, UNDP, Nairobi, Kenya

Ogada T. and Moturic C., (2007) “Improving Access To Technology For Enhanced Industrial Development Of Kenya” Presented to WAITRO Meeting in Sheraton UGANDA

Marti Matsch , “Zero Waste: A New Systems Approach Gaining Global Ground” “ABET Accreditation Yearbook,” Accreditation Board for Engineering and Technology, Inc. New York- 1993

Brenda A. Platt and David Morris, The Economic Benefits of Recycling (Washington, DC: Institute for Local Self-Reliance, February 1993), p. 9. 2. Michael Lewis, Recycling Economic Development through Scrap-Based Manufacturing (Washington, DC: Institute for Local Self-Reliance, February, 1994).

Gupta, Anita (2001) “Improved Competitiveness of Small and Medium-sized Industries through Application of Modern and Efficient Technologies” National Workshop on Promoting Business and Technology Incubation, Phnom Penh,Cambodia

Oyedepo and Kilanko: Proc. ICCEM (2012) 331 - 342

Thermodynamic Analysis of a Gas Turbine Power Plant Modelled with an Evaporative Cooler

[1]Oyedepo, Sunday Olayinka and [2]Kilanko Oluwaseun
[1, 2] Mechanical Engineering Department, Covenant University, Ota, Nigeria
e-mail: Sunday.oyedepo@covenantuniversity.edu.ng,
oluwaseun.kilanko@covenantuniversity.edu.ng

Abstract

Performance of a gas turbine is mainly depends on the inlet air temperature. The power output of a gas turbine depends on the flow of mass through it. Inlet air cooling increases the power output by taking advantage of the gas turbine's feature of higher mass flow rate when the compressor inlet temperature decreases. This is precisely the reason why on hot days, when air is less dense, power output falls off. A rise of 1°C temperature of inlet air decreases the power output by 1%. In this paper the performance enhancement of gas turbine power plants by cooling the compressor intake air with an evaporative cooler is studied. This study investigated the effect of inlet air cooling system on the performance of an existing gas turbine power plant in Nigeria. The results show that for each 5^{o}C decrease of inlet air temperature, net output power increases around 5-10% and the first and second law efficiencies increase around 2-5%. It is shown that the amount of this increase is higher when the pressure ratio is high and turbine inlet temperature is low. The results of this study shows that retrofitting of the existing gas turbine plant with inlet air cooling system gives a better system performance and may prove to be an attractive investment opportunity to the Nigeria government and stakeholders of the plant.

Key words: *Gas Turbine (GT), plant performance, relative humidity, dry bulb temperature*

1. Introduction

The gas turbines are widely being used for producing electricity, operating airplanes and for various industrial applications such as refineries and petrochemical plants (Mahmood and Mahdi, 2009). In aircraft propulsion or drives for vehicles, gas turbines are chosen due to their large power-to-weight and power-to-volume ratio. Furthermore, for certain operating conditions the cycle efficiency of gas turbines is high compared to piston engines. In the field of energy generation, gas turbines have often been chosen in the past when fast start and shut down on demand is required. This is especially needed for compensating peak loads over the daytime. In contrast, steam cycles as used for coal and oil firing or nuclear power are base-load machines since the start and shut down is tremendously longer due to the large heat capacity in the cycle (Büche, 2003).

The basic gas-turbine cycle has low thermal efficiency, so it is important to look for improved gas turbine based cycles (Mahmood and Mahdi, 2009). Therefore, enhancing the performance of Gas turbine was successfully through raising the turbine inlet temperature (TIT) and the compressor pressure ratio and advances in cooling technology and material science caused high turbine inlet temperature conceivable (Ibrahim,et al 2010).

Gas turbines (GTs) have been used for electricity generation in most countries around the world. In the past, their use has been generally limited to generating electricity in periods of peak electricity demand. Gas turbines are ideal for this application as they can be started and stopped quickly enabling them to be brought into service as required to meet energy demand peaks (Jaber et al, 2007). However, due to availability of natural gas at relatively cheap prices compared to distillate fuels, many countries around the world, e.g. Nigeria, use large conventional GTs as base load units, while small ones to meet any shortages in available electricity supplies occurring during an emergency or during the peak load demand periods. Such systems, especially those operating in an open or simple cycle have the disadvantage of being least efficient and so the unit cost of generated electricity is relatively high.

The average efficiency of gas turbine plants in the Nigerian energy utility sector over the past decade was in the range 27-30% (Abam *et al*., 2011). The low efficiencies of the gas turbine plants are tied to many factors which include: operation mode, poor maintenance procedures, age of plant, discrepancies in operating data, high ambient temperature and relative humidity.

It is well known that ambient temperature, humidity and pressure are important factors in

gas turbine performance. Thermodynamic analyses exposed that thermal efficiency and specific output decrease with an increase of humidity and ambient temperature as shown by Tsujikawa and Sawada (1985). Bird and Grabe(1991) have studied the effect of humidity on gas turbine performance and formulated correlations. El-Hadik(1993) [3] carried out a parametric study on the effects of ambient temperature, pressure, humidity and turbine inlet-temperature on power and thermal efficiency. He concluded that the ambient temperature has the greatest effect on gas turbine performance, which increases with the turbine inlet-temperature and pressure ratio. Reductions of power and efficiency due to a 1 K temperature growth were found to be around 0.6% and 0.18%, respectively. The work of Ibrahim, et al (2011) also shows that an increment of 1 °C in the compressor air inlet temperature decreases the gas turbine power output by 1 %. These serve as evident that gas turbine performance is sensitive to the ambient air temperature. As the ambient air temperature rises, less air can be compressed by the compressor since the swallowing capacity of compressor is given, and then the gas turbine output is reduced at a given turbine entry temperature. In addition, the compression work increases because the specific volume of the air increases in proportion to the intake air temperature (Shi, et al, 2010). Generally speaking, the gas turbine is designed to operate with a constant air volume flow in the compressor. When the ambient air temperature increases, its specific mass is reduced, so that the mass flow rate entering the turbine is accordingly decreased. This would, in turn, decrease the power output of the gas turbine. Strictly speaking, the power output is directly dependent on the mass flow rate of the air in the cycle. For each degree Celsius increase of the air temperature, 0.5–0.9% of the power output of the gas turbine cycle is reduced (Hosseini, 2007). The efficiency and power output of a gas turbine during hot condition is less than power output during cold condition. The performance of the plant efficiency is decreasing as the ambient temperature increases, due to the inverse relation between air density and temperature. Cooling the inlet air of gas turbine, decreases the temperature which increases the air density, hence increasing the mass flow rate.

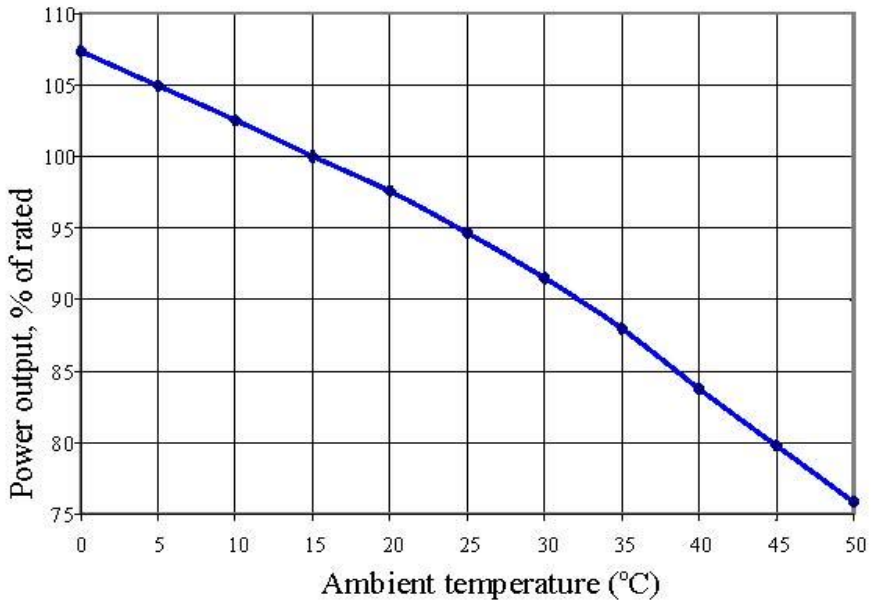

Figure 1: Variations in gas turbine output power with ambient temperature (Al-Tobi, 2009)

Due to these severe ambient conditions, the turbine inlet air cooling is one of many available technologies to improve the performance of the gas turbine power plants by cooling the air at the compressor entry (Farzaneh-Gord and Deymi-Dashtebayaz ,2011). Turbine inlet cooling is defined as cooling the air before it enters the compressor of the gas turbine. The main reason for turbine inlet cooling is to increase the power output of the gas turbine when the ambient temperature is higher than the standard conditions. The rated capacity of all gas turbine is usually based on the standard ambient conditions of 15^{o}C and 14.7 psia (Al-Tobi, 2009) at sea level which is selected by the International Standards Organisation (ISO). Figure 1 shows typical characteristics of gas turbine behaviour with ambient temperature variations. The actual characteristics of a particular gas turbine with ambient temperature depends on its actual design however the general trend and behaviour shown in Figure 1 is still valid for all gas turbines.

Figure 1 shows that the rated capacity of the gas turbine decreases to about 76% when the ambient temperature increased from 15^{o}C to 50^{o}C. This means that the power producers may not be able to meet the demand of their customers at higher ambient temperatures due to this reduction in output power. Note that in hot countries, such as Nigeria, the electricity demand has its peak on the summer due to large demand for air conditioning. Cooling the inlet air to the compressor from 50^{o}C to 15^{o}C will prevent the 24% loss in the output power (Abam et al, 2012).

Therefore, ability to cool the inlet air will facilitate the production of consistent gas turbine power output throughout the year, irrespective of the changes in ambient temperature. Also cooling the inlet air increases the mass flow of air into the gas turbine and at the exhaust outlet. For the same power output, decreasing the inlet air has the effect of decreasing the fuel consumption.

Many researchers have studied different cooling methods to enhance the performance of GT plants operating at high conditions of ambient temperature. Johnson (1988) presented a discussion of the theory and operation of evaporative coolers for industrial gas turbine installations. Calculations of parameters to predict the performance of evaporative cooler were discussed, in addition to installation, operation, feed water quality and the causes and prevention of water carry-over. Ondryas et al., (1991) investigated the impact of using chillers at the air intake to boost gas turbines power in cogeneration plants during high ambient temperatures. Three types of chillers i.e, absorption, vapour-compression and thermal energy storage were studied.

Johnke and Mast (2002) reported that a media cooler can increase the relative humidity of the inlet air to about 90%, thus increasing the power output by 5–10% and the efficiency by 1.5–2.5%. Ameri and Hejazi (2004) have carried out feasibility of installing an absorption chiller system to cool the inlet air to the Chabahar power plant gas turbines. It has been shown that the average power output can be increased by as much as 11.3%. The economical analysis has shown that the internal rate of return (ROR) is 23.4% and the payback period is 4.2 years. Kakaras et al.(2004) have presented a computer simulation of the integration of an innovative absorption chiller technology for reducing the intake-air temperature in gas turbine plants. They concluded that the effect of ambient air temperature variation has the large penalty in the plant's performance for high ambient temperatures.

The influence of ambient temperature on combined cycle power plant performance was investigated by Arrieta and Lora (2005). They showed that a drop in the ambient temperature increases both the electric power generated and efficiency in the plant, and the rise in the temperature of the gas after the supplementary firing increases the generated electric power, but reduces the efficiency. Power augmentation of a typical gas turbine cycle by using a desiccant based evaporative cooling system was studied by Zadpoor and Golshan (2006). The technique requires a desiccant based dehumidifying process to direct the air through an evaporative cooler, which could be either media based or spray type. The performance improvement of the gas turbine cycle for each of these methods, direct evaporative cooler, indirect and direct evaporative cooler and desiccant based evaporative cooler, was studied for different climatic conditions.

The study of (Elliot, 2001) shows that a 1% gain of the output power was obtained for every 1.6°C drop in compressor inlet air temperature using water chillers. Kolp *et al*. (2001) demonstrated the effect of various forms of inlet air cooling and supper charging of 40MW GE LM6000 gas turbine plant. Their results indicate that a 28°C reduction in the compressor inlet air temperature increased the net power output by 30%. In addition, (Mercer, 2002) reported in his study that chillers utilizing thermal storage systems would increase the gas turbine power output by over 25% during peak periods. Similarly evaporative coolers gives an increase of about 10-15% power output, while water fogging a cooling technique will enhance power output by 10-20% (Amell and Cadavid, 2002; Mohanty and Paloso, 1995).

Abam, et al, 2012 carried out performance analysis and components irreversiblities of a 25 MW gas turbine power plant modeled with a spray cooler. The results obtained show that the use of a spray cooler on the existing gas turbine cycle gives a better thermal efficiency and less irreversibility rate in the components system and the entire plant. The power output of the gas turbine plant with spray cooler was found to have increased by over 7%, accompanied by 2.7% increase in machine efficiency with a reduction in specific fuel consumption of 2.05 and 10.03% increase in the energy of exhaust.

Considering the rapid increase in electricity demand in Nigeria and the expected shortages in power supply due to delays in implementation of the major power projects, retrofitting the existing Gas Turbine (GT) power plants in the power sector with inlet-air cooling system is an attractive investment opportunity for the Power Holding Company of Nigeria (PHCN). It is the aim of this study to model an active 33.5MW barge gas turbine plant with an evaporative cooler. Also, the

study investigates the performance enhancement and modification of a grid-connected gas turbine plant operating at Egbin Power Station in Nigeria using the prevailing climatic conditions. The performance of the proposed modified Brayton cycle is compared with base case condition (without inlet air cooling).

2. Materials and Methods

2.1 Data Collection

Operating data for Gas turbine unit were collected from the daily turbine control log sheet for a period of five years (2006 – 2010). The daily average operating variables were statistically analyzed and mean values were computed for the period of January to December, followed by overall average. These are shown in Appendix A. Summary of operating parameters of PB204 unit used for this study is presented in Table 1.The analysis of the plant was divided into different control volumes and performance of the plant was estimated using component-wise modeling. Mass and energy conservation laws were applied to each component and the performance of the plant was determine for the simple system (without evaporative cooler) and for the cooled system (with evaporative cooler).

Table 1: Summary of operating data for the 33.5-MW barge gas turbine power plant

S/N	Operating Parameters	Value	Unit
1	Mass flow rate of air through compressor(m_a)	125.2	Kg/s
2	Temperature of inlet air to compressor (T_1)	304	^oK
3	Pressure of inlet air to compressor(P_1)	0.10132	MPa
4	Outlet temperature of air from compressor(T_2)	622	^oK
5	Outlet pressure of air from compressor (P_2)	0.980	MPa
6	Fuel-gas(natural gas) mass flow rate (m_f)	4.5	Kg/s
7	Fuel- air ratio at full load(on mass basis)	0.036	-
8	Inlet pressure of fuel-gas	1.2	MPa
9	Inlet temperature to gas turbine (T_3)	1219	^oK
10	Turbine outlet gas temperature	750	^oK
11	Exhaust gas temperature	715	^oK
12	Lower Heating Value (LHV)	47,541.57	kJ/kg
13	Isentropic efficiency of Compressor	85	%
14	Isentropic efficiency of Turbine	87	%
15	Combustion efficiency	99	%

2.2 Thermodynamic Model of Gas Turbine Unit (Simple type)

Figure 2 shows the schematic diagram of single shaft gas turbine cycle selected in this study. The compressor inlet temperature is equal to ambient temperature once the base-case neglects the cooling effect and simulates the cycle under ISO conditions (T_0 = 15 °C, P_0 = 101.3 kPa and ϕ = 60 %) and without pressure drop at inlet and exhaust ducts. Thus, the inlet pressure is given by (Ana Paula et al, 2012):

$$P_0 = P_{03} \quad (1)$$

The air and combustion products are assumed to behave as ideal gases.

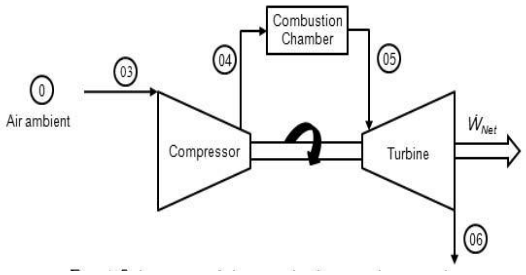

Figure 2 Schematic of the standard gas turbine cycle

The pressure of the air leaving the compressor (P_{04}) is calculated as:

$$P_{04} = r.P_{03} \quad (2)$$

Where r is the compression ratio

Assuming an ideal gas for state 04 and taken isentropic efficiency of compressor to be 0.85, the total temperature of the fluid leaving the compressor having can be evaluated using ideal gas relations

$$T_{04} = \frac{T_{03}}{\eta_c}\left[\left(\frac{P_{04}}{P_{03}}\right)^{\frac{\gamma-1}{\gamma}} - 1\right] + T_{03} \quad (3)$$

Where η_c is the compressor efficiency and γ is the specific heat ratio.

The compressor work is calculated from the mass flow rate and enthalpy change across the compressor as follows:

$$\dot{W}_c = \dot{m}_a.C_{pa}(T_{04} - T_{03}) \quad (4)$$

Where ma is the air mass flow rate and C_{pa} is the specific heat capacity of air which is considered in this study as a temperature variable function and can be fitted by Equation

(5) for the range of 200K<T<800K (Rahman et al.,2011):

$$c_{pa}(T) = 1.04841 - \left(\frac{3.8371T}{10^4}\right) + \left(\frac{9.4537T^2}{10^7}\right) - \left(\frac{5.49031T^3}{10^{10}}\right) + \left(\frac{7.9298T^4}{10^{14}}\right) \quad 5$$

Pressure drop across combustion chamber (ΔP_{cc}) is usually around 2% (Barzegar, et al, 2011). Turbine inlet pressure (P_{05}) can be calculated as:

$P_{05} = P_{04}(1 - \Delta P_{cc})$ 6

Where P_{05} is the turbine entry level pressure in Pa; P_{04} is the combustion chamber inlet temperature, ΔP_{cc}, is pressure drop across the combustion chamber.

The heat delivered by combustion chamber is determined from energy balance:

$$\dot{Q}_{in} = C_{pg}(T_{05} - T_{04}) \quad 7$$

Where C_{pg} is the specific heat capacity of combustion product; the C_{pg} in this work is considered to be a temperature variable function as (Kurt, et al, 2009):

$$c_{pg}(T) = 0.991615 + \left(\frac{6.99703T}{10^5}\right) + \left(\frac{2.7129T^2}{10^7}\right) - \left(\frac{1.22442T^3}{10^{10}}\right) \quad 8$$

The mass flow rate of fuel is computed as (Ana Paula, et al, 2012):

$$\dot{m}_f = \frac{\dot{Q}_{in}}{LHV \times \eta_{com}} \quad 9$$

Where LHV is the lower heating value of the fuel (natural gas) and η_{com} is combustor efficiency

The exhaust gases temperature from gas turbine is given as:

$$T_{06} = T_{05}\left\{1 - \eta_T\left[1 - \left(\frac{P_{05}}{P_{06}}\right)^{\frac{1-\gamma_g}{\gamma_g}}\right]\right\} \quad 10$$

Where η_T is the turbine isentropic efficiency and P_{06} is the ambient temperature

The turbine power is equal to:

$$\dot{W}_T = \dot{m}_g c_{pg}(T_{05} - T_{06}) \quad 11$$

Where $\dot{m}_g$ is the mass flow rate of flue gas and it is given by

$$\dot{m}_g = \dot{m}_a + \dot{m}_f \quad 12$$

The net power obtained from the gas turbine is given by:

$$\dot{W}_{Net} = \dot{W}_T - \dot{W}_C \quad 13$$

The specific fuel consumption (SFC) is determined by equation (14). The Specific fuel consumption compares the ratio of the fuel used by an engine to a certain force such as the amount of power the engine produces. This is a very important economic criterion.

$$SFC = \frac{3600\,\dot{m}_f}{\dot{W}_{Net}} \text{ Kg/kWh} \quad 14$$

Heat rate (HR) of gas turbine cycle is determined by:

$$HR = SFC \times LHV \quad 15$$

The thermal efficiency of the gas turbine is calculated as:

$$\eta_{th} = \frac{\dot{W}_{Net}}{\dot{m}_f \times LHV} \quad 16$$

2.2 Thermodynamic Model of Gas Turbine Unit with Cooling System

Figure 3 is a schematic diagram of gas turbine cycle with cooling system. The gas turbine power plant consists of compressor, combustion chamber and turbine. In this study, the inlet air cooling technique proposed for analysis is evaporative cooling. The performance of the gas turbine will be evaluated with the proposed cooling technique and compared with values of the simple gas turbine.

In the evaporative cooler, water drains through the distribution pad into the media, by gravity action downward through it, and wets enormous area of media surface contacted by air passing through the cooler. The dry air mixes with water becoming saturated where the Dry Bulb Temperature (DBT) of inlet air reaches initial Wet Bulb Temperature (WBT).

It is assumed that the relative humidity of outlet air from the cooler will not exceed 100% despite the inlet air condition. The humidifying efficiency is assumed to be 100%. The gas turbine power plant models are developed on the following assumptions: (i) all components have adiabatic boundaries, (ii) plant performance at ISO conditions, (iii) the air and the combustion products are assume ideal characteristics, (iv) kinetic and potential components of energy are neglected and (v) the ambient conditions of temperature and pressure are 25°C and 1.013 bar.

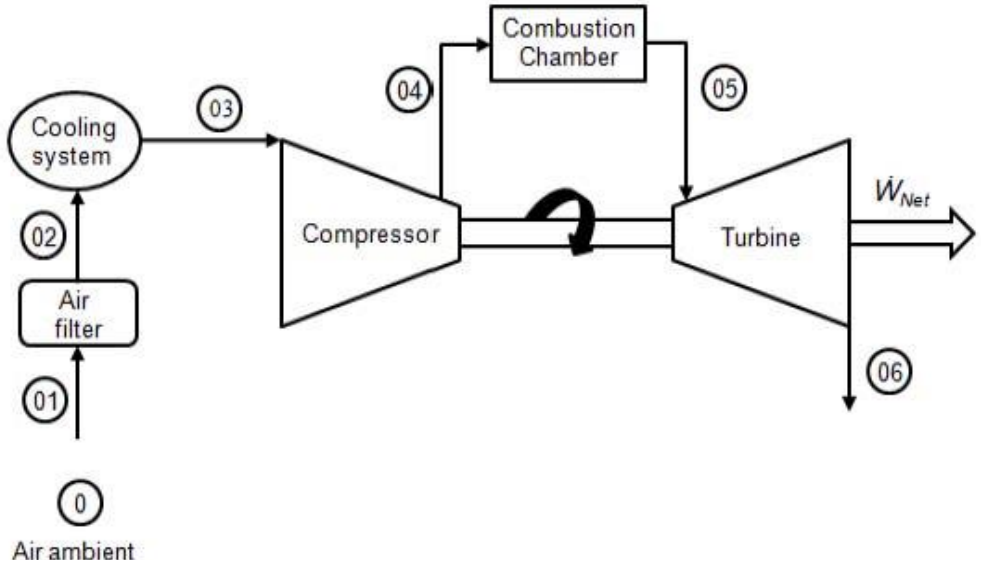

Figure 3 Schematic diagram of the gas turbine cycle with cooling system

2.2.1 Humidifier Model

Cooling in hot and relatively dry climate can be accomplished by evaporative cooling. This is because the cooling technique utilizes the latent heat of vaporization to cool ambient temperature from the dry temperature (Ana Paula, et al, 2012). Evaporative cooling involves passing air across a spray of water or forcing air through a soaked pad that is kept replenished with water (Alok Kumar and Sanjay, 2012). Owing to the low humidity of entering air, a part of the water injected evaporates. The energy required for evaporation is provided by the air stream, which undergoes a reduction in temperature. The following assumptions are made in the humidifier model.

- The relative humidity at the humidifier outlet is 95%
- The pressure drop of air in the humidifier is 1% of the ambient air pressure.

The Common media types of evaporative coolers use a wetted honeycomb- like medium to maximize evaporative surface area and cooling potential. Figure 4 illustrates principle of operation of evaporative cooler. According to Ibrahim et al, 2011, this cooling equipment is placed after the air filter system as shown in Figure 3.This type of arrangement protects the media from the dust and other airborne contaminants that would otherwise impinge upon it. Evaporative cooling involves heat and mass transfer, which occurs when water and the unsaturated air-water mixture of the incoming air are in contact (Hosseini et al., 2007). This transfer is a function of the differences in temperatures and vapour pressures between the air and water. Heat and mass transfer are both operative in the evaporative cooler because of heat transfer from air to water evaporates water, and the water evaporating into the air constitutes mass transfer (Ibrahim et al, 2011).

In evaporative cooling, sensible heat from the air is transferred to water, which becomes latent heat as the water evaporates. The water vapour becomes part of the air and carries the latent heat with it. The air dry-bulb temperature decreases because it gives up the sensible heat. The air wet-bulb temperature is not affected by absorption of latent heat in the water vapour because the water vapour enters the air at air wet-bulb temperature.

Theoretically, the incoming air and water in the evaporative cooler considered as isolated system due to no heat is added to or removed from the system. The process of exchanging the sensible heat of the air for latent heat of evaporation from water is adiabatic (Bhargava and Meher-Homji, 2005). Such system is used as a preferred solution in dry/desert climate, which can be expected to boost the gas turbine power by nearly 12%. Meanwhile, for hot humid climates, the air-cooling is limited to the wet bulb temperature and the capacity of the gas turbine generator may not be increased by more than 5 to 7% in best cases (Johnson, 1989).

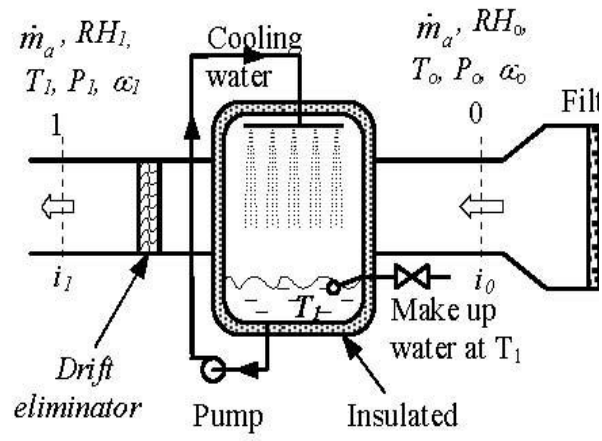

(a)

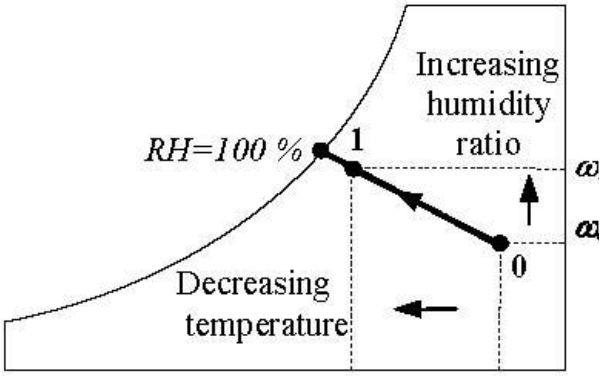

(b)

Figure 4: (a) Schematic of adiabatic evaporative cooler (b) Adiabatic saturation process on the psychometric chart

Applying the mass balance equation across the humidifier control volume boundary gives

$$\omega_{a,e} = \omega_{a,i} + m_w \qquad 17$$

where ω is the specific humidity and is calculated at a certain temperature as

$$\omega = \frac{0.622 P_v}{P - P_v} \qquad 18$$

where $P_{v=}\phi . P_{sat}$ is the partial pressure of vapour, ϕ is the relative humidity and P_{sat} is the saturation pressure of air corresponding to the desired temperature.

The energy balance equation for the humidifier is given by:

$$h_{a,e} = h_{a,i} + (\omega_{a,e} - \omega_{a,i}) h_w \qquad 19$$

Where $h_{a,e}$ and $h_{a,i}$ are the enthalpy of moist air at out-let and inlet of the air humidifier respectively and are calculated as follows

$$h_{a,e} = C_{p,a,e} t_{a,e} + (2500 + 1.88 t_{a,e}) \omega_{a,e}$$

20a

$$h_{a,i} = C_{p,a,in} t_{a,i} + (2500 + 1.88 t_{a,i}) \omega_{a,i}$$

20b

$$T_{a,e} = t_{a,e} + 273$$

20c

The equations (17 – 20) can be solved to determine the value of $T_{a,e}$, $\omega_{a,e}$ and m_w

The inlet air temperature after cooling process (Figure 3) can be calculated as:

$$T_{03} = Tb_{02} - \varepsilon . (Tb_{02} - Tw_{02}) \qquad 21$$

Where Tb_{02} is the dry-bulb temperature, Tw_{02} is the wet- bulb temperature and ε is the cooling effectiveness.

The cooling load associated with the evaporative cooling system results:

$$\dot{Q}_{CL} = \dot{m}_a . C_{pa} (T_{02} - T_{03}) \qquad 22$$

Where $\dot{m}_a$ is the air mass flow rate and C_{pa} is the specific heat of the dry air at constant pressure, determined as a function of the average temperature across the evaporative system.

The working fluid passing through the compressor is assumed to be an ideal mixture of air and water vapour. The total enthalpy of atmospheric air is given as (Abam et al, 2012):

$$h = h_a + \omega \times h_v \cong C_{pa} T_a + \omega h_v \qquad 23$$

where h_a is the enthalpy of dry air, h_v is the enthalpy of water vapour

The enthalpy of water vapour can be evaluated by (Zaki, et al, 2011):

$$h_v = 2501.3 + 1.8723 T_j \quad \text{j refers to state 04 or 05} \qquad 24$$

The total temperature of the fluid leaving the compressor having an isentropic efficiency η_C can be evaluated using ideal gas relation:

$$T_{4s} = T_{03} + \frac{T_{03}}{\eta_C} \left[r_p^{\frac{\gamma - 1}{\gamma}} - 1 \right] \qquad 25$$

Where,

r_p= compression ratio

γ= specific heat ratio

Similarly, the total temperature leaving the turbine having an isentropic efficiency η_T is given by:

$$T_{6s} = T_{05} - \eta_T (T_{05} - T_{06}) \qquad 26$$

The total mass flow rate of humid air is given as:

$$\dot{m}_{ha} = \dot{m}_{da} + \omega \dot{m}_{da} = (1 + \omega) \dot{m}_{da} \qquad 27$$

Where, $\dot{m}_{ha}$ and $\dot{m}_{da}$ are mass flow rates of humid air and dry air respectively. The compressor work for humid air between states 03 and 04is calculated from the mass flow rate and enthalpy change across the compressor:

$$\dot{W}_c = \dot{m}_a (1 + \omega) \times C_{pa} (T_{4s} - T_{03}) + \omega (h_{4s} - h_{03}) \qquad 28$$

The power produced by the turbine due to expansion of hot gases is obtained as:

$$\dot{W}_T = \dot{m}_t C_{pg} (T_{05} - T_{06}) + \omega (h_{05} - h_{06}) \qquad 29$$

Where

$$\dot{m}_t = \dot{m}_a + \dot{m}_v + \dot{m}_f = \dot{m}_a (1 + \omega + f) \qquad 30$$

$$f = \frac{\dot{m}_f}{\dot{m}_a} \quad 31$$

The net power obtained from the gas turbine is given as:

$$\dot{W}_{net} = \dot{W}_T - \dot{W}_C \quad 13$$

The thermal efficiency of the gas turbine is given as:

$$\eta_{th} = \frac{\dot{W}_{net}}{\dot{m}_f \times LHV} \quad 16$$

The specific fuel consumption of the gas turbine is computed by:

$$SFC = \frac{3600 \times \dot{m}_f}{\dot{W}_{net}} kg/kWh \quad 14$$

3. Results and Discussion

The parameter influences in terms of ambient temperature, compression ratio and turbine inlet temperature on the performance of gas turbine cycle power plant are presented in this section. The effects of operation conditions on the network output, specific fuel consumption and efficiency are obtained by the energy-balance utilizing MATLAB10 software. In this study, a single shaft gas turbine is numerically simulated operating with natural gas. Table1 shows the technical parameters for the selected gas turbine unit used to evaluate both the performance of the base-case (without cooling intake air) and evaporative inlet air cooling. Simple gas turbine was simulated employing the ISO conditions without cooling and varying ambient air temperature, turbine inlet temperature and compression ratio.

Effect of ambient temperature

Fig. 5 - 7 shows the effect of ambient temperature on the performance of both simple gas turbine and evaporative cooling inlet conditions. Figure 5 shows that the gas turbine thermal efficiency is affected by ambient temperature due to the change of air density and compressor work. Since a lower ambient temperature leads to a higher air density and a lower compressor work that in turn gives a higher gas turbine output power as shown in Figure 6. It can be seen from Figure 5 that when the ambient temperature increases the thermal efficiency decreases. This is because, the air mass flow rate inlet to compressor increases with decrease of the ambient temperature. So, the fuel mass flow rate will increase, since air to fuel ratio is kept constant. The power increase is less than that of the inlet compressor air mass flow rate; therefore, the specific fuel consumption increases with the increase of ambient temperature (Figure 7). This occurs because of increased losses due to the increased amount of flue gases.

Both net power output and thermal efficiency of simple cycle and evaporative cooling inlet conditions decrease with increase in ambient temperature. Specific fuel consumption of gas turbine cycle increases with increase in ambient temperature. This result shows the importance of low intake air temperature on the gas turbine performance.

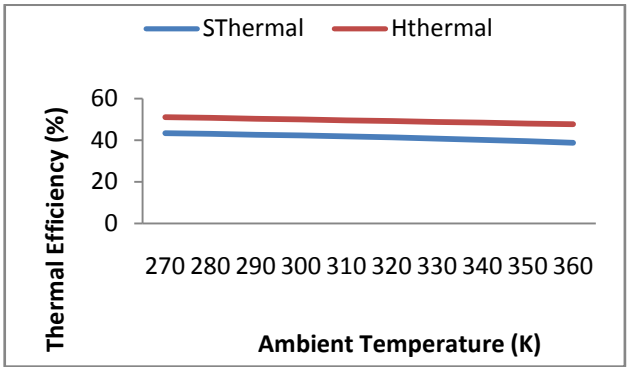

Figure 5: Effect of ambient temperature on gas turbine thermal efficiency

Key: SThermal – simple gas turbine thermal efficiency
Hthermal –humidified gas turbine thermal efficiency

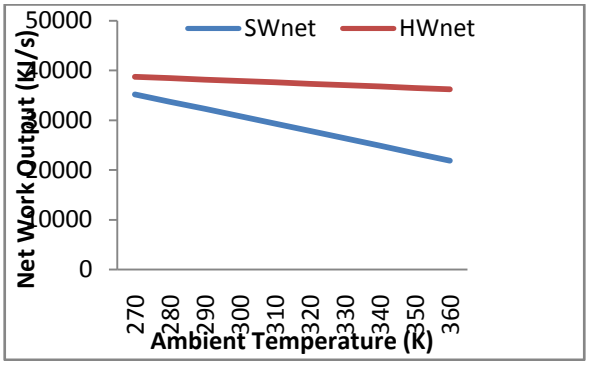

Figure 6: Effect of ambient temperature on Network output of gas turbine cycle

Key: SWnet – simple gas turbine net work output
HWnet – Humidified gas turbine net work output

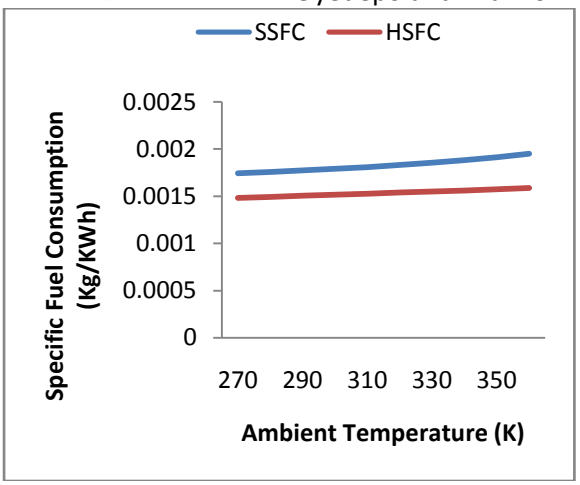

Figure 7: Effect of ambient temperature on specific fuel consumption of gas turbine cycle
Key: SSFC – simple gas turbine specific fuel consumption
HSFC – humified gas turbine specific fuel consumption

From Figure 6 it can be seen that the net work output obtained is lower at ISO conditions, when the intake air is not cooled. This shows that the ambient dryness affects the gas turbine performance providing a higher power output level when the ambient relative humidity is lower. When the evaporative cooling technique is employed, the gas turbine thermal efficiency level is higher in comparison with the base-case as occurred for the power output results.

Effect of Turbine inlet Temperature

Figure 8 shows the relation between the thermal efficiency and turbine inlet temperatures of gas turbine power plants. Thermal efficiency has an ejective relationship with turbine inlet temperature, the efficiency increases when turbine inlet temperature increases, also the decreased in air to fuel ratio caused increased thermal efficiency. Thermal efficiency and network output (Figure 9) increase with increase in turbine inlet temperature. But this increase is limited by metallurgical property of the turbine material. The specific fuel consumption (Figure 10) decreases with increase in turbine inlet temperature. This shows that gas turbine power plant performance can be improved by increasing the turbine inlet temperature.

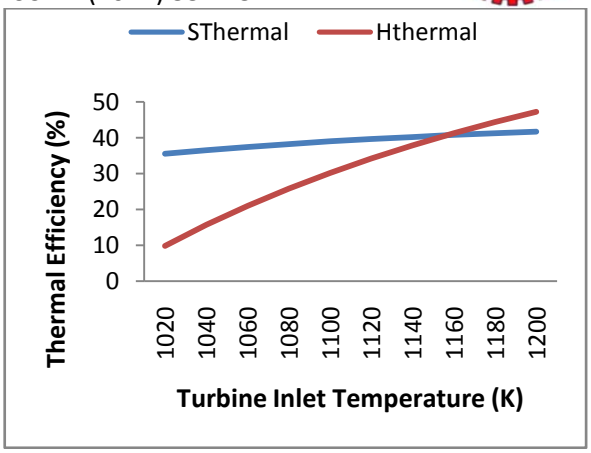

Figure 8: Effect of turbine inlet temperature on thermal efficiency of gas turbine plant

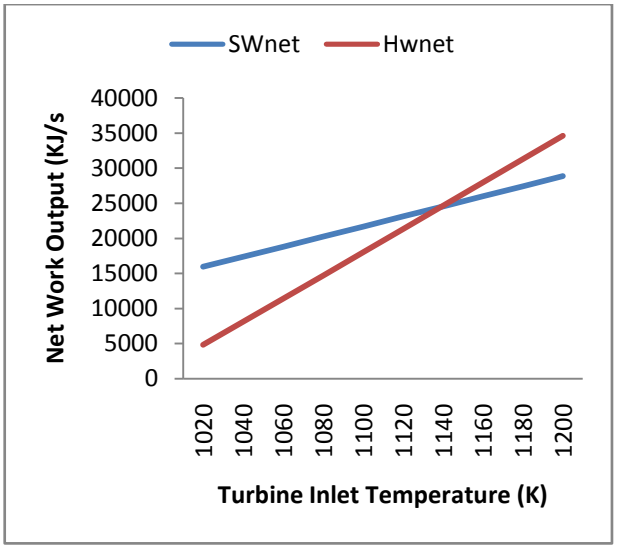

Figure 9: effect of turbine inlet temperature on network output of gas turbine

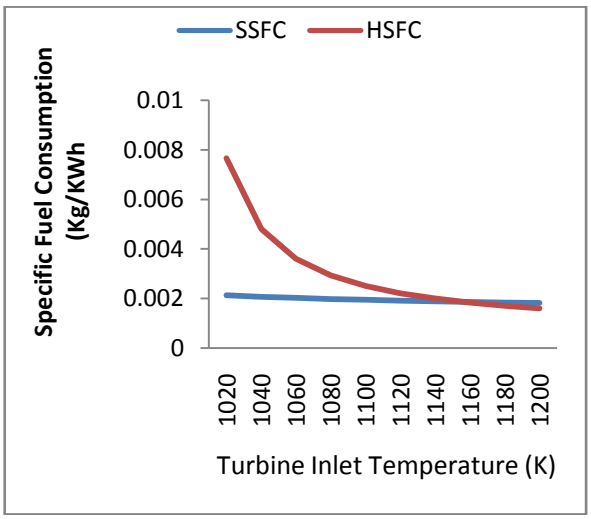

Figure 10: Effect of turbine inlet temperature on specific fuel consumption

4. Conclusion

The influence of operational parameters including the compression ratio, turbine inlet temperature and ambient temperature significantly influence on the performance of gas turbine power plant. The results were summarized as follows.

i) The thermal efficiency decreases and specific fuel consumption increases with the increasing in the ambient temperature.
ii) Increasing the turbine inlet temperature increases the output power and thermal efficiency as a result of increasing the turbine work.
iii) Evaporative cooling system improved the performance of gas turbine power plant as the thermal efficiency and network output are higher than that obtained from simple gas turbine plant
iv) This study shows the significant effect of incorporating air inlet cooling system with simple gas turbine power plant in order to retrofit gas turbine power plant in Nigeria.
v) The inlet air cooling system helps to reduce environmental pollution as the specific fuel consumption is less than that of simple gas turbine plant.

Reference

Abam, F. I., I. U. Ugot and D. I. Igbong (2011) Thermodynamic assessment of grid-based gas turbine power plants in nigeria. J. Emerg. Trends Eng. Applied Sci., 2: 1026-1033.

Mahmood F.G, Mahdi D.D (2009), 'A New Approach for Enhancing Performance of A Gas Turbine (Case Study: Khangiran Refinery)', Appl. Energy, 86: 2750-2759.

Ibrahim, T. K.; Rahman M. M.; Abdalla A. N (2010), 'Study on the effective parameter of gas turbine model with intercooled compression process', Scientific Research and Essays Vol. 5(23), pp. 3760-3770

Jaber, Q.M, Jaber, J.O and Khawaldah, M.A (2007), 'Assessment of Power Augmentation from Gas Turbine Power Plants Using Different Inlet Air Cooling Systems', Jordan Journal of Mechanical and Industrial Engineering , Vol.1 (1): 7 - 15

Shi, X , Agnew, B, Che, D and Gao, J (2010), 'Performance enhancement of conventional combined cycle power plant by inlet air cooling, inter-cooling and LNG cold energy utilization', Applied Thermal Engineering 30: 2003 - 2010

Al-Tobi, I (2009), 'Performance Enhancement of Gas Turbines by Inlet Air Cooling', International Conference on Communication, Computer and Power (ICCCP'09) Muscat, February 15-18: 165 – 170

Abam, F.I, Ugot, I.U and Igbong, D.I (2012), 'Performance Analysis and Components Irreversiblities of a (25 MW) Gas Turbine Power Plant Modeled with a Spray Cooler, American J. of Engineering and Applied Sciences 5 (1): 35-41

Hosseini, R, Beshkani, A and Soltani, M(2007), 'Performance improvement of gas turbines of Fars (Iran) combined cycle power plant by intake air cooling using a media evaporative cooler', Energy Conversion and Management 48: 1055–1064

Bird J and Grabe W (1991), 'Humidity effects on gas turbine performance', ASME Paper No 91-GT-329

Tsujikawa Y and Sawada T (1985), 'Characteristics of hydrogen-fueled gas turbine cycle with intercooler, hydrogen turbine and hydrogen heater', Int J Hydrogen Energy 10(103):677–83

EI-Hadik (1993), 'The impact of atmospheric conditions on gas turbine performance', J Eng Gas Turb Power 112:590–6

Ibrahim, T. K.; Rahman M. M.; Abdalla A. N (2011), 'Improvement of gas turbine performance based on inlet air cooling systems: A technical review', International Journal of Physical Sciences, 6 (4), 620-627

Farzaneh-Gord, M and Deymi-Dashtebayaz, M (2011), 'Effect of various inlet air cooling methods on gas turbine performance', Energy, 36, 1196–1205

Johanson, R.S (1988), "The Theory and Operation of Evaporative Coolers for Industrial Gas Turbine Installations", Gas Turbine and Aero-engine Congress and Exposition, June 5-9, Amsterdam, The Netherlands, Paper No. 88-GT-41

Ondryas, I.S; Wilson, D.A; Kawamoto, M and Haub, G.L (1991), "Options in Gas Turbine

Power Augmentation Using Inlet Air Chilling", Engineering for Gas Turbine and Power, Transaction of the ASME, Vol. 113, 203- 211

Johnke T and Mast M (2002), 'Power boosters—technologies to enhance gas turbine power output on demand, Siemens Power J Online May (2002) <http:// www.siemenswestinghouse.com/download/pool/ mast_engl_3.pdf>

Ameri M and Hejazi S.H (2004), 'The study of capacity enhancement of the Chabahar gas turbine installation using an absorption chiller', Appl Therm Eng, 24:59–68

Kakaras E, Doukelis S and Karellas S (2004), 'Compressor intake-air cooling in gas turbine plants', Energy, 29:2347–58

Arrieta R.P and Lora E.S (2005), 'Influence of ambient temperature on combined cycle power plant performance', Applied Energy, 80:261–72

Zadpoor A.A and Golshan A.H (2006), 'Performance improvement of a gas turbine cycle by using a desiccant-based evaporative cooling system', Energy, 31:2652–64

Elliot, J (2001), Chilled air takes weather out of equation. Diesel and Gas Turbine World Wide Gas Turbine Publications, USA

Kolp, D.A., W.M. Flye and H.A. Guidotti (2001), 'Advantages of air conditioning and supercharging an LM6000 gas turbine Inlet',. J. Eng. Gas Turbine Power Trans. ASME, 117: 513-527

Mercer, M (2002), One stop shop for inlet cooling systems diesel and gas turbine. Worldwide Gas Turbine Publications, USA

Amell, A.A. and Cadavid, F.J (2002), 'Influence of the relative humidity on the air cooling thermal load in gas turbine power plant', Applied Thermal Eng., 22: 1529-1533

Ana Paula P. S, Claudia R. A and Edson L. Z (2012), 'Comparison of Different Gas Turbine Inlet Air Cooling Methods', World Academy of Science, Engineering and Technology 61: 40 - 45

Rahman M.M., Ibrahim T.K., Kadirgama K., Mamat R., and Bakar R. A (2011), 'Influence of operation conditions and ambient temperature on performance of gas turbine power plant', Adv. Mater. Res., 189-193: 3007-3013

Barzegar Avval, H., Ahmadi, I.P., Ghaffarizadeh, A.R and Saidi, M.H (2011), 'Thermo-economic-environmental multiobjective optimization of a gas turbine power plant with preheater using evolutionary algorithm', Int. J. Energy Res., **35**:389–403

Kurt, H., Recebli, Z and Gredik, E(2009), 'Performance analysis of open cycle gas turbines', International Journal of Energy Research, 33(2):285–294.

Alok Kumar M and Sanjay, L. P (2012), 'Parametric Analysis of Cooled Gas Turbine Cycle with Evaporative Inlet Air Cooling', International Journal of Scientific & Engineering Research Volume 3(3):1-8

Büche, D (2003), Multi-Objective Evolutionary Optimization of Gas Turbine Components, Unpublished PhD Thesis, Swiss Federal Institute of Technology, Zürich

APPENDIX A

Station: AES Barge, Egbin, Lagos State

Unit No: PB 204: Year of Commissioning – 2000

Manufacturer: John Brown

Description	Unit	Jan.	Feb.	March	April	May	June	July	Aug	Sept	Oct	Nov	Dec	Avg
Ambient Temperature	^oC	29.0	28.1	32.2	33.3	28.9	29.1	35.0	30.2	31.2	29.9	30.1	28.8	30.48
Ambient Pressure	Bar													1.013
Compressor Disch. Pres.	Bar	8.55	9.86	9.52	8.72	9.53	9.36	8.93	8.65	9.13	9.23	8.69	9.24	9.12
Compressor Outlet Temp	^oC	344.4	354.4	356.7	360.8	370.6	371.6	367.7	372.5	359.6	363.7	350.1	349.8	360.16
Turbine inlet temp (T_3)*	^oC													1137.28
Vol. Flow rate of Fuel	m^3/s	3.08	3.21	3.18	2.96	3.15	2.95	3.00	3.04	2.98	3.01	3.10	3.08	3.06
Turbine outlets temp.(T_4)	^oC	476	483	493	498	476	467	485	464	468	473	489	477	479.08
Power Output	MW	31.3	33.7	32.9	26.8	32.5	20.1	29.4	30.9	28.6	29.6	31.8	31.1	29.89
Density of Air	Kg/m^3													1.17
Density of Fuel	Kg/m^3													0.8420
Fuel Flow Pressure	Bar	11.9	12.1	11.8	12.2	11.7	12.0	12.1	12.2	12.1	12.2	11.8	11.9	12.0
Air Adiabatic Index														1.4

CORROSION INHIBITION Of STAINLESS STEEL(314L) USING MOLASSES

OVRI, J.E.O. and IYASARA,A.C.

DEPARTMENT OF MATERIALS AND METALLURGICAL ENGINEERING
FEDERAL UNIVERSITY OF TECHNOLOGY, OWERRI, NIGERIA

ABSTRACT

The inhibition effect of molasses of varying concentrations (0.2g/L, 0.3g/L, 0.4g/L, 0.5g/L) on the corrosion of austenitic stainless steel (type 316L) in 0.5M tetraoxosulphate(vi)acid (H_2SO_4), Brine (6% NaCl), seawater (3% NaCl) and freshwater media was studied at room temperature. The corrosion rates of the steel were determined using the weight loss method for a period of fifty six days. The solution of the molasses inhibited the corrosion of the stainless steel samples to an extent depending on the concentration of the molasses and the type of medium. The results obtained showed that the higher the concentration of the molasses, the higher the inhibition efficiency (the lower the corrosion rate). The lowest corrosion rates were observed in freshwater medium while H_2SO_4 acid medium showed the highest corrosion rates. The inhibition is attributed to the physical adsorption of the inhibitor (molasses) on the surface of the stainless steel.

KEYWORDS: Inhibition, Molasses, Weight loss, Corrosion rate, Austenitic stainless steel,physical adsorption.

1.0 INTRODUCTION

Corrosion of engineering materials especially metals as a major industrial problem ha posed a serious concern to engineers, scientists and other researchers who are committed to the study of corrosion and its control.
Metals are exposed to the action of acids, bases and brine solutions in different ways and for many reasons. Therefore, the corrosion rates can be controlled or minimized by means of corrosion inhibitors[1].

1.1 Molasses as a corrosion Inhibitor

Inhibitors are known for their specificity of action when added or present in any given corrosive environment. An inhibitor is a substance which when added in small concentrations to an environment decreases the corrosion rate[2]. They are commonly added in small amounts either continuously or intermittently to acids, cooling waters and other environments to minimize or control serious corrosion menace.
Most of the well known inhibitors are natural products of plant origin e.g. molasses, alkaloids, tannins, pigments and amino acids. These inhibitors are known for their efficient characteristics which include non-expensive, ecologically friendly and non-toxic to the environment[(3-7)].
Molasses is a black viscous by-product of the processing of sugar[(4)]. Molasses contains sucrose, reduced sugars, salts (organic and inorganic), colloidal materials, vitamins, amino acids and waxes. The corrosion inhibition action of molasses and other natural plant inhibitors include the following mechanism:

- Adsorbing themselves on the metallic surfaces hence protecting the metallic surfaces by forming a thin film (passivation).
- Increasing the anodic or cathodic polarization behaviours (Tafel slopes).
- Increasing the electrical resistance of the metallic surface
- Reducing the movement or diffusion of ions to the metallic surface.

1.2 Austenitic Stainless Steel

Stainless steel generally denotes a large family of steel containing at least 11.5% chromium[8]. This amount of chromium prevents the formation of rust in unpolluted atmospheres, and it is from this characteristic that the popular designation "stainless" is derived. Stainless steel is corrosion resistant but not resistant to all corroding media (corrodants). Being corrosion resistant is due to a thin transparent film of chromium oxide that forms on the surface[9]. It will withstand oxidizing agents such as nitric acids but is attacked by reducing agents, e.g. hydrochloric acid (HCl), halogen salts such as sodium chloride (NaCl).

According to metallurgical structure, stainless steel is divided into three groups namely; austenitic (FCC) stainless steel, ferritic (BCC) stainless steel and martensitic (FCC or tetragonal) stainless steel[6]. The austenitic stainless steel contains 18% chromium and 8% Nickel, hence is known as 18-8 stainless steel. As a group, austenitic stainless steel is non-magnetic, resistant to atmospheric corrosion, more ductile than the ferritic and martensitic stainless steels and can only be hardened by cold working.

1.3 Objectives of the work

- To determine the inhibition efficiency of molasses on the corrosion of austenitic stainless steel in acidic, salty (brine and seawater) and freshwater environments
- To show that stainless steel is not always corrosion resistant in all environments but can corrode when subjected to severe environments.

2.0 MATERIALS AND METHODS

2.1 Samples preparation

The austenitic stainless steel sample (type 316L) used for this investigation was obtained from Nigerian Foundry, Lagos. It was obtained in sheet of thickness, 0.5cm and cut into coupons of dimension, 5cm X 1.5cm. a hole of 0.35cm was drilled on each coupon through which a twine was passed to aid suspension and total immersion in the media.
The chemical composition of the steel sample is shown in Table 1.

Table 1: Chemical Composition of the Austenitic Stainless Steel (Type 316L)

Element	C	Cr	Ni	Mn	Si	P	S
Wt.(%)	0.08	18.04	8.34	2.00	1.00	0.05	0.03

2.2 Environmental and Inhibitor preparations

Four different environments were used for the investigation. They are standard solutions of

- Brine (6% NaCl solution)
- 0.5M H_2SO_4 acid
- Seawater (3% NaCl solution)
- Freshwater

The brine and H_2SO_4 acid solutions were prepared in the chemistry laboratory of chemistry department, Federal University of Technology, Owerri, Nigeria. The seawater used in this study was obtained from Abonema high sea creek, Port-Harcourt while the freshwater was collected from the local otamiri river in Owerri, Imo State. The chemical analyses of the water samples were performed at SAAT laboratory, Federal university of technology, Owerri.

Table 2: Chemical Analyses of Water samples

Ions	Ca^{2+}	Mg^{2+}	Fe^{2+}	Na^{+}	CO_2	Cl^{-}	O_2^{-}	SO_4^{2-}	HCO_3	NO_3^{-}
Seawater	7.10	3.12	0.29	4.70	0.31	54.36	0.55	2.99	5.23	0.001
Freshwater	1.38	3.34	0.01	1.50	4.25	14.47	5.50	0.40	42.12	0.006

2.3 Experimental Set up and Monitoring

The initial weights of the coupons were taken to the nearest 0.001g on a digital electronic weighing machine (OHAUS Adventurer), degreased and dried in acetone (analar grade).
In each of the environment, five different experiments were setup using the varying concentrations of the molasses including a control (without molasses). The sample coupons were totally immersed in a plastic bowls containing each of the prepared corrosive medium.
The weight loss of each coupon was determined at intervals of seven days for a total of fifty-six days. Thus, the weight loss within the immersion period was determined as the difference between the initial weight prior to immersion and the final weight after immersion, and the corresponding corrosion rate calculated.

3.0 EXPERIMENTAL RESULTS

3.1 Determination of Corrosion Rates

The corrosion rates were calculated using weight loss measurement obtained over the period of the investigation. The following relationship was used for the calculation[10]:.

$$Cr = \frac{534}{D.A.T}$$

Where; Cr = Corrosion rate in mils penetration per year (mpy)
W = Weight loss (g)
D = Density of the metal = 8.4g/cm^3
A = Area of the specimen = 6.68 cm^2
T = Time of exposure (days)

3.2 Calculation of Inhibition Efficiency

The percentage inhibitor efficiency was determined for all the environments at the 56th day (last day) of the experiment. It was calculated by[5]:

$$I\% = \frac{[W_0 - W_1]\ 100}{W_o}$$

Where; I% = percentage Inhibitor efficiency
W_o= Weight loss without inhibitor
W_1 = Weight loss with inhibitor

The results obtained are shown in Tables 3 -6 and presented in Figures 1 –5 with the corresponding variables.

Table 3: Weight loss, Corrosion rate (Cr) and % Inhibitor efficiency (%I) of Austenitic stainless steel exposed to 0.5M H_2SO_4

Medium/coupon No.	**14th day**		**28th day**		**42nd day**		**56th day**		**70th day**		
0.5M H_2SO_4	**Weight loss (mg)**	**Cr X 10^{-3} (mpy)**	**Weight loss (mg)**	**Cr X 10^{-3} (mpy)**	**Weight loss (mg)**	**Cr X 10^{-3} (mpy)**	**Weight loss (mg)**	**Cr X 10^{-3} (mpy)**	**Weight loss (mg)**	**Cr X 10^{-3} (mpy)**	**%I**
S_1	40.00	27.20	50.00	17.00	70.00	15.86	80.00	13.60	100.00	13.60	-
S_2	20.00	13.60	30.00	10.20	40.00	9.10	45.00	7.65	50.00	6.80	27.80
S_3	15.00	10.20	20.00	6.80	30.00	6.80	35.00	5.95	40.00	5.44	33.30
S_4	10.00	6.80	10.00	3.40	15.00	3.34	15.00	2.55	15.00	2.04	45.60
S_5	5.00	3.40	10.00	3.40	10.00	2.27	10.00	1.70	12.00	1.63	56.70

Legend:

S_1 = 0.5M H_2SO_4 without molasses (Control)
S_2 = 0.5M H_2SO_4 with 0.2g/L concentration of molasses
S_3 = 0.5M H_2SO_4 with 0.3g/L concentration of molasses
S_4 = 0.5M H_2SO_4 with 0.4g/L concentration of molasses
S_5 = 0.5M H_2SO_4 with 0.5g/L concentration of molasses

Table 4: Weight loss, Corrosion rate (Cr) and % Inhibitor efficiency (%I) of Austenitic stainless steel exposed to Brine

Medium/coupon No.	**14th day**		**28th day**		**42nd day**		**56th day**		**70th day**		
Brine	**Weight loss (mg)**	**Cr X 10^{-3} (mpy)**	**Weight loss (mg)**	**Cr X 10^{-3} (mpy)**	**Weight loss (mg)**	**Cr X 10^{-3} (mpy)**	**Weight loss (mg)**	**Cr X 10^{-3} (mpy)**	**Weight loss (mg)**	**Cr X 10^{-3} (mpy)**	**%I**
B_1	30.00	20.39	40.00	13.60	60.00	13.60	70.00	11.90	80.00	10.88	-
B_2	20.00	13.60	25.00	8.50	30.00	6.80	40.00	6.80	45.00	6.12	28.60
B_3	15.00	10.20	20.00	6.80	25.00	5.67	25.00	4.25	30.00	4.08	35.70
B_4	8.00	5.44	10.00	3.40	12.00	2.72	15.00	2.55	18.00	2.45	50.00
B_5	4.00	2.72	5.00	1.70	5.00	1.13	6.00	1.02	10.00	1.36	57.10

Legend:
B_1 = Brine without molasses (Control)
B_2 = Brine with 0.2g/L concentration of molasses
B_3 = Brine with 0.3g/L concentration of molasses
B_4 = Brine with 0.4g/L concentration of molasses
B_5 = Brine with 0.5g/L concentration of molasses

Table 5: Weight loss, Corrosion rate (Cr) and % Inhibitor efficiency (%I) of Austenitic stainless steel exposed to seawater

Medium/coupon No.	**14th day**		**28th day**		**42nd day**		**56th day**		**70th day**		
Seawater	**Weight loss (mg)**	**Cr X 10^{-3} (mpy)**	**Weight loss (mg)**	**Cr X 10^{-3} (mpy)**	**Weight loss (mg)**	**Cr X 10^{-3} (mpy)**	**Weight loss (mg)**	**Cr X 10^{-3} (mpy)**	**Weight loss (mg)**	**Cr X 10^{-3} (mpy)**	**%I**
W_1	25.00	17.00	30.00	10.20	40.00	9.06	45.00	7.65	50.00	6.80	-
W_2	15.00	10.20	20.00	6.80	25.00	5.67	25.00	4.25	30.00	4.08	33.30
W_3	10.00	6.80	10.00	3.40	15.00	3.40	15.00	2.55	18.00	2.45	44.40
W_4	5.00	3.40	5.00	1.70	7.00	1.59	10.00	1.70	10.00	1.36	55.60
W_5	5.00	3.40	5.00	1.70	5.00	1.13	8.00	1.19	8.00	1.09	66.70

Legend:
W_1 = Seawater without molasses (Control)
W_2 = Seawater with 0.2g/L concentration of molasses
W_3 = Seawater with 0.3g/L concentration of molasses
W_4 = Seawater with 0.4g/L concentration of molasses
W_5 = Seawater with 0.5g/L concentration of molasses

Table 6: Weight loss, Corrosion rate (Cr) and % Inhibitor efficiency (%I) of Austenitic stainless steel exposed to Freshwater

Medium/coupon No.	14th day		28th day		42nd day		56th day		70th day		
Freshwater	Weight loss (mg)	Cr X 10^{-3} (mpy)	Weight loss (mg)	Cr X 10^{-3} (mpy)	Weight loss (mg)	Cr X 10^{-3} (mpy)	Weight loss (mg)	Cr X 10^{-3} (mpy)	Weight loss (mg)	Cr X 10^{-3} (mpy)	%I
F_1	15.00	10.20	20.00	6.80	25.00	5.67	30.00	5.10	30.00	4.08	-
F_2	10.00	6.80	10.00	3.40	12.00	2.72	15.00	2.55	18.00	2.45	33.30
F_3	8.00	5.44	10.00	3.40	10.00	2.27	12.00	2.04	15.00	2.04	53.30
F_4	5.00	3.40	5.00	1.70	8.00	1.81	10.00	1.70	10.00	1.36	66.67
F_5	2.00	1.36	4.00	1.36	5.00	1.13	5.00	0.85	5.00	0.68	83.33

Legend:

F_1 = Freshwater without molasses (Control)
F_2 = Freshwater with 0.2g/L concentration of molasses
F_3 = Freshwater with 0.3g/L concentration of molasses
F_4 = Freshwater with 0.4g/L concentration of molasses
F_5 = Freshwater with 0.5g/L concentration of molasses

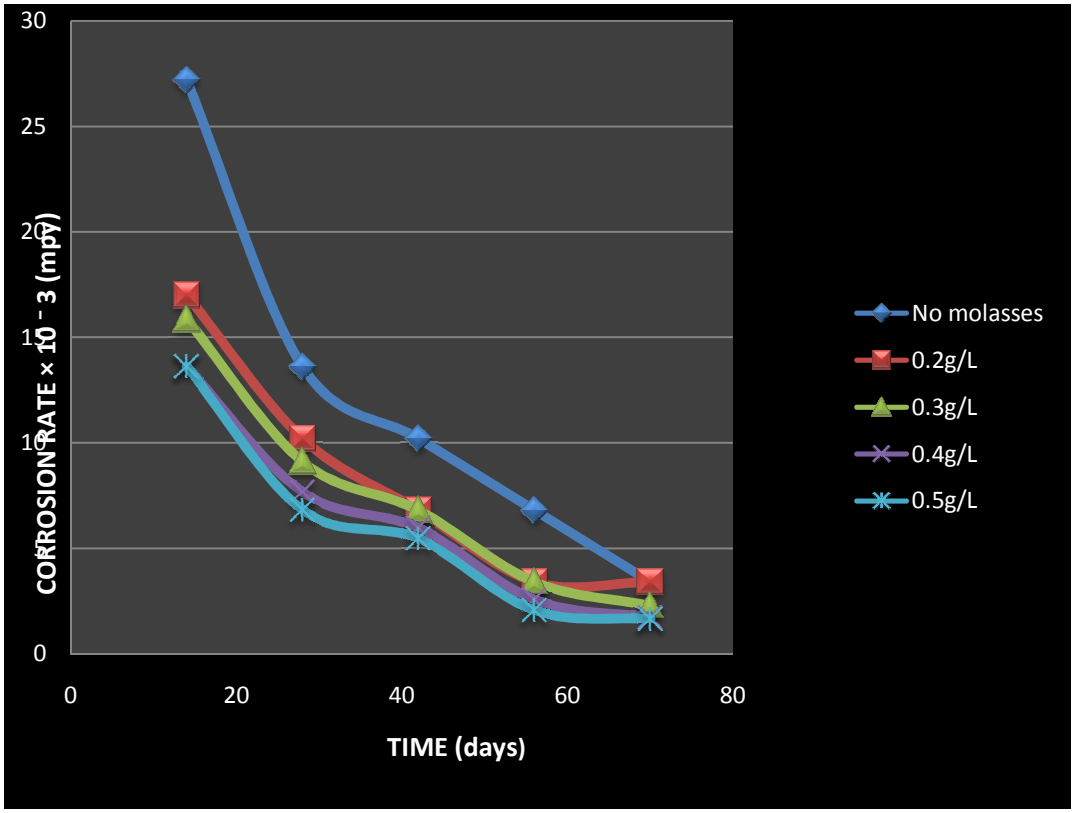

Fig 1. CORROSION RATE (CR) × 10^{-3}(mpy) Vs EXPOSURE TIME (DAYS) OF STEEL EXPOSED TO H_2SO_4

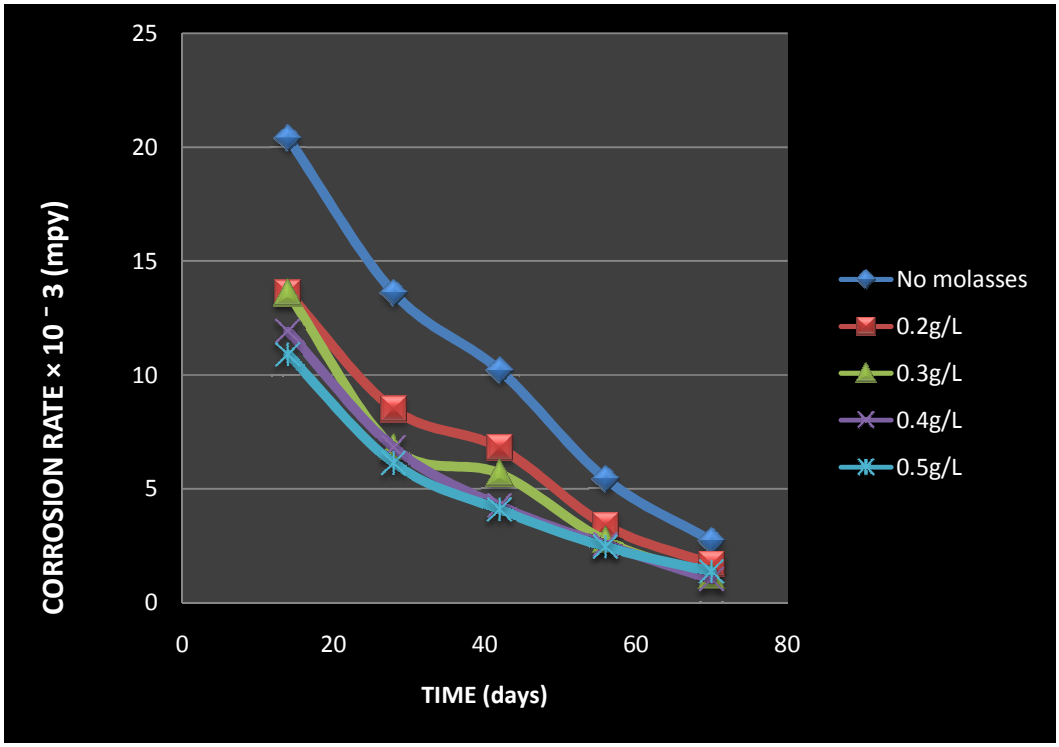

Fig 2. CORROSION RATE (CR) × 10^{-3}(mpy) Vs EXPOSURE TIME (DAYS) OF STEEL EXPOSED TO BRINE

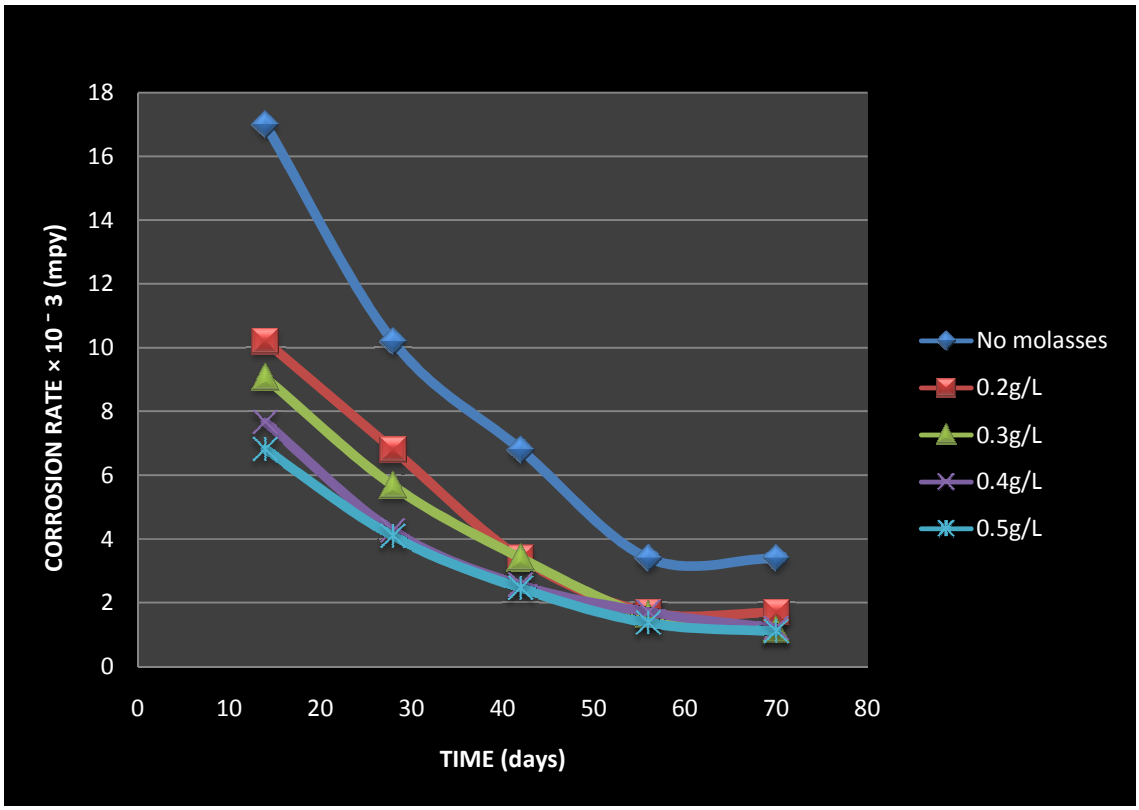

Fig 3. CORROSION RATE (CR) × 10^{-3}(mpy) Vs EXPOSURE TIME (DAYS) OF STEEL EXPOSED TO SEAWATER

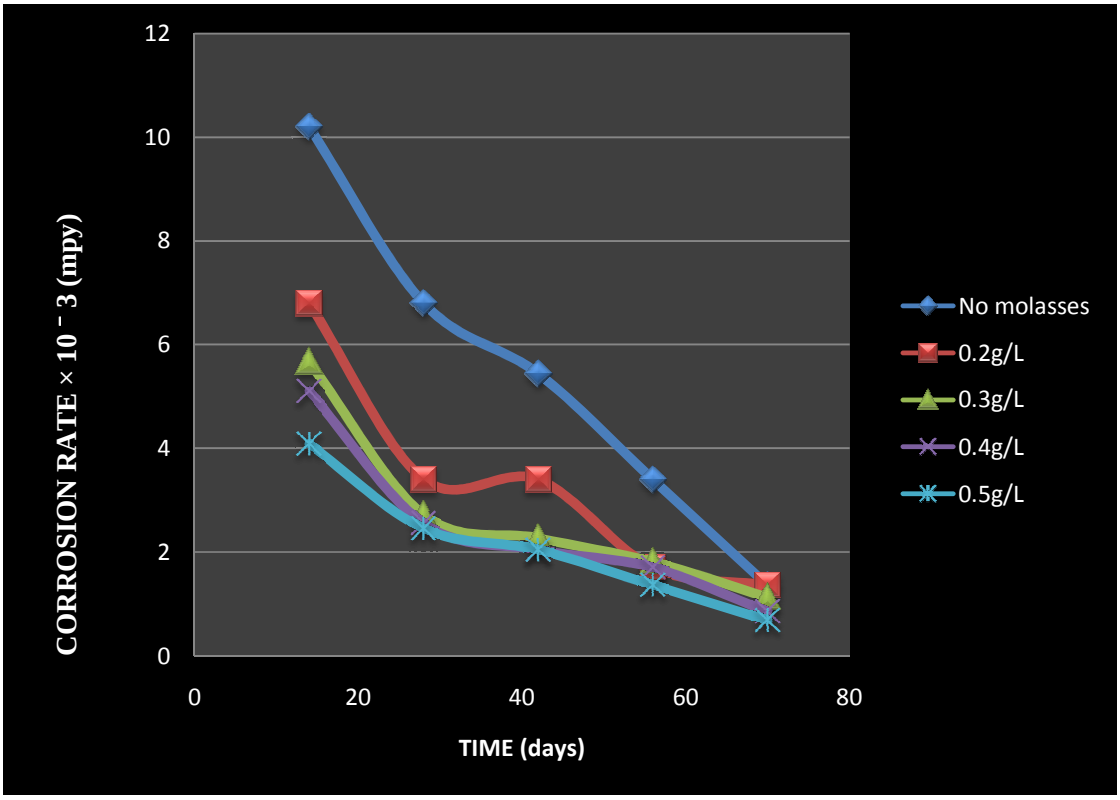

Fig 4. CORROSION RATE (CR) × 10^{-3}(mpy) Vs EXPOSURE TIME (DAYS) OF STEEL EXPOSED TO FRESHWATER

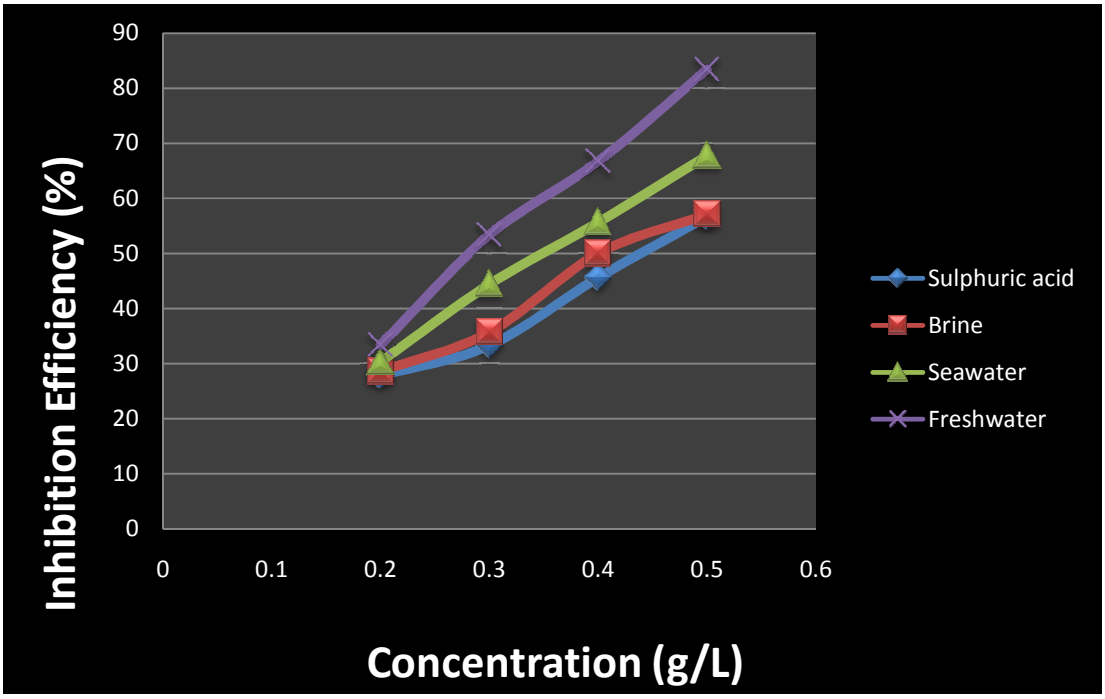

Fig 5. % INHIBITION EFFICIENCY Vs CONCENTRATION (g/L)

4.0 DISCUSSION OF RESULTS

4.1 weight Loss

Tables 3 -6 show the values of weight loss of the steel sample with time for all the media. From the results obtained and presented in the tables, it was observed that the weight loss increases with the time of exposure.

H_2SO_4 acid medium exhibited the highest weight losses (as shown in Table 3), while the lowest weight loss was observed in the freshwater environment (Table 6). The weight loss observed in the steel samples was due to the presence of the aggressive molecular species (ions) contained in the test media[10,11,12,13]. These ions are SO_4^{2-} (from H_2SO_4), Cl^- (from brine and seawater) and OH^- (from freshwater). The SO_4^{2-} ion is the most aggressive and therefore attacks the stainless steel strongly.

Generally, the control experiments (i.e.those media without molasses) recorded higher weight losses more than those media with different concentrations of the inhibitor (molasses).

4.2 Corrosion Rate

The corrosion rates of the steel samples were shown in Tables 3 – 6 and presented in Figures 1 -4. From the plots, corrosion rates decrease sharply with increase in exposure time in all the media. The highest corrosion rate was observed in H_2SO_4 medium due to the presence of the aggressive SO_4^{2-} ions followed by brine and seawater media containing Cl^- ions while the freshwater medium which contains OH^- ions recorded the least corrosion rates.

The higher the concentration of the molasses, the lower the corrosion rate of the steel sample. Molasses is an organic inhibitor, hence adsorption type inhibitor. It adsorbs on the metal surface and depresses both metal dissolution and reduction reactions[14]. Therefore, this blocking effect is due to the blanketing of the metal surface which in turn reduces the active sites on the metal surface upon which anodic and cathodic reactions could occur.

4.3 **Inhibition Efficiency**

Figure 5 shows the variation of inhibition efficiency (I %) with concentration of molasses (g/L). It was observed from the graph that the inhibition efficiency increases with increase in the concentration of the molasses. Thus, the higher the concentration of the molasses, the lower the corrosion rates.The inhibition (decrease in corrosion rate) is attributed to the physical adsorption of the molasses.Consequently,adsorption of the molasses was proposed as the reaction mechanism for the inhibition.However,further work is on-going on the investigation of this reaction mechanism.

5.0 **CONCLUSION**

Based on the results obtained, the following conclusions can be made:

(1) Molasses could best serve as a corrosion inhibitor in freshwater, seawater, brine and H_2SO_4 solutions and performing optimally at 0.5g/L concentration.
(2) Molasses inhibited the corrosion reaction through the mechanism of physical adsorption on the metal (steel) surface.
(3) The inhibition efficiency (I %) of molasses increases with increase in the concentration of the inhibitor.
(4) Austenitic stainless steel is naturally resistant to corrosion to a measurable extent due to its nickel and chromium contents.

REFERENCES

(1) Fontana, M.G and Greene, N.D (1987), Corrosion Engineering, 4th edition. Mc-Graw Hill International Book Coy
(2) Ijomah, M.N.C ,(1991), Elements of Corrosion and Protection. Auto-century publication Co, Enugu.
(3) Ebenso, E.E, et al (2004), Corrosion Inhibition of some plant extract on Aluminium in Acidic medium. J of Corr. Sc & Tech. vol.1.1
(4).http://en.wikipedia.org/wiki/molasses (2011)

(5). C.A. Loto: (1998), The effect of Vernonia Amygdalina (Bitterleaf) solution Extract on the Corrosion Inhibition of Mild steel in 0.05M Hydrochloric and Tetraoxosulphate (iv) Acid, Nigerian Corrosion Journal (NCJ), Vol 1, No. 1 Sept., 19-28.

(6) C.A. Loto, (1990) Corrosion Prevention and Control Journal, Vol 37,5,131.

(7) Olusegun, K., etal: 2004, The Inhibition of Mild Steel corrosion in an Acidic medium by fruit juice of Citrus paradise, Journal of Corrosion science and Technology, 1., 75-78.

(8)Philip, A.S (1983), Corrosion and Protection Handbook. Dekken Inc. New York

(9) Bedricks, A.J. (1979), Corrosion of Stainless Steels.

(10) J.E.O. Ovri, (1998), Corrosion Resistance of Mg MnZn Ferrite in Hostile Environments, Nigerian Corrosion Journal Vol. 1 No. 1, 6 5-72.

(11) A.C. Iyasara: Corrosion Inhibition of Stainless Steel in Different Media using Molasses, B.Eng Dissertation, Federal University of Technology, Owerri, (unpublished).

(12) J.E.O. Ovri, (1998), Corrosion Resistance of Mg MnZn Ferrite in Hostile Environments, Nigerian Corrosion Journal Vol. 1 No. 1, 6 5-72.

(13) J.E.O. Ovri et al , (2010), Corrosion Protection and Control of Reinforcing Steel Rods in Concrete, Global Journal of Engineering and Technology, Vol. 3 No. 3 559-565.

(14**)** Adeyemi, O. and Imosogie B. (2001), Effect of Some Nitrogen- Containing Organic Compounds on Corrosion of Mild Steel in Seawater, Journal of Construction and Material Technology, Vol. 1.2.